



## PDF hosted at the Radboud Repository of the Radboud University Nijmegen

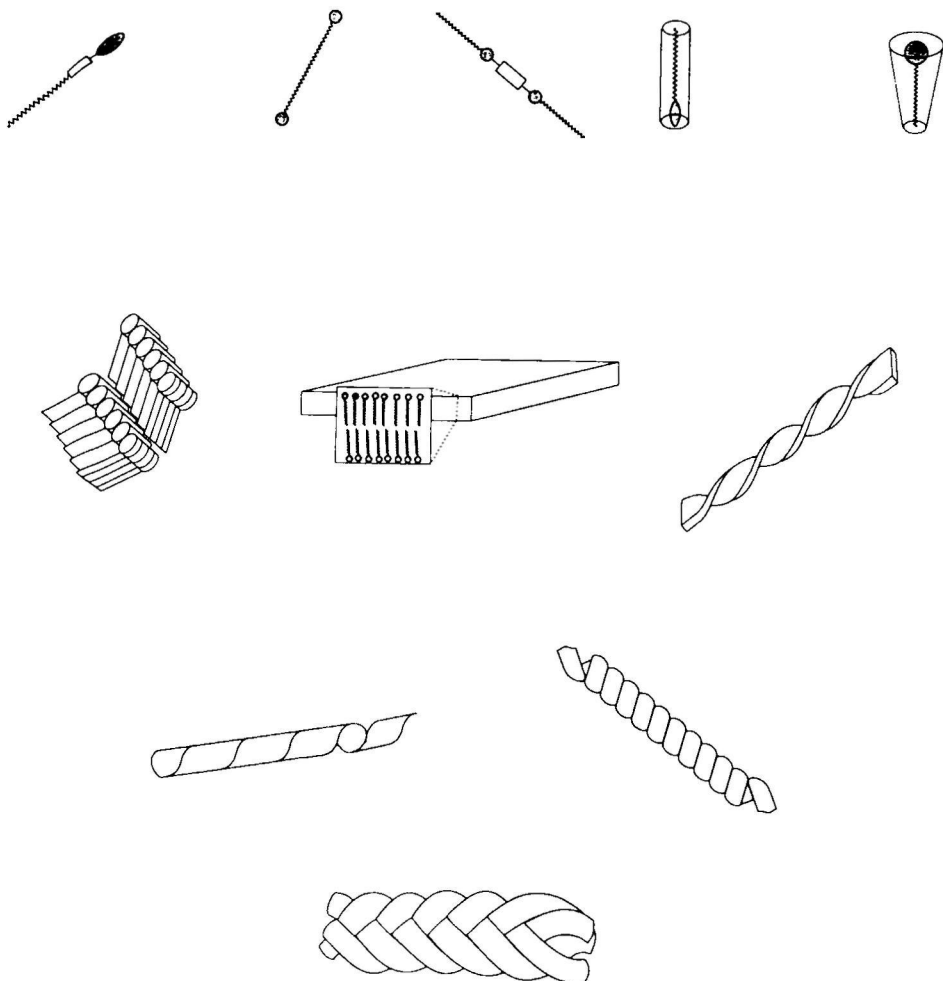
The following full text is a publisher's version.

For additional information about this publication click this link.

<http://hdl.handle.net/2066/146215>

Please be advised that this information was generated on 2017-12-05 and may be subject to change.

# Supramolecular Structures from Gluconamide Building Blocks



Rudi Hafkamp





# **Supramolecular Structures from Gluconamide Building Blocks**

Een Wetenschappelijke Proeve op het Gebied van de  
**Natuurwetenschappen**

**Proefschrift**

ter verkrijging van de graad van doctor aan de Katholieke Universiteit van Nijmegen,  
volgens het besluit van het College van Decanen in het openbaar te verdedigen op  
dinsdag 18 juni 1996, des namiddags om 1 30 precies

door

**Rudolfus Johannes Hendrikus Hafkamp**

Geboren op 6 juli 1966  
te Rheden

Promotor

Prof Dr R J M Nolte

Co-promotor

Dr M C Feiters

Manuscriptcommissie

Dr C F van Nostrum

Dr H A van Doren (NIKO-TNO)

ISBN 90-9009507-1

*Aan degenen die mij altijd hebben gesteund:*

*Henriet en mijn ouders*



# Voorwoord

“Normale” chemici gaan eerst studeren, dan promoveren en pas aan het eind van hun promotie wordt aan een vaste baan gedacht. In mijn geval zijn de zaken wat zig-zaggend verlopen. Door scheikunde in deeltijd te studeren, had ik aan het begin van dit promotieonderzoek universiteiten nauwelijks bij daglicht gezien. Omdat sommige spelregels in het onderzoek bij het bedrijfsleven nu eenmaal anders zijn dan in de academische wereld, kreeg ik in het begin het gevoel bezig te zijn met een geblinddoekte rit over glad ijs. Gelukkig was er een aantal mensen om mij heen die mij niet alleen de blinddoek af deed maar ook schaaften aan de techniek en waarschuwde voor gevaarlijke wakken (!). Door vele aanwijzingen kon ik mijn techniek verbeteren waardoor sneller, efficiënter, zonder angst en vooral met veel enthousiasme door het onderzoek geschaatst kon worden. Verder heb ik veel gehad aan klankborden, luisterende oren en aanmoedigende mensen. Degenen die daarbij hebben geholpen, wil ik hierbij hartelijk danken

Prof. Roeland Nolte, jou heb ik altijd als een hoofdtrainer beschouwd waaraan ik veel heb gehad. Jouw enthousiasme zette me telkens weer aan tot het zoeken naar nieuwe aggregaten in de vorm van vlechtjes, buisjes, ruggegraten en bloemkolen. Daarnaast was de hulp van Dr. Martin Feiters voor mij onontbeerlijk en een stimulans om een ingeslagen weg niet te snel te verlaten. Gelukkig verliep de samenwerking met de labgenoten als Alan, Albert, Bert, (sparring partner) Fokke, Hanny, Hans (2x), Hein, Gerben, Gino, Joost, Nico, Ruud, René (ook dank voor het nakijken van het niet-gepolijste manuscript), Patricia, Peter en Stan alsmede alle studenten erg goed. Bovendien kan ik door hen met veel plezier terug denken aan mijn ‘Nijmeegse tijd’

Hoe lang mijn carrière binnen of buiten de chemie ook gaat duren, “mijn studenten” Bas Kokke en Thien-An Tran Chau zal ik niet snel vergeten. Het door Bas opgebrachte enthousiasme en doorzettingsvermogen om zijn onderzoek tot een goed einde te brengen, zelfs bij een tegenstribbelende katalysator, kan voor iedereen een voorbeeld zijn. Hoewel jouw waardering voor dubieuze films, bloederige grappen en de Sjonnies mij nooit hebben aangesproken, vond ik de daaruit voortvloeiende (luidruchtige) discussies wel erg leuk. De werklust en doelgerichtheid van Thien-An, een half woord was vaak al genoeg, is voor mij een voorbeeld geweest. Verder was je gastvrijheid erg plezierig. Dank aan Dominique Hubert en Bart Nelissen voor het schrijven van een literatuurscriptie waarvan een gedeelte is opgenomen in Hoofdstuk 2.

Waar zouden we zijn zonder de analyse-trein van Helene Amadjais, Peter van Galen, Pieter van der Meer en Ad Swolfs? Samen met Ad Swolfs naar de moleculen kijken met behulp van NMR was niet alleen plezierig maar ook bijzonder leerzaam. Verder helpen vaste krachten als Chris Kroon, Wim van Luyn, Sandra Tjindink en Hans Adams een laboratorium draaiende te houden. Hans Adams is een hele ondersteuning bij de verhuizing van de begane grond naar de eerste verdieping geweest. Voor Gerda Nachtegaal was een duidelijk gestelde vraag al voldoende om direct te gaan meten, ondanks alle inspanningen is er helaas niet uitgekomen wat we ervan verwacht hadden.

Dr. Gordon Chittenden en Prof. Tesser wil ik danken voor het aanreiken van de juiste literatuur en het voeren van leerzame discussies, Henk Regeling voor het aanleren van truuksjes in

de synthese van suikerderivaten en Dr Hans Scheeren en Rene Aben voor het denkwerk bij en gebruik van de hogedruk-apparatuur Mede dankzij het uitvoeren van reacties onder hoge druk heb ik schier onmogelijk te synthetiseren verbindingen toch kunnen maken

In het hier beschreven onderzoek zijn veel experimenten met elektronenmicroscopie uitgevoerd Dit was onmogelijk geweest zonder de hulp van Huub Geurts De apparatuur was altijd operationeel, jij had bijna altijd tijd voor me en was nooit te beroerd om iets te doen wat misschien je taak helemaal niet was (zoals experimenteren met monstervoorbereiding, het keer op keer uitleggen van de technieken aan studenten, promovendi en profs, tot en met het opzoeken van vergelijkbare structuren in de literatuur) Bovendien was het voeren van (stoere) gesprekken over wielrennen altijd leuk

Dank aan Bart Knuiman voor de hulp bij de polymerisatieexperimenten beschreven in Appendix 2 Jan Smits wil bedanken voor de hulp bij het gebruik van de poederdiffractometer Een goede bibliothecaire service was te danken aan Jo en Henk Catherine Crowley dank ik voor de hulp bij correcties in de Engelse taal

Een aantal cruciale metingen zijn buiten de deur uitgevoerd zoals opheldering van een kristalstructuur (zie Hoofdstuk 3) door Dr Huub Kooiman en Dr Ton Spek (RUU), temperatuur-afhankelijke infrarood metingen door Bert Lutz (RUU) en temperatuur-afhankelijke SAXS-metingen door Dr Stephen Picken (Akzo Nobel) Met veel plezier denk ik terug aan de metingen uitgevoerd bij NIKO-TNO in Groningen en aan de samenwerking met Dr Henk van Doren (ook dank voor de correcties van het manuscript) Vanaf het eerste bezoek voelde ik me thuis bij het NIKO, een gevoel dat door jou en je groep van harte ondersteund werd, hiervoor mijn hartelijke dank

Zonder chemie zou er geen leven op aarde zijn, toch is leven naast de chemie voor mij ook belangrijk De nodige ontspanning heb ik beleefd in Deventer, Giethoorn, De Weerribben en de Alblasserwaard met mijn schaatsmaatjes Rob, Jan, Jan, en Wim De juiste aanwijzingen ter verbetering van de techniek, stimulatie tot betere prestaties en gezelligheid heb ik altijd kunnen waarderen

Het feit dat ik altijd terug heb kunnen vallen op familie, zowel tijdens de studies als in de promotietijd, heeft mij altijd het comfortabele gevoel gegeven dat ik er niet alleen voor stond Tot slot wil mijn geliefde Henriët bedanken Als ik van jou niet alle steun en medewerking had gekregen, van afremmen waar nodig tot en met hulp bij het afdrukken van EM-foto's op zaterdagmiddag, was me dit nooit gelukt

*Rudi*



# Contents

## Chapter 1 General introduction

1 1 Introduction to supramolecular chemistry	1
1 2 Liquid crystals	1
1 3 Contents of this thesis	2
1 4 Literature	3

## Chapter 2 Literature survey

2 1 Membrane mimetic chemistry	5
2 2 Amphiphiles	5
2 2 1 Relationship between amphiphilic structure and aggregate morphology	6
2 2 2 Chiral amphiphiles	7
2 2 3 Models for aggregates of chiral amphiphiles	9
2 2 4 Carbohydrate amphiphiles	9
2 3 Thermotropic liquid crystalline properties of carbohydrate amphiphiles	11
2 4 Functional aggregates	12
2 5 Literature	13

## Chapter 3 Thermotropic liquid crystalline properties of *N*-*n*-alkyl-*D*-gluconamides

3 1 Introduction	19
3 2 Experimental	20
3 2 1 Syntheses	20
3 2 2 Metal complexes	30
3 3 Results and discussion	31
3 3 1 Synthesis of imidazole ligand	31
3 3 2 Effect of the length of the alkyl chain on the L C behavior of compounds <b>1</b> and model compounds	33
3 3 3 Characterization of the L C phases of compounds <b>1</b>	39
3 3 4 X-ray structure of compound <b>1a</b>	40
3 3 5 Solution <sup>1</sup> H-NMR study on <b>1a</b>	43
3 3 6 Thermotropic L C behavior of compounds related to imidazolyl gluconamides <b>1</b>	43
3 3 6 1 Different substituents on the terminus of the head group	43
3 3 6 2 Gluconamides with a diacetylene function in the alkyl chain	46
3 3 6 3 <i>n</i> -Alkyl gluconates	47
3 3 6 4 Amide without the carbohydrate part	47
3 3 7 Metallomesogens	48



3 4 Concluding remarks	51
3 5 Literature	52

## **Chapter 4    Suprastructures in water from imidazole containing gluconamides**

4 1 Introduction	55
4 2 Experimental	56
4 2 1 Syntheses	56
4 2 2 Determination of the $pK_a^*$ values	57
4 2 3 UV-vis titrations	58
4 2 4 DSC measurements	58
4 2 5 Electron microscopy	58
4 3 Results and discussion	59
4 3 1 $pK_a$ titrations	59
4 3 2 UV-vis titrations	60
4 3 3 DSC experiments	64
4 3 4 Electron microscopy	69
4 4 Concluding remarks	75
4 5 Literature	77

## **Chapter 5    Positional variation of the imidazole group in gluconamide amphiphiles.                     Effects on the aggregation behavior**

5 1 Introduction	79
5 2 Experimental section	81
5 2 1 Syntheses	81
5 2 2 Measurements of isotherms	85
5 2 3 SAXS experiments	85
5 2 4 Electron microscopy	85
5 3 Results and discussion	86
5 3 1 Preparation of the compounds	86
5 3 2 $pK_a$ determination	88
5 3 3 IR experiments	88
5 3 4 UV-vis spectroscopy	89
5 3 5 Electron microscopy	91
5 3 6 Isotherms	96
5 3 7 X-ray powder diffraction experiments	96
5 3 8 Thermotropic L C behavior	97
5 4 Concluding remarks	97
5 5 Literature	98

## **Chapter 6   Organo-gels from carbohydrate amphiphiles**

6 1 Introduction	101
6 2 Experimental section	105
6 2 1 Syntheses	105
6 2 2 Physical measurements	109
6 3 Results	110
6 3 1 Gelation behavior	110
6 3 2 DSC measurements	113
6 3 3 Electron microscopy	114
6 3 3 1 Gluconamides with aromatic substituents on C <sup>6</sup>	115
6 3 3 2 Gluconamides with aliphatic substituents on C <sup>6</sup>	117
6 3 3 3 Gluconamides without C <sup>6</sup> substituents	120
6 3 4 NMR study	121
6 3 5 X-ray powder diffraction	125
6 3 6 IR experiments	128
6 4 Discussion	131
6 5 Concluding remarks	134
6 6 Literature	135

## **Chapter 7   Catalysis using supramolecular aggregates**

7 1 Introduction	137
7 2 Experimental	138
7 2 1 Syntheses	138
7 2 2 Catalytic aziridinations   General remarks	139
7 2 3 Aziridinations in acetonitrile	139
7 2 4 Aziridinations in chloroform	140
7 2 5 Aziridinations in aqueous dispersions	140
7 2 6 General procedure for the epoxidation reactions	142
7 3 Results and discussion	142
7 3 1 Aziridination in organic solvents	143
7 3 2 Aziridination in water	144
7 3 3 Epoxidation	147
7 4 Concluding remarks	148
7 5 Literature	149

<b>Appendix 1</b>	<b>Suprastructures from Pd complexes made of pyridyl substituted gluconamides</b>	151
	Experimental	152
	Literature	153
<b>Appendix 2</b>	<b>Polymerization of suprastructures</b>	155
	Experimental	156
	Literature	157
<b>Appendix 3</b>	<b>Atomic positional and vibrational parameters (with esd's) for Compound 1a (Chapter 3)</b>	159
<b>Summary</b>		161
<b>Samenvatting</b>		163
<b>Curriculum Vitae</b>		165

# Chapter 1

## General introduction

### 1.1 Introduction to supramolecular chemistry

Traditional synthetic chemistry is concerned with the preparation of single low molecular weight molecules while in polymer chemistry the products have high molecular masses. In both cases the building blocks are linked to each other by covalent bonds. A relatively new field is supramolecular chemistry which is based on non-covalent bonds like H-bridges, electrostatic and van der Waals interactions. One of the pioneers in this type of chemistry, J.-M. Lehn, formulated the new field of research as follows: "Beyond molecular chemistry, based on the covalent bond lies supramolecular chemistry, based on molecular interactions and the intermolecular bond."<sup>1</sup> In other words, in supramolecular chemistry, not only the (physical) properties of the individual compounds are studied but also the change of properties upon and after assembling of molecules are points of interest.

Chemists working in the field of supramolecular chemistry are often inspired by nature since many biological systems like the DNA double helix, a biomembrane or the quaternary structure of a protein are based on non-covalent interactions. As a result of these interactions, self-organization, *i.e.* the spontaneous assembly of monomeric parts towards ordered structures, occurs and is indispensable for living systems. Examples of highly ordered assemblies are cell membranes, DNA double helices and the tobacco mosaic virus.

Supramolecular chemistry can be divided into two areas, host-guest chemistry and the chemistry of molecular aggregates. Host-guest<sup>2</sup> chemistry is concerned with the binding of molecules (guests) in larger (host or receptor) molecules and the designers are mostly inspired by the naturally occurring enzymes. Among the early examples of host-guest complexes are the cation-binding crown ethers discovered by Pedersen.<sup>3</sup> Many receptor molecules have been developed since then, *e.g.* based on Kemp's triacid,<sup>4</sup> cyclodextrines,<sup>5</sup> calixarenes<sup>6</sup> and diphenylglycoluril.<sup>7</sup>

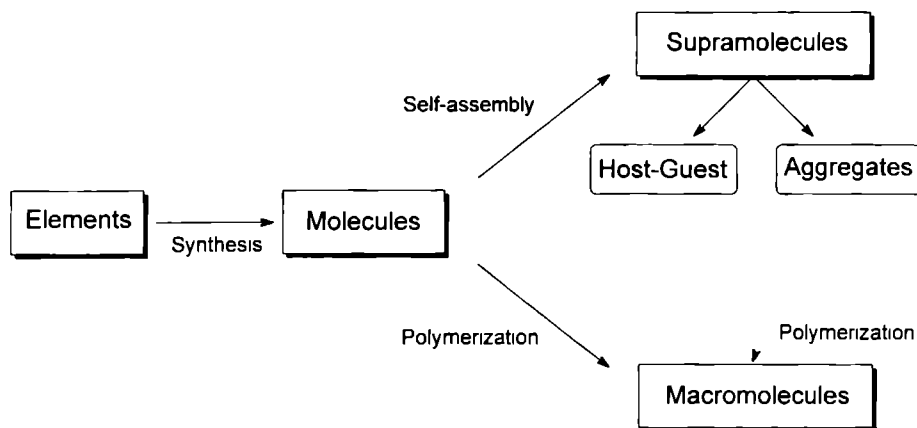
Molecular aggregates are formed by assembling molecular building blocks and, therefore, are to some extent comparable to high molecular weight polymers. In traditional polymer chemistry, however, polymer material is configured in certain shapes *after* the polymerization reaction, while in self-assembling systems the monomeric building blocks determine the form of the molecular aggregate, which may be polymerized afterwards (see Figure 1.1).

### 1.2 Liquid crystals

Liquid crystals (L.C.) are good examples of supramolecular aggregates because it is the organization that makes their physical properties so unique. Liquid crystals can be divided into two types, the thermotropic and lyotropic systems. In the former systems at certain temperatures the molecules are still ordered but the morphology of the phase (mesophase)<sup>\*</sup> is already a fluid

<sup>\*</sup> The L C phase or mesophase is sometimes called the fourth state of matter

liquid Depending on the presence of interacting groups (called mesogenic units), and the shape of the molecules (rodlike or disclike) the compounds form different liquid crystalline phases, calamatic and discotic, respectively



**Figure 1.1** Supramolecular chemistry in the context of synthetic and polymer chemistry

Lyotropic LC systems are dispersions of compounds containing mesogenic groups in a solvent<sup>8</sup> The most investigated building blocks for lyotropic LC systems are amphiphiles (also called surfactants) and constituents of cells (cell wall molecules), although other building blocks are known<sup>9</sup> Aggregation of totally synthetic amphiphiles was for the first time reported by Kunitake<sup>10</sup> and by many groups since then<sup>11</sup> Amphiphilic compounds (from Greek *amphi* = on both sides and *phileo* = to love) consist of two characteristic parts, a hydrophilic head group and a hydrophobic tail The tail usually consists of a long unbranched and sometimes unsaturated alkyl chain while the diversity in head groups is larger Ionic and non-ionic head groups are distinguished, with a further subdivision of the former group in anionic, cationic and zwitterionic head groups The most investigated non-ionic amphiphiles are based on carbohydrates<sup>12</sup>

The main reason for using carbohydrate based amphiphiles is the possibility of expressing their chirality in the supramolecular structure Carbohydrates are attractive chiral building blocks because they are inexpensive (*e.g.* D-glucose is in the price range of ordinary organic solvents such as acetone and methanol) and are obtained with a high enantiomeric purity Carbohydrates in principle are inexhaustible since they are available every year from agricultural crops

### 1.3 Contents of this thesis

The theme of this thesis is the study of the formation and the application of suprastructures from gluconamide derived amphiphiles and their metal complexes In order to increase their applicability, the amphiphiles are in almost every case provided with a metal complexing groups

Following a general literature survey in Chapter 2, the thermotropic properties of C<sup>6</sup>-substituted 2,4,3,5-dimethylene-*N,n*-alkyl-D-gluconamides and their copper complexes are

described in Chapter 3, featuring DSC experiments, temperature-dependent FT-IR, X-ray diffraction experiments and a single crystal structure analysis of an imidazolyl-bismethylene-gluconamide Chapter 4 focuses on the supramolecular structures of C<sup>6</sup>-substituted bismethylene-gluconamides in water, studied by electron microscopy The form of aggregation could be tuned by changing the pH and by the addition of metal ions In Chapter 5, the effect of the location of the metal-complexing imidazole group in the gluconamide on the aggregation behavior of the molecules is described Chapter 6 deals with the formation of organogels based on gluconamides Besides electron microscopy, the rigid gels were investigated by powder diffraction (SAXS), FT-IR and DSC In the final chapter, aggregates of gluconamides are used in catalysis The studied reactions are epoxidations and aziridinations This thesis concludes with summaries in both English and Dutch

## 1.4 Literature

- <sup>1</sup> a) Lehn J-M *Science* **1985**, 227, 849, b) Lehn, J-M *Angew Chem* **1988**, 100, 91, *Ibid Int Ed Eng* **1988**, 27 89
- <sup>2</sup> Cram, D J *Angew Chem* **1988**, 100, 1041, *Ibid Int Ed Eng* **1988**, 27, 1009
- <sup>3</sup> Pedersen C J *J Am Chem Soc* **1967**, 89, 7017
- <sup>4</sup> Rebek, J, Jr *Angew Chem* **1990**, 102, 261, *Ibid Int Ed Eng* **1990**, 29, 245
- <sup>5</sup> Szejtli J *Cyclodextrin Technology* Kluwer Acad Publ Dordrecht **1988**
- <sup>6</sup> Gutsche, C D *Calixarenes*, Royal Society of Chemistry, Cambridge **1989**
- <sup>7</sup> a) Niele F G M *Ph D Thesis University of Utrecht* **1987** b) Sybesma R P *Ph D Thesis University of Nijmegen* **1992**
- <sup>8</sup> a) Madden, T L , Herzfeld, J *Phil Trans R Soc Lond A* **1993**, 344, 357, b) Hoffmann, H *Ber Bunsenges Phys Chem* **1994**, 98, 1433, c) Hoffmann, H , Ulbricht, W *Chemie in unserer Zeit* **1995** 29 76
- <sup>9</sup> Aramid solutions Picken, S J *Ph D Thesis University of Utrecht* **1990**
- <sup>10</sup> Kunitake, T , Okahata, Y *J Am Chem Soc* **1977**, 99, 3860
- <sup>11</sup> For example a) Ringsdorf, H , Schlarb, B , Venzmer, J *Angew Chem* **1988**, 100, 117, *Ibid Int Ed Eng* **1988**, 27, 113 b) Fuhrhop, J -H , Helfrich, W *Chem Rev* **1993**, 93 1565 c) Menger, F M *Angew Chem* **1991** 103, 1104, *Ibid Int Ed Eng* **1991**, 30, 1086
- <sup>12</sup> Jeffrey, G A , Wingert, L M *Liq Crystals* **1992** 12, 179

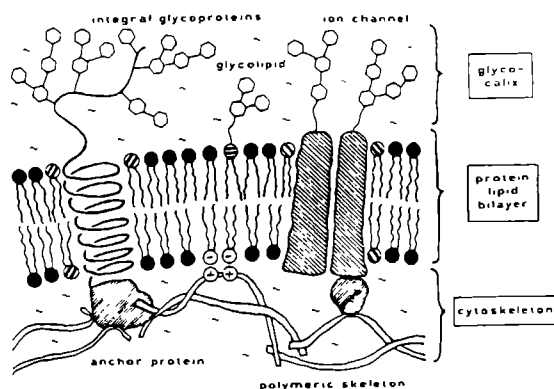


# Chapter 2

## Literature survey

### 2.1 Membrane mimetic chemistry

Twenty years ago it was proposed by Singer and Nicolson<sup>1</sup> that biomembranes are oriented, two-dimensional, viscous solutions of amphiphatic proteins and lipids (called the fluid mosaic model). This model is a conceptual basis for many researchers working in the field of membrane mimetic chemistry.<sup>2</sup> The biomembrane consists of 3 characteristic parts<sup>3</sup>: the glycocalix, the protein lipid bilayer and the cytoskeleton (see Figure 2.1). The main task of the glycocalix is recognition and this part is sometimes called the antenna area of the cells. The cytoskeleton, which is attached to the membrane on the inside of the bilayer, provides the stability of the membrane, while the bilayer of lipids is a host for proteins.



**Figure 2.1** Schematic drawing of membrane (Ref. 3)

The lipids of the bilayer are constructed from polar water-soluble head groups (phosphates or carbohydrates) connected to one or several long aliphatic chains (14 - 24 carbon atoms). Since the discovery by Gebicki and Hicks<sup>4</sup> that artificial membranes can be made from lipid molecules, numerous bilayered systems from synthetic amphiphiles<sup>5</sup> have been reported following the model proposed by Israelachvili (see Figure 2.2).<sup>6</sup>

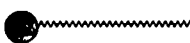
### 2.2 Amphiphiles

Amphiphiles are molecules that combine hydrophilic with hydrophobic parts. Due to this dual character, they can form aggregates in water. The property of amphiphiles to lower the interfacial tension between water and air led to the name surfactants (derived from *surface active agents*), while the name soap molecules originated from their practical applications. The driving force for the clustering of amphiphiles in water has been considered to be the so-called hydrophobic effect,<sup>7</sup> i.e. aggregation of the amphiphiles will liberate the organized shell of water






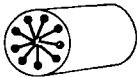


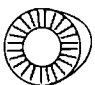


molecules surrounding the aliphatic chains of the individual molecules (called the icebergs) and thereby compensate the loss of entropy caused by the aggregation of the amphiphiles. However, the iceberg theory has been the subject of dispute discussion.<sup>8</sup>

Amphiphilic molecule



Hydrophilic  
headgroup

Hydrophobic  
tail

Shape	Packing parameter $P = v/a_0 l_c$	Aggregate type
	$P < 1/3$ micellar (spherical)	
	$1/3 < P < 1/2$ micellar (globular or cylinder)	
 	$1/2 < P < 1$ bilayers (vesicles)	
	$P > 1$ inverted micelles	

**Figure 2.2** Models for the relationship between molecular structure and aggregation form by Israelachvili,<sup>6</sup>  $v$  = the volume of the hydrophobic part,  $a_0$  is the cross sectional area of the head group and  $l_c$  is the maximal length of the alkyl chain

### 2.2.1 Relationship between amphiphilic structure and aggregate morphology

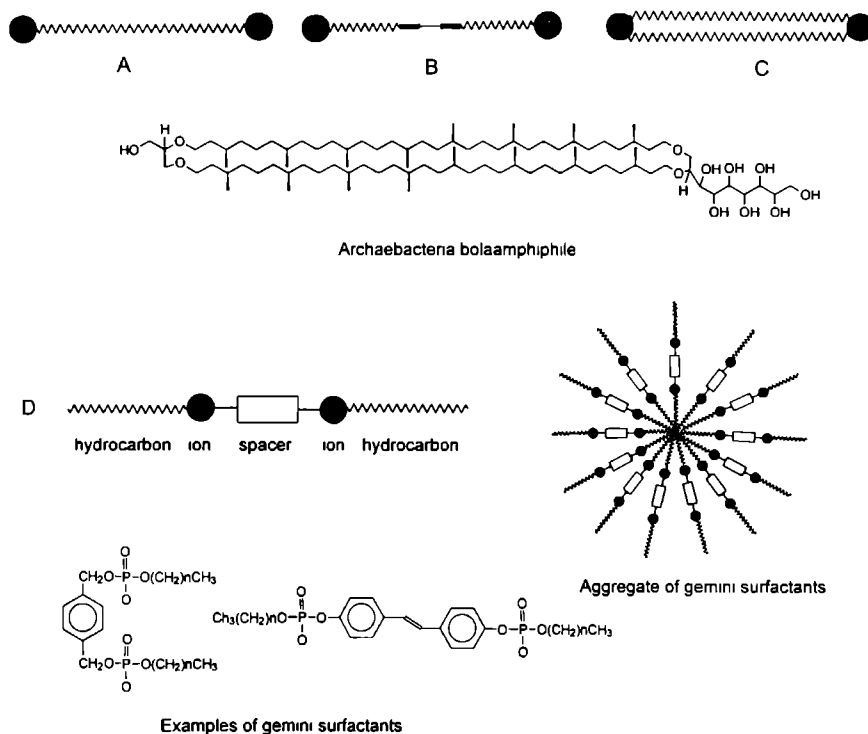
Many structural variations can be applied to amphiphiles without losing the ability to form aggregates. The hydrophilic head group can be anionic *e.g.* phosphate,<sup>4</sup> cationic *e.g.* ammonium,<sup>5</sup> zwitterionic *e.g.* choline<sup>9</sup> or nonionic *e.g.* polyoxyethylene<sup>10</sup> or carbohydrate.<sup>11</sup> The hydrophobic part has been varied by branching the *n*-alkyl chain,<sup>12</sup> introduction of thiol,<sup>13</sup> (polymerizable) alkene,<sup>14,15,16,17</sup> diacetylenic,<sup>18,19,20,21,22,23</sup> or cyclic disulfur<sup>24,25</sup> groups and by changing the hydrogen atoms in the alkyl chains to fluorine atoms.<sup>26,27</sup>

In addition to single and double chained amphiphiles, molecules containing two head groups connected by one or two alkyl chains<sup>28,29</sup> which can be unsaturated (so-called bolaamphiphiles, see Figure 2.3 A-C),<sup>30</sup> were synthesized on inspiration of the archaebacteria (*Sulfolobus solfataricus*) or bixin (recovered from seeds of *Bixa orellana*).<sup>31</sup> Using the unsaturated

bolaamphiphiles an attempt was made to introduce “electron wires” into vesicle membranes,<sup>31</sup> and quinone-containing amphiphiles were prepared in order to form redox-active lipid membranes.<sup>32</sup> With bolaamphiphiles containing unsymmetrical head groups, vesicles with an exterior membrane surface differing from the interior surface were prepared.<sup>33</sup> Amphiphiles in which two head groups are directly linked by a spacer are called gemini surfactants<sup>34</sup> and can, from a structural point of view, be considered as inverted bolaamphiphiles (see Figure 2.3D).

According to the model proposed by Israelachvili,<sup>6</sup> ionic single-chain amphiphiles form micellar solutions, however mixing single-chain compounds forming ion pairs<sup>35</sup> or stacks<sup>36</sup> can also result in bilayers.

In 1981 Kunitake et al.<sup>37</sup> reported that besides a hydrophilic head group and a flexible tail, the presence of a rigid segment, *e.g.* an aromatic group that can give stacking, is essential for the formation of bilayers from single chain amphiphiles.<sup>38</sup>

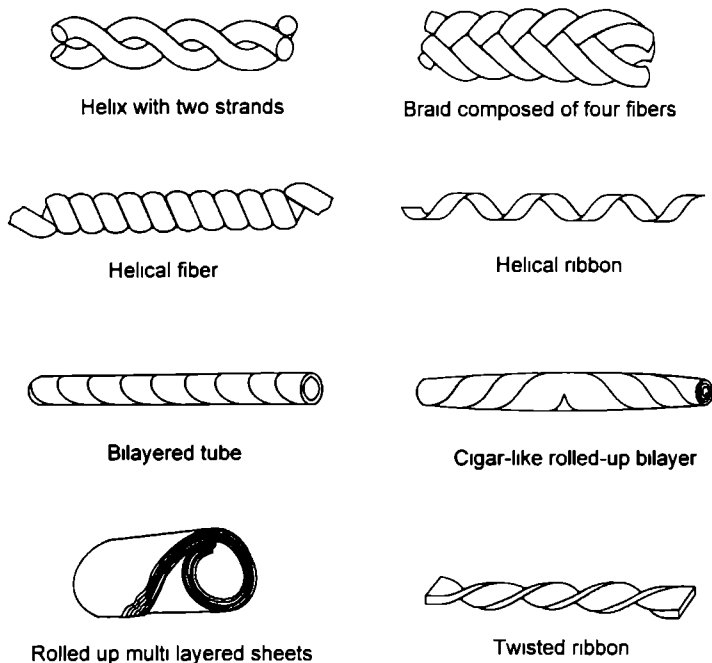


**Figure 2.3** Less common amphiphiles A-C) Bolaamphiphiles , D) Gemini surfactants

### 2.2.2 Chiral amphiphiles

Amphiphilic compounds containing a chiral moiety can express this asymmetry in the suprastructure by the formation of helices, twisted bilayers or tubuli (see Figure 2.4). Creating

asymmetrical assemblies is a challenge for the chemist and many were inspired by nature because helical forms are known from biological systems *e.g.* DNA<sup>39</sup> and collagen,<sup>40</sup> while tubular structures are known from the tobacco mosaic virus (TMV)<sup>41</sup> or the T4 phage.<sup>42</sup>



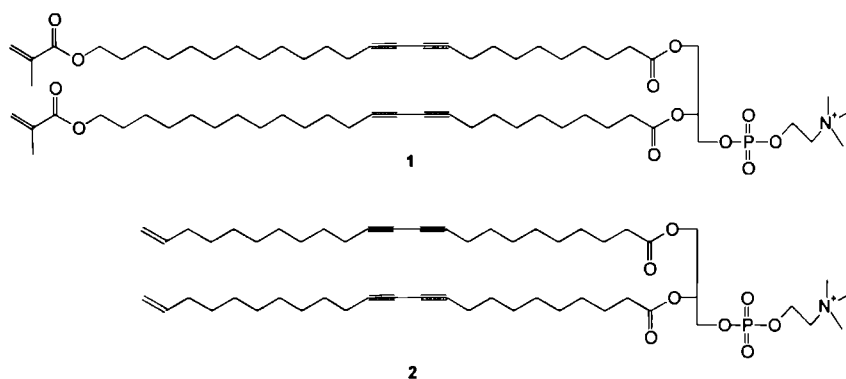
**Figure 2.4** Chiral assemblies from amphiphilic compounds

One of the first synthetic helical suprastructures published was based on the compound 12-hydroxystearic acid.<sup>43</sup> Later chiral amphiphiles based on glutamate,<sup>44</sup> alanine,<sup>45</sup> phospholipids,<sup>46</sup> and carbohydrates<sup>47</sup> have been developed.

The glutamate and alanine derived amphiphiles formed chiral aggregates as was observed by CD spectrometry<sup>44,45,48</sup> and, in addition, the transformation of helical tapes to tubes could be monitored by dark field optical microscopy<sup>49</sup> and electron microscopy.<sup>50</sup> The sense of the helix for the (*L*)-derivative of glutamate was right handed while the (*D*)-enantiomer showed left handed helices. Racemic mixtures did not result in helical forms. This kind of enantiomorphism was also encountered in *n*-alkyl-gluconamide derivatives.<sup>51</sup> The process of the formation of twisted filaments to tube like structures takes in some cases as long as one month,<sup>49</sup> while the change to spherical vesicles occurs almost instantaneously upon heating above the phase transition temperature.<sup>48</sup>

Like the glutamate derived amphiphiles, phosphatidylcholines can form helical shapes<sup>52</sup> and, in combination with aliphatic chains containing diacetylene groups, tubuli are also

formed<sup>46,53</sup> The size of the helices and tubuli can be controlled by variation of the ethanol/water ratio<sup>54</sup> The microstructures could be stabilized by polymerization without losing the suprastructure, indicating an ordered packing of the diacetylene functions<sup>18,55</sup> The microstructures were also influenced by changing the pH<sup>56</sup> or by the addition of metal ions<sup>56,57</sup> It was found that tubuli from diacetylenic phospholipids grow by the wrapping of lipid molecules around a crystalline core<sup>58</sup> Yager et al<sup>59</sup> postulated that the presence of diacetylenic groups enhances the chirality of the phospholipids as they disturb the symmetry in the alkyl chains in such a way that pairs of diacetylene chains can themselves be considered chiral objects<sup>59</sup> The diacetylenic functions are in some cases used only to direct the chirality, as they appeared to be useless for polymerization Introduction of additional polymerizable groups like methacrylate and vinyl (respectively **1** and **2**) resulted in high molecular weight polymers<sup>60</sup>



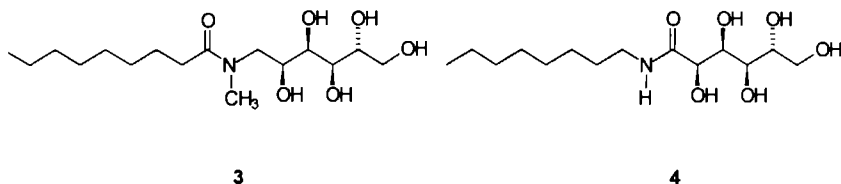
### 2.2.3 Models for aggregates of chiral amphiphiles

Helfrich has explained the regular winding of bilayers to form *ε g* helical structures as the result of a competition between the spontaneous torsion of the bilayer edges and the bending rigidity of the membrane<sup>61</sup> This model was adjusted by considering some of the potential consequences of an intrinsic chiral bending force<sup>62</sup> An intrinsic bending force due to chirality was also postulated by Schnur<sup>63</sup> Yager and Chappell proposed that the bending in their aggregates is due to electrostatic interactions at the edges of the bilayers<sup>64</sup> and highly anisotropic packing interactions<sup>65</sup> Computer modelling studies describing the aggregation of amphiphilic compounds have been published<sup>66,67</sup> A computational model for the chiral packing of molecules in crystals and monolayers has also been published,<sup>68</sup> but no computational model for the packing of amphiphiles in *chiral suprastructures* has been reported so far

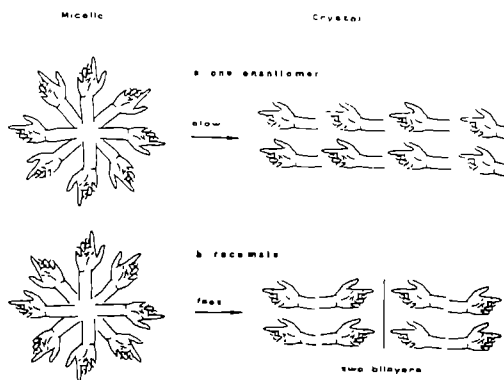
### 2.2.4 Carbohydrate amphiphiles

Amphiphilic compounds based on carbohydrates are attractive alternatives for traditional amphiphilic compounds, because of their excellent biodegradability and their relatively low cost<sup>69</sup> A wide-spread variation of amphiphiles based on alkyl glucosides,<sup>70</sup> with fluorinated alkyl

chains,<sup>71</sup> thioglucosides,<sup>72</sup> sucrose esters,<sup>73</sup> *N*-alkyl-aminoalditols,<sup>74</sup> and gluconamides<sup>47,75,76</sup> has been published. Alkyl glucamides (e.g. octanoyl-*N*-methylglucamide, (OMEGA, 3) and nonanoyl-*N*-methylglucamide (MEGA-10)) appeared to be very useful for dissolving natural membrane components due to their properties as non-ionic detergents and because of their much higher hydrolytic stability than *n*-alkyl-glucosides.<sup>77</sup> Very well investigated types of carbohydrate amphiphiles are the *N,n*-alkyl-D-gluconamides (for example compound 4).



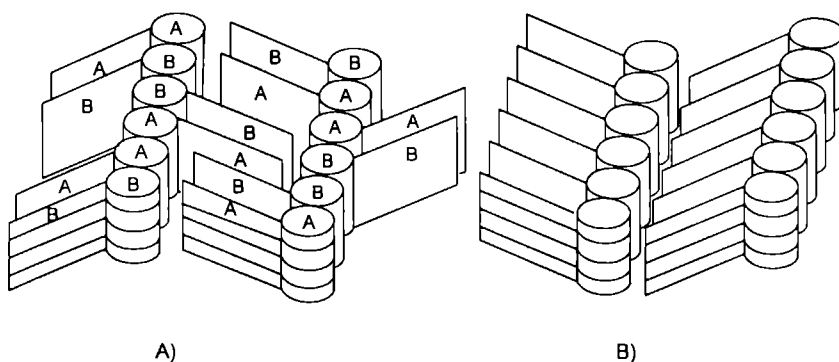
The first electron microscopy study on *N,n*-octyl-D-gluconamide (D-Glu8,<sup>78</sup> note that Glu stands for glucon and is **not** an abbreviation for glutamic acid or glutamate) was described by Pfannemüller and Welte.<sup>76</sup> Fuhrhop and coworkers<sup>51</sup> showed that D-Glu8 forms ropelike structures with a high aspect ratios up to  $10^4$  with bulges and knots. These structures were first proposed as consisting of two intertwined strands,<sup>51</sup> later believed to be a quadruple micellar helix,<sup>79</sup> and are now considered to be a helix of six intertwined strands as the most convincing model.<sup>80</sup> Pure enantiomers formed helices with enantiomorphology (*i.e.* in the case of *N,n*-octyl-D-gluconamide only right handed helices are formed) while racemic mixtures crystallized rapidly, due to the so-called “chiral bilayer effect” (see Figure 2.5)<sup>51</sup>



**Figure 2.5** Chiral bilayer effect (Ref. 51)

Structural variation of the aldonamide and mixing experiments<sup>78,81</sup> led to the conclusion that the solubility and the aggregate type of aldonamides depend directly on the stereochemistry of the head group<sup>81</sup> and that too much bending is not advantageous for molecular ordering.<sup>37</sup> In contrast with findings of Kunitake,<sup>37,38</sup> Fuhrhop concludes that a rigid segment is not needed in order to produce stable fibers.<sup>81</sup> The packing of fibers in the gels made from gluconamide solutions was

also studied by autoradiography,<sup>82</sup>  $^1\text{H}$ -NMR,<sup>83</sup> solid state  $^2\text{H}$ -NMR,<sup>84</sup> solution and solid state  $^{13}\text{C}$ -NMR,<sup>82, 85, 86</sup> FT-IR,<sup>86</sup> X-ray scattering,<sup>86</sup> DSC,<sup>87</sup> viscosity measurements,<sup>87</sup> monolayers in combination with Brewster angle microscope (BAM),<sup>88</sup> single crystal X-ray crystallography<sup>89</sup> and computer modelling (detailed structural analysis with the MATHEMATICA<sup>®</sup> program)<sup>79</sup> Gluconamide amphiphiles have also been polymerized, using incorporated diacetylenic groups,<sup>90</sup> methacrylamide,<sup>91</sup> and acrylate functions<sup>92</sup> The ionic compound *N*-dodecyltartaric acid monoamide showed in a similar way as D-Glu8, micellar fibers that assembled to cloth-like aggregates<sup>93</sup> Double headed bis-gluconamides (bolaamphiphiles) have been synthesized<sup>94</sup> and crystallized<sup>95</sup> showing two conformations of the molecule in the (asymmetric) unit cell Crystals of *N*,*n*-octyl-6-deoxy-D-gluconamide also showed an asymmetric unit containing two molecules (A,B) Molecules A and B formed a complex motif with pairwise alternating orientations and interdigitating antiparallel aliphatic chains (see Figure 2 6A)<sup>96</sup> which is different from the head to tail packing found for *n*-heptyl,<sup>97</sup> *n*-octyl,<sup>89</sup> *n*-nonyl,<sup>89</sup> *n*-decyl,<sup>97</sup> *n*-undecyl,<sup>98</sup> *N*,*n*-dodecyl-D-gluconamide,<sup>88</sup> *N*-cyclohexyl-D-gluconamide,<sup>99</sup> *N*-trideca-5,7-diyne-D-gluconamide,<sup>100</sup> (1*S*,2*S*)-1,2-bis(D-gluconamido)cyclohexane,<sup>101</sup> *n*-nonanyl-*N*-methylglucamide (MEGA-9),<sup>102</sup> *N*,*n*-octyl-D-gulonamide,<sup>103</sup> and *N*,*n*-dodecyl-D-ribonamide, see Figure 2 6B<sup>104</sup>



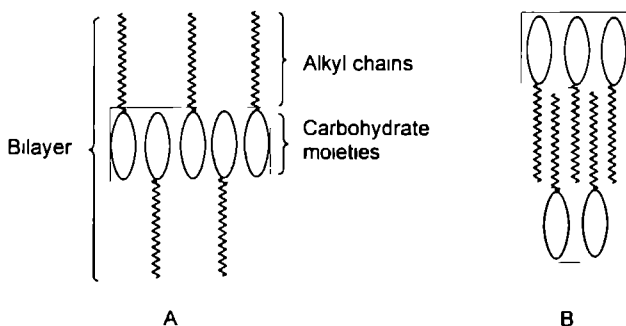
**Figure 2.6** Schematic representation of the crystal packing of gluconamides A) pairwise alternating orientation of the molecules B) head to tail packing

Very characteristic for the crystal structure of the alkyl-gluconamides is the so-called homodromic, quadrilateral hydrogen bond cycle<sup>105</sup> between any molecule and its counterpart in the next cell in the *x*-direction.<sup>89, 98</sup>

### 2.3 Thermotropic liquid crystalline properties of carbohydrate amphiphiles

Carbohydrate amphiphiles also appeared to be successful in the creation of thermotropic liquid crystalline phases<sup>106</sup> Because of their dualistic character, the amphiphilic mesogens are called “schizophrenic molecules”<sup>107</sup> and exhibit amphotropic (derived from *amphiphilic* and *thermotropic*) properties Several types of carbohydrate-derived mesogens have been made, for a

review see Jeffrey.<sup>106,107</sup> *N,n*-Alkyl-D-gluconamides also showed thermotropic L.C. properties.<sup>98,108</sup> The molecules are packed in a L.C. phase that is very common for single tailed carbohydrate amphiphiles, viz the smectic  $A_d$  phase.<sup>106,109</sup> In this phase, a layered structure, containing a rigid core of carbohydrate molecules connected to each other by hydrogen bonds, is separated by alkyl chains (see Figure 2.7A).<sup>108</sup> By systematic variation of the alkyl chains, van Doren came to a revised model for the molecular arrangement in the smectic  $A_d$  phase of carbohydrate derived amphiphiles with a single alkyl chain.<sup>110</sup> In the revised model, the smectic bilayers are identical to the fluid lamellar ( $L_a$ ) lyotropic phase, i.e. partially interdigitized alkyl chains in the core of each layer and carbohydrate moieties on the outside of the bilayer (see Figure 2.7B).



**Figure 2.7** Schematic models of the smectic  $A_d$  phase. Shading denotes the regions of dynamic hydrogen bonding. A) Original model, B) revised model.

The importance of hydrogen bonds in L.C. phases has been discussed recently.<sup>111</sup>

## 2.4 Functional aggregates

Vesicles can be used for sustained release of drugs in medical applications.<sup>112</sup> The stability of the vesicle is critical. Non-polymerized vesicles are too unstable while polymerized vesicles are not permeable enough in order to sustain release.<sup>113</sup> In tubular structures with an impermeable wall, the drug can only diffuse from one end to the other end of the tube. The tubes have a smaller contact surface with the outside matrix than non-polymerized vesicles, which results in a slower release of drugs.<sup>114</sup>

Copper-coated tubular structures prepared from diacetylenic phospholipids have been shown to be very useful in the development of long-term slow-release agents (up to 500 days). Off-shore marine tests showed that rods coated with paint containing small hollow tubules filled with tetracycline (antifouling agent) displayed a remarkable reduction of fouling in comparison with test rods coated with paint containing tetracycline without the hollow tubules.<sup>115</sup>

Metal ions have been used as templates for the formation of (chiral) suprastructures.<sup>57, 116,117,118,119</sup> An interesting application of metal-containing vesicles was shown by Fendler<sup>120</sup> who

enclosed platinum in vesicles and used them for the reduction of methylene blue with hydrogen gas. Singh and Markowitz<sup>121</sup> succeeded in immobilizing colloidal copper on phospholipid tubules by reduction of copper chloride using palladium that was bound to the phospholipids forming the tubules. Both the interior and exterior of the tubules were coated with copper, and nickel, cobalt and gold were immobilized in a similar way. Nickel coated tubes were used for the fabrication of tubule-based field emitting cathodes<sup>122</sup> by mixing the tubules with epoxy resin, and aligning them in a magnetic field of  $\sim 500$  G. After polymerization, the upper part of the resin was etched to expose the nickel-coated tubules and subsequently they were covered with a layer of gold and silver. A stable emission for more than 10 hours was achieved.<sup>116</sup>

Metal-containing aggregates have also been used as a matrix for catalysis.<sup>123</sup> The catalytic applications of suprastructures have been recently reviewed by Feiters.<sup>124</sup> Imidazole-containing aggregates are often used for ester hydrolysis.<sup>117</sup> The first imidazole-functionalized amphiphile reported, was *N*-myristoyl-histidine<sup>125</sup> but this compound appeared only to be catalytically active in combination with micellar cetyltrimethylammonium bromide (CTAB). Enantioselective catalysts containing amphiphiles with imidazole groups based on histidine have been described in the literature.<sup>126,127</sup>

Many vesicular systems containing polypeptides have been investigated.<sup>124</sup> In addition to vesicles or micelles, other aggregate forms like the helical cavities of amylose were used as a matrix for ester hydrolysis with imidazole as a catalyst.<sup>128</sup>

Porphyrins are excellent catalysts for epoxidation reactions<sup>129</sup> and have been successfully incorporated in vesicles while retaining their epoxidation capacities.<sup>130,131</sup> The incorporation of a porphyrine in aggregates of D-Glu-8 failed.<sup>47</sup> Porphyrins covalently bound to 2-aminoglysoamide head groups have been shown to form micellar fibers.<sup>132</sup>

## 2.5 Literature

<sup>1</sup> Singer, S J, Nicolson, G.L. *Science* **1972**, 175, 720.

<sup>2</sup> a) Fendler, J.H. *Membrane Mimetic Chemistry*, John Wiley, New York **1982**; b) Fuhrhop, J.-H., Mathieu, J *Angew Chem* **1984**, 96, 125; *Ibid Int Ed Eng* **1984**, 23, 100

<sup>3</sup> Ringsdorf, H., Schlarb, B ; Venzmer, J. *Angew Chem* **1988**, 100, 117, *Ibid Int Ed Eng* **1988**, 27, 113.

<sup>4</sup> Gebicki, J M , Hicks, M. *Nature* **1973**, 243, 232

<sup>5</sup> The first report of completely synthetic amphiphiles was by Kunitake, cf Kunitake, T., Okahata, Y *J Am Chem Soc* **1977**, 99, 3860, although synthetic emulsifying agents like lecithins were already known since early 50's Baer, E., Kates, M *J Am Chem Soc* **1950**, 72, 942. For early synthetic carbohydrate emulsifying agents see ref 75

<sup>6</sup> a) Israelachvili, J.N.; Mitchell, D.J.; Ninham, B.W, *J Chem Soc , Faraday Trans 2* **1976**, 72, 1525, b) Israelachvili, J N , Marcelja, S; Horn, R.G. *Quart Rev Biophys* **1980**, 13, 121.

<sup>7</sup> Tanford, C *The Hydrophobic Effect*, Wiley Interscience 2<sup>nd</sup> ed., New York **1980**.

<sup>8</sup> Blokzijl, W., Engberts, J B.F.N *Angew Chemie* **1993**, 105, 1610; *Ibid Int Ed Eng* **1993**, 32, 1545 and references cited therein

<sup>9</sup> Inoko, Y ; Mitsui, T. *J Physiol Soc Jpn* **1978**, 44, 1918



- <sup>10</sup> a) Hub, H-H, Hupfer, B, Koch, H, Ringsdorf, H *Angew Chem* **1980**, 92, 962, *Ibid Int Ed Eng* **1980**, 19, 938, b) Echegoyen, L E, Hernandez, J C, Kaifer, A I, Gokel, G W, Echegoyen, L *J Chem Soc Chem Commun* **1988**, 836
- <sup>11</sup> Pfannemüller, B, Welte, W *Chem Phys Lipids* **1985**, 37, 227
- <sup>12</sup> a) Nusselder, J J H, Engberts, J B F N *Langmuir* **1991**, 7, 2089, b) Nusselder, J J H *Ph D Thesis*, University of Groningen **1990**
- <sup>13</sup> Samuel, N K P, Singh, M, Yamaguchi, K, Regen, S L *J Am Chem Soc* **1985**, 107, 42
- <sup>14</sup> Tundo, P, Kippenberger, D J, Klahn, P L, Prieto, N E, Jao, T -C, Fendler, J H *J Am Chem Soc* **1982**, 104, 456
- <sup>15</sup> Regen, S L, Singh, A, Singh, M *J Am Chem Soc* **1982**, 104, 791
- <sup>16</sup> Paleos, C M, Christias, C, Evangelatos, G P *J Polym Sci* **1982**, 20, 2565
- <sup>17</sup> Frankel, D A, Lamparski, H, Liman, U, O'Brien, D F *J Am Chem Soc* **1989**, 111, 9262
- <sup>18</sup> Day, D, Hub, H H, Ringsdorf, H *J Polym Sci Polym Lett Ed* **1978**, 16, 205
- <sup>19</sup> Hupfer, B, Ringsdorf, H, Schupp, H *Chem Phys Lipids* **1984**, 33, 355
- <sup>20</sup> Yager, P, Schoen, P E, Davies, C, Price, R, Singh, A *Biophys J* **1985**, 899
- <sup>21</sup> Kuo, T, O'Brien, D F *J Am Chem Soc* **1988**, 110, 7571
- <sup>22</sup> a) Bader, H, Ringsdorf, H, Skura, J *Angew Chem* **1981**, 93, 109, *Ibid Int Ed Eng* **1981**, 20, 91, b) Frankel, D A, O'Brien, D F *J Am Chem Soc* **1991**, 113, 7436, c) Fuhrhop, J -H, Blumtritt, P, Lehmann, C, Luger, P *J Am Chem Soc* **1991**, 113, 7437
- <sup>23</sup> Rhodes, D G, Frankel, D A, Kuo, T, O'Brien, D F *Langmuir* **1994**, 10, 267
- <sup>24</sup> Regen, S L, Samuel, N K P, Khurana, J M *J Am Chem Soc* **1985**, 107, 5804
- <sup>25</sup> Sadownik, A, Stevely, J, Regen, S L *J Am Chem Soc* **1986**, 108, 7789
- <sup>26</sup> Elbert, R, Folda, T, Ringsdorf, H *J Am Chem Soc* **1984**, 106, 7687
- <sup>27</sup> Ishikawa, Y, Kuwahara, H, Kunitake, T *J Am Chem Soc* **1989**, 111, 8530
- <sup>28</sup> a) Fuoss, R M, Edelson, D J *J Am Chem Soc* **1951**, 73, 269, b) Okahata, Y, Kunitake, T *J Am Chem Soc* **1979**, 101, 5231, c) Hentrich, F, Tschierske, C, Zaschke, H *Angew Chem* **1991**, 103, 429, *Ibid Int Ed Eng* **1991**, 30, 440
- <sup>29</sup> Festag, R, Hessel, V, Lehmann, P, Ringsdorf, H, Wendorff, J H *Recl Trav Chim Pay Bas* **1994**, 113, 222
- <sup>30</sup> a) Bader, H, Ringsdorf, H *Faraday Discuss Chem Soc* **1986**, 82, 1, b) Fuhrhop, J -H, Krull, M, Schulz, A, Möbius, D *Langmuir* **1990**, 6, 497
- <sup>31</sup> Fuhrhop, J -H, Krull, M, Schulz, A, Möbius, D *Langmuir* **1990**, 6, 497
- <sup>32</sup> Fuhrhop, J -H, Hungerbühler, H, Siggel, U *Langmuir* **1990**, 6, 1295
- <sup>33</sup> a) Fuhrhop, J -H, Mathieu, J *J Chem Soc, Chem Commun* **1983**, 144, b) Fuhrhop, J -H, Fritsch, D *Acc Chem Res* **1986**, 19, 130, c) Fuhrhop, J -H, David, H -H, Mathieu, J, Liman, U, Winter, H -J, Boekema, E *J Am Chem Soc* **1986**, 108, 1785, d) Fuhrhop, J -H, Spiroski, D, Boettcher, C *J Am Chem Soc* **1993**, 115, 1600
- <sup>34</sup> Menger, F M, Littau, C A *J Am Chem Soc* **1993**, 115, 10083
- <sup>35</sup> Fukuda, H, Kawata, K, Okuda, H, Regen, S L *J Am Chem Soc* **1990**, 112, 1635
- <sup>36</sup> Schenning A P H J, Feiters, M C, Nolte, R J M *Tetrahedron Lett* **1993**, 34, 7707
- <sup>37</sup> Kunitake, T, Okahata, Y, Shimomura, M, Yasunami, S -I, Takarabe, K *J Am Chem Soc* **1981**, 103, 5401

- <sup>38</sup> Kunitake, T *Angew Chem* **1992**, 104, 692; *Ibid Int Ed Eng* **1992**, 31, 709
- <sup>39</sup> Watson, J D ; Crick, F H C *Nature* **1953**, 171, 737.
- <sup>40</sup> Fraser, R B D *J Mol Biol* **1979**, 129, 463.
- <sup>41</sup> a) Klug, A , Daspar, D L D *Advan Virus Res* **1960**, 7, 274; b) Kushner, D.J *Bacteriological Rev* **1969**, 33, 302; c) Butler, P G J , Klug, A *The assembly of a virus*, Scientific American Inc. **1978**.
- <sup>42</sup> Erickson, R O *Science* **1973**, 181, 705 and references cited therein.
- <sup>43</sup> Hotten, B.W ; Birdsall, D H. *J Colloid Sci* **1952**, 7, 284.
- <sup>44</sup> a) Kunitake, T., Nakashima, N ; Hayashida, S ; Yonemuri, K. *Chem Lett* **1979**, 1413, b) Rhodes, D G , Frankel, D.A , Kuo, T , O'Brien, D.F *Langmuir* **1994**, 10, 267
- <sup>45</sup> Kunitake, T , Nakashima, N ; Morimitsu, K *Chem Lett* **1980**, 1347
- <sup>46</sup> Yager, P , Schoen, P. *Mol Cryst Liq Cryst* **1984**, 106, 371
- <sup>47</sup> a) Fuhrhop, J -H , Helfrich, W. *Chem Rev* **1993**, 93, 1565, b) Fuhrhop, J -H ; Krull, M *Frontiers in Supramolecular Organic Chemistry and Photochemistry* ed. Schneider, H -J , Dürr, H , VCH publ. Weinheim, New York, Basel, Cambridge, p. 223
- <sup>48</sup> a) Kunitake, T , Nakashima, N.; Shimomura, M ; Okahata, Y ; Kano, K., Ogawa, T *J Am Chem Soc* **1980**, 102, 6642; b) Ihara, H , Takafuji, M , Hirayama, C *Langmuir* **1992**, 8, 1548; c) Nakashima, N , Ando, R , Muramatsu, T , Kunitake, T *Langmuir* **1994**, 10, 232
- <sup>49</sup> Nakashima, N., Asakuma, S., Kunitake, T. *J Am Chem Soc* **1985**, 107, 509
- <sup>50</sup> Nakashima, N , Asakuma, S., Kim, J.-M., Kunitake, T *Chem Lett* **1984**, 1709.
- <sup>51</sup> Fuhrhop, J -H ; Schnieder, P ; Rosenberg, J , Boekema, E *J Am Chem Soc* **1987**, 109, 3387
- <sup>52</sup> a) Yanagawa, H., Ogawa, Y , Furuta, H., Tsuno, K. *J. Am Chem Soc* **1989**, 111, 4567, b) Sommerdijk, N A J.M , Buynsters, P J A A ; Pistorius, A M A , Wang, M ; Feiters, M.C ; Nolte, R.J M ; Zwanenburg, B. *J Chem Soc, Chem Commun* **1994**, 1941
- <sup>53</sup> Yager, P., Schoen. P.E., Davies, C.; Price , R ; Singh, A *Biophys J* **1985**, 48, 899
- <sup>54</sup> Georger, J H ; Singh, A.; Price, R.R.; Schnur, J M ; Yager, P ; Schoen, P E *J Am Chem Soc* **1987**, 109, 6169
- <sup>55</sup> Hub, H; Hupfer, B ; Koch, H.; Ringsdorf, H. *J Macromol Sci. Chem* **1981**, A15, 701
- <sup>56</sup> Markowitz, M A ; Schnur, J M ; Singh, A *Chem Phys Lipids* **1992**, 62, 193.
- <sup>57</sup> Markowitz, M A , Baral, S ; Brandow, S., Singh, A. *Thin Solid Films* **1993**, 224, 242
- <sup>58</sup> Yager, P , Price, R.R ; Schnur, J M., Schoen, P E ; Singh, A.; Rhodes, D.G. *Chem Phys Lipids* **1988**, 46, 171.
- <sup>59</sup> Singh, A ; Burke, T.G., Calvert, J.M., Georger, J H.; Herendeen, B., Price, R R , Schoen, P.E , Yager, P *Chem Phys Lipids* **1988**, 47, 135
- <sup>60</sup> Singh, A., Markowitz, M A *New J Chem* **1994**, 18, 377
- <sup>61</sup> Helfrich, W *J Phys Chem* **1986**, 85, 1085.
- <sup>62</sup> Helfrich, W , Prost, J. *Phys Rev A* **1988**, 38, 3065.
- <sup>63</sup> a) Selinger, J V ; Schnur, J. *Phys Rev Lett* **1993**, 71, 4091, b) Schnur, J M., Ratna, B.R , Selinger, J V., Singh, A , Jyothi, G , Easwaran, K.R.K. *Science* **1994**, 264, 945.
- <sup>64</sup> a) Chappell, J S ; Yager, P. *Chem Phys.* **1991**, 150, 73; b) Chappell, J. S.; Yager, P *Biophys J* **1991**, 60, 952
- <sup>65</sup> Chappell, J S.; Yager, P *Chem Phys Lipids* **1991**, 58, 253

- <sup>66</sup> a) Pastor, R.W., Venable, R.M., Karplus, M. *Proc Natl Acad Sci USA* **1991**, *88*, 892; b) Heller, H., Schaefer, M., Schulten, K. *J Phys Chem* **1993**, *97*, 8343; Pohorille, A., Benjamin, I. *J Phys Chem* **1993**, *97*, 2664, c) Os van, N M., Smit, B., Karabornı, S. *Recl Trav Chim Pays-Bas* **1994**, *113*, 181
- <sup>67</sup> a) Sanders, C R., Prestegard, H. *J Am Chem Soc* **1992**, *114*, 7096, b) Hare, B J., Howard, K.P., Prestegard, J H. *Biophys J* **1993**, *64*, 392; c) Buuren, A R., Berendsen, B J. *Langmuir* **1994**, *10*, 1703
- <sup>68</sup> Perlstein, J. *J Am Chem Soc* **1994**, *116*, 455
- <sup>69</sup> a) Kelkenberg, Marl, H. *Tens Surf Det* **1988**, *25*, 8; b) Bekkum, H van, Fuchs, A. *Chem Mag* **1991**, *6/7*, 334, c) Koch, H., Beck, R., Röper, H. *Starch/Starke* **1993**, *2*
- <sup>70</sup> Kataoka, R., Watanabe, Y., Mitaku, S. *Rep Prog Polym Phys Jpn* **1984**, *27*, 699
- <sup>71</sup> a) Mietchen, R.; Prade, H.; Holz, J., Praefcke, K., Blunk, D. *Chem Ber* **1993**, *126*, 1707, b) Zarif, L., Gulik-Krzywicki, T.; Riess, J., Pucci, B., Guedj, C.; Pavia, A A. *Coll Surf A Physicochem Eng Aspects* **1993**, *84*, 107
- <sup>72</sup> a) Saito, S., Tsuchiya, T. *Biochem J* **1984**, *222*, 829; b) Tsuchiya, T., Saito, S. *J Biochem* **1984**, *96*, 1593
- <sup>73</sup> Bjorkling, F., Godtfredsen, S E.; Kirk, O. *J Chem Soc, Chem Commun* **1989**, 934
- <sup>74</sup> Doren, H. A van, Geest, R. van der, Ruijter, C F de, Kellogg, R M., Wynberg, H. *Liq Cryst* **1990**, *8*, 109
- <sup>75</sup> Fieser, M., Fieser, L F., Toromanoff, E., Hirata, Y., Heymann, Tefft, M., Bhattacharya, S. *J Am Chem Soc* **1956**, *78*, 2825
- <sup>76</sup> Pfannemüller, B., Welte, W. *Chem Phys Lipids* **1985**, *37*, 227
- <sup>77</sup> a) Hildreth, J E. *Biochem J* **1982**, *207*, 363; b) Hanatani, M.; Nishifuji, K., Futai, M.; Tsuchiya, T. *J Biochem* **1984**, *95*, 1349
- <sup>78</sup> Fuhrhop, J.-H., Boettcher, C. *J Am Chem Soc* **1990**, *112*, 1768
- <sup>79</sup> Koning, J.; Boettcher, C.; Winkler, H., Zeitler, E., Talmon, Y., Fuhrhop, J.-H. *J Am Chem Soc* **1993**, *115*, 693
- <sup>80</sup> Fuhrhop, J.-H., Koning, J. *Membranes and Molecular Assemblies: The Synkinetic Approach*, part of the series "Monographs in Supramolecular Chemistry", series ed. Stoddart, J F., The Royal Society of Chemistry, Cambridge (UK) **1994**, pag IX
- <sup>81</sup> Fuhrhop, J.-H., Schnieder, P., Boekema, E., Helfrich, W. *J Am Chem Soc* **1988**, *110*, 2861
- <sup>82</sup> Boettcher, C., Boekema, E., Fuhrhop, J.-H. *J Microscopy* **1990**, 173
- <sup>83</sup> a) Svenson, S., Schäfer, A., Fuhrhop, J.-H. *J Chem Soc, Perkin Trans 2* **1994**, 1023, b) Hafkamp, R J H., Feiters, M C., Nolte, R J M. to be published.
- <sup>84</sup> Fuhrhop, J.-H.; Svenson, S.; Boettcher, C., Rössler, E.; Vieth, H.-M. *J Am Chem Soc* **1990**, *112*, 4307
- <sup>85</sup> a) Taravel, F.R., Pfannemüller, B. *Makromol Chem* **1990**, *191*, 3097, b) Svenson, S., Kirste, B., Fuhrhop, J.-H. *J Am Chem Soc* **1994**, *116*, 11969
- <sup>86</sup> Svenson, S., Kőning, J.; Fuhrhop, J.-H. *J Phys Chem* **1994**, *98*, 1022.
- <sup>87</sup> Pfannemüller, B.; Kühn, I. *Makromol Chem* **1988**, *189*, 2433
- <sup>88</sup> Vollhardt, D.; Gutberlet, T., Emrich, G., Fuhrhop, J.-H. *Langmuir* **1995**, *11*, 2661
- <sup>89</sup> a) Zabel, V., Müller-Fahrnow, A., Hilgenfeld, R., Saenger, W., Pfannemüller, B., Enkelmann, V., Welte, W. *Chem Phys Lipids* **1986**, *39*, 313, b) Wang, J.-L.; Lahav, M., Leiserowitz, L. *Angew Chem* **1991**, *103*, 698, *Ibid Int Ed Eng* **1991**, *30*, 696
- <sup>90</sup> Frankel, D.A., O'Brien, D.F. *J Am Chem Soc* **1994**, *116*, 10057
- <sup>91</sup> Loos, M.; Baeyens-Volant, D.; Szalai, E.; David, C. *Makromol Chem* **1990**, *191*, 2917.

- <sup>92</sup> Fuhrhop, J -H , Spiroski, D Schnieder, P *React Polym* **1991**, 15, 215
- <sup>93</sup> Fuhrhop, J -H , Demoulin, C , Rosenberg, J , Boettcher, C *J Am Chem Soc* **1990**, 112, 2827
- <sup>94</sup> Garelli, R , Brisset, F , Rico, I , Lattes, A *Synt Commun* **1993**, 23, 35
- <sup>95</sup> Muller-Fahmow, A , Saenger, W, Fritsch, D , Schnieder, P , Fuhrhop, J -H *Carbohydr Res* **1993**, 242, 11
- <sup>96</sup> Herbst, R , Steiner, T , Pfannemüller, B , Saenger, W *Carbohydr Res* **1995**, 269, 29
- <sup>97</sup> Müller-Fahmow, A , Hilgenfeld, R , Hesse, H , Saenger, W , Pfannemüller, B *Carbohydr Res* **1988**, 176 165
- <sup>98</sup> Jeffrey, G A , Maluszynska, H *Carbohydr Res* **1990**, 207, 211
- <sup>99</sup> Darbon, P N , Odon, Y , Lacombe, J M , Decoster, E , Pavia, A A *Acta Cryst* **1984**, C40, 1105
- <sup>100</sup> Andre, C , Luger, P , Fuhrhop, J -H *Chem Phys Lipids* **1994**,
- <sup>101</sup> André, C , Luger, P , Nehmzow, D , Fuhrhop, J -H *Carbohydr Res* **1994**, 261, 1
- <sup>102</sup> Müller-Fahmow, A , Zabel, V , Steifa, M , Hilgenfeld, R *J Chem Soc Chem Commun* **1986**, 1573
- <sup>103</sup> André, C , Luger, P , Svenson, S , Fuhrhop, J -H *Carbohydr Res* **1992**, 230, 31
- <sup>104</sup> André, C , Luger, P , Bach, R , Fuhrhop, J -H *Carbohydr Res* **1995**, 266, 15
- <sup>105</sup> Flier, J S , Maratos-Flier, E , Pallotta, J A , McIsaac, D *Nature* **1979**, 279, 343
- <sup>106</sup> Jeffrey, G A *Acc Chem Res* **1986**, 19, 168
- <sup>107</sup> Jeffrey, G A , Wingert, L A *Liq Cryst* **1992**, 12, 179
- <sup>108</sup> Pfannemüller, B , Welte, W , Chin, E , Goodby, J W *Liq Cryst* **1986**, 1, 357
- <sup>109</sup> a) Goodby, J W *Mol Cryst Liq Cryst* **1984**, 110, 205, b) Doren, H A van, Geest, R van der, Kellogg, R M , Wynberg, H *Carbohydr Res* **1989**, 194, 71
- <sup>110</sup> Doren, van H A , Wingert, L M *Mol Cryst Liq Cryst* **1991**, 198, 381
- <sup>111</sup> Paleos, C M , Tsiourvas, D *Angew Chem* **1995**, 107, 1839, *Ibid Int Ed Eng* **1995**, 34, 1696
- <sup>112</sup> Lawrance, M J *Chem Soc Rev* **1994**, 417
- <sup>113</sup> Krause, H J , Juliano, R L , Regen, S *J Pharm Sci* **1987**, 76, 1
- <sup>114</sup> Schnur, J M , Price, R , Rudolph, A S *J Controlled Release* **1994**, 28, 3
- <sup>115</sup> Schnur, J M *Science* **1993**, 262, 1669
- <sup>116</sup> For a review of metallomesogens see Espinet, P , Esteruellas, M A , Oro, L A , Serrano, J L , Sola, E *Coord Chem Rev* **1992**, 117, 215, review of discotic structures Giroud-Godquin, A -M., Maitlis, P M *Angew Chem* **1991**, 103, 370, *Ibid Int Ed Eng* **1991**, 30, 375, review of calamitic structures Hudson, S A , Maitlis, P M *Chem Rev* **1993**, 93, 861, review of polymers Oriol, L , Serrano, J L *Adv Mat* **1995**, 7, 348
- <sup>117</sup> Tachibana, T , Kambara, H *J Coll Interface Sci* **1968**, 28, 173
- <sup>118</sup> Zarges, W , Hall, J , Lehn, J -M *Helv Chim Acta* **1991**, 74, 1843, Krämer, R , Lehn, J -M , Marquis-Rigault, A *Proc Natl Acad Sci USA* **1993**, 90, 5394
- <sup>119</sup> Hafkamp, R J H , Feiters, M C , Nolte, R J M *Angew Chem* **1994**, 106, 1054, *Ibid Int Ed Eng* **1994**, 33, 986
- <sup>120</sup> Furihara, K , Fendler, J H *J Am Chem Soc* **1983**, 105, 6152
- <sup>121</sup> Singh, Z , Markowitz, M , Chow, G M *Nanostructured Materials* **1995**, 5, 141
- <sup>122</sup> Kirkpatrick, D A , Bergeron, G L , Czarnaski, M A , Hickman, J J , Chow, G M , Price, R , Ratna, B L , Schoen, P E , Stockton, W B , Baral, S , Ting, A C , Schnur, J M *Appl Phys Lett* **1992**, 60, 1556

- <sup>123</sup> Fendler, J H , Fendler, E J. *Catalysis in Micellar and Macromolecular Systems* Acad. Press, New York **1975**;  
For review of catalysis by micelles and membranes see. Kunitake, T., Shinkai, S. *Adv Phys Org Chem* **1980**, Vol  
A, 435
- <sup>124</sup> Feiters, M.C. *Supramolecular technology and applications*, vol 10, part III, Chap 16, *supramolecular catalysis*  
vol. ed Reinhoudt, D.N., part of the series “*Comprehensive Supramolecular Chemistry*”, ed. Lehn, J.-M , Pergamon  
Press, Elsevier Sci Ltd., Oxford (UK) **1995**.
- <sup>125</sup> a) Ochoa-Solano, A , Romero, G ; Gitler, C *Science* **1967**, 156, 1243, b) Gitler, C., Ochoa-Solano, A *J Am*  
*Chem Soc* **1968**, 90, 5004
- <sup>126</sup> Brown, J M , Bunton, C.A. *J Chem Soc , Chem Commun* **1974**, 969
- <sup>127</sup> a) Cleij, M.C.; Drenth, W , Nolte, R.J.M *Recl Trav Chim Pays-Bas* **1993**, 1, b) Cleij, M C *Ph D Thesis*  
*Univ of Utrecht* **1989**.
- <sup>128</sup> Hui, Y , Zou, W *Frontiers in Supramolecular Organic Chemistry and Photochemistry* ed Schneider, H.-J ,  
Dürr, H , VCH publ Weinheim, New York, Basel, Cambridge, 203
- <sup>129</sup> a) Jørgensen, K A *Chem Rev* **1989**, 89, 431; b) Meunier, B. *Chem Rev* **1992**, 92, 1411
- <sup>130</sup> Sorokin, A B , Khenkin, A M , Marakushev, S.A ; Shilov, A.E., Shteinman, A.A *Dokl Phys Chem* **1984**, 29,  
1101
- <sup>131</sup> Esch, J. van, Roks, M.F.M.; Nolte, R.J M *J Am Chem Soc* **1986**, 108, 6093.
- <sup>132</sup> Fuhrhop, J.-H.; Demoulin, C.; Boettcher, C ; Siggel, U. *J Am Chem. Soc.* **1992**, 114, 4159

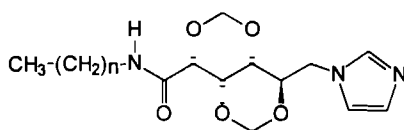
# Chapter 3

## Thermotropic liquid crystalline properties of *N*-*n*-alkyl-D-gluconamides

### 3.1 Introduction

In recent years, the interest in the design and synthesis of supramolecular structures has grown steadily, one of the objectives being the development of new materials<sup>1</sup> and new catalysts<sup>2</sup>. Supramolecular systems<sup>3</sup> have been prepared from a variety of building blocks including surfactants,<sup>4</sup> polymers,<sup>5</sup> rod-like<sup>6</sup> and disk-like mesogens,<sup>7</sup> and other molecules.<sup>8</sup> As part of our program aimed at the development of novel chiral matrices, *e.g.* for catalytic applications, we have undertaken the synthesis and the study of the thermotropic liquid crystalline (LC) properties of gluconamides containing a metal-coordinating group, see **1**. Our interest in gluconamides and related carbohydrates was raised by the recent studies of Fuhrhop and others,<sup>9</sup> which indicate that these compounds can form a great variety of chiral nanometer-sized structures in water. One of the reasons for investigating the thermotropic LC behavior of carbohydrate derivatives<sup>6</sup> is that this type of compounds is likely to form lamellar aggregates<sup>10</sup> which is of interest for the building of supramolecular catalysts in aqueous solutions.<sup>11 12 13</sup>

Although metal complexes with sugar ligands are known since 1951,<sup>14</sup> they were mainly used for the determination of the conformation of the carbohydrate structures and no additional metal complexing group was involved. The goal of the present project was to make metal complexes from gluconamides that are stable, even in aqueous solutions, and therefore it was necessary to couple a metal ligating group to the carbohydrate framework. An excellent candidate for this purpose is imidazole, which is also present in the amino acid histidine and is known to form stable complexes with a great variety of metals.<sup>15</sup>



- 1** a  $n = 7$   
b  $n = 9$   
c  $n = 11$   
d  $n = 11$   
e  $n = 15$   
f  $n = 17$

In this chapter we will show that metal ions coordinated to **1** can induce or stabilize thermotropic LC properties. In addition, interesting architectures can be formed from **1** in water,<sup>16</sup> as will be described in Chapter 4. For a proper evaluation of the physical properties of compounds **1**, we also synthesized a series of related metal complexing carbohydrates.<sup>17</sup> The

liquid crystalline properties of these compounds are also described in this chapter. To the best of our knowledge, the complexes reported here are the first examples of carbohydrate metallomesogens.

### 3.2 Experimental

The syntheses described below were in most cases first attempts, which means that the yields were not optimized and can probably be improved.

Melting points were determined as the average of the onset and the top of the melting peaks of DSC thermograms. IR spectra were recorded on a Biorad Digilab Division FT-IR instrument.  $^1\text{H}$ -NMR spectra were recorded on a Bruker WH-90 or a Bruker WM-400 instrument and the chemical shifts are reported relative to  $(\text{CH}_3)_4\text{Si}$ . Abbreviations used are s, singlet, d, doublet, 2d, double doublet, t, triplet, q, quartet, quin, quintet, m, multiplet.  $^{13}\text{C}$ -NMR spectra were recorded on a Bruker WM-400 or a Bruker WM-500 instrument. Chemical shifts are reported relative to  $(\text{CH}_3)_4\text{Si}$  and calibrated on adamantane.

Mass spectra were recorded on a VG7060E instrument and the elemental analyses were carried out with a Carlo Erba EA 1108 instrument. UV-vis spectra were obtained from a Perkin Elmer Lambda 45 spectrophotometer. Thermograms were recorded on a Perkin Elmer DSC 7 instrument, which was calibrated on indium and zinc. Both heating and cooling runs were recorded with a rate of  $5^\circ\text{C}/\text{min}$ .

Single crystal X-ray diffraction data were collected using an Enraf-Nonius CAD4-Turbo diffractometer on a rotating anode. The crystals were glued on a Lindemann glass capillary and mounted on the diffractometer in a stream of cold nitrogen. The data were optimized to a  $R_{\text{w}}F^2$ -value of 0.224,  $R_F=0.120$ ,  $S=0.90$ , using the SHELXL-93 refinement program.

Chemicals were used as obtained from the supplier, except for the solvents which were distilled prior to use.

#### 3.2.1 Syntheses

***N,n*-Octyl-D-gluconamide (6a).** This compound was synthesized as described in the literature.<sup>18</sup> After 2 recrystallizations from MeOH a colorless crystalline powder was obtained, yield 1.07 g (3.47 mmol, 62.4 %), m.p.  $159.2^\circ\text{C}$ . IR (KBr)  $3532\text{ cm}^{-1}$  ( $(\text{C}^2)\text{OH}$ ),<sup>19</sup> 3358 and 3389 (homodromic H bonding cycle),<sup>20</sup> 1646 (amide I) and 1529 (amide II).  $^1\text{H}$ -NMR (400 MHz, DMSO- $d_6$ , in order to obtain less complex spectra, 1 drop of  $\text{D}_2\text{O}$  was added through which the hydroxyl hydrogen atoms were exchanged for deuterium atoms)  $\delta$  3.956 ppm (d, 1H,  $J_{2,3} = 3.60\text{ Hz}$ ,  $\text{H}^2$ ), 3.877 (2d, 1H,  $J_{3,4} = 2.30\text{ Hz}$ ,  $\text{H}^3$ ), 3.558 (2d, 1H,  $J_{5,6} = 2.80\text{ Hz}$ ,  $J_{6,6} = -11.20\text{ Hz}$ ,  $\text{H}^6$ ), 3.462 ppm (m, 1H,  $J_{5,4} = 8.50\text{ Hz}$ ,  $J_{5,6} = 5.50\text{ Hz}$ ,  $\text{H}^5$ ), 3.440 ppm (m, 1H,  $\text{H}^4$ ), 3.348 (2d, 1H,  $\text{H}^6$ ), 3.033 (8 peaks, 2H,  $-\text{CH}_2-\text{NHCO}$ ), 1.390 (t, 2H,  $-\text{CH}_2-\text{CH}_2-\text{NHCO}$ ), 1.229 (m, 10H,  $\text{CH}_3$ - $(\text{CH}_2)_5$ -), 0.846 (t, 3H,  $\text{CH}_3$ -).  $^{13}\text{C}$ -NMR (100 MHz, DMSO- $d_6$ ) 172.23 ppm ( $-\text{NHCO}-$ ), 73.63 ( $\text{C}^2$ ), 72.41 ( $\text{C}^3$ ), 71.49 ( $\text{C}^5$ ), 70.12 ( $\text{C}^4$ ), 63.38 ( $\text{C}^6$ ), 38.26 ( $-\text{CH}_2-\text{NHCO}-$ ), 31.28, 29.17, 28.78, 28.69, 26.38, 22.12 (methylene carbons from alkyl chain), 14.00 ( $-\text{CH}_3$ ). Anal. Calcd for  $\text{C}_{14}\text{H}_{29}\text{NO}_6$ : C, 54.70, H, 9.51, N, 4.56. Found: C, 54.75, H, 9.50, N, 4.55.

Compounds **6b-6f** were synthesized and purified as mentioned above for **6a**. Starting compounds were the appropriate *n*-alkyl amines. Purification by recrystallization became more difficult in the case of the longer alkyl chain amines, repeated recrystallization, however, generally, yielded pure products.

***N,n*-Decyl-D-gluconamide (6b).** After crystallization, a white crystalline powder was obtained, yield 26.41 g (78.72 mmol, 89.3 %), m.p.  $156.5^\circ\text{C}$ . IR (KBr) showed  $1646\text{ cm}^{-1}$ .

(amide I) and 1529 (amide II), which is similar to **6a**. Anal. Calcd. for  $C_{16}H_{33}NO_6$ : C, 57.29; H, 9.92; N, 4.18. Found: C, 57.27; H, 9.76; N, 4.20.

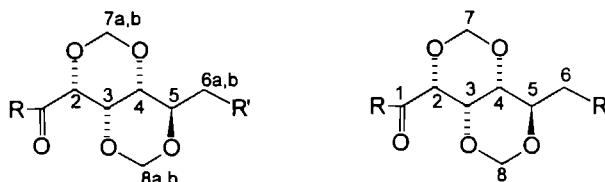
**N,n-Dodecyl-D-gluconamide (6c)**. A crystalline powder was obtained, yield 1.70 g (4.69 mmol, 84.0 %), m.p. 155.5 °C. IR (KBr) showed amide peaks at 1647  $cm^{-1}$  (amide I) and 1529 (amide II). Anal. Calcd. for  $C_{18}H_{37}NO_6$ : C, 59.48; H, 10.26; N, 3.85. Found: C, 59.38; H, 10.20; N, 3.89.

**N,n-Tetradecyl-D-gluconamide (6d)**. After several crystallizations, a crystalline powder was obtained. Yield 17.33 g (44.26 mmol, 91.4 %), m.p. 154.0 °C, IR (KBr) 1647  $cm^{-1}$  (amide I), 1528 (amide II). Anal. Calcd. for  $C_{20}H_{41}NO_6$ : C, 61.35; H, 10.55; N, 3.58. Found: C, 61.30; H, 10.62; N, 3.62.

**N,n-Hexadecyl-D-gluconamide (6e)**. The powder that was obtained in a yield of 14.94 g (35.61 mmol, 62.2 %), consisted of very small crystals, m.p. 151.4 °C, IR (KBr) 1647  $cm^{-1}$  (amide I) and 1527 (amide II). Anal. Calcd. for  $C_{22}H_{45}NO_6$ : C, 62.97; H, 10.81; N, 3.34. Found: C, 62.60; H, 10.81; N, 3.36.

**N,n-Octadecyl-D-gluconamide (6f)**. A white powder was obtained after repeated crystallization (7 times), yield 8.69 g (19.41 mmol, 80.3 %), m.p. 148.5 °C. IR 1624  $cm^{-1}$  (amide I) and 1549 (amide II). Anal. Calcd. for  $C_{24}H_{49}NO_6 \cdot 1.5 MeOH$ : C, 61.79; H, 11.18; N, 2.83. Found: C, 61.98; H, 10.57; N, 3.37.

The carbohydrate skeleton protons and carbon atoms are numbered according to the schemes below.



Numbering schemes for the protons (left) and carbon atoms (right) of the carbohydrate skeleton

In some cases, non first order  $^1H$ -NMR spectra were obtained. The carbohydrate parts of the spectra were therefore simulated by the GeNMR simulation program,<sup>21</sup> and both the chemical shifts and  $J$ -couplings were adjusted until the calculated and measured patterns matched.

**2,4,3,5-Dimethylene-D-gluconic acid (2)**. The synthesis of this compound was described in the literature.<sup>22</sup> After recrystallization from water, crystalline needles were obtained, yield 107.2 g (0.487 mol, 92 %), m.p. 224.5 °C, IR. (KBr) 3428  $cm^{-1}$  (broad, acid OH), 1730 and 1718 ( $C=O$ , double probably due to the presence of more than one conformation), 1178 and 1104 ( $C-O$ , ketal), 1141 ( $C-OH$ , alcohol).  $^1H$ -NMR (DMSO- $d_6$ , 90 MHz)  $\delta$  5.040 ppm (d, 1H,  $J=5.4$  Hz,  $H^{7a}$ ), 4.945 (d, 1H,  $J=6.3$  Hz,  $H^{8a}$ ), 4.760 (d, 2H,  $H^{7b}$  and  $H^{8b}$ ), 4.395 (d, 1H,  $J=2.7$  Hz,  $H^2$ ), 4.090 (broad s, 1H,  $H^3$ ), 3.740 (m, 4H,  $H^{4-6}$ ), EI-MS  $m/z$  221 ( $M+H$ )<sup>+</sup>, 203 ( $M-OH$ )<sup>+</sup>, 189 ( $M-CH_2OH$ )<sup>+</sup>, 175 ( $M-COOH$ )<sup>+</sup>, 85 (cyclic  $-O-CH=CH-CH^+-O-CH_2$ ). Anal. Calcd. for  $C_8H_{12}O_7$ : C, 43.64; H, 5.49. Found: C, 43.57; H, 5.33.



**Methyl-2,4;3,5-dimethylene-D-gluconate (3).** The synthesis of this compound was also described in the literature.<sup>23</sup> After cooling of the reaction mixture, cube-shaped crystals were obtained, yield 26.0 g (0.111 mol, 61 %), m.p. 151.5 °C, IR (KBr) 3501  $\text{cm}^{-1}$  (very sharp, OH), 1757 ( $\text{C=O}$ ).  $^1\text{H-NMR}$  ( $\text{CD}_3\text{OD}$ , 400 MHz)  $\delta$  5.138 ppm (d, 1H,  $J = 6.31\text{ Hz}$ ,  $\text{H}^{\text{7a}}$ ), 5.050 (d, 1H,  $J = 6.31$ ,  $\text{H}^{\text{8a}}$ ), 4.865 (d, 2H,  $\text{H}^{\text{7b}}$  and  $\text{H}^{\text{8b}}$ ), 4.509 (d, 1H,  $J_{2,3} = 2.10$ ,  $\text{H}^2$ ), 4.178 (t, 1H,  $J_{3,2} = 1.66$ ,  $\text{H}^3$ ), 3.880 (m, 3H,  $\text{H}^{\text{4-6a}}$ ), 3.825 (2d, 1H,  $J_1 = 5.66$ ,  $J_2 = -14.20$ , negative  $J$ -coupling was found after simulation,  $\text{H}^{\text{6b}}$ ), 3.768 (s, 3H,  $\text{OCH}_3$ ).  $^{13}\text{C-NMR}$  ( $\text{CD}_3\text{OD}$ , 100 MHz) 169.954 ppm ( $\text{C}^1$ ), 93.220 ( $\text{C}^7$ ), 89.330 ( $\text{C}^8$ ), 78.094 ( $\text{C}^2$ ), 77.482 ( $\text{C}^3$ ), 72.178 ( $\text{C}^5$ ), 69.523 ( $\text{C}^4$ ), 60.221 ( $\text{C}^6$ ), 52.716 ( $\text{OCH}_3$ ). EI-MS  $m/z$  233 ( $\text{M} - \text{H}$ ) $^+$ , 219 ( $\text{M} - \text{CH}_3$ ) $^+$ , 203 ( $\text{M} - \text{OCH}_3$ ) $^+$ , 175 ( $\text{M} - \text{COOCH}_3$ ) $^+$ , 85 (cyclic  $-\text{O}-\text{CH}=\text{CH}-\text{CH}^+-\text{O}-\text{CH}_2$ ). Anal. Calcd. for  $\text{C}_9\text{H}_{14}\text{O}_7$ : C, 46.16; H, 6.02. Found: C, 45.97; H, 5.81.

**2,4;3,5-Dimethylene-N,n-octyl-D-gluconamide (4a).** Compound **2** (20.0 g, 85.4 mmol) was dissolved in 150 ml (10.7 equiv.) of octyl amine and stirred in a nitrogen atmosphere at 95 °C for 2 days. The solution was diluted with ethyl acetate and after one night in the refrigerator, a white precipitate was formed which was filtered and additionally washed with n-hexane. After purification by column chromatography (silica, eluent EtOAc), the white product was washed with n-hexane again, yield 21.75 g (65.63 mmol, 76.9 %) of white crystals, m.p. 99.0 °C (after additional recrystallization from water). IR (KBr) 3486  $\text{cm}^{-1}$  (OH), 3330 (NH), 1660 (amide I), 1550 (amide II), 1180, 1109, 1094 and 1064 (ketal), 1038 ( $\text{C-OH}$ ), IR ( $\text{CHCl}_3$  solution) 3629 (OH), 3426 (NH), 1675 (amide I), 1543 (amide II), 1043 ( $\text{C-OH}$ ).  $^1\text{H-NMR}$  (400 MHz,  $\text{CDCl}_3$ , assignments were made by irradiation on the OH proton and subsequent simulation),  $\delta$  6.601 ppm (t, 1H,  $J = 5.76\text{ Hz}$ ,  $\text{NHCO}$ ), 5.257 (d, 1H,  $J = 6.45$ ,  $\text{H}^{\text{7a}}$ ), 5.082 (d, 1H,  $J = 6.20$ ,  $\text{H}^{\text{8a}}$ ), 4.958 (d, 1H,  $\text{H}^{\text{8b}}$ ), 4.822 (d, 1H,  $\text{H}^{\text{7b}}$ ), 4.236 (t, 1H,  $J_{2,3} = 2.18$ ,  $\text{H}^2$ ), 4.136 (d, 1H,  $J_{3,4} = 0.82$ ,  $\text{H}^3$ ), 4.014 (2d, 1H,  $J_{5,6a} = 6.20$ ,  $J_{5,6b} = 5.78$ ,  $\text{H}^5$ ), 3.890 (7 peaks, 1H,  $J_{6a-6b} = -11.43$ ,  $J_{6a-\text{OH}} = 6.46$ ,  $\text{H}^{\text{6a}}$ ), 3.978 (5 peaks, 1H,  $J_{6b-\text{OH}} = 4.11$ ,  $\text{H}^{\text{6b}}$ ), 3.780 (s, 1H,  $\text{H}^4$ ), 3.292 (q, 2H,  $J = 6.73$ ,  $-\text{CH}_2-\text{NHCO}$ ), 2.877 (2d, 1H, OH), 1.513 (m, 2H,  $-\text{CH}_2-\text{CH}_2-\text{NHCO}$ ), 1.260 (m, 10H,  $\text{CH}_3-(\text{CH}_2)_5-$ ), 0.869 (t, 3H,  $\text{CH}_3$ ).  $^{13}\text{C-NMR}$  ( $\text{CDCl}_3$ , 110 MHz)  $\delta$  167.372 ppm ( $\text{C}^1$ ), 92.150 ( $\text{C}^7$ ), 88.587 ( $\text{C}^8$ ), 77.506 ( $\text{C}^2$ ), 76.104 ( $\text{C}^3$ ), 71.439 ( $\text{C}^5$ ), 67.748 ( $\text{C}^4$ ), 59.926 ( $\text{C}^6$ ), 39.110 ( $-\text{CH}_2-\text{NHCO}$ ), 31.724, 29.322, 29.148, 26.723, 22.576 ( $-(\text{CH}_2)_6-$ ), 14.030 ( $-\text{CH}_3$ ). EI-MS  $m/z$  332 ( $\text{M}+\text{H}$ ) $^+$ , 302 ( $\text{M} - \text{CH}_2\text{OH}$ ) $^+$ , 156 ( $\text{CH}_3-(\text{CH}_2)_7-\text{NHCO}$ ) $^+$ , 85 (cyclic  $-\text{O}-\text{CH}=\text{CH}-\text{CH}^+-\text{O}-\text{CH}_2$ ). Anal. Calcd. for  $\text{C}_{16}\text{H}_{29}\text{NO}_6$ : C, 57.99; H, 8.82; N, 4.23. Found: C, 57.94; H, 8.68; N, 4.26.

Syntheses of **4b-4f** were carried out according to a reaction procedure analogous to that described for **4a**. The starting compounds were the appropriate n-alkyl amines.

**2,4;3,5-Dimethylene-N,n-decyl-D-gluconamide (4b).** Instead of recrystallization from water as was described for the purification of **4a**, this compound was recrystallized from EtOAc which resulted in white crystals, yield 1.71 g (4.75 mmol, 25.5 %), m.p. 102.3 °C. IR (KBr) and  $^1\text{H-NMR}$  (90 MHz,  $\text{CDCl}_3$ ) spectra were analogous to that of **4a** except for  $\delta$  1.254 ppm (m, 16H,  $\text{CH}_3-(\text{CH}_2)_8-$ ), EI-MS  $m/z$  359 ( $\text{M}$ ) $^+$ . Anal. Calcd. for  $\text{C}_{18}\text{H}_{33}\text{NO}_6$ : C, 60.14; H, 9.25; N, 3.90. Found: C, 60.12; H, 9.64; N, 3.93.

**2,4;3,5-Dimethylene-N,n-dodecyl-D-gluconamide (4c).** Purification analogous to that described for **4b**, yield 1.95 g of white crystals (5.03 mmol, 50.2 %), m.p. 103.6 °C. IR (KBr) and  $^1\text{H-NMR}$  (90 MHz,  $\text{CDCl}_3$ ) assignments were similar to that of **4a** except for the number of methylene protons of the alkyl chain  $\delta$  1.252 ppm (m, 20H,  $\text{CH}_3-(\text{CH}_2)_{10}-$ ), EI-MS  $m/z$  387 ( $\text{M}$ ) $^+$ . Anal. Calcd. for  $\text{C}_{20}\text{H}_{37}\text{NO}_6$ : C, 61.99; H, 9.62; N, 3.61. Found: C, 61.72; H, 9.67; N, 3.61.

**2,4;3,5-Dimethylene-N,n-tetradecyl-D-gluconamide (4d).** Purification analogous to that described for **4b**, yield 3.81 g (white crystalline powder, 7.66 mmol, 35.0 %), m.p. 102.8 °C. IR (KBr) and  $^1\text{H-NMR}$  (90 MHz,  $\text{CDCl}_3$ ) assignments similar to those of **4a** except for the

methylene protons of the alkyl chain  $\delta$  1.247 ppm (m, 24H,  $\text{CH}_3\text{-(CH}_2\text{)}_{12}\text{-}$ ), EI-MS  $m/z$  415 ( $\text{M}^+$ ). Anal. Calcd. for  $\text{C}_{22}\text{H}_{41}\text{NO}_6$ : C, 63.59; H, 9.94; N, 3.37. Found: C, 63.23; H, 10.09; N, 3.58.

**2,4;3,5-Dimethylene-*N*,*n*-hexadecyl-D-gluconamide (4e).** Purification analogous to that described for **4b**, yield 5.50 g of white crystalline powder (12.40 mmol, 51.8 %), m.p. 105.5 °C. IR (KBr) and  $^1\text{H-NMR}$  (90 MHz,  $\text{CDCl}_3$ ) spectra were similar to that of **4a** except for the methylene protons of the alkyl chain  $\delta$  1.254 ppm (m, 28H,  $\text{CH}_3\text{-(CH}_2\text{)}_{14}\text{-}$ ), EI-MS  $m/z$  443 ( $\text{M}^+$ ). Anal. Calcd. for  $\text{C}_{24}\text{H}_{45}\text{NO}_6$ : C, 64.98; H, 10.22; N, 3.16. Found: C, 64.98; H, 10.57; N, 3.16.

**2,4;3,5-Dimethylene-*N*,*n*-octadecyl-D-gluconamide (4f).** This compound was purified by column chromatography (silica, eluent MeOH/EtOAc 5:95 v/v) followed by recrystallization from ethyl acetate, yield 0.85 g (white powder, 1.802 mmol, 18.0 %), m.p. 92.0 °C IR (KBr) and  $^1\text{H-NMR}$  (90 MHz,  $\text{CDCl}_3$ ) spectra were analogous to those of **4a** except for the methylene protons of the alkyl chain  $\delta$  1.252 ppm (m, 32H,  $\text{CH}_3\text{-(CH}_2\text{)}_{16}\text{-}$ ), EI-MS  $m/z$  471 ( $\text{M}^+$ ). Anal. Calcd. for  $\text{C}_{26}\text{H}_{49}\text{NO}_6$ : C, 66.21; H, 10.47; N, 2.87. Found: C, 64.34; H, 10.31; N, 3.05

**6-Tosyl-2,4;3,5-dimethylene-*N*,*n*-octyl-D-gluconamide (5a).** To a solution of 15.0 g (45.26 mmol) of **4a** in 150 ml of anhydrous pyridine which was placed in an ice bath, under a nitrogen atmosphere, 9.78 g (51.30 mmol, 1.1 equiv.) of tosyl chloride dissolved in 50 ml of pyridine, was added dropwise. After an additional hour of stirring, the orange solution was stored overnight in the refrigerator. The product was precipitated by pouring the pyridine solution into a mixture of saturated  $\text{NaHCO}_3$  solution and ice. The product was filtered off, dried in vacuum, and used without any further purification, yield 19.065 g (39.26 mmol, 86.7 %), m.p. 116.6 °C IR (KBr)  $3398\text{ cm}^{-1}$  (NH), 1680 (amide I), 1531 (amide II), 1359 and 1176 (S=O),  $^1\text{H-NMR}$  (90 MHz,  $\text{CDCl}_3$ )  $\delta$  7.793 ppm (d, 2H, ArH), 7.368 (d, 2H, ArH), 6.599 (t, 1H, NHCO), 5.230 (d, 1H,  $J=6.3\text{ Hz}$ ,  $\text{H}^{\text{7a}}$ ), 4.896 (d, 1H,  $J=6.8\text{ Hz}$ ,  $\text{H}^{\text{8a}}$ ), 4.786 (d, 2H,  $\text{H}^{\text{8b}}$  and  $\text{H}^{\text{7b}}$ ), 4.215 (m, 3H,  $\text{H}^{\text{5,6a,6b}}$ ), 4.074 (s, 2H,  $\text{H}^{\text{2,3}}$ ), 3.670 (s, 1H,  $\text{H}^{\text{4}}$ ), 2.467 (s, 3H,  $\text{ArCH}_3$ ). EI-MS  $m/z$  485 ( $\text{M}^+$ ), 314 ( $\text{M} - \text{OTs}^+$ ), 156 ( $\text{C}_8\text{H}_{17}\text{-NHCO}^+$ ), 155 ( $\text{SO}_2\text{-C}_6\text{H}_4\text{-CH}_3^+$ ), 85 (cyclic  $-\text{O-CH=CH-CH}^+-\text{O-CH}_2$ ). Anal. Calcd. for  $\text{C}_{23}\text{H}_{35}\text{NO}_8\text{S} \cdot 0.5\text{ H}_2\text{O}$ : C, 55.85; H, 7.34; N, 2.83; S, 6.48 Found: C, 55.63; H, 7.16; N, 2.98; S, 6.27.

The tosylate compounds (**5b-f**) obtained from **4b-f** were prepared by procedures analogous to that of **5a**. The derivatives **5b-d** and **5f** were purified only by washing with water. Since the starting hydroxyl compounds **4b-d** and **4f** do not dissolve in cold water, the products **5b-d** and **5f** were slightly contaminated with the starting hydroxyl compound. Because the contamination was very small and hydroxyl compounds were not affecting the subsequent reactions, these compounds were not further purified.

#### 6-Tosyl-2,4;3,5-dimethylene-*N*,*n*-hexadecyl-D-gluconamide (5e).

Synthesis was analogous to that of compound **5a**. In contrast with **5a-d** and **5f**, this compound was purified first by precipitation from ice/ $\text{NaHCO}_3$  and subsequently with column chromatography (silica, *n*-hexane/EtOAc 1:1, v/v). Yield 6.50 g (10.87 mmol, 78.4 %, m.p. 97.1 °C, EI-MS  $m/z$  597 ( $\text{M}^+$ ), 268 ( $\text{C}_{16}\text{H}_{33}\text{-NHCO}^+$ ), 155 ( $\text{SO}_2\text{-C}_6\text{H}_4\text{-CH}_3^+$ ), 85 (cyclic  $-\text{O-CH=CH-CH}^+-\text{O-CH}_2$ ). Anal. Calcd. for  $\text{C}_{31}\text{H}_{51}\text{NO}_8\text{S}$ : C, 62.28; H, 8.60; N, 2.34; S, 5.36. Found: C, 62.21; H, 8.75; N, 2.36; S, 5.04.

#### 6-Deoxy-6-(1-imidazolyl)-2,4;3,5-dimethylene-*N*,*n*-octyl-D-gluconamide (1a).

Compound **5a** (1.13 g, 2.32 mmol) and 0.50 g (7.28 mmol) of imidazole were dissolved in 7.5 ml chloroform and brought under high pressure (15 kBar) at 50 °C for 2 days. The solution was washed with saturated aqueous  $\text{NaHCO}_3$  and dried over  $\text{Na}_2\text{SO}_4$  and further purified by column chromatography (silica, eluent  $\text{Et}_3\text{N/MeOH/EtOAc}$  1:10:89, v/v/v) followed by recrystallization from diluted aqueous NaOH (pH=8), yield 0.58 g (white needle shaped crystals, 1.52 mmol,

65.6 %, m.p. 134.5 °C IR (KBr) 3332  $\text{cm}^{-1}$  (NH), 3142 (=C-H), 3097 (=C-H), 1667 (amide I), 1545 (amide II), 1187, 1103, 1095 and 1068 (ketal), 993 (=C-H), IR ( $\text{CHCl}_3$  solution), 3426 (NH), 1676 (amide I), 1543 (amide II),  $^1\text{H-NMR}$  (400 MHz,  $\text{CDCl}_3$ , assignments were made by irradiation on proton  $\text{H}^4$ , and recording a COSY spectrum (8K, det F2, 512K evol F1) The spectra did not result in a clear assignment, however, after recording temperature dependent experiments in combination with simulation, the chemical shifts and  $J$ -couplings could be determined unambiguously  $\delta$  7.513 (s, 1H, N=CH-N), 7.105 (s, 1H, -CH<sub>2</sub>-N-CH=CH-N=), 6.965 (s, 1H, -N-CH=CH-N=), 6.530 ppm (t, 1H,  $J = 5.76$  Hz, NHCO), 5.226 (d, 1H,  $J = 6.50$  Hz,  $\text{H}^{7a}$ ), 5.016 (d, 1H,  $J = 6.19$  Hz,  $\text{H}^{8a}$ ), 5.053 (d, 1H,  $\text{H}^{8b}$ ), 4.754 (d, 1H,  $\text{H}^{7b}$ ), 4.330 (2d, 1H,  $J_{6a,5} = 5.50$  Hz,  $J_{6a,6b} = -15.30$  Hz,  $\text{H}^{6a}$ ), 4.219 (m, 1H,  $J_5 = 1.20$  Hz,  $\text{H}^5$ ), 4.211 (m, 1H,  $J_{6b,5} = 10.00$ ,  $\text{H}^{6b}$ ), 4.180 (d, 1H,  $J_3 = 1.00$ ,  $\text{H}^3$ ), 4.130 (d, 1H,  $J_2 = 2.00$  Hz,  $\text{H}^2$ ), 3.530 (t, 1H,  $\text{H}^4$ ), 3.306 (2d, 2H, -CH<sub>2</sub>-NHCO), 1.736 (crystal water), 1.509 (m, 2H, -CH<sub>2</sub>-CH<sub>2</sub>-NHCO), 1.261 (m, 10H, CH<sub>3</sub>-(CH<sub>2</sub>)<sub>5</sub>-), 0.877 (t, 3H, CH<sub>3</sub>)  $^{13}\text{C-NMR}$  ( $\text{CDCl}_3$ , 100 MHz)  $\delta$  167.641 ppm (C<sup>1</sup>), 137.389 (N=CH-N), 135.342 (N-CH=CH-N), 129.780 (N-CH=CH-N), 91.932 (C<sup>7</sup>), 88.003 (C<sup>8</sup>), 77.177 (C<sup>2</sup>), 75.006 (C<sup>3</sup>), 71.118 (C<sup>5</sup>), 66.743 (C<sup>4</sup>), 44.563 (C<sup>6</sup>), 39.008 (-CH<sub>2</sub>-NHCO), 31.616, 29.253, 29.040, 28.913, 26.631, 22.470 (-CH<sub>2</sub>)<sub>6</sub>-), 13.935 (-CH<sub>3</sub>) EI-MS  $m/z$  380 (M - H)<sup>+</sup>, 225 (M - CH<sub>3</sub>-(CH<sub>2</sub>)<sub>7</sub>-NHCO)<sup>+</sup>, Anal. Calcd for C<sub>19</sub>H<sub>31</sub>N<sub>3</sub>O<sub>5</sub> · ½ H<sub>2</sub>O C, 58.44, H, 8.62, N, 10.76 Found C, 58.68, H, 8.18, N, 10.65

Syntheses of **1b-1f** were carried out according to a reaction procedure analogous to that described for **1a**. The starting compounds were the appropriate tosylates (**5b-5f**)

**6-Deoxy-6-(1-imidazolyl)-2,4;3,5-dimethylene-N,n-decyl-D-gluconamide (1b)** After an isolation and purification procedure, which was analogous to that of **1a**, a white crystalline powder was obtained, yield 0.25 g (0.61 mmol, 48.3 %), m.p. 133.9 °C IR (KBr) and  $^1\text{H-NMR}$  (90 MHz,  $\text{CDCl}_3$ ), spectra were similar as those obtained from **1a**, however, the number of protons in the alkyl chain of this compound were different,  $\delta$  1.270 ppm (m, 16H, CH<sub>3</sub>-(CH<sub>2</sub>)<sub>8</sub>-), EI-MS  $m/z$  408 (M - H)<sup>+</sup> Anal. Calcd for C<sub>21</sub>H<sub>33</sub>N<sub>3</sub>O<sub>5</sub> C, 61.59, H, 8.61, N, 10.26 Found C, 61.65, H, 8.62, N, 9.71

**6-Deoxy-6-(1-imidazolyl)-2,4;3,5-dimethylene-N,n-dodecyl-D-gluconamide (1c)**

Isolation of this compound was hampered by the difficult separation of the organic and water layers, therefore 5 min of centrifugation (3300 rpm) was applied. After column chromatography (silica, eluent Et<sub>3</sub>N/MeOH/EtOAc 1:10:89, v/v/v), the compound was recrystallized from EtOAc. Yield was not determined, m.p. 134.3 °C IR (KBr) and  $^1\text{H-NMR}$  (90 MHz,  $\text{CDCl}_3$ ) spectra were similar to those of **1a**, however, the number of protons in the alkyl chain of this compound were different,  $\delta$  1.243 ppm (m, 20H, CH<sub>3</sub>-(CH<sub>2</sub>)<sub>10</sub>-), EI-MS  $m/z$  436 (M - H)<sup>+</sup> Anal. Calcd for C<sub>23</sub>H<sub>39</sub>N<sub>3</sub>O<sub>5</sub> C, 63.13, H, 8.98, N, 9.60 Found C, 63.16, H, 8.88, N, 9.56

**6-Deoxy-6-(1-imidazolyl)-2,4;3,5-dimethylene-N,n-tetradecyl-D-gluconamide (1d)**

The procedure for the isolation and purification was similar to that described for **1c**, yield 0.41 g (white crystalline powder, 0.89 mmol, 36.9 %), m.p. 134.2 °C IR (KBr) and  $^1\text{H-NMR}$  (90 MHz,  $\text{CDCl}_3$ ) spectra were similar to those obtained for **1a**, however, the number of protons in the alkyl chain of this compound were different,  $\delta$  1.233 ppm (m, 24H, CH<sub>3</sub>-(CH<sub>2</sub>)<sub>12</sub>-), EI-MS  $m/z$  464 (M - H)<sup>+</sup> Anal. Calcd for C<sub>25</sub>H<sub>43</sub>N<sub>3</sub>O<sub>5</sub> C, 64.49, H, 9.31, N, 9.02 Found C, 64.58, H, 9.26, N, 8.96

**6-Deoxy-6-(1-imidazolyl)-2,4;3,5-dimethylene-N,n-hexadecyl-D-gluconamide (1e)**

Isolation and purification were similar to the procedure described for **1c**, yield 0.09 g (white crystals, 0.18 mmol, 7.4 %) The conversion was higher, however, due to a poor separation by column chromatography (silica, eluent Et<sub>3</sub>N/MeOH/EtOAc 1:5:94, v/v/v), the amount of pure

product was relatively low, m.p. 131 °C. IR (KBr) and  $^1\text{H-NMR}$  (90 MHz,  $\text{CDCl}_3$ ) spectra were similar to those obtained for **1a**, however, the number of protons in the alkyl chain of this compound were different,  $\delta$  1.224 ppm (m, 28H,  $\text{CH}_3\text{-(CH}_2\text{)}_{14}\text{-}$ ), EI-MS  $m/z$  493 ( $\text{M}^+$ ) Anal Calcd. for  $\text{C}_{27}\text{H}_{47}\text{N}_3\text{O}_5$ : C, 65.69; H, 9.60; N, 8.51. Found: C, 65.96; H, 9.56; N, 8.47.

**6-Deoxy-6-(1-imidazolyl)-2,4,3,5-dimethylene-N,n-octadecyl-D-gluconamide (1f).**

The procedures for the isolation and purification were similar to that described for **1e**, yield 0.65 g (white powder, 1.24 mmol, 68.0 %), m.p. 117 °C. IR (KBr) and  $^1\text{H-NMR}$  (90 MHz,  $\text{CDCl}_3$ ) spectra similar to those obtained for **1a**, however, the number of protons in the alkyl chain of this compound were different,  $\delta$  1.250 ppm (m, 32H,  $\text{CH}_3\text{-(CH}_2\text{)}_{16}\text{-}$ ), EI-MS  $m/z$  521 ( $\text{M}^+$ ). Anal Calcd. for  $\text{C}_{29}\text{H}_{51}\text{N}_3\text{O}_5 \cdot \frac{1}{2} \text{H}_2\text{O}$ : C, 65.61; H, 9.88; N, 7.92. Found: C, 64.42; H, 9.81; N, 8.37.

**6-Deoxy-6-amino-2,4,3,5-dimethylene-N,n-octyl-D-gluconamide (7).** Compound **5a** (0.95 g, 1.88 mmol) was dissolved in 60 ml of MeOH (0 °C) which was saturated with  $\text{NH}_3$  gas (735 mmol). The solution was placed in an autoclave, sealed and heated overnight at 80 °C. The methanol and excess of ammonia were removed by evaporation and in order to isolate the product, the remaining slurry was mixed with aqueous 2N NaOH and  $\text{CHCl}_3$ . After drying the organic layer over  $\text{Na}_2\text{SO}_4$ , the solvent was removed by evaporation. The product was recrystallized from diethyl ether (twice). One spot was detected on TLC with ninhydrine,<sup>24</sup> yield 0.115 g (yellow powder, 0.349 mmol, 18.5 %), m.p. 134 °C. IR (KBr), 3700-3180  $\text{cm}^{-1}$  (top at 3315 ( $\text{NH}_2$ ), 3433 (NH), 1664 (amide I), 1625 ( $\text{NH}_2$ ), 1550 (amide II).  $^1\text{H-NMR}$  (400 MHz,  $\text{CDCl}_3$ ),  $\delta$  6.548 (broad t, 1H,  $\text{NHCO}$ ), 5.261 (d, 1H,  $J_{7a-7b}$  = 6.42 Hz,  $\text{H}^{7a}$ ), 4.958 (2d, 2H,  $J_{8a-8b}$  = 6.39 Hz,  $\text{H}^{8a+8b}$ ), 4.807 (d, 1H,  $\text{H}^{7b}$ ), 4.140 (s, 1H,  $\text{H}^3$ ), 4.115 (d, 1H,  $\text{H}^2$ ), 3.299 (2d,  $J_{5-6a}$  = 8.74 Hz,  $J_{5-6b}$  = 5.84 Hz,  $\text{H}^5$ ), 3.634 (s, 1H,  $\text{H}^4$ ), 3.299 (2d, 2H,  $\text{-CH}_2\text{-NHCO}$ ), 3.215 (m, 1H,  $J_{6a-6b}$  = 13.16 Hz,  $\text{H}^{6a}$ ), 2.848 (2d, 1H,  $\text{H}^{6b}$ ), 1.610 (very broad s, crystal water), 1.513 (septet, 2H,  $\text{-CH}_2\text{-CH}_2\text{-NHCO}$ ) 1.273 (m, 10H,  $\text{CH}_3\text{-(CH}_2\text{)}_6\text{-}$ ), 0.875 (t, 3H,  $\text{CH}_3$ ). EI-MS  $m/z$  330 ( $\text{M}^+$ ), 300 ( $\text{M} - (\text{-CH}_2\text{-NH}_2)^+$ ), 85 (cyclic  $\text{-O-CH=CH-CH}^+\text{-O-CH}_2$ ). Anal. Calcd. for  $\text{C}_{16}\text{H}_{30}\text{N}_2\text{O}_5 \cdot \text{H}_2\text{O}$ : C, 55.14; H, 9.26; N, 8.04. Found: C, 55.97; H, 8.39; N, 7.58.

**6-Phenyl-2,4,3,5-dimethylene-N,n-hexadecyl-D-gluconamide (8).** Compound **5e** (0.658 g, 1.10 mmol) was mixed with 0.580 g (6 equiv.) of phenol and 1.93 g (17 equiv.) of  $\text{Et}_3\text{N}$  and stirred at 115 °C for 3 days in a nitrogen atmosphere. The dark brown oil was diluted with  $\text{CHCl}_3$ , washed with aqueous 1N NaOH and subsequently purified by column chromatography (silica, eluent n-hexane/ $\text{EtOAc}$  3:1, v/v), yield 0.19 g (0.37 mmol, 33.2 %), m.p. 122.6 °C. IR (KBr) 3318  $\text{cm}^{-1}$  (NH), 1655 (amide I), 1602 and 1587 (aromatic C=C), 1537 (amide II), 1250 (phenoxy C-O),  $^1\text{H-NMR}$  (90 MHz,  $\text{CDCl}_3$ )  $\delta$  7.318 ppm (m, 1H, ArH), 6.969 (m, 4H, ArH), 6.552 (t, 1H,  $\text{NHCO}$ ), 5.291 (d, 1H,  $J_{7a-7b}$  = 6.36 Hz,  $\text{H}^{7a}$ ), 5.164 (d, 1H,  $J_{8a-8b}$  = 6.35 Hz,  $\text{H}^{8a}$ ), 5.001 (d, 1H,  $\text{H}^{8b}$ ), 4.849 (d, 1H,  $\text{H}^{7b}$ ), 4.383, 4.295, 4.164 (5H,  $\text{H}^{2,3,5,6a,6b}$ ), 3.889 (s, 1H,  $\text{H}^4$ ). EI-MS  $m/z$  519 ( $\text{M}^+$ ), 426 ( $\text{M} - \text{O-C}_6\text{H}_5$ )<sup>+</sup>, 268 ( $\text{CH}_3\text{-(CH}_2\text{)}_{15}\text{-NHCO}$ )<sup>+</sup>, Anal. Calcd. for  $\text{C}_{30}\text{H}_{49}\text{NO}_6$ : C, 69.33; H, 9.50; N, 2.70. Found: C, 68.90; H, 9.66; N, 2.77.

**6-(4-Pyridyl)-2,4,3,5-dimethylene-N,n-hexadecyl-D-gluconamide (9).** The procedure for the synthesis of this compound was similar to that described for **8**, however, instead of phenol, 0.976 g (5.52 mmol, 3.4 equiv.) of 4-hydroxypyridine and a shorter reaction time (1 night) were used. After column chromatography (silica, eluent  $\text{Et}_3\text{N}/\text{MeOH}/\text{EtOAc}$  1:10:89, v/v), a white crystalline product was obtained, yield 0.21 g (0.40 mmol, 24.7 %), m.p. 130.1 °C. IR (KBr) 3690-3180  $\text{cm}^{-1}$  (top at 3425, peak at 3321, NH), 1655 (amide I), 1594 and 1578 (C=C), 1538 (amide II), 1181, 1107, 1089 and 1070 (ketal),  $^1\text{H-NMR}$  (400 MHz,  $\text{CDCl}_3$ )  $\delta$  8.476 (2d,  $J$  = 4.5 and  $J$  = 1.4 Hz (long range), 2H, ArH), 6.583 (2d, 2H, ArH), 5.291 (d,  $J_{7a-7b}$  = 6.49 Hz, 1H,  $\text{H}^{7a}$ ), 5.108 (d,  $J$  = 6.30 Hz, 1H,  $\text{H}^{8a}$ ), 5.026 (d, 1H,  $\text{H}^{8b}$ ), 4.857 (d, 1H,  $\text{H}^{7b}$ ), 4.364 (2d, 1H,  $\text{H}^{6a}$ ), 4.311

(2d, 1H, H<sup>6b</sup>), 4 311 (m, 2H, H<sup>3'</sup>), 4 177 (d, 1H, H<sup>2</sup>) 3 869 (s, 1H, H<sup>4</sup>), 3 312 (q, 2H, -(CH<sub>2</sub>)<sub>14</sub>-CH<sub>2</sub>-NHCO), 1 516 (2d, 2H, CH<sub>3</sub>-(CH<sub>2</sub>)<sub>13</sub>-CH<sub>2</sub>-), 1 320 (broad s, 26H, CH<sub>3</sub>-(CH<sub>2</sub>)<sub>13</sub>-CH<sub>2</sub>-), 0 900 (t, 3H, CH<sub>3</sub>-) EI-MS *m/z* 520 (M)<sup>+</sup>, 491 (M-C<sub>2</sub>H<sub>5</sub>)<sup>+</sup>, 268 (CH<sub>3</sub>-(CH<sub>2</sub>)<sub>15</sub>-NHCO)<sup>+</sup>, 96 (C<sub>5</sub>H<sub>4</sub>NO hetero tropylium)<sup>+</sup> Anal Calcd for C<sub>29</sub>H<sub>48</sub>N<sub>2</sub>O<sub>6</sub> C, 66 89, H 9 29, N, 5 38 Found C, 66 68, H, 9 13, N, 5 47

**6-(3-Pyridyl)-2,4;3,5-dimethylene-N,n-hexadecyl-D-gluconamide (10)** The procedure described for the synthesis of compound **9** was followed, however, instead of 4-hydroxypyridine, 3-hydroxypyridine was used Yield (after two purifications by column chromatography) 0 13 g of yellow crystals (0 24 mmol, 13 2 %), m p 95 2 °C, IR (KBr) 3427 cm<sup>-1</sup> (NH), 1678 (amide I), 1590, 1567 and 1507 (aromatic, C=C), 1536 (amide II) <sup>1</sup>H-NMR (400 MHz, CDCl<sub>3</sub>) δ 7 774 (s, 1H, ArH), 7 324 (d, 1H, ArH), 7 253 (s, 1H, ArH), 7 226 (2d, 2H, ArH), 6 511 (t, 1H, NHCO), 5 140 (d, *J*<sub>7a-7b</sub> = 6 44 Hz, 1H, H<sup>7a</sup>), 5 080 (d, *J* = 6 14 Hz, 1H, H<sup>8a</sup>), 4 919 (d, 1H, H<sup>8b</sup>), 4 762 (d, 1H, H<sup>7b</sup>), 4 694 (2d, 1H, *J*<sub>6a-5</sub> = 10 00 Hz, *J*<sub>6a-6b</sub> = 13 97 Hz, H<sup>6a</sup>), 4 519 (2d, 1H, *J*<sub>6a-5</sub> = 10 00 Hz, H<sup>6b</sup>), 4 211 (s, 1H, H<sup>2</sup>), 4 159 (d, 1H, H<sup>3</sup>) 3 807 (s, 1H, H<sup>4</sup>), 3 214 (m, 2H, -(CH<sub>2</sub>)<sub>14</sub>-CH<sub>2</sub>-NHCO), 1 419 (2d, 2H, CH<sub>3</sub>-(CH<sub>2</sub>)<sub>13</sub>-CH<sub>2</sub>-), 1 320 (broad s, 26H, CH<sub>3</sub>-(CH<sub>2</sub>)<sub>13</sub>-CH<sub>2</sub>-), 0 900 (t, 3H, CH<sub>3</sub>-) <sup>1</sup>H-NMR did not show the presence of any contamination, however, no satisfactory elemental analysis could be obtained

**6-Deoxy-6-(1-pyrazolyl)-2,4;3,5-dimethylene-N,n-hexadecyl-D-gluconamide (11)** The procedure described for the preparation of **1e** was followed, however, instead of imidazole, 0 462 g (6 78 mmol, 5 equiv) of pyrazole was used Yield 0 01 g (0 01 mmol, 4 %), m p 103 8 °C IR (KBr) 3307 cm<sup>-1</sup> (NH), 1660 (amide I), 1550 (amide II) <sup>1</sup>H-NMR (90 MHz, CDCl<sub>3</sub>) δ 7 538 ppm (d, *J* = 1 59 Hz, 1H, ArH), 7 438 (d, *J* = 2 54, 1H, ArH), 6 538 (t, 1H, NHCO), 6 294 (t, 1H, ArH), 5 225 (d, *J*<sub>7a-7b</sub> = 6 36 Hz, 1H, H<sup>7a</sup>), 5 012 (s, 2H, H<sup>8a,b</sup>), 4 762 (d, 1H, H<sup>7b</sup>), 4 521 (2d, *J*<sub>6a-5</sub> = 7 67 Hz, *J*<sub>6a-6b</sub> = 14 19, 1H, H<sup>6a</sup>), 4 477 (2d, *J*<sub>6b-5</sub> = 6 42 Hz), 4 357 (t, 1H, H<sup>5</sup>), 4 279 (s, 1H, H<sup>2</sup>), 4 134 (d, *J*<sub>2-3</sub> = 1 72 Hz), 3 699 (s, 1H, H<sup>3</sup>) EI-MS *m/z* 493 (M)<sup>+</sup>, 426 (M - O-C<sub>6</sub>H<sub>5</sub>)<sup>+</sup>, 268 (CH<sub>3</sub>-(CH<sub>2</sub>)<sub>15</sub>-NHCO)<sup>+</sup> Anal Calcd for C<sub>30</sub>H<sub>48</sub>N<sub>2</sub>O<sub>7</sub> · H<sub>2</sub>O C, 63 38, H, 9 65, N, 8 21 Found C, 64 16, H, 9 62, N, 8 36

**2,4;3,5-Dimethylene-N,n-hexadecyl-D-gluconamide-6-benzoate (12)** A mixture of 0 084 g (0 598 mmol) of benzoyl chloride in 10 ml of dichloromethane was added dropwise to a stirred solution of 0 200 g (0 45 mmol) of **4e** in 20 ml of dichloromethane containing 0 194 g (4 equiv) of triethyl amine as an additional base, while cooling in an ice bath After 2 hrs of stirring at RT, the solution was refluxed for an additional 2 hrs The reaction was carried out in a dried nitrogen atmosphere After washing the organic layer with water and subsequent drying, the compound was purified by crystallization from ethyl acetate, yield 0 14 g of white crystals (0 26 mmol, 56 7 %), m p 127 7 °C IR (KBr) 3284 cm<sup>-1</sup> (NH), 3072 (=C-H), 1718 (C=O, ester), 1658 (amide I), 1603 and 1585 (C=C), 1548 (amide II), <sup>1</sup>H-NMR (400 MHz, CDCl<sub>3</sub>) δ 8 042 ppm (d, 2H, ArH), 7 590 (t, 1H, ArH), 7 464 (t, 1H, ArH), 6 552 (t, 1H, NHCO), 5 276 (d, *J*<sub>7a-7b</sub> = 6 46 Hz, 1H, H<sup>7a</sup>), 5 059 (d, *J*<sub>8a-8b</sub> = 6 53 Hz, 1H, H<sup>8a</sup>), 5 002 (d, 1H, H<sup>8b</sup>), 4 833 (d, 1H, H<sup>7b</sup>), 4 721 (2d, *J*<sub>6a-5</sub> = 6 23 Hz, *J*<sub>6a-6b</sub> = -11 86, 1H, H<sup>6a</sup>), 4 563 (2d, *J*<sub>6b-5</sub> = 7 05 Hz), 4 342 (t, 1H, H<sup>5a</sup>), 4 279 (broad s, 1H, H<sup>3</sup>), 4 159 (d, *J*<sub>2-3</sub> = 1 48 Hz) EI-MS *m/z* 547 (M)<sup>+</sup>, 268 (CH<sub>3</sub>-(CH<sub>2</sub>)<sub>15</sub>-NHCO)<sup>+</sup>, 225 (M - CH<sub>3</sub>(CH<sub>2</sub>)<sub>15</sub>NHCO)<sup>+</sup>, 85 (cyclic -O-CH=CH-CH<sup>+</sup>-O-CH<sub>2</sub>) Anal Calcd for C<sub>31</sub>H<sub>49</sub>NO<sub>7</sub> C, 67 98, H, 9 02, N, 2 56 Found C, 67 79, H, 8 81, N, 2 63

#### 2,4;3,5-Dimethylene-N,n-hexadecyl-D-gluconamide-6-(3-pyridyl-carboxylate) (13)

The synthesis of this compound starting with 1 484 g (3 35 mmol) of compound **4e**, was analogous to the preparation described for **12** Instead of benzoyl chloride, 0 512 g (3 68 mmol, 1 1 equiv) of 3-pyridinecarboxylic acid chloride was used, yield 0 85 g of white crystals (1 55 mmol, 42 0 %), m p 124 6 °C IR (KBr) 3690-3200 cm<sup>-1</sup> (broad, peak at 3281, NH), 1738

(C=O, ester), 1663 (amide I), 1591 (C=C), 1549 (amide II),  $^1\text{H-NMR}$  (90 MHz,  $\text{CDCl}_3$ )  $\delta$  9.251 ppm (broad s, 1H, ArH), 8.826 (broad s, 1H, ArH, these two peaks were broadened probably due to a dimer formation in which water molecules act as hydrogen bond donors to the pyridyl groups At 2.507 ppm, a broad water molecule peak was visible which integrated to one water molecule per two pyridyl ligands), 8.326 (d, 1H, ArH), 7.450 (2d, 1H, ArH), 6.566 (t, 1H, amide H), patterns and chemical shifts of the methylene bridge and carbohydrate skeleton protons were comparable to those of **11**, 3.311 (double t, 2H,  $(\text{CH}_2)_6\text{-CH}_2\text{-NHCO}$ ), 1.513 (m, 2H,  $(\text{CH}_2)_5\text{-CH}_2\text{-CH}_2\text{NHCO}$ ), 1.263 (broad s, 10H,  $\text{CH}_3\text{-(CH}_2)_5\text{-CH}_2\text{-}$ ), 0.876 (t, 3H,  $\text{CH}_3\text{-}$ ), EI-MS  $m/z$  548 ( $\text{M}^+$ ), 519 ( $\text{M} - \text{C}_2\text{H}_5$ ) $^+$ , 268 ( $\text{CH}_3\text{-(CH}_2)_{15}\text{-NHCO}$ ) $^+$ , 106 ( $\text{COC}_5\text{H}_4\text{N}$ ) $^+$  Anal Calcd for  $\text{C}_{30}\text{H}_{48}\text{N}_2\text{O}_7$  C, 65.67, H, 8.82, N, 5.11 Found C, 65.38, H, 8.90, N, 5.08

**6-Tosyl-2,4;3,5-dimethylene-methyl-D-gluconate (14)** The reaction procedure was similar to that described for **5a**, however, instead of **4a**, 5.244 g (22.4 mmol) of **3** was used. The reaction mixture containing the product was poured into aqueous 1N HCl and extracted with EtOAc and the organic layer was subsequently dried on  $\text{MgSO}_4$ . Yield 6.24 g (pink viscous oil, 16.06 mmol, 71.7%) IR (KBr) 1758  $\text{cm}^{-1}$  (C=O), 1357 and 1178 (S=O),  $^1\text{H-NMR}$  (400 MHz,  $\text{CDCl}_3$ )  $\delta$  7.870 ppm (d, 2H, ArH), 7.350 (d, 2H, ArH), 5.266 (d,  $J_{7a,7b}$  = 6.51 Hz, 1H,  $\text{H}^{7a}$ ), 4.976 (d,  $J_{8a,8b}$  = 6.33 Hz, 1H,  $\text{H}^{8a}$ ), 4.861 (d, 1H,  $\text{H}^{8b}$ ), 4.755 (d, 1H,  $\text{H}^{7b}$ ), 4.275 (m, 3H,  $\text{H}^{5,6a,6b}$ ), 4.120 (m, 1H,  $\text{H}^{2,3}$ ), 3.840 (s, 3H,  $\text{OCH}_3$ ), 3.760 (s, 1H,  $\text{H}^4$ ), 2.480 (s, 3H,  $\text{ArCH}_3$ ) EI-MS  $m/z$  388 ( $\text{M}^+$ ), 155 ( $\text{SO}_2\text{-C}_6\text{H}_4\text{-CH}_3$ ) $^+$ , 85 (cyclic  $-\text{O-CH=CH-CH}^+-\text{O-CH}_2$ ) Anal Calcd for  $\text{C}_{16}\text{H}_{20}\text{O}_9\text{S}$  C, 49.48, H, 5.19, S, 8.26 Found C, 50.03, H, 5.19, S, 8.04

**6-Deoxy-6-(1-imidazolyl)-2,4;3,5-dimethylene-methyl-D-gluconate (15)** The synthesis was analogous to that described for **1a**, however, instead of **5a**, 5.991 g (15.4 mmol) of **14** was used and the product was only purified by column chromatography (silica, eluent  $\text{Et}_3\text{N/MeOH/EtOAc}$  1:5:94, v/v/v), yield 1.00 g (white powder, 3.53 mmol, 22.8%), mp 203 $^{\circ}\text{C}$  (decomp) IR (KBr) 3161 and 3102  $\text{cm}^{-1}$  (=C-H), 1763 (C=O)  $^1\text{H-NMR}$  (400 MHz,  $\text{CDCl}_3$ )  $\delta$  7.527 (s, 1H, N=CH-N), 7.101 (s, 1H, N-CH=CH-N), 6.992 (s, 1H, N-CH=CH-N), 5.241 (d, 1H,  $J$  = 6.58,  $\text{H}^{7a}$ ), 5.080 (d, 1H,  $J$  = 5.42,  $\text{H}^{8a}$ ), 5.030 (d, 1H,  $\text{H}^{8b}$ ), 4.728 (d, 1H,  $\text{H}^{7b}$ ), 4.330 (2d, 1H,  $J_{6a,5}$  = 5.50,  $J_{6a,6b}$  = -15.30,  $\text{H}^{6a}$ ), 4.211 (m, 1H,  $J_{6b,5}$  = 10.00,  $\text{H}^{6b}$ ), 4.180 (d, 1H,  $J_{3,4}$  = 1.00,  $\text{H}^3$ ), 4.130 (d, 1H,  $J_{2,3}$  = 2.00,  $\text{H}^2$ ), 4.219 (m, 1H,  $J_{5,4}$  = 1.20,  $\text{H}^5$ ), 3.530 (t, 1H,  $\text{H}^4$ ), EI-MS  $m/z$  283 ( $\text{M} - \text{H}$ ) $^+$ , 225 ( $\text{M} - \text{COOCH}_3$ ) $^+$ , Anal calcd for  $\text{C}_{12}\text{H}_{16}\text{N}_2\text{O}_6$  C, 50.70, H, 5.67, N, 9.85 Found C, 50.69, H, 5.67, N, 9.82

**6-Deoxy-6-(1-imidazolyl)-2,4;3,5-dimethylene-D-gluconic acid (16)** Compound **15** (0.901 g, 3.33 mmol) was dissolved in a mixture of 75 ml of dioxane/MeOH/aqueous 4N NaOH (15:4:1, v/v/v) $^{25}$  and stirred overnight. After evaporation to dryness, the yellow solid was treated with a cationic exchange resin (Biorad, AG 50 Wx8, 50-100 mesh) and liberated from the resin by treatment with aqueous 1N ammonia solution. Yield (0.88 g) was quantitative, mp 165  $^{\circ}\text{C}$  IR 1606  $\text{cm}^{-1}$  (C=O). No further analyses were carried out.

**6-Deoxy-6-(1-imidazolyl)-2,4;3,5-dimethylene-D-gluconic acid chloride (17)** Compound **16** (0.824 g, 3.05 mmol) was dissolved in 20 ml of  $\text{SOCl}_2$ , and refluxed for 90 min. The excess of thionyl chloride was removed by evaporation. The conversion was monitored by IR (1834  $\text{cm}^{-1}$ , C=O).

**1-Amino-trideca-5,7-diyne (18)** 1-Nitro-trideca-5,7-diyne (1.159 g, 6.19 mmol) which was prepared via oxidative hetero coupling $^{26}$  of 1-iodoheptyne $^{27}$  and 5-cyano-1-pentyne, $^{28}$  was dissolved in 10 ml of THF and added dropwise to a mixture of  $\text{AlH}_3$  $^{29}$  in 10 ml of THF at 0  $^{\circ}\text{C}$ . After overnight stirring at room temperature, a mixture of THF/ $\text{H}_2\text{O}$  (1/1, v/v) was added a few mins later followed by 15 ml of aqueous 1N NaOH. Both the decanted supernatant and the

remaining slurry were extracted with diethyl ether. After the collected organic layers were purified by column chromatography (silica, Et<sub>3</sub>N/MeOH/EtOAc, gradient starting with 1:5:94 up to 1:30:69 v/v), a yellow oil was obtained, yield 0.65 g (3.45 mmol, 55.8 %). IR (KBr) 3368 cm<sup>-1</sup> (very broad, NH), 2250 and 2156 (C≡C). <sup>1</sup>H-NMR (90 MHz, CDCl<sub>3</sub>), 3.20 (m, 2H, CH<sub>2</sub>-NH<sub>2</sub>), 2.18 (m, 4H, -CH<sub>2</sub>C≡C-C≡C-CH<sub>2</sub>-), 1.23 (m, 12H, CH<sub>3</sub>-(CH<sub>2</sub>)<sub>3</sub> + (CH<sub>2</sub>)<sub>2</sub>-CH<sub>2</sub>-NH<sub>2</sub>), 0.83 (t, 3H, CH<sub>3</sub>). No satisfactory mass spectrum could be obtained.

**6-Deoxy-6-(1-imidazolyl)-2,4;3,5-dimethylene-N,n-trideca-5,7-diyne-D-gluconamide**

**(19).** The acid chloride **17** (0.875 g, 3.03 mmol) was mixed with 10 ml of Et<sub>2</sub>O and CH<sub>2</sub>Cl<sub>2</sub> (1:1, v/v) and additionally diluted with 30 ml of anhydrous pyridine. To this slurry a solution of 0.65 g (3.45 mmol) of the amine **18** in 20 ml of pyridine was added dropwise. After stirring overnight at room temperature and subsequent heating at 80 °C for 1.5 hrs., the pyridine was evaporated and the remaining solid was dissolved in chloroform and washed with aqueous 0.01 N NaOH. After separation of the layers by centrifugation for 5 min at 3300 rpm, the organic layer was dried on anhydrous MgSO<sub>4</sub>. The product was purified by column chromatography (silica, Et<sub>3</sub>N/MeOH/EtOAc, 1:5:94 v/v/v) followed by recrystallization from EtOAc. A white powder was obtained, yield 0.46 g (1.04 mmol, 34.2 %), m.p. 129.8 °C. IR (KBr) 3425 cm<sup>-1</sup> (NH), 3150 and 3109 (=C-H), 2255 and 2155 (C≡C), 1687, 1675 (amide I, multiple conformations). <sup>1</sup>H-NMR (400 MHz, CDCl<sub>3</sub>), imidazole: δ 7.531 ppm (s, 1H), 7.099 (s, 1H), and 6.973 (s, 1H), carbohydrate: 5.222 (d, 1H), 5.040 (2d, 2H), 4.757 (d, 1H), 4.358 (2d, 1H), 4.219 (m, 1H), 4.211 (m, 1H), 4.189 (s, 1H), 4.145 (d, 1H), 3.548 (s, 1H) this assignment was by analogy to **6a** except for the alkyl chain protons. 3.333 (10 peaks, 2H, NHCO), 2.279 (m, 2H, C≡C-CH<sub>2</sub>-(CH<sub>2</sub>)<sub>3</sub>NHCO), 2.241 (m, 2H, CH<sub>3</sub>-(CH<sub>2</sub>)<sub>3</sub>-CH<sub>2</sub>-C≡C), 1.599 (m, 4H, C≡C-CH<sub>2</sub>-(CH<sub>2</sub>)<sub>2</sub>-CH<sub>2</sub>NHCO), 1.519 (m, 2H, CH<sub>3</sub>-(CH<sub>2</sub>)<sub>2</sub>-CH<sub>2</sub>-CH<sub>2</sub>-C≡C) 1.350 (m, 4H, CH<sub>3</sub>-(CH<sub>2</sub>)<sub>2</sub>-(CH<sub>2</sub>)<sub>2</sub>-C≡C), 0.895 (t, 3H, -CH<sub>3</sub>), <sup>13</sup>C-NMR (100 MHz, CDCl<sub>3</sub>) carbohydrate and imidazole similar to **5a**, δ 77.912 ppm (C≡C-C≡C-(CH<sub>2</sub>)<sub>3</sub>-NH), 75.062 (CH<sub>3</sub>-(CH<sub>2</sub>)<sub>4</sub>-C≡C-C≡C), 65.802 (C≡C-C≡C-(CH<sub>2</sub>)<sub>3</sub>-NH), 65.050 (CH<sub>3</sub>-(CH<sub>2</sub>)<sub>4</sub>-C≡C-C≡C), 44.748 (C<sup>6</sup>), 38.396 (-CH<sub>2</sub>-NHCO), 30.935, 28.494, 27.948, 25.356, 22095, 19.097, 18.776 (alkyl chain methylene carbons), 13.870 (CH<sub>3</sub>). EI-MS *m/z* 443 (M)<sup>+</sup>, 225 (M - C<sub>13</sub>H<sub>19</sub>-NHCO)<sup>+</sup>, 85 (cyclic -O-CH=CH-CH<sup>+</sup>-O-CH<sub>2</sub>). Anal. calcd. for C<sub>24</sub>H<sub>33</sub>N<sub>3</sub>O<sub>5</sub> · ½H<sub>2</sub>O: C, 63.70; H, 7.57; N, 9.29. Found: C, 63.70; H, 7.49; N, 9.21.

**N,n-Trideca-5,7-diyne-D-gluconamide (20).** Compound **18** (0.568 g, 3.00 mmol) was dissolved in 50 ml of methanol. To the stirred solution, 0.538 g (3.02 mmol) of 1,5-D-gluconolactone was added. After two hrs. of refluxing, the solution was cooled to RT. Crystals appeared in a few hrs., which were collected by filtration. The white crystals were stored in an argon atmosphere at -18 °C. Despite these precautions, the color changed from white to pink in a few days. Yield 0.05 g (0.14 mmol, 4.5 %, not optimized), m.p. 152.5 °C. IR (KBr) 3504 cm<sup>-1</sup> (OH<sup>2</sup>), 3377, 3344 and 3283 (OH), 1654 (amide I), 1541 (amide II). EI-MS *m/z* 369 (M)<sup>+</sup>, 218 (C<sub>13</sub>H<sub>19</sub>-NHCO)<sup>+</sup>. Anal. Calcd. for C<sub>19</sub>H<sub>31</sub>NO<sub>6</sub>: C, 61.77; H, 8.46; N, 3.79. Found: C, 61.44; H, 8.42; N, 3.82.

**6-Deoxy-6-(1-imidazolyl)-2,4;3,5-dimethylene-n-hexadecyl-D-gluconate (21).** The reaction procedure for this compound was similar to that of **19**, however, instead of the amine **18**, 1.550 g (6.39 mmol, 3.8 equiv.) of cetyl alcohol was added to 0.481 g (1.666 mmol) of **17**. Yield 0.04 g (white powder, 0.08 mmol, 5.0 %), m.p. 94.7 °C. IR (KBr) 3130 and 3112 cm<sup>-1</sup> (=C-H), 1760, 1752 (C=O, more conformations). <sup>1</sup>H-NMR (400 MHz, CDCl<sub>3</sub>) imidazole: δ 7.545 (s, 1H), 7.104 (s, 1H) and 6.996 (s, 1H) this assignment was by analogy to that of **1a**, 5.241 (d, 1H, *J* = 6.56 Hz, H<sup>7a</sup>), 5.084 (d, 1H, *J* = 5.28 Hz, H<sup>8a</sup>), 5.012 (d, 1H, H<sup>8b</sup>), 4.717 (d, 1H, H<sup>7b</sup>), 4.246 (m, 5H, H<sup>2,6a,6b</sup> + CH<sub>2</sub>OCO), 4.160 (7 peaks, 1H, H<sup>5</sup>), 3.939 (s, 1H, H<sup>3</sup>), 3.683 (m, 1H, H<sup>4</sup>), 1.771 (incorporated water), 1.675 (6 peaks, 2H, CH<sub>2</sub>-CH<sub>2</sub>-OCO), 1.256 (m, 26H, CH<sub>3</sub>-(CH<sub>2</sub>)<sub>13</sub>-), 0.880 (t, 3H, CH<sub>3</sub>). EI-MS *m/z* 494 (M)<sup>+</sup>, 479, 465, 451, 437, 409, 395, 381, 367, 353, 339, 325

(respectively  $M - (CH_2)_n - CH_3)^+$ , 225 ( $M - C_{16}H_{33} - OCO)^+$ . Anal. Calcd. for  $C_{27}H_{46}N_2O_6$ : C, 65.56; H, 9.57; N, 5.66 Found: C, 66.12; H, 9.58; N, 5.06.

***N,n*-Hexadecyl-6-hydroxy-*n*-hexanoic acid amide (22).** *n*-Hexadecylamine (5.733 g, 23.74 mmol) was mixed with 2.860 g (25.06 mmol) of caprolactone and heated without solvent at 100 °C. After stirring at 100 °C for 2 hrs. in a nitrogen atmosphere, the mixture was cooled and subsequently recrystallized from EtOAc. Recrystallization was repeated for 7 times in order to obtain a pure white crystalline powder, yield n.d., m.p. 92.6 °C. IR (KBr) 3312  $cm^{-1}$  (sharp, NH), 3183 (broad, OH), 1633 (amide I), 1541 (amide II), IR ( $CHCl_3$ ) 3630 (sharp, NH), 3449 (sharp, OH), 1662 (amide I), 1517 (amide II).  $^1H$ -NMR (400 MHz,  $CDCl_3$ )  $\delta$  5.854 ppm (NHCO), 3.631 (t, 2H,  $-CH_2OH$ ), 3.217 (double t, 2H,  $-CH_2NHCO$ ), 2.551 (broad s, 1H,  $-OH$ ), 2.178 (t, 2H,  $(CO)CH_2$ ),  $^{13}C$ -NMR (400 MHz,  $CDCl_3$ )  $\delta$  173.076 ppm (C=O), 62.259 ( $CH_2OH$ ), 39.484 ( $CH_2NH$ ). EI-MS  $m/z$  355 ( $M^+$ ), 337 ( $M - H_2O^+$ ), 268 ( $C_{16}H_{33}NHCO^+$ ). Anal. Calcd. for  $C_{22}H_{45}NO_2 \cdot \frac{1}{2}H_2O$ : C, 74.31; H, 12.75; N, 3.94. Found: C, 73.76; H, 12.48; N, 4.01.

***N,n*-Hexadecyl-6-tosyl-*n*-hexanoic acid amide (23).** Tosylation was carried out using a standard procedure, *eg* as was used for the preparation of **5a**. Instead of pyridine, dichloromethane was used as the solvent for the hydroxyl compound and KOH was added as an additional base. Yield 0.41 g (0.80 mmol, 45 %). IR (KBr) 3326  $cm^{-1}$  (NH), 1644 (amide I), 1533 (amide II), 1363 and 1174 (S=O). Despite a slight contamination with compound **22**, the product was not further purified and used for the synthesis of **24**.

***N,n*-Hexadecyl-6-(1-imidazolyl)-*n*-hexanoic acid amide (24).** This product was synthesized following the procedure described for **1a**. Instead of **5a**, 0.392 g (0.77 mmol) of **23** was used which was dissolved in 4.5 ml of  $CHCl_3$ . The product was purified as was described for **1a**, without recrystallization. Yield 0.05 g (0.12 mmol, 16.1 %), m.p. 65.9 °C IR (KBr) 3317  $cm^{-1}$  (sharp, NH), 3101 and 3047 (=C-H), 1637 (amide I), 1536 (amide II).  $^1H$ -NMR (90 MHz,  $CDCl_3$ )  $\delta$  7.460 ppm (s, 1H, N=CH-N), 7.057 (s, 1H, N=CH-CH-N), 6.911 (s, 1H, N=CH-CH-N), 5.382 (very broad t, 1H, NHCO), 3.927 (t, 2H,  $-CH_2-N=$ ), 3.232 (q, 2H,  $CH_2-(C=O)$ ), 2.139 (t, 2H,  $-CH_2-C=O$ ), 1.935 (t, 2H,  $-CH_2-CH_2-N=$ ), 1.691 (crystal water), 1.240 (m, 32H,  $-(CH_2)_{14}$ - and  $O=C-CH_2-(CH_2)_2-$ ), 0.889 (t, 3H,  $CH_3$ ). EI-MS  $m/z$  405 ( $M^+$ ), 165 ( $CO-(CH_2)_5-N_2C_3H_3^+$ ), 137 ( $-(CH_2)_5-N_2C_3H_3^+$ ), 95 ( $CH_2-CH_2-N_2C_3H_3^+$ ). Anal. Calcd. for  $C_{25}H_{47}N_3O \cdot \frac{1}{2}H_2O$ : C, 72.25; H, 11.68; N, 10.36. Found: C, 72.41; H, 11.67; N, 10.13.

**1-*n*-Hexadecylimidazole (25).** Cetyl alcohol was converted into *n*-hexadecyl tosylate following a standard tosylation procedure (see for instance the synthesis of **23**). The tosylate (1.980 g, 4.99 mmol) was added to a solution of sodium imidazolate in 10 ml of DMF (4.96 mmol) which had been freshly prepared prior to this reaction by treating imidazole with 1 equiv. NaH<sup>\*</sup> in DMF. After a few hrs. stirring at room temperature followed by overnight reaction at 50 °C, a white precipitate (NaOTs) was formed which was removed by filtration. The filtrate was concentrated by evaporation before it was poured into a mixture of ice and saturated  $NaHCO_3$  solution. The product was extracted with dichloromethane and further purified by column chromatography (silica, eluent  $Et_3N/EtOAc$  1:99, v/v). The yellow product was dissolved in dichloromethane and washed with saturated  $NaHCO_3$ , yield 0.38 g of white powder (1.28 mmol, 25.8 %), m.p. 35.8 °C. IR (KBr) 3108  $cm^{-1}$  (=C-H), 2924 and 2853 ( $CH_2$ ), 1718 and 1684 (C=N), 1507 and 1467 (aromate),  $^1H$ -NMR (90 MHz,  $CDCl_3$ )  $\delta$  7.453 ppm (broad s, 1H, N=CH-N- $CH_2$ -), 7.053 (broad s, 1H, N-CH=CH-N- $CH_2$ ), 6.898 (s, 1H, N-CH=CH-N- $CH_2$ ), 3.917 (t, 2H,  $-(CH_2)_{14}-H_2-N$ ), 1.794 (t, 2H,  $-(CH_2)_{13}-CH_2-CH_2-N$ ), 1.254 (broad s, 26H,  $-CH_2-(CH_2)_{13}-CH_2-$ ), 0.880 (t, 3H,  $-CH_3$ ). EI-MS  $m/z$  292 ( $M^+$ ), 277, 263, 249, 235, 221, 207, 193,

\* The NaH was washed with *n*-hexane before use in order to remove the mineral oil in which it is dispersed



179, 165, 151, 137, 123, 109, (M-(CH<sub>2</sub>)<sub>n</sub>-CH<sub>3</sub>, n= 0-12 respectively)<sup>+</sup> Anal Calcd for C<sub>19</sub>H<sub>36</sub>N<sub>2</sub> C, 78.02, H 12.04, N, 9.58 Found C, 78.17, H, 11.90, N, 9.39

### 3.2.2 Metal complexes

**[(1a)<sub>4</sub>Cu][OSO<sub>2</sub>CF<sub>3</sub>]<sub>2</sub> ((1a)<sub>4</sub>Cu)** To a stirred solution of 65.5 mg (0.172 mmol) of **1a** in 0.5 ml of EtOH, 0.043 mmol of [Cu][OSO<sub>2</sub>CF<sub>3</sub>]<sub>2</sub> dissolved in 50 µl EtOH was added. After 30 min, a purple precipitate appeared from the dark blue solution. Unfortunately the oil-like precipitate could not be isolated by filtration. The product was isolated by evaporation of the dispersion to dryness, m.p. 105.8 °C, IR (KBr) 3132 cm<sup>-1</sup> (=C-H), 639 (Cu-N<sub>im</sub>). Elemental analysis failed due to the presence of the triflate anions, however, an indication for the presence of a copper complex with 4 imidazole ligands was the λ<sub>max</sub> observed in the UV-vis spectrum, λ<sub>max</sub> = 595.1 nm (CHCl<sub>3</sub>/MeOH). The loss of weight upon heating was determined in order to estimate the amount of solvent molecules precipitated with the copper salts. After a weight loss of 1.26 %, which equals the evaporation of approx. one molecule of water per complex, the weight was stable from 68 °C up to 150 °C (theoretically 0.95 %).

**[(1b)<sub>4</sub>Cu][OSO<sub>2</sub>CF<sub>3</sub>]<sub>2</sub> ((1b)<sub>4</sub>Cu)** Copper triflate (0.025 mmol) dissolved in 30 µl of EtOH was added to 41.1 mg (0.100 mmol) of **1b** which was dissolved in 0.5 ml of EtOH. A precipitate from the dark blue solution was formed overnight leaving a colorless supernatant. The purple precipitate could be isolated by filtration, yield 77 %, m.p. 130.6 °C IR (KBr) 3132 cm<sup>-1</sup> (=C-H), 638 (Cu-N<sub>im</sub>), UV-vis λ<sub>max</sub> = 610.8 nm (CHCl<sub>3</sub>/MeOH 1:3 (v/v)), loss of weight 2.64 % which is ca. 1 molecule of EtOH per complex (theoretically 2.25 %).

**[(1c)<sub>4</sub>Cu][OSO<sub>2</sub>CF<sub>3</sub>]<sub>2</sub> ((1c)<sub>4</sub>Cu)** Copper triflate (0.028 mmol) was dissolved in 36 µl of EtOH and added to 49.1 mg (0.112 mmol) of **1c** which was dissolved in 0.5 ml of EtOH. A purple precipitate was formed after 15 min, yield 78 %, m.p. 130.5 °C IR (KBr) 3134 cm<sup>-1</sup> (=C-H), 638 (Cu-N<sub>im</sub>), UV-vis λ<sub>max</sub> = 611.4 nm (CHCl<sub>3</sub>/MeOH 1:3 (v/v)), loss of weight 2.43 % which corresponds to 1 molecule of EtOH per complex (theoretically 2.13 %).

**[(1d)<sub>4</sub>Cu][OSO<sub>2</sub>CF<sub>3</sub>]<sub>2</sub> ((1d)<sub>4</sub>Cu)** Copper triflate (0.022 mmol) was dissolved in 24 µl of EtOH and added to 39.5 mg (0.087 mmol) of **1d** which was dissolved in 0.5 ml of EtOH. A purple precipitate was formed overnight, yield 95 %, m.p. 134.6 °C IR (KBr) 3135 cm<sup>-1</sup> (=C-H), 638 (Cu-N<sub>im</sub>), UV-vis λ<sub>max</sub> = 611.1 nm (CHCl<sub>3</sub>/MeOH 1:3 (v/v)), loss of weight 2.82 % which corresponds to 1 molecule of EtOH and 1 molecule of water per complex (theoretically 2.83 %).

**[(1e)<sub>4</sub>Cu][OSO<sub>2</sub>CF<sub>3</sub>]<sub>2</sub> ((1e)<sub>4</sub>Cu)** Copper triflate (0.037 mmol) was dissolved in 47 µl of EtOH and added to 73.2 mg (0.148 mmol) of **1e** which was dissolved in 1.5 ml of EtOH. A purple precipitate was formed after 10 min, yield 90 %, m.p. 127.1 °C IR (KBr) 3135 cm<sup>-1</sup> (=C-H), 638 (Cu-N<sub>im</sub>), UV-vis λ<sub>max</sub> = 610.8 nm (CHCl<sub>3</sub>/MeOH 1:3 (v/v)), loss of weight 2.52 % which corresponds to 1 molecule of EtOH and 1 molecule of water per complex (theoretically 2.70 %).

**[(1f)<sub>4</sub>Cu][OSO<sub>2</sub>CF<sub>3</sub>]<sub>2</sub> ((1f)<sub>4</sub>Cu)** Copper triflate (0.012 mmol) was dissolved in 15 µl of EtOH and added to 24.4 mg (0.047 mmol) of **1f** which was dissolved in 1.3 ml of EtOH. A purple precipitate was formed immediately, yield 90 %, m.p. 125.9 °C IR (KBr) 3135 cm<sup>-1</sup> (=C-H), 638 (Cu-N<sub>im</sub>), UV-vis λ<sub>max</sub> = 611.9 nm (CHCl<sub>3</sub>/MeOH 1:3 (v/v)), no loss of weight was determined.

**[(9)<sub>4</sub>Cu][OSO<sub>2</sub>CF<sub>3</sub>]<sub>2</sub> ((9)<sub>4</sub>Cu)** Copper triflate (0.006 mmol) was dissolved in 1.1 ml of EtOH and added to 12.1 mg (0.023 mmol) of **9** which was dissolved in 0.2 ml of EtOH. A green blue solution was obtained from which the purple product precipitated, yield n.d. No further analytical data are available.

**[(19)<sub>4</sub>Cu][OSO<sub>2</sub>CF<sub>3</sub>]<sub>2</sub> ((19)<sub>4</sub>Cu)** Copper triflate (0.043 mmol) was dissolved in 0.5 ml of EtOH and added to 76.0 mg (0.171 mmol) of **19** which was dissolved in 2 ml of EtOH. The reaction was carried out in a nitrogen atmosphere. No precipitate was formed, and the dark blue solution was therefore evaporated to dryness, UV-vis  $\lambda_{\text{max}}$  = 611.6 nm (CHCl<sub>3</sub>/MeOH 1:3 (v/v))

**[(24)<sub>4</sub>Cu][OSO<sub>2</sub>CF<sub>3</sub>]<sub>2</sub> ((24)<sub>4</sub>Cu)** Upon addition of 0.006 mmol of copper triflate (which was dissolved in 0.4 ml of EtOH) to 9.7 mg (0.024 mmol) of **24** dissolved in 0.5 ml of EtOH, a dark blue solution was obtained. No precipitate was formed and the solution was evaporated to dryness, UV-vis  $\lambda_{\text{max}}$  = 601.9 nm (CHCl<sub>3</sub>/MeOH 1:3 (v/v))

**[(25)<sub>4</sub>Cu][OSO<sub>2</sub>CF<sub>3</sub>]<sub>2</sub> ((25)<sub>4</sub>Cu)** Copper triflate (0.021 mmol) was dissolved in 1 ml of EtOH and added to 24.1 mg (0.084 mmol) of **25** which was dissolved in 0.5 ml of EtOH. After several min a purple precipitate was formed from the dark blue solution leaving a colorless supernatant, yield n.d., UV-vis  $\lambda_{\text{max}}$  = 594.3 nm (CHCl<sub>3</sub>/MeOH 1:3 (v/v))

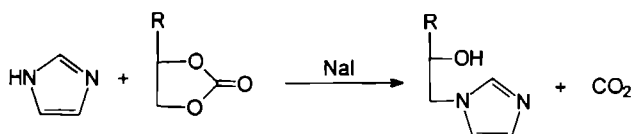
**[(1e)<sub>4</sub>Ni][BF<sub>4</sub>]<sub>2</sub> ((1e)<sub>4</sub>Ni)** A similar procedure was followed as for **(1b)<sub>4</sub>Cu**. 0.0035 mmol of NiBF<sub>4</sub> dissolved in 55  $\mu$ l of EtOH, was added to 10.5 mg (0.0213 mmol) of **1e** which was dissolved in 0.5 ml of EtOH. A pale green precipitate was formed after 15 min, yield n.d. No further analytical data are available.

### 3.3 Results and discussion

#### 3.3.1 Synthesis of imidazole ligand

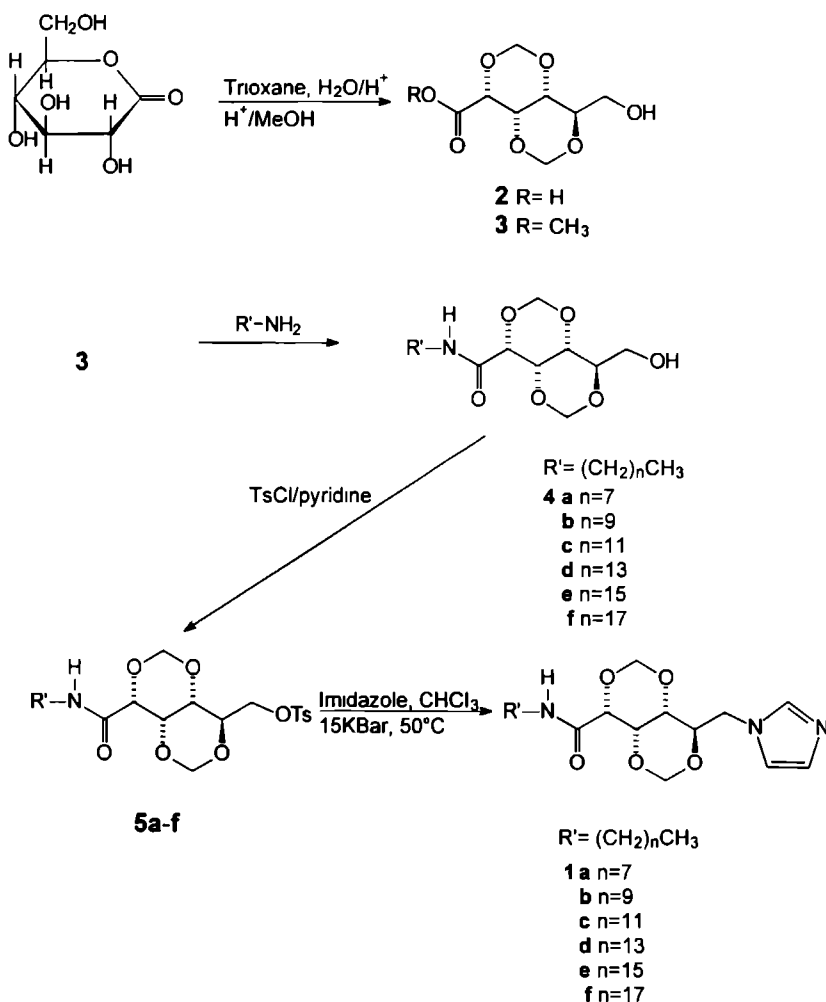
If one wants to replace one of the hydroxyl groups in a glucose molecule by a tosyl group and subsequently by an imidazole group, it is nearly always necessary to protect the other hydroxyl groups from reaction. One of the standard protecting groups is the acetate group which, however, causes problems because of its instability towards bases. The nucleophilic substitution of the tosyl function by the imidazole group can only proceed under basic conditions, and results in removal of one of the acetate groups and the formation of products with 5 or 6 membered rings. Another option is the use of an isopropylidene or acetone clamp, which is known to be stable towards base. As it was our intention to make gluconic acid derivatives with a metal binding ligand at the end of the carbohydrate chain, *viz.* at carbon atom C<sup>6</sup>, and isopropylidene only forms 5 membered rings blocking the OH functions at carbon atoms 2,3 and 5,6, leaving only the OH at carbon atom 4 open for reaction, this protecting group could not be used. A third possibility is to use the benzylidene group,<sup>30</sup> which only blocks 2 of the 5 hydroxyl groups (*viz.* the OH's at carbon atoms 4 and 5). Since in that case the molecule still contains more than one free hydroxyl group, we searched for an alternative route to synthesize the target compounds **1**. This was found in a ring opening reaction of the cyclic carbonate (shown in Scheme 3.1)<sup>31,32</sup>

Scheme 3.1



Although the starting compound *N*-*n*-octyl-2,4-benzylidene-5,6-carbonate-D-gluconamide could easily be obtained, and in a test reaction the carbonate ring of ethylene carbonate could be opened with imidazole yielding 2-(1-imidazolyl)ethanol (see Chapter 4), the desired ring opening of the gluconamide was not achieved. As the last alternative for the protection of the secondary hydroxyl groups we considered methylene bridges at carbon atoms C<sup>2</sup>,C<sup>4</sup> and C<sup>3</sup>,C<sup>5</sup>.<sup>22,23</sup> The advantage of this procedure is that all the secondary hydroxyl groups are now protected with base stable groups and that the primary hydroxyl group is still open for reaction. The big disadvantage is that it is very hard to remove the methylene groups, which can be only achieved partly using strongly acidic conditions (removal of the 3,5 methylene bridge), viz. glacial acetic acid and trifluoroacetic anhydride.<sup>33</sup>

Scheme 3.2



These strong acidic conditions can lead to hydrolysis of the amide bond. The reagent boron trichloride, which is subsequently needed to remove the 2,4 methylene bridge, may react with the imidazole group.

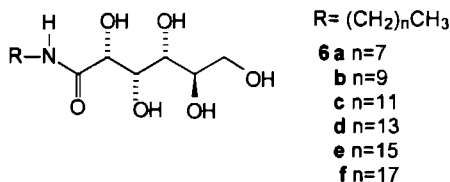
Despite the above mentioned disadvantages we decided to use the methylene protecting group and compounds **1** were synthesized, as shown in Scheme 3.2.

The unprotected hydroxyl group of **4a-f** was tosylated using a standard procedure to give **5a-5f** (Scheme 3.2) and the introduction of the imidazole group was attempted in DMF using a large excess of imidazole (see Chapter 5). This reaction, however, gave a large amount of unwanted side products, *e.g.* 6-deoxy-6,5-didehydro-2,4;3,5-dimethylene-*N,n*-octyl-D-gluconamide (55 %), as the result of an elimination reaction. Enhancing the nucleophilicity of the imidazole by converting it into the corresponding anion did not result in the desired product, probably because this anion reacted with the reactive amide hydrogen, present in **5**.

The elimination could be successfully suppressed when the reaction was carried out under high pressure (15 kBar) at 50 °C. In addition, a higher yield of compounds **1** was obtained (66 % instead of 35 % at normal pressure). We did not remove the protecting groups of **1** because these compounds as such already displayed interesting properties, which are described below and in Chapters 4 and 7.

### 3.3.2 Effect of the length of the alkyl chain on the L.C. behavior of compounds **1** and model compounds

Carbohydrates are excellent building blocks for thermotropic liquid crystalline materials if they are designed keeping in mind the following limitations<sup>34</sup> (i) they must have an *n*-alkyl chain of at least 6 carbon atoms attached to the carbohydrate framework, (ii) they may be cyclic or acyclic but must in most cases contain a number of unprotected hydroxyl functions and (iii) the terminus of the *n*-alkyl chain should not be substituted with polar functional groups such as -OH, -Cl and -C≡N. The model *n*-alkyl gluconamides **6a-f**, meet all these conditions and indeed showed L.C. behavior (see Figure 3.1).



Besides the melting point (m.p.) and the clearing point (c.p.), which is the transition from the L.C. phase to the isotropic (I) phase, additional crystal to crystal ( $K_1 \rightarrow K_2$ ) transitions were observed. The L.C. phases of **6a-f** can be assigned to be smectic A<sub>d</sub> (S<sub>A<sub>d</sub></sub>) on the basis of polarization microscopy studies, which is in agreement with the packing suggested in the literature for the octyl derivative (**6a**).<sup>35</sup> As can be seen in Figure 3.1, the melting points are almost invariant in the

series **6a-f**, whereas the clearing points become higher by elongation of the alkyl chain, which results in a stabilization of the L.C. phases. The rise of the c.p. is most clearly visible for the shorter chain derivatives.<sup>35</sup> Compounds **6** were found to gradually decompose on standing at  $\pm 190^\circ\text{C}$ .

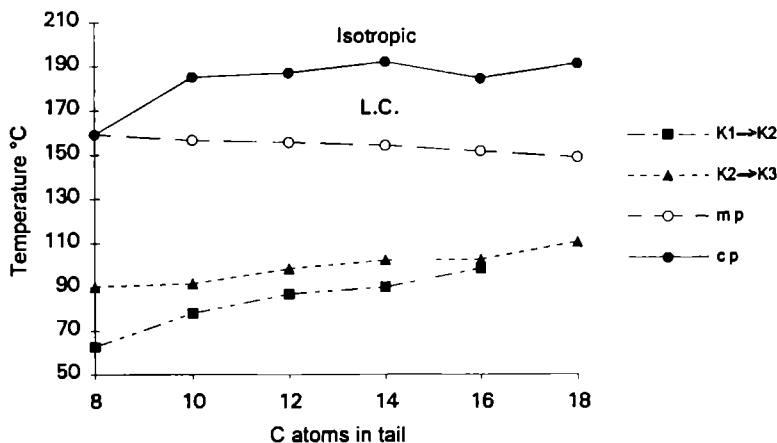


Figure 3.1 Phase transition temperatures of *N*-*n*-alkyl-D-gluconamides

In the literature<sup>34,35</sup> a qualitative model has been proposed for the structural variations that occur when a *N*-alkylgluconamide is heated from the solid phase to the L.C. phase. It is suggested that in the L.C. phase the weaker Van der Waals interactions are broken while the stronger hydrogen bonds remain intact. The latter are only disconnected when the isotropic phase is entered. This theory does not explain why in our case not the melting point but the clearing point is dependent on the length of the alkyl chain. The melting enthalpies of compounds **6** are virtually independent of the length of the alkyl chains (see Table 3.1), which suggests that at the melting points not "the alkyl chains are melting" but the hydrogen bonding scheme of the carbohydrate moiety is changing. Due to partial overlap of peaks, the enthalpy values of the crystal to crystal transitions  $K_1 \rightarrow K_2$  and  $K_2 \rightarrow K_3$  could not be determined accurately which makes that no conclusions can be drawn with regard to the structural variations that take place at these transitions. According to Jeffrey,<sup>36</sup> who studied the packing of *N*,*n*-undecyl-D-gluconamide at different temperatures by powder diffraction, in the first transition a monolayered structure is transformed into a bilayered structure, which would be in agreement with our findings that the temperature of the transition  $K_1 \rightarrow K_2$  is dependent on the length of the alkyl chain. The transition  $K_2 \rightarrow K_3$  is also dependent on the length of the alkyl chain, which suggests another transition involving the alkyl chains.

The type of molecular packing in the L.C.-phase of *N*,*n*-alkyl-D-gluconamides has been intensively discussed in the literature. Baeyens-Volant *et al*<sup>37</sup> have proposed that these

compounds form a monolayered, head to tail packed smectic phase on the bases of the crystal structures of these compounds. On the other hand Pfannemüller *et al.*<sup>35</sup> have reported that *N,n*-alkyl-D-gluconamides exhibit liquid crystalline phases which are miscible with the  $S_{Ad}$  phases of the *n*-alkyl-1-O- $\beta$ -D-glucopyranosides, showing that the packing of the *n*-alkyl-gluconamides and *n*-alkyl-glucopyranosides in the L.C. phase is similar. This has led them to propose a model for the packing of the *n*-alkyl-gluconamide molecules in the L.C. phase (see Figure 3.2).<sup>35,38</sup> This model was supported by data published by Jeffrey *et al.*<sup>36</sup> on the d-spacings of *N,n*-undecyl-D-gluconamide.

**Table 3.1** Thermotropic behavior of *N,n*-alkyl-D-gluconamides<sup>a</sup>

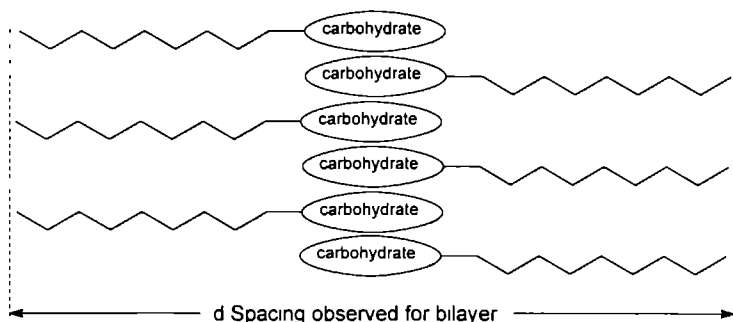
Compound	n <sup>b</sup>	K <sub>1</sub> →K <sub>2</sub> (°C)	K <sub>2</sub> →K <sub>3</sub> (°C)	m p <sup>c</sup> (°C)	c p (°C)
<b>6a</b>	8	62.8	90.3	159.2 (47.2)	140.2 <sup>d</sup>
<b>6b</b>	10	78.1	91.6	156.5 (47.0)	184.9
<b>6c</b>	12	86.7	98.4	155.5 (49.3)	186.7
<b>6d</b>	14	90.0	102.2	154.0 (45.7)	191.8
<b>6e</b>	16	98.5	102.6	151.4 (53.3)	184.3
<b>6f</b>	18	--	110.4	148.5 (50.6)	191.0

<sup>a</sup> Determined from heating runs

<sup>b</sup> Number of carbon atoms in alkyl chain of **6**

<sup>c</sup>  $\Delta H_{\text{melt}}$  (kJ mol<sup>-1</sup>) in parentheses

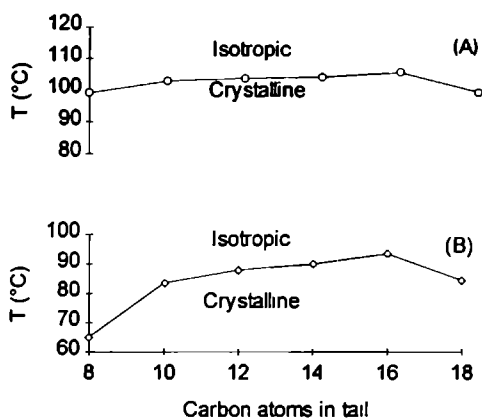
<sup>d</sup> Value obtained upon cooling



**Figure 3.2** Model proposed for  $S_{Ad}$  phase by Pfannemüller<sup>35</sup>

On basis of the molecular requirements formulated by Jeffrey,<sup>34</sup> the methylene protected compounds **4a-f** should show L.C.-behavior. Gluconamides **4a-e**, however, did not show any L.C.-behavior, which is probably due to the fact that these compounds have only one hydroxyl group available for forming hydrogen bonds. Remarkable is the independence of the melting points on the length of the alkyl chain (see Figure 3.3A, and Table 3.2), which suggests that the molecular packing in compounds **4** is similar for the entire series. Compound **4f** did show an enantiotropic L.C. phase (m.p. 99.4 °C) of unknown type (not  $S_A$ ). All compounds crystallized

upon cooling. The solidification points (s.p's) are shown in Figure 3.3B and are summarized in Table 3.2. Surprisingly no trend in the  $\Delta H_{\text{melt}}$  values could be observed (neither in the case of the first heating runs nor in the second heating runs). The  $\Delta H_{\text{solid}}$  values of the crystallizations, however, increased upon elongation of the alkyl chain, which suggests that solidification is dominated by the packing of the alkyl chains and not by the carbohydrate moieties. This was emphasized by the fact that the  $\Delta H_{\text{solid}}$  value of the hexadecyl gluconamide **4e** was almost twice the value of the  $\Delta H_{\text{solid}}$  value of the octyl gluconamide **4a**.



**Figure 3.3** Thermotropic behavior of compounds **4a-f**

A) Melting points, B) solidification points

**Table 3.2** Thermotropic behavior of 2,4,3,5 dimethylene-D-gluconamides (**4**)<sup>a</sup>

Compound	n <sup>b</sup>	m p <sup>c</sup> (°C)	s p <sup>d</sup> (°C)
<b>4a</b>	8	99.1 (33.7)	65.1 (-15.6)
<b>4b</b>	10	102.8 (20.8)	83.6 (-21.5)
<b>4c</b>	12	103.6 (40.5)	88.0 (-24.6)
<b>4d</b>	14	104.0 (27.8)	90.0 (-26.8)
<b>4e</b>	16	105.5 (39.8)	93.5 (-28.3)
<b>4f</b>	18	99.4 (30.8)	84.5 (-20.1)

<sup>a</sup> Data obtained from DSC thermograms

<sup>b</sup> Number of carbon atoms in the alkyl chains of **4**

<sup>c</sup> Melting point obtained from second heating run, melting enthalpy

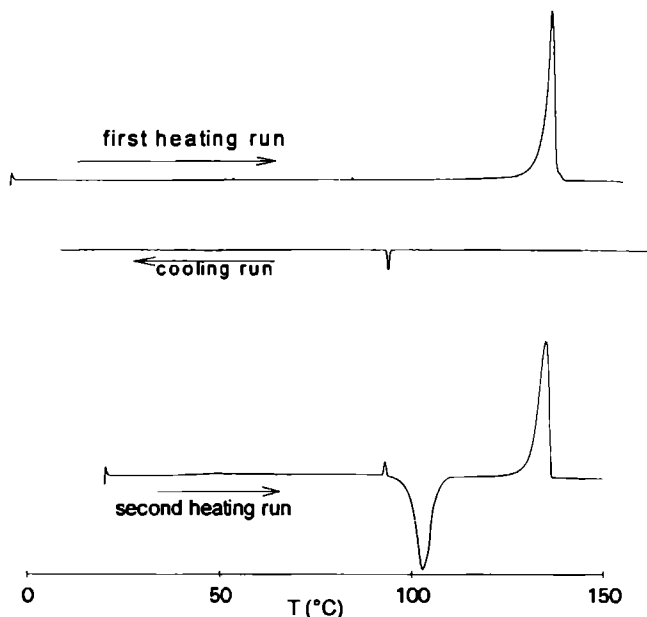
$\Delta H_{\text{melt}}$  (kJ/mol) in parentheses

<sup>d</sup> Solidification point obtained from first cooling run, enthalpy upon solidification

$\Delta H_{\text{solid}}$  (kJ/mol) in parentheses

Gluconamides **1** were crystalline at room temperature and to our surprise some of them showed monotropic<sup>39</sup> L.C. behavior upon cooling from the melt. A remarkable feature was the

hysteresis displayed by these compounds: on cooling the L.C. phase was transformed into a glassy state rather than in a crystalline state. Some of them crystallized at a later time, a nice example being compound **1d** which was heated from the glassy state in the second heating and was found to crystallize just above the c.p. (see Figure 3.4). The mobility of the molecules in the L.C. phase is too low to allow them to rearrange for crystallization. Apparently when the isotropic phase is entered (for **1d** in the second heating run at 93.6 °C), this mobility is acquired and crystallization can occur.



**Figure 3.4** DSC thermogram of compound **1d**.

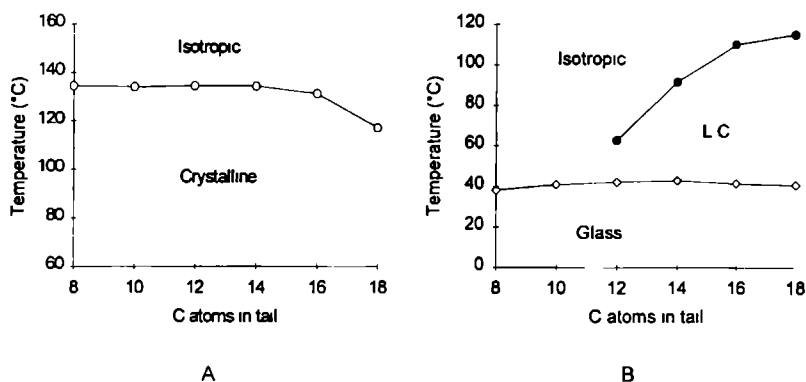
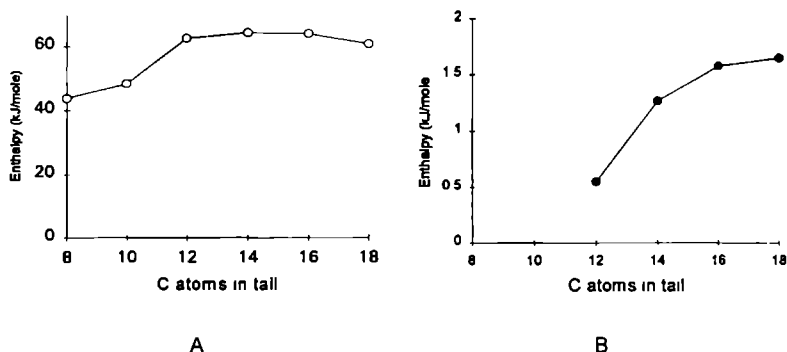
As in the case of the *N,n*-alkyl-D-gluconamides (Table 3.1), the melting points of the series of compounds **1** (except **1f**) are independent on the length of the alkyl chain just as the glass transition temperatures ( $T_g$ 's) are, whereas the clearing points are raised by elongation of the aliphatic chain (see Table 3.3 and Figures 3.5A,B). A possible explanation for the failure of compounds **1a** and **1b** to form L.C. phases is that the system is frozen in a glassy state before the L.C. phase is entered. This can be concluded from the fact that the  $T_g$  line intersects with the c.p. line if the latter is extrapolated to the decyl and octyl derivatives (Figure 3.5B).

The  $\Delta H_{\text{melt}}$  of the compounds that are liquid crystalline (**1c-f**) is not dependent on the length of the alkyl chain. For compounds **1a** and **1b** a slightly lower  $\Delta H_{\text{melt}}$  is observed than for **1c-f** (Figure 3.6A). As can be seen in Figure 3.6B  $\Delta H_{\text{clearing}}$  increases when the number of carbon atoms in compounds **1** is increased.



**Table 3.3** Thermotropic behavior of imidazolyl compounds (**1**)<sup>a</sup>

Compound	n <sup>b</sup>	m p <sup>c</sup> (°C)	c p <sup>d</sup> (°C)	T <sub>g</sub> <sup>e</sup> (°C)
<b>1a</b>	8	134.5 (43.8)	---	38.1
<b>1b</b>	10	134.0 (48.4)	---	40.9
<b>1c</b>	12	134.3 (62.7)	62.7 (-0.55)	42.1
<b>1d</b>	14	134.2 (64.5)	91.6 (-1.27)	42.9
<b>1e</b>	16	131.1 (64.2)	110.0 (-1.58)	41.4
<b>1f</b>	18	117.0 (61.0)	115.0 (-1.65)	40.6

<sup>a</sup> Data obtained from DSC thermograms<sup>b</sup> Number of carbon atoms in the alkyl chains of **1**<sup>c</sup> Melting point obtained from first heating run, melting enthalpy $\Delta H_{\text{melt}}$  (kJ/mole) in parentheses<sup>d</sup> c p obtained from cooling run,  $\Delta H$  clearing (kJ/mol) in parentheses<sup>e</sup> T<sub>g</sub> obtained from cooling run**Figure 3.5** Thermotropic behavior of imidazolyl compounds **1a-f** A) Heating B) Cooling**Figure 3.6** A)  $\Delta H_{\text{melt}}$  and B)  $\Delta H_{\text{clearing}}$  of compounds **1a-f**

### 3.3.3 Characterization of the L.C. phases of compounds 1

According to the textures observed by polarization microscopy, compounds **1c-f** showed  $S_A$  phases. For **1d** this was confirmed by small angle X-ray scattering (SAXS), yielding a d-spacing of the layers of 35.7 Å. Inspection of CPK models revealed that this value is consistent with the presence of interdigitized layers (cf. the model displayed in Figure 3.7) of molecules, which are bent at  $C^2$  with an angle of  $110^\circ$  (cf. crystal structure described below). In both the liquid crystalline state and the isotropic state, broad matching peaks were found at 4.6 Å. The resemblance of these peaks indicates that in both cases the packing of the alkyl chains<sup>19</sup> is not very tight, meaning that, in the smectic phase the alkyl chains are rather disordered.

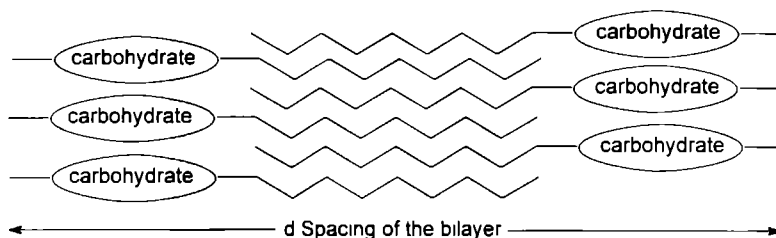
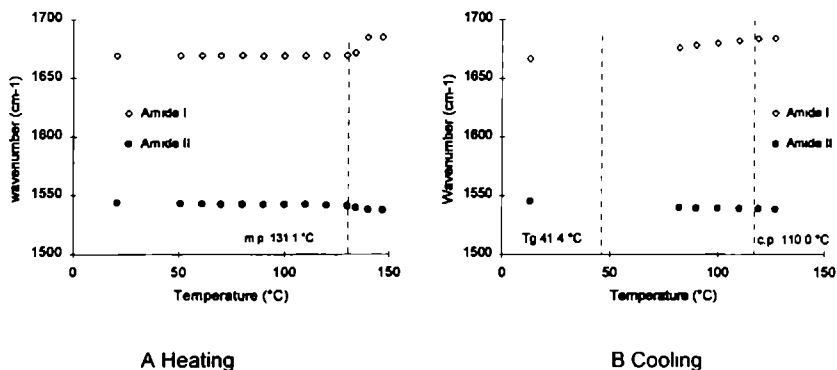


Figure 3.7  $S_A$  phase of compounds 1

In order to further investigate the physical state of the alkyl chains in the L.C. state we performed cross polarization magic angle spinning (CPMAS)  $^{13}\text{C}$ -NMR experiments<sup>40</sup>. With the CPMAS technique it is possible to examine the physical state of molecules or parts of molecules. Unfortunately, the  $S_A$  phases of **1** are monotropic and therefore metastable in the L.C. state. The sample of the compound (**1e**) on which the experiments were carried out crystallized during the measurement, probably because of the rod-like molecules became oriented by the high spinning rates (4500 Hz). The solid state  $^{13}\text{C}$ -NMR and the solution spectrum in  $\text{CDCl}_3$  of **1e** were quite similar although in the solid state the chemical shifts of the imidazole carbon atoms ( $\Delta\delta$  +1.89, -3.22 and +3.87 ppm) and those of the alkyl chains ( $\Delta\delta$  -3.66 ppm) deviated more than average from the shifts of the other carbon atoms (1.22 ppm). This suggests that the imidazole groups interact with each other and that the alkyl chains are closely packed in the solid (crystalline) state.

In order to investigate the existence of hydrogen bonding in the L.C. state, IR-spectroscopy at elevated temperatures<sup>41</sup> was carried out on **1e**. Four different phases were examined: the isotropic phase, the liquid crystalline phase, the crystalline phase and the glass state. The monitored absorptions were the NH stretching, C=O stretching (amide I) and NH bending (amide II) modes. The amide I band showed a shift to a higher wavenumber upon melting (*viz.* from 1669 to 1684  $\text{cm}^{-1}$ ), which is interpreted as being due to a strengthening of the C=O bond (Figure 3.8). This suggests that intermolecular hydrogen bonds are broken when **1e** is melted. The amide II band showed a small shift to a lower value (from 1544 to 1538  $\text{cm}^{-1}$ ). This means that less energy is needed to bend the NH function. The NH vibration at 3343  $\text{cm}^{-1}$  decreased upon melting, while a peak of the non hydrogen bonded NH (at 3435  $\text{cm}^{-1}$ ) came up.

The transition from the isotropic to the L.C. phase (110 °C, see Figure 3.7B) did not have a large effect on the amide I and amide II bands (at 1681 and 1539  $\text{cm}^{-1}$ , respectively) while the shoulder due to the hydrogen bonded NH function (still present in the melted compound) only slightly increased. Further cooling below the glassy state (41.4 °C) resulted in values for the NH vibrations as found in the solid state (3344, with a shoulder at 3472, amide I at 1668 and amide II at 1546  $\text{cm}^{-1}$ ).



**Figure 3.8** IR absorptions observed on heating compound 1e

The absence of shifts observed upon entering the L.C. phase indicates that in this phase no *inter*-molecular hydrogen bonds are present, whereas they do exist in the glassy state. Although the possibility of local crystallization during cooling is always present when dealing with monotropic L.C. phases, it is very unlikely that this had happened in our sample during the measurements because the IR peaks of the alkyl chains in the L.C. and glassy state were broader than in the original crystalline sample, indicating that the packing in the glass was not as regular as in the crystal.<sup>19</sup> The imidazole peaks at 3140 and 3097  $\text{cm}^{-1}$ , which are very sharp in the crystal, fused to one broader peak in the melt (3111  $\text{cm}^{-1}$ ) and in the L.C. phase (3110  $\text{cm}^{-1}$ ), but were separated in the glassy state (3140 and 3102  $\text{cm}^{-1}$ ). This probably means that the imidazole group cannot rotate, move or swing in the crystal and glass but does have this freedom in the melt and L.C. phases.

### 3.3.4 X-ray structure of compound 1a

The exact packing of the molecules in compound 1a was obtained from an X-ray structure determination on a single crystal which was obtained by crystallizing this compound from water. The crystallographic data are presented in Table 3.4, the atomic positional and vibrational parameters are shown in Appendix 3.

**Table 3.4** Crystallographic data for compound **1a**

Formula	C <sub>19</sub> H <sub>31</sub> N <sub>3</sub> O <sub>5</sub> (½ H <sub>2</sub> O not included)
<i>M<sub>r</sub></i>	381.47 (½ H <sub>2</sub> O not included)
space group	P2 <sub>1</sub> 2 <sub>1</sub> 2 <sub>1</sub> (No. 19)
Lattice system	Orthorhombic
Z	4 (+ 2 H <sub>2</sub> O)
a (Å)	5 1230 (13)
b (Å)	7 691 (2)
c (Å)	51 094 (10)
V (Å <sup>3</sup> )	2013.2 (8)
<i>D</i> <sub>calcd</sub> (g cm <sup>-3</sup> )	1.3180 (5)
<i>μ</i> <sub>calcd</sub> (cm <sup>-1</sup> )	0.9
radn (Mo Kα)	0.71073 (graphite mon.)
T (°K)	150
<i>R<sub>F</sub></i> <sup>a</sup>	0.120
<i>R<sub>wF</sub></i> <sup>2b</sup>	0.224
S	0.90

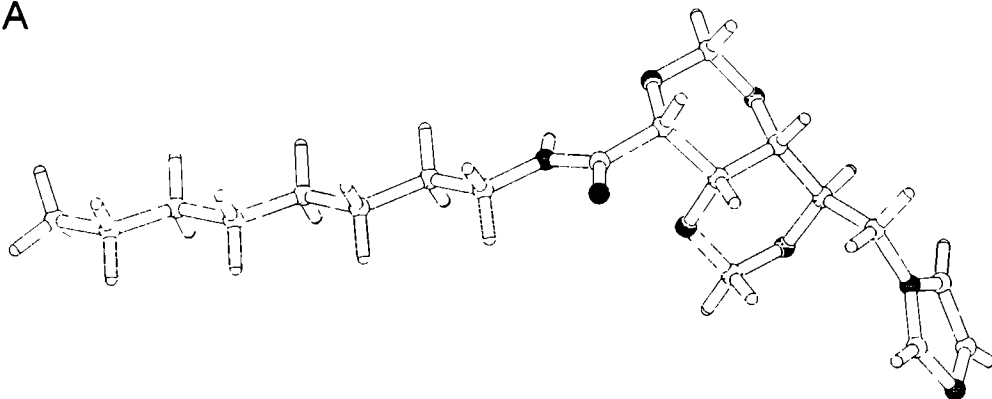
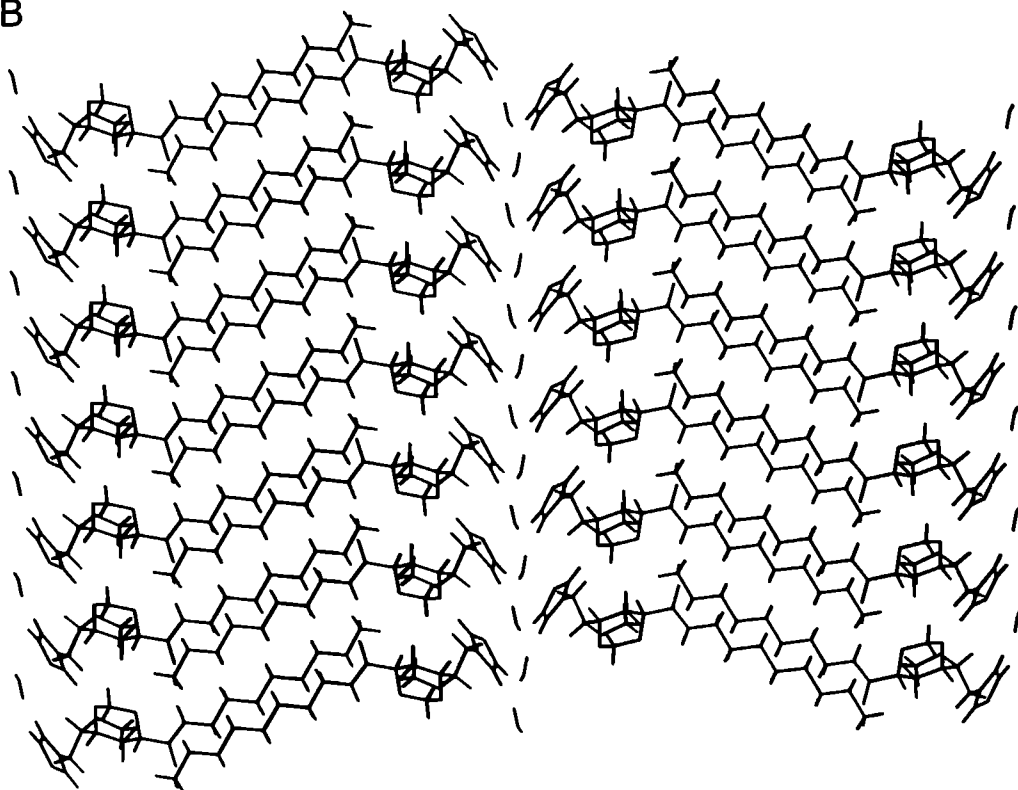
$$^a R_F = \sum |F_o - F_c| / \sum F_o$$

$$^b R_{wF^2} = \sqrt{[\sum w(F_o^2 - F_c^2)^2] / [\sum w(F_o^2)^2]}$$

To our surprise, **1a** crystallized in an interdigitized bilayered structure (see Figure 3.9) which is entirely different from the crystal structures of gluconamide **6a**<sup>18</sup> and related gluconamides,<sup>36,42,43</sup> which display carbohydrate molecules arranged in monolayers. A bilayer structure with interdigitized chains is known to exist for *N*,*n*-octyl-6-deoxy-D-gluconamide<sup>44</sup> and for "double headed" (1*S*,2*S*)-1,2-bis(D-gluconamido) cyclohexane.<sup>45</sup> The alkyl chains of the molecules **1a** do not penetrate in the head group region, but do reach beyond the amide groups which forces these groups to form hydrogen bonding arrays in only one direction, instead of also forming hydrogen bonds with molecules of different arrays. Apparently, the introduction of the dimethylene groups caused a remarkable sharp bend at C<sup>2</sup>. The overall shape of a molecule **1a** is that of a hockey stick (see Figure 3.9A). The sharp bent in the molecule and probably also the disability of **1a** to form a tight hydrogen bonding network creates more space in the tail region. This space is filled by interdigitizing of the tails. A comparable interdigitized packing is found in the well-known liquid crystalline mesogen cholesterol myristate.<sup>46</sup>

Surprising is also the location of the water molecules in the crystal structure of **1a**. These water molecules are hydrogen bonded to the imidazolyl groups and located between different bilayers, in such a way that the stacked gluconamide arrays become separated and the water molecules form layers by themselves. We believe that in the L.C. phase, the hydrogen bonded water molecules form dynamic hydrogen bonding schemes, *i.e.* the H-bonds are no longer fixed in H-bridges between certain pairs of imidazole groups, but are in a process of constantly

breaking up and forming new hydrogen bonds, like water molecules in water. In this way, the water layer between the interdigitized imidazole amphiphile layers acts as a kind of lubricant.

**A****B**

**Figure 3.9** A) Single crystal structure of **1a** B) Packing of **1a**, with interdigitizing alkyl chains and the water molecules between the bilayers

### 3.3.5 Solution $^1\text{H}$ -NMR study on **1a**

In order to determine the structure of **1a** in solution,  $^1\text{H}$ -NMR experiments were carried out in different solvents ( $\text{CDCl}_3$ ,  $\text{CD}_3\text{OD}$ , and  $\text{DMSO}-d_6$ ) and at different temperatures. The  $J$  values obtained from the  $^1\text{H}$ -NMR data were hardly affected by changing the temperature or solvent. As the  $^1\text{H}$ -NMR spectra of **1a** were not first order, the obtained values were checked with a computer simulation program. Dihedral angles were calculated by using the modified Karplus relation published by Altona.<sup>47</sup> Since the torsion angles in crystalline **1a** are known, the virtual  $J$ -couplings of **1a** in the solid state were also calculated (see Table 3.5).

**Table 3.5** Comparison between the dihedral angles of molecules of **1a** in the solid state and in solution

Dihedral angles	X-ray	$^1\text{H}$ -NMR		
	Torsion angles (measured)	$J$ coupling (calc) <sup>a</sup>	$J$ coupling (measured)	Torsion angles (calc)
$\text{H}^2\text{-C}^2\text{-C}^3\text{-H}^3$	$49^\circ$	1.97	1.95	$49^\circ$
$\text{H}^3\text{-C}^3\text{-C}^4\text{-H}^4$	$-48^\circ$	2.03	1.00	$-57^\circ$
$\text{H}^4\text{-C}^4\text{-C}^5\text{-H}^5$	$80^\circ$	0.31	1.20	$94^\circ$
$\text{H}^5\text{-C}^5\text{-C}^6\text{-H}^{6a}$	$48^\circ$	2.89	5.10	$33^\circ$
$\text{H}^6\text{-C}^5\text{-C}^6\text{-H}^{6a}$	$166^\circ$	10.69	9.95	$157^\circ$

<sup>a</sup> Calculated from torsion angles derived from the X-ray data

Given the fact that the values of the calculated torsion angles in solution are not as accurate as the angles obtained from the crystal structure, we may conclude from Table 3.5 that the conformations of the head group of **1a** (including the bend) in the crystalline state and the solution state are quite similar.

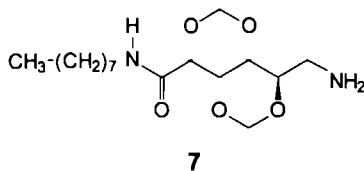
### 3.3.6 Thermotropic L.C. behavior of compounds related to imidazolyl gluconamides **1**

#### 3.3.6.1 Different substituents on the terminus of the head group

The ability of compounds **1** to form L.C. phases is surprising. In this section we will try to establish by applying structural variations in **1** which parts of the molecule are indispensable for the formation of a mesophase.

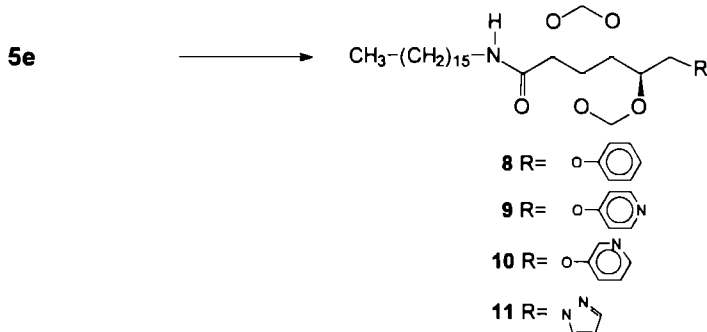
From Figure 3.5B it is clear that for achieving L.C. behavior the imidazole-containing bismethylene protected gluconamides must have alkyl chains of at least 12 carbon atoms length. This length, however, does not guarantee L.C. behavior as can be concluded from the fact that the set of compounds **4a-e** is not L.C. An exception is **4f** which contains an octadecyl chain, but this compound shows a L.C. phase which is different from the smectic phase usually observed for this type of compounds.

All compounds in this section with the exception of compound **7** (which contains an octyl chain) possess a hexadecyl chain, to exclude the possibility that insufficient chain length will prevent the formation of a L.C. phase.



The derivatives **8-11** (see Scheme 3.3), were synthesized by substitution of the tosyl group of gluconamide **5e** by a H-bond accepting aromatic group (except **8**). The rationale behind the synthesis of compounds **9-11** was that water molecules may form *interlayer* hydrogen bonds with the pyridyl and pyrazolyl groups of **9-11** resulting in a structure in which the bilayers are separated by water-layers in a similar way as found for **1a**. The position of the hetero-atom was also varied for both the 5 and 6 membered aromatic rings (**1e** versus **11** and **9** versus **10**). Compound **8** contains a phenyl group and was prepared with the objective to disturb the tight packing of the carbohydrate head groups, which might prevent crystallization resulting in hysteresis upon cooling and the generation of monotropic LC behavior. Although **8** does not have a nitrogen or oxygen atom and therefore is not a potential H-bond acceptor, it still contains an aromatic group that can display  $\pi$ - $\pi$  stacking interactions with similar groups of molecules present in the layers.

Scheme 3.3

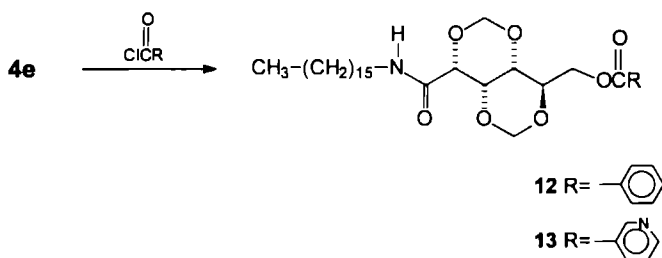


Compound **8** did not show LC behavior and neither did **9**. Apparently,  $\pi$ - $\pi$  stacking was absent or the interaction was too weak to generate LC behavior. The lack of the formation of a mesophase in the case of **9** is surprising, because pyridyl groups are known to form hydrogen bridges<sup>48</sup> and it was expected that water molecules would have formed an additional layer as observed in the X-ray of **1a**. The melting points of compounds **1e** and **9** were found to be almost similar (see Table 3.6), but **9** crystallized at 114 °C, which is above the c.p. of **1e** (110 °C). Compound **8** had a s.p. of 105 °C which is below the c.p. of **1e** and could have given a LC phase if molecules of **8** had been packed in a similar way as molecules of **1e**. Compound **10** behaved

differently from the other compounds and showed an enantiotropic smectic A phase with a m.p. of 95.2 °C and a c.p. of 194 °C. An explanation for the fact that **10** displays thermotropic L.C. behavior and **9** does not, cannot yet be given.

Since **8** does not form a L.C. phase, it can be concluded that a nitrogen atom in the aromatic ring is needed. The absence of L.C. phases in the case of **9** and **11** and the presence of an L.C. phase in the case of **10** suggests that with these type of compounds the nitrogen has to be on the right position of the aromatic ring. The packing of the molecules probably forces the nitrogen centers in a position where hydrogen bonding is possible (**1e** and **10**) or not (**9** and **11**).

Scheme 3.4



**Table 3.6** Thermotropic L C behavior of gluconamides with different C<sup>6</sup> substituents

compound	m p (°C) <sup>a</sup>	c p (°C) <sup>b</sup>
<b>4e</b>	105.5 (39.8)	---
<b>1e</b>	131.1 (64.2)	110.0 (15.8)
<b>7</b>	131.3 (9.9)	---
<b>8</b>	122.6 (40.1)	---
<b>9</b>	130.1 (30.2)	---
<b>10</b>	95.2 (13.2)	194 (27.8)
<b>11</b>	103.8 (26.8)	---
<b>12</b>	127.7 (54.7)	---
<b>13</b>	124.6 (49.5)	---

<sup>a</sup> Melting point,  $\Delta H_{\text{melt}}$  (kJ/mol) in parentheses

<sup>b</sup> Clearing point,  $\Delta H_{\text{clearing}}$  (kJ/mol) in parentheses

The phenyl and meta pyridyl groups were also coupled to the gluconamide framework via an ester linkage (to give compounds **12** and **13**, see Scheme 3.4). Both compounds did not show L.C. behavior although the melting points were in line with the series of compound **1**. We had expected that **12** and **13** would have shown hysteresis (and therefore a L.C. phase), because the rigid methylene protected carbohydrate part is now placed in between 2 rather floppy parts which

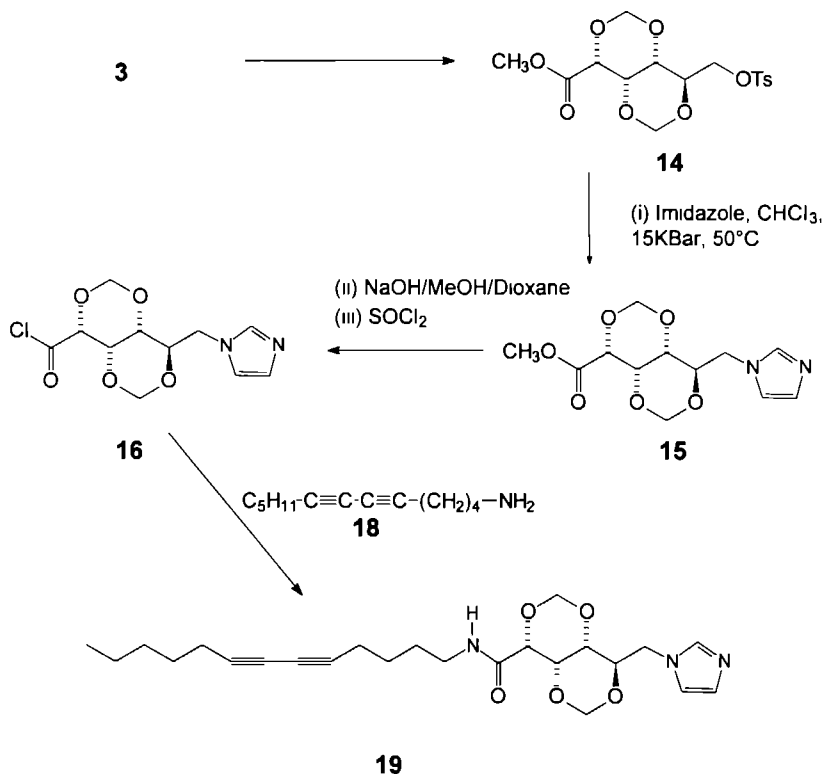


could have prevented crystallization at high temperatures. Unfortunately, the solidification points (s.p.) of **12** and **13** were too high (110.7 and 110.2 °C, respectively). No special trends could be detected in the  $\Delta H_{\text{melt}}$  or  $\Delta H_{\text{clearing}}$  values of compounds **7-13**.

### 3 3 6 2 Gluconamides with a diacetylene function in the alkyl chain

In order to study the effect of a modification in the alkyl chain of the gluconamides **1**, we synthesized compound **19** (Scheme 3.5).

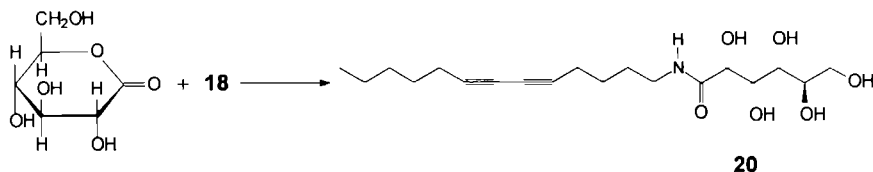
**Scheme 3.5**



Replacing the n-alkyl chain of **1d** by a diacetylene chain in **19** resulted in loss of L.C. behavior. The melting point (129.8 °C) of **19** was similar to the melting points of compounds of **1a-f**, but the diacetylene compound did not show the strong hysteresis needed for monotropic L.C. behavior: upon cooling it crystallized (s.p. 113.9 °C) before the L.C. phase was entered. On the other hand, introduction of the diacetylene function in a non-modified gluconamide derivative **20** (synthesized according to Scheme 3.6) did not result in a loss of L.C. behavior although the mesophase was destabilized by a drop in the c.p. (m.p. 152.5 °C,  $\Delta H_{\text{melt}} = 56.3 \text{ kJ/mol}$ , c.p. 167.8 °C, compare with Table 3.1). This is in line with the postulate<sup>10,37,49</sup> that the interactions of

the tails are disrupted at the clearing point and not at the melting point. We therefore may conclude that diacetylene functions destabilize the L C phase but do not prevent the formation of such a phase as long as this phase is enantiotropic.

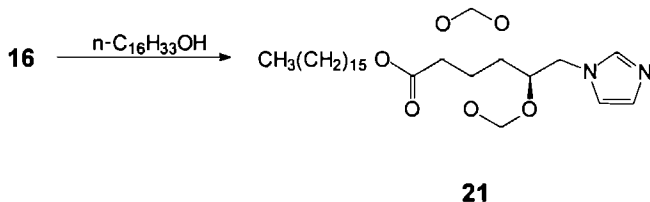
Scheme 3.6



### 3.3.6.3 *n*-Alkyl gluconates

In the literature<sup>35</sup> the ester analog of gluconamide **6a** has been described. Changing the amide function for an ester function did not have a large influence on the thermotropic behavior of the compound. The ester connection in the methylene protected imidazole derivative **21** (synthesized according to Scheme 3.7), however, did have a strong influence on the thermotropic properties. The melting point (94.7 °C) of **21** was found to be strongly decreased with respect to **1e** and was found to lie even below the c.p. of the latter compound. Compound **21**, however, did form a monotropic L C phase ( $S_A$ ) upon cooling (c.p. 88.3 °C), which is what one would expect because the amide function of **1e** does not form *intermolecular* hydrogen bonds in the mesophase (see Section 3.3.3). Despite the decrease of the melting point no *enantiotropic* L C behavior was displayed by **21**. Since **21** and **1e** form L C phases at different temperatures, the ordering of the molecules in the L C phase is probably different.

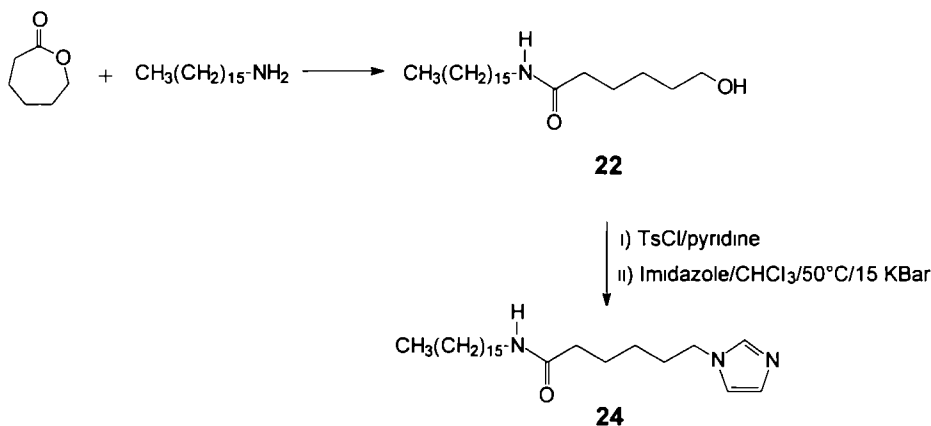
Scheme 3.7



### 3.3.6.4 Amide without the carbohydrate part

In order to investigate the influence the carbohydrate part in compounds **1** on the L C behavior, this rigid moiety was replaced by a flexible *n*-alkyl chain. Compound **24** and reference compound **22** were synthesized as shown in Scheme 3.8. Neither of these compounds showed L C behavior. A similar negative result was obtained in the case of 1-*n*-hexadecylimidazole (**25**).

Scheme 3.8



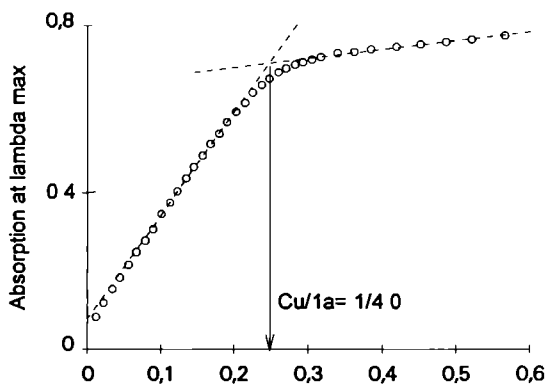
Apparently the inflexible carbohydrate part is necessary to achieve L.C. behavior with this type of compounds.

### 3.3.7 Metallomesogens

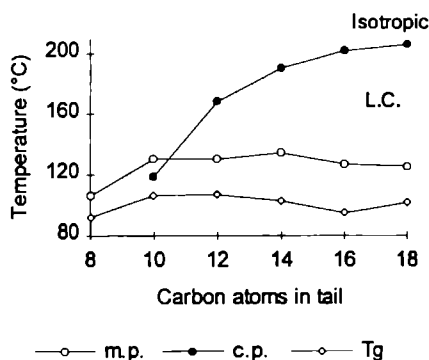
Imidazolyl (Im) compounds **1** were found to give 1/4 (Cu/Im) complexes with copper(II) ions as was determined by UV-vis titrations in methanol (see Figure 3.10).<sup>15</sup> The copper salts used had non-coordinating counter ions, *viz* triflate [ $\text{OSO}_2\text{CF}_3$ ]. For safety reasons this triflate ion was chosen instead of the more commonly used perchlorate anion.<sup>50</sup> Apart from the octyl derivative (**1a**)<sub>4</sub>Cu, all copper complexes of **1** ((**1b**)<sub>4</sub>Cu - (**1f**)<sub>4</sub>Cu) precipitated from dark-blue colored ethanolic solutions, leaving almost colorless supernatants. The complexes (except for (**1f**)<sub>4</sub>Cu) contained approximately one coordinated molecule of ethanol or water which was released at approximately 65 °C, according to thermogravimetric analysis.

Complexes (**1c**)<sub>4</sub>Cu-(**1f**)<sub>4</sub>Cu showed enantiotropic mesophases ( $S_A$ ), while (**1b**)<sub>4</sub>Cu appeared to be monotropic (see Table 3.7 and Figure 3.11). The resemblance of the melting points of compounds **1a-f** with those of the complexes (**1a**)<sub>4</sub>Cu-(**1f**)<sub>4</sub>Cu is remarkable and for both the free ligands, and the copper complexes, the clearing points depend on the length of the alkyl chain (Figure 3.11).

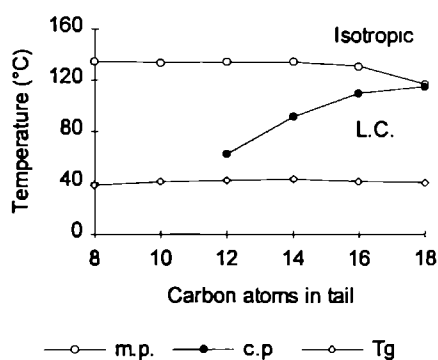
The great similarities in phase behavior (type of L.C. phase, melting points, clearing points and glass transition temperatures in the series of metal free ligands and copper complexes (compare Figure 3.11A and 3.11B) indicates, that the association behavior of the two types of compounds is the same.

Figure 3.10 UV-vis titration of **1a** with  $[\text{Cu}][\text{triflate}]_2$ Table 3.7 Thermotropic behavior of complexes  $(\mathbf{1a})_4\text{Cu}$ – $(\mathbf{1f})_4\text{Cu}$ <sup>a</sup>

Complex	n <sup>b</sup>	m p (°C)	c p (°C)	T <sub>g</sub> (°C)
( <b>1a</b> ) <sub>4</sub> Cu	8	105.8	---	91.8
( <b>1b</b> ) <sub>4</sub> Cu	10	130.6	119.0	106.4
( <b>1c</b> ) <sub>4</sub> Cu	12	130.5	168.2	106.8
( <b>1d</b> ) <sub>4</sub> Cu	14	134.6	190.6	102.7
( <b>1e</b> ) <sub>4</sub> Cu	16	127.1	202.1	94.9
( <b>1f</b> ) <sub>4</sub> Cu	18	125.9	206.4	101.7

<sup>a</sup> Obtained from DSC thermograms<sup>b</sup> Number of carbons in alkyl chain

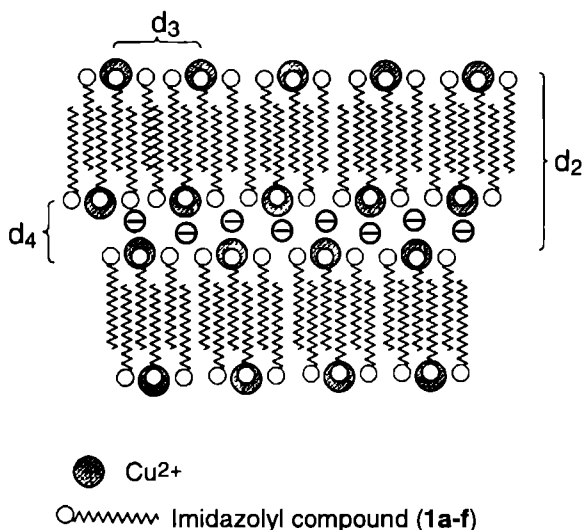
A



B

**Figure 3.11** Thermotropic LC behavior of gluconamides. The melting points were derived from heating curves, the glass transition temperatures from cooling curves. A) complexes  $(\mathbf{1a})_4\text{Cu}$ – $(\mathbf{1f})_4\text{Cu}$ . B) Free ligand.

SAXS experiments at elevated temperatures on **1d** and **(1d)<sub>4</sub>Cu** revealed that the bilayer thicknesses of the copper complex and the imidazolyl ligands in the smectic phase are almost equal (for compounds **1d** and **(1d)<sub>4</sub>Cu** 35.7 and 36.2 Å respectively). In the copper complex **(1d)<sub>4</sub>Cu**, however, besides the broad band corresponding to the spacing of the alkyl chains ( $d_1=4.6$  Å) and the reflection due to the aforementioned bilayer distance ( $d_2=36.2$  Å), two other relatively sharp reflections at  $d_3= 3.4$  Å and at  $d_4= 2.9$  Å were observed. The latter two can be assigned to copper-copper distances. Besides an *inter*-layer copper-copper distance there is also an *intra*-layer copper distance. The intensity of the  $d_4$  peak increased enormously when the sample of **Cu(1d)<sub>4</sub>** was cooled below the glass transition temperature whereas that of  $d_3$  remained exactly the same. Our interpretation is that the  $d_3$  spacing is the *intra*-layer copper-copper distance, which remains the same for the glassy state and the smectic state. In the smectic state the layers can exhibit lateral movement and the *inter*-layer Cu - Cu distance which probably corresponds with  $d_4$ , is not very well defined. By freezing the system into the glassy state the amount of ordering is increased and as a result the  $d_4$  reflection at 2.9 Å is enlarged. In this model (Figure 3.12) ion-rich regions are separated by hydrophobic layers and a molecular laminate<sup>51</sup> is created.



**Figure 3.12** Molecular laminate formed from the copper complexes of compounds **1a-f**

The above proposed model for the arrangement of the copper complexes is similar to that of the metal free ligands as derived from the X-ray structure of **1a**. Upon formation of the copper complex, the water molecules in the assembly of the metal free ligands are replaced by copper ions and counterions, which results in a stabilization of the L.C. phase as can be deduced from the shift of the clearing points to higher temperatures (see Figures 3.11A and B). In the case of the complexes the counterions instead of the water molecules act as the lubricant.

This replacement theory is supported by fact that the copper complex of the diacetylene imidazole derivative,  $(19)_4\text{Cu}$ , and the copper complex of the pyridyl compound,  $(9)_4\text{Cu}$ , do not form a L C phase, like the metal free ligands (**9** and **19**)

The copper complex of **24**,  $(24)_4\text{Cu}$ , showed L C behavior, but in contrast to **1** and  $(1)_4\text{Cu}$ , the amides without the carbohydrate part did not have comparable melting points (65.9 °C for **24** and 118.8 °C for  $(24)_4\text{Cu}$ ). Complex  $(24)_4\text{Cu}$  showed only one clearing point upon heating (139.2 °C,  $\Delta H_{\text{clearing}}$  39.2 kJ/mol complex), but in the cooling run, besides the crystallization point (103.2 °C,  $\Delta H_{\text{solid}}$  147.5 kJ/mol), two phase transitions were detected (130.3 °C,  $\Delta H$  1.6 kJ/mol and 128.3 °C,  $\Delta H$  49.7 kJ/mol). The types of L C phase were not identified, but from the second  $\Delta H_{\text{clearing}}$  value and the high viscosity of the low temperature L C phase it can be concluded that either the mesophase is highly ordered or the layers of molecules are undulated.<sup>52</sup> The copper(II) complex of **25**,  $(25)_4\text{Cu}$ , showed an enantiotropic and highly ordered L C phase between 70.8 and 162.0 °C ( $\Delta H_{\text{clearing}}$  60.4 kJ/mol). The type of phase is not known, but the observed textures were similar to those of  $(24)_4\text{Cu}$ .

A 4:1 complex of **1e** and  $[\text{Ni}][\text{BF}_4]_2$  ( $(1e)_4\text{Ni}$ ) was prepared in an analogous way as the preparation of  $(1e)_4\text{Cu}$ . This complex also showed a L C phase which was, according to observed textures under the polarization microscope, a  $S_A$  phase (m.p. 160.0 °C, c.p. 224.9 °C).

To the best of our knowledge this is the first report both of carbohydrate metallomesogens as well as of mesogens based on imidazole complexes. Other metallomesogens from copper complexes have been described before.<sup>53</sup>

### 3.4 Concluding remarks

As methylene bridges are very rigid and capable of determining the shape of the carbohydrate part in 2,4,3,5-dimethylene-*N*,*n*-alkyl-D-gluconamides, this type of protecting group is also useful to stimulate L C behavior. Although it is generally accepted that hydrogen bonds are important and even required for obtaining carbohydrate liquid crystals,<sup>34</sup> we have shown that with methylene protecting groups a rigid tetraoxa-*cis*-decalin moiety is generated which, in combination with an imidazole function, also creates a L C phase. Incorporation of pyridyl groups also leads to L C phases, due to a hysteresis effect, but the formation of the mesophase is very sensitive to the type of pyridyl group used: a 3-pyridyloxy yields a L C phase, whereas a 4-pyridoxy and a 3-pyridoxy-carboxylate group do not. The introduction of protecting groups affects the hydrogen bonding character of the carbohydrate part, but the typical curves in which the length of alkyl chain is plotted versus the melting or clearing point resemble those of the unmodified *n*-alkyl-D-gluconamides. Our IR experiments showed that the amide functions do not form a hydrogen bonding array in the L C phase, which is remarkable because in traditional carbohydrate liquid crystals such arrays are very important.<sup>48</sup> Apparently, the rigid *cis*-decaline structure of the dimethylene substituted glucon group dominates the packing of the molecules in the same way as the non-protected carbohydrate part does in traditional carbohydrate liquid crystals. This packing behavior is not affected by the introduction of copper ions, which complex to the imidazole groups. In the metal-free systems, the choice of a substituent on carbon atom 6 of

the carbohydrate moiety in order to obtain L.C. behavior is rather subtle. For some as yet unknown reason there has to be a hydrogen bonding or dipole-dipole interaction between the bilayers, otherwise non-hydrogen bonding substituents like phenoxy and benzoate should also have led to L.C. phases. On the other hand, groups with strong hydrogen bonding capacities like hydroxyl and amine groups also failed to form mesophases. Imidazole and pyridine groups which both are weak hydrogen bond acceptors proved to be successful in the formation of L.C. phases. This type of substituents contains a nitrogen atom in the correct position, which can interact with the succeeding layer (possible via H-bonds from water molecules). Water molecules hydrogen bonded by imidazole groups, can act as lubricants in the L.C. phase, by forming a dynamic hydrogen bonded network. Addition of copper(II) ions leads to exchange of the water molecules for copper ions and the L.C. phase is stabilized. In this metallomesogenic system the (non-coordinating) counter ions are acting as a lubricant.

The connection of the alkyl chain to the glucon group can be either an ester or an amide group. The alkyl chain must be flexible and long enough ( $\geq 12$  carbon atoms) otherwise the compound will not show monotropic L.C.-behavior and crystallize or will be trapped in the glassy state before the L.C. phase is entered.

### 3.5 Literature

- <sup>1</sup> Schnur, J M , Shashidhar, R *Adv Mat* **1994**, 6, 971
- <sup>2</sup> Feiters, M C *Supramolecular technology and applications* Vol 10, part III, Chap 16, *Supramolecular catalysis* vol. ed Reinhoudt, D.N. part of the series "Comprehensive Supramolecular Chemistry" ed Lehn, J -M , **1995**
- <sup>3</sup> Lehn, J -M. *Angew Chem* **1988**, 100, 91, *Ibid Int Ed Engl* **1988**, 27, 89.
- <sup>4</sup> a) Fuhrhop, J.-H , Helfrich, W. *Chem Rev* **1993**, 93, 1565, b) Ahuja, R , Caruso, P -L ; Möbius, D , Paulus, W , Ringsdorf, H , Wildburg, G *Angew Chem* **1993**, 105, 1082, *Ibid Int Ed Engl* **1993**, 32, 1033, c) Kunitake, T ; Okahata, Y.; Shimomura, M ; Yasunami, S.-I ; Taharabe, K *J Am Chem Soc* **1981**, 103, 5401, d) Fendler, J.H. *Membrane Mimetic Chemistry*, New York, **1982**; e) Kunitake, T., *Angew Chem* **1992**, 104, 692, *Ibid Int Ed Engl* **1992**, 31, 709; f) Ringsdorf, H , Schlarb, B , Venzmer, J. *Angew Chem* **1988**, 100, 117; *Ibid Int Ed Engl* **1988**, 27, 113
- <sup>5</sup> a) Percec, V ; Tomaros, D., *Compr Polym Sci, suppl Vol I* vol ed. G Allen, *Pergamon Press Oxford* **1992**, 300 , b) O'Brien, D.F , Kuo, T.; Liman, U ; Lamparski, H. *Polym J* **1991**, 23, 619., c) Kwolek, S L ; Morgan, P W ; Schaefer, J.R. *Encycl Polym Sci & Eng* ed. Mark, Bikales, Menges **1987**, 9, 1, d) Zentel, R *Comp Polym Sci* 5, *Pergamon Press Oxford* **1989**, 723.
- <sup>6</sup> Jeffrey, G.A.; Wingert, L M. *Liq Cryst.* **1992**, 12, 179
- <sup>7</sup> Chandrasekhar, S., Ranganath, G.S *Rep Prog Phys.* **1990**, 57
- <sup>8</sup> Zarges, W.; Hall, J., Lehn, J -M. *Helv Chim Acta* **1991**, 74, 1843
- <sup>9</sup> a) Fuhrhop, J.-H.; Schnieder, P.; Rosenberg, J.; Boekema, E *J Am Chem Soc* **1987**, 109, 3387; b) Fuhrhop, J -H , Schnieder, P., Boekema, E.; Helfrich, W. *J Am. Chem Soc* **1988**, 110, 2861, c) Boettcher, C , Boekema, E., Fuhrhop, J.-H. *J Microscopy* **1990**, 160, 173; d) Fuhrhop, J.-H.; Boettcher, C *J Am Chem Soc* **1990**, 112, 1768;

- e) Fuhrhop, J.-H., Svenson, S., Boettcher, C., Rössler, E., Vieth, H.-M. *J Am Chem Soc* **1990**, *112*, 4307, f) Köning, J., Boettcher, C.; Winkler, H.; Zeitler, E.; Talmon, Y.; Fuhrhop, J.-H. *J Am Chem Soc* **1993**, *115*, 693, g) Frankel, D.A., O'Brien, D.F. *J Am Chem Soc* **1991**, *113*, 7436; h) Pfannemüller, B. *Starch/Starke* **1988**, *40*, 476
- <sup>10</sup> Doren, van H. *Ph D Thesis Groningen*, **1989**
- <sup>11</sup> Doren, van H.; Wingert, L.M. *Mol Cryst Liq Cryst* **1991**, *198*, 381; Hentrich, F., Tschierke, C., Zschke, H. *Angew Chemie* **1991**, *103*, 429, *Ibid Int Ed Engl*, **1991**, *30*, 440; Doren, van H., Wingert, L.M. *Recl Trav Chim Pays-Bas* **1994**, *113*, 260; and ref. 10
- <sup>12</sup> For reviews on lamellar phases see: Hoffmann, H. *Ber Bunsenges Phys Chem* **1994**, *98*, 1433, Pas, van de J.C., Buytenhek, C.J., Brouwn, L.F. *Recl Trav Chim Pays-Bas* **1994**, *113*, 231, Thomas, B.N.; Safinya, C.R., Plano, R.J., Clark, N.A. *Science* **1995**, *267*, 1635, Hoffmann, H., Ulbricht, W. *Chemie in Unsere Zeit* **1995**, *29*, 74, Sein, A. *Ph D Thesis Groningen* **1995**
- <sup>13</sup> a) Kunitake, T.; Okahata, Y.; Shimomura, M.; Yasunami, S.-I.; Takarabe, K. *J Am Chem Soc* **1981**, *103*, 5401, b) Kunitake, T. *Angew Chem* **1992**, *104*, 692, *Ibid Int Ed Eng* **1992**, *31*, 709
- <sup>14</sup> Reeves, R.E. *Adv Carbohydr Chem* **1951**, *6*, 107
- <sup>15</sup> Reedijk, J. *Recl Trav Chim Pays-Bas*, **1969**, *88*, 1451
- <sup>16</sup> Hafkamp, R.J.H., Feiters, M.C., Nolte, R.J.M. *Angew Chem* **1994**, *106*, 1054; *Ibid Int Ed Engl* **1994**, *33*, 986
- <sup>17</sup> For reviews on metallomesogens see: (a, general) Espinet, P., Esteruellas, M.A., Oro, L.A.; Serrano, J.L.; Sola, E. *Coord Chem Rev* **1992**, *117*, 215; (b, discotic) Giroud-Godquin, A.-M.; Maitlis, P.M. *Angew Chem* **1991**, *103*, 370, *Ibid Int Ed Eng* **1991**, *30*, 375; (c, calamitic) Hudson, S.A.; Maitlis, P.M. *Chem Rev* **1993**, *93*, 861; (d, polymeric) Oriol, L., Serrano, J.L. *Adv Mat* **1995**, *7*, 348
- <sup>18</sup> Pfannemüller, B., Welte, W. *Chem Phys Lipids* **1985**, *37*, 227.
- <sup>19</sup> Svenson, S., Fuhrhop, J.-H., Köning, J. *J Phys Chem* **1994**, *98*, 1022
- <sup>20</sup> Zabel, V., Müller-Fahmow, A., Hilgenfeld, R., Saenger, W., Pfannemüller, B., Enkelmann, V., Welte, W. *Chem Phys Lipids* **1986**, *39*, 313.
- <sup>21</sup> geNMR V 3.3 (1990), (P.H.M. Budzelaar) NMR simulation package, IvorySoft®, Amsterdam, The Netherlands
- <sup>22</sup> Zief, M., Scattergood, A. *J. Am Chem. Soc* **1947**, *69*, 2132.
- <sup>23</sup> Mehlretter, C.L.; Mellies, R.L.; Rist, C.E.; Hilbert, G.E. *J Am Chem Soc* **1947**, *69*, 2130
- <sup>24</sup> McCaldin, D.J. *Chem Rev* **1960**, *60*, 39.
- <sup>25</sup> Tesser, G.I.; Bolvert-Geers, I.C. *Int J Peptide Protein Res.* **1975**, *7*, 295.
- <sup>26</sup> Brandsma, L. *Acetylenic Chemistry, Studies in Organic Chemistry*, Elsevier Amsterdam **1988**, 21.
- <sup>27</sup> Ref 26 page 59
- <sup>28</sup> Smiley, R.A.; Arnold, C. *J Org Chem* **1960**, *25*, 257
- <sup>29</sup>  $\text{AlH}_3$  was prepared by addition of conc  $\text{H}_2\text{SO}_4$  to  $\text{LiAlH}_4$  in THF, Yoon, N.M.; Brown, H.C. *J Am Chem Soc* **1967**, *90*, 2927
- <sup>30</sup> Chittenden, G.J.F., Univ. of Nijmegen (personal communication).
- <sup>31</sup> For the preparation of cyclic carbonates see a) Komura, H., Yoshino, T., Ishido, Y. *Carbohydrate Res* **1940**, *40*, 391, b) Raaijmakers, H.W.C. *Ph D Thesis, Univ of Nijmegen* **1993**, 115
- <sup>32</sup> For ring opening reactions see Yoshino, T., Inaba, S.; Komura, H.; Ishido, Y. *Bull Chem Soc Japan* **1974**, *47*, 405



- <sup>33</sup> Whistler, Walfrom *Methods in Carbohydrate Chemistry*, Bonner, T G [82], 19, 314
- <sup>34</sup> Jeffrey, G A *Acc Chem Res* 1986, 19, 168
- <sup>35</sup> Pfannemüller, B, Welte, W, Chin, E, Goodby, J W *Liq Cryst* 1986, 1, 357
- <sup>36</sup> Jeffrey, G A, Maluszynska, H *Carbohydr Res* 1990, 207, 211
- <sup>37</sup> Baeyens-Volant, D, Fornasier, R, Szalai, E, David, C *Mol Cryst Liq Cryst* 1985, 135, 93
- <sup>38</sup> Doren, H A van, Wingert, L M *Mol Cryst Liq Cryst* 1991, 198, 381
- <sup>39</sup> Monotropic means that the mesophase is observed only during cooling as a consequence of hysteresis, while with enantiotropic L C phases the mesophase is observed both on heating and cooling
- <sup>40</sup> Svenson, S, Kirste, B, Fuhrhop, J-H *J Am Chem Soc* 1994, 116, 11969
- <sup>41</sup> Lutz, E T G, Maas van der J H *J Mol Struct* 1994, 123
- <sup>42</sup> Müller-Fahrmow, A, Hilgenfeld, R, Hesse, H, Saenger, W, Pfannemüller, B *Carbohydr Res* 1988, 176, 165
- <sup>43</sup> Müller-Fahrmow, A, Saenger, W, Fritsch, D, Schnieder, P, Fuhrhop, J-H *Carbohydr Res* 1993, 242, 11
- <sup>44</sup> Herbst, R, Steiner, T, Pfannemüller, B, Saenger, W *Carbohydr Res* 1995, 269, 165
- <sup>45</sup> Andre, Ch, Luger, P, Nehmzow, D, Fuhrhop, J-H *Carbohydr Res* 1994, 261, 1
- <sup>46</sup> Craven, B M, DeTitta, G T *J Chem Soc Perkin Trans 2* 1976, 814
- <sup>47</sup> Haasnoot, C A G, de Leeuw, F A A M, Altona, C *Tetrahedron* 1980, 36, 2783
- <sup>48</sup> Paleos, C M, Tsiourvas, D *Angew Chem* 1995, 107, 1839, *Ibid Int Ed Eng* 1995, 34, 1696
- <sup>49</sup> Doren, H A van, Geest, R van der, Keuning, C A, Kellog, R M, Wynberg, H *Liq Cryst* 1989, 5, 265
- <sup>50</sup> Wolsey, W C *J Chem Educ* 1973, 50, A335
- <sup>51</sup> Menger, F M, Lee, J-J, Hagen, S *J Am Chem Soc* 1991, 113, 4017
- <sup>52</sup> Neve F, Ghedini, M, Munno, de G, Levelut, A -M *Chem Mater* 1995, 7, 688
- <sup>53</sup> Liquid crystals of copper complexes a) Hoshino, N, Murakami, H, Matsunaga, Y, Maruyama, Y *Inorg Chem* 1990, 29, 1177, b) Galyametdinov, Yu G, Polishchuk, A P, Bikchantaev, I G, Ovchinnikov, I V *J Struct Chem* 1993, 34, 872, c) Maldivi, P, Bonnet, L, Giroud-Godquin, A -M, Ibn-Elhaj, M, Guillon, D, Skoulios, A *Adv Mat* 1993, 5, 909, d) Zheng, H, Lai, C K, Swager, T M *Chem Mat* 1994, 6, 101, e) Alonso, P J, Marcos, M, Martinez, J I, Serrano, J L, Sierra, T *Adv Mat* 1994, 6, 667, f) Neve, F, Ghedini, M, Levelut, A -M, Francescangeli, O *Chem Mat* 1994, 6, 70, g) Molta, M F R, Duarte, M L T S *J Chem Soc Faraday Trans* 1994, 90, 2953

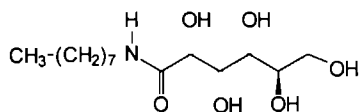
# Chapter 4

## Suprastructures in water from imidazole containing gluconamides

### 4.1 Introduction

Compounds with a hydrophilic and a hydrophobic part are called amphiphilic and can form aggregates in aqueous solution. Carbohydrate derivatives are of great interest as building blocks for amphiphiles because they are chiral and easily accessible in a great variety of structures. Moreover, they can be easily modified using known synthetic methodology. Pfannemüller was the first to synthesize *N*,*n*-alkyl-D-gluconamides of type **1** and to show that these carbohydrate derivatives form helical fibers in water,<sup>1</sup> with a regular twist and a high aspect ratio (up to  $10^4$ ).<sup>3</sup>

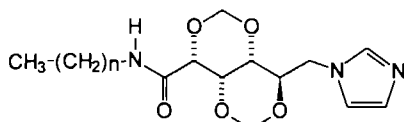
Fuhrhop and coworkers<sup>2</sup> subsequently studied these helical aggregates in great detail by electron microscopy in combination with image analysis,<sup>3</sup> NMR,<sup>4</sup> IR, and powder diffraction<sup>5</sup> and concluded that they consist of micellar fibers. The amphiphiles in the suprastructures are packed in a crystalline order. Variation in the stereochemistry of the head group of the *N*-alkylaldonamides resulted in different suprastructures like stacked bilayers, rolled-up sheets and whisker-type fibers.<sup>6</sup>



**1**

The possibility to tune the structure of the aggregates derived from aldonamides has not been investigated so far, although studies with other systems have been reported in the literature. For instance the sugar analogue *N*,*n*-dodecyltartaric acid monoamide has been shown to form cloth-like aggregates, but only at a pH close to the  $pK_a$  of tartaric acid,<sup>7</sup> suggesting that the structure of the aggregates can be fine-tuned by the pH. In another example, the size and length of hollow tubules made from negatively charged diacetylenic phospholipids could be modified by changing the head group size, the pH, the ionic strength, the type of anion, and the dispersion medium (water-ethanol mixtures).<sup>8</sup> Kunitake has shown that addition of  $Ca^{2+}$  ions to azobenzene phosphate amphiphiles alters the orientation of the head groups in such a way that helical structures are obtained.<sup>9</sup> It has been reported that the length of helical bilayer assemblies prepared from peptide amphiphiles can be shortened by the addition of  $Ba^{2+}$  and  $Ca^{2+}$  ions.<sup>10</sup> 12-Hydroxystearic acid has been shown to form twisted fibers and helical tapes in water.<sup>11</sup> The sense of the twist can be modified by adding metal ions, e.g. complexation of  $Li^+$  ions to D-12-hydroxystearic acid yields fibers with a right-handed twist, whereas complexation of  $Rb^+$  or  $Cs^+$  leads to fibers with a left-handed twist. Phosphatidylserines form aggregates of which the structures can be tuned by addition of calcium ions. In the presence of these ions, scrolls are obtained. Removal of the  $Ca^{2+}$  by EDTA results in vesicles.<sup>12</sup>

In this chapter we show that gluconamide-derivative **2a** forms suprastructures in water which can be tuned by changing the pH or the addition of metal ions.<sup>13</sup>



**2a**  $n = 7$   
**2b**  $n = 11$   
**2c**  $n = 15$

A series of compounds related to **2a** has been synthesized in which the head group, the alkyl chain and the linker between this chain and the carbohydrate moiety has been altered. The influence of these changes on the formation of the suprastructures in water has been investigated with EM and DSC. This chapter also describes the copper complexation behavior of **2a**, which has been studied in detail by UV-vis titrations and by EM.

## 4.2 Experimental

Transmission electron micrographs (TEM) were made on a Philips EM201 instrument (using an acceleration voltage of 60 kV) and a Jeol JEMCXII (60 kV) instrument, while the scanning electron micrographs (SEM) were taken using a JEOL 100 CX II (15 kV) instrument. A Branson 2200 sonication bath was used for sonication. Other analytical instruments were identical to those described in Chapter 3.

Chemicals were used as obtained from the supplier, except for the solvents which were distilled prior to use. The metal perchlorates were obtained as hexahydrates.

### 4.2.1 Syntheses

Compound **1** was prepared according to a literature procedure.<sup>1</sup> The syntheses of compounds **2a**, **2b**, **2c**, **4a**, **4b**, **4c**, and **6** have been described in Chapter 3. For atom labeling see the Experimental from Chapter 3.

**2-(1-Imidazolyl)-ethanol (3).** The synthesis of this compound was adapted from the literature procedure for the preparation of 2-(7-(1,3-dimethylxanthyl))-ethanol.<sup>14</sup> Imidazole (6.838 g, 0.1004 mol), 8.802 g (0.100 mol) of ethylene carbonate and 1.408 g (0.0094 mol) of NaI were heated under stirring for 2 hrs. at reduced pressure in order to remove the liberated CO<sub>2</sub>. The brown syrup was purified by column chromatography (silica, eluent MeOH/EtOAc 1:3, v/v), to yield 2.13 g (0.21 mmol, 19.5 %) of colorless oil. IR (KBr) 3114 cm<sup>-1</sup> (OH), 2936 and 2855 (=C-H), 1513 (C=N), 1081 (C-O), <sup>1</sup>H-NMR (100 MHz, CDCl<sub>3</sub>) δ 7.36 ppm (s, 1H, N<sub>im</sub>-CH=N<sub>im</sub>), 6.93 (s, 1H, CH<sub>2</sub>-N<sub>im</sub>-CH=CH-N<sub>im</sub>=), 6.65 (s, 1H, CH<sub>2</sub>-N<sub>im</sub>-CH=CH-N<sub>im</sub>=), 3.95 (m, 2H, -CH<sub>2</sub>-N<sub>im</sub>), 3.749 (m, 2H, CH<sub>2</sub>-OH).

**6-Deoxy-6-(1-benzimidazolyl)-2,4,3,5-dimethylene-N,n-octyl-D-gluconamide (5).** This compound was prepared following a procedure as described for compound **2a** in Chapter 3. Instead of imidazole, 1.121 g (9.49 mmol, 3.2 equiv.) of benzimidazole was used. Yield 0.22 g (0.51 mmol, 17.0 %) of **5** m.p. 91.9 °C. IR (KBr) 3433 cm<sup>-1</sup> (NH), 3098 and 3050 (=C-H), 1666 (amide I), 1616 (C=C), 1546 (amide II), 1497 (aromatic). <sup>1</sup>H-NMR (400 MHz, CDCl<sub>3</sub>) δ 7.953 ppm (N=CH-N), 7.826 (2d, 1H, ArH), 7.403 (2d, 1H, ArH), 7.319 (m, 2H, ArH), 6.562 (t, 1H, NHCO), 5.202 (d,  $J_{7a-7b}$ =6.50 Hz, 1H, H<sup>7a</sup>), 5.123 (d,  $J_{8a-8b}$ =6.16 Hz, 1H, H<sup>8a</sup>), 5.015 (d, 1H, H<sup>8b</sup>),

4.728 (d, 1H, H<sup>7b</sup>), 4.551 (2d,  $J_{6a-5}$  = 8.06 Hz,  $J_{6a-6b}$  = 14.71, 1H, H<sup>6a</sup>), 4.477 (2d,  $J_{6b-5}$  = 6.47 Hz), 4.379 (m,  $J_{5-4}$  = 1.51 Hz, H<sup>5</sup>), 4.319 (t,  $J_{3-4}$  = 1.34 Hz, 1H, H<sup>3</sup>), 4.157 (d,  $J_{2-3}$  = 1.99 Hz, H<sup>2</sup>), 3.618 (s, 1H, H<sup>4</sup>). <sup>13</sup>C-NMR (100 MHz, CDCl<sub>3</sub>)  $\delta$  166.692 ppm (NHCO), 143.635 (=C-C(=C)-N), 143.009 (N-C=N), 133.564 (=C-C(=C)-N), 123.461, 122.563, 120.672, 109.113 (-CH=CH-), 91.990 (C<sup>7</sup>), 88.358 (C<sup>8</sup>), 77.276 (C<sup>5</sup>), 73.976 (C<sup>2</sup>), 71.494 (C<sup>3</sup>), 66.738 (C<sup>4</sup>) EI-MS  $m/z$  431 (M)<sup>+</sup>, 132 (CH<sub>2</sub>-N<sub>2</sub>C<sub>3</sub>H<sub>5</sub>)<sup>+</sup>, 85 (cyclic -O-CH-CH-CH-O-CH<sub>2</sub>)<sup>+</sup>. Anal. Calcd. for C<sub>19</sub>H<sub>31</sub>N<sub>3</sub>O<sub>5</sub>·H<sub>2</sub>O: C, 61.44; H, 7.85; N, 9.35. Found: C, 61.80; H, 7.63; N, 9.25.

**N,n-Octyl-6-(1-imidazolyl)-n-hexanoic acid amide (7).** This compound was synthesized as described for compound **24** in Chapter 3. Instead of the hexadecyl derivative, 1.275 g (4.26 mmol) of N,n-octyl-6-tosyloxy-n-hexanoic acid amide was used. Yield 0.40 g (2.50 mmol, 58.7 %) of oil. IR (KBr) 3107 and 3066 cm<sup>-1</sup> (=C-H), 1650 (amide I), 1553 (amide II). <sup>1</sup>H-NMR (90 MHz, CDCl<sub>3</sub>)  $\delta$  7.44 ppm (s, 1H, N=CH-N), 7.04 (s, 1H, N=CH-CH-N), 6.891 (s, 1H, N=CH-CH-N), 5.54 (very broad t, 1H, NHCO), 3.94 (t, 2H, -CH<sub>2</sub>-N=), 3.23 (m, 2H, CH<sub>2</sub>-(C=O)), 2.14 (t, 2H, -CH<sub>2</sub>-C=O), 1.81 (t, 2H, -CH<sub>2</sub>-CH<sub>2</sub>-N=), 1.28 (m, 16H, -(CH<sub>2</sub>)<sub>6</sub>- and O=C-CH<sub>2</sub>-(CH<sub>2</sub>)<sub>2</sub>-), 0.87 (t, 3H, CH<sub>3</sub>). EI-MS  $m/z$  293 M<sup>+</sup>, 278, 264, 250, 236, 222, 208, 194 (M - (CH<sub>2</sub>)<sub>n</sub>-CH<sub>3</sub>, n = 0, 1, 2, 3, 4, 5, 6 respectively)<sup>+</sup>, 165 (CO-(CH<sub>2</sub>)<sub>5</sub>-Im)<sup>+</sup>, 137 (-CH<sub>2</sub>)<sub>5</sub>-N<sub>2</sub>C<sub>3</sub>H<sub>3</sub>)<sup>+</sup>, 95 (-CH<sub>2</sub>)<sub>2</sub>-Im)<sup>+</sup>.

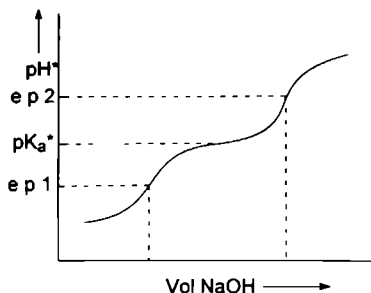
**6-Deoxy-6-(1-imidazolyl)-2,4,3,5-dimethylene-n-octyl-D-gluconate (8).** This compound was synthesized as described for compound **21** in Chapter 3. Instead of n-hexadecan-1-ol, 14 g (8.75 mmol, 6 equiv.) of n-octan-1-ol was used. Yield 0.03 g (0.07 mmol, 5 %) of **8**, m.p. 55.1 °C. IR (KBr) 3136 and 3099 cm<sup>-1</sup> (=C-H), 1757. <sup>1</sup>H-NMR (100 MHz, CDCl<sub>3</sub>)  $\delta$  8.69 ppm (s, 1H, N=CH-N), 8.16 (t, 1H,  $J$ =1.2 Hz, -CH<sub>2</sub>-N-CH=CH-N), 8.06 (t, 1H, -CH<sub>2</sub>-N-CH=CH-N), 4.67 (m, 2H, -CH<sub>2</sub>OH), 4.48 (m, 2H, CH<sub>2</sub>-N). EI-MS  $m/z$  381 (M - H)<sup>+</sup>, 353 (M - C<sub>2</sub>H<sub>5</sub>)<sup>+</sup>, 337 (M - C<sub>3</sub>H<sub>7</sub>)<sup>+</sup>, 325 (M - C<sub>4</sub>H<sub>9</sub>)<sup>+</sup>, 225 (C<sub>8</sub>H<sub>17</sub>OCO)<sup>+</sup>. Anal. Calcd. for C<sub>19</sub>H<sub>30</sub>N<sub>2</sub>O<sub>6</sub>·H<sub>2</sub>O: C, 56.98; H, 8.05; N, 7.00. Found: C, 57.40; H, 7.86; N, 6.55.

#### 4.2.2 Determination of the pK<sub>a</sub>\* values<sup>†</sup>

In order to avoid deviating pK<sub>a</sub> values due to aggregation in the aqueous solutions, a methanol/water (95:5, v/v) mixture was used as the titration solvent. For comparison, methylimidazole and imidazole were also titrated in this medium and were found to have pK<sub>a</sub>\* values of 7.03 and 6.96, respectively, which are similar to their values in water (6.95 for both compounds<sup>15</sup>). The titrations were carried out under a nitrogen atmosphere and the pH electrode was calibrated with a lithium succinate/succinic acid and an ammonium oxalate/oxalic acid buffer (pK<sub>a</sub>\*=7.26 and pK<sub>a</sub>\*= 4.23 respectively).<sup>16</sup> Approximately 0.025 mmol of sample was dissolved in 50 ml of methanol/water (95:5, v/v) containing 0.0012 M HClO<sub>4</sub>. This mixture was titrated with a solution of 0.01 M NaOH in methanol/water (95:5, v/v), which was calibrated with benzoic acid. The curves showed two equivalence points. The first point (e.p.1) was reached when the amount of NaOH added was equivalent to the total amount of HClO<sub>4</sub> minus the amount of imidazolyl compound. The second point (e.p. 2) equaled the total amount of HClO<sub>4</sub>. In the area between the equivalence points, the pH\* is determined by the basic character of the imidazolyl compound. The pH\* value in the middle of this imidazolyl buffered area was taken as the pK<sub>a</sub>\* value (see Figure 4.1).

<sup>\*</sup> Im = imidazolyl

<sup>†</sup> pH and pK<sub>a</sub> values obtained from non-aqueous solutions are denoted with an asterisk



**Figure 4.1** Acid-base titration curve from which the  $pK_a$  value is determined

#### 4.2.3 UV-vis titrations

In a typical titration experiment, an aliquot of 1 ml (100 mM) of a metal salt solution in water was added in steps of 20  $\mu$ l to an aqueous solution of the ligand (2 ml, 50 mM) in a quartz cuvette. After each addition the solution was equilibrated for 1 min. and subsequently UV-vis spectra ( $T = 25^\circ\text{C}$ , slit = 2 nm, scan rate = 120 nm/min) were recorded. The background was recorded with the same solvent mixture as in the titration experiment but without the ligand or metal salt. The reference cuvette contained the same solvent as the measuring cuvette, however, without ligand or metal salt.

#### 4.2.4 DSC measurements

In a typical DSC experiment, 60  $\mu$ l of water was added to 1.5 - 3 mg of compound, which was transferred to a large volume DSC cup (stainless steel). Heating and cooling runs were recorded at a scan rate of  $5^\circ\text{C}/\text{min}$ . The maximum temperature that could be reached was  $130^\circ\text{C}$ . After the runs, the weight was checked, but no loss of weight was observed. In the case of the metal complexes, a metal salt solution was added, instead of pure water.

#### 4.2.5 Electron microscopy

Electron microscopy was performed on dispersions of the amphiphiles in acetic acid/acetate buffered ( $\text{pH}=4.5$ ) solutions or in Tris buffered ( $\text{pH}=8.5$ ) solutions. The metal complexes were prepared in pure water (double distilled or milli-Q<sup>®</sup> quality).

#### TEM experiments

In a typical experiment, ca. 1 mg of amphiphilic compound was dissolved in 0.5 ml of solvent. The mixture was first heated until a clear solution was obtained and then allowed to cool to room temperature. In the case of the metal complexes, a solution containing the metal salt was added to a warm and clear solution of the ligand before the latter solution had cooled to room temperature. The metal salt and amphiphiles were mixed in a stoichiometry that was obtained from the UV-vis titrations,<sup>17, 18</sup> e.g. in the case of  $\text{Cu}(\text{ClO}_4)_2$ , a metal/ligand ratio of 1/4 was used, and in the case of  $\text{CuCl}_2$  a metal/ligand ratio of 1/2.

**Dried-in samples** Mixtures of amphiphiles in acetic acid or Tris buffered solutions and metal complexes in milli-Q water were sonicated<sup>†</sup> at approximately  $70^\circ\text{C}$ . After cooling to room temperature, a drop of the suspension was transferred to a carbon coated 150 Mesh copper grid. After 1 min. the excess of material was blotted off. In samples without metal ions, the contents of the grid were stained with uranyl acetate or covered with Pt deposited at an angle of approximately  $45^\circ$ .

<sup>†</sup> Only samples containing metal ions were sonicated

**Freeze etching.** Suspensions of the amphiphiles in acetic acid or Tris buffered solutions and the metal complexes in milli-Q water were mixed and sonicated for 5 min. at approximately 70 °C, after which the samples were allowed to cool to room temperature. To 0.3 ml of a suspension, one drop of glycerol (cryo-protectant, conc.  $\pm 10\%$ ) was added. A freshly cleaned<sup>†</sup> gold grid, was immersed in the suspension and placed between two freshly cleaned copper plates. The grid and copper plates were cooled very rapidly in a cryojet with liquid propane (-190 °C) that was condensed with liquid nitrogen. The copper plates were quickly pulled apart from the gold grid under high vacuum at -105 °C in a Balzers freeze etching instrument. Subsequently the sample was etched for 5 min. with the freeze fracture knife at -180 °C positioned over the sample in order to sublimate amorphous water molecules. The grid and sheets were covered with a carbon layer of 20 nm, and in addition, Pt diluted with carbon (Pt/C, 3:7, w/w) was deposited at an angle of 45° until a layer of 3 nm was obtained. The material was placed on the surface of a solution of aqueous chromic acid (20 %, w/v). The organic material was oxidized and dissolved in the solution while the replicas remained on the surface. After washing with water (by putting them on a clean water surface), the replicas were transferred to Formvar-coated copper grids.

### SEM experiments

The copper grids with material used in the TEM experiments, were transferred to a SEM specimen (mount) adapter. Subsequently, the sample was covered with a 10 nm gold layer.

## 4.3 Results and discussion

### 4.3.1 pK<sub>a</sub> titrations

As the presence of a charge can have a large influence on the aggregation behavior of an amphiphile<sup>7</sup> we determined the pK<sub>a</sub>-value of the imidazole group in compound **2a** in methanol/water (95.5, v/v). In order to be sure that **2a** is sufficiently protonated the solvent should be buffered at a pH of approximately 2 pH units below the pK<sub>a</sub> (Im) value.

From the titration experiments (see experimental section) it is clear that the pK<sub>a</sub> value of **2a** is very similar to the pK<sub>a</sub> values of imidazole, 1-methyl-imidazole and the model compound **3** (see Table 4.1).

**Table 4.1** pK<sub>a</sub><sup>+</sup>-values of imidazole-containing compounds <sup>a</sup>

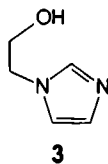
Compound	pK <sub>a</sub> <sup>+</sup>	pK <sub>a</sub> <sup>b</sup>
Imidazole	6.96	6.95
Methylimidazole	7.03	6.95
<b>2a</b>	6.28	
<b>3</b>	6.92	

<sup>a</sup> In methanol/water (95.5, v/v)

<sup>b</sup> In water (see Ref. 5)

Apparently, the presence of a β-oxygen atom in **2a**, a β-hydroxyl group in **3** or a methyl group in methylimidazole has only a small influence on the pK<sub>a</sub> value of the imidazole group. It was assumed, therefore, that the pK<sub>a</sub> values of the imidazole reference compounds in Section 4.3.5 were approximately the same as the pK<sub>a</sub> value of imidazole itself.

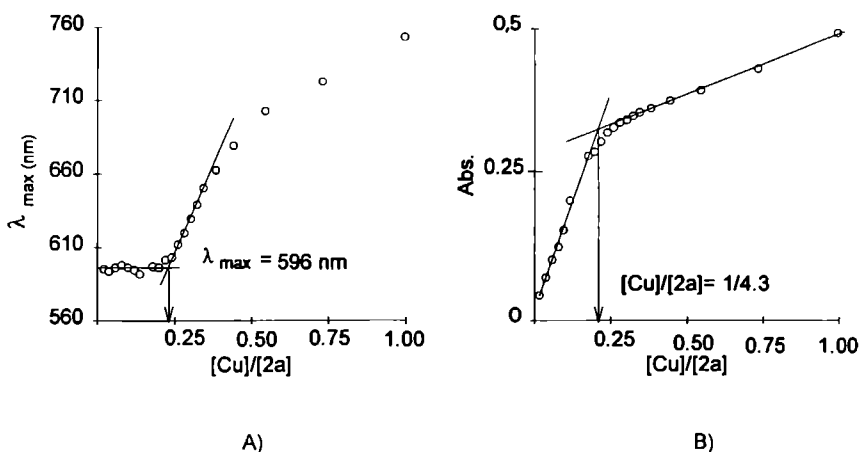
<sup>†</sup> The grids and copper plates were cleaned with conc. hydrochloric acid, then rinsed twice with water and additionally sonicated in acetone (2 min.)



### 4.3.2 UV-vis titrations

#### *Cu(ClO<sub>4</sub>)<sub>2</sub> complexation*

Copper(II) ions can give 1:4 metal-ligand complexes with imidazole compounds.<sup>17</sup> The complex formation can be followed by monitoring a broad band at approximately 600 nm in the UV-vis spectrum, which is indicative of the presence of a  $\text{Cu}(\text{imidazole})_4^{2+}$  complex.<sup>19</sup> Addition of a copper salt with a non-coordinating counter ion (*e.g.* perchlorate) to a solution of **2a** in water, methanol or chloroform was found to give turbid mixtures which prevented accurate UV-vis titrations. In mixtures of organic solvents such as chloroform/methanol (1:2, v/v), however, clear dark blue solutions were obtained and the complexation behavior of **2a** could be determined (see Figure 4.2). During the titration of **2a** with  $\text{Cu}(\text{ClO}_4)_2$  the  $\lambda_{\text{max}}$  gradually shifted from 595 to 750 nm when the  $[\text{Cu}]/[\text{2a}]$  ratio was increased from 1/4 to 1/1. The titrations revealed that at low copper concentrations a 1/4 (Cu/Ligand) complex is present, whereas at high copper concentrations other complexes, *e.g.*  $[\text{Cu}]/[\text{2a}] = 1/3, 1/2$ , or  $1/1$  prevail.<sup>20</sup> Solvent molecules like methanol will probably fill the empty coordination places at the copper(II) centers leading to complexes that have, besides a different  $\lambda_{\text{max}}$ , a weaker chromophoric character. This can be concluded from the curve of the absorbance at  $\lambda_{\text{max}}$  vs. the  $[\text{Cu}]/[\text{2a}]$  ratio which flattens above 1/4 (Figure 4.2)



**Figure 4.2** Titration curves of **2a** with  $\text{Cu}(\text{ClO}_4)_2$ , in a mixture of  $\text{CHCl}_3$  and MeOH (1:2, v/v), A)  $\lambda_{\text{max}}$  vs. the  $[\text{Cu}]/[\text{2a}]$  ratio B) Absorption at  $\lambda_{\text{max}}$  vs. the  $[\text{Cu}]/[\text{2a}]$  ratio

Since it was necessary to carry out the titration of compound **2a** with copper(II) in a mixture of organic solvents we also performed, for comparison, a titration of methylimidazole with copper(II) in an almost similar solvent mixture (see Table 4.2). At low copper concentration 1/4 metal to ligand complexes were formed with methylimidazole, while at higher copper concentrations the  $\lambda_{\text{max}}$  shifted in a way as observed for compound **2a**, indicating a similar complexation behavior as for the latter compound. An oxygen atom which can participate in the copper complexation is situated next to the imidazole group in compound **3**, which makes **3** a better model for compound **2a** than methylimidazole. Compound **3** formed copper complexes that dissolved both in water and in organic solvents without forming turbid mixtures. The titration curves of compound **3** in water, methanol, and in a mixture of chloroform/methanol (1.2. v/v) were almost identical to those of **2a** and MeIm. The  $\lambda_{\text{max}}$  values of all the complexes described in Table 4.2 were very similar indicating that in all cases complexes of the type  $\text{Cu}(\text{imidazole})_4^{2+}$ ,<sup>19</sup> were formed.

**Table 4.2** Complexation stoichiometry of imidazole ligands and Tris with  $\text{Cu}(\text{ClO}_4)_2$  as determined by UV-vis titrations

Ligand	Solvent	Cu/Ligand <sup>a</sup> ratio	$\lambda_{\text{max}}$ (nm) <sup>b</sup>
MeIm	$\text{CHCl}_3/\text{MeOH}$ (1.3, v/v)	1/4 2	610
<b>2a</b>	$\text{CHCl}_3/\text{MeOH}$ (1.2, v/v)	1/4 3	602
<b>3</b>	MeOH	1/4 0	599
<b>3</b>	$\text{CHCl}_3/\text{MeOH}$ (1 3, v/v)	1/4 5	598
<b>3</b>	water (MilliQ)	1/4.3	611

<sup>a</sup> Determined from the intersection of the tangents in the plot of the absorbance at  $\lambda_{\text{max}}$  vs the  $[\text{Cu}]/[\text{Ligand}]$  ratio

<sup>b</sup> Determined from the intersection of the tangents in the plot of  $\lambda_{\text{max}}$  vs the  $[\text{Cu}]/[\text{Ligand}]$  ratio

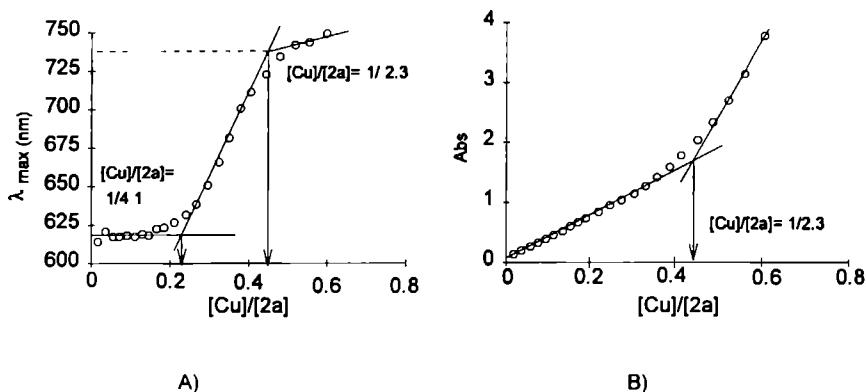
As we used  $\text{Cu}(\text{II})$ -tris(hydroxymethyl)amine (Tris) buffers in many of our experiments (vide infra) we also carried out an UV-vis titrations of **3** with  $\text{Cu}(\text{ClO}_4)_2$  in the presence of this buffer (pH=8.5). The titration curve was similar to that of **3** in pure water. Apparently, Tris is a much weaker ligand<sup>21</sup> for  $\text{Cu}(\text{II})$  than imidazole and the coordinated Tris molecules are completely exchanged for imidazole ligands when the latter are added.

#### *CuCl<sub>2</sub> complexation*

The chloride ions of  $\text{CuCl}_2$  are known to be coordinating anions, causing a complex of **2a** with  $\text{CuCl}_2$  to be different from the complex with  $\text{Cu}(\text{ClO}_4)_2$ . As in the case of the complexes with copper perchlorate and triflate, addition of  $\text{CuCl}_2$  to a solution of **2a** in water resulted in turbid mixtures. From studies carried out by Van Esch in our group<sup>20</sup> we know that monodentate imidazole amphiphiles form a 1/3.4 copper to ligand complexes with  $\text{CuCl}_2$ . A UV-vis titration curve of **2a** with  $\text{CuCl}_2$  in methanol in which the  $\lambda_{\text{max}}$  was plotted against the ratio  $[\text{Cu}]/[\text{2a}]$  showed 2 inflection points, viz at  $[\text{Cu}]/[\text{2a}] = 1/4.1$  and  $1/2.3$ , indicating that both 1/4 and 1/2 complexes were formed (Figure 4.3). A plot of the absorbance at  $\lambda_{\text{max}}$  vs  $[\text{Cu}]/[\text{2a}]$  showed only



one inflection point at the ratio 1/2.3. This may indicate that the extinction coefficients of the 1/4 and 1/2 complexes at  $\lambda_{\max}$  (in the dark blue and bright green region of the UV-vis spectrum, respectively) are very similar. Remarkable is the increase in absorbance which is observed when  $[\text{Cu}]/[\text{2a}]$  is larger than 2.3. In this region  $\lambda_{\max}$  hardly changes. Apparently, the complex of  $\text{CuCl}_2$  ligated by methanol (green)<sup>§</sup> is a strong chromophore.



**Figure 4.3** Titration curves of **2a** with  $\text{CuCl}_2$  in MeOH. A)  $\lambda_{\max}$  vs the  $[\text{Cu}]/[\text{2a}]$  ratio, B) absorbance at  $\lambda_{\max}$  vs the  $[\text{Cu}]/[\text{2a}]$  ratio

#### Complexes of **2a** and model compound **3** with metals other than Cu

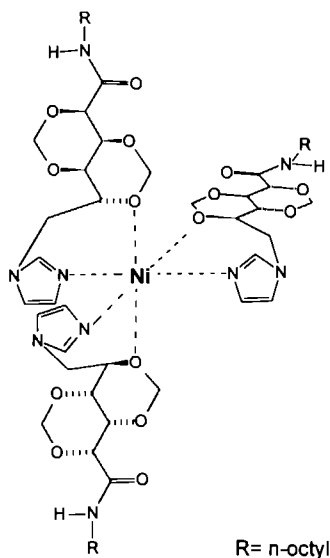
From the literature<sup>17</sup> it is known that imidazole can give 6:1 ligand to metal complexes with  $\text{Co}(\text{ClO}_4)_2$  and  $\text{Ni}(\text{ClO}_4)_2$ .<sup>22</sup> It was of interest therefore to investigate the complexation behavior of **2a** and **3** towards these metal salts. For comparison, experiments were also carried out with imidazole. The UV-vis spectra of both  $[(\text{2a})_n\text{Ni}][\text{ClO}_4]_2$  and  $[(\text{3})_n\text{Ni}][\text{ClO}_4]_2$  showed 2 broad peaks, with  $\lambda_{\max 1} = 380$  nm and  $\lambda_{\max 2}^{\#} = 605$  nm. Both  $\lambda_{\max}$  values gradually shifted to the red during the titration when the  $[\text{Ni}]/[\text{Ligand}]$  ratio was increased from 1/50 to 1/1. This indicates that the complexation stoichiometry changes during the titration. From the plots of the absorbances at  $\lambda_{\max}$  versus the  $[\text{Ni}]/[\text{Ligand}]$  ratios the stoichiometries of the nickel(II) imidazole complexes were determined (see Table 4.3). The results suggest that imidazole itself forms a 4:1 ligand to metal complex (probably square planar<sup>22</sup>), whereas **2a** and **3** act as bidentate ligands giving 3:1 complexes (see Figure 4.4).

<sup>§</sup>  $\text{CuCl}_2$  crystals containing two  $\text{H}_2\text{O}$  molecules are (bright) blue.

<sup>#</sup>  $\lambda_{\max 2}$  was only visible when the  $[\text{Ligand}]/[\text{Ni}]$  ratio was smaller than 10

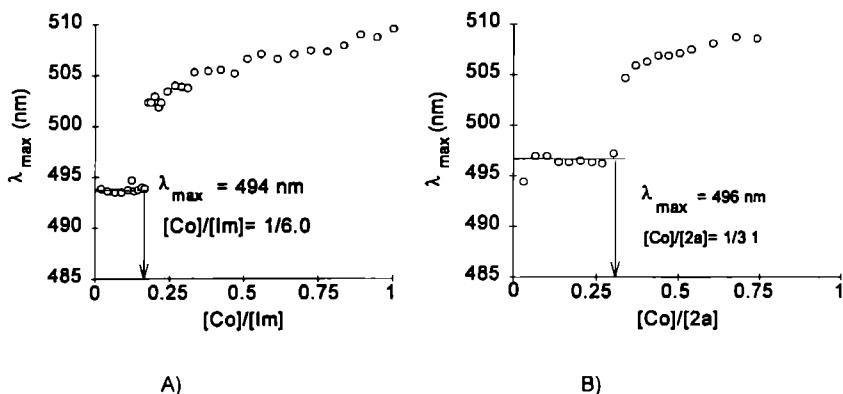
**Table 4.3** Stoichiometry of complexes between imidazole ligands and  $\text{Ni}(\text{ClO}_4)_2$  as determined by UV-vis titrations<sup>a</sup>

Compound	Solvent (v/v)	Ratio $[\text{Ni}]/[\text{Ligand}]$	$\lambda_{\text{max}}$ (nm) <sup>b</sup>
Imidazole	MeOH/H <sub>2</sub> O (1/1)	1/3 6	619
		1/3 8	375
<b>3</b>	MeOH/H <sub>2</sub> O (1/1)	1/3 1	604
		1/3 1	379
<b>2a</b>	MeOH	1/2 8	621
		1/3 2	381

<sup>a</sup> Numbers obtained from the plots of the absorbance at  $\lambda_{\text{max}}$  vs the ratio  $[\text{Ni}]/[\text{Lig}]$ <sup>b</sup> At intersection of tangents (see Figure 4 3), lower line  $\lambda_{\text{max}1}$  upper line  $\lambda_{\text{max}2}$ **Figure 4.4** Proposed structure of the complex  $[\text{Ni}(\mathbf{2a})_3][\text{ClO}_4]_2$ . The nickel ion is six coordinated by 3 nitrogen and 3 oxygen atoms

The titration curves of both imidazole and **2a** with  $\text{Co}(\text{ClO}_4)_2$  in methanol showed an abrupt shift of  $\lambda_{\text{max}}$  (see Figure 4.5), which is in contrast with the titration curves of copper(II) and nickel(II), which displayed gradual shifts. The absence of a gradual shift of  $\lambda_{\text{max}}$  indicates that no mixed complexes are formed at low  $[\text{Co}]/[\text{Ligand}]$  ratios. Figure 4.5 reveals that the cobalt-imidazole complex has a 6:1 ligand to metal stoichiometry and the cobalt - **2a** complex a 3:1 stoichiometry. As only 3 molecules of **2a** are found to coordinate to the cobalt center, other substituents than imidazolyl must participate in the complexation, probably protected hydroxyl

functions as suggested for the coordination of **2a** to nickel(II) (Figure 4.4). Despite the fact that imidazole and **2a** form different complexes, the difference in  $\lambda_{\text{max}}$  for  $[(\text{Im})_6\text{Co}][\text{ClO}_4]_2$  and  $[(\mathbf{2a})_3\text{Co}][\text{ClO}_4]_2$  in methanol was remarkably small.



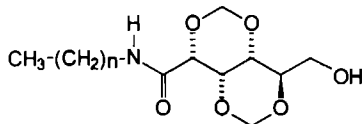
**Figure 4.5** Titration curves of imidazole ligands with  $\text{Co}(\text{ClO}_4)_2$ , A) imidazole, B) compound **2a**

#### 4.3.3 DSC experiments

The temperature at which an amphiphile dissolves in aqueous solution is often called the “Krafft” temperature ( $T_{\text{Krafft}}$ ),<sup>23</sup> which can be determined by using polarizing microscopy or differential scanning calorimetry (DSC). DSC also gives information about the enthalpy of dissolution ( $\Delta H$ )<sub>diss</sub>. In this section the  $T_{\text{Krafft}}$  and ( $\Delta H$ )<sub>diss</sub> of **2a** and related compounds are compared. This study was undertaken because the temperature at which the gluconamide dissolves in aqueous solution is important for the process of self assembly of this kind of molecules. For instance, the helices of *N*,*n*-octyl-*D*-gluconamide (**1**) were obtained by cooling a hot clear solution of **1** in water (1 % w/v) to room temperature.<sup>1,2</sup>

DSC thermograms of **1** in water showed upon heating in the first run two endothermic peaks at 64.3 °C ( $\Delta H = 13.5$  kJ/mol) and 73.4 °C ( $\Delta H = 19.1$  kJ/mol), while only one exothermic peak was found upon cooling (59.9 °C,  $\Delta H = -12.8$  kJ/mol). In the literature<sup>24</sup> the low temperature transition of **1** has been assigned to the splitting of the numerous *intra*- and *intermolecular* hydrogen bonds between the hydroxyl groups in the carbohydrate moieties of the molecules, and the second one to the breaking of the amide hydrogen bonds. This assignment was made with the help of crystallographic studies.<sup>24</sup>

Gluconamide **2a** does not have an extensive hydrogen bonding network that breaks down upon dissolving this compound in water. In order to investigate the effect of the methylene bridges in the absence of the imidazole group, DSC thermograms of gluconamide **4a** in water were recorded. In the heating scan of **4a** only one transition at 51 °C was observed (see Table 4.4).

**4a**  $n = 7$ **b**  $n = 11$ **c**  $n = 15$ 

The lack of a transition at approximately 65 °C was expected, because **4a** cannot form a hydrogen bonding network of the type compound **1** does. More surprising was the relatively low Krafft temperature of **4a**. It shows that the solubility of the gluconamide in water is raised by the introduction of the 2,4;3,5-bismethylene bridges. Like **1**,<sup>25</sup> **4a** has the possibility to form intermolecular amide hydrogen bonds, which are expected to disappear at approximately 75 °C.<sup>24</sup> Apparently, the amide hydrogen bonds in the assembly of **4a** are much weaker than those of **1**, or the amide hydrogen bonds do not influence the solubility of the compounds. Upon cooling no transition was found for compound **4a**, which means that **4a** remained dissolved in the cooling run.

**Table 4.4** Krafft temperatures and enthalpies of dissolution of *N,n*-octyl-D-gluconamides <sup>a</sup>

Compound	$T_{\text{krafft}}$ (°C)	$\Delta H_{\text{diss}}$ (kJ/mol)
<b>1</b>	73.4	32.6
<b>2a</b>	77.9	29.9
<b>4a</b>	51.4	29.4
<b>5</b>	106.4	36.3

<sup>a</sup> Values obtained from DSC thermograms (first heating run)

The  $T_{\text{krafft}}$  of non-protonated **2a** in Tris buffered water (pH=8.5) was found to be higher than that of **4a** and **1** (Table 4.4). This suggests that in crystalline **2a** a strong interaction is present between the imidazole groups. This conclusion is supported by the observation that  $T_{\text{krafft}}$  drops considerably upon protonation of **2a** (see Table 4.5).

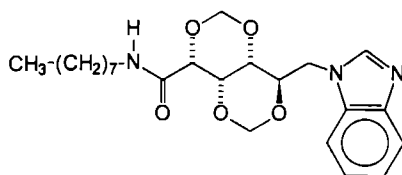
The cooling run of **2a** in Tris buffered solution, did not show any transitions. Despite the lack of transitions in the thermograms, aggregates were formed according to electron microscopy (see Section 4.3.5). This suggests that the transitions are too small to be measured, or that the formation of the aggregates is too slow to be detected by DSC (heating and cooling runs were taken at 5 °C/min.).

**Table 4.5**  $T_{\text{Krafft}}$ , enthalpy and entropy of dissolution of compounds **2**<sup>a</sup>

Compound	Solvent	$T_{\text{Krafft}}$ (°C)	$\Delta H_{\text{diss}}$ (kJ/mol)	$\Delta S_{\text{diss}}$ (J/(mol °K))
<b>2a</b>	Tris buffer <sup>b</sup>	77.4	32.3	92.2
<b>2a</b>	HAc/NaOAc buffer <sup>c</sup>	43.1	56.4	178.4
<b>2b</b>	Tris buffer <sup>b</sup>	95.2	54.2	145.4
<b>2b</b>	HAc/NaOAc buffer <sup>c</sup>	91.5	46.5	127.0
<b>2c</b>	Tris buffer <sup>b</sup>	102.1	62.6	166.9
<b>2c</b>	HAc/NaOAc buffer <sup>c</sup>	99.7	63.4	170.1

<sup>a</sup> Obtained from DSC thermograms (heating and cooling rate 5 °C/min)<sup>b</sup> pH= 8.5<sup>c</sup> pH= 4.5

For comparison, we also recorded DSC thermograms of the benzimidazole derivative **5** in Tris buffered solution at pH=8.5, where **5** is not protonated ( $\text{pK}_{\text{a}}$  5.53<sup>15</sup>). A dramatic increase in  $T_{\text{Krafft}}$  was observed as compared to gluconamide **2a** (see Table 4.4). Gluconamide **5** crystallized in the cooling run at 63.7 °C, which demonstrates that the introduction of an additional aromatic ring reduces the amphiphilic character of the compound.

**5**

The compounds in Table 4.4 all have the same alkyl chain. We may conclude from the data in this table that changes in the carbohydrate part of the molecule have a strong effect on  $T_{\text{Krafft}}$  but only a weak effect on ( $\Delta H_{\text{diss}}$ ). The effect of varying the alkyl chain length was investigated for compounds **2** and **4**. For the former compound elongation of the alkyl chain resulted in higher  $T_{\text{Krafft}}$  and  $\Delta H_{\text{diss}}$  values (see Table 4.5). The same trend was found for compounds **4** although the increases were less dramatic (see Table 4.6).

**Table 4.6**  $T_{\text{Krafft}}$  and  $\Delta H_{\text{diss}}$  and  $\Delta S_{\text{diss}}$  values of compounds **4** in water<sup>a</sup>

Compound	$T_{\text{Krafft}}$ (°C)	$\Delta H_{\text{diss}}$ (kJ/mol)	$\Delta S_{\text{diss}}$ (J/(mol °K))
<b>4a</b>	51.4	29.4	90.6
<b>4b</b>	63.8	36.5	108.4
<b>4c</b>	71.4	40.4	117.3

<sup>a</sup> Values obtained from DSC thermograms (first heating runs)

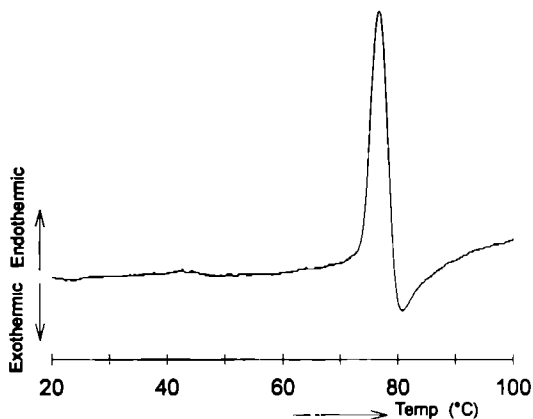
The effect of protonation of the imidazole group on  $T_{\text{krafft}}$  decreased by elongation of the alkyl chain. In Chapter 3 we showed that for a series of homologous liquid crystalline gluconamides the clearing points are dependent and the melting points are independent on the length of the alkyl chain. The melting points of the thermotropic liquid crystalline systems and the  $T_{\text{krafft}}$  values of the lyotropic liquid crystalline systems should show similar trends because in both cases the supramolecular ordering of the molecules is destroyed by passing the transition temperature. It is clear from Tables 4.5 and 4.6 that no such trend exists:  $T_{\text{krafft}}$  depends on the length of the alkyl chain. An explanation for this behavior may be that in the case of the lyotropic systems the entropy effect plays an important role. Tables 4.5 and 4.6 reveal that the entropy of the non protonated **2** and **4** increases upon elongation of the alkyl chain length. This increase in  $\Delta S$  is readily explained because larger molecules must be solvated by more water molecules (reversed hydrophobic effect).

Gluconamides **2b** and **2c** appeared not to be suitable for the formation of supramolecular aggregates in water because these compounds, both in protonated and neutral form, recrystallized very fast from aqueous solutions. Compounds **4b** and **4c** crystallized from water without forming aggregates and were not further investigated by DSC or EM.

### Copper(II) complexes

From the UV-vis titration experiments (vide supra) it is clear that **2a** and  $\text{Cu}(\text{ClO}_4)_2$  ions form  $[(\mathbf{2a})_4\text{Cu}]^{2+}$  complexes. When a mixture of 4 equivalents of **2a** and 1 equivalent of  $\text{Cu}(\text{ClO}_4)_2$  was heated, an endothermic peak at 73.8 °C was observed, directly followed by an exothermic effect peak. The transitions partly overlapped each other (see Figure 4.6). The endothermic peak may be related to the  $T_{\text{krafft}}$  of the complex  $[(\mathbf{2a})_4\text{Cu}][\text{ClO}_4]_2$  and the endothermic peak to the destruction of the complex. Another possibility is that the ligand has to be dissolved before the complex can be formed which would explain why the  $T_{\text{krafft}}$  is very similar to that of the free ligand ( $T_{\text{krafft}}$  77.9 °C, Table 4.4). In the latter case the heat effects are a combination of dissolving **2a** (endothermic effect) and the formation of the complex (exothermic effect). Such a combination of heat effects would be in line with the fact that  $\Delta H_{\text{diss}}$  of the complex\*\* is lower than  $\Delta H_{\text{diss}}$  of the free ligand ( $\Delta H_{\text{diss}}$  for **2a** = 32.3 kJ/mol and  $\Delta H_{\text{diss}}$  for  $[(\mathbf{2a})_4\text{Cu}][\text{ClO}_4]_2$  = 15.8 kJ/mol). A DSC scan of a sample of  $[(\mathbf{2a})_4\text{Cu}][\text{ClO}_4]_2$  that had been precipitated from methanol, showed in water a transition at a much higher temperature (115.6 °C, see Table 4.7, only an endothermic peak was observed). This relatively high transition may indicate that the precipitated complex is hydrated or contains methanol as an additional ligand.

\*\* The  $\Delta H_{\text{diss}}$  was corrected by multiplying it with the factor (Mw complex)/(Mw ligand)



**Figure 4.6** DSC heating scan of **2a** + 0.25 equivalents of  $\text{Cu}(\text{ClO}_4)_2$  in water

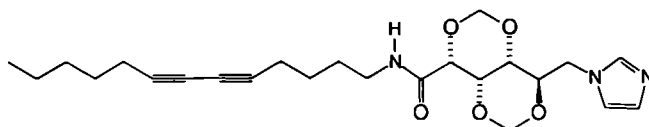
**Table 4.7** DSC of  $\text{Cu}(\text{ClO}_4)_2$  complexes <sup>a</sup>

Ligand	Transition temp in heating run (°C)
<b>2a</b>	73.8
<b>2a<sup>b</sup></b>	115.6
<b>5</b>	102.0
<b>6</b>	84.5

<sup>a</sup> Concentration of the ligands was 1 % w/v

<sup>b</sup> Metal complex was prepared previously by precipitation from methanol

The DSC scan of a mixture of 4 equivalents of the benzimidazole derivative **5** and 1 equivalent of  $\text{Cu}(\text{ClO}_4)_2$  in water showed an endothermic peak at 102 °C which is a similar result as obtained for the free ligand in Tris buffered solution (106.4 °C, Table 4.4). In contrast to the free ligand the copper complex  $[(\mathbf{5})_4\text{Cu}][\text{ClO}_4]_2$  did not crystallize upon cooling. Compound **6**, which is similar to **2** except for the diacetylene function in the aliphatic chain, behaved differently in the DSC runs. For unknown reasons the endothermic peak of the free ligand (103 °C) was much higher than that of the complex (84.5 °C).



**6**

#### 4.3.4 Electron microscopy

Compound **1** is known<sup>1</sup> to form helical ropes which can be visualized by transmission electron microscopy (TEM). The ropes have a regular winding consisting of bulges and knots with diameters of resp. 18.6 and 8.6 nm and a pitch of 22.4 nm.<sup>1,2</sup> There has been discussion as to whether the helical ropes are composed of 2,<sup>2</sup> 4,<sup>5</sup> or 6<sup>26</sup> strands. The current opinion is that the 6 strand model is the most likely one.<sup>26</sup> The aggregates of **1** in water are stabilized by numerous hydrogen bonds,<sup>1</sup> which give the micellar fibers a crystalline core.<sup>5</sup>

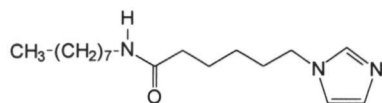
Compound **4a**, which lacks the possibility to form an extensive hydrogen bonding network, dissolved in water, but did not form aggregates according to EM. The solubility of **4a** in water is surprising because four of the five hydroxyl groups are protected. Elongation of the aliphatic chain to dodecyl (**4b**) or hexadecyl (**4c**) decreased the solubility but still no aggregates could be observed by EM.

Gluconamide **2a** also contains protected hydroxyl groups but this compound did form aggregates according to EM. In Tris buffered aqueous solution (pH=8.5) in which **2a** is not protonated, very long fibrous structures were visible (diameter approximately 100 nm length 50  $\mu$ m, see Figure 4.7A). Figure 4.7B shows a fiber that is in the process of being formed from a multi layer tape; for a schematic drawing see Figure 4.7C. The existence of multi-layered structures was shown by freeze fracture experiments in combination with EM (see Figure 4.7B inset). It is not clear from the electron micrographs whether the fibers are hollow or not. Experiments with staining agents as described by Fuhrhop<sup>27</sup> to prove their hollow nature failed. The fibers can assemble to larger tubuli as is shown in Figure 4.7D (arrow shows a fiber which is fused to a tubule). According to this figure the large tubules (diameter approximately 3  $\mu$ m) are hollow.

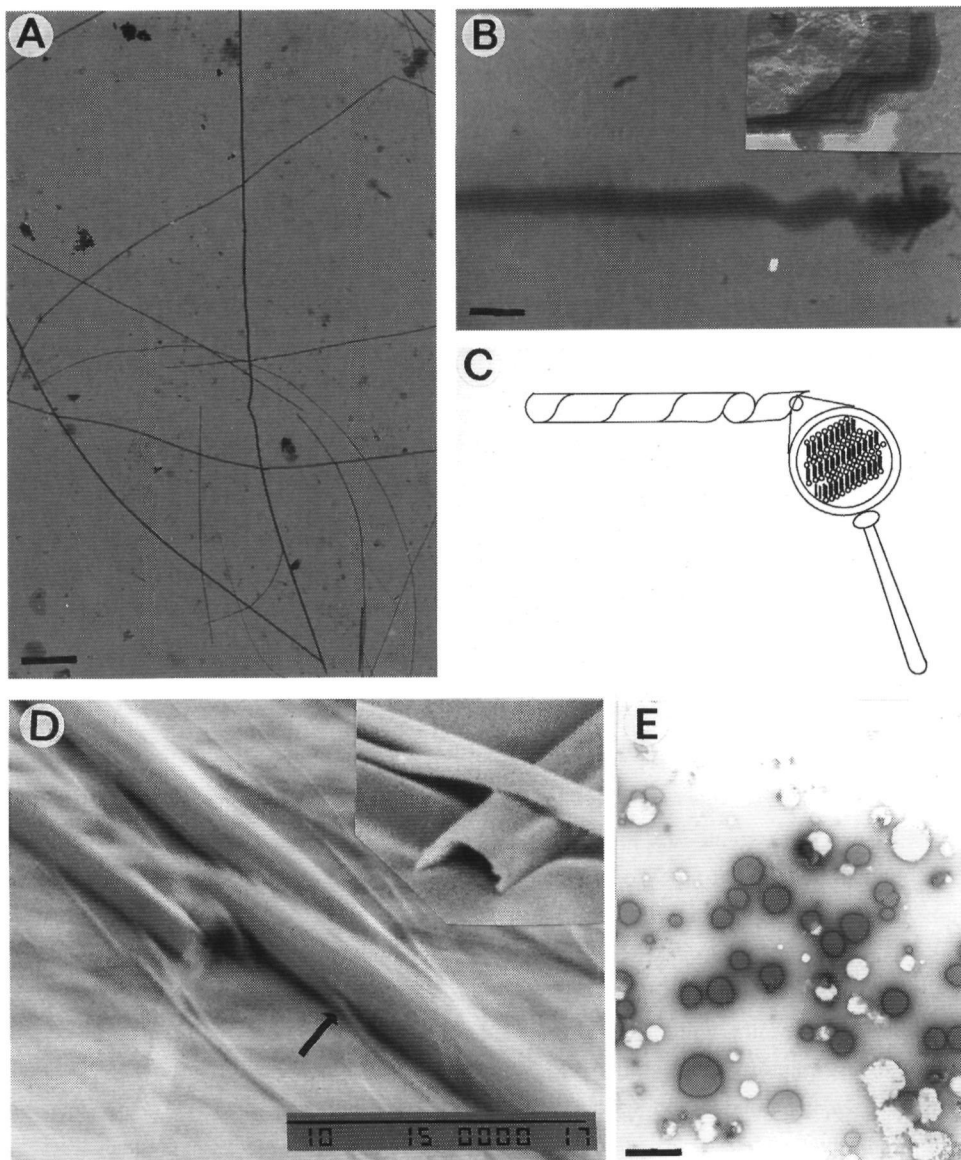
Dissolving compound **2a** in an aqueous acetic acid/sodium acetate buffer (pH=4.5) leads to protonation of the imidazole group. In this buffered solvent vesicles with diameters ranging from 160 to 780 nm were formed (see Figure 4.7E). Apparently upon protonation the diameter of the head group increases in size, making that vesicle structures become thermodynamically more favorable than fiber structures. The architecture of the aggregates formed from compound **2a** thus can be tuned by changing the pH.

The long chain derivatives **2b** and **2c** crystallized upon cooling to room temperature and no suprastructures could be observed by EM. As a reference compound for **2a**, we also studied the imidazole containing amide **7** which lacks the (protected) carbohydrate part. It is likely that the imidazole group in **7** has a similar  $pK_a$  as the imidazole groups in methylimidazole, **2a**, and **3**. Contrary to **2a**, compound **7** did not dissolve in (warm) Tris buffered water (pH=8.5). In aqueous acetic acid/acetate buffer (pH=4.5), **7** dissolved, but EM did not show aggregates. We may conclude therefore, that the carbohydrate moiety is indispensable for the formation of suprastructures, even when its secondary OH groups are protected and cannot form H-bonds. A similar conclusion was drawn with regard to the thermotropic L.C. behavior of the series of compounds **2** (Chapter 3).





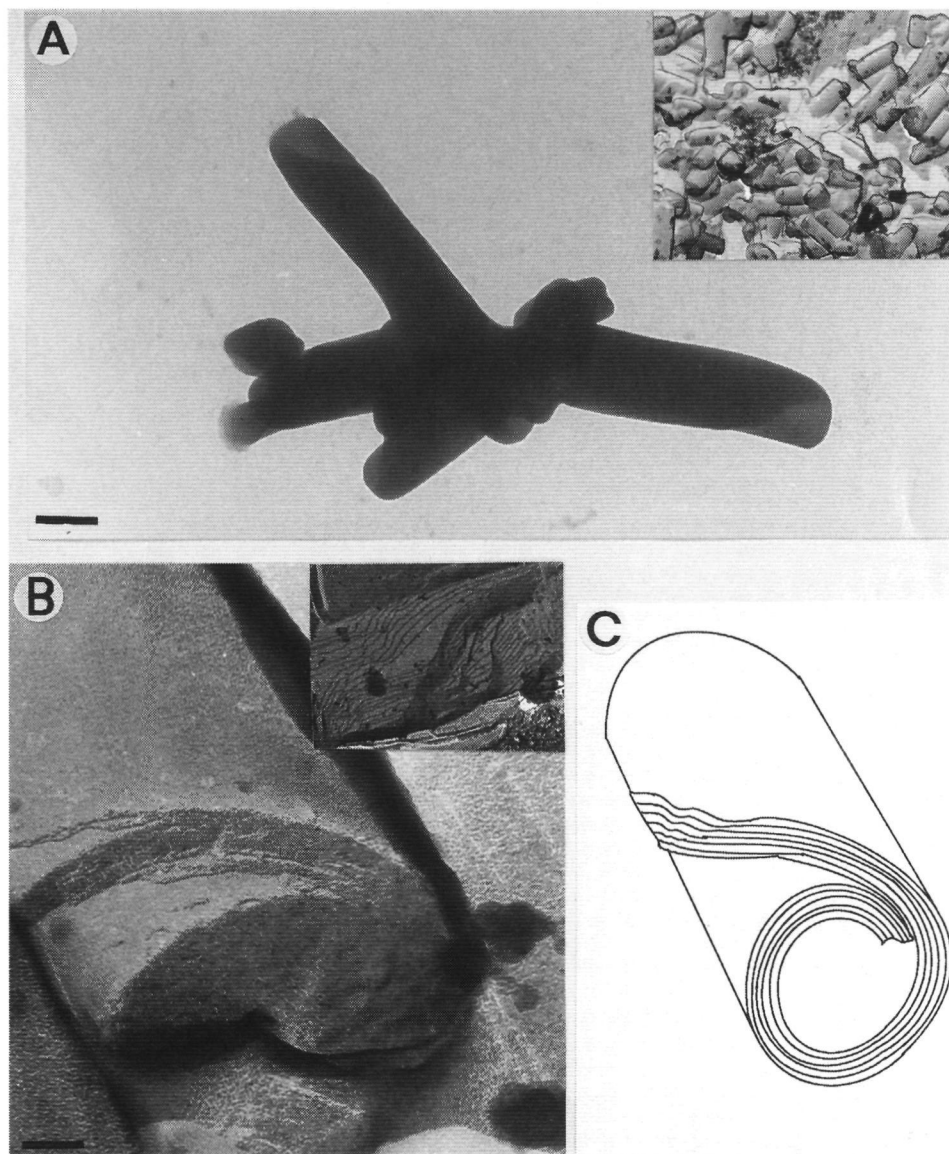
7



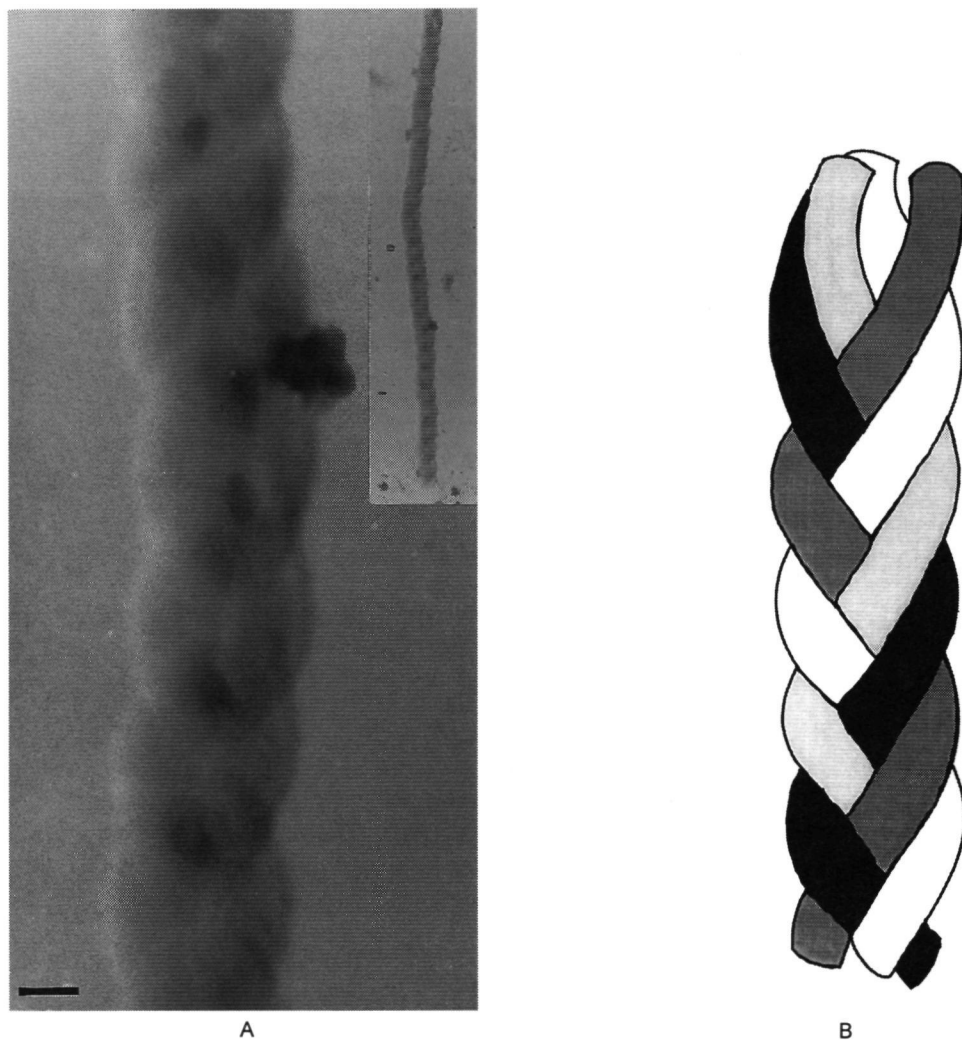
**Figure 4.7** Transmission and Scanning Electron Micrographs (TEM + SEM) of aggregates formed from **2a** in aqueous solutions. A) TEM of fibers of non-protonated **2a**, bar is 3.27  $\mu\text{m}$ . B) Fiber of **2a** in the process of being formed from a tape of multilayers (no staining), bar is 345 nm; inset (freeze fracture technique) shows these multilayers in detail. C) Schematic drawing of the process shown in (B). D) SEM of hollow tubuli and thin fibers of **2a** (bar is 10  $\mu\text{m}$ ); inset shows hollow tube. E) TEM of vesicles formed from **2a** at pH 4.5 (carbon supported hydrophilic copper grid stained with 2 % uranyl acetate), bar is 1.46  $\mu\text{m}$ .

*Copper (II) perchlorate complexes.*

Addition of  $\text{Cu}(\text{ClO}_4)_2$  to a warm clear solution of **2a** in water resulted in the formation of a pale blue turbid mixture. Electron micrographs of this mixture showed, besides multilayered scrolls (Figure 4.8), also a braid-like structure (Figure 4.9).



**Figure 4.8** Scrolls generated from  $[(2\mathbf{a})_4\text{Cu}][\text{ClO}_4]_2$  in water. A) TEM picture of scrolls having diameters of ca. 350 nm. This picture was made without any staining. The wrapping angle of the stretched multilayers is approximately  $45^\circ$ , bar is 230 nm. B) Freeze-fracture electron micrographs of scrolls; inset shows a more detailed picture, bar is 56 nm. C) Schematic drawing of a scroll.



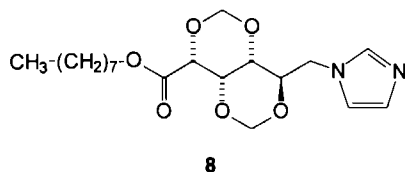
**Figure 4.9** Braided structures formed by  $[(2a)_4Cu][ClO_4]_2$  in water. A) TEM picture without staining; the copper grid was supported with Formvar; bar is 200 nm; the diameter of the braid is 330 nm, the pitch is 980 nm, and the diameter of a single strand is 100 nm, bar is 147 nm. B) Schematic model of the braid.

These micrographs were taken without the use of staining agents: the darkening is due to the presence of the copper ions in the aggregates. Freeze-etching experiments revealed that the scrolls consisted of layers (inset Figure 4.8B). Without copper ions present, **2a** also formed a layered structure (vide supra). This result suggests that the copper ions do not cause any change, but are merely incorporated into a structure that also would have been formed without their presence. A similar phenomenon was observed in the thermotropic L.C. study: long chain derivatives of **2a** formed a smectic phase that was stabilized rather than changed by the addition of copper ions (see

merely incorporated into a structure that also would have been formed without their presence. A similar phenomenon was observed in the thermotropic L.C. study. long chain derivatives of **2a** formed a smectic phase that was stabilized rather than changed by the addition of copper ions (see Chapter 3).<sup>28</sup> Hence, to a great extent the lyotropic and thermotropic liquid crystalline behavior of compounds **2** are comparable. Although the aqueous aggregates both with and without copper have a layered structure, copper has an extra effect: it directs the assembled molecules to a higher organization resulting in scrolls and braids.

The EM picture shown in Figure 4.9 reveals that the braid consists of several strands. A model in which 4 different strands are intertwined seems to match best with the electron micrograph (see Figure 4.9B). Further studies and detailed analysis with the help of a computer are required, however. The individual strands have the same diameter (100 nm) as the fibers formed **2a** without copper ions, which supports the theory that the copper ions stabilize the supramolecular organization and do not change the aggregate structure itself.

We also investigated the self-assembling properties of the copper complexes of a series of reference compounds (**5-8**). Addition of  $\text{Cu}(\text{ClO}_4)_2$  to a mixture of compound **7** resulted in a turbid mixture that turned into a dark blue solution upon cooling to room temperature. Just like in the case without copper ions present, no aggregates were found by EM, again proving that the carbohydrate segment is indispensable for the formation of the supramolecular structures. This result further supports the idea that the ligand and not the copper ion dominates the (molecular) organization. Compound **8** is very similar to **2a** but has an ester linkage between the alkyl chain and the carbohydrate head group. On dispersal in water the copper complex  $[(\mathbf{8})_4\text{Cu}][\text{ClO}_4]_2$  gave vesicles with diameters ranging from 100 to 560 nm (electron micrograph not shown). Thus, the linkage does not have to be an amide group for aggregates to be formed. The shape of the aggregates, however, is influenced by the linkage: an ester function yields vesicles, whereas an amide function leads to scrolls and braids.



This result is of interest because it has been reported in the literature that the amide group does not determine the aggregation behavior of the gluconamide: the thermotropic LC behavior (transition temperature, enthalpy peak size, and peak shape) of n-octylgluconate, the derivative of compound **1** with an ester linkage, was found to be very similar to that of **1**.<sup>29</sup>

The copper complex of the benzimidazole compound **5**, also gave vesicles on dispersal in water. The diameters of the aggregates ranged from 95 nm to 285 nm (electron micrograph not shown). The extra phenyl ring in the head group of the amphiphile apparently prevents that the complex  $[(\mathbf{5})_4\text{Cu}][\text{ClO}_4]_2$  forms braids and scrolls as  $[(\mathbf{2a})_4\text{Cu}][\text{ClO}_4]_2$  does.

The diacetylene derivative **6** was not soluble enough in water ( $T_{\text{kraft}} = 103\text{ }^{\circ}\text{C}$ ) for a proper sample preparation, even not after prolonged heating. According to DSC, the in situ prepared complex  $[(\mathbf{6})_4\text{Cu}][\text{ClO}_4]_2$  crystallized at  $91\text{ }^{\circ}\text{C}$  upon cooling. The isolated copper complex, prepared in ethanol,<sup>30</sup> could not be studied either due to lack of solubility.

#### *Copper (II) complexes with other anions than perchlorate*

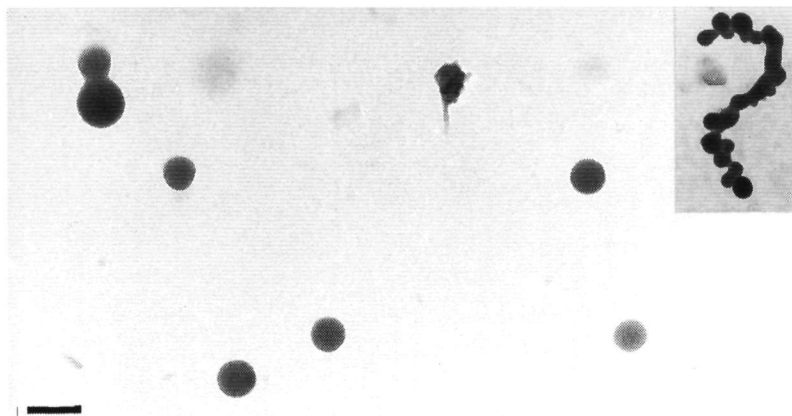
The complex of copper triflate and **2a**<sup>31</sup> is poorly dispersible in water. On the other hand, when the copper complex was made in situ by mixing aqueous solutions of  $\text{Cu}(\text{OSO}_2\text{CF}_3)_2$  and **2a** in a 1:4 metal to ligand ratio, a turbid mixture was obtained. EM showed that this mixture contained ill-defined structures even after 5 minutes of sonication at  $70\text{ }^{\circ}\text{C}$  (pictures not shown).

According to the UV-vis titration experiments described in Section 4.3.2, **2a** can form 1:2 metal to ligand complexes with  $\text{CuCl}_2$ . Mixing this copper salt with **2a** in a 1:2 ratio resulted in rapid precipitation of the complex and no suprastructures were formed. A DSC scan showed an exothermic transition at  $83\text{ }^{\circ}\text{C}$ . Because of this fast precipitation, no further studies were carried out.

#### *Cobalt (II) and nickel complexes*

Mixing  $\text{Co}(\text{ClO}_4)_2$  with **2a** in a 1:3 ratio in water resulted in a turbid mixture that precipitated after cooling in one day. The cobalt complex, however, was easy to redisperse. TEM without staining showed two types of aggregates: vesicle-like structures which appeared greyish under the electron microscope (relatively low cobalt content), and larger, intensely black particles, probably with a high cobalt content (pictures not shown). The latter aggregates were not uniform in size (162 - 920 nm), while the diameter distribution of the grey particles was smaller (70 - 200 nm). Since no additional staining agent was used and the coloring of the particles originates from the cobalt ions only, the grey particles probably are vesicles with a thin wall consisting of only one or a few bilayers and the intensely black particles probably are amorphous agglomerates of cobalt complexes. Besides the grey aggregates, the black particles were still observed after sonication at elevated temperature ( $70\text{ }^{\circ}\text{C}$ ).

Addition of 1 equivalent of  $\text{Ni}(\text{ClO}_4)_2$  to a warm, clear solution of 6 equivalents of **2a** in water gave an opalescent turbid mixture, like most of the metal complexing salts described so far. But unlike the other aqueous metal-containing mixtures, this suspension was stable for weeks. TEM without staining showed that it contained almost perfectly spherical particles. Freshly prepared and aged samples were indistinguishable from each other. The particles were intensely black, which indicates a high nickel content (see Figure 4.10).

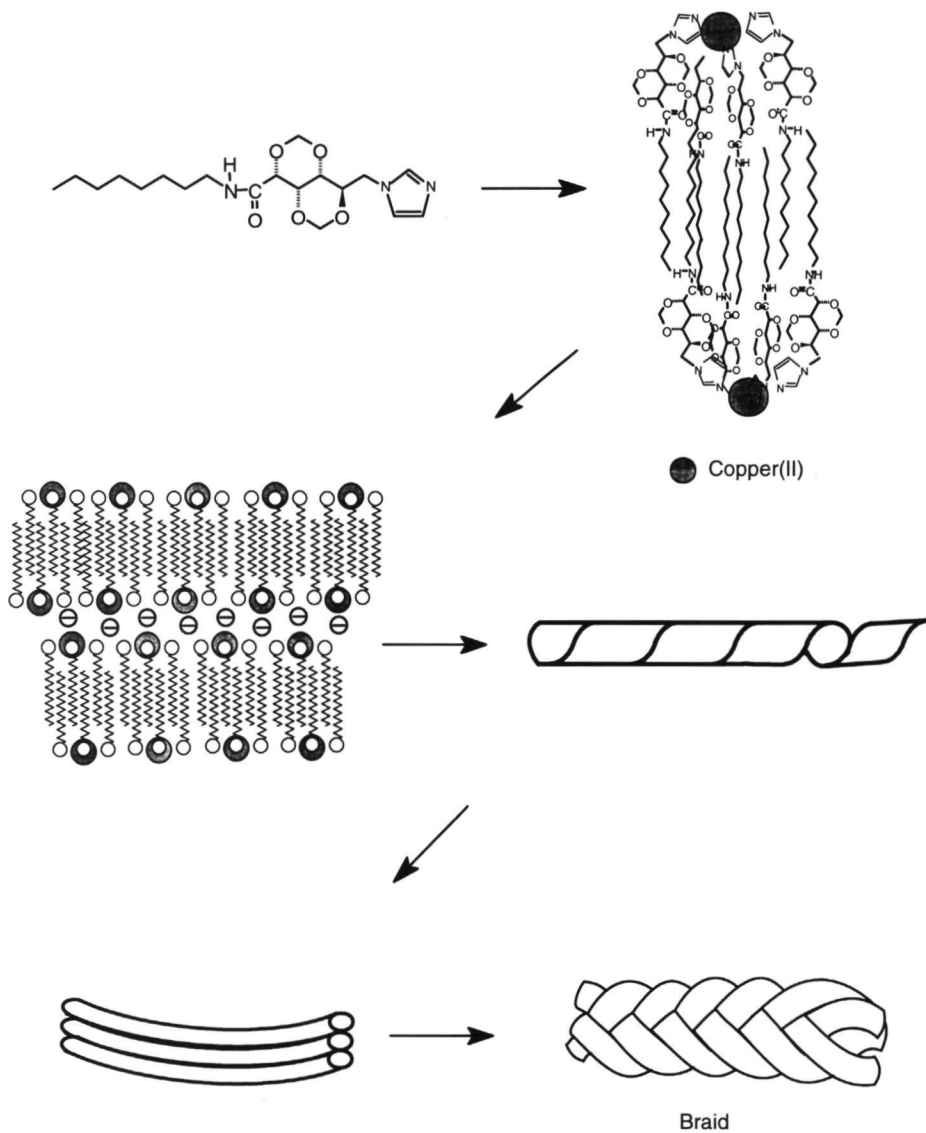


**Figure 4.10** TEM pictures of particles prepared by dispersing of  $[(\mathbf{2a})_3\text{Ni}](\text{ClO}_4)_2$  in water (no additional staining was used). Inset clustering of the particles, bar is 163 nm.

#### 4.4 Concluding remarks

Gluconamide **1** contains five unprotected hydroxyl functions and forms supramolecular aggregates in water with an almost crystalline character.<sup>5</sup> When the hydroxyl functions on carbon atoms 2, 3, 4, and 5 are protected, the compound is still soluble in water but no aggregates are visible by EM. When, however, an imidazole function is introduced on carbon atom 6 fibers, tubes, vesicles, scrolls, and braids can be prepared from the protected gluconamides. The type of aggregate structure depends on the reaction conditions. In slightly basic aqueous solutions fibers are generated that can further assemble to tubes. In acidic solutions vesicles are formed. Addition of copper perchlorate yields scrolls and braids, while nickel and cobalt perchlorate give vesicles. Although the form of the suprastructures is different, in many cases the underlying molecular pattern is the same, *viz.* a layered structure. Apparently, the carbohydrate amphiphile determines the basic mode of molecular assembling, while much of the fine tuning is achieved by the metal ions or protons present.

The most interesting suprastructure discussed in this chapter is the copper containing molecular braid. If we combine the results from the thermotropic L.C. studies described in Chapter 3 with the crystal structure of compound **2a** and the UV-vis titration experiments, we may hypothesize about the way this braid is formed from its molecular components, see Figure 4.11. Steps 1 and 2 follow from the X-ray structure of **2a** and the similarity between the thermotropic LC behavior of the series of compounds **2** and their copper(II) complexes (see Chapter 3). Step 3 (rolling up of the multilayer tape) is supported by the electron micrographs shown in Figure 4.8. Steps 4 and 5 are not supported by any experimental data. Further studies must reveal whether these steps are feasible or whether the braid is formed via a direct route from the multilayer tapes.



**Figure 4.11** Possible route for the formation of the molecular braid.

## 4.5 Literature

- <sup>1</sup> Pfannemüller, B ; Welte, W *Chem Phys Lipids* **1985**, *37*, 227.
- <sup>2</sup> Fuhrhop, J -H ; Schnieder, P , Rosenberg, J., E Boekema *J Am Chem Soc* **1987**, *109*, 3387.
- <sup>3</sup> Köning, J , Boettcher, C ; Winkler, H ; Zeitler, E.; Talmon, Y.; Fuhrhop, J.-H *J Am Chem Soc* **1993**, *115*, 693
- <sup>4</sup> a) Fuhrhop, J -H , Svenson, S.; Boettcher, C , Rössler, E , Vieth, H.-M *J Am Chem Soc* **1990**, *112*, 4307, b) Svenson, S ; Kirste, B , Fuhrhop, J -H *J Am Chem Soc* **1994**, *116*, 11969.
- <sup>5</sup> Svenson, S., Köning, J , Fuhrhop, J -H *J Phys Chem* **1994**, *98*, 1022.
- <sup>6</sup> Fuhrhop, J -H , Boettcher, C. *J Am Chem Soc* **1990**, *112*, 1768
- <sup>7</sup> Fuhrhop, J -H , Demoulin, C ; Rosenberg; Boettcher, C *J Am Chem Soc.* **1990**, *112*, 2827
- <sup>8</sup> a) Yager, P ; Schoen, P E ; Davies, C.; Price, R , Singh, A. *Biophys J* **1985**, *48*, 899; b) Markowitz, M A , Schnur, J M Singh, A. *Chem Phys Lipids* **1992**, *62*, 193.
- <sup>9</sup> Kunitake, T ; Kim, J -M ; Ishikawa, Y *J Chem Soc , Perkin Trans 2* **1991**, 885
- <sup>10</sup> Shimizu, T.; Mori, M , Minamikawa, H., Hato, M *J Chem Soc , Chem Commun* **1990**, 183
- <sup>11</sup> Tachibana, T , Kambara, H *J Colloid Sci* **1968**, *28*, 173.
- <sup>12</sup> Papahadjopoulos, D , Vail, W J ; Jacobsen, K , Poste, G *Biochim Biophys Acta* **1975**, *394*, 483
- <sup>13</sup> Hafkamp, R J H , Feiters, M C ; Nolte, R.J.M *Angew Chem.* **1994**, *106*, 1054, *Ibid Int Ed Engl* **1994**, *33*, 986
- <sup>14</sup> a) Komura, H , Yoshino, T , Ishido, Y *Carbohydrate Res* **1973**, *31*, 154, b) Yoshino, T., Inabe, S , Komura, H., Ishido, Y *Bull Chem Soc Japan* **1974**, *47*, 405.
- <sup>15</sup> *CRC Handbook of Chemistry and Physics 58<sup>th</sup> ed* , Editor R C Weast, CRC Press, Cleveland Ohio, **1977-1978**, D-148
- <sup>16</sup> Perrin, D.; Dempsey, B. *Buffers for pH and metal ion control*, Wiley and Sons, London **1974**.
- <sup>17</sup> Reedijk, J. *Recl Trav Chim. Pays-Bas* **1969**, 1451.
- <sup>18</sup> We initially assumed that the complexation behavior of  $\text{Co}(\text{ClO}_4)_2$  and  $\text{Ni}(\text{ClO}_4)_2$  with **2a** would be similar to that of imidazole as described in the literature (ref 17), and, therefore, **2a** and the metal salts were mixed in a 6:1 (ligand/metal) stoichiometry Later, we learned from UV-vis titrations that the complexation behavior of **2a** is different: with  $\text{Co}(\text{II})$  and with  $\text{Ni}(\text{II})$  3:1 ligand to metal complexes are formed.
- <sup>19</sup> Bernarducci, E., Schwindinger, W.F ; Hughey, IV, J L.; Krogh-Jespersen, K., Schugar, H J. *J Am Chem Soc* **1981**, *103*, 1686
- <sup>20</sup> Esch, J van; Damen, M.; Feiters, M C , Nolte, R.J.M *Recl Trav Chim Pays-Bas* **1994**, *113*, 186
- <sup>21</sup> Arevalillo, A.; Pena, M J. *Electrochim Acta* **1993**, *38*, 957
- <sup>22</sup> Coyle, C L , Stiefel, E I. *The Bioinorganic Chemistry of Nickel*, ed. Lancaster Jr, J.R VCH Publishers, Inc , Weinheim, **1988**, 6
- <sup>23</sup> a) Shinoda, K, Hutchinson, E *J Phys Chem* **1962**, *66*, 577, b) Shinoda, K; Yamaguchi, N ; Carlsson, A. *J Phys Chem* **1989**, *93*, 7216, c) Raaijmakers, H W.C.; Arnouts, E G., Zwanenburg, B; Chittenden, G J F , Doren van, H.A *Recl Trav Chim Pays-Bas* **1995**, *114*, 301
- <sup>24</sup> Pfannemüller, B , Kühn, I *Macromol Chem* **1988**, *189*, 2433.
- <sup>25</sup> Zabel, V; Müller-Fahrmow, A., Hilgenfeld, R ; Saenger, W ; Pfannemüller, B ; Enkelmann, V.; Welte, W *Chem Phys Lipids* **1986**, *39*, 313



<sup>26</sup> Fuhrhop, J -H, Köning, J *Membranes and Molecular Assemblies The Synkinetic Approach*, part of the series "Monographs in Supramolecular Chemistry" series ed Stoddart, J F , The Royal Society of Chemistry, Cambridge (UK) **1994**, pag IX

<sup>27</sup> Fuhrhop, J -H , Spiroski, D , Boettcher, C *J Am Chem Soc* **1993**, *115*, 1600

<sup>28</sup> See Chapter 3, section 3 3 7, compound [(1d)<sub>4</sub>Cu][OTf]<sub>2</sub>

<sup>29</sup> Pfannemüller, B , Welte, W , Chin, E , Goodby, J W *Liq Cryst* **1986**, *1*, 357

<sup>30</sup> Synthesis was described in Chapter 3, compound [(19)<sub>4</sub>Cu][OTf]<sub>2</sub>

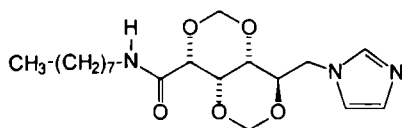
<sup>31</sup> See Chapter 3, Section 3 3 4, compound [(6a)<sub>4</sub>Cu][OTf]<sub>2</sub>

## Chapter 5

### Positional variation of the imidazole group in gluconamide amphiphiles. Effects on the aggregation behavior

#### 5.1 Introduction

In Chapter 3 we described the synthesis and thermotropic liquid crystalline behavior of amphiphilic 6-deoxy-6-(1-imidazolyl)-2,4;3,5-dimethylene-*N*,*n*-octyl-*D*-gluconamides (e.g. **1**) and their copper complexes, e.g.  $\text{Cu}(\textbf{1})_4$ . From both the X-ray structure of **1** and the study of the liquid crystalline properties of a series of compounds related to **1** and  $\text{Cu}(\textbf{1})_4$ , we concluded that in the superstructures of **1** and  $\text{Cu}(\textbf{1})_4$ , the imidazole group plays an important role in the packing of the molecules, viz. via hydrogen bonded water molecules and complexed copper ions.

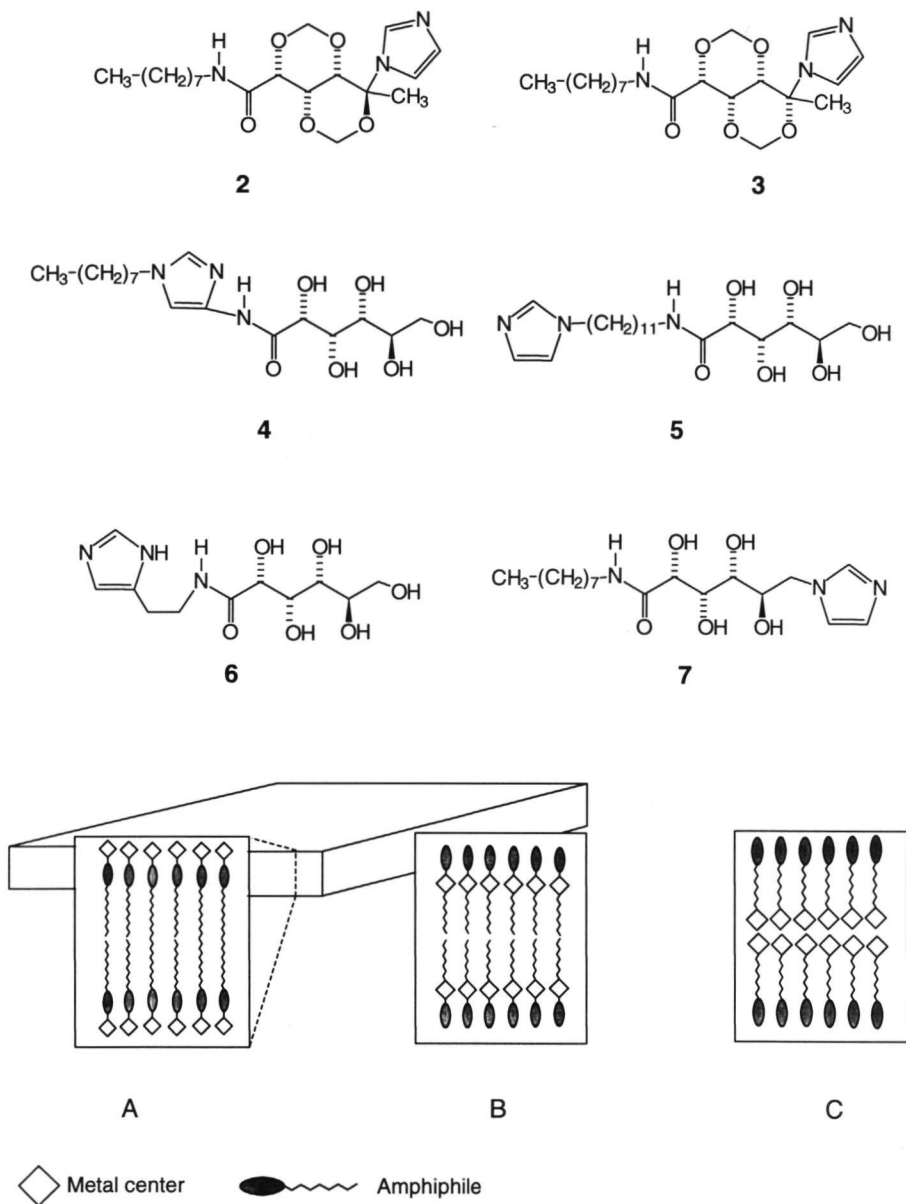


**1**

We also concluded that the rigid *cis*-decaline structure of the methylene protected glucon head group is indispensable for the formation of aggregates in water, because *N*,*n*-octyl-6-(1-imidazolyl)-*n*-hexanoic acid amide and its derived copper complex, which both lack the carbohydrate framework, did not form supramolecular structures in this solvent (see Chapter 4).

In order to investigate the effect of the position of the imidazole group in the amphiphile on the aggregation behavior of this molecule, we prepared and studied gluconamide derivatives **2-6**. Compounds **4-6** were not provided with methylene-protecting groups because of synthetic problems. For reasons of comparison we also synthesized gluconamide **7** and 1-*n*-hexadecylimidazole **8**. In compound **7** the imidazole group is attached to the carbohydrate framework, but in contrast to **1**, this compound lacks the methylene protecting groups.

Metal complexes of amphiphiles<sup>1,2,3</sup> containing imidazole groups are of interest for catalytic applications (see Chapter 7).<sup>4</sup> Another reason for synthesizing compounds **2-6**, therefore, was to see whether these compounds could be used to design new types of amphiphilic catalysts, i.e. catalysts in which the metal center is located at different, but well-defined positions, in the supramolecular aggregate, see Figure 5.1.



**Figure 5.1** Assemblies of amphilic metal complexes in which the metal is located at different positions in the aggregate. A) Metal centers at the aqueous interface as observed for  $\text{Cu(1)}_4$ . B) Metal centers located between the head group region and the aliphatic chain as expected for metal complexes of compound 4. C) Metal centers in the center of the bilayer, as expected for metal complexes of compound 5.

## 5.2 Experimental section

Analytical instruments and electron microscopes were identical to those described in the Chapters 3 and 4.

The  $pK_a^*$  values of compounds **4** and **7** were determined as described in Chapter 4.

### 5.2.1 Syntheses

For numbering of protons and carbon atoms see Chapter 3.

**6-Deoxy-6-iodo-2,4;3,5-dimethylene-*N*,*n*-octyl-D-gluconamide (9).** This compound was synthesized by dissolving 10.039 g (20.67 mmol) of 6-tosyloxy-2,4;3,5-dimethylene-*N*,*n*-octyl-D-gluconamide (the synthesis of this tosylate was described in Chapter 3) and 15.587 g (103.99 mmol) of NaI in 75 ml of anhydrous acetone and stirring overnight in an autoclave at 100 °C. After the precipitated NaOTs had been removed by filtration, the solution was evaporated to dryness. The product was dissolved in chloroform and subsequently washed with water. After drying, a white powder was obtained, yield 8.61 g (19.50 mmol, 94.3 %) of **9**, m.p. 160.9 °C. IR (KBr) 3304  $\text{cm}^{-1}$  (NH), 1657 (amide I), 1549 (amide II), 723 (C-I).  $^1\text{H-NMR}$  (90 MHz,  $\text{CDCl}_3$ )  $\delta$  6.520 ppm (t, 1H, NHCO), 5.264 (d,  $J_{7a-b}$  = 6.62 Hz, 1H,  $\text{H}^{7a}$ ), 4.914 (s, 2H,  $8^{a,b}$ ), 4.838 (d, 1H,  $\text{H}^{7b}$ ), 4.130 (m, 3H,  $\text{H}^{2-4}$ ), 3.900 (s, 1H,  $\text{H}^3$ ), 3.444 (s, 1H,  $\text{H}^6a$ ), 3.356 (s, 1H,  $\text{H}^6b$ ), 3.320 (double t, 2H,  $-\text{CH}_2\text{NHCO}$ ), 1.280 (m, 12H,  $(\text{CH}_2)_6$ ), 0.870 (t, 3H,  $\text{CH}_3$ ). EI-MS  $m/z$  441 ( $\text{M}^+$ ), 156 ( $(\text{CH}_3(\text{CH}_2)_5\text{NHCO})^+$ ), 85 (cyclic  $-\text{O}-\text{CH}=\text{CH}-\text{CH}^+-\text{O}-\text{CH}_2$ ). Anal. Calcd. for  $\text{C}_{16}\text{H}_{28}\text{NO}_5$ : C, 43.63; H, 6.41; N, 3.18. Found: C, 43.75; H, 6.29; N, 3.23.

**6-Deoxy-5-(1-imidazolyl)-2,4;3,5-dimethylene-*N*,*n*-octyl-D-gluconamide (2).** To a solution of 5.079 g (11.51 mmol) of 6-deoxy-6-iodo-2,4;3,5-dimethylene-*N*,*n*-octyl-D-gluconamide (**9**) in 75 ml of DMF was added 7.840 g (115.16 mmol, 10 equiv.) of imidazole and the solution was stirred at 60 °C in a nitrogen atmosphere. After 6 days the temperature was raised to 80 °C and two days later to 100 °C at which it was kept for an additional reaction period of 2 days (10 days of reaction in total). The DMF was removed under reduced pressure and the remaining oil mixed with toluene and subsequently washed with aqueous (saturated)  $\text{NaHCO}_3$  solution. The product was purified by column chromatography (silica, eluent  $\text{Et}_3\text{N}/\text{MeOH}/\text{EtOAc}$  1:5:94, v/v/v). The 3<sup>rd</sup> fraction collected from the column appeared to be compound **2** (white powder), yield 0.11 g (0.29 mmol, 2.5 %), m.p. 152.2 °C. IR (KBr) 3330  $\text{cm}^{-1}$  (NH), 1660 (amide I), 1537 (amide II).  $^1\text{H-NMR}$  (400 MHz,  $\text{CDCl}_3$ )  $\delta$  7.805 ppm (s, 1H,  $\text{N}-\text{CH}=\text{N}$ ), 7.073 (s, 1H,  $\text{N}-\text{CH}=\text{CH}-\text{N}$ ), 7.070 (s, 1H,  $\text{N}-\text{CH}=\text{CH}-\text{N}$ ), 6.541 (t, 1H, NHCO), 5.217 (d, 1H,  $J_{7a-b}$  = 6.83 Hz,  $\text{H}^{7a}$ ), 5.169 (d, 1H,  $J_{8a-b}$  = 4.16 Hz,  $\text{H}^{8a}$ ), 5.152 (d, 1H,  $\text{H}^{8b}$ ), 4.644 (d, 1H,  $\text{H}^{7b}$ ), 4.365 (t, 1H,  $\text{H}^3$ ), 4.122 (d,  $J_{2-3}$  = 1.61 Hz,  $\text{H}^2$ ), 3.617 (s, 1H,  $\text{H}^4$ ), 3.309 (11 peaks, 2H,  $-\text{CH}_2-\text{NHCO}$ ), 1.896 (s, 3H,  $\text{H}^6$ ), 1.501 (5 peaks, 2H,  $-\text{CH}_2-\text{CH}_2-\text{NHCO}$ ), 1.265 (m, 10 H,  $(\text{CH}_2)_5-\text{CH}_3$ ), 0.879 (t, 3H,  $(\text{CH}_2)_5-\text{CH}_3$ ). EI-MS  $m/z$  381 ( $\text{M}^+$ ), 314 ( $\text{M} - \text{imidazolyl}$ ) $^+$ , 156 ( $\text{C}_8\text{H}_{17}\text{NHCO}$ ) $^+$ , 85 (cyclic  $-\text{O}-\text{CH}=\text{CH}-\text{CH}^+-\text{O}-\text{CH}_2$ ). Anal. Calcd. for  $\text{C}_{19}\text{H}_{31}\text{N}_3\text{O}_5$ : C, 59.82; H, 8.19; N, 11.02. Found: C, 59.36; H, 7.89; N, 10.97.

**6-Deoxy-5-(1-imidazolyl)-2,4;3,5-dimethylene-*N*,*n*-octyl-D-idoitonamide (3).** This compound was obtained from the same reaction mixture as compound **2**. The 2<sup>nd</sup> fraction collected from the column (see the synthesis of compound **2**) appeared to be compound **3**; yield 0.25 g (0.66 mmol, 6.7 %) of a highly viscous oil. IR (KBr) 3427  $\text{cm}^{-1}$  (NH), 3115 (C-H), 1666 (amide I), 1543 (amide II).  $^1\text{H-NMR}$  (400 MHz,  $\text{CDCl}_3$ )  $\delta$  7.684 ppm (s, 1H,  $\text{N}-\text{CH}=\text{N}$ ), 7.157 (s, 1H,  $\text{N}-\text{CH}=\text{CH}-\text{N}$ ), 7.029 (s, 1H,  $\text{N}-\text{CH}=\text{CH}-\text{N}$ ), 6.524 (t, 1H, NHCO), 5.384 (d, 1H,  $J_{7a-b}$  = 6.54 Hz,  $\text{H}^{7a}$ ), 5.009 (d, 1H,  $J_{8a-b}$  = 6.73 Hz,  $\text{H}^{8a}$ ), 4.947 (d, 1H,  $\text{H}^{7b}$ ), 4.737 (d, 1H,  $\text{H}^{8b}$ ), 4.232 (d,  $J_{2-3}$  = 1.96 Hz,  $\text{H}^2$ ), 4.160 (t, 1H,  $J_{3-4}$  = 1.46 Hz,  $\text{H}^3$ ), 4.130 (broad s, 1H,  $\text{H}^4$ ), 3.290 (11 peaks, 2H,  $-\text{CH}_2-\text{NHCO}$ ), 1.661 (s, 3H,  $\text{H}^6$ ), 1.500 (5 peaks, 2H,  $-\text{CH}_2-\text{CH}_2-\text{NHCO}$ ), 1.251 (m, 10 H,  $(\text{CH}_2)_5-$

CH<sub>3</sub>), 0.879 (t, 3H, (CH<sub>2</sub>)<sub>5</sub>-CH<sub>3</sub>) EI-MS *m/z* 381 (M)<sup>+</sup>, 314 (M - imidazolyl)<sup>+</sup>, 156 (C<sub>8</sub>H<sub>17</sub>NHCO)<sup>+</sup>, 85 (cyclic -O-CH=CH-CH<sup>+</sup>-O-CH<sub>2</sub>) Anal Calcd for C<sub>19</sub>H<sub>31</sub>N<sub>3</sub>O<sub>5</sub>·H<sub>2</sub>O C, 57.13, H, 8.33, N, 10.52 Found C, 57.83, H, 8.09, N, 10.82

**6-Deoxy-5,6-didehydro-2,4,3,5-dimethylene-N,n-octyl-D-gluconamide (10).** This compound was obtained from the same reaction mixture as compound 2. The 1<sup>st</sup> fraction eluted from the column (see the synthesis of compound 2) appeared to be this elimination product, yield 1.98 g (6.32 mmol, 58.6 %) of white powder, m.p. 111.6 °C IR (KBr) 3293 cm<sup>-1</sup> (very sharp, N-H), 3121, 3089 (-C-H), 1658 (amide I), 1555 (amide II), 863 (=C-H, swing) <sup>1</sup>H-NMR (400 MHz, CDCl<sub>3</sub>) δ 6.565 ppm (broad t, 1H, NHCO), 5.248 (d, 2H, H<sup>7a</sup>+H<sup>8a</sup>), 4.828 (2d, 2H, H<sup>7b</sup>+H<sup>8b</sup>), 4.797 (s, 1H, H<sup>2</sup>), 4.618 (d, 1H, J<sub>2,3</sub> = 1.6 Hz, H<sup>3</sup>), 4.181 (s, 1H, H<sup>4</sup>), 4.100 (s, 2H, =CH<sub>2</sub>), 3.306 (2t, 2H, -CH<sub>2</sub>-NHCO), 1.522 (m, 2H, -CH<sub>2</sub>-CH<sub>2</sub>-NHCO), 1.265 (m, 10H, CH<sub>3</sub>-(CH<sub>2</sub>)<sub>5</sub>-), 0.877 (t, 3H, CH<sub>3</sub>-) Anal Calcd for C<sub>16</sub>H<sub>27</sub>NO<sub>5</sub> C, 61.31, H, 8.68, N, 4.47 Found C, 61.27, H, 8.77, N, 4.63

**6-Deoxy-6-(1-imidazolyl)-N,n-octyl-D-gluconamide (7)** Tosyl chloride (2.255 g, 11.83 mmol) dissolved in 10 ml of pyridine, was added dropwise to a stirred gelated solution of 3.26 g (10.75 mmol) of N,n-octyl-D-gluconamide in 25 ml of pyridine which was cooled in an ice bath. The reaction was carried out in a dry nitrogen atmosphere. After 1 hr of stirring at room temperature and subsequent reaction overnight in the refrigerator, 7.72 g (76.2 mmol, 7 equiv) of acetic acid anhydride was added. After 24 hrs of stirring, the clear solution was poured into a mixture of saturated NaHCO<sub>3</sub> and ice. The precipitate was collected and dried in vacuum. According to <sup>1</sup>H-NMR and IR, 6-deoxy-6-tosyl-N-(octyl)-D-gluconamide tetraacetate (11) was formed. The crude product was used without further purification to avoid deterioration. The tosylate group was substituted by an imidazole group in a high pressure reaction vessel using 3.014 g (4.79 mmol) of tosylate 11 and 0.652 g (9.58 mmol, 2 equiv) of imidazole in 7.5 ml of CHCl<sub>3</sub>. Reaction conditions 15 kBar, 50 °C, 40 hrs. The intermediate product compound (12) was purified by column chromatography (silica, eluent Et<sub>3</sub>N/MeOH/EtOAc 1.5/95, v/v/v), yield 0.66 g (1.26 mmol, 26.4 %). The acetate groups of 12 were removed by treating 0.664 g (1.26 mmol) of this compound with 3.9 mg of NaOMe in 60 ml of MeOH (0.05 equiv NaOMe with respect to the imidazole compound). The deprotected product (7) was purified by recrystallization from EtOAc, yield after deprotection was quantitative, m.p. 104 °C, IR (KBr) 3640-3020 cm<sup>-1</sup> (OH, broad), 3149, 3119 (=C-H), 1646 (Amide I), 1540 (Amide II), <sup>1</sup>H-NMR (CD<sub>3</sub>OD, 400 Mz) δ 7.697 ppm (s, 1H, N-CH=N), 7.184 (s, 1H, N-CH=CH-N), 6.971 (s, 1H, N-CH=CH-N), 4.326 (2d, 1H, J<sub>5,6a</sub> = 3.65 Hz, J<sub>6a,6b</sub> = 14.22 Hz, H<sup>6a</sup>), 4.176 (d, 1H, J<sub>2,3</sub> = 2.36 Hz, H<sup>2</sup>), 4.067 (H<sup>3</sup> mixed with part H<sup>6b</sup>), 4.063 (2d, 1H, J<sub>6b,5</sub> = 7.08 Hz, H<sup>6b</sup>), 3.875 (5 peaks, 1H, H<sup>5</sup>), 3.492 (2d, 1H, J<sub>4,5</sub> = 8.52, H<sup>4</sup>), 3.218 (9 peaks, 2H, (CH<sub>2</sub>)<sub>6</sub>-CH<sub>2</sub>-NHCO), 1.309 (t, 2H, (CH<sub>2</sub>)<sub>5</sub>-CH<sub>2</sub>-CH<sub>2</sub>-NHCO), 0.899 (t, 3H, CH<sub>3</sub>-). No satisfactory mass spectrum (EI or CI) could be obtained. Anal Calcd for C<sub>17</sub>H<sub>31</sub>N<sub>3</sub>O<sub>5</sub>·H<sub>2</sub>O C, 54.38, H, 8.86, N, 11.19 Found C, 54.36, H, 8.55, N, 10.49

**n-Octyl tosylate (13)** n-Octyl alcohol (5.050 g, 38.78 mmol) was tosylated in a standard reaction using 7.67 g (40.23 mmol) of tosyl chloride and 50 ml of pyridine. Yield 9.35 g (32.88 mmol, 84.8 %) of 13. The tosylate was used in the following reaction step without further purification. <sup>1</sup>H-NMR (90 MHz, CDCl<sub>3</sub>) δ 7.778 and 7.324 ppm (2d, J = 8.27 Hz, 2H, ArH), 4.015 (t, J = 6.30 Hz, 2H, -(CH<sub>2</sub>)<sub>6</sub>-CH<sub>2</sub>-OTs), 2.423 (s, 3H, Ar-CH<sub>3</sub>), 1.627 (t, 2H, -(CH<sub>2</sub>)<sub>5</sub>-CH<sub>2</sub>-CH<sub>2</sub>OTs), 1.303 (s, 10H, H<sub>3</sub>C-(CH<sub>2</sub>)<sub>5</sub>-CH<sub>2</sub>-), 0.858 (t, 3H, CH<sub>3</sub>-)

**1-(4-Nitro-1-imidazolyl)-n-octane (14)** To a solution of 1.311 g (11.60 mmol) of 4-nitroimidazole in 10 ml of anhydrous DMF was carefully added 0.46 g (11.50 mmol, 1.0 equiv)

of  $\text{NaH}^+$ . After heating for 30 min. at 60 °C, 2.889 g (10.16 mmol, 0.9 equiv.) of *n*-octyl tosylate (**13**) was added to the clear green solution and the mixture was stirred at 60 °C for 3 days. After this reaction period, a precipitate (sodium tosylate) was removed by filtration. After dilution of the filtrate with toluene and repeated washing with water, the organic layer was dried on  $\text{MgSO}_4$ . The solvent was removed by evaporation and a brown oil remained, which was diluted with *n*-hexane. From this solution white crystals appeared which were light sensitive and therefore were stored in the dark. Yield 2.10 g (9.32 mmol 91.8 %) of **14**, m.p. 44.7 °C. IR (KBr) 3113  $\text{cm}^{-1}$  (imidazole =C-H), 2919 (-CH<sub>2</sub>-) and 2855 (-CH<sub>3</sub>), 1523 and 1333 (-NO<sub>2</sub>), <sup>1</sup>H-NMR (90 MHz,  $\text{CDCl}_3$ )  $\delta$  7.778 ppm (d,  $J=1.4$  Hz long range, 1H, =C(NO<sub>2</sub>)-N=CH-N-(CH<sub>2</sub>)<sub>7</sub>-), 7.425 (d,  $J=1.4$  Hz long range, 1H, N-CH=C-NO<sub>2</sub>), 4.019 (t,  $J=7.1$  Hz, 2H, -(CH<sub>2</sub>)<sub>6</sub>-CH<sub>2</sub>-N), 1.850 (t,  $J=7.1$  Hz, 2H, H<sub>3</sub>C-(CH<sub>2</sub>)<sub>5</sub>-CH<sub>2</sub>-CH<sub>2</sub>), 1.285 (s, 10H, H<sub>3</sub>C-(CH<sub>2</sub>)<sub>5</sub>-CH<sub>2</sub>), 0.874 (t, 3H, CH<sub>3</sub>-). EI-MS  $m/z$  225 (M)<sup>+</sup>, 179 (M - NO<sub>2</sub>)<sup>+</sup>. Anal. Calcd. for C<sub>11</sub>H<sub>19</sub>N<sub>3</sub>O<sub>2</sub>: C, 58.65; H, 8.50; N, 8.65. Found: C, 58.31; H, 8.30; N, 8.25.

**1-(4-Amino-1-imidazolyl)-*n*-octane (15).** A solution of 2.11 g (9.35 mmol) of **14** in 50 ml of 1,4-dioxane was purged for several min. with a flow of nitrogen. The nitro group was reduced with Pd/C and H<sub>2</sub>.<sup>5</sup> According to TLC (hexane/EtOAc, 1:1, v/v, UV detection and detection with ninhydrine<sup>6</sup>) the reduction was completed after 3 hrs. The mixture was filtered over Celite and concentrated under reduced pressure. Because the product appeared to be air sensitive, it was used for the next step without isolation or further characterization.

**1-(*n*-Octyl)-4-imidazolyl-*N*-D-gluconamide (4).** A clear solution of 2.0 g (10.24 mmol) of **15** in 25 ml of 1,4-dioxane was heated to reflux and 2.01 g (6.54 mmol, 1.2 equiv.) of 1,5-D-gluconolactone was added. After refluxing overnight the solvent was evaporated under reduced pressure. The product was diluted with chloroform and washed with aqueous saturated NaHCO<sub>3</sub>. The brown precipitate at the interface of the aqueous and the organic layer was collected by filtration. The brown precipitate was washed with chloroform and alkaline water until a white powder remained, which was subsequently recrystallized from methanol. Yield 1.35 g (3.62 mmol, 38.7 %), m.p. 172.3 °C. IR (KBr) 3620-3000  $\text{cm}^{-1}$  (OH), 3161 and 3134 (imidazole =C-H), 2927 (-CH<sub>2</sub>-), 1670 (Amide I), 1578 (Amide II), <sup>1</sup>H-NMR (400 MHz, DMSO-*d*<sub>6</sub> after addition of a drop of D<sub>2</sub>O)  $\delta$  9.195 ppm (s, 1H, NHCO), 7.407 (d,  $J=1.4$  Hz long range, 1H, N<sub>im</sub>-CH=C(N<sub>im</sub>)-NH-CO), 7.215 (d,  $J=1.4$  Hz long range, 1H, -(CH<sub>2</sub>)<sub>7</sub>-N<sub>im</sub>-CH=N<sub>im</sub>-CH), 4.141 (d, 1H,  $J_{2,3}=3.64$  Hz, H<sup>2</sup>), 3.935 (2d, 1H,  $J_{3,4}=2.46$  Hz, H<sup>3</sup>), 3.879 (t, 2H, -(CH<sub>2</sub>)<sub>6</sub>-CH<sub>2</sub>-N), 3.568 (2d, 1H,  $J_{6a,5}=2.73$  Hz, H<sup>6a</sup>), 3.507 (m, 1H,  $J_{4,5}=8.35$  Hz, H<sup>4</sup>, H<sup>4</sup>-H<sup>5</sup> are overlapping, however, the same pattern was obtained after simulation with the program GeNMR<sup>®</sup>), 3.498 (m, 1H, H<sup>5</sup>), 3.379 (2d, 1H,  $J_{6a,6b}=-10.95$ , H<sup>6b</sup>), 1.650 (t, 2H, H<sub>3</sub>C-(CH<sub>2</sub>)<sub>5</sub>-CH<sub>2</sub>-CH<sub>2</sub>), 1.204 (s, 10H, H<sub>3</sub>C-(CH<sub>2</sub>)<sub>5</sub>-CH<sub>2</sub>), 0.813 (t, 3H, CH<sub>3</sub>-), <sup>13</sup>C-NMR (110 MHz, DMSO-*d*<sub>6</sub>)  $\delta$  169.22 ppm (-C=O), 136.82 (N<sub>im</sub>-CH-N<sub>im</sub>), 133.08 (-CH<sub>2</sub>-N<sub>im</sub>-CH=C(N<sub>im</sub>)-), 120.60 (-CH<sub>2</sub>-N<sub>im</sub>-CH=C(N<sub>im</sub>)-NHCO-), 73.45 (C=O-CH(OH)-), 72.23 (C=O-CH(OH)-CH(OH)-), 71.52 (C=O-(CH(OH))<sub>2</sub>-CH(OH)-), 70.22 (C=O-(CH(OH))<sub>3</sub>-CH(OH)-), 46.21 (-CH<sub>2</sub>-N<sub>imidazole</sub>), 13.76 (CH<sub>3</sub>-). Anal. Calcd. for C<sub>17</sub>H<sub>31</sub>N<sub>3</sub>O<sub>6</sub>: C, 54.68; H, 8.37; N, 11.25. Found: C, 54.71; H, 8.24; N, 11.02.

**11-(*t*-Butyloxyamido)-*n*-undecan-1-ol (16).** In 30 min., 4.29 g (30.0 mmol, 1.5 equiv.) of *t*-butyloxycarboxy azide in 50 ml of dioxane was added dropwise to a solution of 4.03 g (21.5 mmol) of 11-amino-undecan-1-ol in 40 ml of water. After stirring overnight at room temperature, the dioxane and the excess of *t*-butyloxycarboxy azide were removed under reduced pressure. The water-layer was extracted 3 times with 50 ml of diethyl ether. The collected organic layers were dried ( $\text{MgSO}_4$ ) and concentrated to give a yellow powder. Yield 2.90 g (10.1 mmol,

<sup>†</sup> The NaH was dispersed in mineral oil (60 %) and was washed twice with anhydrous diethyl ether prior to use

46.9 %), m.p. 36.4 °C. IR (KBr) 3381  $\text{cm}^{-1}$  (NH), 2982 ( $\text{CH}_3$  from *t*-butoxy group), 2921 ( $\text{CH}_2$ ), 1690 ( $\text{C}=\text{O}$ ), 1523 (NH).  $^1\text{H-NMR}$  (100 MHz,  $\text{CDCl}_3$ )  $\delta$  4.48 ppm (broad t, 1H, NHCO), 3.64 (t, 2H,  $-\text{CH}_2\text{-OH}$ ), 3.10 (q, 2H,  $-\text{CH}_2\text{-NHCO}$ ), 1.44 (s, 9H,  $(\text{CH}_3)_3$ ), 1.28 (broad s, 18H,  $-(\text{CH}_2)_9$ ). Anal. Calcd. for  $\text{C}_{16}\text{H}_{33}\text{NO}_3$ : C, 66.86; H, 11.57; N, 4.87. Found: C, 67.15; H, 11.62; N, 4.76.

**11-(*t*-Butyloxyamido)-*n*-undecyl tosylate (17).** In 30 min., a solution of 2.51 g (13.14 mmol, 1.1 equiv.) of tosyl chloride in 15 ml of pyridine was added dropwise to a solution of 3.41 g (11.86 mmol) of **16** in 30 ml of anhydrous pyridine which was cooled in an ice bath. The reaction vessel was purged with dried nitrogen gas. After an additional 60 min. of stirring, the clear mixture was placed overnight in the refrigerator for completion of the reaction. The solution was poured out into a mixture of ice and saturated  $\text{NaHCO}_3$ . The oily product was extracted with chloroform and the organic layer was dried on  $\text{MgSO}_4$ . The product was purified by column chromatography (silica, eluent EtOAc/hexane 1:5, v/v). Yield 1.83 g (4.26 mmol, 36.0 %) of **17**, m.p. 44.5 °C. IR (KBr) 3377  $\text{cm}^{-1}$  (NH), 1688 ( $\text{C}=\text{O}$ ), 1523 (NH), 1364 ( $\text{S}=\text{O}$ ).  $^1\text{H-NMR}$  (100 MHz,  $\text{CDCl}_3$ )  $\delta$  7.79 ppm (d, 2H, ArH), 7.34 (d, 2H, ArH), 4.48 (broad t, 1H, NHCO), 4.01 (t, 2H,  $-\text{CH}_2\text{-OTs}$ ), 3.10 (pseudo q, 2H,  $-\text{CH}_2\text{-NHCO}$ ), 2.45 (s, 3H, Ar- $\text{CH}_3$ ), 1.44 (s, 9H,  $(\text{CH}_3)_3$ ), 1.22 (broad s, 18H,  $-(\text{CH}_2)_9$ ). Anal. Calcd. for  $\text{C}_{23}\text{H}_{39}\text{NO}_5\text{S}$ : C, 62.55; H, 8.90; N, 3.17; S, 7.26. Found: C, 62.46; H, 8.57; N, 3.26; S, 6.88.

**11-(*t*-Butyloxyamido)-*n*-undecylimidazole (18).** Imidazole (0.40 g, 5.90 mmol) was converted into its sodium salt with sodium hydride (0.248 g, 1.05 equiv., washed twice with *n*-hexane in order to remove the mineral oil) in 50 ml of anhydrous DMF (60 °C, 0.5 hr.). To this green solution, 1.30 g (2.94 mmol, 0.5 equiv.) of **17** was added. After overnight reaction at 60 °C, the DMF was removed by evaporation and the remaining pale yellow powder was dissolved in chloroform. The organic layer was washed twice with water and dried on  $\text{Na}_2\text{SO}_4$ . After evaporation of the solvent, **18** was obtained as a pale yellow powder, which according to  $^1\text{H-NMR}$ , was slightly contaminated with DMF. Despite this contamination, **18** was used in the next reaction step. IR (KBr) 3112  $\text{cm}^{-1}$  ( $=\text{C-H}$ ), 1702 ( $\text{C}=\text{O}$ ), 1507 (NH),  $^1\text{H-NMR}$  (100 MHz,  $\text{CDCl}_3$ )  $\delta$  7.46 ppm (s, 1H,  $\text{N}=\text{CH-N}$ ), 7.06 (t (long range), 1H,  $\text{N-CH}=\text{CH-N-CH}_2$ ), 6.91 (t (long range), 1H,  $\text{N-CH}=\text{CH-N-CH}_2$ ), 3.92 (t, 2H,  $-\text{CH}_2\text{-Im}$ ), 3.09 (q, 2H,  $-\text{CH}_2\text{-NHCO}$ ). Due to the contamination with DMF no satisfactory elemental analysis was obtained.

**11-Imidazolyl-*n*-undecylamine (19).** To a mixture of 15 ml of TFA and 15 ml of  $\text{CH}_2\text{Cl}_2$  was added a solution of 0.91 g (2.70 mmol) of **18** in 20 ml of  $\text{CH}_2\text{Cl}_2$ . After 1 hr. of stirring at 0 °C the mixture was diluted with 50 ml of  $\text{CH}_2\text{Cl}_2$ . The organic solution was washed 3 times with aqueous 4N NaOH until the pH was  $\pm 10$ . The organic layer was dried ( $\text{Na}_2\text{SO}_4$ ) and concentrated to give a pale yellow powder which was not further purified, yield 0.302 g (105 %) of **19**. IR (KBr) 3344  $\text{cm}^{-1}$  (NH), 3096 ( $=\text{C-H}$ ),  $^1\text{H-NMR}$  (100 MHz,  $\text{CDCl}_3$ )  $\delta$  7.39 ppm (broad s, 1H,  $\text{N}=\text{CH-N}$ ), 7.98 (broad s, 1H,  $\text{N-CH}=\text{CH-N-CH}_2$ ), 6.83 (broad s, 1H,  $\text{N-CH}=\text{CH-N-CH}_2$ ), 2.60 (broad t, 2H,  $-\text{CH}_2\text{-NH}_2$ ). No satisfactory elemental analysis could be obtained due to contamination with small amounts of DMF.

***N*-(11-(1-Imidazolyl)-*n*-undecyl)-*D*-gluconamide (5).** A mixture of 0.401 g (1.47 mmol) of **19**, 0.278 g (1.56 mmol) of 1,5-*D*-gluconolactone and 0.208 g (2.06 mmol) of  $\text{Et}_3\text{N}$  in 50 ml of methanol was refluxed overnight. The solution was concentrated, which resulted in precipitation. The precipitate was filtered and purified by column chromatography (eluent  $\text{Et}_3\text{N}/\text{MeOH}/\text{CHCl}_3$  1:15:84, v/v/v) to give a yellow powder, yield 0.26 g (0.59 mmol, 40.3 %) of **5**, m.p. 107 °C. IR (KBr) 3640-3040  $\text{cm}^{-1}$  (OH), 3150 and 3140 ( $=\text{C-H}$ ), 2920 ( $-\text{CH}_2-$ ), 1641 (Amide I), 1535 (Amide II),  $^1\text{H-NMR}$  (400 MHz,  $\text{CD}_3\text{OD}$ )  $\delta$  7.680 ppm (s, 1H,  $\text{N}=\text{CH-N-CH}_2$ ), 7.130 (s, 1H,  $\text{N-CH}=\text{CH-N-CH}_2$ ), 6.980 (s, 1H,  $\text{N-CH}=\text{CH-N-CH}_2$ ), 4.205 (d, 1H,  $J_{2,3} = 3.05 \text{ Hz}$ ,  $\text{H}^2$ ), 4.090 (t,

$^1\text{H}$ ,  $J_{3-4} = 2.54$  Hz,  $\text{H}^4$ ), 4.020 (t, 2H,  $-(\text{CH}_2)_{10}-\text{CH}_2-\text{N}_{\text{im}}$ ), 3.780 (2d, 1H,  $J_{6a-5} = 2.70$  Hz,  $J_{6a-6b} = -10.94$  Hz,  $\text{H}^{6a}$ ), 3.696 (m, 1H,  $J_{4-5} = 8.58$  Hz,  $\text{H}^4$ , overlapping with  $\text{H}^5$ , values checked with GeNMR), 3.680 (m, 1H,  $\text{H}^5$ ), 3.623 (2d, 1H,  $J_{5-6b} = 5.01$  Hz,  $\text{H}^{6b}$ ), 3.230 (m, 2H,  $-\text{CH}_2-\text{NHCO}$ ), 1.790 (t, 2H,  $-(\text{CH}_2)_9-\text{CH}_2-\text{CH}_2-\text{N}_{\text{im}}$ ), 1.530 (t, 2H,  $\text{CH}_2-\text{CH}_2-\text{NHCO}$ ), 1.310 (broad s, 14H,  $-\text{CH}_2-(\text{CH}_2)_7-\text{CH}_2-$ ),  $^{13}\text{C}$ -NMR (110 MHz,  $\text{CD}_3\text{OD}$ )  $\delta$  175.00 ppm ( $-\text{C}=\text{O}$ ), , 138.27 ( $\text{N}_{\text{im}}=\text{CH}-\text{N}_{\text{im}}$ ), 128.61 ( $\text{N}_{\text{im}}-\text{CH}=\text{CH}-\text{N}_{\text{im}}-\text{CH}_2-$ ), 120.60 ( $\text{N}_{\text{im}}-\text{CH}=\text{CH}-\text{N}_{\text{im}}-\text{CH}_2-$ ), 75.35 ( $\text{O}=\text{C}-\text{CH}(\text{OH})-$ ), 74.32 ( $\text{O}=\text{C}-\text{CH}(\text{OH})-\text{CH}(\text{OH})-$ ), 74.07 ( $\text{O}=\text{C}-(\text{CH}(\text{OH}))_2-\text{CH}(\text{OH})-$ ), 73.01 ( $\text{O}=\text{C}-(\text{CH}(\text{OH}))_3-\text{CH}(\text{OH})-$ ), 48.07 ( $-\text{CH}_2-\text{N}_{\text{imidazole}}$ ), 40.11 ( $-\text{CH}_2-\text{NHCO}$ ). Anal. Calcd. for  $\text{C}_{20}\text{H}_{37}\text{N}_3\text{O}_6 \cdot \frac{1}{2} \text{H}_2\text{O}$ : C, 56.58; H, 9.02; N, 9.90. Found: C, 56.83; H, 8.62; N, 10.08.

**N-(2-(2-Imidazolyl)-ethyl)-D-gluconamide (6).** To 0.695 g (3.78 mmol) of histamine dihydrochloride were added 0.673 g (3.78 mmol, 1 equiv.) of 1,5-D-gluconolactone, 30 ml of methanol, and 0.946 g (9.35 mmol, 2.5 equiv.) of  $\text{Et}_3\text{N}$  (the latter in order to liberate the histamine from its hydrochloride salt). After 30 min. refluxing a clear solution was obtained. After refluxing for an additional 30 min. the solution was cooled. White crystals were formed which were washed with cold methanol. Yield 0.79 g (2.72 mmol, 72.6 %) of **6**, m.p. 161.1 °C. IR (KBr) 3670–2800  $\text{cm}^{-1}$  (broad, with peaks at 3476, 3379, 3324 and 3212, OH), 2960 and 2939 ( $=\text{C}-\text{H}$ ), 1645 (amide I), 1590 (aromate), 1529 (amide II).  $^1\text{H}$ -NMR (400 MHz,  $\text{DMSO}-d_6$ ),  $\delta$  7.739 ppm (t, 1H,  $\text{NHCO}$ , which disappeared after addition of one drop of  $\text{D}_2\text{O}$ ), ( $\text{DMSO}-d_6 + 1$  drop of  $\text{D}_2\text{O}$ )  $\delta$  7.536 ppm (s, 1H,  $\text{N}_{\text{im}}-\text{CH}-\text{N}_{\text{im}}$ ), 6.809 (s, 1H,  $\text{N}_{\text{im}}-\text{CH}-\text{C}(\text{CH}_2)-\text{N}_{\text{im}}$ ), 3.966 (d, 1H,  $J_{2-3} = 3.70$  Hz,  $\text{H}^2$ ), 3.873 (2d, 1H,  $J_{3-4} = 2.04$ ,  $\text{H}^3$ ), 3.557 (2d, 1H,  $J_{6a-5} = 2.54$  Hz,  $J_{6a-6b} = -10.92$  Hz,  $\text{H}_{6a}$ ), 3.461 (m, 2H,  $\text{H}^{4+5}$ ), 3.358 (m, 1H,  $\text{H}^{6b}$ ), 3.284 (t, 2H,  $J = 6.98$  Hz,  $-\text{CH}_2-\text{NHCO}$ ), 2.629 (t,  $J = 7.138$  Hz,  $-\text{CH}_2-\text{CH}_2-\text{NHCO}$ ). Anal. Calcd. for  $\text{C}_{11}\text{H}_{19}\text{N}_3\text{O}_6 \cdot \frac{1}{3} \text{H}_2\text{O}$ : C, 44.74; H, 6.71; N, 14.23. Found: C, 45.06; H, 6.45; N, 13.68.

**1-n-Hexadecylimidazole (8).** Synthesis of this compound was described in Chapter 3.

### 5.2.2 Measurements of isotherms

Isotherms were recorded on a home-built Langmuir trough equipped with a Wilhelmy balance. The trough was filled with Milli-Q<sup>®</sup> water, which was in some cases adjusted with  $\text{H}_2\text{SO}_4$  to pH=1 or buffered with Tris (pH=9). The compounds were dissolved in methanol (conc. of 2.5 mM) and an accurate amount of 40  $\mu\text{l}$  solution was added dropwise on the subphase (195  $\text{cm}^2$ ). After 5 min. of stabilization, the compression was started. The temperature deviation was within 0.2 °C, and on a clean surface the surface pressure ( $\pi$ ) stayed below 0.1 mN/m.

### 5.2.3 SAXS experiments

X-ray powder diffractograms were recorded on a Philips PW1710 powder diffractometer with a Ni filtered Cu source (40 kV, 55 mA,  $\lambda=1.54060$  Å). The aqueous suspensions were transferred to a silicon sample holder and rapidly lyophilized in a vacuum desiccator under high vacuum and in the presence of  $\text{P}_2\text{O}_5$ .

### 5.2.4 Electron microscopy

The equipment that was used for electron microscopy experiments, has been described in Chapter 4. The sample preparation was similar to the procedure described in Chapter 4, Section 4.2.5.

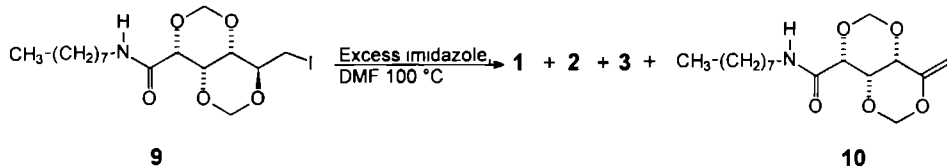


### 5.3 Results and discussion

#### 5.3.1 Preparation of the compounds

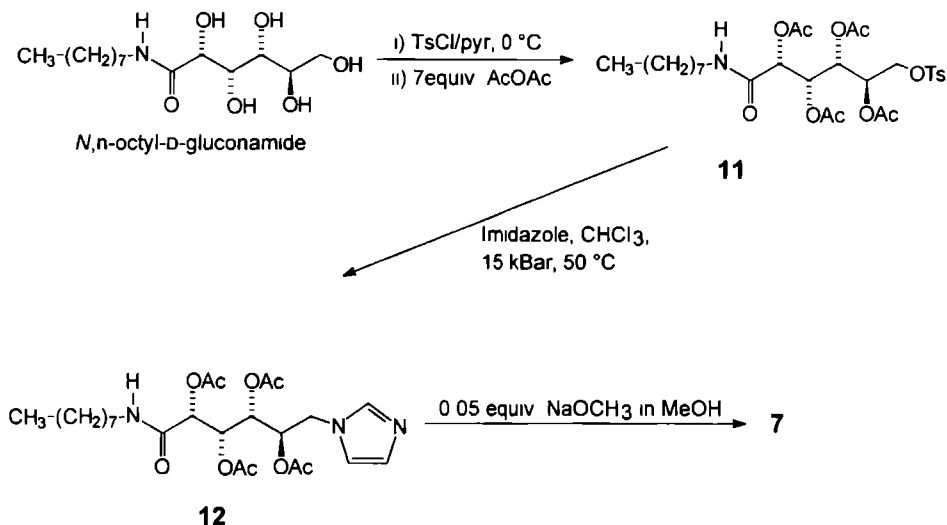
The synthesis of **1** has been described in Chapter 3. The attachment of the imidazole group to the gluconamide framework of **1** was carried out at 15 kBar to minimize the amount of elimination product. The reaction can also be carried out at normal pressure in DMF at 100 °C, with the disadvantage of low yields. If the tosylate in the above mentioned reaction (see Chapter 3) was substituted by an iodide (Scheme 5.1) the yield of **1** increased but the elimination product (**10**) was still the major component. In addition to **1** also compounds **2** and **3** (Scheme 5.1) were obtained, which could be isolated by column chromatography.

Scheme 5.1



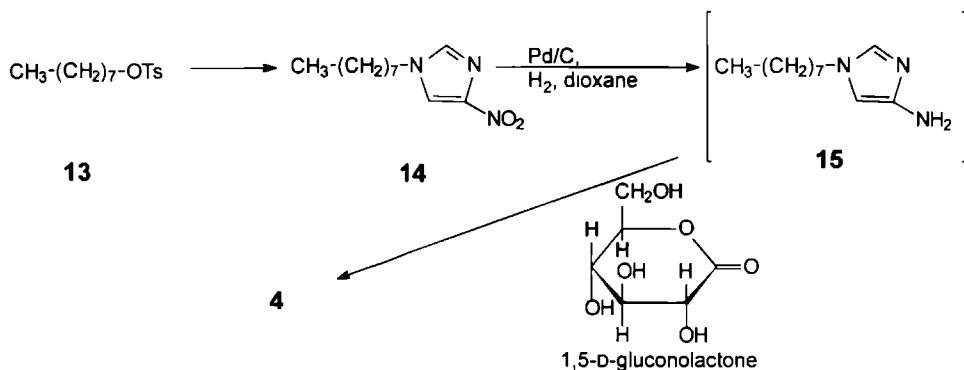
The synthesis of the non-protected 6-deoxy gluconamide **7** was performed as described in Scheme 5.2. The introduction of the imidazole group could be successfully carried out at high pressure.

Scheme 5.2



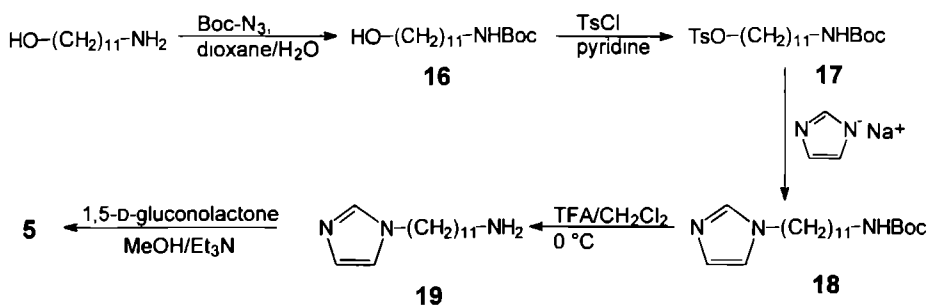
The synthesis of compound **4**, which has an imidazole group located between its head group and its alkyl chain, is outlined in Scheme 5.3. Compound **15**, which carries an amino substituted imidazole group, is air sensitive, and, therefore, was used in the subsequent reaction step to **4** without isolation.

Scheme 5.3



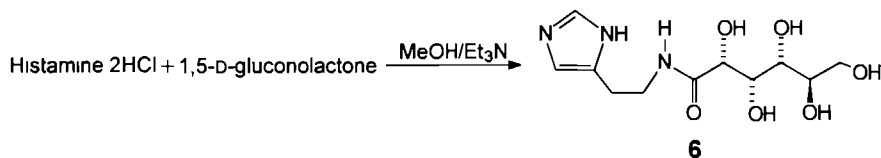
Compound **5**, in which the imidazole group is connected to the end of the alkyl chain, was synthesized according to Scheme 5.4.

Scheme 5.4



The synthesis of compound **6**, in which the imidazole group is connected to the amide nitrogen via an ethylene spacer is described in Scheme 5.5. Compound **6** by itself is not amphiphilic, but in combination with other metal ligating molecules, *e.g.* 1-imidazolyl-*n*-hexadecane (**8**) and metal ions, it may show amphiphilic behavior.

Scheme 5-5



### 5.3.2 $pK_a$ determination

The apparent  $pK_a$  ( $pK_a^*$ ) of **1** in a methanol-water mixture (95:1, v/v), is 6.28 which is only slightly lower than the  $pK_a$  values of imidazole and methyl imidazole (see Chapter 4).<sup>7</sup> The  $pK_a^*$  of compound **7** (7.02) was found to be rather similar to that of **1**. Apparently, the influence of the free hydroxyl groups in **7** on the acid-base character of the imidazole group is insignificant, although both types of groups are located next to each other. We assumed, therefore, that the  $pK_a^*$  values of compounds **2**, **3**, **5** and **6** were similar to those of imidazole and methylimidazole. Titration of compound **4**, in which the imidazole group is placed between the aliphatic chain and the amide function, did not result in the expected titration curve for imidazole-containing compounds (see Chapter 4, Figure 4.1). Instead of the usual buffer zone between the two inflection points, only one steep rise in  $pH^*$  was observed. The titration curve turned out to be similar to the titration of the blanco, which means that in solution **4** is not able to accept a proton from the titrant  $HClO_4$ . This lack of protonation may be due to the fact that the  $N^2$  nitrogen atom of the imidazole group is blocked because it is involved in an intramolecular hydrogen bond with the amide hydrogen atom. IR-experiments confirmed this hypothesis (see next Section).

### 5.3.3 IR experiments

Compound **4** and *N*,*n*-octyl-D-gluconamide were recrystallized from deuterated methanol in order to exchange the hydroxyl and amide hydrogens for deuterium atoms. The IR-spectrum of deuterium exchanged *N*,*n*-octyl-D-gluconamide showed a considerable shift of the hydroxyl stretching vibrations, viz from a broad peak between 3620 and 3100  $cm^{-1}$  to one between 2750 and 2150  $cm^{-1}$ . The amide II peak (N-H bend) was shifted from 1528 to 1463  $cm^{-1}$  upon deuterium exchange of *N*,*n*-octyl-D-gluconamide. The IR-spectrum of **4** recrystallized from  $CD_3OD$  also showed a shift of the hydroxyl stretching vibrations, viz. from a set of peaks between 3680 and 3180  $cm^{-1}$  to a set of peaks between 2680 and 2030  $cm^{-1}$ . In contrast to *N*,*n*-octyl-D-gluconamide, deuterium exchanged **4** did not show a shift of the amide II vibration, indicating that the amide hydrogen was not exchanged for deuterium. This lack of exchange is probably due to the presence of a very strong *intramolecular* hydrogen bond with the imidazole group in **4** (vide supra).

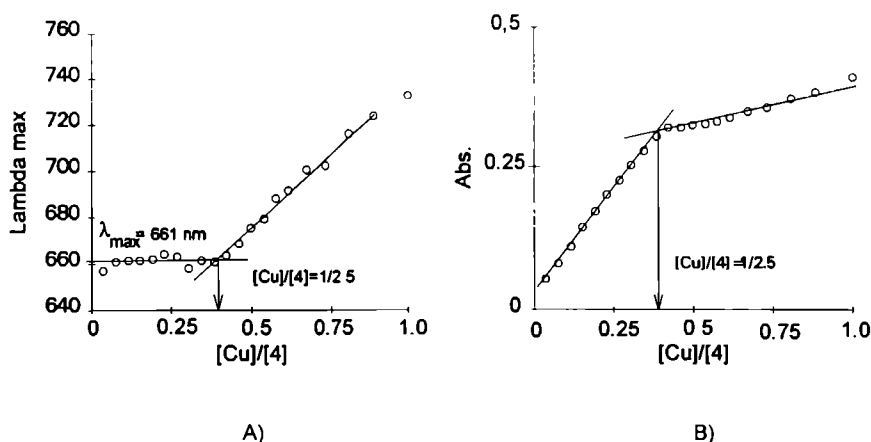
### 5.3.4 UV-vis spectroscopy

In order to determine the stoichiometry of the Cu(II) imidazole complexes, UV-vis titrations were carried out with compounds **1**, **4**, **6**, and **7** monitoring the d-d transition at approximately 600 nm.<sup>8</sup>

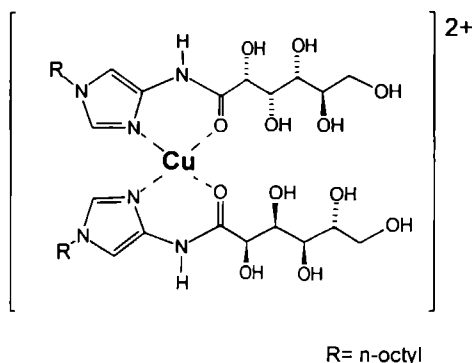
We assumed that the copper complexation behavior of compounds **2** and **3** was similar to that of **1**, *i.e.* 4 ligands surrounding the copper ion in Cu(ClO<sub>4</sub>)<sub>2</sub> (Chapter 4). The copper complexation of compound **7**, which formed 1/4 (Cu/Ligand) complexes with Cu(ClO<sub>4</sub>)<sub>2</sub>, is rather similar to the complexation behavior of compound **1** (Table 5 1). Apparently, the hydroxyl groups do not dramatically disturb the stoichiometry of the copper complex, although the free hydroxyl groups could have acted as additional ligating groups.

Compound **4** showed a deviating copper complexation behavior. In the graphs of the  $\lambda_{\max}$  and the absorption at  $\lambda_{\max}$  versus the copper perchlorate/ligand ratio inflection points were found at a Cu/ligand ratio of 1/2.5, indicating the formation of 1:2 or 1:3 complexes (see Figure 5.2). Although it is known from the literature that copper(II) ions can be ligated by 3 imidazole groups,<sup>9</sup> we believe that in our case, it is probable that 1:2 copper-ligand complexes are present, due to crowding of the ligands. It is not unlikely that in the case of the 1:2 complexes the oxygen atoms of the amide function take part in the complexation (*cf.* Figure 5.3).

Graphs of  $\lambda_{\max}$  and the absorption at  $\lambda_{\max}$  plotted versus the copper/ligand ratio obtained from a UV-vis titration of **4** with CuCl<sub>2</sub>, showed inflection points at a Cu/ligand ratio of 1/2.5, indicating that in the case of this metal salt similar copper complexes are obtained as in the case of Cu(ClO<sub>4</sub>)<sub>2</sub>. It should be noted that the  $\lambda_{\max}$  values of both the Cu(ClO<sub>4</sub>)<sub>2</sub> and CuCl<sub>2</sub> complexes (661 and 672 nm, respectively, the solutions are green), are different from those of the traditional blue-colored imidazole copper(II) complexes.



**Figure 5.2** UV-vis titration of [Cu][ClO<sub>4</sub>]<sub>2</sub> with **4** in methanol, A)  $\lambda_{\max}$  vs the [Cu]/[4] ratio B) Absorption at  $\lambda_{\max}$  vs the [Cu]/[4] ratio



**Figure 5.3** Possible structure of the complex of **4** with Cu(II) ions

**Table 5.1** Stoichiometry of complexes between Cu(ClO<sub>4</sub>)<sub>2</sub> and various imidazole ligands <sup>a</sup>

Ligand	Solvent <sup>b</sup>	Complexation	$\lambda_{\max}$ of complex (nm)
Melm <sup>c</sup>	H <sub>2</sub> O/MeOH (1.4)	1/4 1	610
<b>1</b>	CHCl <sub>3</sub> /MeOH (1 3)	1/4 4	602
<b>4</b>	CHCl <sub>3</sub> /MeOH (1 3)	1/2 5	661
<b>6</b>	H <sub>2</sub> O	1/4 0	585
<b>7</b>	CHCl <sub>3</sub> /MeOH (1 1)	1/3 7	613

<sup>a</sup> Obtained from UV-vis titrations. Cu(II)/ligand ratios were determined from the intersection of the tangents in the curves of  $\lambda_{\max}$  vs the Cu/ligand ratio (e.g. see Fig 5.2A)

<sup>b</sup> Ratio of solvents (v/v) in parenthesis

<sup>c</sup> 1-Methylimidazole

Compound **6** was titrated with Cu(ClO<sub>4</sub>)<sub>2</sub> in water, and showed an inflection point at 1/4.0 (Table 5.1). Apparently, the carbonyl oxygen atom of the amide function in this compound is not in a favorable position to participate in the complexation of the copper(II) center. In contrast to the 1:2 copper-ligand complexes obtained from gluconamide **4**, the copper complex of **6** displayed a dark blue color. In order to investigate the possibility of forming a mixed complex of copper(II) with **6** and 1-n-hexadecylimidazole (**8**), UV-vis spectra of the pure complexes of [(**6**)<sub>4</sub>Cu][ClO<sub>4</sub>]<sub>2</sub>, ((**6**)<sub>4</sub>Cu) and [(**8**)<sub>4</sub>Cu][ClO<sub>4</sub>]<sub>2</sub>, ((**8**)<sub>4</sub>Cu) were recorded as well as of a mixture of **6**, **8** and Cu(ClO<sub>4</sub>)<sub>2</sub> in a (2+2):1 ratio. The solvent appeared to be a limiting factor for the preparation of the afore mentioned complexes. Solvent mixtures of chloroform and methanol resulted in precipitation of both (**6**)<sub>4</sub>Cu and (**8**)<sub>4</sub>Cu. All complexes, therefore, were prepared in DMSO (the concentrations of the Cu complexes of **7**, **8** and combinations of these ligands were kept the same). The  $\lambda_{\max}$  values of the complexes are given in Table 5.2. It should be noted that the  $\lambda_{\max}$  values of the mixed complex are in between those of the pure complexes, but not at the arithmetical average. Although this is not yet a definite proof we believe that complexes with

mixed ligands were formed. Attempts to confirm the formation of mixed copper complexes with FAB-MS failed.

**Table 5.2**  $\lambda_{\max}$  Values of complexes between  $\text{Cu}(\text{ClO}_4)_2$  and various imidazole ligands

Complex <sup>a</sup>	$\lambda_{\max}$ (nm)
$[(1)_4\text{Cu}][\text{ClO}_4]_2$	647
$[(4)_2\text{Cu}][\text{ClO}_4]_2$	678
$[(6)_4\text{Cu}][\text{ClO}_4]_2$	650
$[(7)_4\text{Cu}][\text{ClO}_4]_2$	684
$[(8)_4\text{Cu}][\text{ClO}_4]_2$	677
$[(6)_2+(8)_2\text{Cu}][\text{ClO}_4]_2$	657

<sup>a</sup> In DMSO The concentration of the complexes is 45 mmolar

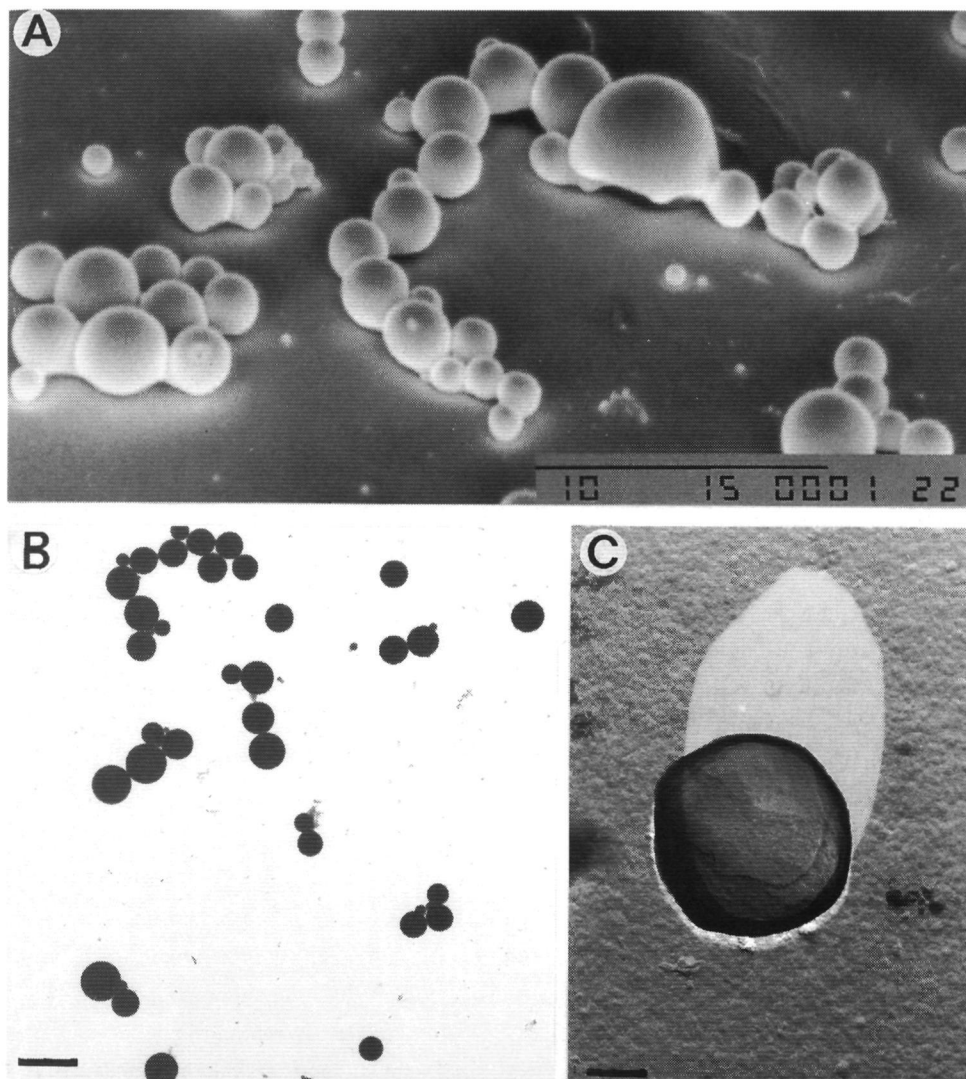
### 5.3.5 Electron microscopy

In Chapter 4, we reported that gluconamides containing imidazole groups can form vesicles, fibers, tubes or braids depending on the pH or the addition of metal ions. In this section the aggregates of compounds **2-8** and their copper complexes in aqueous solutions are described as visualized by transition electron microscopy (TEM). In addition, an attempt to prepare amphiphilic complexes in water by mixing **6** and **8** in combination with  $\text{Cu}(\text{ClO}_4)_2$ , is presented.

*6-Deoxy-5-(1-imidazolyl)-2,4,3,5-dimethylene-N,n-octyl-D-gluconamide (2)*. This compound dissolved readily in both warm ( $T = 60^\circ\text{C}$ ) acetic acid/sodium acetate buffered ( $\text{pH}=4.5$ ) water and warm Tris buffered ( $\text{pH}=8.5$ ) water. In both cases the solution remained clear upon cooling and no well-defined supramolecular structures of either the protonated form of **2** in acetate buffer or the non-protonated form of **2** in Tris buffer could be discerned by TEM. Upon addition of 0.25 equivalents of  $\text{Cu}(\text{ClO}_4)_2$  to a hot ( $T=80^\circ\text{C}$ ), clear aqueous solution of **2**, a pale blue turbid suspension was obtained. After sonicating the suspension for 5 minutes at  $70^\circ\text{C}$ , perfectly spherical vesicles with diameters ranging from 270 to 7000 nm, were observed by SEM (see Figure 5.4A). From the intense black color of the TEM pictures which were made without addition of staining agents, it was concluded that the aggregates contained copper ions (Figure 5.4B). Freeze-etching experiments revealed that the vesicles were multilamellar aggregates (Figure 5.4C). The vesicular suspension was stable for a short period only and started to precipitate after one day standing at room temperature.

*6-Deoxy-5-(1-imidazolyl)-2,4,3,5-dimethylene-N,n-octyl-D-idoitnamide (3)*. Despite the change of the carbohydrate framework from gluconamide to idoitnamide, and the change in stereochemical environment of the imidazole group, the aggregation behavior of compound **3** was very similar to that of compound **2**. Both the protonated (in acetate buffered solution) and neutral form (in Tris buffered solution) of **3** remained dissolved in water without forming aggregates when the warm clear aqueous solutions of this compound were cooled to room temperature.

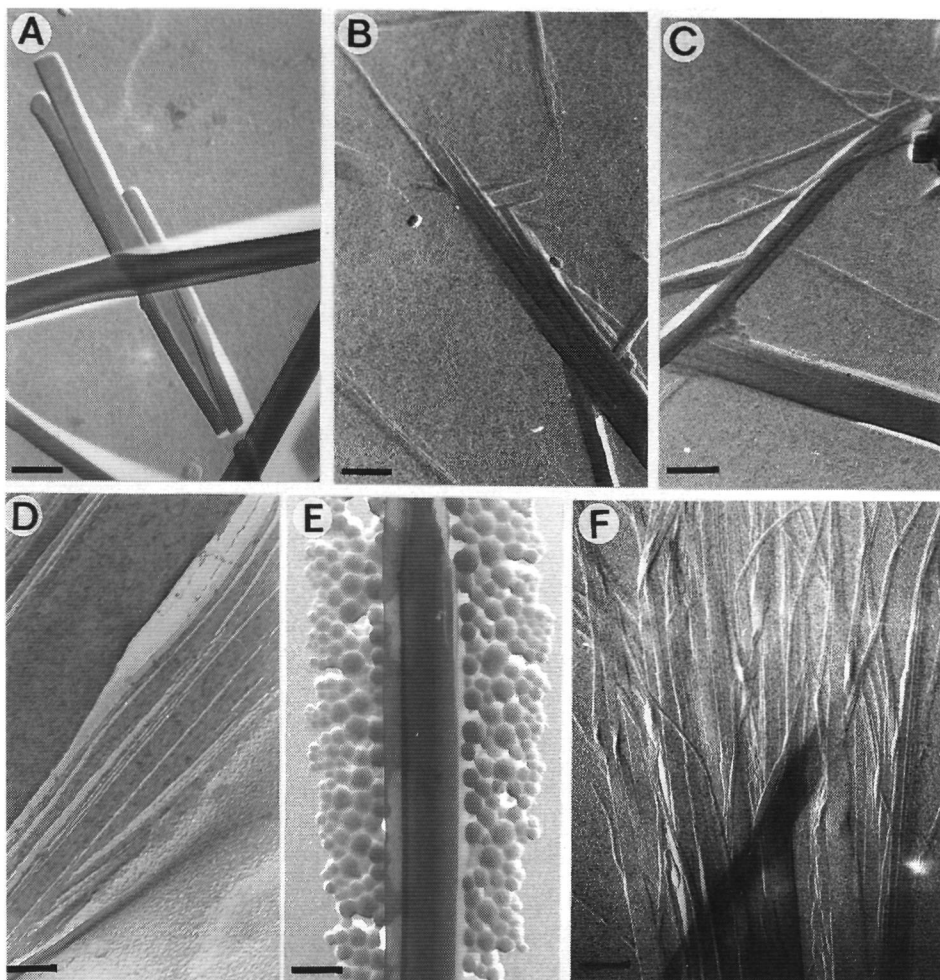
According to TEM and SEM, the copper complex ( $[(3)_4\text{Cu}][\text{ClO}_4]_2$ ) self-assembled in water to give multi lamellar spherical vesicles with a broad size distribution (pictures not shown). The diameters of the aggregates ranged from 130 nm - 6800 nm.



**Figure 5.4** Electron micrographs of vesicles of  $[(2)_4\text{Cu}][\text{ClO}_4]_2$ . A) SEM picture, bar is 10  $\mu\text{m}$ . B) TEM picture of dried vesicles, bar is 2.60  $\mu\text{m}$ . C) Freeze-etched electron micrograph showing multilamellar vesicles, bar is 298 nm.

*1-(n-Octyl)-4-imidazolyl-N-D-gluconamide (4)*. This compound dissolved in hot water and formed a gel upon cooling to room temperature. The gel crystallized after a few hours. TEM pictures taken from the gel showed ribbons (Figure 5.5A), which were composed of fibers (Figures 5.5B and C). According to freeze-etching experiments, the ribbons had a multilayer

structure (Figure 5.5D). The same type of ribbons was formed on cooling a warm clear solution of **4** in methanol (pictures not shown).



**Figure 5.5** TEM pictures of **4** in water (Pt shadowing), A) ribbons, bar is 275 nm, B) + C) ribbons showing fibers at their ends (bars are 260 and 250 nm, respectively), D) electron micrographs of a freeze-etched ribbon, bar is 75 nm, E) ribbons and vesicles obtained from an aqueous mixture of **4** and  $\text{Co}(\text{ClO}_4)_2$  (molar ratio  $\text{Co}/4 = 1/6$ ), bar is 231 nm, F) fibers formed in a mixture of **4** and  $\text{Ni}(\text{ClO}_4)_2$  in water (molar ratio  $\text{Ni}/4 = 1/4$ ), bar is 244 nm.

The 1:2 metal to ligand complex of **4** and  $\text{Cu}(\text{ClO}_4)_2$  yielded vesicles in water with an uniform diameter of 90 nm (pictures not shown). Mixing **4** and  $\text{Co}(\text{ClO}_4)_2$  in water in a 1:6 metal to ligand ratio<sup>10</sup> gave, according to TEM, both ribbons and vesicles (Figure 5.5E). Adding  $\text{Ni}(\text{ClO}_4)_2$  to a hot clear solution of **4** in a 1:4 metal to ligand ratio yielded after cooling ribbons and fibers (Figure 5.5F), while mixing  $\text{Mn}(\text{ClO}_4)_2$  and **4** in a 1:6 metal to ligand ratio gave fibers



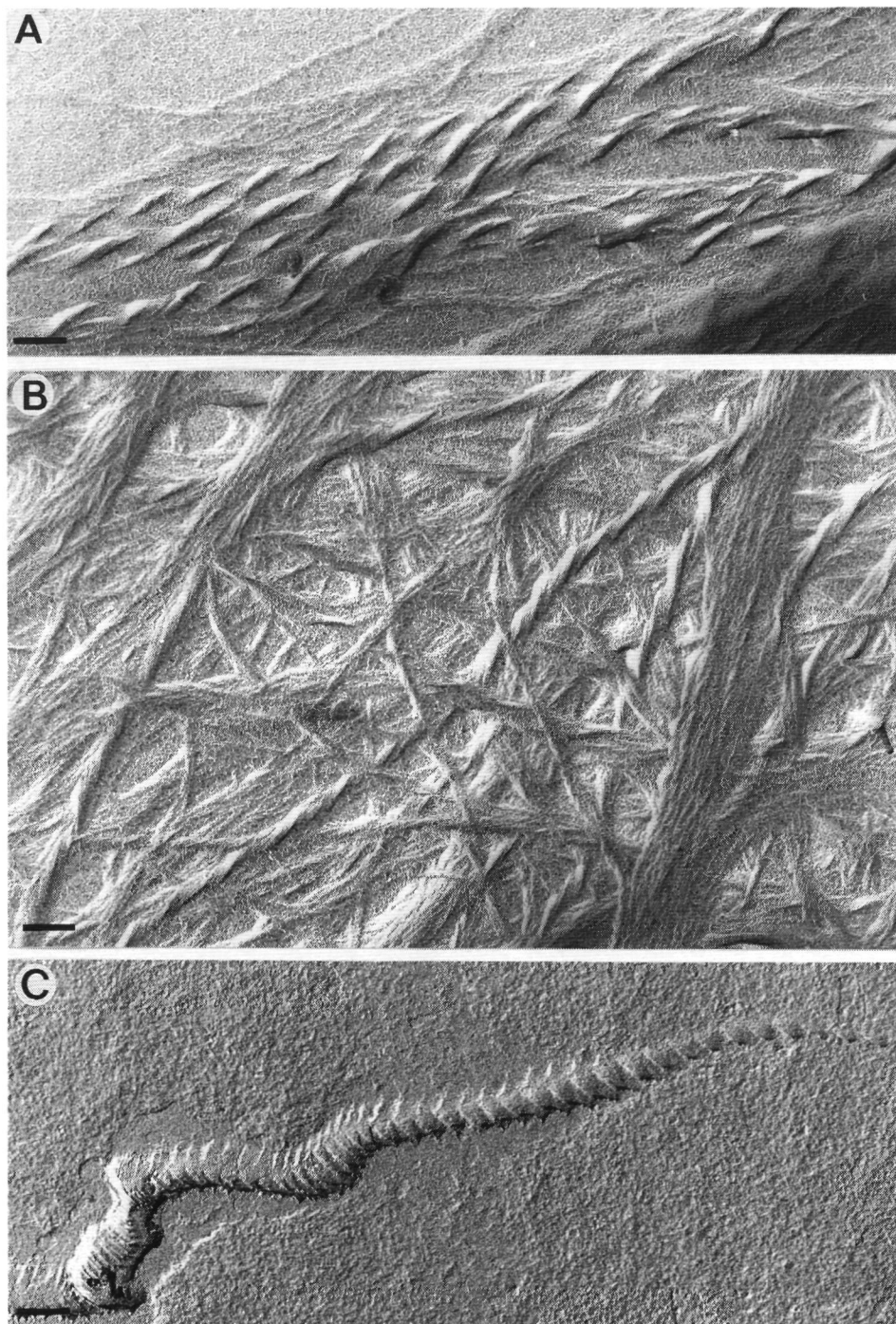
only (pictures not shown) The complexation behavior of  $\text{Co}(\text{ClO}_4)_2$ ,  $\text{Mn}(\text{ClO}_4)_2$  and  $\text{Ni}(\text{ClO}_4)_2$  with **4** was not studied further in detail All dispersions gave precipitates after a while

*N*-(11-(1-Imidazolyl)-*n*-undecyl)-*D*-gluconamide (**5**) This compound was readily soluble in acidic (acetic acid/sodium acetate buffer, pH=4.5) and alkaline (Tris buffer, pH=8.5) solutions Both the protonated (acetate buffer) and the neutral form (Tris buffer) of **5** did not form turbid solutions or gels in water like *N*,*n*-octyl-*D*-gluconamide and *N*,*n*-dodecyl-*D*-gluconamide did The suspension of neutral **5** was investigated with TEM Amorphous droplets with irregular offshoots were visible Although TEM showed some irregularly shaped structures, we believe that these are formed during the quick drying process, because the aqueous solution of **5** remained clear even after cooling, indicating that **5** did not form superstructures in solution Addition of  $\text{Cu}(\text{ClO}_4)_2$  (1:4 metal to ligand ratio),  $\text{Co}(\text{ClO}_4)_2$  (1:6 ratio),  $\text{Ni}(\text{ClO}_4)_2$  (1:4 ratio),  $\text{Mn}(\text{ClO}_4)_2$  (1:6 ratio) and  $\text{Zn}(\text{ClO}_4)_2$  (1:4) to hot clear solutions of **5** in water in all cases resulted in turbid mixtures in which no well-defined aggregates could be observed by TEM, except for the Mn complex in which case planar bilayer structures were visible (picture not shown)

*Mixture of N*-(2-(2-imidazolyl)-ethyl)-*D*-gluconamide (**6**) and 1-imidazolyl-hexadecane (**8**). Before studying the aggregation behavior of mixed complexes of compounds **6** and **8** with  $\text{Cu}(\text{ClO}_4)_2$ , we first prepared the separate complexes  $[(\mathbf{6})_4\text{Cu}][\text{ClO}_4]_2$  ( $(\mathbf{6})_4\text{Cu}$ ) and  $[(\mathbf{8})_4\text{Cu}][\text{ClO}_4]_2$  ( $(\mathbf{8})_4\text{Cu}$ ) and investigated these complexes with TEM Complex  $(\mathbf{6})_4\text{Cu}$  dissolved in water without giving suprastructures while  $(\mathbf{8})_4\text{Cu}$  formed ill-defined droplets (no vesicles)<sup>11</sup> A mixture of **6** (2 equiv), **8** (2 equiv) and  $\text{Cu}(\text{ClO}_4)_2$  (1 equiv) in water,<sup>12</sup> however, showed the presence of vesicles with diameters in the range of 150 to 500 nm (pictures not shown)

In order to obtain further information about the physical properties of the complexes we also recorded DSC thermograms of  $(\mathbf{6})_4\text{Cu}$  and  $(\mathbf{8})_4\text{Cu}$ , separately and the mixed complex of **6** and **8** with  $\text{Cu}(\text{ClO}_4)_2$  in water The complex  $(\mathbf{6})_4\text{Cu}$  dissolved in water at room temperature giving a dark blue solution, which showed no phase transition upon heating or cooling, while the complex  $(\mathbf{8})_4\text{Cu}$  in water was found to display a broad transition between 32 and 74 °C (maximum at 56 °C) The mixed complex of **6**, **8** and  $\text{Cu}(\text{ClO}_4)_2$  (2:2:1 molar ratio) in water showed on heating a thermogram which was almost similar to that of  $(\mathbf{8})_4\text{Cu}$  in water Thus the phase transition temperatures in the mixed complex are merely determined by ligand **8**, i.e. by the aliphatic chain and not by the carbohydrate head group A strong influence of the aliphatic tail on the aggregation behavior of gluconamide amphiphiles was also found in the thermotropic LC behavior of these compounds (see Chapter 3)

6-Deoxy-6-(1-imidazolyl)-*N*,*n*-octyl-*D*-gluconamide (**7**) This compound was dissolved in an acetic acid/sodium acetate buffer (pH=4.5, **7** is protonated) but formed no aggregates after cooling In a Tris buffered solution of **7** (pH=8.5, **7** is in neutral form) twisted ribbons with regular twists in one direction and fibers were visible by TEM (see Figure 5.6A and B) The copper complex  $[(\mathbf{7})_4\text{Cu}][\text{ClO}_4]_2$  showed, after freeze-etching, an interesting but rather strange aggregate (Figure 5.6C), which is probably a helix or a braid torn apart during the freeze-etching experiment



**Figure 5.6** TEM pictures of **7** and its copper (II) complex in water (Pt shadowing) A) twisted ribbons and B) fibers of **7**. C) Freeze-etched electron micrograph of  $[(7)_4Cu][ClO_4]_2$  dispersed in water.

### 5.3.6 Isotherms

In order to investigate why compound **5** fails to exhibit amphiphilic behavior, isotherms were recorded using the Langmuir film balance technique. For comparison similar experiments were carried out with *N*,*n*-dodecyl-D-gluconamide and compound **8** in the neutral and charged form. The latter compound appeared to form unstable monolayers both on an aqueous subphase which was buffered with Tris (pH=8.5, **8** in the neutral form) and on a subphase buffered with acetic acid/sodium acetate (pH=4.5, **8** is positively charged). *N*-*n*-Dodecyl-D-gluconamide showed an isotherm without any plateau area. From the onset of the surface pressure - surface area curve a molecular area of  $19.9 \text{ \AA}^2$  could be calculated, which did not change very much when the temperature or pH was changed. When **5** was spread on a Tris buffered subphase the surface pressure did not increase upon decreasing the surface area, which indicated that the molecules dissolved in the subphase without forming a monolayer. A similar result was obtained on an acetate buffered subphase indicating that the monolayer was not stable. Because of this negative result no further experiments were carried out with **5**.

### 5.3.7 X-ray powder diffraction experiments

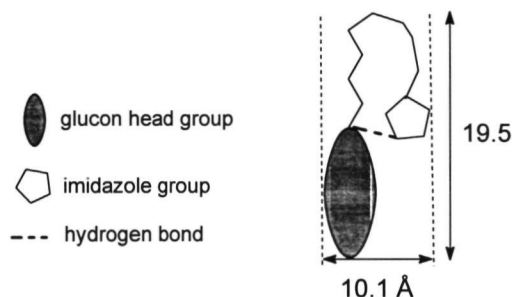
Powder diffractograms of lyophilized unprotonated **7** were recorded which showed that this compound is packed in layers with an interlayer distance similar to that of compound **1** (see Table 5.3 and Chapter 3). This suggests that the alkyl chains of **7** are interdigitized (Table 5.3). Although lyophilization can disturb the packing, we believe that by rapid cooling of the samples the ordering of the molecules in the aggregates is maintained. For lyophilized **4** a periodicity of  $38.5 \text{ \AA}$  was measured, which indicates that the molecules are packed in bilayers with their tails facing each other.<sup>13</sup> This packing is similar to the packing of *N*,*n*-octyl-D-gluconamide in aqueous aggregates,<sup>14</sup> but different from the monolayered head to tail packing found in the crystal structures of gluconamides, e.g. *N*,*n*-undecyl-D-gluconamide ( $19.5 \text{ \AA}$ ).<sup>13</sup>

**Table 5.3** Results of powder diffraction experiments on lyophilized samples of various gluconamides

Compound	d (Å)	Packing mode
<b>1</b>	25.5	bilayer (interdigitized)
<b>4</b>	38.5	bilayer (tail to tail)
<b>7</b>	26.5	bilayer (interdigitized)
<b>5H<sup>+</sup></b>	10.1 and 19.7	folded chain

Compound **5**, freeze-dried from Tris buffered solution, did not give a useful diffractogram indicating that the packing of the molecules was irregular. To our surprise lyophilization of **5** from an acetate buffered solution gave (according to the powder diffractogram), a highly ordered sample. Two periodicities, viz.  $10.1 \text{ \AA}$  and  $19.7 \text{ \AA}$ , were observed. According to CPK models,  $19.7 \text{ \AA}$  is a too small length for a stretched out molecule and, hence, also for molecules packed in an interdigitized bilayer. This length may indicate, however, that the alkyl chains of the

molecules are folded back, allowing the imidazole groups to form intramolecular hydrogen bonds with the amide groups. The 10 Å periodicity derived from the powder diffractograms, is also consistent with an alkyl chain that is folded back (see Figure 5.7). This folding disturbs the length-width ratio which is outside the range required for amphiphilic behavior of the molecule,<sup>15</sup> and is probably the reason why **5** does not form a stable monolayer on the air water interface and does not form aggregates in water.



**Figure 5.7** Schematic drawing of gluconamide **5** with a folded alkyl chain.

### 5.3.8 Thermotropic L.C. behavior

Experiments in the literature<sup>16</sup> and our own experiments,<sup>17</sup> have indicated that the amide function in a gluconamide is not very important for generating thermotropic L.C. behavior. The presence of a long alkyl chain and a glucon head group is thought to be sufficient for the molecules to display this behavior. DSC experiments carried out on **4** showed that this compound is not liquid crystalline although it had the required properties. Despite the absence of an intermolecular amide hydrogen bonding array, the melting point of **4** (172.3 °C) is higher than that of comparable non-modified gluconamides (e.g. *N*,*n*-octyl-D-gluconamide, m.p. 159.2 °C or *N*,*n*-undecyl-D-gluconamide m.p. 156.7 °C<sup>16</sup>). Apparently the interaction between the imidazole groups of neighboring molecules is very strong. Compound **5** did not show thermotropic L.C. behavior either, which is probably due to the folding of the alkyl chain, that prevents the molecules to adopt the rod-shaped form required for generating liquid crystalline behavior.

### 5.4 Concluding remarks

In the previous chapters we have shown that the imidazole groups in our gluconamides are of great importance to obtain (tunable) aggregation behavior in aqueous solution and to generate thermotropic L.C. behavior.<sup>17</sup> Based on the results described in this chapter, we may add to this that also the location of the imidazole group in the gluconamide is important for the aggregation behavior of this molecule. The ability to form highly organized aggregates is lost when in the gluconamide the imidazole group is moved from carbon atom C<sup>6</sup> to carbon atom C<sup>5</sup> (compare the generation of non-uniform sized vesicles from [(2)<sub>4</sub>Cu][ClO<sub>4</sub>]<sub>2</sub> with the braids formed from [(1)<sub>4</sub>Cu][ClO<sub>4</sub>]<sub>2</sub> (see Chapter 4). In the case of **5**, where the imidazole is located at the terminus of the hydrophobic part of the molecule, the alkyl chain was shown to folded back and to form an

intramolecular hydrogen bond with the amide function. As a result the conformation of the gluconamide was not fit for proper amphiphilic character.<sup>15</sup> A possible solution to overcome this problem is the introduction of a rigid segment in the alkyl chain, *e.g.* diacetylene function, but also in this case the risk of losing amphiphilic character is present (see Chapter 4).

In compound **4**, the imidazole is located between the head group and the alkyl chain. The carbohydrate part including the amide group of this compound is similar to that of *N*,*n*-octyl-D-gluconamide. One would expect, therefore, similar aggregation behavior for these two compounds,<sup>18</sup> because the hydroxyl groups in both cases can form inter-molecular hydrogen bonds which are important for the aggregation process, especially in aqueous solutions.<sup>19</sup> In theory, the packing of the molecules of **4** in the aggregates should be looser than that in aggregates of *N*,*n*-octyl-D-gluconamide, because the imidazole group is more bulky than one or two methylene groups. Remarkably, the packing in the former case appeared to be tighter than that in the latter case. An indication for this is the melting point of **4** which was found to be higher than that of the unmodified gluconamide, and melting points reflect the strength of the crystal packing (see Chapter 3). The aggregation behavior of **4** was not dependent on the solvent (methanol or water), whereas the aggregation of *N*,*n*-octyl-D-gluconamide was (see Chapter 6). The imidazole groups of molecules of **4** presumably show  $\pi$ - $\pi$  stacking interactions as they do in the aggregates of gluconamide **1** (see Chapters 3 and 6).

It is questionable whether it is possible to use **4** as an amphiphilic matrix for the anchoring of catalytically active metal complexes as was suggested in the Introduction. The metal complexing behavior of this compound is disturbed due to its bulkiness (only 1:2 metal to ligand complexes with  $\text{Cu}(\text{ClO}_4)_2$  were observed), and this bulkiness will prevent further coordination of substrates, which is necessary for catalysis. In addition, dissociation of **4** from the coordination sphere of the metal, which is needed for aziridination reactions (see Chapter 7), is very unlikely given the inflexibility of the ligand. This inflexibility was demonstrated by the presence of a strong hydrogen bond between the amide function in **4** and the imidazole group.

In principle, it is possible to create amphiphilic metal complexes by binding ligand molecules with different character, *i.e.* hydrophobic and hydrophylic, to a metal center. We have demonstrated that this idea is viable by mixing the hydrophobic imidazole derivative **8** and the hydrophylic imidazolyl derivate **6**, in water with copper (II) ions. The resulting complex displayed amphiphilic behavior and formed vesicles.

## 5.5 Literature

<sup>1</sup> Kunitake, T., Ishikawa, Y.; Shimomura, M. *J Am Chem Soc* **1986**, *108*, 327

<sup>2</sup> a) Menger, F M., Lee, J.-J.; Hagen, S. *J Am Chem Soc* **1991**, *113*, 4017, b) Kimizuka, N., Handa, T., Ichinose, I., Kunitake, T. *Angew Chem* **1994**, *106*, 2576, *Ibid Int Ed Eng* **1994**, *33*, 2483

<sup>3</sup> Ishikawa, Y., Kunitake, T. *J Am Chem Soc* **1986**, *108*, 8300.

<sup>4</sup> a) Brown, J M., Bunton, C.A. *J Chem Soc., Chem Commun* **1974**, 969; b) Kunitake, T., Ihara, H., Okahata, Y. *J Am Chem Soc* **1983**, *105*, 6070; c) Cleij, M.C., Drenth, W., Nolte, R.J.M. *Recl Trav Chim Pays-Bas* **1993** *112*, 1

- <sup>5</sup> Al-Shaar, A H M , Gilmour, D W , Lythgoe, D J , McClenaghan, I , Ramsden, C A *J Chem Soc Perkin Trans I* **1992**, 2779
- <sup>6</sup> McCaldin, D J *Chem Rev* **1960**, 60, 39
- <sup>7</sup> The pK<sub>a</sub>\* of imidazole in methanol/water is 6.96, see Chapter 4 and CRC Handbook of Chem and Phys 51<sup>st</sup> edition, Ed R C Weast, CRC Press, Cleveland Ohio, **1970**, D-118
- <sup>8</sup> Bernarducci, E , Schwindinger, W F , Hughey, IV, J L , Krogh-Jespersen, K , Schugar, H J *J Am Chem Soc* **1981**, 103, 1686
- <sup>9</sup> Tang, C C , Davalian, D , Huang, P , Breslow, R *J Am Chem Soc* **1978**, 100, 3918
- <sup>10</sup> The stoichiometry of the complexes between imidazole ligands and Co(ClO<sub>4</sub>)<sub>2</sub>, Ni(ClO<sub>4</sub>)<sub>2</sub>, and Mn(ClO<sub>4</sub>)<sub>2</sub> is (ligand to metal) 6 : 1, 4 : 1, and 6 : 1, respectively, cf Reedyk, J *Recl Trav Chim Pays-Bas*, **1969**, 1451
- <sup>11</sup> Compound **8** did not dissolve in water, not even after prolonged heating. The ligand, therefore, was dissolved in methanol, mixed with [Cu][ClO<sub>4</sub>]<sub>2</sub> (which resulted in a turbid mixture) and injected in water
- <sup>12</sup> The components were mixed before adding the copper(II) salt. Compound **8** was brought in water by injection
- <sup>13</sup> A tail-to-tail packing of *N*-n-undecyl-D-gluconamide shows a periodicity of 39.5 Å, see also Jeffrey, G A , Maluszinska, H *Carbohydr Res* **1990**, 207, 211
- <sup>14</sup> Svenson, S , Köning, J , Fuhrhop, J -H *J Phys Chem* **1994**, 98, 1022
- <sup>15</sup> Israelachvili, J N , Marcelja, S , Horn, R G *Quart Rev Biophys* **1980**, 13, 121
- <sup>16</sup> Pfannemüller, B , Welte, W , Chin, E , Goodby, J W *Liq Cryst* **1986**, 1, 357
- <sup>17</sup> See Chapters 3 and 4
- <sup>18</sup> a) Pfannemüller, B , Kühn, I *Macromol Chem* **1988**, 189, 2433, b) Tavel, F T , Pfannemüller, B *Macromol Chem* **1990**, 191, 3097
- <sup>19</sup> a) Fuhrhop, J -H , Schnieder, P , Rosenberg, J , Boekema, E *J Am Chem Soc* **1987**, 109, 3387, b) Fuhrhop, J -H , Schnieder, P , Boekema, E , Helfrich, W *J Am Chem Soc* **1988**, 110, 2861, c) Fuhrhop, J -H , Boettcher, C *J Am Chem Soc* **1990**, 112, 1768-1776, d) Köning, J , Boettcher, C , Winkler, H , Zeitler, E , Talmon, Y , Fuhrhop, J -H *J Am Chem Soc* **1993**, 115, 693, e) Svenson, S , Kirste, B , Fuhrhop, J -H *J Am Chem Soc* **1994**, 116, 11969, g) Frankel, D A , O'Brien, D F *J Am Chem Soc* **1994**, 116, 10057



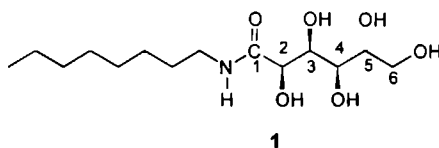
# Chapter 6

## Organo-gels from carbohydrate amphiphiles

### 6.1 Introduction

In supramolecular chemistry, assemblies of molecules held together by non-covalent interactions such as electrostatic interactions, VanderWaals interactions and H-bonding are receiving great interest. Amphiphiles consisting of a carbohydrate head group<sup>1</sup> to which an aliphatic alkyl chain is connected by an amide function are known to form fibrous aggregates upon dispersion in water<sup>2,3</sup>. Recently, we described imidazole containing carbohydrate amphiphiles which self assemble to give aggregates of which the structure can be tuned by changing the solvent conditions and by addition of copper ions<sup>4</sup>.

The behavior of supramolecular aggregates to some extent is comparable to that of macromolecules, for example repetitive units linked to each other by non-covalent or covalent bonds, can give a network resulting in a gel-like structure. A difference, however, is that gels obtained from supramolecules can be disintegrated by addition of a cosolvent or by raising the temperature because the connections are non-covalent bonds, whereas network structures obtained from macromolecules disintegrate only by breaking chemical bonds.



*N*-octyl-D-gluconamide **1** is known to form a highly viscous gel in aqueous solutions. Using transition electron microscopy (TEM) in combination with image analysis,<sup>5</sup> DSC<sup>6</sup> and NMR<sup>7</sup> it was proposed that this gel consists of 4 intertwined superhelices.<sup>8</sup> The self-assembly of **1** into helices has been ascribed to the formation of an intermolecular hydrogen bonding network, from which, during the aggregation, water molecules are expelled.<sup>2,9</sup> Different proposals regarding the packing arrangement of the gluconamide molecules in the aggregates have been made, viz head to tail<sup>10</sup> as found in the crystal structure<sup>11</sup> of **1** and head to head<sup>12</sup> which is seen more commonly for amphiphilic molecules in water. We believe that the latter packing is the most likely one given the powder diffraction experiments on lyophilized fibers which were recently published in the literature.<sup>10</sup>

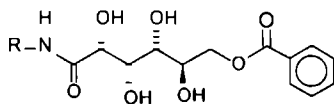
Neither the length of the alkyl chain nor the introduction of a diacetylene function into this chain was found to have a dramatic influence upon the aggregation behavior of molecules of type **1** in water.<sup>13</sup> Variations in the head group, however, dramatically changed the type of clustering.<sup>5a,13</sup> Gluconamide **1** has also been reported to gelate in 1,2-xylene,<sup>5</sup> forming bilayer scrolls, but this organogel was found to be very unstable.<sup>5</sup> Unfortunately, **1** is scarcely soluble in



common organic solvents like acetone, chloroform and dioxane, and, therefore, is not an ideal molecule for an extensive study of its gelation effects in organic solvents

Gelation in organic solvents has so far been observed for lecithins,<sup>14</sup> cholesterol derivatives,<sup>15</sup> peptides,<sup>16</sup> two-component gelling agents,<sup>17</sup> calixarenes,<sup>18</sup> semifluorinated *n*-alkanes<sup>19</sup> or silanes,<sup>20</sup> phenols<sup>21a</sup> and phthalocyanines<sup>21b</sup>. Despite the fact that a relatively broad range of compounds displays gelation, no rules of thumb for the design of such compounds have been given in the literature. This contrasts the situation for the classical amphiphilic compounds where such rules have been proposed.<sup>22</sup> Some factors, however, are known to stimulate gelation behavior, *viz* the possibility to form hydrogen bonds (as found in amide<sup>17</sup> and urethane<sup>16c</sup> gels) and a rod-shape geometry of the building block.<sup>15b</sup>

As part of our program aimed at the design and synthesis of supramolecular structures from carbohydrate amphiphiles and more particularly the fine-tuning of these structures, we synthesized compound **2a**. To our surprise **2a** formed gels at low concentrations in common organic solvents like chloroform, ethyl acetate and acetone. The introduction of the benzoate ester apparently changed the characteristic features of the carbohydrate moiety which is now located between two hydrophobic groups: the alkyl chain connected via the amide function and the ester group coupled at the C<sup>6</sup> end of the carbohydrate group.

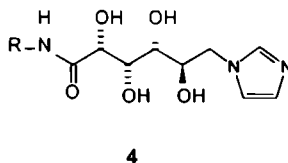
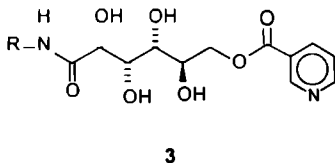


**2a** R= n-octyl  
**2b** R= n-hexadecyl

Stimulated by this finding we decided to study in more detail the organogel forming properties of *n*-alkyl-D-gluconamides. The results are described in this chapter. The investigations have been carried out using electron microscopy (EM), differential scanning calorimetry (DSC), NMR, UV-vis spectroscopy, X-ray powder diffraction (SAXS) and FT-IR. In order to be able to understand the driving forces behind organogel formation and hopefully to present suggestions for the design of new amphiphilic organo-gelators, a number of gluconamide derivatives based on gluconamide **1** have been synthesized and investigated. The rationale behind the choice of derivatives is presented below.

#### *Derivatives with aromatic nitrogen substituents on C<sup>6</sup>*

In order to probe the influence of an electron donor site in the aromatic head group, compounds **3** (pyridyl group) and **4** (imidazolyl group) have been synthesized.

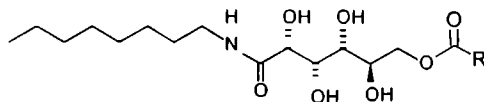


R = n-octyl

From investigations on the aggregation behavior of the imidazolyl compound **11** in water (see below) we know that the imidazole function plays an important role in the self assembly behavior of the amphiphiles (see Chapters 3 and 4). A crystal structure of **11** revealed that H-bonding by entrapped water molecules is important for the aggregation behavior of this compound. By comparing **3** and **4** with gluconamide **2**, we hoped to get insight in the influence of H-bonding by entrapped water molecules on the gelation behavior. Besides that, pyridyl and imidazolyl groups are metal complexing groups and therefore **3** and **4** are potentially interacting building blocks for catalytic systems which is part of another research program, see Chapter 7.

#### Derivatives with aliphatic substituents on C<sup>6</sup>

The benzoate ester (**2a**), 3-pyridine carboxylic ester (**3**) and imidazolyl (**4**) substituents are all aromatic moieties and can display  $\pi$ - $\pi$  stacking interactions. For comparison we have also synthesized a series of aliphatic ester functionalized gluconamides compounds **5-6**, which cannot give  $\pi$ - $\pi$  stacking. To investigate the effect of a bulky substituent we have also prepared compound **7**. The n-octanoic ester (see **6**) also is a relatively bulky group, but for compound **6** still a tight packing of the head groups can be expected because non-branched aliphatic chains tend to aggregate in a regular manner.



**5** R = CH<sub>3</sub>

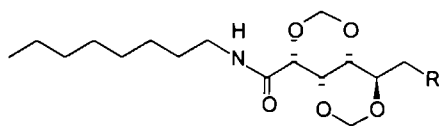
**6** R = (CH<sub>2</sub>)<sub>6</sub>ClCH<sub>3</sub>

**7** R =

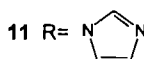
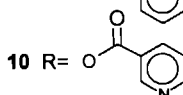
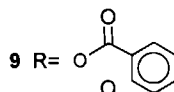
#### Methylene protected derivatives

Although the hydroxyl functions in carbohydrates of type **1** are generally considered to be important for the formation of a hydrogen bonding network,<sup>1,13</sup> we found that carbohydrate amphiphiles with protected hydroxyl groups can still form suprastructures in water (see Chapter 4).<sup>4</sup> The 2,4,3,5 dimethylene gluconamides **8-11** all have their secondary hydroxyl groups protected but contain the same functional groups that are present in **1**, **2a**, **3** and **4** (hydroxyl).

benzoyl, 3-pyridyl, and imidazolyl respectively) These compounds therefore have been included in this study for reasons of comparison

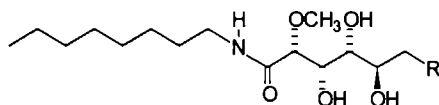


**8** R= OH

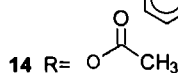
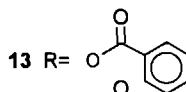


#### *Derivatives protected on C<sup>2</sup> with a methoxy group*

Compound **12** is special in the sense that it contains a methoxy group on the carbon atom C<sup>2</sup> which prohibits 1,3-*syndiaxial* interactions<sup>5a,7b 12 23</sup> between the -OH functions on C<sup>2</sup> and on C<sup>4</sup>. These *syndiaxial* interactions are believed to induce a bend in the glucon head group leading to a sickle-type of conformation<sup>23</sup>. We decided to include this compound in our study. It should be noted that the bulkiness of the methoxy group by itself can cause a bending in the head group. In general a disturbed linearity of the head group will increase the solubility of the amphiphile in water and may contribute to the formation of highly curved aggregates like helical micellar rods<sup>5a</sup>.



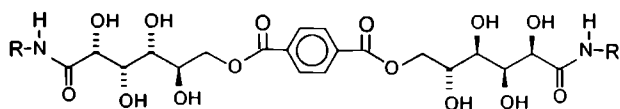
**12** R= OH



Too much bending, however, will not be advantageous for molecular ordering,<sup>22b</sup> which makes it difficult to predict the behavior of **12**. For comparison, we also prepared the derivatives **13** and **14**, which contain a benzoate and acetate function on C<sup>6</sup> respectively.

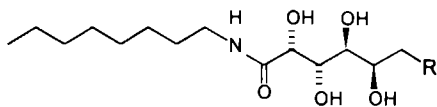
### Dimers of *N*,*n*-octyl-*D*-gluconamides

The introduction of an aliphatic substituent on the head group, as in **6** gives a gluconamide with two equally long alkyl chains at either end. In addition to compound **6**, we also prepared **15** which contains two *N*,*n*-octyl-*D*-gluconamide moieties linked up together at their head groups via a terephthalate spacer. This type of amphiphile has been previously reported by Menger and was named gemini surfactant.<sup>24</sup> For gemini surfactants, inverted bilayer structures with both alkyl chains facing the solvent can be expected.<sup>25</sup> Packing constraints are important in the understanding of the process of building up the aggregates.<sup>12, 13, 22a</sup> From the crystal structures of several gluconamides with aliphatic chains it is known that these molecules tend to crystallize in a head to tail manner.<sup>26</sup> Using **6** and **15** we hoped to obtain a monolayered packing of the amphiphiles, which has a head to head ordering. The idea is somewhat similar to the membrane spanning bolaamphiphiles,<sup>27</sup> which form monolayers of molecules having head groups on both ends. Since in **6** the head group is in the center, this molecule could be called a reversed bolaamphiphile, while **15** fits the gemini surfactant description.<sup>24</sup>

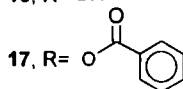


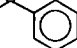
**15** R= *n*-octyl

For comparison we also synthesized the galactonamides **16** and **17**. Open-chain galactonamides do not have a bent head group like gluconamides have. In the case of compound **16** this results in a decreased solubility in water and a complete insolubility in 1,2-xylene. The low tensile gel which can be prepared at low concentrations in water, has been reported to contain helically twisted ribbons.<sup>5a</sup>



**16**, R= OH



**17**, R= 

## 6.2 Experimental section

### 6.2.1 Syntheses

All solvents were distilled before use and dried on Mol Sieves 3 or 4 Å. Special care was taken with pyridine (distilled from CaH<sub>2</sub>), because this solvent is hygroscopic.

Analytical instruments and electron microscopes used, were identical to those described in the previous chapters.

The melting points were obtained from DSC measurements (the average of onset and peak of the melting transition). The synthesis of compound **1** has been described by Pfannemüller et al.<sup>2</sup>

***N,n*-Octyl-D-gluconamide-6-benzoate (2a).** Benzoyl chloride (1 306 g, 9.29 mmol 1.08 equiv.) was dissolved in 5 ml of pyridine and added dropwise to a cooled (ice bath) and stirred gelated solution of 2.650 g (8.62 mmol) of *N,n*-octyl-D-gluconamide (**1**) in 40 ml of pyridine. The apparatus was purged with dried nitrogen gas. Over a period of 2 hrs. whilst stirring in which the temperature was raised from 0 to 60 °C, the resulting clear yellow mixture was poured into ± 600 ml of saturated NaHCO<sub>3</sub>/icewater. The precipitate was purified by column chromatography (silica gel, eluent CHCl<sub>3</sub>/MeOH 95:5, v/v), yield 3.22 g (7.83 mmol, 90 %), m.p. 145.9 °C IR (KBr) 3660-3030 cm<sup>-1</sup> broad (OH), 1720/1703 (C=O, ester), probably more than one conformation in the solid state, only one peak in solution (THF) 1722, 1666 (amide I), 1546 (amide II). <sup>1</sup>H-NMR (DMSO-d<sub>6</sub>) δ 8.014 ppm (d, 2H, ArH), 7.636 (2 d, 1H, ArH), 7.516 (t, 2H, ArH), carbohydrate skeleton protons see Table 6.6, 3.063 (9 peaks, 2H, -(CH<sub>2</sub>)<sub>6</sub>-CH<sub>2</sub>-NHCO), 1.397 (t, 2H, -(CH<sub>2</sub>)<sub>5</sub>-CH<sub>2</sub>-CH<sub>2</sub>NHCO), 1.226 (broad s, 10H, CH<sub>3</sub>-(CH<sub>2</sub>)<sub>5</sub>-CH<sub>2</sub>-), 0.842 (t, 3H, CH<sub>3</sub>-). EI-MS *m/z* 412 (M+H)<sup>+</sup>, 156 (C<sub>8</sub>H<sub>17</sub>-NHC=O)<sup>+</sup>, 105 (ArC=O)<sup>+</sup>, 77 (C<sub>6</sub>H<sub>5</sub>). Anal. Calcd. for C<sub>21</sub>H<sub>33</sub>NO<sub>7</sub>: C, 61.30; H, 8.08; N, 3.40. Found: C, 61.22; H, 7.97; N, 3.40.

***N,n*-Dodecyl-D-gluconamide-6-benzoate (2b).** For the synthesis of this compound the procedure described for compound **2a** was followed using 3.081 g (8.476 mmol) of *N,n*-dodecyl-D-gluconamide (for the synthesis of this compound see Chapter 3) and 1.059 g (7.534 mmol) of benzoyl chloride. Yield 0.23 g (0.49 mmol, 6.5 %, not optimized), m.p. 153.0 °C. IR (KBr) similar to the spectrum found for **2a**. <sup>1</sup>H-NMR similar to the NMR spectrum obtained for **2a**, except for the integral of the methylene protons of the alkyl chain, which was equivalent to 18 protons. EI-MS *m/z* 468 (M+H)<sup>+</sup>, 212 (C<sub>8</sub>H<sub>17</sub>-NHC=O)<sup>+</sup>, 105 (ArC=O)<sup>+</sup>, 77 (C<sub>6</sub>H<sub>5</sub>). Anal. Calcd for C<sub>25</sub>H<sub>41</sub>NO<sub>7</sub>: C, 64.22; H, 8.84; N, 3.00. Found: C, 64.28; H, 8.97; N, 2.95.

***N,n*-Octyl-D-gluconamide-6-(3-pyridyl)-carboxylate (3).** This compound was prepared in an analogous manner to compound **2a** using 3.023 g (9.83 mmol) **1** and 1.1417 g (10.01 mmol) of 3-pyridinecarboxyl chloride (prepared from 3-pyridinecarboxylic (nicotinic) acid and thionyl chloride) instead of benzoyl chloride. The removal of the excess of pyridine (70 ml) was carried out under reduced pressure and at elevated temperature. Yield 0.35 g (0.85 mmol, 9 %, not optimized), after column chromatography (silica, eluent Et<sub>3</sub>N/EtOH/CHCl<sub>3</sub>, 1:20:79 v/v/v), m.p. 155.9 °C. IR (KBr) 3600-3050 cm<sup>-1</sup>, broad (OH), 1711 (C=O, ester), 1624 (amide I), 1540 (amide II). <sup>1</sup>H-NMR (DMSO-d<sub>6</sub>) δ 9.160 ppm (d, 1H, ArH), 8.651 (2d, 1H, ArH), 8.347 (2d, 1H, ArH), 7.636 (t, 1H, NHCO), 7.574 (2d, 1H, ArH), carbohydrate skeleton protons see Table 6.6, 3.073 (9 peaks, 2H, -(CH<sub>2</sub>)<sub>6</sub>-CH<sub>2</sub>-NHCO), 1.404 (t, 2H, (CH<sub>2</sub>)<sub>5</sub>-CH<sub>2</sub>-CH<sub>2</sub>NHCO), 1.262 (broad s, 10H, CH<sub>3</sub>-(CH<sub>2</sub>)<sub>5</sub>-CH<sub>2</sub>-), 0.846 (t, 3H, CH<sub>3</sub>-); EI-MS *m/z* 412 M<sup>+</sup>, 156 (C<sub>8</sub>H<sub>17</sub>-NHC=O)<sup>+</sup>, 106 (PyrC=O)<sup>+</sup>, 78 (Pyr)<sup>+</sup>. Anal. Calcd. for C<sub>20</sub>H<sub>32</sub>N<sub>2</sub>O<sub>7</sub>: C, 58.24; H, 7.82; N, 6.79. Found C, 58.25, H, 7.64; N, 6.76.

**6-Deoxy-6-(1-imidazolyl)-*N,n*-octyl-D-gluconamide (4).** The synthesis and characterization of this compound are described in Chapter 5.

***N,n*-Octyl-D-gluconamide-6-acetate (5).** Acetic acid anhydride (1.031 g, 10.1 mmol, 1.01 equiv.) was dissolved in 15 ml of pyridine and added dropwise to a stirred (partly gelated) solution of 1.030 g (10.0 mmol) of *N,n*-octyl-D-gluconamide in 60 ml of pyridine at room temperature. The reaction vessel was purged with dry nitrogen. After 2 hrs. of stirring the solvent was evaporated at elevated temperature. The crude product was purified by column chromatography (silica gel, eluent CHCl<sub>3</sub>/MeOH, 9:1 v/v) and recrystallized from EtOAc. Yield

0.40 g (1.14 mmol, 11 %, not optimized), m.p. 130 °C IR (KBr) 3650-3030  $\text{cm}^{-1}$  broad (OH), 1736 (C=O, ester), 1640 (amide I), 1550 (amide II)  $^1\text{H-NMR}$  (DMSO- $d_6$ )  $\delta$  7.598 ppm (t, 1H, NHCO), carbohydrate skeleton protons see Table 6.6, 3.053 (9 peaks, 2H,  $(\text{CH}_2)_6\text{-CH}_2\text{-NH}$ ), 1.994 (s, 3H, O-CO- $\text{CH}_3$ ), 1.389 (t, 2H,  $-(\text{CH}_2)_5\text{-CH}_2\text{-CH}_2\text{NHCO}$ ), 1.227 (broad s, 10H,  $\text{CH}_3\text{-(CH}_2)_5\text{-CH}_2\text{-}$ ), 0.846 (t, 3H,  $\text{CH}_3\text{-}$ ), EI-MS  $m/z$  350 ( $\text{M}+\text{H}$ ) $^+$ , 276 ( $\text{C}_8\text{H}_{17}\text{-NHCO(CHOH)}_4$ ) $^+$ , 156 ( $\text{C}_8\text{H}_{17}\text{-NHC=O}$ ) $^+$ , 43 ( $\text{CH}_3\text{C=O}$ ) $^+$ , Anal. Calcd for  $\text{C}_{16}\text{H}_{31}\text{NO}_7$ : C, 55.00, H, 8.94, N, 4.01. Found: C, 54.57, H, 9.01, N, 4.41.

***N,n*-Octyl-D-gluconamide-6-(*n*-octalate) (6).** The synthetic procedure was analogous to that described for compound **2a**. Instead of benzoyl chloride, 1.633 g (10.04 mmol) of caprylyl chloride (prepared from octanoic acid and thionyl chloride, distilled prior to use) and 3.093 g (10.06 mmol) of **1** were used. To keep the acid chloride mixture fluid, gentle heating was applied. The vessel, however, containing the gluconamide mixture to which the caprolyl chloride was added, was kept at 0 °C. The precipitate obtained from pouring the clear reaction mixture into  $\text{NaHCO}_3/\text{ice}$  was purified by column chromatography (silica, eluent  $\text{CHCl}_3/\text{MeOH}$ , 9:1 v/v) and recrystallized from EtOAc. Yield 0.18 g (0.42 mmol, 4 %, not optimized), m.p. 146.8 °C IR (KBr) 3640-3060  $\text{cm}^{-1}$  broad (OH), 1736 (C=O, ester), 1640 (amide I), 1545 (amide II),  $^1\text{H-NMR}$  (DMSO- $d_6$ )  $\delta$  7.604 ppm (t, 1H, NHCO), for the carbohydrate skeleton protons see Table 6.6, 3.056 (10 peaks, 2H,  $-(\text{CH}_2)_6\text{-CH}_2\text{-NH}$ ), 2.274 (t, 2H, O-CO- $\text{CH}_2\text{--}(\text{CH}_2)_5$ ), 1.377 (t, 2H,  $(\text{CH}_2)_5\text{-CH}_2\text{-CH}_2\text{NHCO}$ ), 1.265 (broad s, 18H,  $(\text{CH}_2)_5\text{-CH}_2\text{-NHCO}$  and O-CO- $\text{CH}_2\text{-(CH}_2)_5$ ), 0.846 (t, 6H,  $\text{CH}_3\text{-}$ ), EI-MS  $m/z$  433 ( $\text{M}^+$ ), 156 ( $\text{C}_8\text{H}_{17}\text{-NHC=O}$ ) $^+$ , 127 ( $\text{CH}_3\text{-(CH}_2)_6\text{-C=O}$ ) $^+$ , Anal. Calcd for  $\text{C}_{22}\text{H}_{43}\text{NO}_7$ : C, 60.94, H, 10.00, N, 3.23. Found: C, 60.03, H, 10.01, N, 3.38.

***N,n*-Octyl-D-gluconamide-6-cyclohexanoate (7).** The synthetic procedure was analogous to that of compound **2a**, using 2.658 g (8.65 mmol) of **1**, and 1.337 g (9.12 mmol) of cyclohexanecarboxyl chloride (prepared from cyclohexanecarboxylic acid and thionyl chloride and distilled prior to use) instead of benzoyl chloride. Yield 2.16 g (5.18 mmol, 60 %) The compound was purified by column chromatography (silica eluent  $\text{CHCl}_3/\text{MeOH}$ , 96:4 v/v) m.p. 122.3 °C IR (KBr) 3650-3100  $\text{cm}^{-1}$  broad (OH), 1715 (C=O, ester), 1626 (amide I), 1544 (amide II)  $^1\text{H-NMR}$  (DMSO- $d_6$ )  $\delta$  7.614 ppm (t, 1H, NHCO), for the carbohydrate skeleton protons see Table 6.6, 2.289 (9 peaks, 1H,  $\text{OCHC}_5\text{H}_{10}$ ), 1.812 (d, 2H, cyclohexyl  $\text{CH}_2$ ), 1.655 (2d, 2H, cyclohexyl  $\text{CH}_2$ ), 1.570 (d, 1H, C-H from cyclohexyl group), 1.41-1.29 (7H, C-H +  $2\text{*CH}_2$  from cyclohexyl group +  $(\text{CH}_2)_5\text{-CH}_2\text{-CH}_2\text{NHCO}$ ), 1.231 (broad s, 10H,  $\text{CH}_3\text{-(CH}_2)_5\text{-CH}_2\text{-}$ ), 0.846 (t, 3H,  $\text{CH}_3\text{-}$ ), EI-MS  $m/z$  417 ( $\text{M}^+$ ), 290 ( $\text{C}_8\text{H}_{17}\text{-NHCO(CHOH)}_4\text{CH}_2$ ) $^+$ , 276 ( $\text{C}_8\text{H}_{17}\text{-NHCO(CHOH)}_4$ ) $^+$ , 156 ( $\text{C}_8\text{H}_{17}\text{-NHC=O}$ ) $^+$ , 111 ( $\text{C}_6\text{H}_{11}\text{C=O}$ ) $^+$ , 83 ( $\text{C}_6\text{H}_{11}$ ) $^+$ . Anal. Calcd for  $\text{C}_{21}\text{H}_{39}\text{NO}_7$ : C, 60.41, H, 9.41, N, 3.35. Found: C, 60.48, H, 9.41, N, 3.29.

The syntheses and characterization of compounds **8** and **11** are described in Chapter 3.<sup>4</sup>

**2,4,3,5-Dimethylene-*N,n*-octyl-D-gluconamide-6-benzoate (9)** Benzoyl chloride, 0.853 g (5.93 mmol, 2 equiv.) was dissolved in 10 ml of chloroform and added dropwise to a stirred solution of 0.826 g (2.49 mmol) of 2,4,3,5-dimethylene-*N,n*-octyl-D-gluconamide (**8**) and 0.258 g (2.55 mmol) of triethyl amine in 20 ml of chloroform which was placed in an ice bath. The reaction vessel was purged with dried nitrogen gas. After stirring overnight at room temperature and additional refluxing for 2 hrs., the mixture was washed with water, and the compound was purified by recrystallization from ethyl acetate. Yield 0.50 g (1.15 mmol, 46 %, not optimized), m.p. 148.0 °C IR (KBr) 3285  $\text{cm}^{-1}$  sharp (NH), 1719 (C=O, ester), 1660 (amide I), 1549 (amide II)  $^1\text{H-NMR}$  ( $\text{CDCl}_3$ )  $\delta$  8.042 ppm (d, 2H, ArH), 7.590 (t, 1H, ArH), 7.464 (t, 1H, ArH), 6.552 (t, 1H, amide H), 5.276 and 4.833 (2 times d, 2H, methylene bridge H), 5.059 and 5.002 (2 times d, 2H, methylene bridge H) for the carbohydrate skeleton protons see Table 6.6, 3.309 (q, 2H,  $-(\text{CH}_2)_6\text{-CH}_2\text{-NHCO}$ ), 1.510 (m, 2H,  $(\text{CH}_2)_5\text{-CH}_2\text{-CH}_2\text{NHCO}$ ), 1.262 (broad s,

10H,  $\text{CH}_3\text{-(CH}_2\text{)}_5\text{-CH}_2\text{-}$ ), 0 875 (t, 3H,  $\text{CH}_3\text{-}$ ) EI-MS  $m/z$  435 ( $\text{M}^+$ ), 156 ( $\text{C}_8\text{H}_{17}\text{-NHC=O}^+$ ), 105 ( $\text{C}_6\text{H}_5\text{C=O}^+$ ), 77 ( $\text{C}_6\text{H}_5^+$ ), Anal Calcd for  $\text{C}_{23}\text{H}_{33}\text{NO}_7$  C, 63 43, H, 7 64, N, 3 22 Found C, 63 43, H, 7 56, N, 3 22

**2,4,3,5-Dimethylene-*N,n*-octyl-D-gluconamide-6-(3-pyridyl) carboxylate (10)** The synthetic procedure was analogous to that described for compound 9 In the present case 0 829 g (2 50 mmol) of 8 and 0 386 g (2 73 mmol) of 3-pyridine-carboxylic acid chloride were used The crude product was purified by column chromatography (silica, eluent EtOAc/MeOH, 95 5 v/v), yield 0 25 g (0 57 g, 49 %, not optimized), m p 135 2 °C IR (KBr) 3281  $\text{cm}^{-1}$  sharp (NH), 1723 (C=O, ester), 1661 (amide I), 1549 (amide II),  $^1\text{H-NMR}$  ( $\text{CDCl}_3$ )  $\delta$  9 251 ppm (broad s, 1H, ArH), 8 826 (broad s, 1H, ArH) these two peaks are broadened probably due to dimer formation, in which water acts as a hydrogen bond donor to the pyridyl groups, at 2 507 ppm, a broad peak due to a water molecule is visible which integrates to one water molecule per two pyridyl ligands, 8 326 (d, 1H, ArH), 7 450 (2d, 1H, ArH), 6 566 (t, 1H, amide H), the patterns and chemical shifts of the methylene bridge and carbohydrate skeleton protons are similar to those of 9, 3 311 (q, 2H,  $\text{-(CH}_2\text{)}_6\text{-CH}_2\text{-NHCO}$ ), 1 513 (m, 2H,  $\text{-(CH}_2\text{)}_5\text{-CH}_2\text{-CH}_2\text{NHCO}$ ), 1 263 (broad s, 10H,  $\text{CH}_3\text{-(CH}_2\text{)}_5\text{-CH}_2\text{-}$ ), 0 876 (t, 3H,  $\text{CH}_3\text{-}$ ), EI-MS  $m/z$  350 ( $\text{M+H}^+$ ), 276 ( $\text{C}_8\text{H}_{17}\text{-NHCO(CHOH)}_4^+$ ), 156 ( $\text{C}_8\text{H}_{17}\text{-NHC=O}^+$ ), 43 ( $\text{CH}_3\text{C=O}^+$ ), Anal Calcd for  $\text{C}_{22}\text{H}_{32}\text{N}_2\text{O}_7 \cdot \frac{1}{2} \text{H}_2\text{O}$  C, 59 31, H, 7 47, N, 6 29 Found C, 59 44, H, 7 36, N, 6 31

**2-Methoxy-*N,n*-octyl-D-gluconamide (12)** To a mixture of 4 140 g (13 47 mmol) of *N,n*-octyl-D-gluconamide (1) and 1 105 g (19 70 mmol, 1 5 equiv) of powdered KOH in 35 ml of DMSO, was added dropwise 1 758 g (13 94 mmol, 1 03 equiv) of dimethyl sulfate<sup>28</sup> dissolved in 15 ml of DMSO After stirring the reaction mixture for 4 hrs, ethanol was added to inactivate the excess of dimethyl sulfate Prior to evaporation of DMSO the excess KOH was neutralized with 1 30 g (21 65 mmol) of acetic acid anhydride The residue was purified by column chromatography (silica, eluent  $\text{CHCl}_3/\text{MeOH}$ , 93 7 v/v), yield 0 61 g (1 89 mmol, 14 %), m p 129 2 °C IR (KBr) 3660-3060  $\text{cm}^{-1}$  broad (OH), 1656 (amide I), 1564 (amide II)  $^1\text{H-NMR}$  ( $\text{DMSO-}d_6$ )  $\delta$  7 840 ppm (t, 1H, NHCO), for the carbohydrate skeleton protons see Table 6 6, 3 260 (s, 3H,  $\text{OCH}_3$ ), 3 057 (m, 2H, 2H,  $\text{(CH}_2\text{)}_6\text{-CH}_2\text{-NHCO}$ ), 1 398 (t, 2H,  $\text{(CH}_2\text{)}_5\text{-CH}_2\text{-CH}_2\text{NHCO}$ ), 1 230 (broad s, 10H,  $\text{CH}_3\text{-(CH}_2\text{)}_5\text{-CH}_2\text{-}$ ), 0 844 (t, 3H,  $\text{CH}_3\text{-}$ ), EI-MS  $m/z$  321 ( $\text{M+H}^+$ ), 276 ( $\text{C}_8\text{H}_{17}\text{-NHCO(CHOCH}_3\text{)(CHOH)}_3\text{CH}_2\text{OH}^+$ ), 260 ( $\text{C}_8\text{H}_{17}\text{-NHCO(CHOCH}_3\text{)(CHOH)}_2^+$ ), 230 ( $\text{C}_8\text{H}_{17}\text{-NHCO(CHOCH}_3\text{)CHOH}^+$ ), 156 ( $\text{C}_8\text{H}_{17}\text{-NHC=O}^+$ ) Anal Calcd for  $\text{C}_{15}\text{H}_{31}\text{NO}_6$  C, 56 05, H, 9 72, N, 4 36 Found C, 56 04, H, 9 79, N, 4 42

**2-Methoxy-*N,n*-octyl-D-gluconamide-6-benzoate (13)** This compound was synthesized as described for compound 2a In this procedure 0 219 g (1 56 mmol) of benzoyl chloride and 0 338 g (1 05 mmol) of compound 8 were used The work up and purification procedure was similar to that described for compound 5 Yield 0 13 g (0 31 mmol, 29 %), m p 111 3 °C IR (KBr) 3660-3020  $\text{cm}^{-1}$  broad (OH), 1697 (C=O, ester), 1654 (amide I), 1539 (amide II)  $^1\text{H-NMR}$  (90 MHz,  $\text{CDCl}_3$ )  $\delta$  8 058 ppm (d, 2H, ArH), 7 483 (m, 3H, ArH), 6 787 (t, 1H, NH-CO), 3 450 (s, 3H,  $\text{OCH}_3$ ), 1 258 (broad s, 10H,  $\text{CH}_3\text{-(CH}_2\text{)}_5\text{-CH}_2\text{-}$ ), 0 875 (t, 3H,  $\text{CH}_3\text{-}$ ) EI-MS  $m/z$  426 ( $\text{M+H}^+$ ), 290 ( $\text{C}_8\text{H}_{17}\text{-NHCO(CHOCH}_3\text{)(CHOH)}_3^+$ ), 260 ( $\text{C}_8\text{H}_{17}\text{-NHCO(CHOCH}_3\text{)(CHOH)}_2^+$ ), 230 ( $\text{C}_8\text{H}_{17}\text{-NHCO(CHOCH}_3\text{)CHOH}^+$ ), 156 ( $\text{C}_8\text{H}_{17}\text{-NHC=O}^+$ ), 105 ( $\text{ArC=O}^+$ ) 77 ( $\text{C}_6\text{H}_5^+$ ) Anal Calcd for  $\text{C}_{22}\text{H}_{35}\text{NO}_7$  C, 62 09, H, 8 29, N, 3 29 Found C, 61 94, H, 8 26, N, 3 23

**2-Methoxy-*N,n*-octyl-D-gluconamide-6-acetate (14)** The synthetic procedure was analogous to that described for compound 5, using 0 171 g (1 67 mmol) of acetic anhydride and 0 493 g (1 54 mmol) of compound 12 The work up and purification procedure was similar to that for compound 7 Yield 0 17 g (0 47 mmol, 30 %), m p 101 9 °C IR (KBr) 3660-3125  $\text{cm}^{-1}$  broad (OH), 1717 (C=O, ester), 1650 (amide I), 1539 (amide II)  $^1\text{H-NMR}$  ( $\text{DMSO-}d_6$ )  $\delta$  7 614 ppm (t,

1H, NHCO), for the carbohydrate skeleton protons see Table 6.6, 3.263 (s, 3H, OCH<sub>3</sub>), 3.059 (m, 2H, -(CH<sub>2</sub>)<sub>6</sub>-CH<sub>2</sub>-NHCO), 1.991 (s, 3H, OCOCH<sub>3</sub>), 1.402 (t, 2H, (CH<sub>2</sub>)<sub>5</sub>-CH<sub>2</sub>-CH<sub>2</sub>NHCO), 1.232 (broad s, 10H, CH<sub>3</sub>-(CH<sub>2</sub>)<sub>5</sub>-CH<sub>2</sub>-), 0.843 (t, 3H, CH<sub>3</sub>-). EI-MS: *m/z* 363 (M+H)<sup>+</sup>, 290 (C<sub>8</sub>H<sub>17</sub>-NHCO(CHOCH<sub>3</sub>)(CHOH)<sub>3</sub>)<sup>+</sup>, 260 (C<sub>8</sub>H<sub>17</sub>-NHCO(CHOCH<sub>3</sub>)(CHOH)<sub>2</sub>)<sup>+</sup>, 230 (C<sub>8</sub>H<sub>17</sub>-NHCO(CHOCH<sub>3</sub>)(CHOH))<sup>+</sup>, 201 (C<sub>8</sub>H<sub>17</sub>-NHCO(CHOCH<sub>3</sub>))<sup>+</sup>, 156 (C<sub>8</sub>H<sub>17</sub>-NHC=O)<sup>+</sup>, 43 (CH<sub>3</sub>C=O). Anal. Calcd. for C<sub>17</sub>H<sub>33</sub>NO<sub>7</sub>: C, 56.18; H, 9.15; N, 3.85. Found: C, 56.03; H, 9.14; N, 3.88.

**Di-(6-*N*,*n*-octyl-D-gluconamide)-terephthalate (15).** To a partly gelated solution of 2.538 g (8.23 mmol) of **1** in 40 ml of pyridine, was added dropwise over a period of 20 min. 0.883 g (4.35 mmol) of terephthaloyl dichloride which was dissolved in 10 ml of DMF. After stirring for 1 hr. at 0 °C and an additional 1 hr. at room temperature, the clear yellow solution was heated for 2 hrs. at 60 °C. After cooling the clear solution was poured into ± 500 ml of saturated NaHCO<sub>3</sub>/ice and the precipitate was washed with hot methanol. Yield 1.13 g (1.51 mmol, 37 %), m.p. 203.4 °C (dec.). IR (KBr) cm<sup>-1</sup> 3650-3030 broad (OH), 1724/1701 (C=O, ester); since the peak of the ester function was split into two values, it was assumed that this function is present in the solid state in more than one conformation, 1624 (amide I), 1543 (amide II). <sup>1</sup>H-NMR (DMSO-d<sub>6</sub>) δ 8.133 ppm (s, 4H, ArH), 7.628 (t, 2H, ArH), for the carbohydrate skeleton protons see Table 6.6, 3.065 (9 peaks, 2H, (CH<sub>2</sub>)<sub>6</sub>-CH<sub>2</sub>-NHCO), 1.396 (t, 2H, (CH<sub>2</sub>)<sub>5</sub>-CH<sub>2</sub>-CH<sub>2</sub>NHCO), 1.223 (broad s, 10H, CH<sub>3</sub>-(CH<sub>2</sub>)<sub>5</sub>-CH<sub>2</sub>-), 0.837 (t, 3H, CH<sub>3</sub>-); EI-MS *m/z* 744 (M+H)<sup>+</sup>, 156 (C<sub>8</sub>H<sub>17</sub>-NHC=O)<sup>+</sup>, 105 (ArC=O)<sup>+</sup>, 77 (C<sub>6</sub>H<sub>5</sub>). Anal. Calcd. for C<sub>36</sub>H<sub>60</sub>N<sub>2</sub>O<sub>14</sub>: C, 58.03; H, 8.12; N, 3.76. Found: C, 57.59; H, 7.92; N, 3.66.

***N*,*n*-Octyl-D-galactonamide (16).** The synthesis and characterization of this compound has been described in the literature<sup>5a</sup> The analytical data (<sup>1</sup>H-NMR, IR, elemental analysis) were satisfactory.

***N*,*n*-Octyl-D-galactonamide-6-benzoate (17).** The synthetic procedure for this compound was similar to that described for compound **2a**. In the present case 0.765 g (5.44 mmol) of benzoyl chloride and 1.520 g (4.94 mmol) of *N*,*n*-octyl-D-galactonamide<sup>5a</sup> (compound **16**) were used. The precipitate obtained after pouring the reaction mixture into saturated NaHCO<sub>3</sub>/ice was purified by column chromatography (silica, eluent CHCl<sub>3</sub>/MeOH, 93:7 v/v), followed by recrystallization. Yield 0.33 g (0.80 mmol, 16 %), m.p. 188.2 °C (dec.). IR (KBr) 3669-3020 cm<sup>-1</sup> broad (OH), 1721/1711 (2×C=O, ester), 1665/1624 (amide I), 1543 (amide II). <sup>1</sup>H-NMR (DMSO-d<sub>6</sub>) δ 7.988 ppm (d, 2H, ArH), 7.650 (t, 1H, ArH), 7.522 (t, 2H, ArH), 5.169 (d, 1H, O<sup>2</sup>H), 4.711 (d, 1H, O<sup>5</sup>H), 4.510 (d, 1H, O<sup>4</sup>H), 4.397 (d, 1H, O<sup>3</sup>H), 4.297 (2d, 1H, C<sup>6</sup>H), 4.226 (2d, 1H, C<sup>6</sup>H), 4.143 (d, 1H, C<sup>2</sup>H), 4.061 (q, 1H, C<sup>5</sup>H), 3.854 (t, 1H, C<sup>3</sup>H), 3.476 (t, 1H, C<sup>4</sup>H), 3.077 (m, 2H, (CH<sub>2</sub>)<sub>6</sub>-CH<sub>2</sub>-NHCO), 1.399 (t, 2H, (CH<sub>2</sub>)<sub>5</sub>-CH<sub>2</sub>-CH<sub>2</sub>NHCO), 1.234 (broad s, 10H, CH<sub>3</sub>-(CH<sub>2</sub>)<sub>5</sub>-CH<sub>2</sub>-), 0.845 (t, 3H, CH<sub>3</sub>-); EI-MS *m/z* 411 (M)<sup>+</sup>, 156 (C<sub>8</sub>H<sub>17</sub>-NHC=O)<sup>+</sup>, 105 (ArC=O)<sup>+</sup>, 77 (C<sub>6</sub>H<sub>5</sub>). Anal. Calcd. for C<sub>21</sub>H<sub>33</sub>NO<sub>7</sub>·0.5H<sub>2</sub>O: C, 59.98; H, 8.15; N, 3.33. Found: C, 60.02; H, 7.87; N, 3.39.

## 6.2.2 Physical measurements

### Determination of *T*<sub>gel</sub>

A typical procedure for the preparation of the organogels was as follows: in a test tube, approximately 0.5 ml of solvent was added to 5 mg of powdered sample. The tube was closed and gently heated, in most cases until the mixture started to boil. Subsequently, the mixture was vortexed until a clear solution was obtained and thereafter allowed to cool to room temperature. When the gel had a viscosity high enough to turn the test tube upside down without damaging the structure, the sol-to-gel temperature was determined according to a method described in the



literature<sup>29</sup> A glass ball was placed on top of the gel and the test tube was subsequently placed in a thermostatted water bath and heated at 1.5 °C/min. The temperature at which the ball started to fall through the gel was denoted as  $T_{\text{gel}}$ .

#### *DSC measurements*

The thermograms were recorded on a Perkin Elmer DSC 7 instrument using closed stainless steel cups. Gelator (0.5 mg) was placed in the cups and 50  $\mu\text{L}$  of solvent was added with the help of a pipette. After sealing the cups were heated to 20 °C above the boiling point of the solvent, before the first run was recorded. The scan rate for both the heating and cooling runs was 5 °C/min. At least 2 heating and 2 cooling runs per sample were recorded. Loss of solvent during the runs was checked by weighing the cups before and after the measurements. In all cases no loss of weight was found. For the calibration of the instrument cyclohexane and indium samples were used.

The thermograms of the samples without solvent were recorded in 30  $\mu\text{L}$  aluminium pans. Calibration was carried out with zinc and indium samples (scan rate of 5 °C/min).

#### *Electron Microscopy*

The electron micrographs were recorded on TEM Philips EM201 and TEM Jeol JEMCXII instruments. The gels were transferred to carbon-coated 150 mesh copper grids. After 30 sec. of acclimatization the excess material was removed and the grids were covered with Pt deposited at an angle of 45°.

#### *X-ray powder diffraction*

X-ray powder diffractograms were recorded on a Philips PW1710 powder diffractometer with a Ni filtered Cu source (40 KV, 55 mA,  $\lambda = 1.54060 \text{ \AA}$ ). The 1 % (weight/volume) gels were transferred to a silicon sample holder and rapidly dried under high vacuum.

#### *FT-IR spectroscopy*

FT-IR spectra were recorded on a Bio Rad Digilab Division (FTS-25) instrument. The gels and solutions were measured between NaCl windows and corrected for the solvents. Solid samples were measured as KBr pellets.

## **6.3 Results**

### **6.3.1 Gelation behavior**

Compounds **1-17** were studied with regard to their gelation behavior in 5 organic solvents. The results are compiled in Table 6.1. The gels obtained were either clear or slightly turbid. Those possessing a viscosity so high that the test tube could be turned upside down without damaging the structure are denoted as (G) in Table 6.1. Gels with this behavior could be made from the gluconamide (**1**), the benzoate (**2a**), the cyclohexanoate (**7**) and the C<sup>2</sup> methoxy protected derivative **12**. The gels obtained from the imidazole and acetate derivatives **4** and **5** showed a significantly higher viscosity than expected for a solution or a vesicular dispersion, but were not as viscous as the afore mentioned gels, those are earmarked as (T). In some cases the compound remained dissolved (S) upon cooling without forming a gel while others formed crystalline powders within one hour (R). Insolubility is denoted as (I).

Compound **1** is capable of forming a very strong hydrogen bonding network which can only be split by very polar solvents like water and ethanol or by high temperature, *i.e.* in solvents

with high boiling points like 1,2-xylene (b.p. 144 °C). Introduction of substituents on the gluconamide framework leads to enhancement of the solubility (see Table 6.1). Both aromatic and aliphatic substituents on carbon atom C<sup>6</sup> gave soluble products, which in some cases recrystallized from ethyl acetate, but formed gels in 1,2-xylene and chloroform. When the secondary hydroxyl groups of the gluconamide derivatives were protected, the compounds became too soluble for most organic solvents and in most cases no gels or turbid mixtures were formed upon cooling. Even protection of only one of the hydroxyl groups (*viz* C<sup>2</sup>), increased the solubility too much for the formation of gels (except for compound **12** in 1,2-xylene). n-Hexane turned out not to be a suitable solvent for the formation of organo-gels. Even **6** and **15** did not dissolve in this solvent, which is somewhat surprising, since in both compounds the hydrophilic carbohydrate moiety is located in between two hydrophobic alkyl chains which should give **6** a relatively hydrophobic character.

**Table 6.1** Gelation behavior of gluconamides in organic solvents <sup>a</sup>

Compound	Protected <sup>b</sup>	Substituent <sup>c</sup>	n-hexane	1,2-xylene	CHCl <sub>3</sub>	EtOAc	EtOH
<b>1</b>	No	OH	I	G	I	I	R
<b>2a</b>	No	Aromatic	I	G	G	G	G
<b>3</b>	No	Aromatic	I	R	I	R	S
<b>4</b>	No	Aromatic	I	T	G	R	S
<b>5</b>	No	Aliphatic	I	G <sup>d</sup>	G <sup>d</sup>	R	S
<b>6</b>	No	Aliphatic	I	S	T	R	R
<b>7</b>	No	Aliphatic	I	G	G	G	S
<b>8</b>	Dimethylene	OH	R	T	S	S	S
<b>9</b>	Dimethylene	Aromatic	R	S	S	S	S
<b>10</b>	Dimethylene	Aromatic	R	S	S	S	S
<b>11</b>	Dimethylene	Aromatic	I	R	S	S	S
<b>12</b>	C <sup>2</sup> methoxy	OH	I	G	S	S	S
<b>13</b>	C <sup>2</sup> methoxy	Aromatic	I	R	S	S	S
<b>14</b>	C <sup>2</sup> methoxy	Aliphatic	I	R	S	S	S
<b>15</b>	No	Dimer	I	I	I	I	I
<b>(16)<sup>e</sup></b>	No	OH	I	I	I	I	R
<b>(17)<sup>e</sup></b>	No	Aromatic	I	T	T	R	R

<sup>a</sup> G the compound gels the solvent resulting in a high viscosity mixture upon cooling S compound dissolves without gelation I the compound is insoluble after prolonged heating R compound recrystallizes upon cooling within 1 h T upon cooling a turbid mixture with a slightly increased viscosity is obtained, but no gel is formed

<sup>b</sup> Protection of the hydroxyl groups

<sup>c</sup> Substituents on the C<sup>6</sup> of the carbohydrate

<sup>d</sup> Gel with low viscosity

<sup>e</sup> Galactonamide derivatives

In fact the octyl derivative **6** was hardly soluble in any solvent: only in boiling chloroform a clear solution could be obtained, which turned cloudy and viscous but did not form a firm gel. The gemini surfactant **15** was insoluble in almost every solvent, only in DMSO this compound could be dissolved. Apparently the packing in the solid phase is very strong, which was also evident from the very high melting point (203 °C, dec.) of this compound. Introduction of a benzoyl group in the gluconamide resulted in gelation of almost every solvent. Placing the benzoyl function on the galactonamide framework (**17**) resulted in an increase of the solubility of the compound, but unlike the gluconamide derivative, gelation was weak. Only in 1,2-xylene a gel with a very low tensile strength was formed.

All gels were thermoreversible, *i.e.* they turned into clear, low viscosity solutions upon heating and gelation returned after cooling. The temperature at which the gel vanishes is denoted as the gel-to-sol temperature  $T_{\text{gel}}$ . For the benzoate derivative **2a**, we studied  $T_{\text{gel}}$  in a variety of solvents (Table 6.2). We tried to relate physical constants like polarization index according to Snyder,<sup>30</sup> Rohrschneider constants,<sup>31</sup> dielectrical constants, surface tension and boiling points of the solvents to the  $T_{\text{gel}}$  values, but unfortunately no clear correlation could be obtained.

**Table 6.2** Temperatures at which the gel of the benzoate derivative **2a** vanishes in different solvents <sup>a</sup>

Solvent	$T_{\text{gel}}$ (°C) <sup>b</sup>	Pol index <sup>c</sup>	Boiling point (°C) <sup>e</sup>
Water	R	9 0	100
Methanol	17	6 6	65
Ethanol	28	5 2	79
Acetonitril	50	6 2	82
Acetone	28	5 4	56
Dioxane	15	4 8	101
Chloroform	66	4 4	62
Ethyl acetate	42	4 3	77
Tetrahydrofurane	S	4 2	66
Dichloromethane	43	3 4	40
Toluene	101	2 3	111
Ether	I	--- <sup>d</sup>	35
n-Hexane	I	--- <sup>d</sup>	69
Benzene	95	--- <sup>d</sup>	80
1,2-Xylene	102	--- <sup>d</sup>	144

<sup>a</sup> Determined by the Takahashi method, see Ref 29

<sup>b</sup> Explanation of symbols see Table 6 1

<sup>c</sup> Polarization index according to Snyder, see Ref 30

<sup>d</sup> Polarization index not known

<sup>e</sup> Boiling points of pure solvents.

In contrast to the gels of **1** in water and in 1,2-xylene where precipitation occurred after a couple of days,<sup>5,6</sup> the gels of **2a** in various solvents were very stable and did not change over a

period of several months. Transition electron microscopy (TEM) pictures of an aged sample in chloroform showed exactly the same texture as TEM carried out on a freshly prepared sample. The stability of the gel was only affected by raising the temperature.

In some cases (chloroform, dichloromethane, and benzene see Table 6.2) the  $T_{\text{gel}}$  of **2a** exceeded the boiling point of the solvent. Boiling only occurred upon decomposition of the gel ( $T_{\text{gel}} = \text{boiling}$ ).

Elongation of the alkyl chain length from n-octyl to n-hexadecyl in compound (**2b**) resulted in a slower gelation process. Only after one day of conditioning at ambient temperature, a gel in chloroform was formed, which is considerably slower than the time required for the octyl derivative **2a**, which gelled within several minutes upon cooling. This effect was also observed in aqueous gels of unsubstituted *N,n*-alkyl-D-gluconamides, which tend to crystallize with a rate depending on the length of the alkyl chain,<sup>2</sup> and in gels of maltobionamides, of which the fibers of the long chain compounds are not as regularly oriented as those of the short chain ones.<sup>2</sup>

### 6.3.2 DSC measurements

In order to obtain information about the enthalpy changes that accompany the formation and collapse of the gels, differential scanning calorimetry (DSC) experiments were carried out with compound **2a**. Both the heating and cooling curves showed in all cases very broad peaks, indicating that the transitions took place gradually. This can be attributed to the relatively low degree of ordering that is present in the gel, compared to the crystalline structures, which normally give sharp peaks (*e.g.* crystal-crystal transitions or melting). Although the large peak width reduced the accuracy of the thermograms,<sup>32</sup> certain trends could be distinguished.

**Table 6.3** Heat transformation upon gel formation,  $\Delta H(\text{gel})$  for **2a** in various solvents, obtained from DSC cooling thermograms

Solvent	kJ/mole gelator <sup>a</sup>
Dichloromethane	- 19
Chloroform	- 21
Ethanol	(14) <sup>b</sup>
Benzene	- 44
Toluene	- 37
1,2-Xylene	- 38

<sup>a</sup> Corrected to 50  $\mu\text{l}$  1 % gel (values  $\pm$  15 %)

<sup>b</sup> Value obtained upon heating. Gel formation upon cooling was too slow for accurate DSC measurements

The  $\Delta H(\text{gel})$  values were measured in several solvents. Thermograms of the gels showed that in chlorinated solvents  $\Delta H(\text{gel})$  is much lower than in aromatic solvents. In the case of ethanol an even lower  $\Delta H(\text{gel})$  value was observed (see Table 6.3). The latter is probably due to the fact that ethanol can accept and donate hydrogen bonds and hence disturb the *inter*-molecular hydrogen bonding network of **2a**. In order to investigate the influence of H-bonding from the

solvent, it would be of interest to do experiments in other solvents that are either H-bond donating or H-bond accepting. Compound **2a** dissolved in H-bonding accepting solvents like DMSO or THF but, unfortunately, remained in solution upon cooling, while gelation in dioxane was too slow (2 days) for performing accurate DSC measurements. On the other hand **2a** did not dissolve at all in water (H-bond donating) while gelation in methanol again was too slow (16 hrs.) for accurate DSC recording. For comparison we recorded the energy transfer that takes place when the aqueous gel of **1** is dissolved. As can be seen in Table 6.4 the energy transfers of **1** in water and **2a** in ethanol are in the same range.

**Table 6.4** Heat transfer upon dissolving the gels of **1** and **2a** <sup>a</sup>

Compound	kJ/mole gelator
<b>1</b> in water	11
<b>2a</b> in ethanol	14

<sup>a</sup> Data obtained from DSC heating thermograms

We also measured  $\Delta H(\text{gel})$  values for other gelators than **2a** in an organic solvent. In order to make it possible to compare different gelators in one solvent, experiments were carried out in 1,2-xylene. Since not every compound described so far gelled in 1,2-xylene, the choice was limited to **1**, **2a**, **12**, and **17**. Table 6.5 shows that the  $\Delta H(\text{gel})$  upon disruption of the gels in 1,2-xylene is nearly independent of the gelator type. Even the galactonamide derivative (compound **17**) does not deviate from this trend, although this compound formed a turbid mixture instead of a highly viscous gel.

**Table 6.5** Heat transfer upon formation of the gels in 1,2-xylene obtained from DSC cooling thermograms

Compound	kJ/mol gelator
<b>1</b>	- 42
<b>2a</b>	- 38
<b>12</b>	- 38
<b>17</b> <sup>a</sup>	- 37

<sup>a</sup> This compound does not form a highly viscous gel, but a turbid mixture

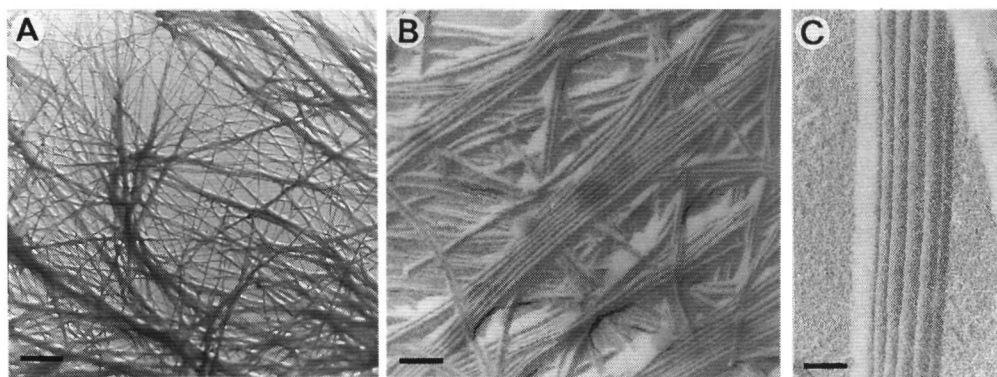
### 6.3.3 Electron microscopy

The high viscosity of the gels suggests that network structures are formed from the gluconamide building blocks, which we decided to investigate by transmission electron microscopy (TEM) in combination with Pt shadowing. In the following the TEM pictures obtained from the various compounds are discussed in some detail.

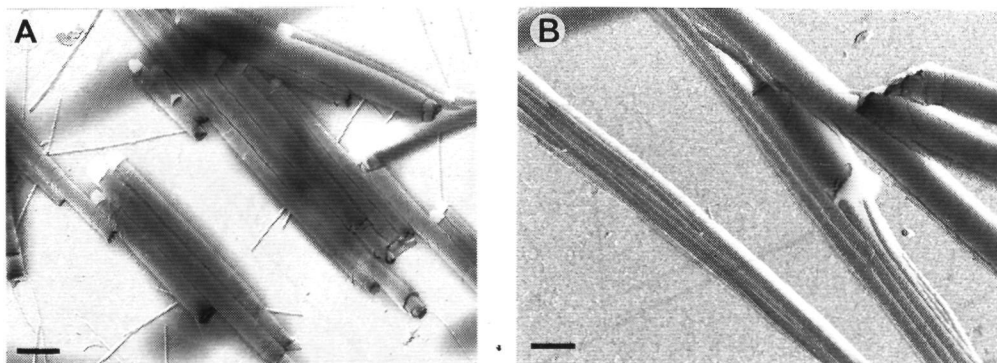
### 6.3.3.1 Gluconamides with aromatic substituents on C<sup>6</sup>

#### Benzoate derivatives **2a** and **2b**

The TEM pictures of the organogels formed from the benzoate derivative **2a** showed a network of whisker-type fibers (see Figure 6.1A, TEM picture, of a gel from **2a** in chloroform). Despite the relatively low concentration (1 % w/v), the network is finely meshed, which explains why the gel is rigid and why it can exist above the boiling point of the solvent without collapsing. The fibers are often bundled like the strings in a rope (see Figure 6.1B), but neither the individual fibers nor the bundles of fibers showed chirality. Apparently, in contrast with **1** in water, the chirality of the head group of **2a** is not expressed in the supramolecular structure. The fibers have an average diameter of 31 nm and hence must be composed of more than one monolayer or bilayer (2.4 nm and 4.9 nm, respectively, as estimated from CPK models) or must be hollow. From the TEM micrographs it can not be distinguished if the rodlike structures of **2a** are hollow tubes, or solid rods.



**Figure 6.1** TEM pictures of a gel of **2a** in chloroform (Pt shadowing). A) network of fibers, bar is 1.5  $\mu\text{m}$ . B) Bundles of whisker-type fibers, bar is 240 nm. C) Intertwined bundles of fibers; bar is 80 nm.



**Figure 6.2** TEM pictures of a gel of **2b** in chloroform (Pt shadowing). A) Cigar-like tubes from rolled-up multilayers; bar is 870 nm. B) Whisker-type fibers and cigar-like tubes, bar is 340 nm.

More insight would have been obtained if freeze-fracture and negative staining experiments could have been performed, but the organic solvent like chloroform prohibited the

application of these preparative techniques. The aspect ratio (length to width) of the fibers was very high, viz up to 500. Although the  $T_{\text{gel}}$  and  $\Delta H(\text{gel})$  values were dependent on the solvent, the shapes of the textures were not. Micrographs recorded from gels of **2a** in ethyl acetate, ethanol, or 1,2-xylene all showed fiber-like structures with the same dimensions as those seen for **2a** in chloroform.

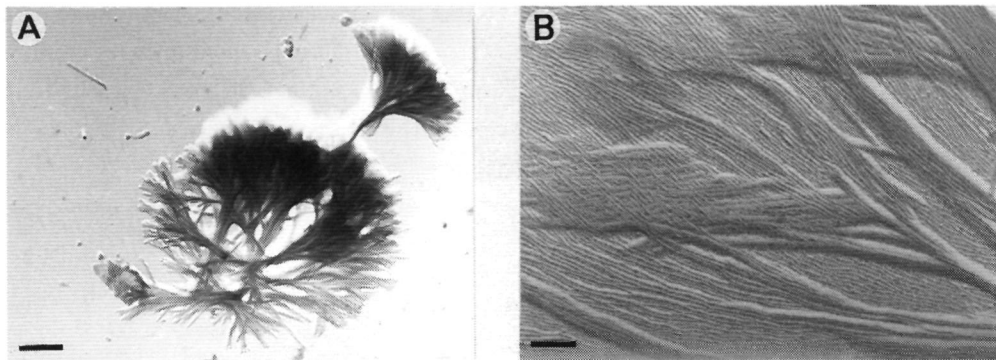
In electron micrographs of gels of **2b** two aggregation forms could be discerned: cigar-like rolled up multilayers (see Figure 6 2A) and whisker-type fibers (see Figure 6 2B) which were also present in gels of **2a** in chloroform (see Figure 6 1B). The multi-layered cigar-like structures had diameters ranging from 200 to 500 nm, whereas the fibers had a much smaller average diameter of 65 nm. These fibers must either consist of several layers or be hollow, because the estimated monolayer thickness is only 3.1 nm.

### *3-Pyridyl-carboxylate derivative 3*

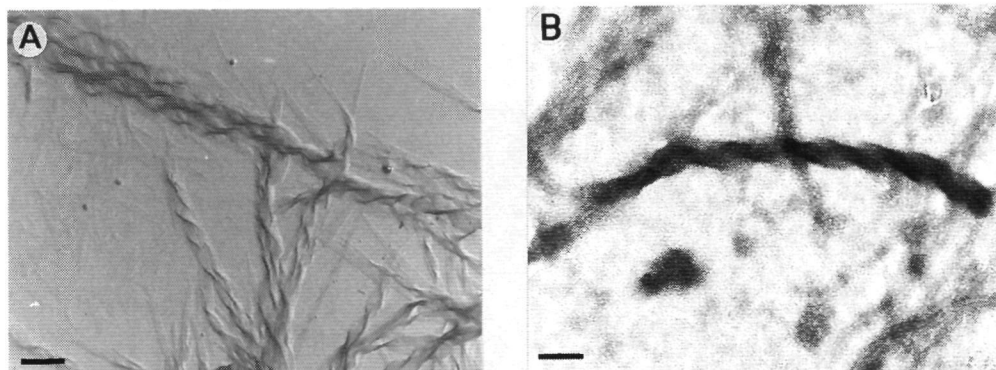
A TEM picture of a gel of **3** in dioxane showed fiber-like structures which assembled to form larger rod-like aggregates (the diameter of the fibers was approximately 10 nm, the average diameter of the rods was 40 nm, see Figure 6 3). Gluconamide **2a** also formed rod-like structures of approximately 30 nm, but the finer fibers of 10 nm as observed in the gels of the pyridine-carboxylic acid ester **3** were absent in the gels of **2a**. Chiral suprastructures like chiral twists or helical ropes, were not observed for compound **3**.

### *Imidazolyl derivative 4*

Compound **4** which contains the aromatic substituent imidazole was found to gelate in chloroform (see Section 6 3 1). TEM pictures of the gels revealed the presence of twisted ribbon-like structures (see Figure 6 4A). The direction of the twist was for all ribbons similar. For comparison we also studied the aggregation behavior of **4** in aqueous solution. The imidazole group of **4** has a  $\text{p}K_{\text{a}} = 7.02$  (see Chapter 5) and will be partly protonated in neutral water. In order to study the effect of protonation on the aggregation behavior as was done for the imidazole compound **11** (see Chapter 4), **4** was dissolved in Tris buffered ( $\text{pH} = 8.5$ ) and acetic acid/sodium acetate buffered ( $\text{pH} = 4.5$ ) water. In the former solution, compound **4** slowly formed a gel in which the same type of twisted ribbons were present as in the gel in chloroform. Attempts to obtain freeze etched electron micrographs of **4** in Tris buffered water failed, presumably because the alkyl chains in the bilayers intercalate, which prohibits clear fracturing. Staining of the samples with uranyl acetate, resulted in micrographs with relatively contrast-rich regions (Figure 6 4B). This might indicate that in the aggregates the hydrophilic parts of **4**, which bind the uranyl acetate, are in direct contact with the aqueous phase. We believe that the aggregates of **4** in chloroform have a similar molecular arrangement as the aggregates in water. The hydrophilic head groups of **4** and not the hydrophobic alkyl chains are probably facing the chloroform phase. Aggregation of **4** in water was found to be much slower than aggregation in chloroform or in dichloromethane. The clear solution of neutral **4** in water gelled only after 1 day, whereas the clear solution of **4** in chloroform gelled within 1 hour. Dissolving **4** in the acetate buffer of  $\text{pH} = 4.5$  resulted in a clear solution without the formation of any aggregates.



**Figure 6.3** TEM picture of a gel of **3** in 1,4-dioxane. A) Overview bar is 570 nm. B) Visible are rods which are build up from fibers. (Pt shadowing); bar is 140 nm.



**Figure 6.4** TEM pictures of **4**. A) Gel in chloroform. Visible are twisted ribbons (Pt shadowing), bar is 212 nm. B) Gel in Tris buffered solution pH 8.5 (neg. staining with  $\text{U}(\text{OAc})_2$  1 %). Visible are twisted ribbons; bar is 73 nm.

### 6.3.3.2 Gluconamides with aliphatic substituents on $\text{C}^6$

#### *Acetyl derivative 5*

Compound **5** has a relative small hydrophobic substituent on carbon atom  $\text{C}^6$  of the glucon moiety. It is therefore not surprising that **5** is readily soluble in water at elevated temperatures and is capable of forming a gel upon cooling. Compound **5** also gels in organic solvents (*vide supra*). Gels formed from **5** in water and in chloroform were investigated by TEM. The aqueous gel of **5** had a lower viscosity than the gel obtained from **1** in water or from **2a** in chloroform. Electron micrographs of **5** in water showed the presence of multilayered ribbons, which rolled up to give helices (not shown). In chloroform similar types of chiral aggregates were present (see Figure 6.5A + 6.5B). This would suggest that the way compound **5** aggregates is solvent independent. Apparently, small hydrophobic groups (imidazole, see above, and acetate) allow the gluconamides to form gels in both water and chloroform. These groups do not disturb the packing of **5** and as a result the molecular chirality can be expressed in the suprastructures.

#### *n-Octyl derivative 6*

Since the size, shape, and structure of the substituent are important for the generation of the suprastructures, it was of interest to investigate what type of aggregates were present in gels of compound **6**, which has a longer alkyl substituent than **5**. Micrographs of a turbid mixture of **6**





# **Supramolecular Structures from Gluconamide Building Blocks**

Een Wetenschappelijke Proeve op het Gebied van de  
**Natuurwetenschappen**

**Proefschrift**

ter verkrijging van de graad van doctor aan de Katholieke Universiteit van Nijmegen,  
volgens het besluit van het College van Decanen in het openbaar te verdedigen op  
dinsdag 18 juni 1996, des namiddags om 1 30 precies

door

**Rudolfus Johannes Hendrikus Hafkamp**

Geboren op 6 juli 1966  
te Rheden

Promotor

Prof Dr R J M Nolte

Co-promotor

Dr M C Feiters

Manuscriptcommissie

Dr C F van Nostrum

Dr H A van Doren (NIKO-TNO)

ISBN 90-9009507-1

*Aan degenen die mij altijd hebben gesteund:*

*Henriet en mijn ouders*



# Voorwoord

“Normale” chemici gaan eerst studeren, dan promoveren en pas aan het eind van hun promotie wordt aan een vaste baan gedacht. In mijn geval zijn de zaken wat zig-zaggend verlopen. Door scheikunde in deeltijd te studeren, had ik aan het begin van dit promotieonderzoek universiteiten nauwelijks bij daglicht gezien. Omdat sommige spelregels in het onderzoek bij het bedrijfsleven nu eenmaal anders zijn dan in de academische wereld, kreeg ik in het begin het gevoel bezig te zijn met een geblinddoekte rit over glad ijs. Gelukkig was er een aantal mensen om mij heen die mij niet alleen de blinddoek af deed maar ook schaaftte aan de techniek en waarschuwde voor gevaarlijke wakken (!). Door vele aanwijzingen kon ik mijn techniek verbeteren waardoor sneller, efficiënter, zonder angst en vooral met veel enthousiasme door het onderzoek geschaatst kon worden. Verder heb ik veel gehad aan klankborden, luisterende oren en aanmoedigende mensen. Degenen die daarbij hebben geholpen, wil ik hierbij hartelijk danken

Prof. Roeland Nolte, jou heb ik altijd als een hoofdtrainer beschouwd waaraan ik veel heb gehad. Jouw enthousiasme zette me telkens weer aan tot het zoeken naar nieuwe aggregaten in de vorm van vlechtjes, buisjes, ruggegraten en bloemkolen. Daarnaast was de hulp van Dr. Martin Feiters voor mij onontbeerlijk en een stimulans om een ingeslagen weg niet te snel te verlaten. Gelukkig verliep de samenwerking met de labgenoten als Alan, Albert, Bert, (sparring partner) Fokke, Hanny, Hans (2x), Hein, Gerben, Gino, Joost, Nico, Ruud, René (ook dank voor het nakijken van het niet-gepolijste manuscript), Patricia, Peter en Stan alsmede alle studenten erg goed. Bovendien kan ik door hen met veel plezier terug denken aan mijn ‘Nijmeegse tijd’

Hoe lang mijn carrière binnen of buiten de chemie ook gaat duren, “mijn studenten” Bas Kokke en Thien-An Tran Chau zal ik niet snel vergeten. Het door Bas opgebrachte enthousiasme en doorzettingsvermogen om zijn onderzoek tot een goed einde te brengen, zelfs bij een tegenstribbelende katalysator, kan voor iedereen een voorbeeld zijn. Hoewel jouw waardering voor dubieuze films, bloederige grappen en de Sjonnie's mij nooit hebben aangesproken, vond ik de daaruit voortvloeiende (luidruchtige) discussies wel erg leuk. De werklust en doelgerichtheid van Thien-An, een half woord was vaak al genoeg, is voor mij een voorbeeld geweest. Verder was je gastvrijheid erg plezierig. Dank aan Dominique Hubert en Bart Nelissen voor het schrijven van een literatuurscriptie waarvan een gedeelte is opgenomen in Hoofdstuk 2.

Waar zouden we zijn zonder de analyse-trein van Helene Amadjais, Peter van Galen, Pieter van der Meer en Ad Swolfs? Samen met Ad Swolfs naar de moleculen kijken met behulp van NMR was niet alleen plezierig maar ook bijzonder leerzaam. Verder helpen vaste krachten als Chris Kroon, Wim van Luyn, Sandra Tjindink en Hans Adams een laboratorium draaiende te houden. Hans Adams is een hele ondersteuning bij de verhuizing van de begane grond naar de eerste verdieping geweest. Voor Gerda Nachtegaal was een duidelijk gestelde vraag al voldoende om direct te gaan meten, ondanks alle inspanningen is er helaas niet uitgekomen wat we ervan verwacht hadden.

Dr. Gordon Chittenden en Prof. Tesser wil ik danken voor het aanreiken van de juiste literatuur en het voeren van leerzame discussies, Henk Regeling voor het aanleren van truuksjes in

de synthese van suikerderivaten en Dr Hans Scheeren en Rene Aben voor het denkwerk bij en gebruik van de hogedruk-apparatuur Mede dankzij het uitvoeren van reacties onder hoge druk heb ik schier onmogelijk te synthetiseren verbindingen toch kunnen maken

In het hier beschreven onderzoek zijn veel experimenten met elektronenmicroscopie uitgevoerd Dit was onmogelijk geweest zonder de hulp van Huub Geurts De apparatuur was altijd operationeel, jij had bijna altijd tijd voor me en was nooit te beroerd om iets te doen wat misschien je taak helemaal niet was (zoals experimenteren met monstervoorbereiding, het keer op keer uitleggen van de technieken aan studenten, promovendi en profs, tot en met het opzoeken van vergelijkbare structuren in de literatuur) Bovendien was het voeren van (stoere) gesprekken over wielrennen altijd leuk

Dank aan Bart Knuiman voor de hulp bij de polymerisatieexperimenten beschreven in Appendix 2 Jan Smits wil bedanken voor de hulp bij het gebruik van de poederdiffractometer Een goede bibliothecaire service was te danken aan Jo en Henk Catherine Crowley dank ik voor de hulp bij correcties in de Engelse taal

Een aantal cruciale metingen zijn buiten de deur uitgevoerd zoals opheldering van een kristalstructuur (zie Hoofdstuk 3) door Dr Huub Kooiman en Dr Ton Spek (RUU), temperatuur-afhankelijke infrarood metingen door Bert Lutz (RUU) en temperatuur-afhankelijke SAXS-metingen door Dr Stephen Picken (Akzo Nobel) Met veel plezier denk ik terug aan de metingen uitgevoerd bij NIKO-TNO in Groningen en aan de samenwerking met Dr Henk van Doren (ook dank voor de correcties van het manuscript) Vanaf het eerste bezoek voelde ik me thuis bij het NIKO, een gevoel dat door jou en je groep van harte ondersteund werd, hiervoor mijn hartelijke dank

Zonder chemie zou er geen leven op aarde zijn, toch is leven naast de chemie voor mij ook belangrijk De nodige ontspanning heb ik beleefd in Deventer, Giethoorn, De Weerribben en de Alblasserwaard met mijn schaatsmaatjes Rob, Jan, Jan, en Wim De juiste aanwijzingen ter verbetering van de techniek, stimulatie tot betere prestaties en gezelligheid heb ik altijd kunnen waarderen

Het feit dat ik altijd terug heb kunnen vallen op familie, zowel tijdens de studies als in de promotietijd, heeft mij altijd het comfortabele gevoel gegeven dat ik er niet alleen voor stond Tot slot wil mijn geliefde Henriët bedanken Als ik van jou niet alle steun en medewerking had gekregen, van afremmen waar nodig tot en met hulp bij het afdrukken van EM-foto's op zaterdagmiddag, was me dit nooit gelukt

*Rudi*



# Contents

## Chapter 1 General introduction

1 1 Introduction to supramolecular chemistry	1
1 2 Liquid crystals	1
1 3 Contents of this thesis	2
1 4 Literature	3

## Chapter 2 Literature survey

2 1 Membrane mimetic chemistry	5
2 2 Amphiphiles	5
2 2 1 Relationship between amphiphilic structure and aggregate morphology	6
2 2 2 Chiral amphiphiles	7
2 2 3 Models for aggregates of chiral amphiphiles	9
2 2 4 Carbohydrate amphiphiles	9
2 3 Thermotropic liquid crystalline properties of carbohydrate amphiphiles	11
2 4 Functional aggregates	12
2 5 Literature	13

## Chapter 3 Thermotropic liquid crystalline properties of *N*-*n*-alkyl-*D*-gluconamides

3 1 Introduction	19
3 2 Experimental	20
3 2 1 Syntheses	20
3 2 2 Metal complexes	30
3 3 Results and discussion	31
3 3 1 Synthesis of imidazole ligand	31
3 3 2 Effect of the length of the alkyl chain on the L C behavior of compounds <b>1</b> and model compounds	33
3 3 3 Characterization of the L C phases of compounds <b>1</b>	39
3 3 4 X-ray structure of compound <b>1a</b>	40
3 3 5 Solution <sup>1</sup> H-NMR study on <b>1a</b>	43
3 3 6 Thermotropic L C behavior of compounds related to imidazolyl gluconamides <b>1</b>	43
3 3 6 1 Different substituents on the terminus of the head group	43
3 3 6 2 Gluconamides with a diacetylene function in the alkyl chain	46
3 3 6 3 <i>n</i> -Alkyl gluconates	47
3 3 6 4 Amide without the carbohydrate part	47
3 3 7 Metallomesogens	48



3 4 Concluding remarks	51
3 5 Literature	52

## **Chapter 4    Suprastructures in water from imidazole containing gluconamides**

4 1 Introduction	55
4 2 Experimental	56
4 2 1 Syntheses	56
4 2 2 Determination of the $pK_a^*$ values	57
4 2 3 UV-vis titrations	58
4 2 4 DSC measurements	58
4 2 5 Electron microscopy	58
4 3 Results and discussion	59
4 3 1 $pK_a$ titrations	59
4 3 2 UV-vis titrations	60
4 3 3 DSC experiments	64
4 3 4 Electron microscopy	69
4 4 Concluding remarks	75
4 5 Literature	77

## **Chapter 5    Positional variation of the imidazole group in gluconamide amphiphiles.                     Effects on the aggregation behavior**

5 1 Introduction	79
5 2 Experimental section	81
5 2 1 Syntheses	81
5 2 2 Measurements of isotherms	85
5 2 3 SAXS experiments	85
5 2 4 Electron microscopy	85
5 3 Results and discussion	86
5 3 1 Preparation of the compounds	86
5 3 2 $pK_a$ determination	88
5 3 3 IR experiments	88
5 3 4 UV-vis spectroscopy	89
5 3 5 Electron microscopy	91
5 3 6 Isotherms	96
5 3 7 X-ray powder diffraction experiments	96
5 3 8 Thermotropic L C behavior	97
5 4 Concluding remarks	97
5 5 Literature	98

## **Chapter 6   Organo-gels from carbohydrate amphiphiles**

6 1 Introduction	101
6 2 Experimental section	105
6 2 1 Syntheses	105
6 2 2 Physical measurements	109
6 3 Results	110
6 3 1 Gelation behavior	110
6 3 2 DSC measurements	113
6 3 3 Electron microscopy	114
6 3 3 1 Gluconamides with aromatic substituents on C <sup>6</sup>	115
6 3 3 2 Gluconamides with aliphatic substituents on C <sup>6</sup>	117
6 3 3 3 Gluconamides without C <sup>6</sup> substituents	120
6 3 4 NMR study	121
6 3 5 X-ray powder diffraction	125
6 3 6 IR experiments	128
6 4 Discussion	131
6 5 Concluding remarks	134
6 6 Literature	135

## **Chapter 7   Catalysis using supramolecular aggregates**

7 1 Introduction	137
7 2 Experimental	138
7 2 1 Syntheses	138
7 2 2 Catalytic aziridinations   General remarks	139
7 2 3 Aziridinations in acetonitrile	139
7 2 4 Aziridinations in chloroform	140
7 2 5 Aziridinations in aqueous dispersions	140
7 2 6 General procedure for the epoxidation reactions	142
7 3 Results and discussion	142
7 3 1 Aziridination in organic solvents	143
7 3 2 Aziridination in water	144
7 3 3 Epoxidation	147
7 4 Concluding remarks	148
7 5 Literature	149

<b>Appendix 1</b>	<b>Suprastructures from Pd complexes made of pyridyl substituted gluconamides</b>	151
	Experimental	152
	Literature	153
<b>Appendix 2</b>	<b>Polymerization of suprastructures</b>	155
	Experimental	156
	Literature	157
<b>Appendix 3</b>	<b>Atomic positional and vibrational parameters (with esd's) for Compound 1a (Chapter 3)</b>	159
<b>Summary</b>		161
<b>Samenvatting</b>		163
<b>Curriculum Vitae</b>		165

# Chapter 1

## General introduction

### 1.1 Introduction to supramolecular chemistry

Traditional synthetic chemistry is concerned with the preparation of single low molecular weight molecules while in polymer chemistry the products have high molecular masses. In both cases the building blocks are linked to each other by covalent bonds. A relatively new field is supramolecular chemistry which is based on non-covalent bonds like H-bridges, electrostatic and van der Waals interactions. One of the pioneers in this type of chemistry, J.-M. Lehn, formulated the new field of research as follows: "Beyond molecular chemistry, based on the covalent bond lies supramolecular chemistry, based on molecular interactions and the intermolecular bond."<sup>1</sup> In other words, in supramolecular chemistry, not only the (physical) properties of the individual compounds are studied but also the change of properties upon and after assembling of molecules are points of interest.

Chemists working in the field of supramolecular chemistry are often inspired by nature since many biological systems like the DNA double helix, a biomembrane or the quaternary structure of a protein are based on non-covalent interactions. As a result of these interactions, self-organization, *i.e.* the spontaneous assembly of monomeric parts towards ordered structures, occurs and is indispensable for living systems. Examples of highly ordered assemblies are cell membranes, DNA double helices and the tobacco mosaic virus.

Supramolecular chemistry can be divided into two areas, host-guest chemistry and the chemistry of molecular aggregates. Host-guest<sup>2</sup> chemistry is concerned with the binding of molecules (guests) in larger (host or receptor) molecules and the designers are mostly inspired by the naturally occurring enzymes. Among the early examples of host-guest complexes are the cation-binding crown ethers discovered by Pedersen.<sup>3</sup> Many receptor molecules have been developed since then, *e.g.* based on Kemp's triacid,<sup>4</sup> cyclodextrines,<sup>5</sup> calixarenes<sup>6</sup> and diphenylglycoluril.<sup>7</sup>

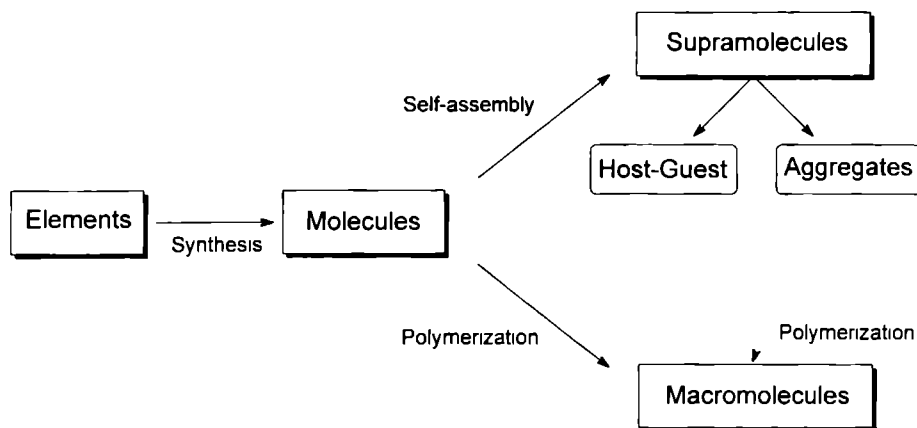
Molecular aggregates are formed by assembling molecular building blocks and, therefore, are to some extent comparable to high molecular weight polymers. In traditional polymer chemistry, however, polymer material is configured in certain shapes *after* the polymerization reaction, while in self-assembling systems the monomeric building blocks determine the form of the molecular aggregate, which may be polymerized afterwards (see Figure 1.1).

### 1.2 Liquid crystals

Liquid crystals (L.C.) are good examples of supramolecular aggregates because it is the organization that makes their physical properties so unique. Liquid crystals can be divided into two types, the thermotropic and lyotropic systems. In the former systems at certain temperatures the molecules are still ordered but the morphology of the phase (mesophase)<sup>\*</sup> is already a fluid

<sup>\*</sup> The L C phase or mesophase is sometimes called the fourth state of matter

liquid Depending on the presence of interacting groups (called mesogenic units), and the shape of the molecules (rodlike or disclike) the compounds form different liquid crystalline phases, calamatic and discotic, respectively



**Figure 1.1** Supramolecular chemistry in the context of synthetic and polymer chemistry

Lyotropic LC systems are dispersions of compounds containing mesogenic groups in a solvent<sup>8</sup> The most investigated building blocks for lyotropic LC systems are amphiphiles (also called surfactants) and constituents of cells (cell wall molecules), although other building blocks are known<sup>9</sup> Aggregation of totally synthetic amphiphiles was for the first time reported by Kunitake<sup>10</sup> and by many groups since then<sup>11</sup> Amphiphilic compounds (from Greek *amphi* = on both sides and *phileo* = to love) consist of two characteristic parts, a hydrophilic head group and a hydrophobic tail The tail usually consists of a long unbranched and sometimes unsaturated alkyl chain while the diversity in head groups is larger Ionic and non-ionic head groups are distinguished, with a further subdivision of the former group in anionic, cationic and zwitterionic head groups The most investigated non-ionic amphiphiles are based on carbohydrates<sup>12</sup>

The main reason for using carbohydrate based amphiphiles is the possibility of expressing their chirality in the supramolecular structure Carbohydrates are attractive chiral building blocks because they are inexpensive (*e.g.* D-glucose is in the price range of ordinary organic solvents such as acetone and methanol) and are obtained with a high enantiomeric purity Carbohydrates in principle are inexhaustible since they are available every year from agricultural crops

### 1.3 Contents of this thesis

The theme of this thesis is the study of the formation and the application of suprastructures from gluconamide derived amphiphiles and their metal complexes In order to increase their applicability, the amphiphiles are in almost every case provided with a metal complexing groups

Following a general literature survey in Chapter 2, the thermotropic properties of C<sup>6</sup>-substituted 2,4,3,5-dimethylene-*N,n*-alkyl-D-gluconamides and their copper complexes are

described in Chapter 3, featuring DSC experiments, temperature-dependent FT-IR, X-ray diffraction experiments and a single crystal structure analysis of an imidazolyl-bismethylene-gluconamide Chapter 4 focuses on the supramolecular structures of C<sup>6</sup>-substituted bismethylene-gluconamides in water, studied by electron microscopy The form of aggregation could be tuned by changing the pH and by the addition of metal ions In Chapter 5, the effect of the location of the metal-complexing imidazole group in the gluconamide on the aggregation behavior of the molecules is described Chapter 6 deals with the formation of organogels based on gluconamides Besides electron microscopy, the rigid gels were investigated by powder diffraction (SAXS), FT-IR and DSC In the final chapter, aggregates of gluconamides are used in catalysis The studied reactions are epoxidations and aziridinations This thesis concludes with summaries in both English and Dutch

## 1.4 Literature

- <sup>1</sup> a) Lehn J-M *Science* **1985**, 227, 849, b) Lehn, J -M *Angew Chem* **1988**, 100, 91, *Ibid Int Ed Eng* **1988**, 27 89
- <sup>2</sup> Cram, D J *Angew Chem* **1988**, 100, 1041, *Ibid Int Ed Eng* **1988**, 27, 1009
- <sup>3</sup> Pedersen C J *J Am Chem Soc* **1967**, 89, 7017
- <sup>4</sup> Rebek, J, Jr *Angew Chem* **1990**, 102, 261, *Ibid Int Ed Eng* **1990**, 29, 245
- <sup>5</sup> Szejtli J *Cyclodextrin Technology* Kluwer Acad Publ Dordrecht **1988**
- <sup>6</sup> Gutsche, C D *Calixarenes*, Royal Society of Chemistry, Cambridge **1989**
- <sup>7</sup> a) Niele F G M *Ph D Thesis University of Utrecht* **1987** b) Sybesma R P *Ph D Thesis University of Nijmegen* **1992**
- <sup>8</sup> a) Madden, T L , Herzfeld, J *Phil Trans R Soc Lond A* **1993**, 344, 357, b) Hoffmann, H *Ber Bunsenges Phys Chem* **1994**, 98, 1433, c) Hoffmann, H , Ulbricht, W *Chemie in unserer Zeit* **1995** 29 76
- <sup>9</sup> Aramid solutions Picken, S J *Ph D Thesis University of Utrecht* **1990**
- <sup>10</sup> Kunitake, T , Okahata, Y *J Am Chem Soc* **1977**, 99, 3860
- <sup>11</sup> For example a) Ringsdorf, H , Schlarb, B , Venzmer, J *Angew Chem* **1988**, 100, 117, *Ibid Int Ed Eng* **1988**, 27, 113 b) Fuhrhop, J -H , Helfrich, W *Chem Rev* **1993**, 93 1565 c) Menger, F M *Angew Chem* **1991** 103, 1104, *Ibid Int Ed Eng* **1991**, 30, 1086
- <sup>12</sup> Jeffrey, G A , Wingert, L M *Liq Crystals* **1992** 12, 179

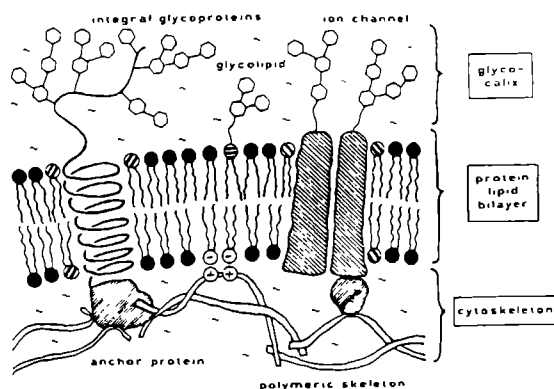


# Chapter 2

## Literature survey

### 2.1 Membrane mimetic chemistry

Twenty years ago it was proposed by Singer and Nicolson<sup>1</sup> that biomembranes are oriented, two-dimensional, viscous solutions of amphiphatic proteins and lipids (called the fluid mosaic model). This model is a conceptual basis for many researchers working in the field of membrane mimetic chemistry.<sup>2</sup> The biomembrane consists of 3 characteristic parts<sup>3</sup>: the glycocalix, the protein lipid bilayer and the cytoskeleton (see Figure 2.1). The main task of the glycocalix is recognition and this part is sometimes called the antenna area of the cells. The cytoskeleton, which is attached to the membrane on the inside of the bilayer, provides the stability of the membrane, while the bilayer of lipids is a host for proteins.



**Figure 2.1** Schematic drawing of membrane (Ref. 3)

The lipids of the bilayer are constructed from polar water-soluble head groups (phosphates or carbohydrates) connected to one or several long aliphatic chains (14 - 24 carbon atoms). Since the discovery by Gebicki and Hicks<sup>4</sup> that artificial membranes can be made from lipid molecules, numerous bilayered systems from synthetic amphiphiles<sup>5</sup> have been reported following the model proposed by Israelachvili (see Figure 2.2).<sup>6</sup>

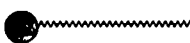
### 2.2 Amphiphiles

Amphiphiles are molecules that combine hydrophilic with hydrophobic parts. Due to this dual character, they can form aggregates in water. The property of amphiphiles to lower the interfacial tension between water and air led to the name surfactants (derived from *surface active agents*), while the name soap molecules originated from their practical applications. The driving force for the clustering of amphiphiles in water has been considered to be the so-called hydrophobic effect,<sup>7</sup> i.e. aggregation of the amphiphiles will liberate the organized shell of water






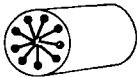


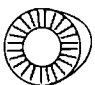


molecules surrounding the aliphatic chains of the individual molecules (called the icebergs) and thereby compensate the loss of entropy caused by the aggregation of the amphiphiles. However, the iceberg theory has been the subject of dispute discussion.<sup>8</sup>

Amphiphilic molecule



Hydrophilic  
headgroup

Hydrophobic  
tail

Shape	Packing parameter $P = v/a_0 l_c$	Aggregate type
	$P < 1/3$ micellar (spherical)	
	$1/3 < P < 1/2$ micellar (globular or cylinder)	
 	$1/2 < P < 1$ bilayers (vesicles)	
	$P > 1$ inverted micelles	

**Figure 2.2** Models for the relationship between molecular structure and aggregation form by Israelachvili,<sup>6</sup>  $v$  = the volume of the hydrophobic part,  $a_0$  is the cross sectional area of the head group and  $l_c$  is the maximal length of the alkyl chain

### 2.2.1 Relationship between amphiphilic structure and aggregate morphology

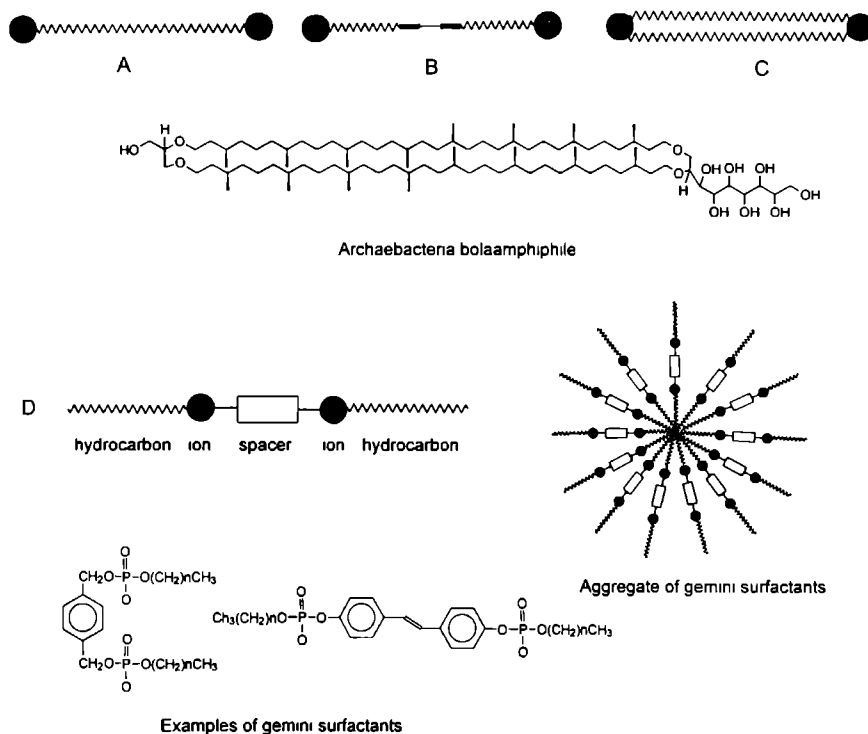
Many structural variations can be applied to amphiphiles without losing the ability to form aggregates. The hydrophilic head group can be anionic *e.g.* phosphate,<sup>4</sup> cationic *e.g.* ammonium,<sup>5</sup> zwitterionic *e.g.* choline<sup>9</sup> or nonionic *e.g.* polyoxyethylene<sup>10</sup> or carbohydrate.<sup>11</sup> The hydrophobic part has been varied by branching the *n*-alkyl chain,<sup>12</sup> introduction of thiol,<sup>13</sup> (polymerizable) alkene,<sup>14,15,16,17</sup> diacetylenic,<sup>18,19,20,21,22,23</sup> or cyclic disulfur<sup>24,25</sup> groups and by changing the hydrogen atoms in the alkyl chains to fluorine atoms.<sup>26,27</sup>

In addition to single and double chained amphiphiles, molecules containing two head groups connected by one or two alkyl chains<sup>28,29</sup> which can be unsaturated (so-called bolaamphiphiles, see Figure 2.3 A-C),<sup>30</sup> were synthesized on inspiration of the archaebacteria (*Sulfolobus solfataricus*) or bixin (recovered from seeds of *Bixa orellana*).<sup>31</sup> Using the unsaturated

bolaamphiphiles an attempt was made to introduce “electron wires” into vesicle membranes,<sup>31</sup> and quinone-containing amphiphiles were prepared in order to form redox-active lipid membranes.<sup>32</sup> With bolaamphiphiles containing unsymmetrical head groups, vesicles with an exterior membrane surface differing from the interior surface were prepared.<sup>33</sup> Amphiphiles in which two head groups are directly linked by a spacer are called gemini surfactants<sup>34</sup> and can, from a structural point of view, be considered as inverted bolaamphiphiles (see Figure 2.3D).

According to the model proposed by Israelachvili,<sup>6</sup> ionic single-chain amphiphiles form micellar solutions, however mixing single-chain compounds forming ion pairs<sup>35</sup> or stacks<sup>36</sup> can also result in bilayers.

In 1981 Kunitake et al.<sup>37</sup> reported that besides a hydrophilic head group and a flexible tail, the presence of a rigid segment, *e.g.* an aromatic group that can give stacking, is essential for the formation of bilayers from single chain amphiphiles.<sup>38</sup>

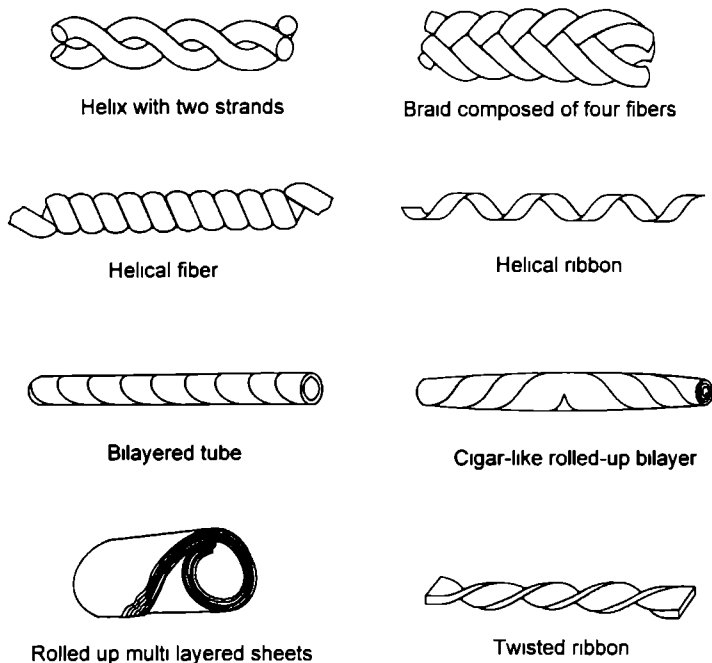


**Figure 2.3** Less common amphiphiles A-C) Bolaamphiphiles , D) Gemini surfactants

### 2.2.2 Chiral amphiphiles

Amphiphilic compounds containing a chiral moiety can express this asymmetry in the suprastructure by the formation of helices, twisted bilayers or tubuli (see Figure 2.4). Creating

asymmetrical assemblies is a challenge for the chemist and many were inspired by nature because helical forms are known from biological systems *e.g.* DNA<sup>39</sup> and collagen,<sup>40</sup> while tubular structures are known from the tobacco mosaic virus (TMV)<sup>41</sup> or the T4 phage.<sup>42</sup>



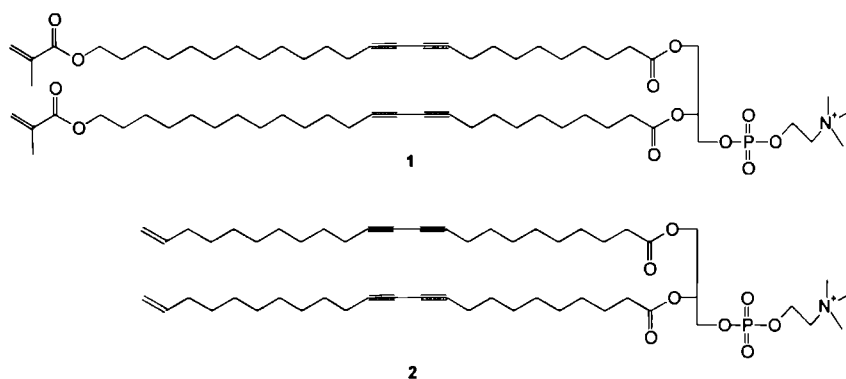
**Figure 2.4** Chiral assemblies from amphiphilic compounds

One of the first synthetic helical suprastructures published was based on the compound 12-hydroxystearic acid.<sup>43</sup> Later chiral amphiphiles based on glutamate,<sup>44</sup> alanine,<sup>45</sup> phospholipids,<sup>46</sup> and carbohydrates<sup>47</sup> have been developed.

The glutamate and alanine derived amphiphiles formed chiral aggregates as was observed by CD spectrometry<sup>44,45,48</sup> and, in addition, the transformation of helical tapes to tubes could be monitored by dark field optical microscopy<sup>49</sup> and electron microscopy.<sup>50</sup> The sense of the helix for the (*L*)-derivative of glutamate was right handed while the (*D*)-enantiomer showed left handed helices. Racemic mixtures did not result in helical forms. This kind of enantiomorphism was also encountered in *n*-alkyl-gluconamide derivatives.<sup>51</sup> The process of the formation of twisted filaments to tube like structures takes in some cases as long as one month,<sup>49</sup> while the change to spherical vesicles occurs almost instantaneously upon heating above the phase transition temperature.<sup>48</sup>

Like the glutamate derived amphiphiles, phosphatidylcholines can form helical shapes<sup>52</sup> and, in combination with aliphatic chains containing diacetylene groups, tubuli are also

formed<sup>46,53</sup> The size of the helices and tubuli can be controlled by variation of the ethanol/water ratio<sup>54</sup> The microstructures could be stabilized by polymerization without losing the suprastructure, indicating an ordered packing of the diacetylene functions<sup>18,55</sup> The microstructures were also influenced by changing the pH<sup>56</sup> or by the addition of metal ions<sup>56,57</sup> It was found that tubuli from diacetylenic phospholipids grow by the wrapping of lipid molecules around a crystalline core<sup>58</sup> Yager et al<sup>59</sup> postulated that the presence of diacetylenic groups enhances the chirality of the phospholipids as they disturb the symmetry in the alkyl chains in such a way that pairs of diacetylene chains can themselves be considered chiral objects<sup>59</sup> The diacetylenic functions are in some cases used only to direct the chirality, as they appeared to be useless for polymerization Introduction of additional polymerizable groups like methacrylate and vinyl (respectively **1** and **2**) resulted in high molecular weight polymers<sup>60</sup>



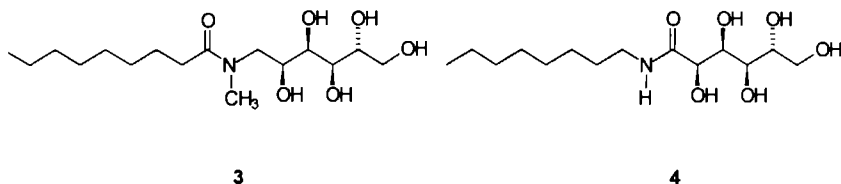
### 2.2.3 Models for aggregates of chiral amphiphiles

Helfrich has explained the regular winding of bilayers to form *ε g* helical structures as the result of a competition between the spontaneous torsion of the bilayer edges and the bending rigidity of the membrane<sup>61</sup> This model was adjusted by considering some of the potential consequences of an intrinsic chiral bending force<sup>62</sup> An intrinsic bending force due to chirality was also postulated by Schnur<sup>63</sup> Yager and Chappell proposed that the bending in their aggregates is due to electrostatic interactions at the edges of the bilayers<sup>64</sup> and highly anisotropic packing interactions<sup>65</sup> Computer modelling studies describing the aggregation of amphiphilic compounds have been published<sup>66,67</sup> A computational model for the chiral packing of molecules in crystals and monolayers has also been published,<sup>68</sup> but no computational model for the packing of amphiphiles in *chiral suprastructures* has been reported so far

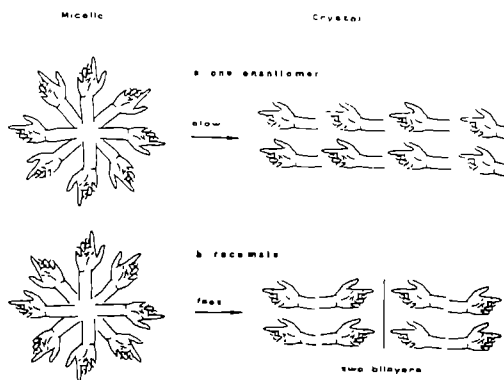
### 2.2.4 Carbohydrate amphiphiles

Amphiphilic compounds based on carbohydrates are attractive alternatives for traditional amphiphilic compounds, because of their excellent biodegradability and their relatively low cost<sup>69</sup> A wide-spread variation of amphiphiles based on alkyl glucosides,<sup>70</sup> with fluorinated alkyl

chains,<sup>71</sup> thioglucosides,<sup>72</sup> sucrose esters,<sup>73</sup> *N*-alkyl-aminoalditols,<sup>74</sup> and gluconamides<sup>47,75,76</sup> has been published. Alkyl glucamides (e.g. octanoyl-*N*-methylglucamide, (OMEGA, 3) and nonanoyl-*N*-methylglucamide (MEGA-10)) appeared to be very useful for dissolving natural membrane components due to their properties as non-ionic detergents and because of their much higher hydrolytic stability than *n*-alkyl-glucosides.<sup>77</sup> Very well investigated types of carbohydrate amphiphiles are the *N,n*-alkyl-D-gluconamides (for example compound 4).



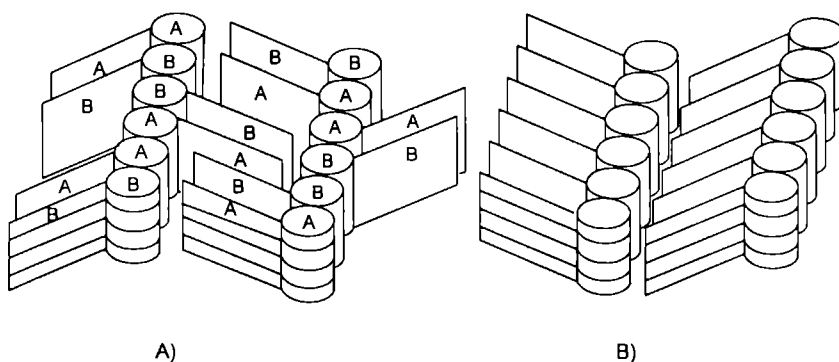
The first electron microscopy study on *N,n*-octyl-D-gluconamide (D-Glu8,<sup>78</sup> note that Glu stands for glucon and is **not** an abbreviation for glutamic acid or glutamate) was described by Pfannemüller and Welte.<sup>76</sup> Fuhrhop and coworkers<sup>51</sup> showed that D-Glu8 forms ropelike structures with a high aspect ratios up to  $10^4$  with bulges and knots. These structures were first proposed as consisting of two intertwined strands,<sup>51</sup> later believed to be a quadruple micellar helix,<sup>79</sup> and are now considered to be a helix of six intertwined strands as the most convincing model.<sup>80</sup> Pure enantiomers formed helices with enantiomorphology (*i.e.* in the case of *N,n*-octyl-D-gluconamide only right handed helices are formed) while racemic mixtures crystallized rapidly, due to the so-called “chiral bilayer effect” (see Figure 2.5)<sup>51</sup>



**Figure 2.5** Chiral bilayer effect (Ref. 51)

Structural variation of the aldonamide and mixing experiments<sup>78,81</sup> led to the conclusion that the solubility and the aggregate type of aldonamides depend directly on the stereochemistry of the head group<sup>81</sup> and that too much bending is not advantageous for molecular ordering.<sup>37</sup> In contrast with findings of Kunitake,<sup>37,38</sup> Fuhrhop concludes that a rigid segment is not needed in order to produce stable fibers.<sup>81</sup> The packing of fibers in the gels made from gluconamide solutions was

also studied by autoradiography,<sup>82</sup>  $^1\text{H}$ -NMR,<sup>83</sup> solid state  $^2\text{H}$ -NMR,<sup>84</sup> solution and solid state  $^{13}\text{C}$ -NMR,<sup>82, 85, 86</sup> FT-IR,<sup>86</sup> X-ray scattering,<sup>86</sup> DSC,<sup>87</sup> viscosity measurements,<sup>87</sup> monolayers in combination with Brewster angle microscope (BAM),<sup>88</sup> single crystal X-ray crystallography<sup>89</sup> and computer modelling (detailed structural analysis with the MATHEMATICA<sup>®</sup> program)<sup>79</sup> Gluconamide amphiphiles have also been polymerized, using incorporated diacetylenic groups,<sup>90</sup> methacrylamide,<sup>91</sup> and acrylate functions<sup>92</sup> The ionic compound *N*-dodecyltartaric acid monoamide showed in a similar way as D-Glu8, micellar fibers that assembled to cloth-like aggregates<sup>93</sup> Double headed bis-gluconamides (bolaamphiphiles) have been synthesized<sup>94</sup> and crystallized<sup>95</sup> showing two conformations of the molecule in the (asymmetric) unit cell Crystals of *N*,*n*-octyl-6-deoxy-D-gluconamide also showed an asymmetric unit containing two molecules (A,B) Molecules A and B formed a complex motif with pairwise alternating orientations and interdigitating antiparallel aliphatic chains (see Figure 2 6A)<sup>96</sup> which is different from the head to tail packing found for *n*-heptyl,<sup>97</sup> *n*-octyl,<sup>89</sup> *n*-nonyl,<sup>89</sup> *n*-decyl,<sup>97</sup> *n*-undecyl,<sup>98</sup> *N*,*n*-dodecyl-D-gluconamide,<sup>88</sup> *N*-cyclohexyl-D-gluconamide,<sup>99</sup> *N*-trideca-5,7-diyne-D-gluconamide,<sup>100</sup> (1*S*,2*S*)-1,2-bis(D-gluconamido)cyclohexane,<sup>101</sup> *n*-nonanyl-*N*-methylglucamide (MEGA-9),<sup>102</sup> *N*,*n*-octyl-D-gulonamide,<sup>103</sup> and *N*,*n*-dodecyl-D-ribonamide, see Figure 2 6B<sup>104</sup>



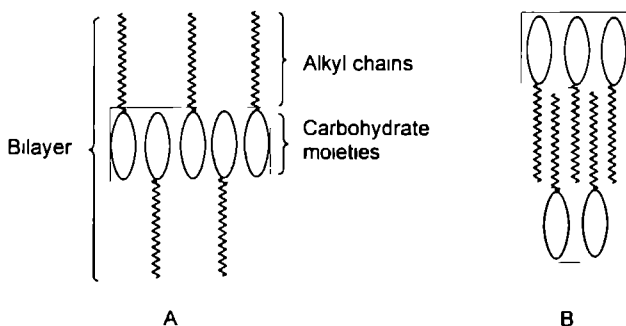
**Figure 2.6** Schematic representation of the crystal packing of gluconamides A) pairwise alternating orientation of the molecules B) head to tail packing

Very characteristic for the crystal structure of the alkyl-gluconamides is the so-called homodromic, quadrilateral hydrogen bond cycle<sup>105</sup> between any molecule and its counterpart in the next cell in the *x*-direction.<sup>89, 98</sup>

### 2.3 Thermotropic liquid crystalline properties of carbohydrate amphiphiles

Carbohydrate amphiphiles also appeared to be successful in the creation of thermotropic liquid crystalline phases<sup>106</sup> Because of their dualistic character, the amphiphilic mesogens are called “schizophrenic molecules”<sup>107</sup> and exhibit amphotropic (derived from *amphiphilic* and *thermotropic*) properties Several types of carbohydrate-derived mesogens have been made, for a

review see Jeffrey.<sup>106,107</sup> *N,n*-Alkyl-D-gluconamides also showed thermotropic L.C. properties.<sup>98,108</sup> The molecules are packed in a L.C. phase that is very common for single tailed carbohydrate amphiphiles, viz the smectic  $A_d$  phase.<sup>106,109</sup> In this phase, a layered structure, containing a rigid core of carbohydrate molecules connected to each other by hydrogen bonds, is separated by alkyl chains (see Figure 2.7A).<sup>108</sup> By systematic variation of the alkyl chains, van Doren came to a revised model for the molecular arrangement in the smectic  $A_d$  phase of carbohydrate derived amphiphiles with a single alkyl chain.<sup>110</sup> In the revised model, the smectic bilayers are identical to the fluid lamellar ( $L_a$ ) lyotropic phase, i.e. partially interdigitized alkyl chains in the core of each layer and carbohydrate moieties on the outside of the bilayer (see Figure 2.7B).



**Figure 2.7** Schematic models of the smectic  $A_d$  phase. Shading denotes the regions of dynamic hydrogen bonding. A) Original model, B) revised model.

The importance of hydrogen bonds in L.C. phases has been discussed recently.<sup>111</sup>

## 2.4 Functional aggregates

Vesicles can be used for sustained release of drugs in medical applications.<sup>112</sup> The stability of the vesicle is critical. Non-polymerized vesicles are too unstable while polymerized vesicles are not permeable enough in order to sustain release.<sup>113</sup> In tubular structures with an impermeable wall, the drug can only diffuse from one end to the other end of the tube. The tubes have a smaller contact surface with the outside matrix than non-polymerized vesicles, which results in a slower release of drugs.<sup>114</sup>

Copper-coated tubular structures prepared from diacetylenic phospholipids have been shown to be very useful in the development of long-term slow-release agents (up to 500 days). Off-shore marine tests showed that rods coated with paint containing small hollow tubules filled with tetracycline (antifouling agent) displayed a remarkable reduction of fouling in comparison with test rods coated with paint containing tetracycline without the hollow tubules.<sup>115</sup>

Metal ions have been used as templates for the formation of (chiral) suprastructures.<sup>57, 116,117,118,119</sup> An interesting application of metal-containing vesicles was shown by Fendler<sup>120</sup> who

enclosed platinum in vesicles and used them for the reduction of methylene blue with hydrogen gas. Singh and Markowitz<sup>121</sup> succeeded in immobilizing colloidal copper on phospholipid tubules by reduction of copper chloride using palladium that was bound to the phospholipids forming the tubules. Both the interior and exterior of the tubules were coated with copper, and nickel, cobalt and gold were immobilized in a similar way. Nickel coated tubes were used for the fabrication of tubule-based field emitting cathodes<sup>122</sup> by mixing the tubules with epoxy resin, and aligning them in a magnetic field of  $\sim 500$  G. After polymerization, the upper part of the resin was etched to expose the nickel-coated tubules and subsequently they were covered with a layer of gold and silver. A stable emission for more than 10 hours was achieved.<sup>116</sup>

Metal-containing aggregates have also been used as a matrix for catalysis.<sup>123</sup> The catalytic applications of suprastructures have been recently reviewed by Feiters.<sup>124</sup> Imidazole-containing aggregates are often used for ester hydrolysis.<sup>117</sup> The first imidazole-functionalized amphiphile reported, was *N*-myristoyl-histidine<sup>125</sup> but this compound appeared only to be catalytically active in combination with micellar cetyltrimethylammonium bromide (CTAB). Enantioselective catalysts containing amphiphiles with imidazole groups based on histidine have been described in the literature.<sup>126,127</sup>

Many vesicular systems containing polypeptides have been investigated.<sup>124</sup> In addition to vesicles or micelles, other aggregate forms like the helical cavities of amylose were used as a matrix for ester hydrolysis with imidazole as a catalyst.<sup>128</sup>

Porphyrins are excellent catalysts for epoxidation reactions<sup>129</sup> and have been successfully incorporated in vesicles while retaining their epoxidation capacities.<sup>130,131</sup> The incorporation of a porphyrine in aggregates of D-Glu-8 failed.<sup>47</sup> Porphyrins covalently bound to 2-aminoglysoamide head groups have been shown to form micellar fibers.<sup>132</sup>

## 2.5 Literature

<sup>1</sup> Singer, S J, Nicolson, G.L. *Science* **1972**, 175, 720.

<sup>2</sup> a) Fendler, J.H. *Membrane Mimetic Chemistry*, John Wiley, New York **1982**; b) Fuhrhop, J.-H., Mathieu, J *Angew Chem* **1984**, 96, 125; *Ibid Int Ed Eng* **1984**, 23, 100

<sup>3</sup> Ringsdorf, H., Schlarb, B ; Venzmer, J. *Angew Chem* **1988**, 100, 117, *Ibid Int Ed Eng* **1988**, 27, 113.

<sup>4</sup> Gebicki, J M , Hicks, M. *Nature* **1973**, 243, 232

<sup>5</sup> The first report of completely synthetic amphiphiles was by Kunitake, cf Kunitake, T., Okahata, Y *J Am Chem Soc* **1977**, 99, 3860, although synthetic emulsifying agents like lecithins were already known since early 50's Baer, E., Kates, M *J Am Chem Soc* **1950**, 72, 942. For early synthetic carbohydrate emulsifying agents see ref 75

<sup>6</sup> a) Israelachvili, J.N.; Mitchell, D.J.; Ninham, B.W, *J Chem Soc , Faraday Trans 2* **1976**, 72, 1525, b) Israelachvili, J N , Marcelja, S; Horn, R.G. *Quart Rev Biophys* **1980**, 13, 121.

<sup>7</sup> Tanford, C *The Hydrophobic Effect*, Wiley Interscience 2<sup>nd</sup> ed., New York **1980**.

<sup>8</sup> Blokzijl, W., Engberts, J B.F.N *Angew Chemie* **1993**, 105, 1610; *Ibid Int Ed Eng* **1993**, 32, 1545 and references cited therein

<sup>9</sup> Inoko, Y ; Mitsui, T. *J Physiol Soc Jpn* **1978**, 44, 1918



- <sup>10</sup> a) Hub, H-H, Hupfer, B, Koch, H, Ringsdorf, H *Angew Chem* **1980**, 92, 962, *Ibid Int Ed Eng* **1980**, 19, 938, b) Echegoyen, L E, Hernandez, J C, Kaifer, A I, Gokel, G W, Echegoyen, L *J Chem Soc Chem Commun* **1988**, 836
- <sup>11</sup> Pfannemüller, B, Welte, W *Chem Phys Lipids* **1985**, 37, 227
- <sup>12</sup> a) Nusselder, J J H, Engberts, J B F N *Langmuir* **1991**, 7, 2089, b) Nusselder, J J H *Ph D Thesis*, University of Groningen **1990**
- <sup>13</sup> Samuel, N K P, Singh, M, Yamaguchi, K, Regen, S L *J Am Chem Soc* **1985**, 107, 42
- <sup>14</sup> Tundo, P, Kippenberger, D J, Klahn, P L, Prieto, N E, Jao, T -C, Fendler, J H *J Am Chem Soc* **1982**, 104, 456
- <sup>15</sup> Regen, S L, Singh, A, Singh, M *J Am Chem Soc* **1982**, 104, 791
- <sup>16</sup> Paleos, C M, Christias, C, Evangelatos, G P *J Polym Sci* **1982**, 20, 2565
- <sup>17</sup> Frankel, D A, Lamparski, H, Liman, U, O'Brien, D F *J Am Chem Soc* **1989**, 111, 9262
- <sup>18</sup> Day, D, Hub, H H, Ringsdorf, H *J Polym Sci Polym Lett Ed* **1978**, 16, 205
- <sup>19</sup> Hupfer, B, Ringsdorf, H, Schupp, H *Chem Phys Lipids* **1984**, 33, 355
- <sup>20</sup> Yager, P, Schoen, P E, Davies, C, Price, R, Singh, A *Biophys J* **1985**, 899
- <sup>21</sup> Kuo, T, O'Brien, D F *J Am Chem Soc* **1988**, 110, 7571
- <sup>22</sup> a) Bader, H, Ringsdorf, H, Skura, J *Angew Chem* **1981**, 93, 109, *Ibid Int Ed Eng* **1981**, 20, 91, b) Frankel, D A, O'Brien, D F *J Am Chem Soc* **1991**, 113, 7436, c) Fuhrhop, J -H, Blumtritt, P, Lehmann, C, Luger, P *J Am Chem Soc* **1991**, 113, 7437
- <sup>23</sup> Rhodes, D G, Frankel, D A, Kuo, T, O'Brien, D F *Langmuir* **1994**, 10, 267
- <sup>24</sup> Regen, S L, Samuel, N K P, Khurana, J M *J Am Chem Soc* **1985**, 107, 5804
- <sup>25</sup> Sadownik, A, Stevely, J, Regen, S L *J Am Chem Soc* **1986**, 108, 7789
- <sup>26</sup> Elbert, R, Folda, T, Ringsdorf, H *J Am Chem Soc* **1984**, 106, 7687
- <sup>27</sup> Ishikawa, Y, Kuwahara, H, Kunitake, T *J Am Chem Soc* **1989**, 111, 8530
- <sup>28</sup> a) Fuoss, R M, Edelson, D J *J Am Chem Soc* **1951**, 73, 269, b) Okahata, Y, Kunitake, T *J Am Chem Soc* **1979**, 101, 5231, c) Hentrich, F, Tschierske, C, Zäschke, H *Angew Chem* **1991**, 103, 429, *Ibid Int Ed Eng* **1991**, 30, 440
- <sup>29</sup> Festag, R, Hessel, V, Lehmann, P, Ringsdorf, H, Wendorff, J H *Recl Trav Chim Pay Bas* **1994**, 113, 222
- <sup>30</sup> a) Bader, H, Ringsdorf, H *Faraday Discuss Chem Soc* **1986**, 82, 1, b) Fuhrhop, J -H, Krull, M, Schulz, A, Möbius, D *Langmuir* **1990**, 6, 497
- <sup>31</sup> Fuhrhop, J -H, Krull, M, Schulz, A, Möbius, D *Langmuir* **1990**, 6, 497
- <sup>32</sup> Fuhrhop, J -H, Hungerbühler, H, Siggel, U *Langmuir* **1990**, 6, 1295
- <sup>33</sup> a) Fuhrhop, J -H, Mathieu, J *J Chem Soc, Chem Commun* **1983**, 144, b) Fuhrhop, J -H, Fritsch, D *Acc Chem Res* **1986**, 19, 130, c) Fuhrhop, J -H, David, H -H, Mathieu, J, Liman, U, Winter, H -J, Boekema, E *J Am Chem Soc* **1986**, 108, 1785, d) Fuhrhop, J -H, Spiroski, D, Boettcher, C *J Am Chem Soc* **1993**, 115, 1600
- <sup>34</sup> Menger, F M, Littau, C A *J Am Chem Soc* **1993**, 115, 10083
- <sup>35</sup> Fukuda, H, Kawata, K, Okuda, H, Regen, S L *J Am Chem Soc* **1990**, 112, 1635
- <sup>36</sup> Schenning A P H J, Feiters, M C, Nolte, R J M *Tetrahedron Lett* **1993**, 34, 7707
- <sup>37</sup> Kunitake, T, Okahata, Y, Shimomura, M, Yasunami, S -I, Takarabe, K *J Am Chem Soc* **1981**, 103, 5401

- <sup>38</sup> Kunitake, T *Angew Chem* **1992**, 104, 692; *Ibid Int Ed Eng* **1992**, 31, 709
- <sup>39</sup> Watson, J D ; Crick, F H C *Nature* **1953**, 171, 737.
- <sup>40</sup> Fraser, R B D *J Mol Biol* **1979**, 129, 463.
- <sup>41</sup> a) Klug, A , Daspar, D L D *Advan Virus Res* **1960**, 7, 274; b) Kushner, D.J *Bacteriological Rev* **1969**, 33, 302; c) Butler, P G J , Klug, A *The assembly of a virus*, Scientific American Inc. **1978**.
- <sup>42</sup> Erickson, R O *Science* **1973**, 181, 705 and references cited therein.
- <sup>43</sup> Hotten, B.W ; Birdsall, D H. *J Colloid Sci* **1952**, 7, 284.
- <sup>44</sup> a) Kunitake, T., Nakashima, N ; Hayashida, S ; Yonemuri, K. *Chem Lett* **1979**, 1413, b) Rhodes, D G , Frankel, D.A , Kuo, T , O'Brien, D.F *Langmuir* **1994**, 10, 267
- <sup>45</sup> Kunitake, T , Nakashima, N ; Morimitsu, K *Chem Lett* **1980**, 1347
- <sup>46</sup> Yager, P , Schoen, P. *Mol Cryst Liq Cryst* **1984**, 106, 371
- <sup>47</sup> a) Fuhrhop, J -H , Helfrich, W. *Chem Rev* **1993**, 93, 1565, b) Fuhrhop, J -H ; Krull, M *Frontiers in Supramolecular Organic Chemistry and Photochemistry* ed. Schneider, H -J , Dürr, H , VCH publ. Weinheim, New York, Basel, Cambridge, p. 223
- <sup>48</sup> a) Kunitake, T , Nakashima, N.; Shimomura, M ; Okahata, Y ; Kano, K., Ogawa, T *J Am Chem Soc* **1980**, 102, 6642; b) Ihara, H , Takafuji, M , Hirayama, C *Langmuir* **1992**, 8, 1548; c) Nakashima, N , Ando, R , Muramatsu, T , Kunitake, T *Langmuir* **1994**, 10, 232
- <sup>49</sup> Nakashima, N., Asakuma, S., Kunitake, T. *J Am Chem Soc* **1985**, 107, 509
- <sup>50</sup> Nakashima, N , Asakuma, S., Kim, J.-M., Kunitake, T *Chem Lett* **1984**, 1709.
- <sup>51</sup> Fuhrhop, J -H ; Schnieder, P ; Rosenberg, J , Boekema, E *J Am Chem Soc* **1987**, 109, 3387
- <sup>52</sup> a) Yanagawa, H., Ogawa, Y , Furuta, H., Tsuno, K. *J. Am Chem Soc* **1989**, 111, 4567, b) Sommerdijk, N A J.M , Buynsters, P J A A ; Pistorius, A M A , Wang, M ; Feiters, M.C ; Nolte, R.J M ; Zwanenburg, B. *J Chem Soc, Chem Commun* **1994**, 1941
- <sup>53</sup> Yager, P., Schoen. P.E., Davies, C.; Price , R ; Singh, A *Biophys J* **1985**, 48, 899
- <sup>54</sup> Georger, J H ; Singh, A.; Price, R.R.; Schnur, J M ; Yager, P ; Schoen, P E *J Am Chem Soc* **1987**, 109, 6169
- <sup>55</sup> Hub, H; Hupfer, B ; Koch, H.; Ringsdorf, H. *J Macromol Sci. Chem* **1981**, A15, 701
- <sup>56</sup> Markowitz, M A ; Schnur, J M ; Singh, A *Chem Phys Lipids* **1992**, 62, 193.
- <sup>57</sup> Markowitz, M A , Baral, S ; Brandow, S., Singh, A. *Thin Solid Films* **1993**, 224, 242
- <sup>58</sup> Yager, P , Price, R.R ; Schnur, J M., Schoen, P E ; Singh, A.; Rhodes, D.G. *Chem Phys Lipids* **1988**, 46, 171.
- <sup>59</sup> Singh, A ; Burke, T.G., Calvert, J.M., Georger, J H.; Herendeen, B., Price, R R , Schoen, P.E , Yager, P *Chem Phys Lipids* **1988**, 47, 135
- <sup>60</sup> Singh, A., Markowitz, M A *New J Chem* **1994**, 18, 377
- <sup>61</sup> Helfrich, W *J Phys Chem* **1986**, 85, 1085.
- <sup>62</sup> Helfrich, W , Prost, J. *Phys Rev A* **1988**, 38, 3065.
- <sup>63</sup> a) Selinger, J V ; Schnur, J. *Phys Rev Lett* **1993**, 71, 4091, b) Schnur, J M., Ratna, B.R , Selinger, J V., Singh, A , Jyothi, G , Easwaran, K.R.K. *Science* **1994**, 264, 945.
- <sup>64</sup> a) Chappell, J S ; Yager, P. *Chem Phys.* **1991**, 150, 73; b) Chappell, J. S.; Yager, P *Biophys J* **1991**, 60, 952
- <sup>65</sup> Chappell, J S.; Yager, P *Chem Phys Lipids* **1991**, 58, 253

- <sup>66</sup> a) Pastor, R.W., Venable, R.M., Karplus, M. *Proc Natl Acad Sci USA* **1991**, *88*, 892; b) Heller, H., Schaefer, M., Schulten, K. *J Phys Chem* **1993**, *97*, 8343; Pohorille, A., Benjamin, I. *J Phys Chem* **1993**, *97*, 2664, c) Os van, N M., Smit, B., Karabornı, S. *Recl Trav Chim Pays-Bas* **1994**, *113*, 181
- <sup>67</sup> a) Sanders, C R., Prestegard, H. *J Am Chem Soc* **1992**, *114*, 7096, b) Hare, B J., Howard, K.P., Prestegard, J H. *Biophys J* **1993**, *64*, 392; c) Buuren, A R., Berendsen, B J. *Langmuir* **1994**, *10*, 1703
- <sup>68</sup> Perlstein, J. *J Am Chem Soc* **1994**, *116*, 455
- <sup>69</sup> a) Kelkenberg, Marl, H. *Tens Surf Det* **1988**, *25*, 8; b) Bekkum, H van, Fuchs, A. *Chem Mag* **1991**, *6/7*, 334, c) Koch, H., Beck, R., Röper, H. *Starch/Starke* **1993**, *2*
- <sup>70</sup> Kataoka, R., Watanabe, Y., Mitaku, S. *Rep Prog Polym Phys Jpn* **1984**, *27*, 699
- <sup>71</sup> a) Mietchen, R.; Prade, H.; Holz, J., Praefcke, K., Blunk, D. *Chem Ber* **1993**, *126*, 1707, b) Zarif, L., Gulik-Krzywicki, T.; Riess, J., Pucci, B., Guedj, C.; Pavia, A A. *Coll Surf A Physicochem Eng Aspects* **1993**, *84*, 107
- <sup>72</sup> a) Saito, S., Tsuchiya, T. *Biochem J* **1984**, *222*, 829; b) Tsuchiya, T., Saito, S. *J Biochem* **1984**, *96*, 1593
- <sup>73</sup> Bjorkling, F., Godtfredsen, S E.; Kirk, O. *J Chem Soc, Chem Commun* **1989**, 934
- <sup>74</sup> Doren, H. A van, Geest, R. van der, Ruijter, C F de, Kellogg, R M., Wynberg, H. *Liq Cryst* **1990**, *8*, 109
- <sup>75</sup> Fieser, M., Fieser, L F., Toromanoff, E., Hirata, Y., Heymann, Tefft, M., Bhattacharya, S. *J Am Chem Soc* **1956**, *78*, 2825
- <sup>76</sup> Pfannemüller, B., Welte, W. *Chem Phys Lipids* **1985**, *37*, 227
- <sup>77</sup> a) Hildreth, J E. *Biochem J* **1982**, *207*, 363; b) Hanatani, M.; Nishifuji, K., Futai, M.; Tsuchiya, T. *J Biochem* **1984**, *95*, 1349
- <sup>78</sup> Fuhrhop, J.-H., Boettcher, C. *J Am Chem Soc* **1990**, *112*, 1768
- <sup>79</sup> Koning, J.; Boettcher, C.; Winkler, H., Zeitler, E., Talmon, Y., Fuhrhop, J.-H. *J Am Chem Soc* **1993**, *115*, 693
- <sup>80</sup> Fuhrhop, J.-H., Koning, J. *Membranes and Molecular Assemblies: The Synkinetic Approach*, part of the series "Monographs in Supramolecular Chemistry", series ed. Stoddart, J F., The Royal Society of Chemistry, Cambridge (UK) **1994**, pag IX
- <sup>81</sup> Fuhrhop, J.-H., Schnieder, P., Boekema, E., Helfrich, W. *J Am Chem Soc* **1988**, *110*, 2861
- <sup>82</sup> Boettcher, C., Boekema, E., Fuhrhop, J.-H. *J Microscopy* **1990**, 173
- <sup>83</sup> a) Svenson, S., Schäfer, A., Fuhrhop, J.-H. *J Chem Soc, Perkin Trans 2* **1994**, 1023, b) Hafkamp, R J H., Feiters, M C., Nolte, R J M. to be published.
- <sup>84</sup> Fuhrhop, J.-H.; Svenson, S.; Boettcher, C., Rössler, E.; Vieth, H.-M. *J Am Chem Soc* **1990**, *112*, 4307
- <sup>85</sup> a) Taravel, F.R., Pfannemüller, B. *Makromol Chem* **1990**, *191*, 3097, b) Svenson, S., Kirste, B., Fuhrhop, J.-H. *J Am Chem Soc* **1994**, *116*, 11969
- <sup>86</sup> Svenson, S., Köning, J.; Fuhrhop, J.-H. *J Phys Chem* **1994**, *98*, 1022.
- <sup>87</sup> Pfannemüller, B.; Kühn, I. *Makromol Chem* **1988**, *189*, 2433
- <sup>88</sup> Vollhardt, D.; Gutberlet, T., Emrich, G., Fuhrhop, J.-H. *Langmuir* **1995**, *11*, 2661
- <sup>89</sup> a) Zabel, V., Müller-Fahrnow, A., Hilgenfeld, R., Saenger, W., Pfannemüller, B., Enkelmann, V., Welte, W. *Chem Phys Lipids* **1986**, *39*, 313, b) Wang, J.-L.; Lahav, M., Leiserowitz, L. *Angew Chem* **1991**, *103*, 698, *Ibid Int Ed Eng* **1991**, *30*, 696
- <sup>90</sup> Frankel, D.A., O'Brien, D.F. *J Am Chem Soc* **1994**, *116*, 10057
- <sup>91</sup> Loos, M.; Baeyens-Volant, D.; Szalai, E.; David, C. *Makromol Chem* **1990**, *191*, 2917.

- <sup>92</sup> Fuhrhop, J.-H., Spiroski, D., Schnieder, P. *React Polym* **1991**, *15*, 215
- <sup>93</sup> Fuhrhop, J.-H., Demoulin, C., Rosenberg, J., Boettcher, C. *J Am Chem Soc* **1990**, *112*, 2827
- <sup>94</sup> Garelli, R., Brisset, F., Rico, I., Lattes, A. *Synt Commun* **1993**, *23*, 35
- <sup>95</sup> Muller-Fahmow, A., Saenger, W., Fritsch, D., Schnieder, P., Fuhrhop, J.-H. *Carbohydr Res* **1993**, *242*, 11
- <sup>96</sup> Herbst, R., Steiner, T., Pfannemüller, B., Saenger, W. *Carbohydr Res* **1995**, *269*, 29
- <sup>97</sup> Müller-Fahmow, A., Hilgenfeld, R., Hesse, H., Saenger, W., Pfannemüller, B. *Carbohydr Res* **1988**, *176*, 165
- <sup>98</sup> Jeffrey, G. A., Maluszynska, H. *Carbohydr Res* **1990**, *207*, 211
- <sup>99</sup> Darbon, P. N., Odon, Y., Lacombe, J. M., Decoster, E., Pavia, A. A. *Acta Cryst* **1984**, *C40*, 1105
- <sup>100</sup> Andre, C., Luger, P., Fuhrhop, J.-H. *Chem Phys Lipids* **1994**,
- <sup>101</sup> André, C., Luger, P., Nehmzow, D., Fuhrhop, J.-H. *Carbohydr Res* **1994**, *261*, 1
- <sup>102</sup> Müller-Fahmow, A., Zabel, V., Steifa, M., Hilgenfeld, R. *J Chem Soc Chem Commun* **1986**, 1573
- <sup>103</sup> André, C., Luger, P., Svenson, S., Fuhrhop, J.-H. *Carbohydr Res* **1992**, *230*, 31
- <sup>104</sup> André, C., Luger, P., Bach, R., Fuhrhop, J.-H. *Carbohydr Res* **1995**, *266*, 15
- <sup>105</sup> Flier, J. S., Maratos-Flier, E., Pallotta, J. A., McIsaac, D. *Nature* **1979**, *279*, 343
- <sup>106</sup> Jeffrey, G. A. *Acc Chem Res* **1986**, *19*, 168
- <sup>107</sup> Jeffrey, G. A., Wingert, L. A. *Liq Cryst* **1992**, *12*, 179
- <sup>108</sup> Pfannemüller, B., Welte, W., Chin, E., Goodby, J. W. *Liq Cryst* **1986**, *1*, 357
- <sup>109</sup> a) Goodby, J. W. *Mol Cryst Liq Cryst* **1984**, *110*, 205, b) Doren, H. A., van, Geest, R., van der, Kellogg, R. M., Wynberg, H. *Carbohydr Res* **1989**, *194*, 71
- <sup>110</sup> Doren, van H. A., Wingert, L. M. *Mol Cryst Liq Cryst* **1991**, *198*, 381
- <sup>111</sup> Paleos, C. M., Tsiourvas, D. *Angew Chem* **1995**, *107*, 1839, *Ibid Int Ed Eng* **1995**, *34*, 1696
- <sup>112</sup> Lawrance, M. J. *Chem Soc Rev* **1994**, 417
- <sup>113</sup> Krause, H. J., Juliano, R. L., Regen, S. *J Pharm Sci* **1987**, *76*, 1
- <sup>114</sup> Schnur, J. M., Price, R., Rudolph, A. S. *J Controlled Release* **1994**, *28*, 3
- <sup>115</sup> Schnur, J. M. *Science* **1993**, *262*, 1669
- <sup>116</sup> For a review of metallomesogens see Espinet, P., Esteruelas, M. A., Oro, L. A., Serrano, J. L., Sola, E. *Coord Chem Rev* **1992**, *117*, 215, review of discotic structures Giroud-Godquin, A.-M., Maitlis, P. M. *Angew Chem* **1991**, *103*, 370, *Ibid Int Ed Eng* **1991**, *30*, 375, review of calamitic structures Hudson, S. A., Maitlis, P. M. *Chem Rev* **1993**, *93*, 861, review of polymers Oriol, L., Serrano, J. L. *Adv Mat* **1995**, *7*, 348
- <sup>117</sup> Tachibana, T., Kambara, H. *J Coll Interface Sci* **1968**, *28*, 173
- <sup>118</sup> Zarges, W., Hall, J., Lehn, J.-M. *Helv Chim Acta* **1991**, *74*, 1843, Krämer, R., Lehn, J.-M., Marquis-Rigault, A. *Proc Natl Acad Sci USA* **1993**, *90*, 5394
- <sup>119</sup> Hafkamp, R. J. H., Feiters, M. C., Nolte, R. J. M. *Angew Chem* **1994**, *106*, 1054, *Ibid Int Ed Eng* **1994**, *33*, 986
- <sup>120</sup> Furihara, K., Fendler, J. H. *J Am Chem Soc* **1983**, *105*, 6152
- <sup>121</sup> Singh, Z., Markowitz, M., Chow, G. M. *Nanostructured Materials* **1995**, *5*, 141
- <sup>122</sup> Kirkpatrick, D. A., Bergeron, G. L., Czarnaski, M. A., Hickman, J. J., Chow, G. M., Price, R., Ratna, B. L., Schoen, P. E., Stockton, W. B., Baral, S., Ting, A. C., Schnur, J. M. *Appl Phys Lett* **1992**, *60*, 1556

- <sup>123</sup> Fendler, J H , Fendler, E J. *Catalysis in Micellar and Macromolecular Systems* Acad. Press, New York **1975**;  
For review of catalysis by micelles and membranes see. Kunitake, T., Shinkai, S. *Adv Phys Org Chem* **1980**, Vol  
A, 435
- <sup>124</sup> Feiters, M.C. *Supramolecular technology and applications*, vol 10, part III, Chap 16, *supramolecular catalysis*  
vol. ed Reinhoudt, D.N., part of the series "Comprehensive Supramolecular Chemistry", ed. Lehn, J.-M , Pergamon  
Press, Elsevier Sci Ltd., Oxford (UK) **1995**.
- <sup>125</sup> a) Ochoa-Solano, A , Romero, G ; Gitler, C *Science* **1967**, 156, 1243, b) Gitler, C., Ochoa-Solano, A *J Am*  
*Chem Soc* **1968**, 90, 5004
- <sup>126</sup> Brown, J M , Bunton, C.A. *J Chem Soc , Chem Commun* **1974**, 969
- <sup>127</sup> a) Cleij, M.C.; Drenth, W , Nolte, R.J.M *Recl Trav Chim Pays-Bas* **1993**, 1, b) Cleij, M C *Ph D Thesis*  
*Univ of Utrecht* **1989**.
- <sup>128</sup> Hui, Y , Zou, W *Frontiers in Supramolecular Organic Chemistry and Photochemistry* ed Schneider, H.-J ,  
Dürr, H , VCH publ Weinheim, New York, Basel, Cambridge, 203
- <sup>129</sup> a) Jørgensen, K A *Chem Rev* **1989**, 89, 431; b) Meunier, B. *Chem Rev* **1992**, 92, 1411
- <sup>130</sup> Sorokin, A B , Khenkin, A M , Marakushev, S.A ; Shilov, A.E., Shteinman, A.A *Dokl Phys Chem* **1984**, 29,  
1101
- <sup>131</sup> Esch, J. van, Roks, M.F.M.; Nolte, R.J M *J Am Chem Soc* **1986**, 108, 6093.
- <sup>132</sup> Fuhrhop, J.-H.; Demoulin, C.; Boettcher, C ; Siggel, U. *J Am Chem. Soc.* **1992**, 114, 4159

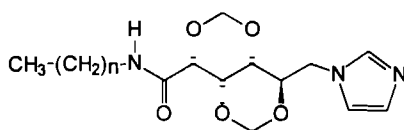
# Chapter 3

## Thermotropic liquid crystalline properties of *N*-*n*-alkyl-D-gluconamides

### 3.1 Introduction

In recent years, the interest in the design and synthesis of supramolecular structures has grown steadily, one of the objectives being the development of new materials<sup>1</sup> and new catalysts<sup>2</sup>. Supramolecular systems<sup>3</sup> have been prepared from a variety of building blocks including surfactants,<sup>4</sup> polymers,<sup>5</sup> rod-like<sup>6</sup> and disk-like mesogens,<sup>7</sup> and other molecules.<sup>8</sup> As part of our program aimed at the development of novel chiral matrices, *e.g.* for catalytic applications, we have undertaken the synthesis and the study of the thermotropic liquid crystalline (LC) properties of gluconamides containing a metal-coordinating group, see **1**. Our interest in gluconamides and related carbohydrates was raised by the recent studies of Fuhrhop and others,<sup>9</sup> which indicate that these compounds can form a great variety of chiral nanometer-sized structures in water. One of the reasons for investigating the thermotropic LC behavior of carbohydrate derivatives<sup>6</sup> is that this type of compounds is likely to form lamellar aggregates<sup>10</sup> which is of interest for the building of supramolecular catalysts in aqueous solutions.<sup>11 12 13</sup>

Although metal complexes with sugar ligands are known since 1951,<sup>14</sup> they were mainly used for the determination of the conformation of the carbohydrate structures and no additional metal complexing group was involved. The goal of the present project was to make metal complexes from gluconamides that are stable, even in aqueous solutions, and therefore it was necessary to couple a metal ligating group to the carbohydrate framework. An excellent candidate for this purpose is imidazole, which is also present in the amino acid histidine and is known to form stable complexes with a great variety of metals.<sup>15</sup>



- 1** a *n* = 7  
b *n* = 9  
c *n* = 11  
d *n* = 11  
e *n* = 15  
f *n* = 17

In this chapter we will show that metal ions coordinated to **1** can induce or stabilize thermotropic LC properties. In addition, interesting architectures can be formed from **1** in water,<sup>16</sup> as will be described in Chapter 4. For a proper evaluation of the physical properties of compounds **1**, we also synthesized a series of related metal complexing carbohydrates.<sup>17</sup> The

liquid crystalline properties of these compounds are also described in this chapter. To the best of our knowledge, the complexes reported here are the first examples of carbohydrate metallomesogens.

### 3.2 Experimental

The syntheses described below were in most cases first attempts, which means that the yields were not optimized and can probably be improved.

Melting points were determined as the average of the onset and the top of the melting peaks of DSC thermograms. IR spectra were recorded on a Biorad Digilab Division FT-IR instrument.  $^1\text{H}$ -NMR spectra were recorded on a Bruker WH-90 or a Bruker WM-400 instrument and the chemical shifts are reported relative to  $(\text{CH}_3)_4\text{Si}$ . Abbreviations used are s, singlet, d, doublet, 2d, double doublet, t, triplet, q, quartet, quin, quintet, m, multiplet.  $^{13}\text{C}$ -NMR spectra were recorded on a Bruker WM-400 or a Bruker WM-500 instrument. Chemical shifts are reported relative to  $(\text{CH}_3)_4\text{Si}$  and calibrated on adamantane.

Mass spectra were recorded on a VG7060E instrument and the elemental analyses were carried out with a Carlo Erba EA 1108 instrument. UV-vis spectra were obtained from a Perkin Elmer Lambda 45 spectrophotometer. Thermograms were recorded on a Perkin Elmer DSC 7 instrument, which was calibrated on indium and zinc. Both heating and cooling runs were recorded with a rate of  $5\text{ }^\circ\text{C}/\text{min}$ .

Single crystal X-ray diffraction data were collected using an Enraf-Nonius CAD4-Turbo diffractometer on a rotating anode. The crystals were glued on a Lindemann glass capillary and mounted on the diffractometer in a stream of cold nitrogen. The data were optimized to a  $R_{\text{w}}^2$ -value of 0.224,  $R_F=0.120$ ,  $S=0.90$ , using the SHELXL-93 refinement program.

Chemicals were used as obtained from the supplier, except for the solvents which were distilled prior to use.

#### 3.2.1 Syntheses

***N,n*-Octyl-D-gluconamide (6a).** This compound was synthesized as described in the literature.<sup>18</sup> After 2 recrystallizations from MeOH a colorless crystalline powder was obtained, yield 1.07 g (3.47 mmol, 62.4 %), m.p.  $159.2\text{ }^\circ\text{C}$ . IR (KBr)  $3532\text{ cm}^{-1}$  ( $(\text{C}^2)\text{OH}$ ),<sup>19</sup> 3358 and 3389 (homodromic H bonding cycle),<sup>20</sup> 1646 (amide I) and 1529 (amide II).  $^1\text{H}$ -NMR (400 MHz, DMSO- $d_6$ , in order to obtain less complex spectra, 1 drop of  $\text{D}_2\text{O}$  was added through which the hydroxyl hydrogen atoms were exchanged for deuterium atoms)  $\delta$  3.956 ppm (d, 1H,  $J_{2,3} = 3.60\text{ Hz}$ ,  $\text{H}^2$ ), 3.877 (2d, 1H,  $J_{3,4} = 2.30\text{ Hz}$ ,  $\text{H}^3$ ), 3.558 (2d, 1H,  $J_{5,6} = 2.80\text{ Hz}$ ,  $J_{6,6} = -11.20\text{ Hz}$ ,  $\text{H}^6$ ), 3.462 ppm (m, 1H,  $J_{5,4} = 8.50\text{ Hz}$ ,  $J_{5,6} = 5.50\text{ Hz}$ ,  $\text{H}^5$ ), 3.440 ppm (m, 1H,  $\text{H}^4$ ), 3.348 (2d, 1H,  $\text{H}^6$ ), 3.033 (8 peaks, 2H,  $-\text{CH}_2-\text{NHCO}$ ), 1.390 (t, 2H,  $-\text{CH}_2-\text{CH}_2-\text{NHCO}$ ), 1.229 (m, 10H,  $\text{CH}_3$ - $(\text{CH}_2)_5$ -), 0.846 (t, 3H,  $\text{CH}_3$ -).  $^{13}\text{C}$ -NMR (100 MHz, DMSO- $d_6$ ) 172.23 ppm ( $-\text{NHCO}-$ ), 73.63 ( $\text{C}^2$ ), 72.41 ( $\text{C}^3$ ), 71.49 ( $\text{C}^5$ ), 70.12 ( $\text{C}^4$ ), 63.38 ( $\text{C}^6$ ), 38.26 ( $-\text{CH}_2-\text{NHCO}-$ ), 31.28, 29.17, 28.78, 28.69, 26.38, 22.12 (methylene carbons from alkyl chain), 14.00 ( $-\text{CH}_3$ ). Anal. Calcd for  $\text{C}_{14}\text{H}_{29}\text{NO}_6$ : C, 54.70, H, 9.51, N, 4.56. Found: C, 54.75, H, 9.50, N, 4.55.

Compounds **6b-6f** were synthesized and purified as mentioned above for **6a**. Starting compounds were the appropriate *n*-alkyl amines. Purification by recrystallization became more difficult in the case of the longer alkyl chain amines, repeated recrystallization, however, generally, yielded pure products.

***N,n*-Decyl-D-gluconamide (6b).** After crystallization, a white crystalline powder was obtained, yield 26.41 g (78.72 mmol, 89.3 %), m.p.  $156.5\text{ }^\circ\text{C}$ . IR (KBr) showed  $1646\text{ cm}^{-1}$ .

(amide I) and 1529 (amide II), which is similar to **6a**. Anal. Calcd. for  $C_{16}H_{33}NO_6$ : C, 57.29; H, 9.92; N, 4.18. Found: C, 57.27; H, 9.76; N, 4.20.

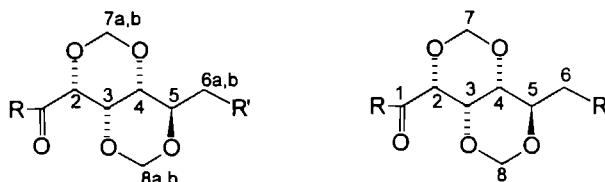
**N,n-Dodecyl-D-gluconamide (6c)**. A crystalline powder was obtained, yield 1.70 g (4.69 mmol, 84.0 %), m.p. 155.5 °C. IR (KBr) showed amide peaks at 1647  $cm^{-1}$  (amide I) and 1529 (amide II). Anal. Calcd. for  $C_{18}H_{37}NO_6$ : C, 59.48; H, 10.26; N, 3.85. Found: C, 59.38; H, 10.20; N, 3.89.

**N,n-Tetradecyl-D-gluconamide (6d)**. After several crystallizations, a crystalline powder was obtained. Yield 17.33 g (44.26 mmol, 91.4 %), m.p. 154.0 °C, IR (KBr) 1647  $cm^{-1}$  (amide I), 1528 (amide II). Anal. Calcd. for  $C_{20}H_{41}NO_6$ : C, 61.35; H, 10.55; N, 3.58. Found: C, 61.30; H, 10.62; N, 3.62.

**N,n-Hexadecyl-D-gluconamide (6e)**. The powder that was obtained in a yield of 14.94 g (35.61 mmol, 62.2 %), consisted of very small crystals, m.p. 151.4 °C, IR (KBr) 1647  $cm^{-1}$  (amide I) and 1527 (amide II). Anal. Calcd. for  $C_{22}H_{45}NO_6$ : C, 62.97; H, 10.81; N, 3.34. Found: C, 62.60; H, 10.81; N, 3.36.

**N,n-Octadecyl-D-gluconamide (6f)**. A white powder was obtained after repeated crystallization (7 times), yield 8.69 g (19.41 mmol, 80.3 %), m.p. 148.5 °C. IR 1624  $cm^{-1}$  (amide I) and 1549 (amide II). Anal. Calcd. for  $C_{24}H_{49}NO_6 \cdot 1.5$  MeOH: C, 61.79; H, 11.18; N, 2.83. Found: C, 61.98; H, 10.57; N, 3.37.

The carbohydrate skeleton protons and carbon atoms are numbered according to the schemes below.



Numbering schemes for the protons (left) and carbon atoms (right) of the carbohydrate skeleton

In some cases, non first order  $^1H$ -NMR spectra were obtained. The carbohydrate parts of the spectra were therefore simulated by the GeNMR simulation program,<sup>21</sup> and both the chemical shifts and  $J$ -couplings were adjusted until the calculated and measured patterns matched.

**2,4,3,5-Dimethylene-D-gluconic acid (2)**. The synthesis of this compound was described in the literature.<sup>22</sup> After recrystallization from water, crystalline needles were obtained, yield 107.2 g (0.487 mol, 92 %), m.p. 224.5 °C, IR. (KBr) 3428  $cm^{-1}$  (broad, acid OH), 1730 and 1718 ( $C=O$ , double probably due to the presence of more than one conformation), 1178 and 1104 ( $C-O$ , ketal), 1141 ( $C-OH$ , alcohol).  $^1H$ -NMR (DMSO- $d_6$ , 90 MHz)  $\delta$  5.040 ppm (d, 1H,  $J=5.4$  Hz,  $H^{7a}$ ), 4.945 (d, 1H,  $J=6.3$  Hz,  $H^{8a}$ ), 4.760 (d, 2H,  $H^{7b}$  and  $H^{8b}$ ), 4.395 (d, 1H,  $J=2.7$  Hz,  $H^2$ ), 4.090 (broad s, 1H,  $H^3$ ), 3.740 (m, 4H,  $H^{4-6}$ ), EI-MS  $m/z$  221 ( $M+H$ )<sup>+</sup>, 203 ( $M-OH$ )<sup>+</sup>, 189 ( $M-CH_2OH$ )<sup>+</sup>, 175 ( $M-COOH$ )<sup>+</sup>, 85 (cyclic  $-O-CH=CH-CH^+-O-CH_2$ ). Anal. Calcd. for  $C_8H_{12}O_7$ : C, 43.64; H, 5.49. Found: C, 43.57; H, 5.33.



**Methyl-2,4;3,5-dimethylene-D-gluconate (3).** The synthesis of this compound was also described in the literature.<sup>23</sup> After cooling of the reaction mixture, cube-shaped crystals were obtained, yield 26.0 g (0.111 mol, 61 %), m.p. 151.5 °C, IR (KBr) 3501  $\text{cm}^{-1}$  (very sharp, OH), 1757 ( $\text{C}=\text{O}$ ).  $^1\text{H-NMR}$  ( $\text{CD}_3\text{OD}$ , 400 MHz)  $\delta$  5.138 ppm (d, 1H,  $J = 6.31\text{ Hz}$ ,  $\text{H}^{\text{7a}}$ ), 5.050 (d, 1H,  $J = 6.31$ ,  $\text{H}^{\text{8a}}$ ), 4.865 (d, 2H,  $\text{H}^{\text{7b}}$  and  $\text{H}^{\text{8b}}$ ), 4.509 (d, 1H,  $J_{2,3} = 2.10$ ,  $\text{H}^2$ ), 4.178 (t, 1H,  $J_{3,2} = 1.66$ ,  $\text{H}^3$ ), 3.880 (m, 3H,  $\text{H}^{\text{4-6a}}$ ), 3.825 (2d, 1H,  $J_1 = 5.66$ ,  $J_2 = -14.20$ , negative  $J$ -coupling was found after simulation,  $\text{H}^{\text{6b}}$ ), 3.768 (s, 3H,  $\text{OCH}_3$ ).  $^{13}\text{C-NMR}$  ( $\text{CD}_3\text{OD}$ , 100 MHz) 169.954 ppm ( $\text{C}^1$ ), 93.220 ( $\text{C}^7$ ), 89.330 ( $\text{C}^8$ ), 78.094 ( $\text{C}^2$ ), 77.482 ( $\text{C}^3$ ), 72.178 ( $\text{C}^5$ ), 69.523 ( $\text{C}^4$ ), 60.221 ( $\text{C}^6$ ), 52.716 ( $\text{OCH}_3$ ). EI-MS  $m/z$  233 ( $\text{M} - \text{H}$ ) $^+$ , 219 ( $\text{M} - \text{CH}_3$ ) $^+$ , 203 ( $\text{M} - \text{OCH}_3$ ) $^+$ , 175 ( $\text{M} - \text{COOCH}_3$ ) $^+$ , 85 (cyclic  $-\text{O}-\text{CH}=\text{CH}-\text{CH}^+-\text{O}-\text{CH}_2$ ). Anal. Calcd. for  $\text{C}_9\text{H}_{14}\text{O}_7$ : C, 46.16; H, 6.02. Found: C, 45.97; H, 5.81.

**2,4;3,5-Dimethylene-N,n-octyl-D-gluconamide (4a).** Compound **2** (20.0 g, 85.4 mmol) was dissolved in 150 ml (10.7 equiv.) of octyl amine and stirred in a nitrogen atmosphere at 95 °C for 2 days. The solution was diluted with ethyl acetate and after one night in the refrigerator, a white precipitate was formed which was filtered and additionally washed with n-hexane. After purification by column chromatography (silica, eluent EtOAc), the white product was washed with n-hexane again, yield 21.75 g (65.63 mmol, 76.9 %) of white crystals, m.p. 99.0 °C (after additional recrystallization from water). IR (KBr) 3486  $\text{cm}^{-1}$  (OH), 3330 (NH), 1660 (amide I), 1550 (amide II), 1180, 1109, 1094 and 1064 (ketal), 1038 ( $\text{C}-\text{OH}$ ), IR ( $\text{CHCl}_3$  solution) 3629 (OH), 3426 (NH), 1675 (amide I), 1543 (amide II), 1043 ( $\text{C}-\text{OH}$ ).  $^1\text{H-NMR}$  (400 MHz,  $\text{CDCl}_3$ , assignments were made by irradiation on the OH proton and subsequent simulation),  $\delta$  6.601 ppm (t, 1H,  $J = 5.76\text{ Hz}$ ,  $\text{NHCO}$ ), 5.257 (d, 1H,  $J = 6.45$ ,  $\text{H}^{\text{7a}}$ ), 5.082 (d, 1H,  $J = 6.20$ ,  $\text{H}^{\text{8a}}$ ), 4.958 (d, 1H,  $\text{H}^{\text{8b}}$ ), 4.822 (d, 1H,  $\text{H}^{\text{7b}}$ ), 4.236 (t, 1H,  $J_{2,3} = 2.18$ ,  $\text{H}^2$ ), 4.136 (d, 1H,  $J_{3,4} = 0.82$ ,  $\text{H}^3$ ), 4.014 (2d, 1H,  $J_{5,6a} = 6.20$ ,  $J_{5,6b} = 5.78$ ,  $\text{H}^5$ ), 3.890 (7 peaks, 1H,  $J_{6a-6b} = -11.43$ ,  $J_{6a-\text{OH}} = 6.46$ ,  $\text{H}^{\text{6a}}$ ), 3.978 (5 peaks, 1H,  $J_{6b-\text{OH}} = 4.11$ ,  $\text{H}^{\text{6b}}$ ), 3.780 (s, 1H,  $\text{H}^4$ ), 3.292 (q, 2H,  $J = 6.73$ ,  $-\text{CH}_2-\text{NHCO}$ ), 2.877 (2d, 1H, OH), 1.513 (m, 2H,  $-\text{CH}_2-\text{CH}_2-\text{NHCO}$ ), 1.260 (m, 10H,  $\text{CH}_3-(\text{CH}_2)_5-$ ), 0.869 (t, 3H,  $\text{CH}_3$ ).  $^{13}\text{C-NMR}$  ( $\text{CDCl}_3$ , 110 MHz)  $\delta$  167.372 ppm ( $\text{C}^1$ ), 92.150 ( $\text{C}^7$ ), 88.587 ( $\text{C}^8$ ), 77.506 ( $\text{C}^2$ ), 76.104 ( $\text{C}^3$ ), 71.439 ( $\text{C}^5$ ), 67.748 ( $\text{C}^4$ ), 59.926 ( $\text{C}^6$ ), 39.110 ( $-\text{CH}_2-\text{NHCO}$ ), 31.724, 29.322, 29.148, 26.723, 22.576 ( $-(\text{CH}_2)_6-$ ), 14.030 ( $-\text{CH}_3$ ). EI-MS  $m/z$  332 ( $\text{M}+\text{H}$ ) $^+$ , 302 ( $\text{M} - \text{CH}_2\text{OH}$ ) $^+$ , 156 ( $\text{CH}_3-(\text{CH}_2)_7-\text{NHCO}$ ) $^+$ , 85 (cyclic  $-\text{O}-\text{CH}=\text{CH}-\text{CH}^+-\text{O}-\text{CH}_2$ ). Anal. Calcd. for  $\text{C}_{16}\text{H}_{29}\text{NO}_6$ : C, 57.99; H, 8.82; N, 4.23. Found: C, 57.94; H, 8.68; N, 4.26.

Syntheses of **4b-4f** were carried out according to a reaction procedure analogous to that described for **4a**. The starting compounds were the appropriate n-alkyl amines.

**2,4;3,5-Dimethylene-N,n-decyl-D-gluconamide (4b).** Instead of recrystallization from water as was described for the purification of **4a**, this compound was recrystallized from EtOAc which resulted in white crystals, yield 1.71 g (4.75 mmol, 25.5 %), m.p. 102.3 °C. IR (KBr) and  $^1\text{H-NMR}$  (90 MHz,  $\text{CDCl}_3$ ) spectra were analogous to that of **4a** except for  $\delta$  1.254 ppm (m, 16H,  $\text{CH}_3-(\text{CH}_2)_8-$ ), EI-MS  $m/z$  359 ( $\text{M}$ ) $^+$ . Anal. Calcd. for  $\text{C}_{18}\text{H}_{33}\text{NO}_6$ : C, 60.14; H, 9.25; N, 3.90. Found: C, 60.12; H, 9.64; N, 3.93.

**2,4;3,5-Dimethylene-N,n-dodecyl-D-gluconamide (4c).** Purification analogous to that described for **4b**, yield 1.95 g of white crystals (5.03 mmol, 50.2 %), m.p. 103.6 °C. IR (KBr) and  $^1\text{H-NMR}$  (90 MHz,  $\text{CDCl}_3$ ) assignments were similar to that of **4a** except for the number of methylene protons of the alkyl chain  $\delta$  1.252 ppm (m, 20H,  $\text{CH}_3-(\text{CH}_2)_{10}-$ ), EI-MS  $m/z$  387 ( $\text{M}$ ) $^+$ . Anal. Calcd. for  $\text{C}_{20}\text{H}_{37}\text{NO}_6$ : C, 61.99; H, 9.62; N, 3.61. Found: C, 61.72; H, 9.67; N, 3.61.

**2,4;3,5-Dimethylene-N,n-tetradecyl-D-gluconamide (4d).** Purification analogous to that described for **4b**, yield 3.81 g (white crystalline powder, 7.66 mmol, 35.0 %), m.p. 102.8 °C. IR (KBr) and  $^1\text{H-NMR}$  (90 MHz,  $\text{CDCl}_3$ ) assignments similar to those of **4a** except for the

methylene protons of the alkyl chain  $\delta$  1.247 ppm (m, 24H,  $\text{CH}_3\text{-(CH}_2\text{)}_{12}\text{-}$ ), EI-MS  $m/z$  415 ( $\text{M}^+$ ). Anal. Calcd. for  $\text{C}_{22}\text{H}_{41}\text{NO}_6$ : C, 63.59; H, 9.94; N, 3.37. Found: C, 63.23; H, 10.09; N, 3.58.

**2,4;3,5-Dimethylene-*N*,*n*-hexadecyl-D-gluconamide (4e).** Purification analogous to that described for **4b**, yield 5.50 g of white crystalline powder (12.40 mmol, 51.8 %), m.p. 105.5 °C. IR (KBr) and  $^1\text{H-NMR}$  (90 MHz,  $\text{CDCl}_3$ ) spectra were similar to that of **4a** except for the methylene protons of the alkyl chain  $\delta$  1.254 ppm (m, 28H,  $\text{CH}_3\text{-(CH}_2\text{)}_{14}\text{-}$ ), EI-MS  $m/z$  443 ( $\text{M}^+$ ). Anal. Calcd. for  $\text{C}_{24}\text{H}_{45}\text{NO}_6$ : C, 64.98; H, 10.22; N, 3.16. Found: C, 64.98; H, 10.57; N, 3.16.

**2,4;3,5-Dimethylene-*N*,*n*-octadecyl-D-gluconamide (4f).** This compound was purified by column chromatography (silica, eluent MeOH/EtOAc 5:95 v/v) followed by recrystallization from ethyl acetate, yield 0.85 g (white powder, 1.802 mmol, 18.0 %), m.p. 92.0 °C IR (KBr) and  $^1\text{H-NMR}$  (90 MHz,  $\text{CDCl}_3$ ) spectra were analogous to those of **4a** except for the methylene protons of the alkyl chain  $\delta$  1.252 ppm (m, 32H,  $\text{CH}_3\text{-(CH}_2\text{)}_{16}\text{-}$ ), EI-MS  $m/z$  471 ( $\text{M}^+$ ). Anal. Calcd. for  $\text{C}_{26}\text{H}_{49}\text{NO}_6$ : C, 66.21; H, 10.47; N, 2.87. Found: C, 64.34; H, 10.31; N, 3.05

**6-Tosyl-2,4;3,5-dimethylene-*N*,*n*-octyl-D-gluconamide (5a).** To a solution of 15.0 g (45.26 mmol) of **4a** in 150 ml of anhydrous pyridine which was placed in an ice bath, under a nitrogen atmosphere, 9.78 g (51.30 mmol, 1.1 equiv.) of tosyl chloride dissolved in 50 ml of pyridine, was added dropwise. After an additional hour of stirring, the orange solution was stored overnight in the refrigerator. The product was precipitated by pouring the pyridine solution into a mixture of saturated  $\text{NaHCO}_3$  solution and ice. The product was filtered off, dried in vacuum, and used without any further purification, yield 19.065 g (39.26 mmol, 86.7 %), m.p. 116.6 °C IR (KBr)  $3398\text{ cm}^{-1}$  (NH), 1680 (amide I), 1531 (amide II), 1359 and 1176 (S=O),  $^1\text{H-NMR}$  (90 MHz,  $\text{CDCl}_3$ )  $\delta$  7.793 ppm (d, 2H, ArH), 7.368 (d, 2H, ArH), 6.599 (t, 1H, NHCO), 5.230 (d, 1H,  $J=6.3\text{ Hz}$ ,  $\text{H}^{\text{7a}}$ ), 4.896 (d, 1H,  $J=6.8\text{ Hz}$ ,  $\text{H}^{\text{8a}}$ ), 4.786 (d, 2H,  $\text{H}^{\text{8b}}$  and  $\text{H}^{\text{7b}}$ ), 4.215 (m, 3H,  $\text{H}^{\text{5,6a,6b}}$ ), 4.074 (s, 2H,  $\text{H}^{\text{2,3}}$ ), 3.670 (s, 1H,  $\text{H}^{\text{4}}$ ), 2.467 (s, 3H,  $\text{ArCH}_3$ ). EI-MS  $m/z$  485 ( $\text{M}^+$ ), 314 ( $\text{M} - \text{OTs}^+$ ), 156 ( $\text{C}_8\text{H}_{17}\text{-NHCO}^+$ ), 155 ( $\text{SO}_2\text{-C}_6\text{H}_4\text{-CH}_3^+$ ), 85 (cyclic  $-\text{O-CH=CH-CH}^+-\text{O-CH}_2$ ). Anal. Calcd. for  $\text{C}_{23}\text{H}_{35}\text{NO}_8\text{S} \cdot 0.5\text{ H}_2\text{O}$ : C, 55.85; H, 7.34; N, 2.83; S, 6.48 Found: C, 55.63; H, 7.16; N, 2.98; S, 6.27.

The tosylate compounds (**5b-f**) obtained from **4b-f** were prepared by procedures analogous to that of **5a**. The derivatives **5b-d** and **5f** were purified only by washing with water. Since the starting hydroxyl compounds **4b-d** and **4f** do not dissolve in cold water, the products **5b-d** and **5f** were slightly contaminated with the starting hydroxyl compound. Because the contamination was very small and hydroxyl compounds were not affecting the subsequent reactions, these compounds were not further purified.

#### 6-Tosyl-2,4;3,5-dimethylene-*N*,*n*-hexadecyl-D-gluconamide (5e).

Synthesis was analogous to that of compound **5a**. In contrast with **5a-d** and **5f**, this compound was purified first by precipitation from ice/ $\text{NaHCO}_3$  and subsequently with column chromatography (silica, *n*-hexane/EtOAc 1:1, v/v). Yield 6.50 g (10.87 mmol, 78.4 %, m.p. 97.1 °C, EI-MS  $m/z$  597 ( $\text{M}^+$ ), 268 ( $\text{C}_{16}\text{H}_{33}\text{-NHCO}^+$ ), 155 ( $\text{SO}_2\text{-C}_6\text{H}_4\text{-CH}_3^+$ ), 85 (cyclic  $-\text{O-CH=CH-CH}^+-\text{O-CH}_2$ ). Anal. Calcd. for  $\text{C}_{31}\text{H}_{51}\text{NO}_8\text{S}$ : C, 62.28; H, 8.60; N, 2.34; S, 5.36. Found: C, 62.21; H, 8.75; N, 2.36; S, 5.04.

#### 6-Deoxy-6-(1-imidazolyl)-2,4;3,5-dimethylene-*N*,*n*-octyl-D-gluconamide (1a).

Compound **5a** (1.13 g, 2.32 mmol) and 0.50 g (7.28 mmol) of imidazole were dissolved in 7.5 ml chloroform and brought under high pressure (15 kBar) at 50 °C for 2 days. The solution was washed with saturated aqueous  $\text{NaHCO}_3$  and dried over  $\text{Na}_2\text{SO}_4$  and further purified by column chromatography (silica, eluent  $\text{Et}_3\text{N/MeOH/EtOAc}$  1:10:89, v/v/v) followed by recrystallization from diluted aqueous NaOH (pH=8), yield 0.58 g (white needle shaped crystals, 1.52 mmol,

65.6 %, m.p. 134.5 °C IR (KBr) 3332  $\text{cm}^{-1}$  (NH), 3142 (=C-H), 3097 (=C-H), 1667 (amide I), 1545 (amide II), 1187, 1103, 1095 and 1068 (ketal), 993 (=C-H), IR ( $\text{CHCl}_3$  solution), 3426 (NH), 1676 (amide I), 1543 (amide II),  $^1\text{H-NMR}$  (400 MHz,  $\text{CDCl}_3$ , assignments were made by irradiation on proton  $\text{H}^4$ , and recording a COSY spectrum (8K, det F2, 512K evol F1) The spectra did not result in a clear assignment, however, after recording temperature dependent experiments in combination with simulation, the chemical shifts and  $J$ -couplings could be determined unambiguously  $\delta$  7.513 (s, 1H, N=CH-N), 7.105 (s, 1H, -CH<sub>2</sub>-N-CH=CH-N=), 6.965 (s, 1H, -N-CH=CH-N=), 6.530 ppm (t, 1H,  $J = 5.76$  Hz, NHCO), 5.226 (d, 1H,  $J = 6.50$  Hz,  $\text{H}^{7a}$ ), 5.016 (d, 1H,  $J = 6.19$  Hz,  $\text{H}^{8a}$ ), 5.053 (d, 1H,  $\text{H}^{8b}$ ), 4.754 (d, 1H,  $\text{H}^{7b}$ ), 4.330 (2d, 1H,  $J_{6a,5} = 5.50$  Hz,  $J_{6a,6b} = -15.30$  Hz,  $\text{H}^{6a}$ ), 4.219 (m, 1H,  $J_5 = 1.20$  Hz,  $\text{H}^5$ ), 4.211 (m, 1H,  $J_{6b,5} = 10.00$ ,  $\text{H}^{6b}$ ), 4.180 (d, 1H,  $J_3 = 1.00$ ,  $\text{H}^3$ ), 4.130 (d, 1H,  $J_2 = 2.00$  Hz,  $\text{H}^2$ ), 3.530 (t, 1H,  $\text{H}^4$ ), 3.306 (2d, 2H, -CH<sub>2</sub>-NHCO), 1.736 (crystal water), 1.509 (m, 2H, -CH<sub>2</sub>-CH<sub>2</sub>-NHCO), 1.261 (m, 10H, CH<sub>3</sub>-(CH<sub>2</sub>)<sub>5</sub>-), 0.877 (t, 3H, CH<sub>3</sub>)  $^{13}\text{C-NMR}$  ( $\text{CDCl}_3$ , 100 MHz)  $\delta$  167.641 ppm (C<sup>1</sup>), 137.389 (N=CH-N), 135.342 (N-CH=CH-N), 129.780 (N-CH=CH-N), 91.932 (C<sup>7</sup>), 88.003 (C<sup>8</sup>), 77.177 (C<sup>2</sup>), 75.006 (C<sup>3</sup>), 71.118 (C<sup>5</sup>), 66.743 (C<sup>4</sup>), 44.563 (C<sup>6</sup>), 39.008 (-CH<sub>2</sub>-NHCO), 31.616, 29.253, 29.040, 28.913, 26.631, 22.470 (-CH<sub>2</sub>)<sub>6</sub>-), 13.935 (-CH<sub>3</sub>) EI-MS  $m/z$  380 (M - H)<sup>+</sup>, 225 (M - CH<sub>3</sub>-(CH<sub>2</sub>)<sub>7</sub>-NHCO)<sup>+</sup>, Anal. Calcd for C<sub>19</sub>H<sub>31</sub>N<sub>3</sub>O<sub>5</sub> · ½ H<sub>2</sub>O C, 58.44, H, 8.62, N, 10.76 Found C, 58.68, H, 8.18, N, 10.65

Syntheses of **1b-1f** were carried out according to a reaction procedure analogous to that described for **1a**. The starting compounds were the appropriate tosylates (**5b-5f**)

**6-Deoxy-6-(1-imidazolyl)-2,4;3,5-dimethylene-N,n-decyl-D-gluconamide (1b)** After an isolation and purification procedure, which was analogous to that of **1a**, a white crystalline powder was obtained, yield 0.25 g (0.61 mmol, 48.3 %), m.p. 133.9 °C IR (KBr) and  $^1\text{H-NMR}$  (90 MHz,  $\text{CDCl}_3$ ), spectra were similar as those obtained from **1a**, however, the number of protons in the alkyl chain of this compound were different,  $\delta$  1.270 ppm (m, 16H, CH<sub>3</sub>-(CH<sub>2</sub>)<sub>8</sub>-), EI-MS  $m/z$  408 (M - H)<sup>+</sup> Anal. Calcd for C<sub>21</sub>H<sub>33</sub>N<sub>3</sub>O<sub>5</sub> C, 61.59, H, 8.61, N, 10.26 Found C, 61.65, H, 8.62, N, 9.71

**6-Deoxy-6-(1-imidazolyl)-2,4;3,5-dimethylene-N,n-dodecyl-D-gluconamide (1c)**

Isolation of this compound was hampered by the difficult separation of the organic and water layers, therefore 5 min of centrifugation (3300 rpm) was applied. After column chromatography (silica, eluent Et<sub>3</sub>N/MeOH/EtOAc 1:10:89, v/v/v), the compound was recrystallized from EtOAc. Yield was not determined, m.p. 134.3 °C IR (KBr) and  $^1\text{H-NMR}$  (90 MHz,  $\text{CDCl}_3$ ) spectra were similar to those of **1a**, however, the number of protons in the alkyl chain of this compound were different,  $\delta$  1.243 ppm (m, 20H, CH<sub>3</sub>-(CH<sub>2</sub>)<sub>10</sub>-), EI-MS  $m/z$  436 (M - H)<sup>+</sup> Anal. Calcd for C<sub>23</sub>H<sub>39</sub>N<sub>3</sub>O<sub>5</sub> C, 63.13, H, 8.98, N, 9.60 Found C, 63.16, H, 8.88, N, 9.56

**6-Deoxy-6-(1-imidazolyl)-2,4;3,5-dimethylene-N,n-tetradecyl-D-gluconamide (1d)**

The procedure for the isolation and purification was similar to that described for **1c**, yield 0.41 g (white crystalline powder, 0.89 mmol, 36.9 %), m.p. 134.2 °C IR (KBr) and  $^1\text{H-NMR}$  (90 MHz,  $\text{CDCl}_3$ ) spectra were similar to those obtained for **1a**, however, the number of protons in the alkyl chain of this compound were different,  $\delta$  1.233 ppm (m, 24H, CH<sub>3</sub>-(CH<sub>2</sub>)<sub>12</sub>-), EI-MS  $m/z$  464 (M - H)<sup>+</sup> Anal. Calcd for C<sub>25</sub>H<sub>43</sub>N<sub>3</sub>O<sub>5</sub> C, 64.49, H, 9.31, N, 9.02 Found C, 64.58, H, 9.26, N, 8.96

**6-Deoxy-6-(1-imidazolyl)-2,4;3,5-dimethylene-N,n-hexadecyl-D-gluconamide (1e)**

Isolation and purification were similar to the procedure described for **1c**, yield 0.09 g (white crystals, 0.18 mmol, 7.4 %) The conversion was higher, however, due to a poor separation by column chromatography (silica, eluent Et<sub>3</sub>N/MeOH/EtOAc 1:5:94, v/v/v), the amount of pure

product was relatively low, m.p. 131 °C. IR (KBr) and  $^1\text{H-NMR}$  (90 MHz,  $\text{CDCl}_3$ ) spectra were similar to those obtained for **1a**, however, the number of protons in the alkyl chain of this compound were different,  $\delta$  1.224 ppm (m, 28H,  $\text{CH}_3\text{-(CH}_2\text{)}_{14}\text{-}$ ), EI-MS  $m/z$  493 ( $\text{M}^+$ ) Anal Calcd. for  $\text{C}_{27}\text{H}_{47}\text{N}_3\text{O}_5$ : C, 65.69; H, 9.60; N, 8.51. Found: C, 65.96; H, 9.56; N, 8.47.

**6-Deoxy-6-(1-imidazolyl)-2,4,3,5-dimethylene-N,n-octadecyl-D-gluconamide (1f).**

The procedures for the isolation and purification were similar to that described for **1e**, yield 0.65 g (white powder, 1.24 mmol, 68.0 %), m.p. 117 °C. IR (KBr) and  $^1\text{H-NMR}$  (90 MHz,  $\text{CDCl}_3$ ) spectra similar to those obtained for **1a**, however, the number of protons in the alkyl chain of this compound were different,  $\delta$  1.250 ppm (m, 32H,  $\text{CH}_3\text{-(CH}_2\text{)}_{16}\text{-}$ ), EI-MS  $m/z$  521 ( $\text{M}^+$ ). Anal Calcd. for  $\text{C}_{29}\text{H}_{51}\text{N}_3\text{O}_5 \cdot \frac{1}{2} \text{H}_2\text{O}$ : C, 65.61; H, 9.88; N, 7.92. Found: C, 64.42; H, 9.81; N, 8.37.

**6-Deoxy-6-amino-2,4,3,5-dimethylene-N,n-octyl-D-gluconamide (7).** Compound **5a** (0.95 g, 1.88 mmol) was dissolved in 60 ml of MeOH (0 °C) which was saturated with  $\text{NH}_3$  gas (735 mmol). The solution was placed in an autoclave, sealed and heated overnight at 80 °C. The methanol and excess of ammonia were removed by evaporation and in order to isolate the product, the remaining slurry was mixed with aqueous 2N NaOH and  $\text{CHCl}_3$ . After drying the organic layer over  $\text{Na}_2\text{SO}_4$ , the solvent was removed by evaporation. The product was recrystallized from diethyl ether (twice). One spot was detected on TLC with ninhydrine,<sup>24</sup> yield 0.115 g (yellow powder, 0.349 mmol, 18.5 %), m.p. 134 °C. IR (KBr), 3700-3180  $\text{cm}^{-1}$  (top at 3315 ( $\text{NH}_2$ ), 3433 (NH), 1664 (amide I), 1625 ( $\text{NH}_2$ ), 1550 (amide II).  $^1\text{H-NMR}$  (400 MHz,  $\text{CDCl}_3$ ),  $\delta$  6.548 (broad t, 1H,  $\text{NHCO}$ ), 5.261 (d, 1H,  $J_{7a-7b}$  = 6.42 Hz,  $\text{H}^{7a}$ ), 4.958 (2d, 2H,  $J_{8a-8b}$  = 6.39 Hz,  $\text{H}^{8a+8b}$ ), 4.807 (d, 1H,  $\text{H}^{7b}$ ), 4.140 (s, 1H,  $\text{H}^3$ ), 4.115 (d, 1H,  $\text{H}^2$ ), 3.299 (2d,  $J_{5-6a}$  = 8.74 Hz,  $J_{5-6b}$  = 5.84 Hz,  $\text{H}^5$ ), 3.634 (s, 1H,  $\text{H}^4$ ), 3.299 (2d, 2H,  $-\text{CH}_2\text{-NHCO}$ ), 3.215 (m, 1H,  $J_{6a-6b}$  = 13.16 Hz,  $\text{H}^{6a}$ ), 2.848 (2d, 1H,  $\text{H}^{6b}$ ), 1.610 (very broad s, crystal water), 1.513 (septet, 2H,  $-\text{CH}_2\text{-CH}_2\text{-NHCO}$ ) 1.273 (m, 10H,  $\text{CH}_3\text{-(CH}_2\text{)}_6\text{-}$ ), 0.875 (t, 3H,  $\text{CH}_3$ ). EI-MS  $m/z$  330 ( $\text{M}^+$ ), 300 ( $\text{M} - (-\text{CH}_2\text{-NH}_2)^+$ ), 85 (cyclic  $-\text{O-CH=CH-CH}^+-\text{O-CH}_2$ ). Anal. Calcd. for  $\text{C}_{16}\text{H}_{30}\text{N}_2\text{O}_5 \cdot \text{H}_2\text{O}$ : C, 55.14; H, 9.26; N, 8.04. Found: C, 55.97; H, 8.39; N, 7.58.

**6-Phenyl-2,4,3,5-dimethylene-N,n-hexadecyl-D-gluconamide (8).** Compound **5e** (0.658 g, 1.10 mmol) was mixed with 0.580 g (6 equiv.) of phenol and 1.93 g (17 equiv.) of  $\text{Et}_3\text{N}$  and stirred at 115 °C for 3 days in a nitrogen atmosphere. The dark brown oil was diluted with  $\text{CHCl}_3$ , washed with aqueous 1N NaOH and subsequently purified by column chromatography (silica, eluent n-hexane/ $\text{EtOAc}$  3:1, v/v), yield 0.19 g (0.37 mmol, 33.2 %), m.p. 122.6 °C. IR (KBr) 3318  $\text{cm}^{-1}$  (NH), 1655 (amide I), 1602 and 1587 (aromatic  $\text{C=C}$ ), 1537 (amide II), 1250 (phenoxy  $\text{C-O}$ ),  $^1\text{H-NMR}$  (90 MHz,  $\text{CDCl}_3$ )  $\delta$  7.318 ppm (m, 1H, ArH), 6.969 (m, 4H, ArH), 6.552 (t, 1H,  $\text{NHCO}$ ), 5.291 (d, 1H,  $J_{7a-7b}$  = 6.36 Hz,  $\text{H}^{7a}$ ), 5.164 (d, 1H,  $J_{8a-8b}$  = 6.35 Hz,  $\text{H}^{8a}$ ), 5.001 (d, 1H,  $\text{H}^{8b}$ ), 4.849 (d, 1H,  $\text{H}^{7b}$ ), 4.383, 4.295, 4.164 (5H,  $\text{H}^{2,3,5,6a,6b}$ ), 3.889 (s, 1H,  $\text{H}^4$ ). EI-MS  $m/z$  519 ( $\text{M}^+$ ), 426 ( $\text{M} - \text{O-C}_6\text{H}_5$ )<sup>+</sup>, 268 ( $\text{CH}_3\text{-(CH}_2\text{)}_{15}\text{-NHCO}$ )<sup>+</sup>, Anal. Calcd. for  $\text{C}_{30}\text{H}_{49}\text{NO}_6$ : C, 69.33; H, 9.50; N, 2.70. Found: C, 68.90; H, 9.66; N, 2.77.

**6-(4-Pyridyl)-2,4,3,5-dimethylene-N,n-hexadecyl-D-gluconamide (9).** The procedure for the synthesis of this compound was similar to that described for **8**, however, instead of phenol, 0.976 g (5.52 mmol, 3.4 equiv.) of 4-hydroxypyridine and a shorter reaction time (1 night) were used. After column chromatography (silica, eluent  $\text{Et}_3\text{N/MeOH/EtOAc}$  1:10:89, v/v), a white crystalline product was obtained, yield 0.21 g (0.40 mmol, 24.7 %), m.p. 130.1 °C. IR (KBr) 3690-3180  $\text{cm}^{-1}$  (top at 3425, peak at 3321, NH), 1655 (amide I), 1594 and 1578 ( $\text{C=C}$ ), 1538 (amide II), 1181, 1107, 1089 and 1070 (ketal),  $^1\text{H-NMR}$  (400 MHz,  $\text{CDCl}_3$ )  $\delta$  8.476 (2d,  $J$  = 4.5 and  $J$  = 1.4 Hz (long range), 2H, ArH), 6.583 (2d, 2H, ArH), 5.291 (d,  $J_{7a-7b}$  = 6.49 Hz, 1H,  $\text{H}^{7a}$ ), 5.108 (d,  $J$  = 6.30 Hz, 1H,  $\text{H}^{8a}$ ), 5.026 (d, 1H,  $\text{H}^{8b}$ ), 4.857 (d, 1H,  $\text{H}^{7b}$ ), 4.364 (2d, 1H,  $\text{H}^{6a}$ ), 4.311

(2d, 1H, H<sup>6b</sup>), 4 311 (m, 2H, H<sup>3'</sup>), 4 177 (d, 1H, H<sup>2</sup>) 3 869 (s, 1H, H<sup>4</sup>), 3 312 (q, 2H, -(CH<sub>2</sub>)<sub>14</sub>-CH<sub>2</sub>-NHCO), 1 516 (2d, 2H, CH<sub>3</sub>-(CH<sub>2</sub>)<sub>13</sub>-CH<sub>2</sub>-), 1 320 (broad s, 26H, CH<sub>3</sub>-(CH<sub>2</sub>)<sub>13</sub>-CH<sub>2</sub>-), 0 900 (t, 3H, CH<sub>3</sub>-) EI-MS *m/z* 520 (M)<sup>+</sup>, 491 (M-C<sub>2</sub>H<sub>5</sub>)<sup>+</sup>, 268 (CH<sub>3</sub>-(CH<sub>2</sub>)<sub>15</sub>-NHCO)<sup>+</sup>, 96 (C<sub>5</sub>H<sub>4</sub>NO hetero tropylium)<sup>+</sup> Anal Calcd for C<sub>29</sub>H<sub>48</sub>N<sub>2</sub>O<sub>6</sub> C, 66 89, H 9 29, N, 5 38 Found C, 66 68, H, 9 13, N, 5 47

**6-(3-Pyridyl)-2,4;3,5-dimethylene-N,n-hexadecyl-D-gluconamide (10)** The procedure described for the synthesis of compound **9** was followed, however, instead of 4-hydroxypyridine, 3-hydroxypyridine was used. Yield (after two purifications by column chromatography) 0 13 g of yellow crystals (0 24 mmol, 13 2 %), m p 95 2 °C, IR (KBr) 3427 cm<sup>-1</sup> (NH), 1678 (amide I), 1590, 1567 and 1507 (aromatic, C=C), 1536 (amide II) <sup>1</sup>H-NMR (400 MHz, CDCl<sub>3</sub>) δ 7 774 (s, 1H, ArH), 7 324 (d, 1H, ArH), 7 253 (s, 1H, ArH), 7 226 (2d, 2H, ArH), 6 511 (t, 1H, NHCO), 5 140 (d, *J*<sub>7a-7b</sub> = 6 44 Hz, 1H, H<sup>7a</sup>), 5 080 (d, *J* = 6 14 Hz, 1H, H<sup>8a</sup>), 4 919 (d, 1H, H<sup>8b</sup>), 4 762 (d, 1H, H<sup>7b</sup>), 4 694 (2d, 1H, *J*<sub>6a-5</sub> = 10 00 Hz, *J*<sub>6a-6b</sub> = 13 97 Hz, H<sup>6a</sup>), 4 519 (2d, 1H, *J*<sub>6a-5</sub> = 10 00 Hz, H<sup>6b</sup>), 4 211 (s, 1H, H<sup>2</sup>), 4 159 (d, 1H, H<sup>3</sup>) 3 807 (s, 1H, H<sup>4</sup>), 3 214 (m, 2H, -(CH<sub>2</sub>)<sub>14</sub>-CH<sub>2</sub>-NHCO), 1 419 (2d, 2H, CH<sub>3</sub>-(CH<sub>2</sub>)<sub>13</sub>-CH<sub>2</sub>-), 1 320 (broad s, 26H, CH<sub>3</sub>-(CH<sub>2</sub>)<sub>13</sub>-CH<sub>2</sub>-), 0 900 (t, 3H, CH<sub>3</sub>-) <sup>1</sup>H-NMR did not show the presence of any contamination, however, no satisfactory elemental analysis could be obtained

**6-Deoxy-6-(1-pyrazolyl)-2,4;3,5-dimethylene-N,n-hexadecyl-D-gluconamide (11)** The procedure described for the preparation of **1e** was followed, however, instead of imidazole, 0 462 g (6 78 mmol, 5 equiv) of pyrazole was used. Yield 0 01 g (0 01 mmol, 4 %), m p 103 8 °C IR (KBr) 3307 cm<sup>-1</sup> (NH), 1660 (amide I), 1550 (amide II) <sup>1</sup>H-NMR (90 MHz, CDCl<sub>3</sub>) δ 7 538 ppm (d, *J* = 1 59 Hz, 1H, ArH), 7 438 (d, *J* = 2 54, 1H, ArH), 6 538 (t, 1H, NHCO), 6 294 (t, 1H, ArH), 5 225 (d, *J*<sub>7a-7b</sub> = 6 36 Hz, 1H, H<sup>7a</sup>), 5 012 (s, 2H, H<sup>8a,b</sup>), 4 762 (d, 1H, H<sup>7b</sup>), 4 521 (2d, *J*<sub>6a-5</sub> = 7 67 Hz, *J*<sub>6a-6b</sub> = 14 19, 1H, H<sup>6a</sup>), 4 477 (2d, *J*<sub>6b-5</sub> = 6 42 Hz), 4 357 (t, 1H, H<sup>5</sup>), 4 279 (s, 1H, H<sup>2</sup>), 4 134 (d, *J*<sub>2-3</sub> = 1 72 Hz), 3 699 (s, 1H, H<sup>3</sup>) EI-MS *m/z* 493 (M)<sup>+</sup>, 426 (M - O-C<sub>6</sub>H<sub>5</sub>)<sup>+</sup>, 268 (CH<sub>3</sub>-(CH<sub>2</sub>)<sub>15</sub>-NHCO)<sup>+</sup> Anal Calcd for C<sub>30</sub>H<sub>48</sub>N<sub>2</sub>O<sub>7</sub> · H<sub>2</sub>O C, 63 38, H, 9 65, N, 8 21 Found C, 64 16, H, 9 62, N, 8 36

**2,4;3,5-Dimethylene-N,n-hexadecyl-D-gluconamide-6-benzoate (12)** A mixture of 0 084 g (0 598 mmol) of benzoyl chloride in 10 ml of dichloromethane was added dropwise to a stirred solution of 0 200 g (0 45 mmol) of **4e** in 20 ml of dichloromethane containing 0 194 g (4 equiv) of triethyl amine as an additional base, while cooling in an ice bath. After 2 hrs of stirring at RT, the solution was refluxed for an additional 2 hrs. The reaction was carried out in a dried nitrogen atmosphere. After washing the organic layer with water and subsequent drying, the compound was purified by crystallization from ethyl acetate, yield 0 14 g of white crystals (0 26 mmol, 56 7 %), m p 127 7 °C IR (KBr) 3284 cm<sup>-1</sup> (NH), 3072 (=C-H), 1718 (C=O, ester), 1658 (amide I), 1603 and 1585 (C=C), 1548 (amide II), <sup>1</sup>H-NMR (400 MHz, CDCl<sub>3</sub>) δ 8 042 ppm (d, 2H, ArH), 7 590 (t, 1H, ArH), 7 464 (t, 1H, ArH), 6 552 (t, 1H, NHCO), 5 276 (d, *J*<sub>7a-7b</sub> = 6 46 Hz, 1H, H<sup>7a</sup>), 5 059 (d, *J*<sub>8a-8b</sub> = 6 53 Hz, 1H, H<sup>8a</sup>), 5 002 (d, 1H, H<sup>8b</sup>), 4 833 (d, 1H, H<sup>7b</sup>), 4 721 (2d, *J*<sub>6a-5</sub> = 6 23 Hz, *J*<sub>6a-6b</sub> = -11 86, 1H, H<sup>6a</sup>), 4 563 (2d, *J*<sub>6b-5</sub> = 7 05 Hz), 4 342 (t, 1H, H<sup>5a</sup>), 4 279 (broad s, 1H, H<sup>3</sup>), 4 159 (d, *J*<sub>2-3</sub> = 1 48 Hz) EI-MS *m/z* 547 (M)<sup>+</sup>, 268 (CH<sub>3</sub>-(CH<sub>2</sub>)<sub>15</sub>-NHCO)<sup>+</sup>, 225 (M - CH<sub>3</sub>(CH<sub>2</sub>)<sub>15</sub>NHCO)<sup>+</sup>, 85 (cyclic -O-CH=CH-CH<sup>+</sup>-O-CH<sub>2</sub>) Anal Calcd for C<sub>31</sub>H<sub>49</sub>NO<sub>7</sub> C, 67 98, H, 9 02, N, 2 56 Found C, 67 79, H, 8 81, N, 2 63

#### 2,4;3,5-Dimethylene-N,n-hexadecyl-D-gluconamide-6-(3-pyridyl-carboxylate) (13)

The synthesis of this compound starting with 1 484 g (3 35 mmol) of compound **4e**, was analogous to the preparation described for **12**. Instead of benzoyl chloride, 0 512 g (3 68 mmol, 1 1 equiv) of 3-pyridinecarboxylic acid chloride was used, yield 0 85 g of white crystals (1 55 mmol, 42 0 %), m p 124 6 °C IR (KBr) 3690-3200 cm<sup>-1</sup> (broad, peak at 3281, NH), 1738

(C=O, ester), 1663 (amide I), 1591 (C=C), 1549 (amide II),  $^1\text{H-NMR}$  (90 MHz,  $\text{CDCl}_3$ )  $\delta$  9.251 ppm (broad s, 1H, ArH), 8.826 (broad s, 1H, ArH, these two peaks were broadened probably due to a dimer formation in which water molecules act as hydrogen bond donors to the pyridyl groups At 2.507 ppm, a broad water molecule peak was visible which integrated to one water molecule per two pyridyl ligands), 8.326 (d, 1H, ArH), 7.450 (2d, 1H, ArH), 6.566 (t, 1H, amide H), patterns and chemical shifts of the methylene bridge and carbohydrate skeleton protons were comparable to those of **11**, 3.311 (double t, 2H,  $(\text{CH}_2)_6\text{-CH}_2\text{-NHCO}$ ), 1.513 (m, 2H,  $(\text{CH}_2)_5\text{-CH}_2\text{-CH}_2\text{NHCO}$ ), 1.263 (broad s, 10H,  $\text{CH}_3\text{-(CH}_2)_5\text{-CH}_2\text{-}$ ), 0.876 (t, 3H,  $\text{CH}_3\text{-}$ ), EI-MS  $m/z$  548 ( $\text{M}^+$ ), 519 ( $\text{M} - \text{C}_2\text{H}_5$ ) $^+$ , 268 ( $\text{CH}_3\text{-(CH}_2)_{15}\text{-NHCO}$ ) $^+$ , 106 ( $\text{COC}_5\text{H}_4\text{N}$ ) $^+$  Anal Calcd for  $\text{C}_{30}\text{H}_{48}\text{N}_2\text{O}_7$  C, 65.67, H, 8.82, N, 5.11 Found C, 65.38, H, 8.90, N, 5.08

**6-Tosyl-2,4;3,5-dimethylene-methyl-D-gluconate (14)** The reaction procedure was similar to that described for **5a**, however, instead of **4a**, 5.244 g (22.4 mmol) of **3** was used. The reaction mixture containing the product was poured into aqueous 1N HCl and extracted with EtOAc and the organic layer was subsequently dried on  $\text{MgSO}_4$ . Yield 6.24 g (pink viscous oil, 16.06 mmol, 71.7%) IR (KBr) 1758  $\text{cm}^{-1}$  (C=O), 1357 and 1178 (S=O),  $^1\text{H-NMR}$  (400 MHz,  $\text{CDCl}_3$ )  $\delta$  7.870 ppm (d, 2H, ArH), 7.350 (d, 2H, ArH), 5.266 (d,  $J_{7a,7b}$  = 6.51 Hz, 1H,  $\text{H}^{7a}$ ), 4.976 (d,  $J_{8a,8b}$  = 6.33 Hz, 1H,  $\text{H}^{8a}$ ), 4.861 (d, 1H,  $\text{H}^{8b}$ ), 4.755 (d, 1H,  $\text{H}^{7b}$ ), 4.275 (m, 3H,  $\text{H}^{5,6a,6b}$ ), 4.120 (m, 1H,  $\text{H}^{2,3}$ ), 3.840 (s, 3H,  $\text{OCH}_3$ ), 3.760 (s, 1H,  $\text{H}^4$ ), 2.480 (s, 3H,  $\text{ArCH}_3$ ) EI-MS  $m/z$  388 ( $\text{M}^+$ ), 155 ( $\text{SO}_2\text{-C}_6\text{H}_4\text{-CH}_3$ ) $^+$ , 85 (cyclic  $\text{-O-CH=CH-CH}^+\text{-O-CH}_2$ ) Anal Calcd for  $\text{C}_{16}\text{H}_{20}\text{O}_9\text{S}$  C, 49.48, H, 5.19, S, 8.26 Found C, 50.03, H, 5.19, S, 8.04

**6-Deoxy-6-(1-imidazolyl)-2,4;3,5-dimethylene-methyl-D-gluconate (15)** The synthesis was analogous to that described for **1a**, however, instead of **5a**, 5.991 g (15.4 mmol) of **14** was used and the product was only purified by column chromatography (silica, eluent  $\text{Et}_3\text{N/MeOH/EtOAc}$  1:5:94, v/v/v), yield 1.00 g (white powder, 3.53 mmol, 22.8%), mp 203 $^{\circ}\text{C}$  (decomp) IR (KBr) 3161 and 3102  $\text{cm}^{-1}$  (=C-H), 1763 (C=O)  $^1\text{H-NMR}$  (400 MHz,  $\text{CDCl}_3$ )  $\delta$  7.527 (s, 1H, N=CH-N), 7.101 (s, 1H, N-CH=CH-N), 6.992 (s, 1H, N-CH=CH-N), 5.241 (d, 1H,  $J$  = 6.58,  $\text{H}^{7a}$ ), 5.080 (d, 1H,  $J$  = 5.42,  $\text{H}^{8a}$ ), 5.030 (d, 1H,  $\text{H}^{8b}$ ), 4.728 (d, 1H,  $\text{H}^{7b}$ ), 4.330 (2d, 1H,  $J_{6a,5}$  = 5.50,  $J_{6a,6b}$  = -15.30,  $\text{H}^{6a}$ ), 4.211 (m, 1H,  $J_{6b,5}$  = 10.00,  $\text{H}^{6b}$ ), 4.180 (d, 1H,  $J_{3,4}$  = 1.00,  $\text{H}^3$ ), 4.130 (d, 1H,  $J_{2,3}$  = 2.00,  $\text{H}^2$ ), 4.219 (m, 1H,  $J_{5,4}$  = 1.20,  $\text{H}^5$ ), 3.530 (t, 1H,  $\text{H}^4$ ), EI-MS  $m/z$  283 ( $\text{M} - \text{H}$ ) $^+$ , 225 ( $\text{M} - \text{COOCH}_3$ ) $^+$ , Anal calcd for  $\text{C}_{12}\text{H}_{16}\text{N}_2\text{O}_6$  C, 50.70, H, 5.67, N, 9.85 Found C, 50.69, H, 5.67, N, 9.82

**6-Deoxy-6-(1-imidazolyl)-2,4;3,5-dimethylene-D-gluconic acid (16)** Compound **15** (0.901 g, 3.33 mmol) was dissolved in a mixture of 75 ml of dioxane/MeOH/aqueous 4N NaOH (15:4:1, v/v/v) $^{25}$  and stirred overnight. After evaporation to dryness, the yellow solid was treated with a cationic exchange resin (Biorad, AG 50 Wx8, 50-100 mesh) and liberated from the resin by treatment with aqueous 1N ammonia solution. Yield (0.88 g) was quantitative, mp 165  $^{\circ}\text{C}$  IR 1606  $\text{cm}^{-1}$  (C=O). No further analyses were carried out.

**6-Deoxy-6-(1-imidazolyl)-2,4;3,5-dimethylene-D-gluconic acid chloride (17)** Compound **16** (0.824 g, 3.05 mmol) was dissolved in 20 ml of  $\text{SOCl}_2$ , and refluxed for 90 min. The excess of thionyl chloride was removed by evaporation. The conversion was monitored by IR (1834  $\text{cm}^{-1}$ , C=O).

**1-Amino-trideca-5,7-diyne (18)** 1-Nitro-trideca-5,7-diyne (1.159 g, 6.19 mmol) which was prepared via oxidative hetero coupling $^{26}$  of 1-iodoheptyne $^{27}$  and 5-cyano-1-pentyne, $^{28}$  was dissolved in 10 ml of THF and added dropwise to a mixture of  $\text{AlH}_3$  $^{29}$  in 10 ml of THF at 0  $^{\circ}\text{C}$ . After overnight stirring at room temperature, a mixture of THF/ $\text{H}_2\text{O}$  (1/1, v/v) was added a few mins later followed by 15 ml of aqueous 1N NaOH. Both the decanted supernatant and the

remaining slurry were extracted with diethyl ether. After the collected organic layers were purified by column chromatography (silica, Et<sub>3</sub>N/MeOH/EtOAc, gradient starting with 1:5:94 up to 1:30:69 v/v), a yellow oil was obtained, yield 0.65 g (3.45 mmol, 55.8 %). IR (KBr) 3368 cm<sup>-1</sup> (very broad, NH), 2250 and 2156 (C≡C). <sup>1</sup>H-NMR (90 MHz, CDCl<sub>3</sub>), 3.20 (m, 2H, CH<sub>2</sub>-NH<sub>2</sub>), 2.18 (m, 4H, -CH<sub>2</sub>C≡C-C≡C-CH<sub>2</sub>-), 1.23 (m, 12H, CH<sub>3</sub>-(CH<sub>2</sub>)<sub>3</sub> + (CH<sub>2</sub>)<sub>2</sub>-CH<sub>2</sub>-NH<sub>2</sub>), 0.83 (t, 3H, CH<sub>3</sub>). No satisfactory mass spectrum could be obtained.

**6-Deoxy-6-(1-imidazolyl)-2,4;3,5-dimethylene-N,n-trideca-5,7-diyne-D-gluconamide**

**(19).** The acid chloride **17** (0.875 g, 3.03 mmol) was mixed with 10 ml of Et<sub>2</sub>O and CH<sub>2</sub>Cl<sub>2</sub> (1:1, v/v) and additionally diluted with 30 ml of anhydrous pyridine. To this slurry a solution of 0.65 g (3.45 mmol) of the amine **18** in 20 ml of pyridine was added dropwise. After stirring overnight at room temperature and subsequent heating at 80 °C for 1.5 hrs., the pyridine was evaporated and the remaining solid was dissolved in chloroform and washed with aqueous 0.01 N NaOH. After separation of the layers by centrifugation for 5 min at 3300 rpm, the organic layer was dried on anhydrous MgSO<sub>4</sub>. The product was purified by column chromatography (silica, Et<sub>3</sub>N/MeOH/EtOAc, 1:5:94 v/v/v) followed by recrystallization from EtOAc. A white powder was obtained, yield 0.46 g (1.04 mmol, 34.2 %), m.p. 129.8 °C. IR (KBr) 3425 cm<sup>-1</sup> (NH), 3150 and 3109 (=C-H), 2255 and 2155 (C≡C), 1687, 1675 (amide I, multiple conformations). <sup>1</sup>H-NMR (400 MHz, CDCl<sub>3</sub>), imidazole: δ 7.531 ppm (s, 1H), 7.099 (s, 1H), and 6.973 (s, 1H), carbohydrate: 5.222 (d, 1H), 5.040 (2d, 2H), 4.757 (d, 1H), 4.358 (2d, 1H), 4.219 (m, 1H), 4.211 (m, 1H), 4.189 (s, 1H), 4.145 (d, 1H), 3.548 (s, 1H) this assignment was by analogy to **6a** except for the alkyl chain protons. 3.333 (10 peaks, 2H, NHCO), 2.279 (m, 2H, C≡C-CH<sub>2</sub>-(CH<sub>2</sub>)<sub>3</sub>NHCO), 2.241 (m, 2H, CH<sub>3</sub>-(CH<sub>2</sub>)<sub>3</sub>-CH<sub>2</sub>-C≡C), 1.599 (m, 4H, C≡C-CH<sub>2</sub>-(CH<sub>2</sub>)<sub>2</sub>-CH<sub>2</sub>NHCO), 1.519 (m, 2H, CH<sub>3</sub>-(CH<sub>2</sub>)<sub>2</sub>-CH<sub>2</sub>-CH<sub>2</sub>-C≡C) 1.350 (m, 4H, CH<sub>3</sub>-(CH<sub>2</sub>)<sub>2</sub>-(CH<sub>2</sub>)<sub>2</sub>-C≡C), 0.895 (t, 3H, -CH<sub>3</sub>), <sup>13</sup>C-NMR (100 MHz, CDCl<sub>3</sub>) carbohydrate and imidazole similar to **5a**, δ 77.912 ppm (C≡C-C≡C-(CH<sub>2</sub>)<sub>3</sub>-NH), 75.062 (CH<sub>3</sub>-(CH<sub>2</sub>)<sub>4</sub>-C≡C-C≡C), 65.802 (C≡C-C≡C-(CH<sub>2</sub>)<sub>3</sub>-NH), 65.050 (CH<sub>3</sub>-(CH<sub>2</sub>)<sub>4</sub>-C≡C-C≡C), 44.748 (C<sup>6</sup>), 38.396 (-CH<sub>2</sub>-NHCO), 30.935, 28.494, 27.948, 25.356, 22095, 19.097, 18.776 (alkyl chain methylene carbons), 13.870 (CH<sub>3</sub>). EI-MS *m/z* 443 (M)<sup>+</sup>, 225 (M - C<sub>13</sub>H<sub>19</sub>-NHCO)<sup>+</sup>, 85 (cyclic -O-CH=CH-CH<sup>+</sup>-O-CH<sub>2</sub>). Anal. calcd. for C<sub>24</sub>H<sub>33</sub>N<sub>3</sub>O<sub>5</sub> · ½H<sub>2</sub>O: C, 63.70; H, 7.57; N, 9.29. Found: C, 63.70; H, 7.49; N, 9.21.

**N,n-Trideca-5,7-diyne-D-gluconamide (20).** Compound **18** (0.568 g, 3.00 mmol) was dissolved in 50 ml of methanol. To the stirred solution, 0.538 g (3.02 mmol) of 1,5-D-gluconolactone was added. After two hrs. of refluxing, the solution was cooled to RT. Crystals appeared in a few hrs., which were collected by filtration. The white crystals were stored in an argon atmosphere at -18 °C. Despite these precautions, the color changed from white to pink in a few days. Yield 0.05 g (0.14 mmol, 4.5 %, not optimized), m.p. 152.5 °C. IR (KBr) 3504 cm<sup>-1</sup> (OH<sup>2</sup>), 3377, 3344 and 3283 (OH), 1654 (amide I), 1541 (amide II). EI-MS *m/z* 369 (M)<sup>+</sup>, 218 (C<sub>13</sub>H<sub>19</sub>-NHCO)<sup>+</sup>. Anal. Calcd. for C<sub>19</sub>H<sub>31</sub>NO<sub>6</sub>: C, 61.77; H, 8.46; N, 3.79. Found: C, 61.44; H, 8.42; N, 3.82.

**6-Deoxy-6-(1-imidazolyl)-2,4;3,5-dimethylene-n-hexadecyl-D-gluconate (21).** The reaction procedure for this compound was similar to that of **19**, however, instead of the amine **18**, 1.550 g (6.39 mmol, 3.8 equiv.) of cetyl alcohol was added to 0.481 g (1.666 mmol) of **17**. Yield 0.04 g (white powder, 0.08 mmol, 5.0 %), m.p. 94.7 °C. IR (KBr) 3130 and 3112 cm<sup>-1</sup> (=C-H), 1760, 1752 (C=O, more conformations). <sup>1</sup>H-NMR (400 MHz, CDCl<sub>3</sub>) imidazole: δ 7.545 (s, 1H), 7.104 (s, 1H) and 6.996 (s, 1H) this assignment was by analogy to that of **1a**, 5.241 (d, 1H, *J* = 6.56 Hz, H<sup>7a</sup>), 5.084 (d, 1H, *J* = 5.28 Hz, H<sup>8a</sup>), 5.012 (d, 1H, H<sup>8b</sup>), 4.717 (d, 1H, H<sup>7b</sup>), 4.246 (m, 5H, H<sup>2,6a,6b</sup> + CH<sub>2</sub>OCO), 4.160 (7 peaks, 1H, H<sup>5</sup>), 3.939 (s, 1H, H<sup>3</sup>), 3.683 (m, 1H, H<sup>4</sup>), 1.771 (incorporated water), 1.675 (6 peaks, 2H, CH<sub>2</sub>-CH<sub>2</sub>-OCO), 1.256 (m, 26H, CH<sub>3</sub>-(CH<sub>2</sub>)<sub>13</sub>-), 0.880 (t, 3H, CH<sub>3</sub>). EI-MS *m/z* 494 (M)<sup>+</sup>, 479, 465, 451, 437, 409, 395, 381, 367, 353, 339, 325

(respectively  $M - (CH_2)_n - CH_3)^+$ , 225 ( $M - C_{16}H_{33} - OCO)^+$ . Anal. Calcd. for  $C_{27}H_{46}N_2O_6$ : C, 65.56; H, 9.57; N, 5.66. Found: C, 66.12; H, 9.58; N, 5.06.

**N,n-Hexadecyl-6-hydroxy-n-hexanoic acid amide (22).** n-Hexadecylamine (5.733 g, 23.74 mmol) was mixed with 2.860 g (25.06 mmol) of caprolactone and heated without solvent at 100 °C. After stirring at 100 °C for 2 hrs. in a nitrogen atmosphere, the mixture was cooled and subsequently recrystallized from EtOAc. Recrystallization was repeated for 7 times in order to obtain a pure white crystalline powder, yield n.d., m.p. 92.6 °C. IR (KBr) 3312  $cm^{-1}$  (sharp, NH), 3183 (broad, OH), 1633 (amide I), 1541 (amide II), IR ( $CHCl_3$ ) 3630 (sharp, NH), 3449 (sharp, OH), 1662 (amide I), 1517 (amide II).  $^1H$ -NMR (400 MHz,  $CDCl_3$ )  $\delta$  5.854 ppm (NHCO), 3.631 (t, 2H,  $-CH_2OH$ ), 3.217 (double t, 2H,  $-CH_2NHCO$ ), 2.551 (broad s, 1H,  $-OH$ ), 2.178 (t, 2H,  $(CO)CH_2$ ),  $^{13}C$ -NMR (400 MHz,  $CDCl_3$ )  $\delta$  173.076 ppm (C=O), 62.259 ( $CH_2OH$ ), 39.484 ( $CH_2NH$ ). EI-MS  $m/z$  355 ( $M^+$ ), 337 ( $M - H_2O^+$ ), 268 ( $C_{16}H_{33}NHCO^+$ ). Anal. Calcd. for  $C_{22}H_{45}NO_2 \cdot \frac{1}{2}H_2O$ : C, 74.31; H, 12.75; N, 3.94. Found: C, 73.76; H, 12.48; N, 4.01.

**N,n-Hexadecyl-6-tosyl-n-hexanoic acid amide (23).** Tosylation was carried out using a standard procedure, *e.g.* as was used for the preparation of **5a**. Instead of pyridine, dichloromethane was used as the solvent for the hydroxyl compound and KOH was added as an additional base. Yield 0.41 g (0.80 mmol, 45 %). IR (KBr) 3326  $cm^{-1}$  (NH), 1644 (amide I), 1533 (amide II), 1363 and 1174 (S=O). Despite a slight contamination with compound **22**, the product was not further purified and used for the synthesis of **24**.

**N,n-Hexadecyl-6-(1-imidazolyl)-n-hexanoic acid amide (24).** This product was synthesized following the procedure described for **1a**. Instead of **5a**, 0.392 g (0.77 mmol) of **23** was used which was dissolved in 4.5 ml of  $CHCl_3$ . The product was purified as was described for **1a**, without recrystallization. Yield 0.05 g (0.12 mmol, 16.1 %), m.p. 65.9 °C. IR (KBr) 3317  $cm^{-1}$  (sharp, NH), 3101 and 3047 (=C-H), 1637 (amide I), 1536 (amide II).  $^1H$ -NMR (90 MHz,  $CDCl_3$ )  $\delta$  7.460 ppm (s, 1H, N=CH-N), 7.057 (s, 1H, N=CH-CH-N), 6.911 (s, 1H, N=CH-CH-N), 5.382 (very broad t, 1H, NHCO), 3.927 (t, 2H,  $-CH_2-N=$ ), 3.232 (q, 2H,  $CH_2-(C=O)$ ), 2.139 (t, 2H,  $-CH_2-C=O$ ), 1.935 (t, 2H,  $-CH_2-CH_2-N=$ ), 1.691 (crystal water), 1.240 (m, 32H,  $-(CH_2)_{14}$ - and  $O=C-CH_2-(CH_2)_2-$ ), 0.889 (t, 3H,  $CH_3$ ). EI-MS  $m/z$  405 ( $M^+$ ), 165 ( $CO-(CH_2)_5-N_2C_3H_3^+$ ), 137 ( $-(CH_2)_5-N_2C_3H_3^+$ ), 95 ( $CH_2-CH_2-N_2C_3H_3^+$ ). Anal. Calcd. for  $C_{25}H_{47}N_3O \cdot \frac{1}{2}H_2O$ : C, 72.25; H, 11.68; N, 10.36. Found: C, 72.41; H, 11.67; N, 10.13.

**1-n-Hexadecylimidazole (25).** Cetyl alcohol was converted into n-hexadecyl tosylate following a standard tosylation procedure (see for instance the synthesis of **23**). The tosylate (1.980 g, 4.99 mmol) was added to a solution of sodium imidazolate in 10 ml of DMF (4.96 mmol) which had been freshly prepared prior to this reaction by treating imidazole with 1 equiv. NaH in DMF. After a few hrs. stirring at room temperature followed by overnight reaction at 50 °C, a white precipitate (NaOTs) was formed which was removed by filtration. The filtrate was concentrated by evaporation before it was poured into a mixture of ice and saturated  $NaHCO_3$  solution. The product was extracted with dichloromethane and further purified by column chromatography (silica, eluent  $Et_3N/EtOAc$  1:99, v/v). The yellow product was dissolved in dichloromethane and washed with saturated  $NaHCO_3$ , yield 0.38 g of white powder (1.28 mmol, 25.8 %), m.p. 35.8 °C. IR (KBr) 3108  $cm^{-1}$  (=C-H), 2924 and 2853 ( $CH_2$ ), 1718 and 1684 (C=N), 1507 and 1467 (aromate),  $^1H$ -NMR (90 MHz,  $CDCl_3$ )  $\delta$  7.453 ppm (broad s, 1H, N=CH-N- $CH_2$ -), 7.053 (broad s, 1H, N-CH=CH-N- $CH_2$ ), 6.898 (s, 1H, N-CH=CH-N- $CH_2$ ), 3.917 (t, 2H,  $-(CH_2)_{14}-H_2-N$ ), 1.794 (t, 2H,  $-(CH_2)_{13}-CH_2-CH_2-N$ ), 1.254 (broad s, 26H,  $-CH_2-(CH_2)_{13}-CH_2-$ ), 0.880 (t, 3H,  $-CH_3$ ). EI-MS  $m/z$  292 ( $M^+$ ), 277, 263, 249, 235, 221, 207, 193,

\* The NaH was washed with n-hexane before use in order to remove the mineral oil in which it is dispersed



179, 165, 151, 137, 123, 109, (M-(CH<sub>2</sub>)<sub>n</sub>-CH<sub>3</sub>, n= 0-12 respectively)<sup>+</sup> Anal Calcd for C<sub>19</sub>H<sub>36</sub>N<sub>2</sub> C, 78.02, H 12.04, N, 9.58 Found C, 78.17, H, 11.90, N, 9.39

### 3.2.2 Metal complexes

**[(1a)<sub>4</sub>Cu][OSO<sub>2</sub>CF<sub>3</sub>]<sub>2</sub> ((1a)<sub>4</sub>Cu)** To a stirred solution of 65.5 mg (0.172 mmol) of **1a** in 0.5 ml of EtOH, 0.043 mmol of [Cu][OSO<sub>2</sub>CF<sub>3</sub>]<sub>2</sub> dissolved in 50 µl EtOH was added. After 30 min, a purple precipitate appeared from the dark blue solution. Unfortunately the oil-like precipitate could not be isolated by filtration. The product was isolated by evaporation of the dispersion to dryness, m.p. 105.8 °C, IR (KBr) 3132 cm<sup>-1</sup> (=C-H), 639 (Cu-N<sub>im</sub>). Elemental analysis failed due to the presence of the triflate anions, however, an indication for the presence of a copper complex with 4 imidazole ligands was the λ<sub>max</sub> observed in the UV-vis spectrum, λ<sub>max</sub> = 595.1 nm (CHCl<sub>3</sub>/MeOH). The loss of weight upon heating was determined in order to estimate the amount of solvent molecules precipitated with the copper salts. After a weight loss of 1.26 %, which equals the evaporation of approx. one molecule of water per complex, the weight was stable from 68 °C up to 150 °C (theoretically 0.95 %).

**[(1b)<sub>4</sub>Cu][OSO<sub>2</sub>CF<sub>3</sub>]<sub>2</sub> ((1b)<sub>4</sub>Cu)** Copper triflate (0.025 mmol) dissolved in 30 µl of EtOH was added to 41.1 mg (0.100 mmol) of **1b** which was dissolved in 0.5 ml of EtOH. A precipitate from the dark blue solution was formed overnight leaving a colorless supernatant. The purple precipitate could be isolated by filtration, yield 77 %, m.p. 130.6 °C IR (KBr) 3132 cm<sup>-1</sup> (=C-H), 638 (Cu-N<sub>im</sub>), UV-vis λ<sub>max</sub> = 610.8 nm (CHCl<sub>3</sub>/MeOH 1:3 (v/v)), loss of weight 2.64 % which is ca. 1 molecule of EtOH per complex (theoretically 2.25 %).

**[(1c)<sub>4</sub>Cu][OSO<sub>2</sub>CF<sub>3</sub>]<sub>2</sub> ((1c)<sub>4</sub>Cu)** Copper triflate (0.028 mmol) was dissolved in 36 µl of EtOH and added to 49.1 mg (0.112 mmol) of **1c** which was dissolved in 0.5 ml of EtOH. A purple precipitate was formed after 15 min, yield 78 %, m.p. 130.5 °C IR (KBr) 3134 cm<sup>-1</sup> (=C-H), 638 (Cu-N<sub>im</sub>), UV-vis λ<sub>max</sub> = 611.4 nm (CHCl<sub>3</sub>/MeOH 1:3 (v/v)), loss of weight 2.43 % which corresponds to 1 molecule of EtOH per complex (theoretically 2.13 %).

**[(1d)<sub>4</sub>Cu][OSO<sub>2</sub>CF<sub>3</sub>]<sub>2</sub> ((1d)<sub>4</sub>Cu)** Copper triflate (0.022 mmol) was dissolved in 24 µl of EtOH and added to 39.5 mg (0.087 mmol) of **1d** which was dissolved in 0.5 ml of EtOH. A purple precipitate was formed overnight, yield 95 %, m.p. 134.6 °C IR (KBr) 3135 cm<sup>-1</sup> (=C-H), 638 (Cu-N<sub>im</sub>), UV-vis λ<sub>max</sub> = 611.1 nm (CHCl<sub>3</sub>/MeOH 1:3 (v/v)), loss of weight 2.82 % which corresponds to 1 molecule of EtOH and 1 molecule of water per complex (theoretically 2.83 %).

**[(1e)<sub>4</sub>Cu][OSO<sub>2</sub>CF<sub>3</sub>]<sub>2</sub> ((1e)<sub>4</sub>Cu)** Copper triflate (0.037 mmol) was dissolved in 47 µl of EtOH and added to 73.2 mg (0.148 mmol) of **1e** which was dissolved in 1.5 ml of EtOH. A purple precipitate was formed after 10 min, yield 90 %, m.p. 127.1 °C IR (KBr) 3135 cm<sup>-1</sup> (=C-H), 638 (Cu-N<sub>im</sub>), UV-vis λ<sub>max</sub> = 610.8 nm (CHCl<sub>3</sub>/MeOH 1:3 (v/v)), loss of weight 2.52 % which corresponds to 1 molecule of EtOH and 1 molecule of water per complex (theoretically 2.70 %).

**[(1f)<sub>4</sub>Cu][OSO<sub>2</sub>CF<sub>3</sub>]<sub>2</sub> ((1f)<sub>4</sub>Cu)** Copper triflate (0.012 mmol) was dissolved in 15 µl of EtOH and added to 24.4 mg (0.047 mmol) of **1f** which was dissolved in 1.3 ml of EtOH. A purple precipitate was formed immediately, yield 90 %, m.p. 125.9 °C IR (KBr) 3135 cm<sup>-1</sup> (=C-H), 638 (Cu-N<sub>im</sub>), UV-vis λ<sub>max</sub> = 611.9 nm (CHCl<sub>3</sub>/MeOH 1:3 (v/v)), no loss of weight was determined.

**[(9)<sub>4</sub>Cu][OSO<sub>2</sub>CF<sub>3</sub>]<sub>2</sub> ((9)<sub>4</sub>Cu)** Copper triflate (0.006 mmol) was dissolved in 1.1 ml of EtOH and added to 12.1 mg (0.023 mmol) of **9** which was dissolved in 0.2 ml of EtOH. A green blue solution was obtained from which the purple product precipitated, yield n.d. No further analytical data are available.

**[(19)<sub>4</sub>Cu][OSO<sub>2</sub>CF<sub>3</sub>]<sub>2</sub> ((19)<sub>4</sub>Cu)** Copper triflate (0.043 mmol) was dissolved in 0.5 ml of EtOH and added to 76.0 mg (0.171 mmol) of **19** which was dissolved in 2 ml of EtOH. The reaction was carried out in a nitrogen atmosphere. No precipitate was formed, and the dark blue solution was therefore evaporated to dryness, UV-vis  $\lambda_{\text{max}}$  = 611.6 nm (CHCl<sub>3</sub>/MeOH 1:3 (v/v)).

**[(24)<sub>4</sub>Cu][OSO<sub>2</sub>CF<sub>3</sub>]<sub>2</sub> ((24)<sub>4</sub>Cu)** Upon addition of 0.006 mmol of copper triflate (which was dissolved in 0.4 ml of EtOH) to 9.7 mg (0.024 mmol) of **24** dissolved in 0.5 ml of EtOH, a dark blue solution was obtained. No precipitate was formed and the solution was evaporated to dryness, UV-vis  $\lambda_{\text{max}}$  = 601.9 nm (CHCl<sub>3</sub>/MeOH 1:3 (v/v)).

**[(25)<sub>4</sub>Cu][OSO<sub>2</sub>CF<sub>3</sub>]<sub>2</sub> ((25)<sub>4</sub>Cu)** Copper triflate (0.021 mmol) was dissolved in 1 ml of EtOH and added to 24.1 mg (0.084 mmol) of **25** which was dissolved in 0.5 ml of EtOH. After several min, a purple precipitate was formed from the dark blue solution leaving a colorless supernatant, yield n.d., UV-vis  $\lambda_{\text{max}}$  = 594.3 nm (CHCl<sub>3</sub>/MeOH 1:3 (v/v)).

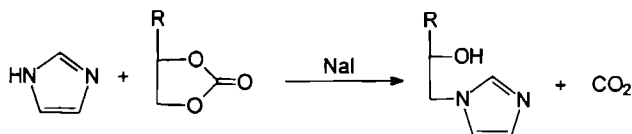
**[(1e)<sub>4</sub>Ni][BF<sub>4</sub>]<sub>2</sub> ((1e)<sub>4</sub>Ni)** A similar procedure was followed as for **(1b)<sub>4</sub>Cu**. 0.0035 mmol of NiBF<sub>4</sub> dissolved in 55  $\mu$ l of EtOH, was added to 10.5 mg (0.0213 mmol) of **1e** which was dissolved in 0.5 ml of EtOH. A pale green precipitate was formed after 15 min, yield n.d. No further analytical data are available.

### 3.3 Results and discussion

#### 3.3.1 Synthesis of imidazole ligand

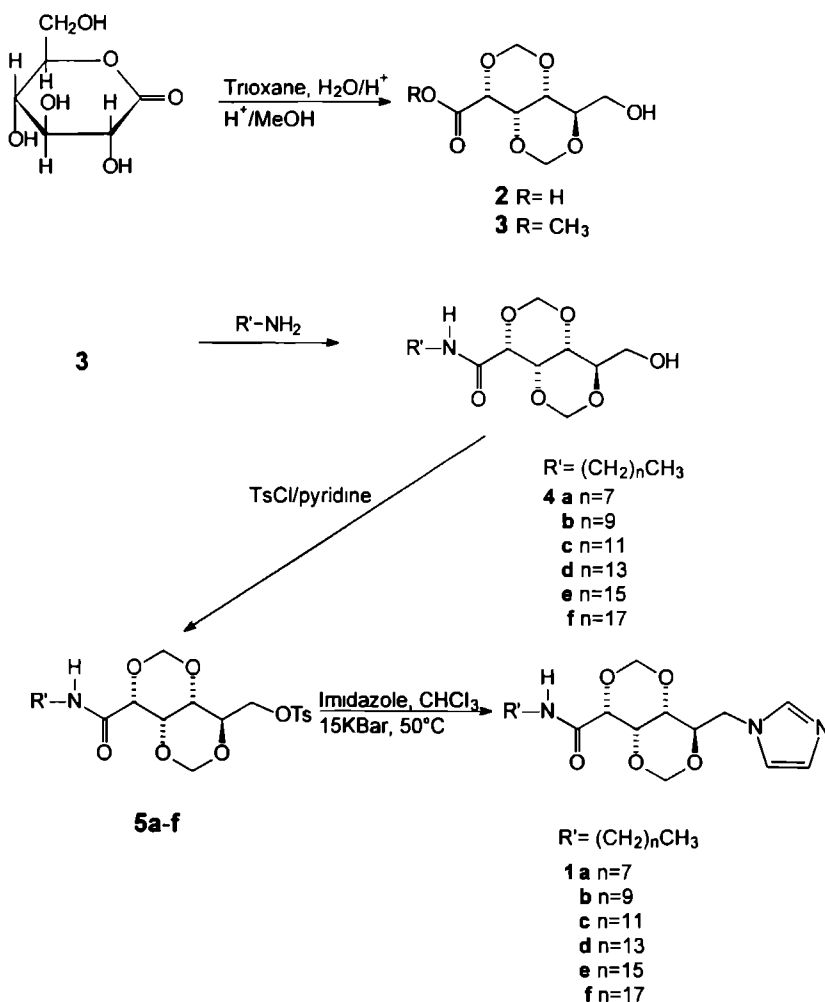
If one wants to replace one of the hydroxyl groups in a glucose molecule by a tosyl group and subsequently by an imidazole group, it is nearly always necessary to protect the other hydroxyl groups from reaction. One of the standard protecting groups is the acetate group which, however, causes problems because of its instability towards bases. The nucleophilic substitution of the tosyl function by the imidazole group can only proceed under basic conditions, and results in removal of one of the acetate groups and the formation of products with 5 or 6 membered rings. Another option is the use of an isopropylidene or acetone clamp, which is known to be stable towards base. As it was our intention to make gluconic acid derivatives with a metal binding ligand at the end of the carbohydrate chain, *viz.* at carbon atom C<sup>6</sup>, and isopropylidene only forms 5 membered rings blocking the OH functions at carbon atoms 2,3 and 5,6, leaving only the OH at carbon atom 4 open for reaction, this protecting group could not be used. A third possibility is to use the benzylidene group,<sup>30</sup> which only blocks 2 of the 5 hydroxyl groups (*viz.* the OH's at carbon atoms 4 and 5). Since in that case the molecule still contains more than one free hydroxyl group, we searched for an alternative route to synthesize the target compounds **1**. This was found in a ring opening reaction of the cyclic carbonate (shown in Scheme 3.1).<sup>31,32</sup>

Scheme 3.1



Although the starting compound *N*-*n*-octyl-2,4-benzylidene-5,6-carbonate-D-gluconamide could easily be obtained, and in a test reaction the carbonate ring of ethylene carbonate could be opened with imidazole yielding 2-(1-imidazolyl)ethanol (see Chapter 4), the desired ring opening of the gluconamide was not achieved. As the last alternative for the protection of the secondary hydroxyl groups we considered methylene bridges at carbon atoms C<sup>2</sup>,C<sup>4</sup> and C<sup>3</sup>,C<sup>5</sup>.<sup>22,23</sup> The advantage of this procedure is that all the secondary hydroxyl groups are now protected with base stable groups and that the primary hydroxyl group is still open for reaction. The big disadvantage is that it is very hard to remove the methylene groups, which can be only achieved partly using strongly acidic conditions (removal of the 3,5 methylene bridge), viz. glacial acetic acid and trifluoroacetic anhydride.<sup>33</sup>

Scheme 3.2



These strong acidic conditions can lead to hydrolysis of the amide bond. The reagent boron trichloride, which is subsequently needed to remove the 2,4 methylene bridge, may react with the imidazole group.

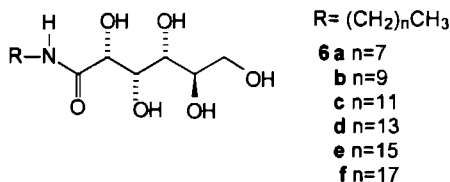
Despite the above mentioned disadvantages we decided to use the methylene protecting group and compounds **1** were synthesized, as shown in Scheme 3.2.

The unprotected hydroxyl group of **4a-f** was tosylated using a standard procedure to give **5a-5f** (Scheme 3.2) and the introduction of the imidazole group was attempted in DMF using a large excess of imidazole (see Chapter 5). This reaction, however, gave a large amount of unwanted side products, *e.g.* 6-deoxy-6,5-didehydro-2,4;3,5-dimethylene-*N,n*-octyl-D-gluconamide (55 %), as the result of an elimination reaction. Enhancing the nucleophilicity of the imidazole by converting it into the corresponding anion did not result in the desired product, probably because this anion reacted with the reactive amide hydrogen, present in **5**.

The elimination could be successfully suppressed when the reaction was carried out under high pressure (15 kBar) at 50 °C. In addition, a higher yield of compounds **1** was obtained (66 % instead of 35 % at normal pressure). We did not remove the protecting groups of **1** because these compounds as such already displayed interesting properties, which are described below and in Chapters 4 and 7.

### 3.3.2 Effect of the length of the alkyl chain on the L.C. behavior of compounds **1** and model compounds

Carbohydrates are excellent building blocks for thermotropic liquid crystalline materials if they are designed keeping in mind the following limitations<sup>34</sup> (i) they must have an *n*-alkyl chain of at least 6 carbon atoms attached to the carbohydrate framework, (ii) they may be cyclic or acyclic but must in most cases contain a number of unprotected hydroxyl functions and (iii) the terminus of the *n*-alkyl chain should not be substituted with polar functional groups such as -OH, -Cl and -C≡N. The model *n*-alkyl gluconamides **6a-f**, meet all these conditions and indeed showed L.C. behavior (see Figure 3.1).



Besides the melting point (m.p.) and the clearing point (c.p.), which is the transition from the L.C. phase to the isotropic (I) phase, additional crystal to crystal ( $K_1 \rightarrow K_2$ ) transitions were observed. The L.C. phases of **6a-f** can be assigned to be smectic A<sub>d</sub> (S<sub>A<sub>d</sub></sub>) on the basis of polarization microscopy studies, which is in agreement with the packing suggested in the literature for the octyl derivative (**6a**).<sup>35</sup> As can be seen in Figure 3.1, the melting points are almost invariant in the

series **6a-f**, whereas the clearing points become higher by elongation of the alkyl chain, which results in a stabilization of the L.C. phases. The rise of the c.p. is most clearly visible for the shorter chain derivatives.<sup>35</sup> Compounds **6** were found to gradually decompose on standing at  $\pm 190^\circ\text{C}$ .

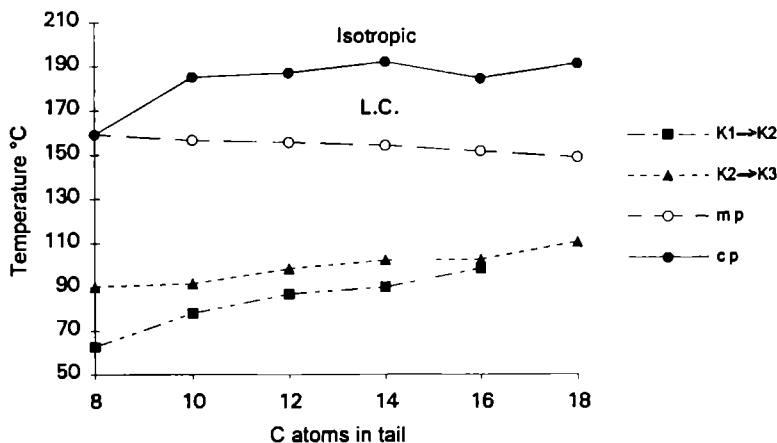


Figure 3.1 Phase transition temperatures of *N*-*n*-alkyl-D-gluconamides

In the literature<sup>34,35</sup> a qualitative model has been proposed for the structural variations that occur when a *N*-alkylgluconamide is heated from the solid phase to the L.C. phase. It is suggested that in the L.C. phase the weaker Van der Waals interactions are broken while the stronger hydrogen bonds remain intact. The latter are only disconnected when the isotropic phase is entered. This theory does not explain why in our case not the melting point but the clearing point is dependent on the length of the alkyl chain. The melting enthalpies of compounds **6** are virtually independent of the length of the alkyl chains (see Table 3.1), which suggests that at the melting points not "the alkyl chains are melting" but the hydrogen bonding scheme of the carbohydrate moiety is changing. Due to partial overlap of peaks, the enthalpy values of the crystal to crystal transitions  $K_1 \rightarrow K_2$  and  $K_2 \rightarrow K_3$  could not be determined accurately which makes that no conclusions can be drawn with regard to the structural variations that take place at these transitions. According to Jeffrey,<sup>36</sup> who studied the packing of *N*,*n*-undecyl-D-gluconamide at different temperatures by powder diffraction, in the first transition a monolayered structure is transformed into a bilayered structure, which would be in agreement with our findings that the temperature of the transition  $K_1 \rightarrow K_2$  is dependent on the length of the alkyl chain. The transition  $K_2 \rightarrow K_3$  is also dependent on the length of the alkyl chain, which suggests another transition involving the alkyl chains.

The type of molecular packing in the L.C.-phase of *N*,*n*-alkyl-D-gluconamides has been intensively discussed in the literature. Baeyens-Volant *et al*<sup>37</sup> have proposed that these

compounds form a monolayered, head to tail packed smectic phase on the bases of the crystal structures of these compounds. On the other hand Pfannemüller *et al.*<sup>35</sup> have reported that *N,n*-alkyl-D-gluconamides exhibit liquid crystalline phases which are miscible with the  $S_{Ad}$  phases of the *n*-alkyl-1-O- $\beta$ -D-glucopyranosides, showing that the packing of the *n*-alkyl-gluconamides and *n*-alkyl-glucopyranosides in the L.C. phase is similar. This has led them to propose a model for the packing of the *n*-alkyl-gluconamide molecules in the L.C. phase (see Figure 3.2).<sup>35,38</sup> This model was supported by data published by Jeffrey *et al.*<sup>36</sup> on the d-spacings of *N,n*-undecyl-D-gluconamide.

**Table 3.1** Thermotropic behavior of *N,n*-alkyl-D-gluconamides<sup>a</sup>

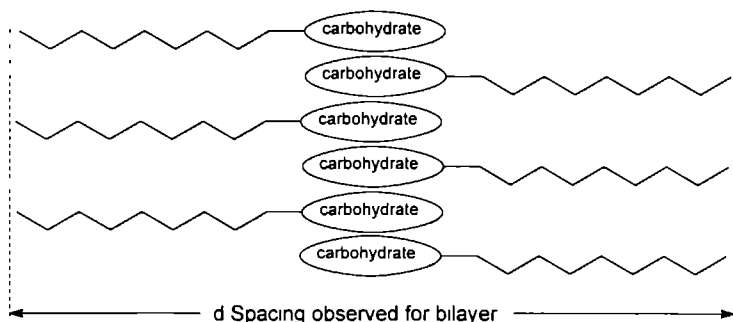
Compound	n <sup>b</sup>	K <sub>1</sub> →K <sub>2</sub> (°C)	K <sub>2</sub> →K <sub>3</sub> (°C)	m p <sup>c</sup> (°C)	c p (°C)
<b>6a</b>	8	62.8	90.3	159.2 (47.2)	140.2 <sup>d</sup>
<b>6b</b>	10	78.1	91.6	156.5 (47.0)	184.9
<b>6c</b>	12	86.7	98.4	155.5 (49.3)	186.7
<b>6d</b>	14	90.0	102.2	154.0 (45.7)	191.8
<b>6e</b>	16	98.5	102.6	151.4 (53.3)	184.3
<b>6f</b>	18	--	110.4	148.5 (50.6)	191.0

<sup>a</sup> Determined from heating runs

<sup>b</sup> Number of carbon atoms in alkyl chain of **6**

<sup>c</sup>  $\Delta H_{\text{melt}}$  (kJ mol<sup>-1</sup>) in parentheses

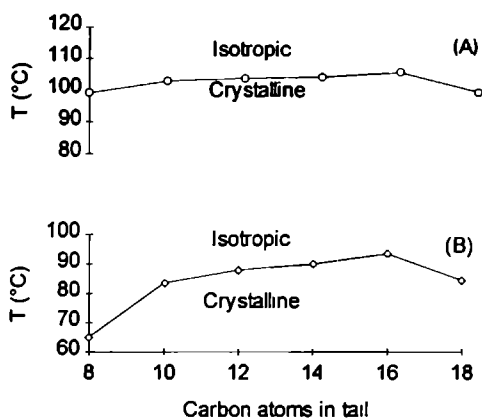
<sup>d</sup> Value obtained upon cooling



**Figure 3.2** Model proposed for  $S_{Ad}$  phase by Pfannemüller<sup>35</sup>

On basis of the molecular requirements formulated by Jeffrey,<sup>34</sup> the methylene protected compounds **4a-f** should show L.C.-behavior. Gluconamides **4a-e**, however, did not show any L.C.-behavior, which is probably due to the fact that these compounds have only one hydroxyl group available for forming hydrogen bonds. Remarkable is the independence of the melting points on the length of the alkyl chain (see Figure 3.3A, and Table 3.2), which suggests that the molecular packing in compounds **4** is similar for the entire series. Compound **4f** did show an enantiotropic L.C. phase (m.p. 99.4 °C) of unknown type (not  $S_A$ ). All compounds crystallized

upon cooling. The solidification points (s.p's) are shown in Figure 3.3B and are summarized in Table 3.2. Surprisingly no trend in the  $\Delta H_{\text{melt}}$  values could be observed (neither in the case of the first heating runs nor in the second heating runs). The  $\Delta H_{\text{solid}}$  values of the crystallizations, however, increased upon elongation of the alkyl chain, which suggests that solidification is dominated by the packing of the alkyl chains and not by the carbohydrate moieties. This was emphasized by the fact that the  $\Delta H_{\text{solid}}$  value of the hexadecyl gluconamide **4e** was almost twice the value of the  $\Delta H_{\text{solid}}$  value of the octyl gluconamide **4a**.



**Figure 3.3** Thermotropic behavior of compounds **4a-f**

A) Melting points, B) solidification points

**Table 3.2** Thermotropic behavior of 2,4,3,5 dimethylene-D-gluconamides (**4**)<sup>a</sup>

Compound	n <sup>b</sup>	m p <sup>c</sup> (°C)	s p <sup>d</sup> (°C)
<b>4a</b>	8	99.1 (33.7)	65.1 (-15.6)
<b>4b</b>	10	102.8 (20.8)	83.6 (-21.5)
<b>4c</b>	12	103.6 (40.5)	88.0 (-24.6)
<b>4d</b>	14	104.0 (27.8)	90.0 (-26.8)
<b>4e</b>	16	105.5 (39.8)	93.5 (-28.3)
<b>4f</b>	18	99.4 (30.8)	84.5 (-20.1)

<sup>a</sup> Data obtained from DSC thermograms

<sup>b</sup> Number of carbon atoms in the alkyl chains of **4**

<sup>c</sup> Melting point obtained from second heating run, melting enthalpy

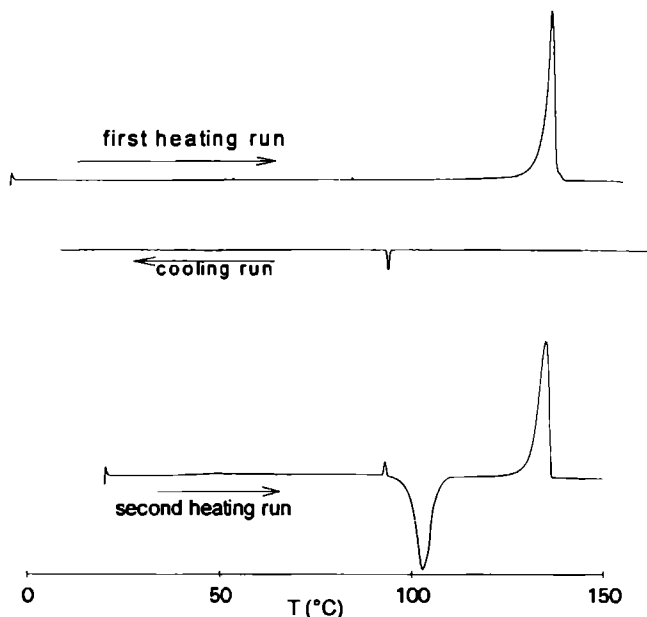
$\Delta H_{\text{melt}}$  (kJ/mol) in parentheses

<sup>d</sup> Solidification point obtained from first cooling run, enthalpy upon solidification

$\Delta H_{\text{solid}}$  (kJ/mol) in parentheses

Gluconamides **1** were crystalline at room temperature and to our surprise some of them showed monotropic<sup>39</sup> L.C. behavior upon cooling from the melt. A remarkable feature was the

hysteresis displayed by these compounds: on cooling the L.C. phase was transformed into a glassy state rather than in a crystalline state. Some of them crystallized at a later time, a nice example being compound **1d** which was heated from the glassy state in the second heating and was found to crystallize just above the c.p. (see Figure 3.4). The mobility of the molecules in the L.C. phase is too low to allow them to rearrange for crystallization. Apparently when the isotropic phase is entered (for **1d** in the second heating run at 93.6 °C), this mobility is acquired and crystallization can occur.



**Figure 3.4** DSC thermogram of compound **1d**.

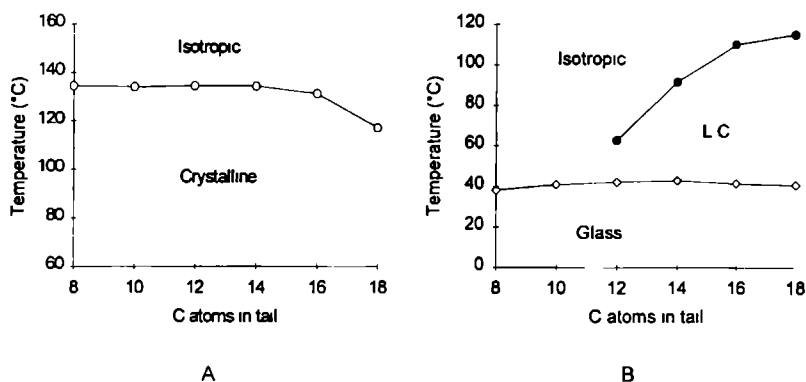
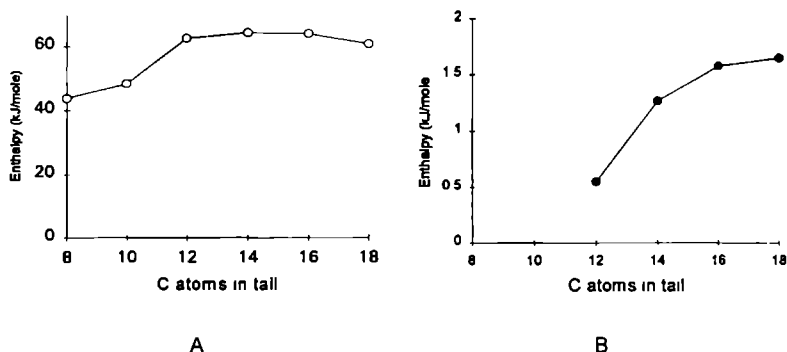
As in the case of the *N,n*-alkyl-D-gluconamides (Table 3.1), the melting points of the series of compounds **1** (except **1f**) are independent on the length of the alkyl chain just as the glass transition temperatures ( $T_g$ 's) are, whereas the clearing points are raised by elongation of the aliphatic chain (see Table 3.3 and Figures 3.5A,B). A possible explanation for the failure of compounds **1a** and **1b** to form L.C. phases is that the system is frozen in a glassy state before the L.C. phase is entered. This can be concluded from the fact that the  $T_g$  line intersects with the c.p. line if the latter is extrapolated to the decyl and octyl derivatives (Figure 3.5B).

The  $\Delta H_{\text{melt}}$  of the compounds that are liquid crystalline (**1c-f**) is not dependent on the length of the alkyl chain. For compounds **1a** and **1b** a slightly lower  $\Delta H_{\text{melt}}$  is observed than for **1c-f** (Figure 3.6A). As can be seen in Figure 3.6B  $\Delta H_{\text{clearing}}$  increases when the number of carbon atoms in compounds **1** is increased.



**Table 3.3** Thermotropic behavior of imidazolyl compounds (**1**)<sup>a</sup>

Compound	n <sup>b</sup>	m p <sup>c</sup> (°C)	c p <sup>d</sup> (°C)	T <sub>g</sub> <sup>e</sup> (°C)
<b>1a</b>	8	134.5 (43.8)	---	38.1
<b>1b</b>	10	134.0 (48.4)	---	40.9
<b>1c</b>	12	134.3 (62.7)	62.7 (-0.55)	42.1
<b>1d</b>	14	134.2 (64.5)	91.6 (-1.27)	42.9
<b>1e</b>	16	131.1 (64.2)	110.0 (-1.58)	41.4
<b>1f</b>	18	117.0 (61.0)	115.0 (-1.65)	40.6

<sup>a</sup> Data obtained from DSC thermograms<sup>b</sup> Number of carbon atoms in the alkyl chains of **1**<sup>c</sup> Melting point obtained from first heating run, melting enthalpy $\Delta H_{\text{melt}}$  (kJ/mole) in parentheses<sup>d</sup> c p obtained from cooling run,  $\Delta H$  clearing (kJ/mol) in parentheses<sup>e</sup> T<sub>g</sub> obtained from cooling run**Figure 3.5** Thermotropic behavior of imidazolyl compounds **1a-f** A) Heating B) Cooling**Figure 3.6** A)  $\Delta H_{\text{melt}}$  and B)  $\Delta H_{\text{clearing}}$  of compounds **1a-f**

### 3.3.3 Characterization of the L.C. phases of compounds 1

According to the textures observed by polarization microscopy, compounds **1c-f** showed  $S_A$  phases. For **1d** this was confirmed by small angle X-ray scattering (SAXS), yielding a d-spacing of the layers of 35.7 Å. Inspection of CPK models revealed that this value is consistent with the presence of interdigitized layers (cf. the model displayed in Figure 3.7) of molecules, which are bent at  $C^2$  with an angle of  $110^\circ$  (cf. crystal structure described below). In both the liquid crystalline state and the isotropic state, broad matching peaks were found at 4.6 Å. The resemblance of these peaks indicates that in both cases the packing of the alkyl chains<sup>19</sup> is not very tight, meaning that, in the smectic phase the alkyl chains are rather disordered.

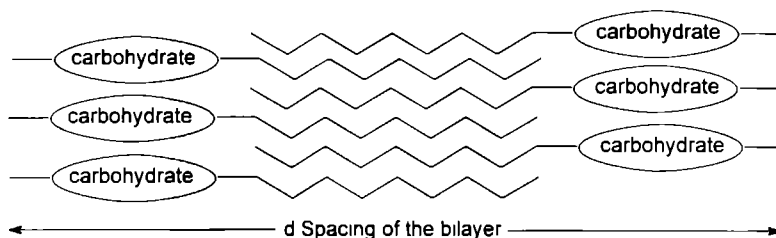
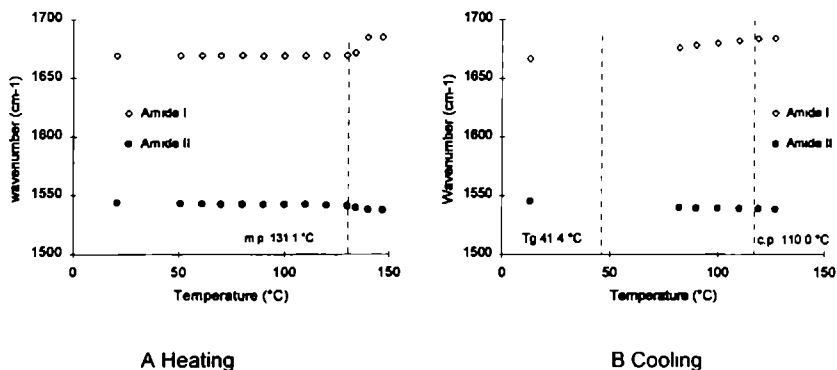


Figure 3.7  $S_A$  phase of compounds 1

In order to further investigate the physical state of the alkyl chains in the L.C. state we performed cross polarization magic angle spinning (CPMAS)  $^{13}\text{C}$ -NMR experiments<sup>40</sup>. With the CPMAS technique it is possible to examine the physical state of molecules or parts of molecules. Unfortunately, the  $S_A$  phases of **1** are monotropic and therefore metastable in the L.C. state. The sample of the compound (**1e**) on which the experiments were carried out crystallized during the measurement, probably because of the rod-like molecules became oriented by the high spinning rates (4500 Hz). The solid state  $^{13}\text{C}$ -NMR and the solution spectrum in  $\text{CDCl}_3$  of **1e** were quite similar although in the solid state the chemical shifts of the imidazole carbon atoms ( $\Delta\delta$  +1.89, -3.22 and +3.87 ppm) and those of the alkyl chains ( $\Delta\delta$  -3.66 ppm) deviated more than average from the shifts of the other carbon atoms (1.22 ppm). This suggests that the imidazole groups interact with each other and that the alkyl chains are closely packed in the solid (crystalline) state.

In order to investigate the existence of hydrogen bonding in the L.C. state, IR-spectroscopy at elevated temperatures<sup>41</sup> was carried out on **1e**. Four different phases were examined: the isotropic phase, the liquid crystalline phase, the crystalline phase and the glass state. The monitored absorptions were the NH stretching, C=O stretching (amide I) and NH bending (amide II) modes. The amide I band showed a shift to a higher wavenumber upon melting (*viz.* from 1669 to 1684  $\text{cm}^{-1}$ ), which is interpreted as being due to a strengthening of the C=O bond (Figure 3.8). This suggests that intermolecular hydrogen bonds are broken when **1e** is melted. The amide II band showed a small shift to a lower value (from 1544 to 1538  $\text{cm}^{-1}$ ). This means that less energy is needed to bend the NH function. The NH vibration at 3343  $\text{cm}^{-1}$  decreased upon melting, while a peak of the non hydrogen bonded NH (at 3435  $\text{cm}^{-1}$ ) came up.

The transition from the isotropic to the L.C. phase (110 °C, see Figure 3.7B) did not have a large effect on the amide I and amide II bands (at 1681 and 1539  $\text{cm}^{-1}$ , respectively) while the shoulder due to the hydrogen bonded NH function (still present in the melted compound) only slightly increased. Further cooling below the glassy state (41.4 °C) resulted in values for the NH vibrations as found in the solid state (3344, with a shoulder at 3472, amide I at 1668 and amide II at 1546  $\text{cm}^{-1}$ ).



**Figure 3.8** IR absorptions observed on heating compound 1e

The absence of shifts observed upon entering the L.C. phase indicates that in this phase no *inter*-molecular hydrogen bonds are present, whereas they do exist in the glassy state. Although the possibility of local crystallization during cooling is always present when dealing with monotropic L.C. phases, it is very unlikely that this had happened in our sample during the measurements because the IR peaks of the alkyl chains in the L.C. and glassy state were broader than in the original crystalline sample, indicating that the packing in the glass was not as regular as in the crystal.<sup>19</sup> The imidazole peaks at 3140 and 3097  $\text{cm}^{-1}$ , which are very sharp in the crystal, fused to one broader peak in the melt (3111  $\text{cm}^{-1}$ ) and in the L.C. phase (3110  $\text{cm}^{-1}$ ), but were separated in the glassy state (3140 and 3102  $\text{cm}^{-1}$ ). This probably means that the imidazole group cannot rotate, move or swing in the crystal and glass but does have this freedom in the melt and L.C. phases.

### 3.3.4 X-ray structure of compound 1a

The exact packing of the molecules in compound 1a was obtained from an X-ray structure determination on a single crystal which was obtained by crystallizing this compound from water. The crystallographic data are presented in Table 3.4, the atomic positional and vibrational parameters are shown in Appendix 3.

**Table 3.4** Crystallographic data for compound **1a**

Formula	C <sub>19</sub> H <sub>31</sub> N <sub>3</sub> O <sub>5</sub> (½ H <sub>2</sub> O not included)
<i>M<sub>r</sub></i>	381.47 (½ H <sub>2</sub> O not included)
space group	P2 <sub>1</sub> 2 <sub>1</sub> 2 <sub>1</sub> (No. 19)
Lattice system	Orthorhombic
Z	4 (+ 2 H <sub>2</sub> O)
a (Å)	5 1230 (13)
b (Å)	7 691 (2)
c (Å)	51 094 (10)
V (Å <sup>3</sup> )	2013.2 (8)
<i>D</i> <sub>calcd</sub> (g cm <sup>-3</sup> )	1.3180 (5)
μ <sub>calcd</sub> (cm <sup>-1</sup> )	0.9
radn (Mo Kα)	0.71073 (graphite mon.)
T (°K)	150
<i>R<sub>F</sub></i> <sup>a</sup>	0.120
<i>R</i> <sub>wF<sup>2</sup></sub> <sup>b</sup>	0.224
S	0.90

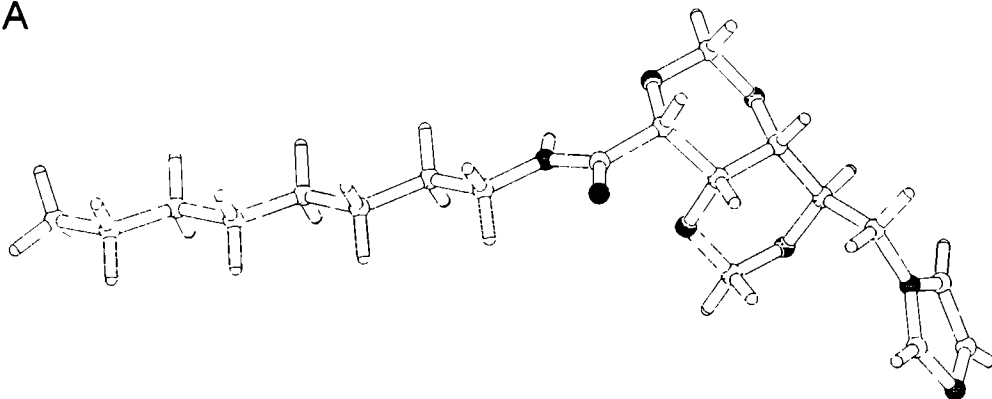
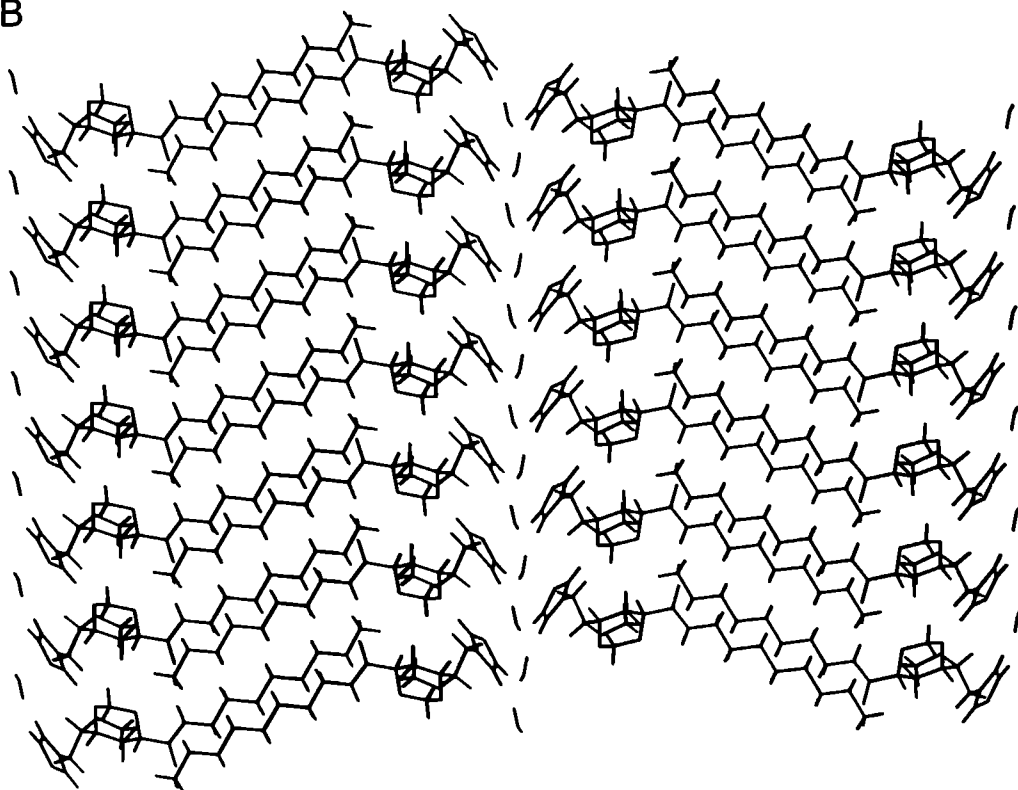
$$^a R_F = \sum |F_o - F_c| / \sum F_o$$

$$^b R_{wF^2} = \sqrt{[\sum w(F_o^2 - F_c^2)^2] / [\sum w(F_o^2)^2]}$$

To our surprise, **1a** crystallized in an interdigitized bilayered structure (see Figure 3.9) which is entirely different from the crystal structures of gluconamide **6a**<sup>18</sup> and related gluconamides,<sup>36,42,43</sup> which display carbohydrate molecules arranged in monolayers. A bilayer structure with interdigitized chains is known to exist for *N*,*n*-octyl-6-deoxy-D-gluconamide<sup>44</sup> and for "double headed" (1*S*,2*S*)-1,2-bis(D-gluconamido) cyclohexane.<sup>45</sup> The alkyl chains of the molecules **1a** do not penetrate in the head group region, but do reach beyond the amide groups which forces these groups to form hydrogen bonding arrays in only one direction, instead of also forming hydrogen bonds with molecules of different arrays. Apparently, the introduction of the dimethylene groups caused a remarkable sharp bend at C<sup>2</sup>. The overall shape of a molecule **1a** is that of a hockey stick (see Figure 3.9A). The sharp bent in the molecule and probably also the disability of **1a** to form a tight hydrogen bonding network creates more space in the tail region. This space is filled by interdigitizing of the tails. A comparable interdigitized packing is found in the well-known liquid crystalline mesogen cholesterol myristate.<sup>46</sup>

Surprising is also the location of the water molecules in the crystal structure of **1a**. These water molecules are hydrogen bonded to the imidazolyl groups and located between different bilayers, in such a way that the stacked gluconamide arrays become separated and the water molecules form layers by themselves. We believe that in the L.C. phase, the hydrogen bonded water molecules form dynamic hydrogen bonding schemes, *i.e.* the H-bonds are no longer fixed in H-bridges between certain pairs of imidazole groups, but are in a process of constantly

breaking up and forming new hydrogen bonds, like water molecules in water. In this way, the water layer between the interdigitized imidazole amphiphile layers acts as a kind of lubricant.

**A****B**

**Figure 3.9** A) Single crystal structure of **1a** B) Packing of **1a**, with interdigitizing alkyl chains and the water molecules between the bilayers

### 3.3.5 Solution $^1\text{H}$ -NMR study on **1a**

In order to determine the structure of **1a** in solution,  $^1\text{H}$ -NMR experiments were carried out in different solvents ( $\text{CDCl}_3$ ,  $\text{CD}_3\text{OD}$ , and  $\text{DMSO}-d_6$ ) and at different temperatures. The  $J$  values obtained from the  $^1\text{H}$ -NMR data were hardly affected by changing the temperature or solvent. As the  $^1\text{H}$ -NMR spectra of **1a** were not first order, the obtained values were checked with a computer simulation program. Dihedral angles were calculated by using the modified Karplus relation published by Altona.<sup>47</sup> Since the torsion angles in crystalline **1a** are known, the virtual  $J$ -couplings of **1a** in the solid state were also calculated (see Table 3.5).

**Table 3.5** Comparison between the dihedral angles of molecules of **1a** in the solid state and in solution

Dihedral angles	X-ray	$^1\text{H}$ -NMR		
	Torsion angles (measured)	$J$ coupling (calc) <sup>a</sup>	$J$ coupling (measured)	Torsion angles (calc)
$\text{H}^2\text{-C}^2\text{-C}^3\text{-H}^3$	$49^\circ$	1.97	1.95	$49^\circ$
$\text{H}^3\text{-C}^3\text{-C}^4\text{-H}^4$	$-48^\circ$	2.03	1.00	$-57^\circ$
$\text{H}^4\text{-C}^4\text{-C}^5\text{-H}^5$	$80^\circ$	0.31	1.20	$94^\circ$
$\text{H}^5\text{-C}^5\text{-C}^6\text{-H}^{6a}$	$48^\circ$	2.89	5.10	$33^\circ$
$\text{H}^6\text{-C}^5\text{-C}^6\text{-H}^{6a}$	$166^\circ$	10.69	9.95	$157^\circ$

<sup>a</sup> Calculated from torsion angles derived from the X-ray data

Given the fact that the values of the calculated torsion angles in solution are not as accurate as the angles obtained from the crystal structure, we may conclude from Table 3.5 that the conformations of the head group of **1a** (including the bend) in the crystalline state and the solution state are quite similar.

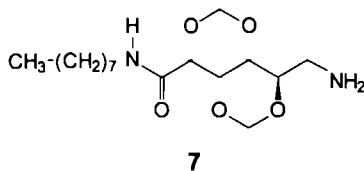
### 3.3.6 Thermotropic L.C. behavior of compounds related to imidazolyl gluconamides **1**

#### 3.3.6.1 Different substituents on the terminus of the head group

The ability of compounds **1** to form L.C. phases is surprising. In this section we will try to establish by applying structural variations in **1** which parts of the molecule are indispensable for the formation of a mesophase.

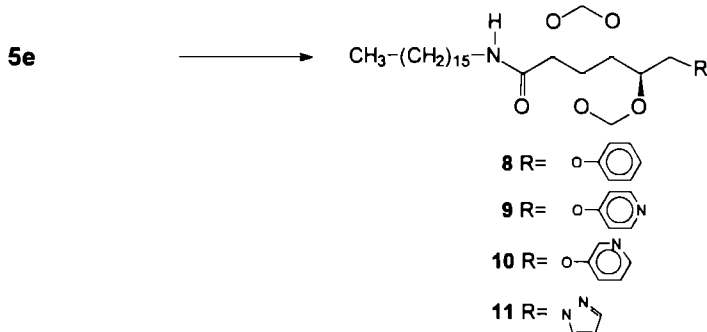
From Figure 3.5B it is clear that for achieving L.C. behavior the imidazole-containing bismethylene protected gluconamides must have alkyl chains of at least 12 carbon atoms length. This length, however, does not guarantee L.C. behavior as can be concluded from the fact that the set of compounds **4a-e** is not L.C. An exception is **4f** which contains an octadecyl chain, but this compound shows a L.C. phase which is different from the smectic phase usually observed for this type of compounds.

All compounds in this section with the exception of compound **7** (which contains an octyl chain) possess a hexadecyl chain, to exclude the possibility that insufficient chain length will prevent the formation of a L.C. phase.



The derivatives **8-11** (see Scheme 3.3), were synthesized by substitution of the tosyl group of gluconamide **5e** by a H-bond accepting aromatic group (except **8**). The rationale behind the synthesis of compounds **9-11** was that water molecules may form *interlayer* hydrogen bonds with the pyridyl and pyrazolyl groups of **9-11** resulting in a structure in which the bilayers are separated by water-layers in a similar way as found for **1a**. The position of the hetero-atom was also varied for both the 5 and 6 membered aromatic rings (**1e** versus **11** and **9** versus **10**). Compound **8** contains a phenyl group and was prepared with the objective to disturb the tight packing of the carbohydrate head groups, which might prevent crystallization resulting in hysteresis upon cooling and the generation of monotropic LC behavior. Although **8** does not have a nitrogen or oxygen atom and therefore is not a potential H-bond acceptor, it still contains an aromatic group that can display  $\pi$ - $\pi$  stacking interactions with similar groups of molecules present in the layers.

Scheme 3.3

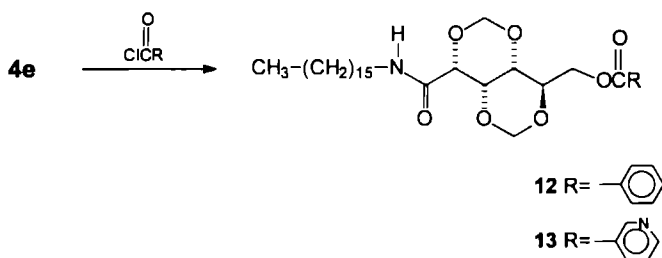


Compound **8** did not show LC behavior and neither did **9**. Apparently,  $\pi$ - $\pi$  stacking was absent or the interaction was too weak to generate LC behavior. The lack of the formation of a mesophase in the case of **9** is surprising, because pyridyl groups are known to form hydrogen bridges<sup>48</sup> and it was expected that water molecules would have formed an additional layer as observed in the X-ray of **1a**. The melting points of compounds **1e** and **9** were found to be almost similar (see Table 3.6), but **9** crystallized at 114 °C, which is above the c.p. of **1e** (110 °C). Compound **8** had a s.p. of 105 °C which is below the c.p. of **1e** and could have given a LC phase if molecules of **8** had been packed in a similar way as molecules of **1e**. Compound **10** behaved

differently from the other compounds and showed an enantiotropic smectic A phase with a m.p. of 95.2 °C and a c.p. of 194 °C. An explanation for the fact that **10** displays thermotropic L.C. behavior and **9** does not, cannot yet be given.

Since **8** does not form a L.C. phase, it can be concluded that a nitrogen atom in the aromatic ring is needed. The absence of L.C. phases in the case of **9** and **11** and the presence of an L.C. phase in the case of **10** suggests that with these type of compounds the nitrogen has to be on the right position of the aromatic ring. The packing of the molecules probably forces the nitrogen centers in a position where hydrogen bonding is possible (**1e** and **10**) or not (**9** and **11**).

Scheme 3.4



**Table 3.6** Thermotropic L C behavior of gluconamides with different C<sup>6</sup> substituents

compound	m p (°C) <sup>a</sup>	c p (°C) <sup>b</sup>
<b>4e</b>	105.5 (39.8)	---
<b>1e</b>	131.1 (64.2)	110.0 (15.8)
<b>7</b>	131.3 (9.9)	---
<b>8</b>	122.6 (40.1)	---
<b>9</b>	130.1 (30.2)	---
<b>10</b>	95.2 (13.2)	194 (27.8)
<b>11</b>	103.8 (26.8)	---
<b>12</b>	127.7 (54.7)	---
<b>13</b>	124.6 (49.5)	---

<sup>a</sup> Melting point,  $\Delta H_{\text{melt}}$  (kJ/mol) in parentheses

<sup>b</sup> Clearing point,  $\Delta H_{\text{clearing}}$  (kJ/mol) in parentheses

The phenyl and meta pyridyl groups were also coupled to the gluconamide framework via an ester linkage (to give compounds **12** and **13**, see Scheme 3.4). Both compounds did not show L.C. behavior although the melting points were in line with the series of compound **1**. We had expected that **12** and **13** would have shown hysteresis (and therefore a L.C. phase), because the rigid methylene protected carbohydrate part is now placed in between 2 rather floppy parts which

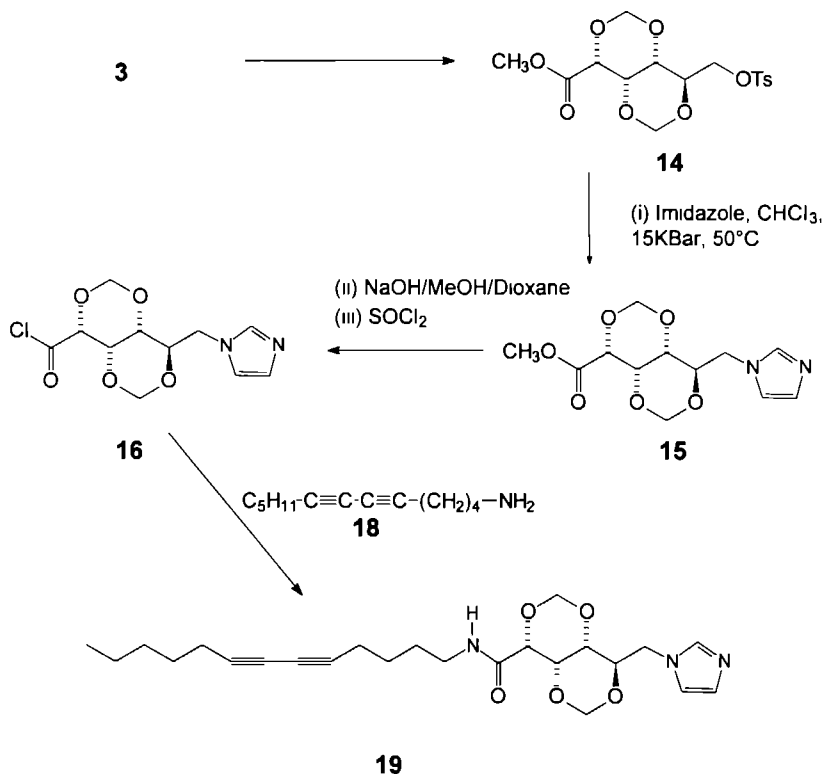


could have prevented crystallization at high temperatures. Unfortunately, the solidification points (s.p.) of **12** and **13** were too high (110.7 and 110.2 °C, respectively). No special trends could be detected in the  $\Delta H_{\text{melt}}$  or  $\Delta H_{\text{clearing}}$  values of compounds **7-13**.

### 3 3 6 2 Gluconamides with a diacetylene function in the alkyl chain

In order to study the effect of a modification in the alkyl chain of the gluconamides **1**, we synthesized compound **19** (Scheme 3.5).

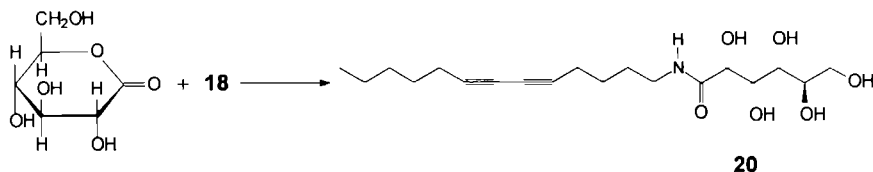
**Scheme 3.5**



Replacing the n-alkyl chain of **1d** by a diacetylene chain in **19** resulted in loss of L.C. behavior. The melting point (129.8 °C) of **19** was similar to the melting points of compounds of **1a-f**, but the diacetylene compound did not show the strong hysteresis needed for monotropic L.C. behavior: upon cooling it crystallized (s.p. 113.9 °C) before the L.C. phase was entered. On the other hand, introduction of the diacetylene function in a non-modified gluconamide derivative **20** (synthesized according to Scheme 3.6) did not result in a loss of L.C. behavior although the mesophase was destabilized by a drop in the c.p. (m.p. 152.5 °C,  $\Delta H_{\text{melt}} = 56.3$  kJ/mol, c.p. 167.8 °C, compare with Table 3.1). This is in line with the postulate<sup>10,37,49</sup> that the interactions of

the tails are disrupted at the clearing point and not at the melting point. We therefore may conclude that diacetylene functions destabilize the L C phase but do not prevent the formation of such a phase as long as this phase is enantiotropic.

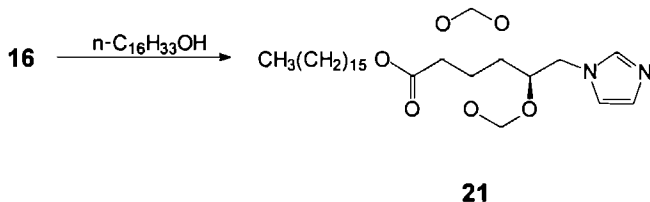
Scheme 3.6



### 3.3.6.3 *n*-Alkyl gluconates

In the literature<sup>35</sup> the ester analog of gluconamide **6a** has been described. Changing the amide function for an ester function did not have a large influence on the thermotropic behavior of the compound. The ester connection in the methylene protected imidazole derivative **21** (synthesized according to Scheme 3.7), however, did have a strong influence on the thermotropic properties. The melting point (94.7 °C) of **21** was found to be strongly decreased with respect to **1e** and was found to lie even below the c.p. of the latter compound. Compound **21**, however, did form a monotropic L C phase (S<sub>A</sub>) upon cooling (c.p. 88.3 °C), which is what one would expect because the amide function of **1e** does not form *intermolecular* hydrogen bonds in the mesophase (see Section 3.3.3). Despite the decrease of the melting point no *enantiotropic* L C behavior was displayed by **21**. Since **21** and **1e** form L C phases at different temperatures, the ordering of the molecules in the L C phase is probably different.

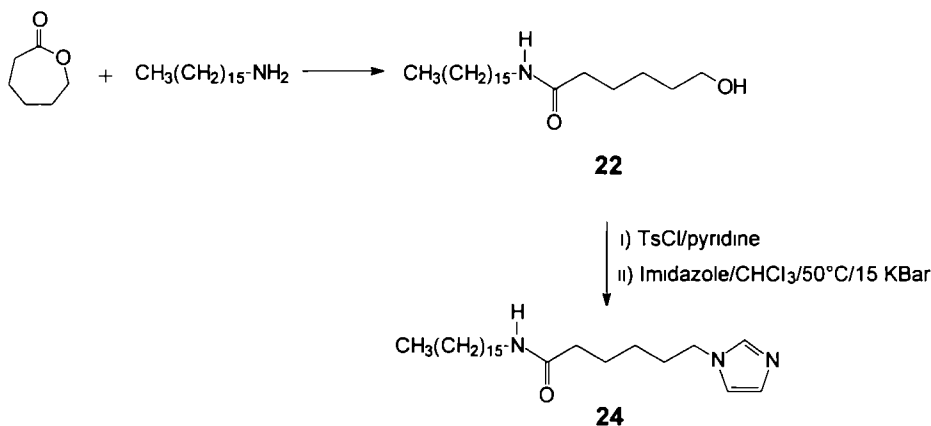
Scheme 3.7



### 3.3.6.4 Amide without the carbohydrate part

In order to investigate the influence the carbohydrate part in compounds **1** on the L C behavior, this rigid moiety was replaced by a flexible *n*-alkyl chain. Compound **24** and reference compound **22** were synthesized as shown in Scheme 3.8. Neither of these compounds showed L C behavior. A similar negative result was obtained in the case of 1-*n*-hexadecylimidazole (**25**).

Scheme 3.8



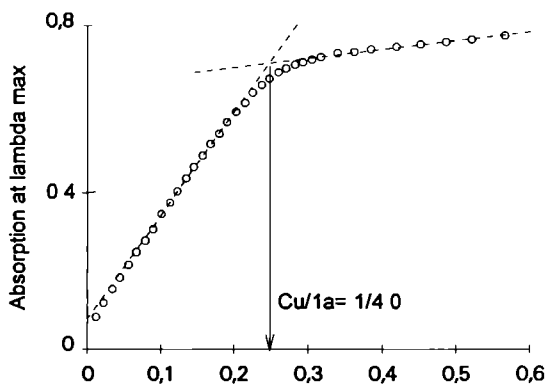
Apparently the inflexible carbohydrate part is necessary to achieve L.C. behavior with this type of compounds.

### 3.3.7 Metallomesogens

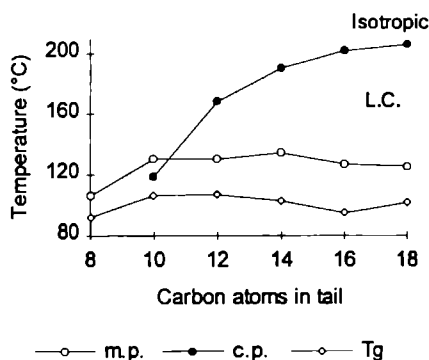
Imidazolyl (Im) compounds **1** were found to give 1/4 (Cu/Im) complexes with copper(II) ions as was determined by UV-vis titrations in methanol (see Figure 3.10).<sup>15</sup> The copper salts used had non-coordinating counter ions, *viz* triflate [OSO<sub>2</sub>CF<sub>3</sub>]. For safety reasons this triflate ion was chosen instead of the more commonly used perchlorate anion.<sup>50</sup> Apart from the octyl derivative (**1a**)<sub>4</sub>Cu, all copper complexes of **1** ((**1b**)<sub>4</sub>Cu - (**1f**)<sub>4</sub>Cu) precipitated from dark-blue colored ethanolic solutions, leaving almost colorless supernatants. The complexes (except for (**1f**)<sub>4</sub>Cu) contained approximately one coordinated molecule of ethanol or water which was released at approximately 65 °C, according to thermogravimetric analysis.

Complexes (**1c**)<sub>4</sub>Cu-(**1f**)<sub>4</sub>Cu showed enantiotropic mesophases (S<sub>A</sub>), while (**1b**)<sub>4</sub>Cu appeared to be monotropic (see Table 3.7 and Figure 3.11). The resemblance of the melting points of compounds **1a-f** with those of the complexes (**1a**)<sub>4</sub>Cu-(**1f**)<sub>4</sub>Cu is remarkable and for both the free ligands, and the copper complexes, the clearing points depend on the length of the alkyl chain (Figure 3.11).

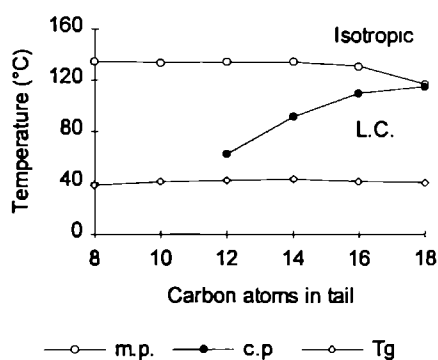
The great similarities in phase behavior (type of L.C. phase, melting points, clearing points and glass transition temperatures in the series of metal free ligands and copper complexes (compare Figure 3.11A and 3.11B) indicates, that the association behavior of the two types of compounds is the same.

Figure 3.10 UV-vis titration of **1a** with  $[\text{Cu}][\text{triflate}]_2$ Table 3.7 Thermotropic behavior of complexes  $(\mathbf{1a})_4\text{Cu}$ – $(\mathbf{1f})_4\text{Cu}$ <sup>a</sup>

Complex	n <sup>b</sup>	m p (°C)	c p (°C)	T <sub>g</sub> (°C)
( <b>1a</b> ) <sub>4</sub> Cu	8	105.8	---	91.8
( <b>1b</b> ) <sub>4</sub> Cu	10	130.6	119.0	106.4
( <b>1c</b> ) <sub>4</sub> Cu	12	130.5	168.2	106.8
( <b>1d</b> ) <sub>4</sub> Cu	14	134.6	190.6	102.7
( <b>1e</b> ) <sub>4</sub> Cu	16	127.1	202.1	94.9
( <b>1f</b> ) <sub>4</sub> Cu	18	125.9	206.4	101.7

<sup>a</sup> Obtained from DSC thermograms<sup>b</sup> Number of carbons in alkyl chain

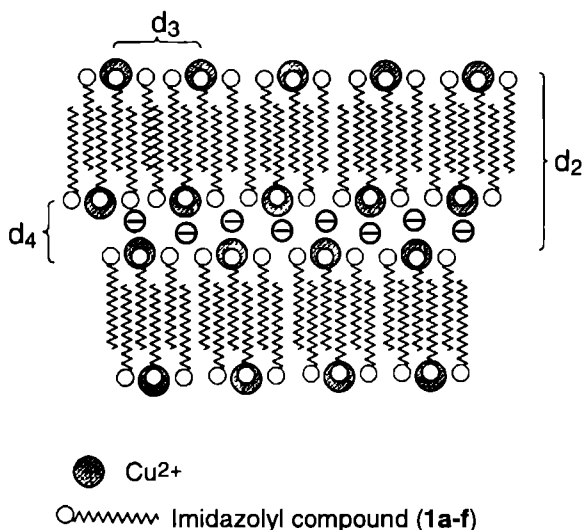
A



B

**Figure 3.11** Thermotropic LC behavior of gluconamides. The melting points were derived from heating curves, the glass transition temperatures from cooling curves. A) complexes  $(\mathbf{1a})_4\text{Cu}$ – $(\mathbf{1f})_4\text{Cu}$ . B) Free ligand.

SAXS experiments at elevated temperatures on **1d** and **(1d)<sub>4</sub>Cu** revealed that the bilayer thicknesses of the copper complex and the imidazolyl ligands in the smectic phase are almost equal (for compounds **1d** and **(1d)<sub>4</sub>Cu** 35.7 and 36.2 Å respectively). In the copper complex **(1d)<sub>4</sub>Cu**, however, besides the broad band corresponding to the spacing of the alkyl chains ( $d_1=4.6$  Å) and the reflection due to the aforementioned bilayer distance ( $d_2=36.2$  Å), two other relatively sharp reflections at  $d_3= 3.4$  Å and at  $d_4= 2.9$  Å were observed. The latter two can be assigned to copper-copper distances. Besides an *inter*-layer copper-copper distance there is also an *intra*-layer copper distance. The intensity of the  $d_4$  peak increased enormously when the sample of **Cu(1d)<sub>4</sub>** was cooled below the glass transition temperature whereas that of  $d_3$  remained exactly the same. Our interpretation is that the  $d_3$  spacing is the *intra*-layer copper-copper distance, which remains the same for the glassy state and the smectic state. In the smectic state the layers can exhibit lateral movement and the *inter*-layer Cu - Cu distance which probably corresponds with  $d_4$ , is not very well defined. By freezing the system into the glassy state the amount of ordering is increased and as a result the  $d_4$  reflection at 2.9 Å is enlarged. In this model (Figure 3.12) ion-rich regions are separated by hydrophobic layers and a molecular laminate<sup>51</sup> is created.



**Figure 3.12** Molecular laminate formed from the copper complexes of compounds **1a-f**

The above proposed model for the arrangement of the copper complexes is similar to that of the metal free ligands as derived from the X-ray structure of **1a**. Upon formation of the copper complex, the water molecules in the assembly of the metal free ligands are replaced by copper ions and counterions, which results in a stabilization of the L.C. phase as can be deduced from the shift of the clearing points to higher temperatures (see Figures 3.11A and B). In the case of the complexes the counterions instead of the water molecules act as the lubricant.

This replacement theory is supported by fact that the copper complex of the diacetylene imidazole derivative,  $(19)_4\text{Cu}$ , and the copper complex of the pyridyl compound,  $(9)_4\text{Cu}$ , do not form a L C phase, like the metal free ligands (**9** and **19**)

The copper complex of **24**,  $(24)_4\text{Cu}$ , showed L C behavior, but in contrast to **1** and  $(1)_4\text{Cu}$ , the amides without the carbohydrate part did not have comparable melting points (65.9 °C for **24** and 118.8 °C for  $(24)_4\text{Cu}$ ). Complex  $(24)_4\text{Cu}$  showed only one clearing point upon heating (139.2 °C,  $\Delta H_{\text{clearing}}$  39.2 kJ/mol complex), but in the cooling run, besides the crystallization point (103.2 °C,  $\Delta H_{\text{solid}}$  147.5 kJ/mol), two phase transitions were detected (130.3 °C,  $\Delta H$  1.6 kJ/mol and 128.3 °C,  $\Delta H$  49.7 kJ/mol). The types of L C phase were not identified, but from the second  $\Delta H_{\text{clearing}}$  value and the high viscosity of the low temperature L C phase it can be concluded that either the mesophase is highly ordered or the layers of molecules are undulated.<sup>52</sup> The copper(II) complex of **25**,  $(25)_4\text{Cu}$ , showed an enantiotropic and highly ordered L C phase between 70.8 and 162.0 °C ( $\Delta H_{\text{clearing}}$  60.4 kJ/mol). The type of phase is not known, but the observed textures were similar to those of  $(24)_4\text{Cu}$ .

A 4:1 complex of **1e** and  $[\text{Ni}][\text{BF}_4]_2$  ( $(1e)_4\text{Ni}$ ) was prepared in an analogous way as the preparation of  $(1e)_4\text{Cu}$ . This complex also showed a L C phase which was, according to observed textures under the polarization microscope, a  $S_A$  phase (m.p. 160.0 °C, c.p. 224.9 °C).

To the best of our knowledge this is the first report both of carbohydrate metallomesogens as well as of mesogens based on imidazole complexes. Other metallomesogens from copper complexes have been described before.<sup>53</sup>

### 3.4 Concluding remarks

As methylene bridges are very rigid and capable of determining the shape of the carbohydrate part in 2,4,3,5-dimethylene-*N*,*n*-alkyl-D-gluconamides, this type of protecting group is also useful to stimulate L C behavior. Although it is generally accepted that hydrogen bonds are important and even required for obtaining carbohydrate liquid crystals,<sup>34</sup> we have shown that with methylene protecting groups a rigid tetraoxa-*cis*-decalin moiety is generated which, in combination with an imidazole function, also creates a L C phase. Incorporation of pyridyl groups also leads to L C phases, due to a hysteresis effect, but the formation of the mesophase is very sensitive to the type of pyridyl group used: a 3-pyridyloxy yields a L C phase, whereas a 4-pyridoxy and a 3-pyridoxy-carboxylate group do not. The introduction of protecting groups affects the hydrogen bonding character of the carbohydrate part, but the typical curves in which the length of alkyl chain is plotted versus the melting or clearing point resemble those of the unmodified *n*-alkyl-D-gluconamides. Our IR experiments showed that the amide functions do not form a hydrogen bonding array in the L C phase, which is remarkable because in traditional carbohydrate liquid crystals such arrays are very important.<sup>48</sup> Apparently, the rigid *cis*-decaline structure of the dimethylene substituted glucon group dominates the packing of the molecules in the same way as the non-protected carbohydrate part does in traditional carbohydrate liquid crystals. This packing behavior is not affected by the introduction of copper ions, which complex to the imidazole groups. In the metal-free systems, the choice of a substituent on carbon atom 6 of

the carbohydrate moiety in order to obtain L.C. behavior is rather subtle. For some as yet unknown reason there has to be a hydrogen bonding or dipole-dipole interaction between the bilayers, otherwise non-hydrogen bonding substituents like phenoxy and benzoate should also have led to L.C. phases. On the other hand, groups with strong hydrogen bonding capacities like hydroxyl and amine groups also failed to form mesophases. Imidazole and pyridine groups which both are weak hydrogen bond acceptors proved to be successful in the formation of L.C. phases. This type of substituents contains a nitrogen atom in the correct position, which can interact with the succeeding layer (possible via H-bonds from water molecules). Water molecules hydrogen bonded by imidazole groups, can act as lubricants in the L.C. phase, by forming a dynamic hydrogen bonded network. Addition of copper(II) ions leads to exchange of the water molecules for copper ions and the L.C. phase is stabilized. In this metallomesogenic system the (non-coordinating) counter ions are acting as a lubricant.

The connection of the alkyl chain to the glucon group can be either an ester or an amide group. The alkyl chain must be flexible and long enough ( $\geq 12$  carbon atoms) otherwise the compound will not show monotropic L.C.-behavior and crystallize or will be trapped in the glassy state before the L.C. phase is entered.

### 3.5 Literature

<sup>1</sup> Schnur, J M , Shashidhar, R *Adv Mat* **1994**, *6*, 971

<sup>2</sup> Feiters, M C *Supramolecular technology and applications* Vol 10, part III, Chap 16, *Supramolecular catalysis* vol. ed Reinhoudt, D.N. part of the series "Comprehensive Supramolecular Chemistry" ed Lehn, J -M , **1995**

<sup>3</sup> Lehn, J -M. *Angew Chem* **1988**, *100*, 91, *Ibid Int Ed Engl* **1988**, *27*, 89.

<sup>4</sup> a) Fuhrhop, J.-H , Helfrich, W. *Chem Rev* **1993**, *93*, 1565, b) Ahuja, R , Caruso, P -L ; Möbius, D , Paulus, W , Ringsdorf, H , Wildburg, G *Angew Chem* **1993**, *105*, 1082 , *Ibid Int Ed Engl* **1993**, *32*, 1033, c) Kunitake, T ; Okahata, Y.; Shimomura, M ; Yasunami, S.-I ; Taharabe, K *J Am Chem Soc* **1981**, *103*, 5401, d) Fendler, J.H. *Membrane Mimetic Chemistry*, New York, **1982**; e) Kunitake, T., *Angew Chem* **1992**, *104*, 692, *Ibid Int Ed Engl* **1992**, *31*, 709; f) Ringsdorf, H , Schlarb, B , Venzmer, J. *Angew Chem* **1988**, *100*, 117; *Ibid Int Ed Engl* **1988**, *27*, 113

<sup>5</sup> a) Percec, V ; Tomaros, D., *Compr Polym Sci, suppl Vol I* vol ed. G Allen, *Pergamon Press Oxford* **1992**, 300 , b) O'Brien, D.F , Kuo, T.; Liman, U ; Lamparski, H. *Polym J* **1991**, *23*, 619., c) Kwolek, S L ; Morgan, P W ; Schaefer, J.R. *Encycl Polym Sci & Eng* ed. Mark, Bikales, Menges **1987**, *9*, 1, d) Zentel, R *Comp Polym Sci* 5, *Pergamon Press Oxford* **1989**, 723.

<sup>6</sup> Jeffrey, G.A.; Wingert, L M. *Liq Cryst.* **1992**, *12*, 179

<sup>7</sup> Chandrasekhar, S., Ranganath, G.S *Rep Prog Phys.* **1990**, 57

<sup>8</sup> Zarges, W.; Hall, J., Lehn, J -M. *Helv Chim Acta* **1991**, *74*, 1843

<sup>9</sup> a) Fuhrhop, J.-H.; Schnieder, P.; Rosenberg, J.; Boekema, E *J Am Chem Soc* **1987**, *109*, 3387; b) Fuhrhop, J -H , Schnieder, P., Boekema, E.; Helfrich, W. *J Am. Chem Soc* **1988**, *110*, 2861, c) Boettcher, C , Boekema, E., Fuhrhop, J.-H. *J Microscopy* **1990**, *160*, 173; d) Fuhrhop, J.-H.; Boettcher, C *J Am Chem Soc* **1990**, *112*, 1768;

- e) Fuhrhop, J.-H., Svenson, S., Boettcher, C., Rössler, E., Vieth, H.-M. *J Am Chem Soc* **1990**, *112*, 4307, f) Köning, J., Boettcher, C.; Winkler, H.; Zeitler, E.; Talmon, Y.; Fuhrhop, J.-H. *J Am Chem Soc* **1993**, *115*, 693, g) Frankel, D.A., O'Brien, D.F. *J Am Chem Soc* **1991**, *113*, 7436; h) Pfannemüller, B. *Starch/Starke* **1988**, *40*, 476
- <sup>10</sup> Doren, van H. *Ph D Thesis Groningen*, **1989**
- <sup>11</sup> Doren, van H.; Wingert, L.M. *Mol Cryst Liq Cryst* **1991**, *198*, 381; Hentrich, F., Tschierke, C., Zschke, H. *Angew Chemie* **1991**, *103*, 429, *Ibid Int Ed Engl*, **1991**, *30*, 440; Doren, van H., Wingert, L.M. *Recl Trav Chim Pays-Bas* **1994**, *113*, 260; and ref. 10
- <sup>12</sup> For reviews on lamellar phases see: Hoffmann, H. *Ber Bunsenges Phys Chem* **1994**, *98*, 1433, Pas, van de J.C., Buytenhek, C.J., Brouwn, L.F. *Recl Trav Chim Pays-Bas* **1994**, *113*, 231, Thomas, B.N.; Safinya, C.R., Plano, R.J., Clark, N.A. *Science* **1995**, *267*, 1635, Hoffmann, H., Ulbricht, W. *Chemie in Unsere Zeit* **1995**, *29*, 74, Sein, A. *Ph D Thesis Groningen* **1995**
- <sup>13</sup> a) Kunitake, T.; Okahata, Y.; Shimomura, M.; Yasunami, S.-I., Takarabe, K. *J Am Chem Soc* **1981**, *103*, 5401, b) Kunitake, T. *Angew Chem* **1992**, *104*, 692, *Ibid Int Ed Eng* **1992**, *31*, 709
- <sup>14</sup> Reeves, R.E. *Adv Carbohydr Chem* **1951**, *6*, 107
- <sup>15</sup> Reedijk, J. *Recl Trav Chim Pays-Bas*, **1969**, *88*, 1451
- <sup>16</sup> Hafkamp, R.J.H., Feiters, M.C., Nolte, R.J.M. *Angew Chem* **1994**, *106*, 1054; *Ibid Int Ed Engl* **1994**, *33*, 986
- <sup>17</sup> For reviews on metallomesogens see: (a, general) Espinet, P., Esteruellas, M.A., Oro, L.A.; Serrano, J.L.; Sola, E. *Coord Chem Rev* **1992**, *117*, 215; (b, discotic) Giroud-Godquin, A.-M.; Maitlis, P.M. *Angew Chem* **1991**, *103*, 370, *Ibid Int Ed Eng* **1991**, *30*, 375; (c, calamitic) Hudson, S.A.; Maitlis, P.M. *Chem Rev* **1993**, *93*, 861; (d, polymeric) Oriol, L., Serrano, J.L. *Adv Mat* **1995**, *7*, 348
- <sup>18</sup> Pfannemüller, B., Welte, W. *Chem Phys Lipids* **1985**, *37*, 227.
- <sup>19</sup> Svenson, S., Fuhrhop, J.-H., Köning, J. *J Phys Chem* **1994**, *98*, 1022
- <sup>20</sup> Zabel, V., Müller-Fahmow, A., Hilgenfeld, R., Saenger, W., Pfannemüller, B., Enkelmann, V., Welte, W. *Chem Phys Lipids* **1986**, *39*, 313.
- <sup>21</sup> geNMR V 3.3 (1990), (P.H.M. Budzelaar) NMR simulation package, IvorySoft®, Amsterdam, The Netherlands
- <sup>22</sup> Zief, M., Scattergood, A. *J. Am Chem. Soc* **1947**, *69*, 2132.
- <sup>23</sup> Mehlretter, C.L.; Mellies, R.L.; Rist, C.E.; Hilbert, G.E. *J Am Chem Soc* **1947**, *69*, 2130
- <sup>24</sup> McCaldin, D.J. *Chem Rev* **1960**, *60*, 39.
- <sup>25</sup> Tesser, G.I.; Bolvert-Geers, I.C. *Int J Peptide Protein Res.* **1975**, *7*, 295.
- <sup>26</sup> Brandsma, L. *Acetylenic Chemistry, Studies in Organic Chemistry*, Elsevier Amsterdam **1988**, 21.
- <sup>27</sup> Ref 26 page 59
- <sup>28</sup> Smiley, R.A.; Arnold, C. *J Org Chem* **1960**, *25*, 257
- <sup>29</sup>  $\text{AlH}_3$  was prepared by addition of conc  $\text{H}_2\text{SO}_4$  to  $\text{LiAlH}_4$  in THF, Yoon, N.M.; Brown, H.C. *J Am Chem Soc* **1967**, *90*, 2927
- <sup>30</sup> Chittenden, G.J.F., Univ. of Nijmegen (personal communication).
- <sup>31</sup> For the preparation of cyclic carbonates see a) Komura, H., Yoshino, T., Ishido, Y. *Carbohydrate Res* **1940**, *40*, 391, b) Raaijmakers, H.W.C. *Ph D Thesis, Univ of Nijmegen* **1993**, 115
- <sup>32</sup> For ring opening reactions see Yoshino, T., Inaba, S.; Komura, H.; Ishido, Y. *Bull Chem Soc Japan* **1974**, *47*, 405



- <sup>33</sup> Whistler, Walfrom *Methods in Carbohydrate Chemistry*, Bonner, T G [82], 19, 314
- <sup>34</sup> Jeffrey, G A *Acc Chem Res* 1986, 19, 168
- <sup>35</sup> Pfannemüller, B, Welte, W, Chin, E, Goodby, J W *Liq Cryst* 1986, 1, 357
- <sup>36</sup> Jeffrey, G A, Maluszynska, H *Carbohydr Res* 1990, 207, 211
- <sup>37</sup> Baeyens-Volant, D, Fornasier, R, Szalai, E, David, C *Mol Cryst Liq Cryst* 1985, 135, 93
- <sup>38</sup> Doren, H A van, Wingert, L M *Mol Cryst Liq Cryst* 1991, 198, 381
- <sup>39</sup> Monotropic means that the mesophase is observed only during cooling as a consequence of hysteresis, while with enantiotropic L C phases the mesophase is observed both on heating and cooling
- <sup>40</sup> Svenson, S, Kirste, B, Fuhrhop, J-H *J Am Chem Soc* 1994, 116, 11969
- <sup>41</sup> Lutz, E T G, Maas van der J H *J Mol Struct* 1994, 123
- <sup>42</sup> Müller-Fahrmow, A, Hilgenfeld, R, Hesse, H, Saenger, W, Pfannemüller, B *Carbohydr Res* 1988, 176, 165
- <sup>43</sup> Müller-Fahrmow, A, Saenger, W, Fritsch, D, Schnieder, P, Fuhrhop, J-H *Carbohydr Res* 1993, 242, 11
- <sup>44</sup> Herbst, R, Steiner, T, Pfannemüller, B, Saenger, W *Carbohydr Res* 1995, 269, 165
- <sup>45</sup> Andre, Ch, Luger, P, Nehmzow, D, Fuhrhop, J-H *Carbohydr Res* 1994, 261, 1
- <sup>46</sup> Craven, B M, DeTitta, G T *J Chem Soc Perkin Trans 2* 1976, 814
- <sup>47</sup> Haasnoot, C A G, de Leeuw, F A A M, Altona, C *Tetrahedron* 1980, 36, 2783
- <sup>48</sup> Paleos, C M, Tsiourvas, D *Angew Chem* 1995, 107, 1839, *Ibid Int Ed Eng* 1995, 34, 1696
- <sup>49</sup> Doren, H A van, Geest, R van der, Keuning, C A, Kellog, R M, Wynberg, H *Liq Cryst* 1989, 5, 265
- <sup>50</sup> Wolsey, W C *J Chem Educ* 1973, 50, A335
- <sup>51</sup> Menger, F M, Lee, J-J, Hagen, S *J Am Chem Soc* 1991, 113, 4017
- <sup>52</sup> Neve F, Ghedini, M, Munno, de G, Levelut, A -M *Chem Mater* 1995, 7, 688
- <sup>53</sup> Liquid crystals of copper complexes a) Hoshino, N, Murakami, H, Matsunaga, Y, Maruyama, Y *Inorg Chem* 1990, 29, 1177, b) Galyametdinov, Yu G, Polishchuk, A P, Bikchantaev, I G, Ovchinnikov, I V *J Struct Chem* 1993, 34, 872, c) Maldivi, P, Bonnet, L, Giroud-Godquin, A -M, Ibn-Elhaj, M, Guillon, D, Skoulios, A *Adv Mat* 1993, 5, 909, d) Zheng, H, Lai, C K, Swager, T M *Chem Mat* 1994, 6, 101, e) Alonso, P J, Marcos, M, Martinez, J I, Serrano, J L, Sierra, T *Adv Mat* 1994, 6, 667, f) Neve, F, Ghedini, M, Levelut, A -M, Francescangeli, O *Chem Mat* 1994, 6, 70, g) Molta, M F R, Duarte, M L T S *J Chem Soc Faraday Trans* 1994, 90, 2953

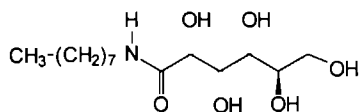
# Chapter 4

## Suprastructures in water from imidazole containing gluconamides

### 4.1 Introduction

Compounds with a hydrophilic and a hydrophobic part are called amphiphilic and can form aggregates in aqueous solution. Carbohydrate derivatives are of great interest as building blocks for amphiphiles because they are chiral and easily accessible in a great variety of structures. Moreover, they can be easily modified using known synthetic methodology. Pfannemüller was the first to synthesize *N*,*n*-alkyl-D-gluconamides of type **1** and to show that these carbohydrate derivatives form helical fibers in water,<sup>1</sup> with a regular twist and a high aspect ratio (up to  $10^4$ ).<sup>3</sup>

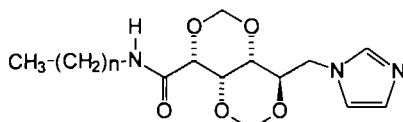
Fuhrhop and coworkers<sup>2</sup> subsequently studied these helical aggregates in great detail by electron microscopy in combination with image analysis,<sup>3</sup> NMR,<sup>4</sup> IR, and powder diffraction<sup>5</sup> and concluded that they consist of micellar fibers. The amphiphiles in the suprastructures are packed in a crystalline order. Variation in the stereochemistry of the head group of the *N*-alkylaldonamides resulted in different suprastructures like stacked bilayers, rolled-up sheets and whisker-type fibers.<sup>6</sup>



**1**

The possibility to tune the structure of the aggregates derived from aldonamides has not been investigated so far, although studies with other systems have been reported in the literature. For instance the sugar analogue *N*,*n*-dodecyltartaric acid monoamide has been shown to form cloth-like aggregates, but only at a pH close to the  $pK_a$  of tartaric acid,<sup>7</sup> suggesting that the structure of the aggregates can be fine-tuned by the pH. In another example, the size and length of hollow tubules made from negatively charged diacetylenic phospholipids could be modified by changing the head group size, the pH, the ionic strength, the type of anion, and the dispersion medium (water-ethanol mixtures).<sup>8</sup> Kunitake has shown that addition of  $Ca^{2+}$  ions to azobenzene phosphate amphiphiles alters the orientation of the head groups in such a way that helical structures are obtained.<sup>9</sup> It has been reported that the length of helical bilayer assemblies prepared from peptide amphiphiles can be shortened by the addition of  $Ba^{2+}$  and  $Ca^{2+}$  ions.<sup>10</sup> 12-Hydroxystearic acid has been shown to form twisted fibers and helical tapes in water.<sup>11</sup> The sense of the twist can be modified by adding metal ions, e.g. complexation of  $Li^+$  ions to D-12-hydroxystearic acid yields fibers with a right-handed twist, whereas complexation of  $Rb^+$  or  $Cs^+$  leads to fibers with a left-handed twist. Phosphatidylserines form aggregates of which the structures can be tuned by addition of calcium ions. In the presence of these ions, scrolls are obtained. Removal of the  $Ca^{2+}$  by EDTA results in vesicles.<sup>12</sup>

In this chapter we show that gluconamide-derivative **2a** forms suprastructures in water which can be tuned by changing the pH or the addition of metal ions.<sup>13</sup>



**2a**  $n = 7$   
**b**  $n = 11$   
**c**  $n = 15$

A series of compounds related to **2a** has been synthesized in which the head group, the alkyl chain and the linker between this chain and the carbohydrate moiety has been altered. The influence of these changes on the formation of the suprastructures in water has been investigated with EM and DSC. This chapter also describes the copper complexation behavior of **2a**, which has been studied in detail by UV-vis titrations and by EM.

## 4.2 Experimental

Transmission electron micrographs (TEM) were made on a Philips EM201 instrument (using an acceleration voltage of 60 kV) and a Jeol JEMCXII (60 kV) instrument, while the scanning electron micrographs (SEM) were taken using a JEOL 100 CX II (15 kV) instrument. A Branson 2200 sonication bath was used for sonication. Other analytical instruments were identical to those described in Chapter 3.

Chemicals were used as obtained from the supplier, except for the solvents which were distilled prior to use. The metal perchlorates were obtained as hexahydrates.

### 4.2.1 Syntheses

Compound **1** was prepared according to a literature procedure.<sup>1</sup> The syntheses of compounds **2a**, **2b**, **2c**, **4a**, **4b**, **4c**, and **6** have been described in Chapter 3. For atom labeling see the Experimental from Chapter 3.

**2-(1-Imidazolyl)-ethanol (3).** The synthesis of this compound was adapted from the literature procedure for the preparation of 2-(7-(1,3-dimethylxanthyl))-ethanol.<sup>14</sup> Imidazole (6.838 g, 0.1004 mol), 8.802 g (0.100 mol) of ethylene carbonate and 1.408 g (0.0094 mol) of NaI were heated under stirring for 2 hrs. at reduced pressure in order to remove the liberated CO<sub>2</sub>. The brown syrup was purified by column chromatography (silica, eluent MeOH/EtOAc 1:3, v/v), to yield 2.13 g (0.21 mmol, 19.5 %) of colorless oil. IR (KBr) 3114 cm<sup>-1</sup> (OH), 2936 and 2855 (=C-H), 1513 (C=N), 1081 (C-O), <sup>1</sup>H-NMR (100 MHz, CDCl<sub>3</sub>)  $\delta$  7.36 ppm (s, 1H, N<sub>im</sub>-CH=N<sub>im</sub>), 6.93 (s, 1H, CH<sub>2</sub>-N<sub>im</sub>-CH=CH-N<sub>im</sub>=), 6.65 (s, 1H, CH<sub>2</sub>-N<sub>im</sub>-CH=CH-N<sub>im</sub>=), 3.95 (m, 2H, -CH<sub>2</sub>-N<sub>im</sub>), 3.749 (m, 2H, CH<sub>2</sub>-OH).

**6-Deoxy-6-(1-benzimidazolyl)-2,4,3,5-dimethylene-N,n-octyl-D-gluconamide (5).** This compound was prepared following a procedure as described for compound **2a** in Chapter 3. Instead of imidazole, 1.121 g (9.49 mmol, 3.2 equiv.) of benzimidazole was used. Yield 0.22 g (0.51 mmol, 17.0 %) of **5** m.p. 91.9 °C. IR (KBr) 3433 cm<sup>-1</sup> (NH), 3098 and 3050 (=C-H), 1666 (amide I), 1616 (C=C), 1546 (amide II), 1497 (aromatic). <sup>1</sup>H-NMR (400 MHz, CDCl<sub>3</sub>)  $\delta$  7.953 ppm (N=CH-N), 7.826 (2d, 1H, ArH), 7.403 (2d, 1H, ArH), 7.319 (m, 2H, ArH), 6.562 (t, 1H, NHCO), 5.202 (d,  $J_{7a-7b}$ =6.50 Hz, 1H, H<sup>7a</sup>), 5.123 (d,  $J_{8a-8b}$ =6.16 Hz, 1H, H<sup>8a</sup>), 5.015 (d, 1H, H<sup>8b</sup>),

4.728 (d, 1H, H<sup>7b</sup>), 4.551 (2d,  $J_{6a-5}$  = 8.06 Hz,  $J_{6a-6b}$  = 14.71, 1H, H<sup>6a</sup>), 4.477 (2d,  $J_{6b-5}$  = 6.47 Hz), 4.379 (m,  $J_{5-4}$  = 1.51 Hz, H<sup>5</sup>), 4.319 (t,  $J_{3-4}$  = 1.34 Hz, 1H, H<sup>3</sup>), 4.157 (d,  $J_{2-3}$  = 1.99 Hz, H<sup>2</sup>), 3.618 (s, 1H, H<sup>4</sup>). <sup>13</sup>C-NMR (100 MHz, CDCl<sub>3</sub>)  $\delta$  166.692 ppm (NHCO), 143.635 (=C-C(=C)-N), 143.009 (N-C=N), 133.564 (=C-C(=C)-N), 123.461, 122.563, 120.672, 109.113 (-CH=CH-), 91.990 (C<sup>7</sup>), 88.358 (C<sup>8</sup>), 77.276 (C<sup>5</sup>), 73.976 (C<sup>2</sup>), 71.494 (C<sup>3</sup>), 66.738 (C<sup>4</sup>). EI-MS  $m/z$  431 (M)<sup>+</sup>, 132 (CH<sub>2</sub>-N<sub>2</sub>C<sub>3</sub>H<sub>5</sub>)<sup>+</sup>, 85 (cyclic -O-CH-CH-CH-O-CH<sub>2</sub>)<sup>+</sup>. Anal. Calcd. for C<sub>19</sub>H<sub>31</sub>N<sub>3</sub>O<sub>5</sub>·H<sub>2</sub>O: C, 61.44; H, 7.85; N, 9.35. Found: C, 61.80; H, 7.63; N, 9.25.

***N*,n-Octyl-6-(1-imidazolyl)-n-hexanoic acid amide (7).** This compound was synthesized as described for compound **24** in Chapter 3. Instead of the hexadecyl derivative, 1.275 g (4.26 mmol) of *N*,n-octyl-6-tosyloxy-n-hexanoic acid amide was used. Yield 0.40 g (2.50 mmol, 58.7 %) of oil. IR (KBr) 3107 and 3066 cm<sup>-1</sup> (=C-H), 1650 (amide I), 1553 (amide II). <sup>1</sup>H-NMR (90 MHz, CDCl<sub>3</sub>)  $\delta$  7.44 ppm (s, 1H, N=CH-N), 7.04 (s, 1H, N=CH-CH-N), 6.891 (s, 1H, N=CH-CH-N), 5.54 (very broad t, 1H, NHCO), 3.94 (t, 2H, -CH<sub>2</sub>-N=), 3.23 (m, 2H, CH<sub>2</sub>-(C=O)), 2.14 (t, 2H, -CH<sub>2</sub>-C=O), 1.81 (t, 2H, -CH<sub>2</sub>-CH<sub>2</sub>-N=), 1.28 (m, 16H, -(CH<sub>2</sub>)<sub>6</sub>- and O=C-CH<sub>2</sub>-(CH<sub>2</sub>)<sub>2</sub>-), 0.87 (t, 3H, CH<sub>3</sub>). EI-MS  $m/z$  293 M<sup>+</sup>, 278, 264, 250, 236, 222, 208, 194 (M - (CH<sub>2</sub>)<sub>n</sub>-CH<sub>3</sub>, n = 0, 1, 2, 3, 4, 5, 6 respectively)<sup>+</sup>, 165 (CO-(CH<sub>2</sub>)<sub>5</sub>-Im)<sup>+</sup>, 137 (-CH<sub>2</sub>)<sub>5</sub>-N<sub>2</sub>C<sub>3</sub>H<sub>3</sub>)<sup>+</sup>, 95 (-CH<sub>2</sub>)<sub>2</sub>-Im)<sup>+</sup>.

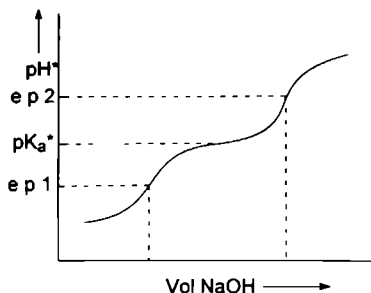
**6-Deoxy-6-(1-imidazolyl)-2,4,3,5-dimethylene-n-octyl-D-gluconate (8).** This compound was synthesized as described for compound **21** in Chapter 3. Instead of n-hexadecan-1-ol, 14 g (8.75 mmol, 6 equiv.) of n-octan-1-ol was used. Yield 0.03 g (0.07 mmol, 5 %) of **8**, m.p. 55.1 °C. IR (KBr) 3136 and 3099 cm<sup>-1</sup> (=C-H), 1757. <sup>1</sup>H-NMR (100 MHz, CDCl<sub>3</sub>)  $\delta$  8.69 ppm (s, 1H, N=CH-N), 8.16 (t, 1H,  $J$ =1.2 Hz, -CH<sub>2</sub>-N-CH=CH-N), 8.06 (t, 1H, -CH<sub>2</sub>-N-CH=CH-N), 4.67 (m, 2H, -CH<sub>2</sub>OH), 4.48 (m, 2H, CH<sub>2</sub>-N). EI-MS  $m/z$  381 (M - H)<sup>+</sup>, 353 (M - C<sub>2</sub>H<sub>5</sub>)<sup>+</sup>, 337 (M - C<sub>3</sub>H<sub>7</sub>)<sup>+</sup>, 325 (M - C<sub>4</sub>H<sub>9</sub>)<sup>+</sup>, 225 (C<sub>8</sub>H<sub>17</sub>OCO)<sup>+</sup>. Anal. Calcd. for C<sub>19</sub>H<sub>30</sub>N<sub>2</sub>O<sub>6</sub>·H<sub>2</sub>O: C, 56.98; H, 8.05; N, 7.00. Found: C, 57.40; H, 7.86; N, 6.55.

#### 4.2.2 Determination of the pK<sub>a</sub>\* values<sup>†</sup>

In order to avoid deviating pK<sub>a</sub> values due to aggregation in the aqueous solutions, a methanol/water (95:5, v/v) mixture was used as the titration solvent. For comparison, methylimidazole and imidazole were also titrated in this medium and were found to have pK<sub>a</sub>\* values of 7.03 and 6.96, respectively, which are similar to their values in water (6.95 for both compounds<sup>15</sup>). The titrations were carried out under a nitrogen atmosphere and the pH electrode was calibrated with a lithium succinate/succinic acid and an ammonium oxalate/oxalic acid buffer (pK<sub>a</sub>\*=7.26 and pK<sub>a</sub>\*= 4.23 respectively).<sup>16</sup> Approximately 0.025 mmol of sample was dissolved in 50 ml of methanol/water (95:5, v/v) containing 0.0012 M HClO<sub>4</sub>. This mixture was titrated with a solution of 0.01 M NaOH in methanol/water (95:5, v/v), which was calibrated with benzoic acid. The curves showed two equivalence points. The first point (e.p.1) was reached when the amount of NaOH added was equivalent to the total amount of HClO<sub>4</sub> minus the amount of imidazolyl compound. The second point (e.p. 2) equaled the total amount of HClO<sub>4</sub>. In the area between the equivalence points, the pH\* is determined by the basic character of the imidazolyl compound. The pH\* value in the middle of this imidazolyl buffered area was taken as the pK<sub>a</sub>\* value (see Figure 4.1).

<sup>\*</sup> Im = imidazolyl

<sup>†</sup> pH and pK<sub>a</sub> values obtained from non-aqueous solutions are denoted with an asterisk



**Figure 4.1** Acid-base titration curve from which the  $pK_a$  value is determined

#### 4.2.3 UV-vis titrations

In a typical titration experiment, an aliquot of 1 ml (100 mM) of a metal salt solution in water was added in steps of 20  $\mu$ l to an aqueous solution of the ligand (2 ml, 50 mM) in a quartz cuvette. After each addition the solution was equilibrated for 1 min. and subsequently UV-vis spectra ( $T = 25^\circ\text{C}$ , slit = 2 nm, scan rate = 120 nm/min) were recorded. The background was recorded with the same solvent mixture as in the titration experiment but without the ligand or metal salt. The reference cuvette contained the same solvent as the measuring cuvette, however, without ligand or metal salt.

#### 4.2.4 DSC measurements

In a typical DSC experiment, 60  $\mu$ l of water was added to 1.5 - 3 mg of compound, which was transferred to a large volume DSC cup (stainless steel). Heating and cooling runs were recorded at a scan rate of  $5^\circ\text{C}/\text{min}$ . The maximum temperature that could be reached was  $130^\circ\text{C}$ . After the runs, the weight was checked, but no loss of weight was observed. In the case of the metal complexes, a metal salt solution was added, instead of pure water.

#### 4.2.5 Electron microscopy

Electron microscopy was performed on dispersions of the amphiphiles in acetic acid/acetate buffered ( $\text{pH} = 4.5$ ) solutions or in Tris buffered ( $\text{pH} = 8.5$ ) solutions. The metal complexes were prepared in pure water (double distilled or milli-Q<sup>®</sup> quality).

#### TEM experiments

In a typical experiment, ca. 1 mg of amphiphilic compound was dissolved in 0.5 ml of solvent. The mixture was first heated until a clear solution was obtained and then allowed to cool to room temperature. In the case of the metal complexes, a solution containing the metal salt was added to a warm and clear solution of the ligand before the latter solution had cooled to room temperature. The metal salt and amphiphiles were mixed in a stoichiometry that was obtained from the UV-vis titrations,<sup>17, 18</sup> e.g. in the case of  $\text{Cu}(\text{ClO}_4)_2$ , a metal/ligand ratio of 1/4 was used, and in the case of  $\text{CuCl}_2$  a metal/ligand ratio of 1/2.

**Dried-in samples** Mixtures of amphiphiles in acetic acid or Tris buffered solutions and metal complexes in milli-Q water were sonicated<sup>†</sup> at approximately  $70^\circ\text{C}$ . After cooling to room temperature, a drop of the suspension was transferred to a carbon coated 150 Mesh copper grid. After 1 min. the excess of material was blotted off. In samples without metal ions, the contents of the grid were stained with uranyl acetate or covered with Pt deposited at an angle of approximately  $45^\circ$ .

<sup>†</sup> Only samples containing metal ions were sonicated

**Freeze etching.** Suspensions of the amphiphiles in acetic acid or Tris buffered solutions and the metal complexes in milli-Q water were mixed and sonicated for 5 min. at approximately 70 °C, after which the samples were allowed to cool to room temperature. To 0.3 ml of a suspension, one drop of glycerol (cryo-protectant, conc.  $\pm$  10 %) was added. A freshly cleaned<sup>†</sup> gold grid, was immersed in the suspension and placed between two freshly cleaned copper plates. The grid and copper plates were cooled very rapidly in a cryojet with liquid propane (-190 °C) that was condensed with liquid nitrogen. The copper plates were quickly pulled apart from the gold grid under high vacuum at -105 °C in a Balzers freeze etching instrument. Subsequently the sample was etched for 5 min. with the freeze fracture knife at -180 °C positioned over the sample in order to sublimate amorphous water molecules. The grid and sheets were covered with a carbon layer of 20 nm, and in addition, Pt diluted with carbon (Pt/C, 3:7, w/w) was deposited at an angle of 45° until a layer of 3 nm was obtained. The material was placed on the surface of a solution of aqueous chromic acid (20 %, w/v). The organic material was oxidized and dissolved in the solution while the replicas remained on the surface. After washing with water (by putting them on a clean water surface), the replicas were transferred to Formvar-coated copper grids.

## SEM experiments

The copper grids with material used in the TEM experiments, were transferred to a SEM specimen (mount) adapter. Subsequently, the sample was covered with a 10 nm gold layer.

## 4.3 Results and discussion

### 4.3.1 pK<sub>a</sub> titrations

As the presence of a charge can have a large influence on the aggregation behavior of an amphiphile<sup>7</sup> we determined the pK<sub>a</sub>-value of the imidazole group in compound **2a** in methanol/water (95.5, v/v). In order to be sure that **2a** is sufficiently protonated the solvent should be buffered at a pH of approximately 2 pH units below the pK<sub>a</sub> (Im) value.

From the titration experiments (see experimental section) it is clear that the pK<sub>a</sub> value of **2a** is very similar to the pK<sub>a</sub> values of imidazole, 1-methyl-imidazole and the model compound **3** (see Table 4.1).

**Table 4.1** pK<sub>a</sub><sup>\*</sup>-values of imidazole-containing compounds <sup>a</sup>

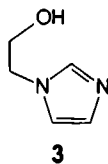
Compound	pK <sub>a</sub> <sup>*</sup>	pK <sub>a</sub> <sup>b</sup>
Imidazole	6.96	6.95
Methylimidazole	7.03	6.95
<b>2a</b>	6.28	
<b>3</b>	6.92	

<sup>a</sup> In methanol/water (95.5, v/v)

<sup>b</sup> In water (see Ref. 5)

Apparently, the presence of a β-oxygen atom in **2a**, a β-hydroxyl group in **3** or a methyl group in methylimidazole has only a small influence on the pK<sub>a</sub> value of the imidazole group. It was assumed, therefore, that the pK<sub>a</sub> values of the imidazole reference compounds in Section 4.3.5 were approximately the same as the pK<sub>a</sub> value of imidazole itself.

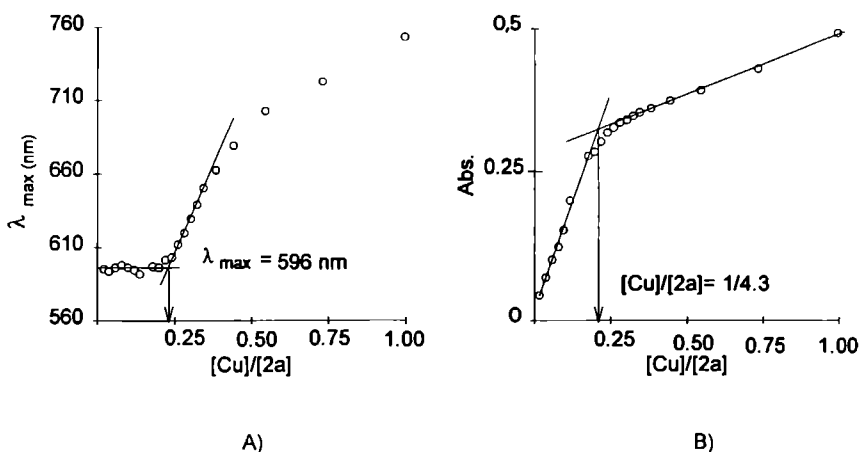
<sup>†</sup> The grids and copper plates were cleaned with conc. hydrochloric acid, then rinsed twice with water and additionally sonicated in acetone (2 min.)



### 4.3.2 UV-vis titrations

#### *Cu(ClO<sub>4</sub>)<sub>2</sub> complexation*

Copper(II) ions can give 1:4 metal-ligand complexes with imidazole compounds.<sup>17</sup> The complex formation can be followed by monitoring a broad band at approximately 600 nm in the UV-vis spectrum, which is indicative of the presence of a  $\text{Cu}(\text{imidazole})_4^{2+}$  complex.<sup>19</sup> Addition of a copper salt with a non-coordinating counter ion (*e.g.* perchlorate) to a solution of **2a** in water, methanol or chloroform was found to give turbid mixtures which prevented accurate UV-vis titrations. In mixtures of organic solvents such as chloroform/methanol (1:2, v/v), however, clear dark blue solutions were obtained and the complexation behavior of **2a** could be determined (see Figure 4.2). During the titration of **2a** with  $\text{Cu}(\text{ClO}_4)_2$  the  $\lambda_{\text{max}}$  gradually shifted from 595 to 750 nm when the  $[\text{Cu}]/[\text{2a}]$  ratio was increased from 1/4 to 1/1. The titrations revealed that at low copper concentrations a 1/4 (Cu/Ligand) complex is present, whereas at high copper concentrations other complexes, *e.g.*  $[\text{Cu}]/[\text{2a}] = 1/3, 1/2$ , or  $1/1$  prevail.<sup>20</sup> Solvent molecules like methanol will probably fill the empty coordination places at the copper(II) centers leading to complexes that have, besides a different  $\lambda_{\text{max}}$ , a weaker chromophoric character. This can be concluded from the curve of the absorbance at  $\lambda_{\text{max}}$  vs. the  $[\text{Cu}]/[\text{2a}]$  ratio which flattens above 1/4 (Figure 4.2)



**Figure 4.2** Titration curves of **2a** with  $\text{Cu}(\text{ClO}_4)_2$ , in a mixture of  $\text{CHCl}_3$  and MeOH (1:2, v/v), A)  $\lambda_{\text{max}}$  vs. the  $[\text{Cu}]/[\text{2a}]$  ratio B) Absorption at  $\lambda_{\text{max}}$  vs. the  $[\text{Cu}]/[\text{2a}]$  ratio

Since it was necessary to carry out the titration of compound **2a** with copper(II) in a mixture of organic solvents we also performed, for comparison, a titration of methylimidazole with copper(II) in an almost similar solvent mixture (see Table 4.2). At low copper concentration 1/4 metal to ligand complexes were formed with methylimidazole, while at higher copper concentrations the  $\lambda_{\max}$  shifted in a way as observed for compound **2a**, indicating a similar complexation behavior as for the latter compound. An oxygen atom which can participate in the copper complexation is situated next to the imidazole group in compound **3**, which makes **3** a better model for compound **2a** than methylimidazole. Compound **3** formed copper complexes that dissolved both in water and in organic solvents without forming turbid mixtures. The titration curves of compound **3** in water, methanol, and in a mixture of chloroform/methanol (1.2, v/v) were almost identical to those of **2a** and MeIm. The  $\lambda_{\max}$  values of all the complexes described in Table 4.2 were very similar indicating that in all cases complexes of the type  $\text{Cu}(\text{imidazole})_4^{2+}$ ,<sup>19</sup> were formed.

**Table 4.2** Complexation stoichiometry of imidazole ligands and Tris with  $\text{Cu}(\text{ClO}_4)_2$  as determined by UV-vis titrations

Ligand	Solvent	Cu/Ligand <sup>a</sup> ratio	$\lambda_{\max}$ (nm) <sup>b</sup>
MeIm	$\text{CHCl}_3/\text{MeOH}$ (1.3, v/v)	1/4 2	610
<b>2a</b>	$\text{CHCl}_3/\text{MeOH}$ (1.2, v/v)	1/4 3	602
<b>3</b>	MeOH	1/4 0	599
<b>3</b>	$\text{CHCl}_3/\text{MeOH}$ (1.3, v/v)	1/4 5	598
<b>3</b>	water (MilliQ)	1/4.3	611

<sup>a</sup> Determined from the intersection of the tangents in the plot of the absorbance at  $\lambda_{\max}$  vs the  $[\text{Cu}]/[\text{Ligand}]$  ratio

<sup>b</sup> Determined from the intersection of the tangents in the plot of  $\lambda_{\max}$  vs the  $[\text{Cu}]/[\text{Ligand}]$  ratio

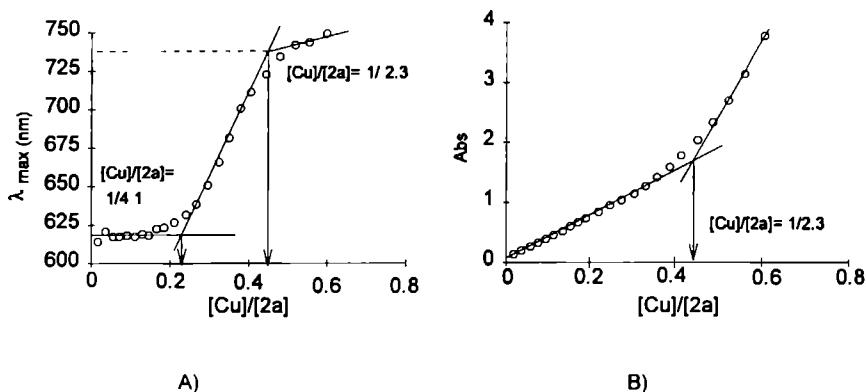
As we used  $\text{Cu}(\text{II})$ -tris(hydroxymethyl)amine (Tris) buffers in many of our experiments (vide infra) we also carried out an UV-vis titrations of **3** with  $\text{Cu}(\text{ClO}_4)_2$  in the presence of this buffer (pH=8.5). The titration curve was similar to that of **3** in pure water. Apparently, Tris is a much weaker ligand<sup>21</sup> for  $\text{Cu}(\text{II})$  than imidazole and the coordinated Tris molecules are completely exchanged for imidazole ligands when the latter are added.

#### *CuCl<sub>2</sub> complexation*

The chloride ions of  $\text{CuCl}_2$  are known to be coordinating anions, causing a complex of **2a** with  $\text{CuCl}_2$  to be different from the complex with  $\text{Cu}(\text{ClO}_4)_2$ . As in the case of the complexes with copper perchlorate and triflate, addition of  $\text{CuCl}_2$  to a solution of **2a** in water resulted in turbid mixtures. From studies carried out by Van Esch in our group<sup>20</sup> we know that monodentate imidazole amphiphiles form a 1/3.4 copper to ligand complexes with  $\text{CuCl}_2$ . A UV-vis titration curve of **2a** with  $\text{CuCl}_2$  in methanol in which the  $\lambda_{\max}$  was plotted against the ratio  $[\text{Cu}]/[\text{2a}]$  showed 2 inflection points, viz at  $[\text{Cu}]/[\text{2a}] = 1/4.1$  and  $1/2.3$ , indicating that both 1/4 and 1/2 complexes were formed (Figure 4.3). A plot of the absorbance at  $\lambda_{\max}$  vs  $[\text{Cu}]/[\text{2a}]$  showed only



one inflection point at the ratio 1/2.3. This may indicate that the extinction coefficients of the 1/4 and 1/2 complexes at  $\lambda_{\max}$  (in the dark blue and bright green region of the UV-vis spectrum, respectively) are very similar. Remarkable is the increase in absorbance which is observed when  $[\text{Cu}]/[\text{2a}]$  is larger than 2.3. In this region  $\lambda_{\max}$  hardly changes. Apparently, the complex of  $\text{CuCl}_2$  ligated by methanol (green)<sup>§</sup> is a strong chromophore.



**Figure 4.3** Titration curves of **2a** with  $\text{CuCl}_2$  in MeOH. A)  $\lambda_{\max}$  vs the  $[\text{Cu}]/[\text{2a}]$  ratio, B) absorbance at  $\lambda_{\max}$  vs the  $[\text{Cu}]/[\text{2a}]$  ratio

#### Complexes of **2a** and model compound **3** with metals other than Cu

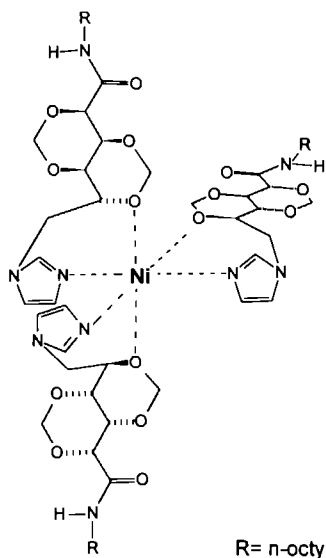
From the literature<sup>17</sup> it is known that imidazole can give 6:1 ligand to metal complexes with  $\text{Co}(\text{ClO}_4)_2$  and  $\text{Ni}(\text{ClO}_4)_2$ .<sup>22</sup> It was of interest therefore to investigate the complexation behavior of **2a** and **3** towards these metal salts. For comparison, experiments were also carried out with imidazole. The UV-vis spectra of both  $[(\text{2a})_n\text{Ni}][\text{ClO}_4]_2$  and  $[(\text{3})_n\text{Ni}][\text{ClO}_4]_2$  showed 2 broad peaks, with  $\lambda_{\max 1} = 380$  nm and  $\lambda_{\max 2}^{\#} = 605$  nm. Both  $\lambda_{\max}$  values gradually shifted to the red during the titration when the  $[\text{Ni}]/[\text{Ligand}]$  ratio was increased from 1/50 to 1/1. This indicates that the complexation stoichiometry changes during the titration. From the plots of the absorbances at  $\lambda_{\max}$  versus the  $[\text{Ni}]/[\text{Ligand}]$  ratios the stoichiometries of the nickel(II) imidazole complexes were determined (see Table 4.3). The results suggest that imidazole itself forms a 4:1 ligand to metal complex (probably square planar<sup>22</sup>), whereas **2a** and **3** act as bidentate ligands giving 3:1 complexes (see Figure 4.4).

<sup>§</sup>  $\text{CuCl}_2$  crystals containing two  $\text{H}_2\text{O}$  molecules are (bright) blue.

<sup>#</sup>  $\lambda_{\max 2}$  was only visible when the  $[\text{Ligand}]/[\text{Ni}]$  ratio was smaller than 10

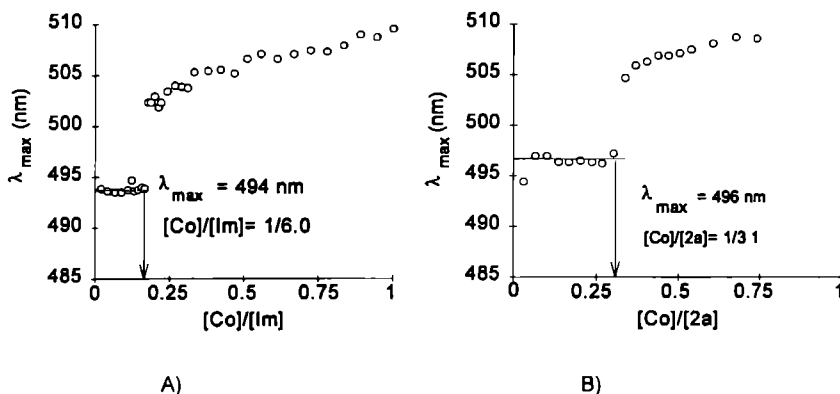
**Table 4.3** Stoichiometry of complexes between imidazole ligands and  $\text{Ni}(\text{ClO}_4)_2$  as determined by UV-vis titrations<sup>a</sup>

Compound	Solvent (v/v)	Ratio $[\text{Ni}]/[\text{Ligand}]$	$\lambda_{\text{max}}$ (nm) <sup>b</sup>
Imidazole	MeOH/H <sub>2</sub> O (1/1)	1/3 6	619
		1/3 8	375
<b>3</b>	MeOH/H <sub>2</sub> O (1/1)	1/3 1	604
		1/3 1	379
<b>2a</b>	MeOH	1/2 8	621
		1/3 2	381

<sup>a</sup> Numbers obtained from the plots of the absorbance at  $\lambda_{\text{max}}$  vs the ratio  $[\text{Ni}]/[\text{Lig}]$ <sup>b</sup> At intersection of tangents (see Figure 4 3), lower line  $\lambda_{\text{max}1}$  upper line  $\lambda_{\text{max}2}$ **Figure 4.4** Proposed structure of the complex  $[\text{Ni}(\mathbf{2a})_3][\text{ClO}_4]_2$ . The nickel ion is six coordinated by 3 nitrogen and 3 oxygen atoms

The titration curves of both imidazole and **2a** with  $\text{Co}(\text{ClO}_4)_2$  in methanol showed an abrupt shift of  $\lambda_{\text{max}}$  (see Figure 4.5), which is in contrast with the titration curves of copper(II) and nickel(II), which displayed gradual shifts. The absence of a gradual shift of  $\lambda_{\text{max}}$  indicates that no mixed complexes are formed at low  $[\text{Co}]/[\text{Ligand}]$  ratios. Figure 4.5 reveals that the cobalt-imidazole complex has a 6:1 ligand to metal stoichiometry and the cobalt - **2a** complex a 3:1 stoichiometry. As only 3 molecules of **2a** are found to coordinate to the cobalt center, other substituents than imidazolyl must participate in the complexation, probably protected hydroxyl

functions as suggested for the coordination of **2a** to nickel(II) (Figure 4.4). Despite the fact that imidazole and **2a** form different complexes, the difference in  $\lambda_{\text{max}}$  for  $[(\text{Im})_6\text{Co}][\text{ClO}_4]_2$  and  $[(\mathbf{2a})_3\text{Co}][\text{ClO}_4]_2$  in methanol was remarkably small.



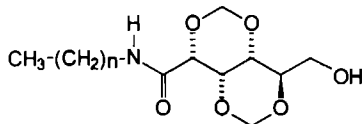
**Figure 4.5** Titration curves of imidazole ligands with  $\text{Co}(\text{ClO}_4)_2$ , A) imidazole, B) compound **2a**

#### 4.3.3 DSC experiments

The temperature at which an amphiphile dissolves in aqueous solution is often called the “Krafft” temperature ( $T_{\text{Krafft}}$ ),<sup>23</sup> which can be determined by using polarizing microscopy or differential scanning calorimetry (DSC). DSC also gives information about the enthalpy of dissolution ( $\Delta H$ )<sub>diss</sub>. In this section the  $T_{\text{Krafft}}$  and ( $\Delta H$ )<sub>diss</sub> of **2a** and related compounds are compared. This study was undertaken because the temperature at which the gluconamide dissolves in aqueous solution is important for the process of self assembly of this kind of molecules. For instance, the helices of *N*,*n*-octyl-*D*-gluconamide (**1**) were obtained by cooling a hot clear solution of **1** in water (1 % w/v) to room temperature.<sup>1,2</sup>

DSC thermograms of **1** in water showed upon heating in the first run two endothermic peaks at 64.3 °C ( $\Delta H = 13.5$  kJ/mol) and 73.4 °C ( $\Delta H = 19.1$  kJ/mol), while only one exothermic peak was found upon cooling (59.9 °C,  $\Delta H = -12.8$  kJ/mol). In the literature<sup>24</sup> the low temperature transition of **1** has been assigned to the splitting of the numerous *intra*- and *intermolecular* hydrogen bonds between the hydroxyl groups in the carbohydrate moieties of the molecules, and the second one to the breaking of the amide hydrogen bonds. This assignment was made with the help of crystallographic studies.<sup>24</sup>

Gluconamide **2a** does not have an extensive hydrogen bonding network that breaks down upon dissolving this compound in water. In order to investigate the effect of the methylene bridges in the absence of the imidazole group, DSC thermograms of gluconamide **4a** in water were recorded. In the heating scan of **4a** only one transition at 51 °C was observed (see Table 4.4).

**4a**  $n = 7$ **4b**  $n = 11$ **4c**  $n = 15$ 

The lack of a transition at approximately 65 °C was expected, because **4a** cannot form a hydrogen bonding network of the type compound **1** does. More surprising was the relatively low Krafft temperature of **4a**. It shows that the solubility of the gluconamide in water is raised by the introduction of the 2,4;3,5-bismethylene bridges. Like **1**,<sup>25</sup> **4a** has the possibility to form intermolecular amide hydrogen bonds, which are expected to disappear at approximately 75 °C.<sup>24</sup> Apparently, the amide hydrogen bonds in the assembly of **4a** are much weaker than those of **1**, or the amide hydrogen bonds do not influence the solubility of the compounds. Upon cooling no transition was found for compound **4a**, which means that **4a** remained dissolved in the cooling run.

**Table 4.4** Krafft temperatures and enthalpies of dissolution of *N,n*-octyl-D-gluconamides <sup>a</sup>

Compound	$T_{\text{krafft}}$ (°C)	$\Delta H_{\text{diss}}$ (kJ/mol)
<b>1</b>	73.4	32.6
<b>2a</b>	77.9	29.9
<b>4a</b>	51.4	29.4
<b>5</b>	106.4	36.3

<sup>a</sup> Values obtained from DSC thermograms (first heating run)

The  $T_{\text{krafft}}$  of non-protonated **2a** in Tris buffered water (pH=8.5) was found to be higher than that of **4a** and **1** (Table 4.4). This suggests that in crystalline **2a** a strong interaction is present between the imidazole groups. This conclusion is supported by the observation that  $T_{\text{krafft}}$  drops considerably upon protonation of **2a** (see Table 4.5).

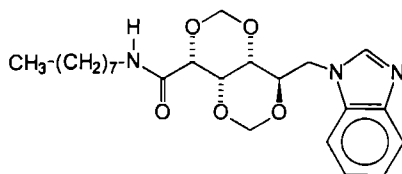
The cooling run of **2a** in Tris buffered solution, did not show any transitions. Despite the lack of transitions in the thermograms, aggregates were formed according to electron microscopy (see Section 4.3.5). This suggests that the transitions are too small to be measured, or that the formation of the aggregates is too slow to be detected by DSC (heating and cooling runs were taken at 5 °C/min.).

**Table 4.5**  $T_{\text{Krafft}}$ , enthalpy and entropy of dissolution of compounds **2**<sup>a</sup>

Compound	Solvent	$T_{\text{Krafft}}$ (°C)	$\Delta H_{\text{diss}}$ (kJ/mol)	$\Delta S_{\text{diss}}$ (J/(mol °K))
<b>2a</b>	Tris buffer <sup>b</sup>	77.4	32.3	92.2
<b>2a</b>	HAc/NaOAc buffer <sup>c</sup>	43.1	56.4	178.4
<b>2b</b>	Tris buffer <sup>b</sup>	95.2	54.2	145.4
<b>2b</b>	HAc/NaOAc buffer <sup>c</sup>	91.5	46.5	127.0
<b>2c</b>	Tris buffer <sup>b</sup>	102.1	62.6	166.9
<b>2c</b>	HAc/NaOAc buffer <sup>c</sup>	99.7	63.4	170.1

<sup>a</sup> Obtained from DSC thermograms (heating and cooling rate 5 °C/min)<sup>b</sup> pH= 8.5<sup>c</sup> pH= 4.5

For comparison, we also recorded DSC thermograms of the benzimidazole derivative **5** in Tris buffered solution at pH=8.5, where **5** is not protonated ( $\text{pK}_{\text{a}}$  5.53<sup>15</sup>). A dramatic increase in  $T_{\text{Krafft}}$  was observed as compared to gluconamide **2a** (see Table 4.4). Gluconamide **5** crystallized in the cooling run at 63.7 °C, which demonstrates that the introduction of an additional aromatic ring reduces the amphiphilic character of the compound.

**5**

The compounds in Table 4.4 all have the same alkyl chain. We may conclude from the data in this table that changes in the carbohydrate part of the molecule have a strong effect on  $T_{\text{Krafft}}$  but only a weak effect on ( $\Delta H_{\text{diss}}$ ). The effect of varying the alkyl chain length was investigated for compounds **2** and **4**. For the former compound elongation of the alkyl chain resulted in higher  $T_{\text{Krafft}}$  and  $\Delta H_{\text{diss}}$  values (see Table 4.5). The same trend was found for compounds **4** although the increases were less dramatic (see Table 4.6).

**Table 4.6**  $T_{\text{Krafft}}$  and  $\Delta H_{\text{diss}}$  and  $\Delta S_{\text{diss}}$  values of compounds **4** in water<sup>a</sup>

Compound	$T_{\text{Krafft}}$ (°C)	$\Delta H_{\text{diss}}$ (kJ/mol)	$\Delta S_{\text{diss}}$ (J/(mol °K))
<b>4a</b>	51.4	29.4	90.6
<b>4b</b>	63.8	36.5	108.4
<b>4c</b>	71.4	40.4	117.3

<sup>a</sup> Values obtained from DSC thermograms (first heating runs)

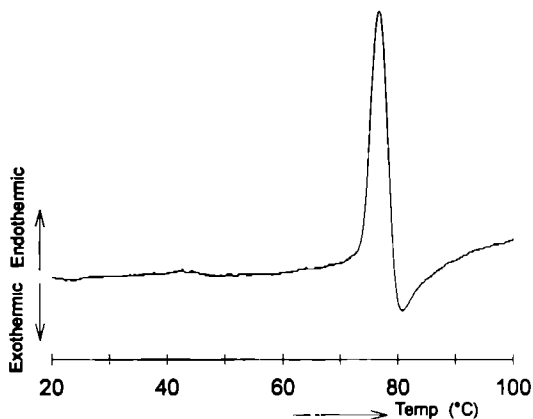
The effect of protonation of the imidazole group on  $T_{\text{krafft}}$  decreased by elongation of the alkyl chain. In Chapter 3 we showed that for a series of homologous liquid crystalline gluconamides the clearing points are dependent and the melting points are independent on the length of the alkyl chain. The melting points of the thermotropic liquid crystalline systems and the  $T_{\text{krafft}}$  values of the lyotropic liquid crystalline systems should show similar trends because in both cases the supramolecular ordering of the molecules is destroyed by passing the transition temperature. It is clear from Tables 4.5 and 4.6 that no such trend exists:  $T_{\text{krafft}}$  depends on the length of the alkyl chain. An explanation for this behavior may be that in the case of the lyotropic systems the entropy effect plays an important role. Tables 4.5 and 4.6 reveal that the entropy of the non protonated **2** and **4** increases upon elongation of the alkyl chain length. This increase in  $\Delta S$  is readily explained because larger molecules must be solvated by more water molecules (reversed hydrophobic effect).

Gluconamides **2b** and **2c** appeared not to be suitable for the formation of supramolecular aggregates in water because these compounds, both in protonated and neutral form, recrystallized very fast from aqueous solutions. Compounds **4b** and **4c** crystallized from water without forming aggregates and were not further investigated by DSC or EM.

### Copper(II) complexes

From the UV-vis titration experiments (vide supra) it is clear that **2a** and  $\text{Cu}(\text{ClO}_4)_2$  ions form  $[(\mathbf{2a})_4\text{Cu}]^{2+}$  complexes. When a mixture of 4 equivalents of **2a** and 1 equivalent of  $\text{Cu}(\text{ClO}_4)_2$  was heated, an endothermic peak at 73.8 °C was observed, directly followed by an exothermic effect peak. The transitions partly overlapped each other (see Figure 4.6). The endothermic peak may be related to the  $T_{\text{krafft}}$  of the complex  $[(\mathbf{2a})_4\text{Cu}][\text{ClO}_4]_2$  and the endothermic peak to the destruction of the complex. Another possibility is that the ligand has to be dissolved before the complex can be formed which would explain why the  $T_{\text{krafft}}$  is very similar to that of the free ligand ( $T_{\text{krafft}}$  77.9 °C, Table 4.4). In the latter case the heat effects are a combination of dissolving **2a** (endothermic effect) and the formation of the complex (exothermic effect). Such a combination of heat effects would be in line with the fact that  $\Delta H_{\text{diss}}$  of the complex\*\* is lower than  $\Delta H_{\text{diss}}$  of the free ligand ( $\Delta H_{\text{diss}}$  for **2a** = 32.3 kJ/mol and  $\Delta H_{\text{diss}}$  for  $[(\mathbf{2a})_4\text{Cu}][\text{ClO}_4]_2$  = 15.8 kJ/mol). A DSC scan of a sample of  $[(\mathbf{2a})_4\text{Cu}][\text{ClO}_4]_2$  that had been precipitated from methanol, showed in water a transition at a much higher temperature (115.6 °C, see Table 4.7, only an endothermic peak was observed). This relatively high transition may indicate that the precipitated complex is hydrated or contains methanol as an additional ligand.

\*\* The  $\Delta H_{\text{diss}}$  was corrected by multiplying it with the factor (Mw complex)/(Mw ligand)



**Figure 4.6** DSC heating scan of **2a** + 0.25 equivalents of  $\text{Cu}(\text{ClO}_4)_2$  in water

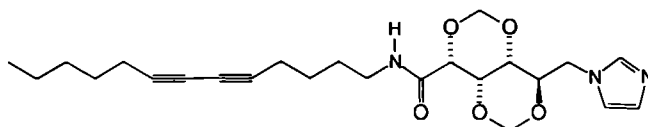
**Table 4.7** DSC of  $\text{Cu}(\text{ClO}_4)_2$  complexes <sup>a</sup>

Ligand	Transition temp in heating run (°C)
<b>2a</b>	73.8
<b>2a<sup>b</sup></b>	115.6
<b>5</b>	102.0
<b>6</b>	84.5

<sup>a</sup> Concentration of the ligands was 1 % w/v

<sup>b</sup> Metal complex was prepared previously by precipitation from methanol

The DSC scan of a mixture of 4 equivalents of the benzimidazole derivative **5** and 1 equivalent of  $\text{Cu}(\text{ClO}_4)_2$  in water showed an endothermic peak at 102 °C which is a similar result as obtained for the free ligand in Tris buffered solution (106.4 °C, Table 4.4). In contrast to the free ligand the copper complex  $[(\mathbf{5})_4\text{Cu}][\text{ClO}_4]_2$  did not crystallize upon cooling. Compound **6**, which is similar to **2** except for the diacetylene function in the aliphatic chain, behaved differently in the DSC runs. For unknown reasons the endothermic peak of the free ligand (103 °C) was much higher than that of the complex (84.5 °C).



**6**

#### 4.3.4 Electron microscopy

Compound **1** is known<sup>1</sup> to form helical ropes which can be visualized by transmission electron microscopy (TEM). The ropes have a regular winding consisting of bulges and knots with diameters of resp. 18.6 and 8.6 nm and a pitch of 22.4 nm.<sup>1,2</sup> There has been discussion as to whether the helical ropes are composed of 2,<sup>2</sup> 4,<sup>5</sup> or 6<sup>26</sup> strands. The current opinion is that the 6 strand model is the most likely one.<sup>26</sup> The aggregates of **1** in water are stabilized by numerous hydrogen bonds,<sup>1</sup> which give the micellar fibers a crystalline core.<sup>5</sup>

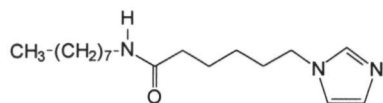
Compound **4a**, which lacks the possibility to form an extensive hydrogen bonding network, dissolved in water, but did not form aggregates according to EM. The solubility of **4a** in water is surprising because four of the five hydroxyl groups are protected. Elongation of the aliphatic chain to dodecyl (**4b**) or hexadecyl (**4c**) decreased the solubility but still no aggregates could be observed by EM.

Gluconamide **2a** also contains protected hydroxyl groups but this compound did form aggregates according to EM. In Tris buffered aqueous solution (pH=8.5) in which **2a** is not protonated, very long fibrous structures were visible (diameter approximately 100 nm length 50  $\mu$ m, see Figure 4.7A). Figure 4.7B shows a fiber that is in the process of being formed from a multi layer tape; for a schematic drawing see Figure 4.7C. The existence of multi-layered structures was shown by freeze fracture experiments in combination with EM (see Figure 4.7B inset). It is not clear from the electron micrographs whether the fibers are hollow or not. Experiments with staining agents as described by Fuhrhop<sup>27</sup> to prove their hollow nature failed. The fibers can assemble to larger tubuli as is shown in Figure 4.7D (arrow shows a fiber which is fused to a tubule). According to this figure the large tubules (diameter approximately 3  $\mu$ m) are hollow.

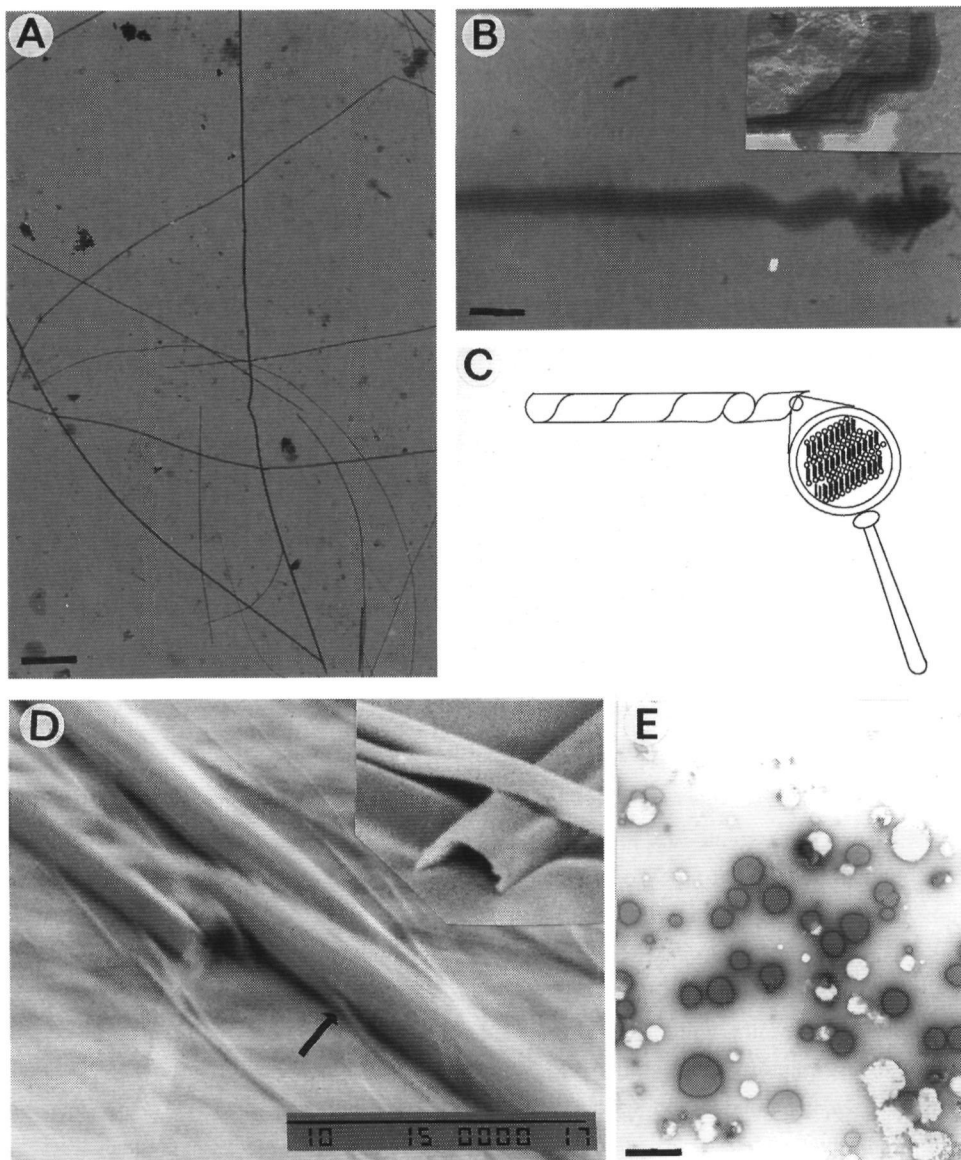
Dissolving compound **2a** in an aqueous acetic acid/sodium acetate buffer (pH=4.5) leads to protonation of the imidazole group. In this buffered solvent vesicles with diameters ranging from 160 to 780 nm were formed (see Figure 4.7E). Apparently upon protonation the diameter of the head group increases in size, making that vesicle structures become thermodynamically more favorable than fiber structures. The architecture of the aggregates formed from compound **2a** thus can be tuned by changing the pH.

The long chain derivatives **2b** and **2c** crystallized upon cooling to room temperature and no suprastructures could be observed by EM. As a reference compound for **2a**, we also studied the imidazole containing amide **7** which lacks the (protected) carbohydrate part. It is likely that the imidazole group in **7** has a similar  $pK_a$  as the imidazole groups in methylimidazole, **2a**, and **3**. Contrary to **2a**, compound **7** did not dissolve in (warm) Tris buffered water (pH=8.5). In aqueous acetic acid/acetate buffer (pH=4.5), **7** dissolved, but EM did not show aggregates. We may conclude therefore, that the carbohydrate moiety is indispensable for the formation of suprastructures, even when its secondary OH groups are protected and cannot form H-bonds. A similar conclusion was drawn with regard to the thermotropic L.C. behavior of the series of compounds **2** (Chapter 3).





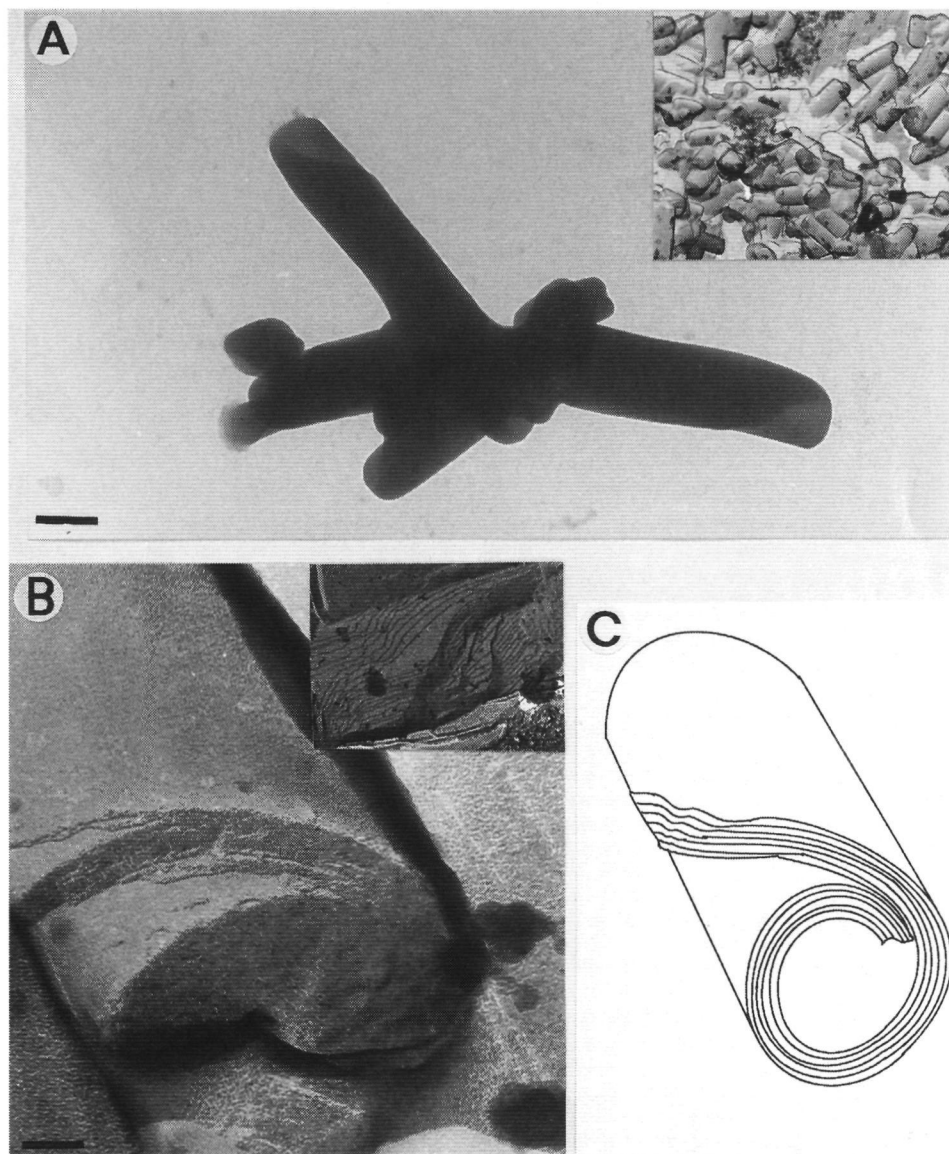
7



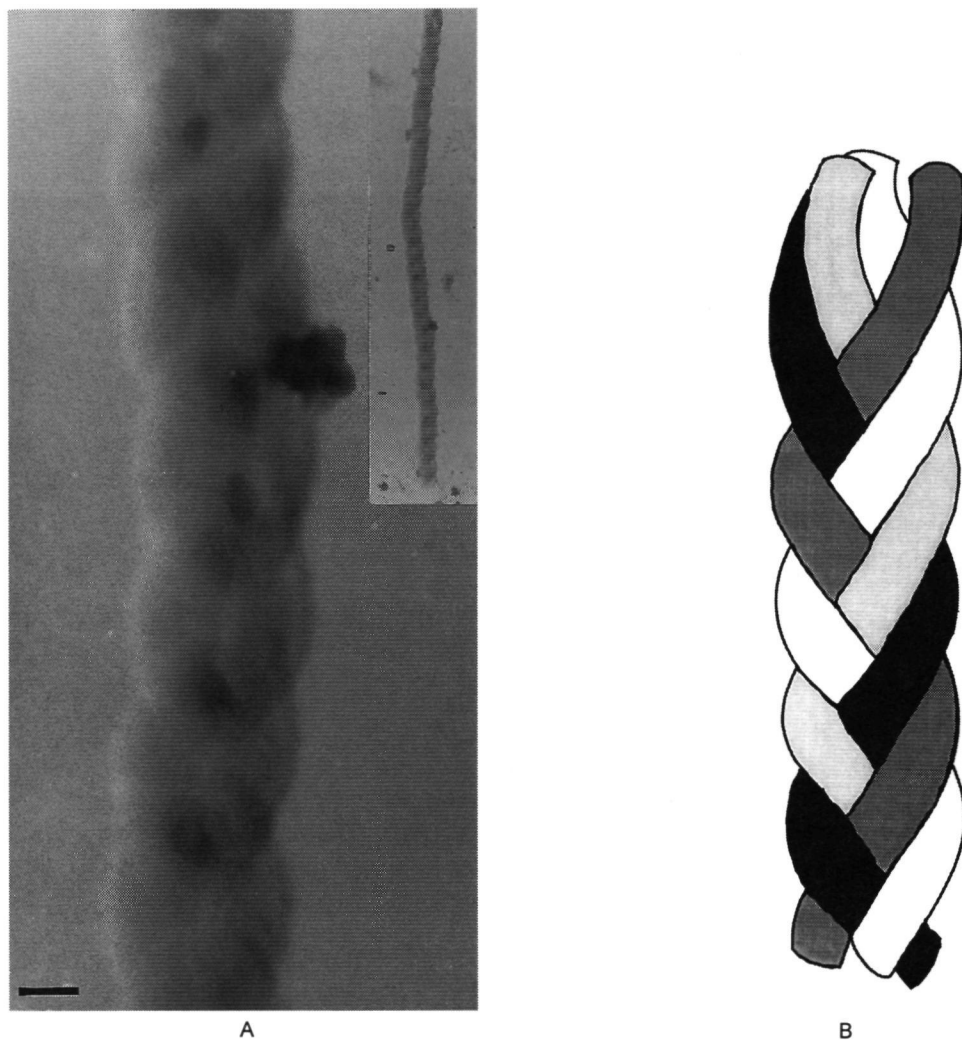
**Figure 4.7** Transmission and Scanning Electron Micrographs (TEM + SEM) of aggregates formed from **2a** in aqueous solutions. A) TEM of fibers of non-protonated **2a**, bar is 3.27  $\mu\text{m}$ . B) Fiber of **2a** in the process of being formed from a tape of multilayers (no staining), bar is 345 nm; inset (freeze fracture technique) shows these multilayers in detail. C) Schematic drawing of the process shown in (B). D) SEM of hollow tubuli and thin fibers of **2a** (bar is 10  $\mu\text{m}$ ); inset shows hollow tube. E) TEM of vesicles formed from **2a** at pH 4.5 (carbon supported hydrophilic copper grid stained with 2 % uranyl acetate), bar is 1.46  $\mu\text{m}$ .

*Copper (II) perchlorate complexes.*

Addition of  $\text{Cu}(\text{ClO}_4)_2$  to a warm clear solution of **2a** in water resulted in the formation of a pale blue turbid mixture. Electron micrographs of this mixture showed, besides multilayered scrolls (Figure 4.8), also a braid-like structure (Figure 4.9).



**Figure 4.8** Scrolls generated from  $[(2\mathbf{a})_4\text{Cu}][\text{ClO}_4]_2$  in water. A) TEM picture of scrolls having diameters of ca. 350 nm. This picture was made without any staining. The wrapping angle of the stretched multilayers is approximately  $45^\circ$ , bar is 230 nm. B) Freeze-fracture electron micrographs of scrolls; inset shows a more detailed picture, bar is 56 nm. C) Schematic drawing of a scroll.



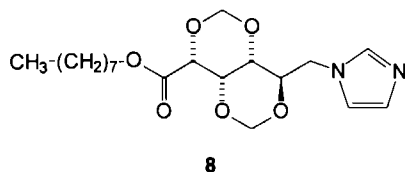
**Figure 4.9** Braided structures formed by  $[(2a)_4Cu][ClO_4]_2$  in water. A) TEM picture without staining; the copper grid was supported with Formvar; bar is 200 nm; the diameter of the braid is 330 nm, the pitch is 980 nm, and the diameter of a single strand is 100 nm, bar is 147 nm. B) Schematic model of the braid.

These micrographs were taken without the use of staining agents: the darkening is due to the presence of the copper ions in the aggregates. Freeze-etching experiments revealed that the scrolls consisted of layers (inset Figure 4.8B). Without copper ions present, **2a** also formed a layered structure (vide supra). This result suggests that the copper ions do not cause any change, but are merely incorporated into a structure that also would have been formed without their presence. A similar phenomenon was observed in the thermotropic L.C. study: long chain derivatives of **2a** formed a smectic phase that was stabilized rather than changed by the addition of copper ions (see

merely incorporated into a structure that also would have been formed without their presence. A similar phenomenon was observed in the thermotropic L.C. study. long chain derivatives of **2a** formed a smectic phase that was stabilized rather than changed by the addition of copper ions (see Chapter 3).<sup>28</sup> Hence, to a great extent the lyotropic and thermotropic liquid crystalline behavior of compounds **2** are comparable. Although the aqueous aggregates both with and without copper have a layered structure, copper has an extra effect: it directs the assembled molecules to a higher organization resulting in scrolls and braids.

The EM picture shown in Figure 4.9 reveals that the braid consists of several strands. A model in which 4 different strands are intertwined seems to match best with the electron micrograph (see Figure 4.9B). Further studies and detailed analysis with the help of a computer are required, however. The individual strands have the same diameter (100 nm) as the fibers formed **2a** without copper ions, which supports the theory that the copper ions stabilize the supramolecular organization and do not change the aggregate structure itself.

We also investigated the self-assembling properties of the copper complexes of a series of reference compounds (**5-8**). Addition of  $\text{Cu}(\text{ClO}_4)_2$  to a mixture of compound **7** resulted in a turbid mixture that turned into a dark blue solution upon cooling to room temperature. Just like in the case without copper ions present, no aggregates were found by EM, again proving that the carbohydrate segment is indispensable for the formation of the supramolecular structures. This result further supports the idea that the ligand and not the copper ion dominates the (molecular) organization. Compound **8** is very similar to **2a** but has an ester linkage between the alkyl chain and the carbohydrate head group. On dispersal in water the copper complex  $[(\mathbf{8})_4\text{Cu}][\text{ClO}_4]_2$  gave vesicles with diameters ranging from 100 to 560 nm (electron micrograph not shown). Thus, the linkage does not have to be an amide group for aggregates to be formed. The shape of the aggregates, however, is influenced by the linkage: an ester function yields vesicles, whereas an amide function leads to scrolls and braids.



This result is of interest because it has been reported in the literature that the amide group does not determine the aggregation behavior of the gluconamide: the thermotropic LC behavior (transition temperature, enthalpy peak size, and peak shape) of n-octylgluconate, the derivative of compound **1** with an ester linkage, was found to be very similar to that of **1**.<sup>29</sup>

The copper complex of the benzimidazole compound **5**, also gave vesicles on dispersal in water. The diameters of the aggregates ranged from 95 nm to 285 nm (electron micrograph not shown). The extra phenyl ring in the head group of the amphiphile apparently prevents that the complex  $[(\mathbf{5})_4\text{Cu}][\text{ClO}_4]_2$  forms braids and scrolls as  $[(\mathbf{2a})_4\text{Cu}][\text{ClO}_4]_2$  does.

The diacetylene derivative **6** was not soluble enough in water ( $T_{\text{kraft}} = 103\text{ }^{\circ}\text{C}$ ) for a proper sample preparation, even not after prolonged heating. According to DSC, the in situ prepared complex  $[(\mathbf{6})_4\text{Cu}][\text{ClO}_4]_2$  crystallized at  $91\text{ }^{\circ}\text{C}$  upon cooling. The isolated copper complex, prepared in ethanol,<sup>30</sup> could not be studied either due to lack of solubility.

#### *Copper (II) complexes with other anions than perchlorate*

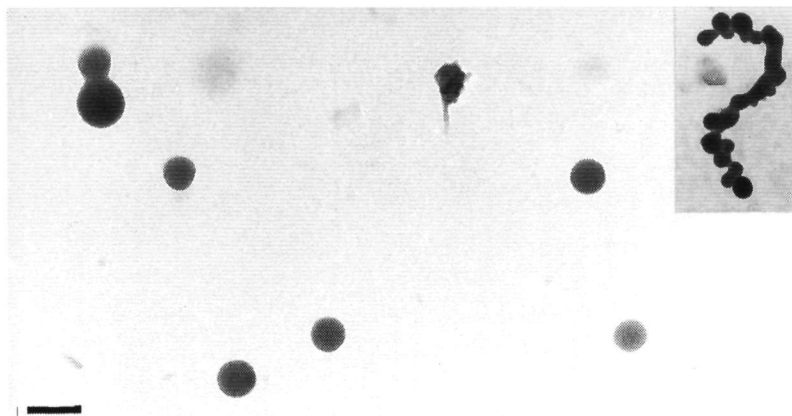
The complex of copper triflate and **2a**<sup>31</sup> is poorly dispersible in water. On the other hand, when the copper complex was made in situ by mixing aqueous solutions of  $\text{Cu}(\text{OSO}_2\text{CF}_3)_2$  and **2a** in a 1:4 metal to ligand ratio, a turbid mixture was obtained. EM showed that this mixture contained ill-defined structures even after 5 minutes of sonication at  $70\text{ }^{\circ}\text{C}$  (pictures not shown).

According to the UV-vis titration experiments described in Section 4.3.2, **2a** can form 1:2 metal to ligand complexes with  $\text{CuCl}_2$ . Mixing this copper salt with **2a** in a 1:2 ratio resulted in rapid precipitation of the complex and no suprastructures were formed. A DSC scan showed an exothermic transition at  $83\text{ }^{\circ}\text{C}$ . Because of this fast precipitation no further studies were carried out.

#### *Cobalt (II) and nickel complexes*

Mixing  $\text{Co}(\text{ClO}_4)_2$  with **2a** in a 1:3 ratio in water resulted in a turbid mixture that precipitated after cooling in one day. The cobalt complex, however, was easy to redisperse. TEM without staining showed two types of aggregates: vesicle-like structures which appeared greyish under the electron microscope (relatively low cobalt content), and larger, intensely black particles, probably with a high cobalt content (pictures not shown). The latter aggregates were not uniform in size (162 - 920 nm), while the diameter distribution of the grey particles was smaller (70 - 200 nm). Since no additional staining agent was used and the coloring of the particles originates from the cobalt ions only, the grey particles probably are vesicles with a thin wall consisting of only one or a few bilayers and the intensely black particles probably amorphous agglomerates of cobalt complexes. Besides the grey aggregates, the black particles were still observed after sonication at elevated temperature ( $70\text{ }^{\circ}\text{C}$ ).

Addition of 1 equivalent of  $\text{Ni}(\text{ClO}_4)_2$  to a warm clear solution of 6 equivalents of **2a** in water gave an opalescent turbid mixture, like most of the metal complexing salts described so far. But unlike the other aqueous metal containing mixtures, this suspension was stable for weeks. TEM without staining showed that it contained almost perfectly spherical particles. Freshly prepared and aged samples were indistinguishable from each other. The particles were intensely black, which indicates a high nickel content (see Figure 4.10).

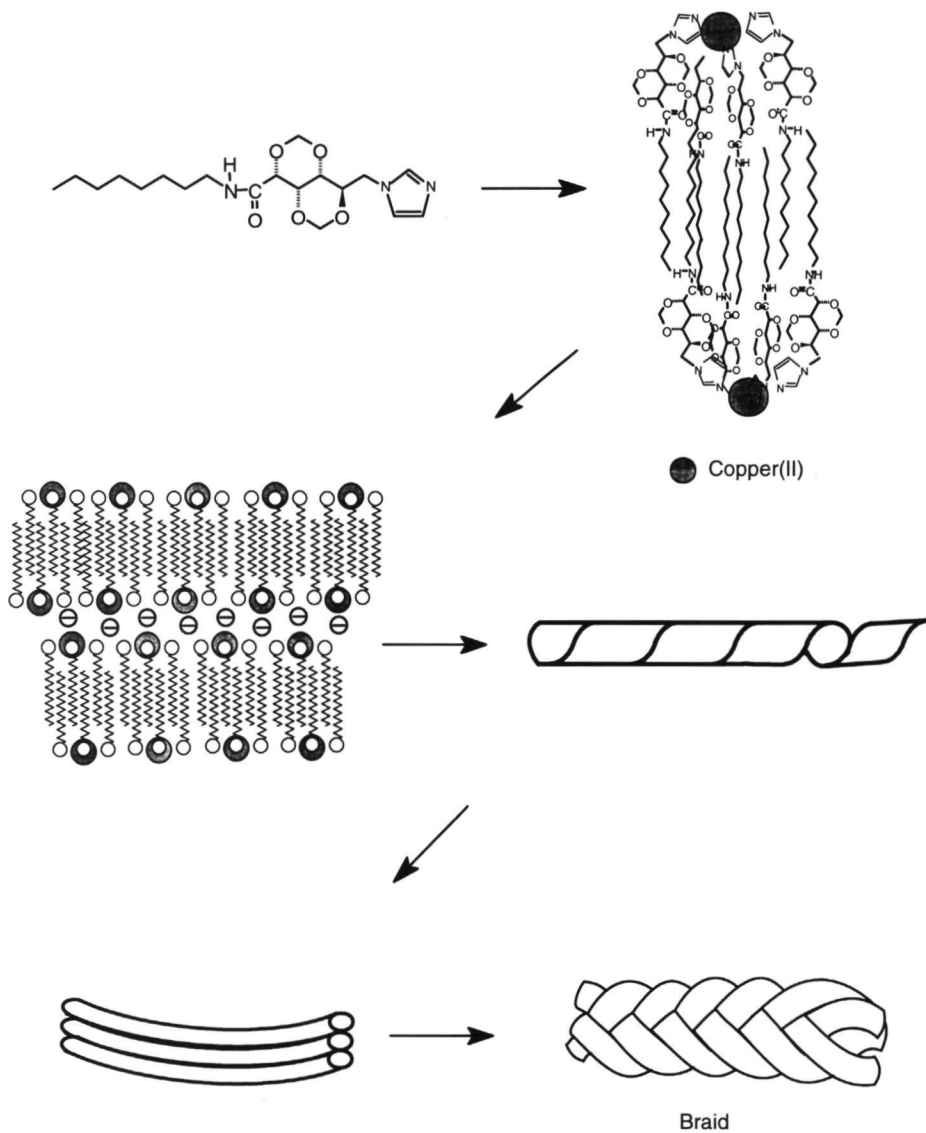


**Figure 4.10** TEM pictures of particles prepared by dispersing of  $[(\mathbf{2a})_3\text{Ni}][\text{ClO}_4]_2$  in water (no additional staining was used). Inset clustering of the particles, bar is 163 nm.

#### 4.4 Concluding remarks

Gluconamide **1** contains five unprotected hydroxyl functions and forms supramolecular aggregates in water with an almost crystalline character.<sup>5</sup> When the hydroxyl functions on carbon atoms 2, 3, 4, and 5 are protected, the compound is still soluble in water but no aggregates are visible by EM. When, however, an imidazole function is introduced on carbon atom 6 fibers, tubes, vesicles, scrolls, and braids can be prepared from the protected gluconamides. The type of aggregate structure depends on the reaction conditions. In slightly basic aqueous solutions fibers are generated that can further assemble to tubes. In acidic solutions vesicles are formed. Addition of copper perchlorate yields scrolls and braids, while nickel and cobalt perchlorate give vesicles. Although the form of the suprastructures is different, in many cases the underlying molecular pattern is the same, *viz.* a layered structure. Apparently, the carbohydrate amphiphile determines the basic mode of molecular assembling, while much of the fine tuning is achieved by the metal ions or protons present.

The most interesting suprastructure discussed in this chapter is the copper containing molecular braid. If we combine the results from the thermotropic L.C. studies described in Chapter 3 with the crystal structure of compound **2a** and the UV-vis titration experiments, we may hypothesize about the way this braid is formed from its molecular components, see Figure 4.11. Steps 1 and 2 follow from the X-ray structure of **2a** and the similarity between the thermotropic LC behavior of the series of compounds **2** and their copper(II) complexes (see Chapter 3). Step 3 (rolling up of the multilayer tape) is supported by the electron micrographs shown in Figure 4.8. Steps 4 and 5 are not supported by any experimental data. Further studies must reveal whether these steps are feasible or whether the braid is formed via a direct route from the multilayer tapes.



**Figure 4.11** Possible route for the formation of the molecular braid.

## 4.5 Literature

- <sup>1</sup> Pfannemüller, B ; Welte, W *Chem Phys Lipids* **1985**, 37, 227.
- <sup>2</sup> Fuhrhop, J -H ; Schnieder, P , Rosenberg, J., E Boekema *J Am Chem Soc* **1987**, 109, 3387.
- <sup>3</sup> Köning, J , Boettcher, C ; Winkler, H ; Zeitler, E.; Talmon, Y.; Fuhrhop, J.-H *J Am Chem Soc* **1993**, 115, 693
- <sup>4</sup> a) Fuhrhop, J -H , Svenson, S.; Boettcher, C , Rössler, E , Vieth, H.-M *J Am Chem Soc* **1990**, 112, 4307, b) Svenson, S ; Kirste, B , Fuhrhop, J -H *J Am Chem Soc* **1994**, 116, 11969.
- <sup>5</sup> Svenson, S., Köning, J , Fuhrhop, J -H *J Phys Chem* **1994**, 98, 1022.
- <sup>6</sup> Fuhrhop, J -H , Boettcher, C. *J Am Chem Soc* **1990**, 112, 1768
- <sup>7</sup> Fuhrhop, J -H , Demoulin, C ; Rosenberg; Boettcher, C *J Am Chem Soc.* **1990**, 112, 2827
- <sup>8</sup> a) Yager, P ; Schoen, P E ; Davies, C.; Price, R , Singh, A. *Biophys J* **1985**, 48, 899; b) Markowitz, M A , Schnur, J M Singh, A. *Chem Phys Lipids* **1992**, 62, 193.
- <sup>9</sup> Kunitake, T ; Kim, J -M ; Ishikawa, Y *J Chem Soc , Perkin Trans 2* **1991**, 885
- <sup>10</sup> Shimizu, T.; Mori, M , Minamikawa, H., Hato, M *J Chem Soc , Chem Commun* **1990**, 183
- <sup>11</sup> Tachibana, T , Kambara, H *J Colloid Sci* **1968**, 28, 173.
- <sup>12</sup> Papahadjopoulos, D , Vail, W J ; Jacobsen, K , Poste, G *Biochim Biophys Acta* **1975**, 394, 483
- <sup>13</sup> Hafkamp, R J H , Feiters, M C ; Nolte, R.J.M *Angew Chem.* **1994**, 106, 1054, *Ibid Int Ed Engl* **1994**, 33, 986
- <sup>14</sup> a) Komura, H , Yoshino, T , Ishido, Y *Carbohydrate Res* **1973**, 31, 154, b) Yoshino, T., Inabe, S , Komura, H., Ishido, Y *Bull Chem Soc Japan* **1974**, 47, 405.
- <sup>15</sup> *CRC Handbook of Chemistry and Physics 58<sup>th</sup> ed* , Editor R C Weast, CRC Press, Cleveland Ohio, **1977-1978**, D-148
- <sup>16</sup> Perrin, D.; Dempsey, B. *Buffers for pH and metal ion control*, Wiley and Sons, London **1974**.
- <sup>17</sup> Reedijk, J. *Recl Trav Chim. Pays-Bas* **1969**, 1451.
- <sup>18</sup> We initially assumed that the complexation behavior of  $\text{Co}(\text{ClO}_4)_2$  and  $\text{Ni}(\text{ClO}_4)_2$  with **2a** would be similar to that of imidazole as described in the literature (ref 17), and, therefore, **2a** and the metal salts were mixed in a 6:1 (ligand/metal) stoichiometry. Later, we learned from UV-vis titrations that the complexation behavior of **2a** is different: with  $\text{Co}(\text{II})$  and with  $\text{Ni}(\text{II})$  3:1 ligand to metal complexes are formed.
- <sup>19</sup> Bernarducci, E., Schwindinger, W.F ; Hughey, IV, J L.; Krogh-Jespersen, K., Schugar, H J. *J Am Chem Soc* **1981**, 103, 1686
- <sup>20</sup> Esch, J van; Damen, M.; Feiters, M C , Nolte, R.J.M *Recl Trav Chim Pays-Bas* **1994**, 113, 186
- <sup>21</sup> Arevalillo, A.; Pena, M J. *Electrochim Acta* **1993**, 38, 957
- <sup>22</sup> Coyle, C L , Stiefel, E I. *The Bioinorganic Chemistry of Nickel*, ed. Lancaster Jr, J.R VCH Publishers, Inc , Weinheim, **1988**, 6
- <sup>23</sup> a) Shinoda, K, Hutchinson, E *J Phys Chem* **1962**, 66, 577, b) Shinoda, K; Yamaguchi, N ; Carlsson, A. *J Phys Chem* **1989**, 93, 7216, c) Raaijmakers, H W.C.; Arnouts, E G., Zwanenburg, B; Chittenden, G J F , Doren van, H.A *Recl Trav Chim Pays-Bas* **1995**, 114, 301
- <sup>24</sup> Pfannemüller, B , Kühn, I *Macromol Chem* **1988**, 189, 2433.
- <sup>25</sup> Zabel, V; Müller-Fahrmow, A., Hilgenfeld, R ; Saenger, W ; Pfannemüller, B ; Enkelmann, V.; Welte, W *Chem Phys Lipids* **1986**, 39, 313



<sup>26</sup> Fuhrhop, J -H, Köning, J *Membranes and Molecular Assemblies The Synkinetic Approach*, part of the series "Monographs in Supramolecular Chemistry" series ed Stoddart, J F , The Royal Society of Chemistry, Cambridge (UK) **1994**, pag IX

<sup>27</sup> Fuhrhop, J -H , Spiroski, D , Boettcher, C *J Am Chem Soc* **1993**, *115*, 1600

<sup>28</sup> See Chapter 3, section 3 3 7, compound [(1d)<sub>4</sub>Cu][OTf]<sub>2</sub>

<sup>29</sup> Pfannemüller, B , Welte, W , Chin, E , Goodby, J W *Liq Cryst* **1986**, *1*, 357

<sup>30</sup> Synthesis was described in Chapter 3, compound [(19)<sub>4</sub>Cu][OTf]<sub>2</sub>

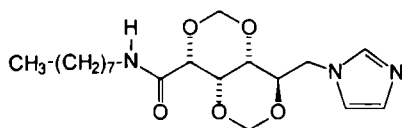
<sup>31</sup> See Chapter 3, Section 3 3 4, compound [(6a)<sub>4</sub>Cu][OTf]<sub>2</sub>

## Chapter 5

### Positional variation of the imidazole group in gluconamide amphiphiles. Effects on the aggregation behavior

#### 5.1 Introduction

In Chapter 3 we described the synthesis and thermotropic liquid crystalline behavior of amphiphilic 6-deoxy-6-(1-imidazolyl)-2,4;3,5-dimethylene-*N*,*n*-octyl-D-gluconamides (e.g. **1**) and their copper complexes, e.g. Cu(**1**)<sub>4</sub>. From both the X-ray structure of **1** and the study of the liquid crystalline properties of a series of compounds related to **1** and Cu(**1**)<sub>4</sub>, we concluded that in the superstructures of **1** and Cu(**1**)<sub>4</sub>, the imidazole group plays an important role in the packing of the molecules, viz. via hydrogen bonded water molecules and complexed copper ions.

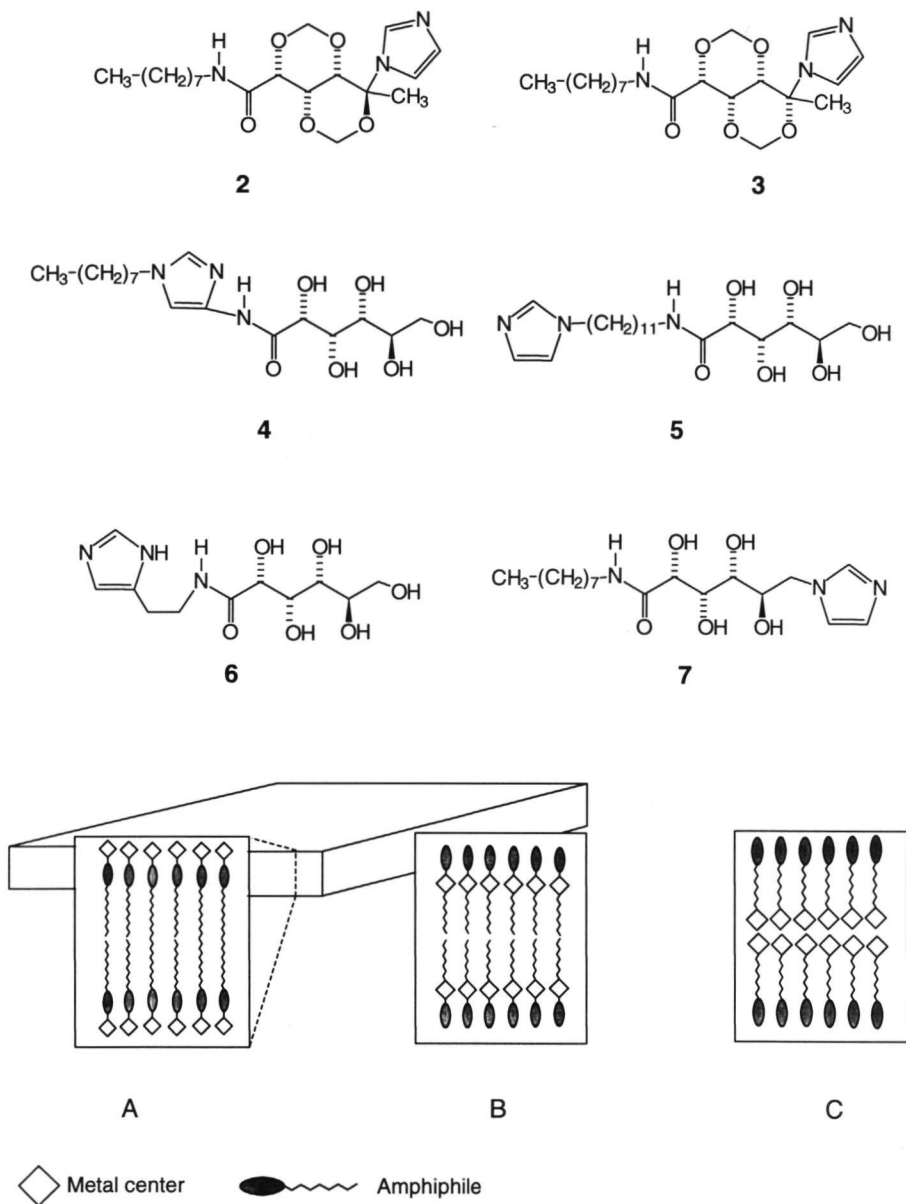


**1**

We also concluded that the rigid *cis*-decaline structure of the methylene protected glucon head group is indispensable for the formation of aggregates in water, because *N*,*n*-octyl-6-(1-imidazolyl)-*n*-hexanoic acid amide and its derived copper complex, which both lack the carbohydrate framework, did not form supramolecular structures in this solvent (see Chapter 4).

In order to investigate the effect of the position of the imidazole group in the amphiphile on the aggregation behavior of this molecule, we prepared and studied gluconamide derivatives **2-6**. Compounds **4-6** were not provided with methylene-protecting groups because of synthetic problems. For reasons of comparison we also synthesized gluconamide **7** and 1-*n*-hexadecylimidazole **8**. In compound **7** the imidazole group is attached to the carbohydrate framework, but in contrast to **1**, this compound lacks the methylene protecting groups.

Metal complexes of amphiphiles<sup>1,2,3</sup> containing imidazole groups are of interest for catalytic applications (see Chapter 7).<sup>4</sup> Another reason for synthesizing compounds **2-6**, therefore, was to see whether these compounds could be used to design new types of amphiphilic catalysts, i.e. catalysts in which the metal center is located at different, but well-defined positions, in the supramolecular aggregate, see Figure 5.1.



**Figure 5.1** Assemblies of amphilic metal complexes in which the metal is located at different positions in the aggregate. A) Metal centers at the aqueous interface as observed for  $\text{Cu(1)}_4$ . B) Metal centers located between the head group region and the aliphatic chain as expected for metal complexes of compound 4. C) Metal centers in the center of the bilayer, as expected for metal complexes of compound 5.

## 5.2 Experimental section

Analytical instruments and electron microscopes were identical to those described in the Chapters 3 and 4.

The  $pK_a^*$  values of compounds **4** and **7** were determined as described in Chapter 4.

### 5.2.1 Syntheses

For numbering of protons and carbon atoms see Chapter 3.

**6-Deoxy-6-iodo-2,4;3,5-dimethylene-*N*,*n*-octyl-D-gluconamide (9).** This compound was synthesized by dissolving 10.039 g (20.67 mmol) of 6-tosyloxy-2,4;3,5-dimethylene-*N*,*n*-octyl-D-gluconamide (the synthesis of this tosylate was described in Chapter 3) and 15.587 g (103.99 mmol) of NaI in 75 ml of anhydrous acetone and stirring overnight in an autoclave at 100 °C. After the precipitated NaOTs had been removed by filtration, the solution was evaporated to dryness. The product was dissolved in chloroform and subsequently washed with water. After drying, a white powder was obtained, yield 8.61 g (19.50 mmol, 94.3 %) of **9**, m.p. 160.9 °C. IR (KBr) 3304  $\text{cm}^{-1}$  (NH), 1657 (amide I), 1549 (amide II), 723 (C-I).  $^1\text{H-NMR}$  (90 MHz,  $\text{CDCl}_3$ )  $\delta$  6.520 ppm (t, 1H, NHCO), 5.264 (d,  $J_{7a-b}$  = 6.62 Hz, 1H,  $\text{H}^{7a}$ ), 4.914 (s, 2H,  $8^{a,b}$ ), 4.838 (d, 1H,  $\text{H}^{7b}$ ), 4.130 (m, 3H,  $\text{H}^{2-4}$ ), 3.900 (s, 1H,  $\text{H}^3$ ), 3.444 (s, 1H,  $\text{H}^6a$ ), 3.356 (s, 1H,  $\text{H}^6b$ ), 3.320 (double t, 2H,  $-\text{CH}_2\text{NHCO}$ ), 1.280 (m, 12H,  $(\text{CH}_2)_6$ ), 0.870 (t, 3H,  $\text{CH}_3$ ). EI-MS  $m/z$  441 ( $\text{M}^+$ ), 156 ( $(\text{CH}_3(\text{CH}_2)_5\text{NHCO})^+$ ), 85 (cyclic  $-\text{O}-\text{CH}=\text{CH}-\text{CH}^+-\text{O}-\text{CH}_2$ ). Anal. Calcd. for  $\text{C}_{16}\text{H}_{28}\text{NO}_5$ : C, 43.63; H, 6.41; N, 3.18. Found: C, 43.75; H, 6.29; N, 3.23.

**6-Deoxy-5-(1-imidazolyl)-2,4;3,5-dimethylene-*N*,*n*-octyl-D-gluconamide (2).** To a solution of 5.079 g (11.51 mmol) of 6-deoxy-6-iodo-2,4;3,5-dimethylene-*N*,*n*-octyl-D-gluconamide (**9**) in 75 ml of DMF was added 7.840 g (115.16 mmol, 10 equiv.) of imidazole and the solution was stirred at 60 °C in a nitrogen atmosphere. After 6 days the temperature was raised to 80 °C and two days later to 100 °C at which it was kept for an additional reaction period of 2 days (10 days of reaction in total). The DMF was removed under reduced pressure and the remaining oil mixed with toluene and subsequently washed with aqueous (saturated)  $\text{NaHCO}_3$  solution. The product was purified by column chromatography (silica, eluent  $\text{Et}_3\text{N}/\text{MeOH}/\text{EtOAc}$  1:5:94, v/v/v). The 3<sup>rd</sup> fraction collected from the column appeared to be compound **2** (white powder), yield 0.11 g (0.29 mmol, 2.5 %), m.p. 152.2 °C. IR (KBr) 3330  $\text{cm}^{-1}$  (NH), 1660 (amide I), 1537 (amide II).  $^1\text{H-NMR}$  (400 MHz,  $\text{CDCl}_3$ )  $\delta$  7.805 ppm (s, 1H,  $\text{N}-\text{CH}=\text{N}$ ), 7.073 (s, 1H,  $\text{N}-\text{CH}=\text{CH}-\text{N}$ ), 7.070 (s, 1H,  $\text{N}-\text{CH}=\text{CH}-\text{N}$ ), 6.541 (t, 1H, NHCO), 5.217 (d, 1H,  $J_{7a-b}$  = 6.83 Hz,  $\text{H}^{7a}$ ), 5.169 (d, 1H,  $J_{8a-b}$  = 4.16 Hz,  $\text{H}^{8a}$ ), 5.152 (d, 1H,  $\text{H}^{8b}$ ), 4.644 (d, 1H,  $\text{H}^{7b}$ ), 4.365 (t, 1H,  $\text{H}^3$ ), 4.122 (d,  $J_{2-3}$  = 1.61 Hz,  $\text{H}^2$ ), 3.617 (s, 1H,  $\text{H}^4$ ), 3.309 (11 peaks, 2H,  $-\text{CH}_2-\text{NHCO}$ ), 1.896 (s, 3H,  $\text{H}^6$ ), 1.501 (5 peaks, 2H,  $-\text{CH}_2-\text{CH}_2-\text{NHCO}$ ), 1.265 (m, 10 H,  $(\text{CH}_2)_5-\text{CH}_3$ ), 0.879 (t, 3H,  $(\text{CH}_2)_5-\text{CH}_3$ ). EI-MS  $m/z$  381 ( $\text{M}^+$ ), 314 ( $\text{M} - \text{imidazolyl}$ ) $^+$ , 156 ( $\text{C}_8\text{H}_{17}\text{NHCO}$ ) $^+$ , 85 (cyclic  $-\text{O}-\text{CH}=\text{CH}-\text{CH}^+-\text{O}-\text{CH}_2$ ). Anal. Calcd. for  $\text{C}_{19}\text{H}_{31}\text{N}_3\text{O}_5$ : C, 59.82; H, 8.19; N, 11.02. Found: C, 59.36; H, 7.89; N, 10.97.

**6-Deoxy-5-(1-imidazolyl)-2,4;3,5-dimethylene-*N*,*n*-octyl-D-idoitonamide (3).** This compound was obtained from the same reaction mixture as compound **2**. The 2<sup>nd</sup> fraction collected from the column (see the synthesis of compound **2**) appeared to be compound **3**; yield 0.25 g (0.66 mmol, 6.7 %) of a highly viscous oil. IR (KBr) 3427  $\text{cm}^{-1}$  (NH), 3115 (C-H), 1666 (amide I), 1543 (amide II).  $^1\text{H-NMR}$  (400 MHz,  $\text{CDCl}_3$ )  $\delta$  7.684 ppm (s, 1H,  $\text{N}-\text{CH}=\text{N}$ ), 7.157 (s, 1H,  $\text{N}-\text{CH}=\text{CH}-\text{N}$ ), 7.029 (s, 1H,  $\text{N}-\text{CH}=\text{CH}-\text{N}$ ), 6.524 (t, 1H, NHCO), 5.384 (d, 1H,  $J_{7a-b}$  = 6.54 Hz,  $\text{H}^{7a}$ ), 5.009 (d, 1H,  $J_{8a-b}$  = 6.73 Hz,  $\text{H}^{8a}$ ), 4.947 (d, 1H,  $\text{H}^{7b}$ ), 4.737 (d, 1H,  $\text{H}^{8b}$ ), 4.232 (d,  $J_{2-3}$  = 1.96 Hz,  $\text{H}^2$ ), 4.160 (t, 1H,  $J_{3-4}$  = 1.46 Hz,  $\text{H}^3$ ), 4.130 (broad s, 1H,  $\text{H}^4$ ), 3.290 (11 peaks, 2H,  $-\text{CH}_2-\text{NHCO}$ ), 1.661 (s, 3H,  $\text{H}^6$ ), 1.500 (5 peaks, 2H,  $-\text{CH}_2-\text{CH}_2-\text{NHCO}$ ), 1.251 (m, 10 H,  $(\text{CH}_2)_5-$

CH<sub>3</sub>), 0,879 (t, 3H, (CH<sub>2</sub>)<sub>5</sub>-CH<sub>3</sub>) EI-MS *m/z* 381 (M)<sup>+</sup>, 314 (M - imidazolyl)<sup>+</sup>, 156 (C<sub>8</sub>H<sub>17</sub>NHCO)<sup>+</sup>, 85 (cyclic -O-CH=CH-CH<sup>+</sup>-O-CH<sub>2</sub>) Anal Calcd for C<sub>19</sub>H<sub>31</sub>N<sub>3</sub>O<sub>5</sub>·H<sub>2</sub>O C, 57 13, H, 8 33, N, 10 52 Found C, 57 83, H, 8 09, N, 10 82

**6-Deoxy-5,6-didehydro-2,4,3,5-dimethylene-N,n-octyl-D-gluconamide (10).** This compound was obtained from the same reaction mixture as compound 2. The 1<sup>st</sup> fraction eluted from the column (see the synthesis of compound 2) appeared to be this elimination product, yield 1 98 g (6 32 mmol, 58 6 %) of white powder, m p 111 6 °C IR (KBr) 3293 cm<sup>-1</sup> (very sharp, N-H), 3121, 3089 (-C-H), 1658 (amide I), 1555 (amide II), 863 (=C-H, swing) <sup>1</sup>H-NMR (400 MHz, CDCl<sub>3</sub>) δ 6 565 ppm (broad t, 1H, NHCO), 5 248 (d, 2H, H<sup>7a</sup>+H<sup>8a</sup>), 4 828 (2d, 2H, H<sup>7b</sup>+H<sup>8b</sup>), 4 797 (s, 1H, H<sup>2</sup>), 4,618 (d, 1H, J<sub>2,3</sub> = 1 6 Hz, H<sup>3</sup>), 4 181 (s, 1H, H<sup>4</sup>), 4 100 (s, 2H, =CH<sub>2</sub>), 3 306 (2t, 2H, -CH<sub>2</sub>-NHCO), 1 522 (m, 2H, -CH<sub>2</sub>-CH<sub>2</sub>-NHCO), 1 265 (m 10 H, CH<sub>3</sub>-(CH<sub>2</sub>)<sub>5</sub>-), 0 877 (t, 3H, CH<sub>3</sub>-) Anal Calcd for C<sub>16</sub>H<sub>27</sub>NO<sub>5</sub> C, 61 31, H, 8 68, N, 4 47 Found C, 61 27, H, 8 77, N, 4 63

**6-Deoxy-6-(1-imidazolyl)-N,n-octyl-D-gluconamide (7)** Tosyl chloride (2 255 g, 11 83 mmol) dissolved in 10 ml of pyridine, was added dropwise to a stirred gelated solution of 3 26 g (10 75 mmol) of N,n-octyl-D-gluconamide in 25 ml of pyridine which was cooled in an ice bath. The reaction was carried out in a dry nitrogen atmosphere. After 1 hr of stirring at room temperature and subsequent reaction overnight in the refrigerator, 7 72 g (76 2 mmol, 7 equiv) of acetic acid anhydride was added. After 24 hrs of stirring, the clear solution was poured into a mixture of saturated NaHCO<sub>3</sub> and ice. The precipitate was collected and dried in vacuum. According to <sup>1</sup>H-NMR and IR, 6-deoxy-6-tosyl-N-(octyl)-D-gluconamide tetraacetate (11) was formed. The crude product was used without further purification to avoid deterioration. The tosylate group was substituted by an imidazole group in a high pressure reaction vessel using 3 014 g (4 79 mmol) of tosylate 11 and 0 652 g (9 58 mmol, 2 equiv) of imidazole in 7 5 ml of CHCl<sub>3</sub>. Reaction conditions 15 kBar, 50 °C, 40 hrs. The intermediate product compound (12) was purified by column chromatography (silica, eluent Et<sub>3</sub>N/MeOH/EtOAc 1 5 95, v/v/v), yield 0 66 g (1 26 mmol, 26 4 %). The acetate groups of 12 were removed by treating 0 664 g (1 26 mmol) of this compound with 3 9 mg of NaOMe in 60 ml of MeOH (0 05 equiv NaOMe with respect to the imidazole compound). The deprotected product (7) was purified by recrystallization from EtOAc, yield after deprotection was quantitative, m p 104 °C, IR (KBr) 3640-3020 cm<sup>-1</sup> (OH, broad), 3149, 3119 (=C-H), 1646 (Amide I), 1540 (Amide II), <sup>1</sup>H-NMR (CD<sub>3</sub>OD, 400 Mz), δ 7 697 ppm (s, 1H, N-CH=N), 7 184 (s, 1H, N-CH=CH-N), 6 971 (s, 1H, N-CH=CH-N), 4 326 (2d, 1H, J<sub>5,6a</sub> = 3 65 Hz, J<sub>6a,6b</sub> = 14 22 Hz, H<sup>6a</sup>), 4 176 (d, 1H, J<sub>2,3</sub> = 2 36 Hz, H<sup>2</sup>), 4 067 (H<sup>3</sup> mixed with part H<sup>6b</sup>), 4 063 (2d, 1H, J<sub>6b,5</sub> = 7 08 Hz, H<sup>6b</sup>), 3 875 (5 peaks, 1H, H<sup>5</sup>), 3 492 (2d, 1H, J<sub>4,5</sub> = 8 52, H<sup>4</sup>), 3 218 (9 peaks, 2H, (CH<sub>2</sub>)<sub>6</sub>-CH<sub>2</sub>-NHCO), 1 309 (t, 2H, (CH<sub>2</sub>)<sub>5</sub>-CH<sub>2</sub>-CH<sub>2</sub>-NHCO), 0 899 (t, 3H, CH<sub>3</sub>-). No satisfactory mass spectrum (EI or CI) could be obtained. Anal Calcd for C<sub>17</sub>H<sub>31</sub>N<sub>3</sub>O<sub>5</sub>·H<sub>2</sub>O C, 54 38, H, 8 86, N, 11 19 Found C, 54 36, H, 8 55, N, 10 49

**n-Octyl tosylate (13)** n-Octyl alcohol (5 050 g, 38 78 mmol) was tosylated in a standard reaction using 7 67 g (40 23 mmol) of tosyl chloride and 50 ml of pyridine. Yield 9 35 g (32 88 mmol, 84 8 %) of 13. The tosylate was used in the following reaction step without further purification. <sup>1</sup>H-NMR (90 MHz, CDCl<sub>3</sub>) δ 7 778 and 7 324 ppm (2d, J = 8 27 Hz, 2H, ArH), 4 015 (t, J = 6 30 Hz, 2H, -(CH<sub>2</sub>)<sub>6</sub>-CH<sub>2</sub>-OTs), 2 423 (s, 3H, Ar-CH<sub>3</sub>), 1 627 (t, 2H, -(CH<sub>2</sub>)<sub>5</sub>-CH<sub>2</sub>-CH<sub>2</sub>OTs), 1 303 (s, 10H, H<sub>3</sub>C-(CH<sub>2</sub>)<sub>5</sub>-CH<sub>2</sub>-), 0 858 (t, 3H, CH<sub>3</sub>-)

**1-(4-Nitro-1-imidazolyl)-n-octane (14)** To a solution of 1 311 g (11 60 mmol) of 4-nitroimidazole in 10 ml of anhydrous DMF was carefully added 0 46 g (11 50 mmol, 1 0 equiv)

of  $\text{NaH}^+$ . After heating for 30 min. at 60 °C, 2.889 g (10.16 mmol, 0.9 equiv.) of *n*-octyl tosylate (**13**) was added to the clear green solution and the mixture was stirred at 60 °C for 3 days. After this reaction period, a precipitate (sodium tosylate) was removed by filtration. After dilution of the filtrate with toluene and repeated washing with water, the organic layer was dried on  $\text{MgSO}_4$ . The solvent was removed by evaporation and a brown oil remained, which was diluted with *n*-hexane. From this solution white crystals appeared which were light sensitive and therefore were stored in the dark. Yield 2.10 g (9.32 mmol 91.8 %) of **14**, m.p. 44.7 °C. IR (KBr) 3113  $\text{cm}^{-1}$  (imidazole =C-H), 2919 (-CH<sub>2</sub>-) and 2855 (-CH<sub>3</sub>), 1523 and 1333 (-NO<sub>2</sub>), <sup>1</sup>H-NMR (90 MHz,  $\text{CDCl}_3$ )  $\delta$  7.778 ppm (d,  $J=1.4$  Hz long range, 1H, =C(NO<sub>2</sub>)-N=CH-N-(CH<sub>2</sub>)<sub>7</sub>-), 7.425 (d,  $J=1.4$  Hz long range, 1H, N-CH=C-NO<sub>2</sub>), 4.019 (t,  $J=7.1$  Hz, 2H, -(CH<sub>2</sub>)<sub>6</sub>-CH<sub>2</sub>-N), 1.850 (t,  $J=7.1$  Hz, 2H, H<sub>3</sub>C-(CH<sub>2</sub>)<sub>5</sub>-CH<sub>2</sub>-CH<sub>2</sub>), 1.285 (s, 10H, H<sub>3</sub>C-(CH<sub>2</sub>)<sub>5</sub>-CH<sub>2</sub>), 0.874 (t, 3H, CH<sub>3</sub>-). EI-MS  $m/z$  225 (M)<sup>+</sup>, 179 (M - NO<sub>2</sub>)<sup>+</sup>. Anal. Calcd. for C<sub>11</sub>H<sub>19</sub>N<sub>3</sub>O<sub>2</sub>: C, 58.65; H, 8.50; N, 8.65. Found: C, 58.31; H, 8.30; N, 8.25.

**1-(4-Amino-1-imidazolyl)-*n*-octane (15).** A solution of 2.11 g (9.35 mmol) of **14** in 50 ml of 1,4-dioxane was purged for several min. with a flow of nitrogen. The nitro group was reduced with Pd/C and H<sub>2</sub>.<sup>5</sup> According to TLC (hexane/EtOAc, 1:1, v/v, UV detection and detection with ninhydrine<sup>6</sup>) the reduction was completed after 3 hrs. The mixture was filtered over Celite and concentrated under reduced pressure. Because the product appeared to be air sensitive, it was used for the next step without isolation or further characterization.

**1-(*n*-Octyl)-4-imidazolyl-*N*-D-gluconamide (4).** A clear solution of 2.0 g (10.24 mmol) of **15** in 25 ml of 1,4-dioxane was heated to reflux and 2.01 g (6.54 mmol, 1.2 equiv.) of 1,5-D-gluconolactone was added. After refluxing overnight the solvent was evaporated under reduced pressure. The product was diluted with chloroform and washed with aqueous saturated NaHCO<sub>3</sub>. The brown precipitate at the interface of the aqueous and the organic layer was collected by filtration. The brown precipitate was washed with chloroform and alkaline water until a white powder remained, which was subsequently recrystallized from methanol. Yield 1.35 g (3.62 mmol, 38.7 %), m.p. 172.3 °C. IR (KBr) 3620-3000  $\text{cm}^{-1}$  (OH), 3161 and 3134 (imidazole =C-H), 2927 (-CH<sub>2</sub>-), 1670 (Amide I), 1578 (Amide II), <sup>1</sup>H-NMR (400 MHz, DMSO-*d*<sub>6</sub> after addition of a drop of D<sub>2</sub>O)  $\delta$  9.195 ppm (s, 1H, NHCO), 7.407 (d,  $J=1.4$  Hz long range, 1H, N<sub>im</sub>-CH=C(N<sub>im</sub>)-NH-CO), 7.215 (d,  $J=1.4$  Hz long range, 1H, -(CH<sub>2</sub>)<sub>7</sub>-N<sub>im</sub>-CH=N<sub>im</sub>-CH), 4.141 (d, 1H,  $J_{2,3}=3.64$  Hz, H<sup>2</sup>), 3.935 (2d, 1H,  $J_{3,4}=2.46$  Hz, H<sup>3</sup>), 3.879 (t, 2H, -(CH<sub>2</sub>)<sub>6</sub>-CH<sub>2</sub>-N), 3.568 (2d, 1H,  $J_{6a,5}=2.73$  Hz, H<sup>6a</sup>), 3.507 (m, 1H,  $J_{4,5}=8.35$  Hz, H<sup>4</sup>, H<sup>4</sup>-H<sup>5</sup> are overlapping, however, the same pattern was obtained after simulation with the program GeNMR<sup>®</sup>), 3.498 (m, 1H, H<sup>5</sup>), 3.379 (2d, 1H,  $J_{6a,6b}=-10.95$ , H<sup>6b</sup>), 1.650 (t, 2H, H<sub>3</sub>C-(CH<sub>2</sub>)<sub>5</sub>-CH<sub>2</sub>-CH<sub>2</sub>), 1.204 (s, 10H, H<sub>3</sub>C-(CH<sub>2</sub>)<sub>5</sub>-CH<sub>2</sub>), 0.813 (t, 3H, CH<sub>3</sub>-), <sup>13</sup>C-NMR (110 MHz, DMSO-*d*<sub>6</sub>)  $\delta$  169.22 ppm (-C=O), 136.82 (N<sub>im</sub>-CH-N<sub>im</sub>), 133.08 (-CH<sub>2</sub>-N<sub>im</sub>-CH=C(N<sub>im</sub>)-), 120.60 (-CH<sub>2</sub>-N<sub>im</sub>-CH=C(N<sub>im</sub>)-NHCO-), 73.45 (C=O-CH(OH)-), 72.23 (C=O-CH(OH)-CH(OH)-), 71.52 (C=O-(CH(OH))<sub>2</sub>-CH(OH)-), 70.22 (C=O-(CH(OH))<sub>3</sub>-CH(OH)-), 46.21 (-CH<sub>2</sub>-N<sub>imidazole</sub>), 13.76 (CH<sub>3</sub>-). Anal. Calcd. for C<sub>17</sub>H<sub>31</sub>N<sub>3</sub>O<sub>6</sub>: C, 54.68; H, 8.37; N, 11.25. Found: C, 54.71; H, 8.24; N, 11.02.

**11-(*t*-Butyloxyamido)-*n*-undecan-1-ol (16).** In 30 min., 4.29 g (30.0 mmol, 1.5 equiv.) of *t*-butyloxycarboxy azide in 50 ml of dioxane was added dropwise to a solution of 4.03 g (21.5 mmol) of 11-amino-undecan-1-ol in 40 ml of water. After stirring overnight at room temperature, the dioxane and the excess of *t*-butyloxycarboxy azide were removed under reduced pressure. The water-layer was extracted 3 times with 50 ml of diethyl ether. The collected organic layers were dried ( $\text{MgSO}_4$ ) and concentrated to give a yellow powder. Yield 2.90 g (10.1 mmol,

<sup>†</sup> The NaH was dispersed in mineral oil (60 %) and was washed twice with anhydrous diethyl ether prior to use

46.9 %), m.p. 36.4 °C. IR (KBr) 3381  $\text{cm}^{-1}$  (NH), 2982 ( $\text{CH}_3$  from *t*-butoxy group), 2921 ( $\text{CH}_2$ ), 1690 ( $\text{C}=\text{O}$ ), 1523 (NH).  $^1\text{H-NMR}$  (100 MHz,  $\text{CDCl}_3$ )  $\delta$  4.48 ppm (broad t, 1H, NHCO), 3.64 (t, 2H,  $-\text{CH}_2\text{-OH}$ ), 3.10 (q, 2H,  $-\text{CH}_2\text{-NHCO}$ ), 1.44 (s, 9H,  $(\text{CH}_3)_3$ ), 1.28 (broad s, 18H,  $-(\text{CH}_2)_9$ ). Anal. Calcd. for  $\text{C}_{16}\text{H}_{33}\text{NO}_3$ : C, 66.86; H, 11.57; N, 4.87. Found: C, 67.15; H, 11.62; N, 4.76.

**11-(*t*-Butyloxyamido)-*n*-undecyl tosylate (17).** In 30 min., a solution of 2.51 g (13.14 mmol, 1.1 equiv.) of tosyl chloride in 15 ml of pyridine was added dropwise to a solution of 3.41 g (11.86 mmol) of **16** in 30 ml of anhydrous pyridine which was cooled in an ice bath. The reaction vessel was purged with dried nitrogen gas. After an additional 60 min. of stirring, the clear mixture was placed overnight in the refrigerator for completion of the reaction. The solution was poured out into a mixture of ice and saturated  $\text{NaHCO}_3$ . The oily product was extracted with chloroform and the organic layer was dried on  $\text{MgSO}_4$ . The product was purified by column chromatography (silica, eluent EtOAc/hexane 1:5, v/v). Yield 1.83 g (4.26 mmol, 36.0 %) of **17**, m.p. 44.5 °C. IR (KBr) 3377  $\text{cm}^{-1}$  (NH), 1688 ( $\text{C}=\text{O}$ ), 1523 (NH), 1364 ( $\text{S}=\text{O}$ ).  $^1\text{H-NMR}$  (100 MHz,  $\text{CDCl}_3$ )  $\delta$  7.79 ppm (d, 2H, ArH), 7.34 (d, 2H, ArH), 4.48 (broad t, 1H, NHCO), 4.01 (t, 2H,  $-\text{CH}_2\text{-OTs}$ ), 3.10 (pseudo q, 2H,  $-\text{CH}_2\text{-NHCO}$ ), 2.45 (s, 3H, Ar- $\text{CH}_3$ ), 1.44 (s, 9H,  $(\text{CH}_3)_3$ ), 1.22 (broad s, 18H,  $-(\text{CH}_2)_9$ ). Anal. Calcd. for  $\text{C}_{23}\text{H}_{39}\text{NO}_5\text{S}$ : C, 62.55; H, 8.90; N, 3.17; S, 7.26. Found: C, 62.46; H, 8.57; N, 3.26; S, 6.88.

**11-(*t*-Butyloxyamido)-*n*-undecylimidazole (18).** Imidazole (0.40 g, 5.90 mmol) was converted into its sodium salt with sodium hydride (0.248 g, 1.05 equiv., washed twice with *n*-hexane in order to remove the mineral oil) in 50 ml of anhydrous DMF (60 °C, 0.5 hr.). To this green solution, 1.30 g (2.94 mmol, 0.5 equiv.) of **17** was added. After overnight reaction at 60 °C, the DMF was removed by evaporation and the remaining pale yellow powder was dissolved in chloroform. The organic layer was washed twice with water and dried on  $\text{Na}_2\text{SO}_4$ . After evaporation of the solvent, **18** was obtained as a pale yellow powder, which according to  $^1\text{H-NMR}$ , was slightly contaminated with DMF. Despite this contamination, **18** was used in the next reaction step. IR (KBr) 3112  $\text{cm}^{-1}$  ( $=\text{C-H}$ ), 1702 ( $\text{C}=\text{O}$ ), 1507 (NH),  $^1\text{H-NMR}$  (100 MHz,  $\text{CDCl}_3$ )  $\delta$  7.46 ppm (s, 1H,  $\text{N}=\text{CH-N}$ ), 7.06 (t (long range), 1H,  $\text{N-CH}=\text{CH-N-CH}_2$ ), 6.91 (t (long range), 1H,  $\text{N-CH}=\text{CH-N-CH}_2$ ), 3.92 (t, 2H,  $-\text{CH}_2\text{-Im}$ ), 3.09 (q, 2H,  $-\text{CH}_2\text{-NHCO}$ ). Due to the contamination with DMF no satisfactory elemental analysis was obtained.

**11-Imidazolyl-*n*-undecylamine (19).** To a mixture of 15 ml of TFA and 15 ml of  $\text{CH}_2\text{Cl}_2$  was added a solution of 0.91 g (2.70 mmol) of **18** in 20 ml of  $\text{CH}_2\text{Cl}_2$ . After 1 hr. of stirring at 0 °C the mixture was diluted with 50 ml of  $\text{CH}_2\text{Cl}_2$ . The organic solution was washed 3 times with aqueous 4N NaOH until the pH was  $\pm 10$ . The organic layer was dried ( $\text{Na}_2\text{SO}_4$ ) and concentrated to give a pale yellow powder which was not further purified, yield 0.302 g (105 %) of **19**. IR (KBr) 3344  $\text{cm}^{-1}$  (NH), 3096 ( $=\text{C-H}$ ),  $^1\text{H-NMR}$  (100 MHz,  $\text{CDCl}_3$ )  $\delta$  7.39 ppm (broad s, 1H,  $\text{N}=\text{CH-N}$ ), 7.98 (broad s, 1H,  $\text{N-CH}=\text{CH-N-CH}_2$ ), 6.83 (broad s, 1H,  $\text{N-CH}=\text{CH-N-CH}_2$ ), 2.60 (broad t, 2H,  $-\text{CH}_2\text{-NH}_2$ ). No satisfactory elemental analysis could be obtained due to contamination with small amounts of DMF.

***N*-(11-(1-Imidazolyl)-*n*-undecyl)-*D*-gluconamide (5).** A mixture of 0.401 g (1.47 mmol) of **19**, 0.278 g (1.56 mmol) of 1,5-*D*-gluconolactone and 0.208 g (2.06 mmol) of  $\text{Et}_3\text{N}$  in 50 ml of methanol was refluxed overnight. The solution was concentrated, which resulted in precipitation. The precipitate was filtered and purified by column chromatography (eluent  $\text{Et}_3\text{N}/\text{MeOH}/\text{CHCl}_3$  1:15:84, v/v/v) to give a yellow powder, yield 0.26 g (0.59 mmol, 40.3 %) of **5**, m.p. 107 °C. IR (KBr) 3640-3040  $\text{cm}^{-1}$  (OH), 3150 and 3140 ( $=\text{C-H}$ ), 2920 ( $-\text{CH}_2-$ ), 1641 (Amide I), 1535 (Amide II),  $^1\text{H-NMR}$  (400 MHz,  $\text{CD}_3\text{OD}$ )  $\delta$  7.680 ppm (s, 1H,  $\text{N}=\text{CH-N-CH}_2$ ), 7.130 (s, 1H,  $\text{N-CH}=\text{CH-N-CH}_2$ ), 6.980 (s, 1H,  $\text{N-CH}=\text{CH-N-CH}_2$ ), 4.205 (d, 1H,  $J_{2,3} = 3.05 \text{ Hz}$ ,  $\text{H}^2$ ), 4.090 (t,

$^1\text{H}$ ,  $J_{3-4} = 2.54$  Hz,  $\text{H}^4$ ), 4.020 (t, 2H,  $-(\text{CH}_2)_{10}-\text{CH}_2-\text{N}_{\text{im}}$ ), 3.780 (2d, 1H,  $J_{6a-5} = 2.70$  Hz,  $J_{6a-6b} = -10.94$  Hz,  $\text{H}^{6a}$ ), 3.696 (m, 1H,  $J_{4-5} = 8.58$  Hz,  $\text{H}^4$ , overlapping with  $\text{H}^5$ , values checked with GeNMR), 3.680 (m, 1H,  $\text{H}^5$ ), 3.623 (2d, 1H,  $J_{5-6b} = 5.01$  Hz,  $\text{H}^{6b}$ ), 3.230 (m, 2H,  $-\text{CH}_2-\text{NHCO}$ ), 1.790 (t, 2H,  $-(\text{CH}_2)_9-\text{CH}_2-\text{CH}_2-\text{N}_{\text{im}}$ ), 1.530 (t, 2H,  $\text{CH}_2-\text{CH}_2-\text{NHCO}$ ), 1.310 (broad s, 14H,  $-\text{CH}_2-(\text{CH}_2)_7-\text{CH}_2-$ ),  $^{13}\text{C}$ -NMR (110 MHz,  $\text{CD}_3\text{OD}$ )  $\delta$  175.00 ppm ( $-\text{C}=\text{O}$ ), , 138.27 ( $\text{N}_{\text{im}}=\text{CH}-\text{N}_{\text{im}}$ ), 128.61 ( $\text{N}_{\text{im}}-\text{CH}=\text{CH}-\text{N}_{\text{im}}-\text{CH}_2-$ ), 120.60 ( $\text{N}_{\text{im}}-\text{CH}=\text{CH}-\text{N}_{\text{im}}-\text{CH}_2-$ ), 75.35 ( $\text{O}=\text{C}-\text{CH}(\text{OH})-$ ), 74.32 ( $\text{O}=\text{C}-\text{CH}(\text{OH})-\text{CH}(\text{OH})-$ ), 74.07 ( $\text{O}=\text{C}-(\text{CH}(\text{OH}))_2-\text{CH}(\text{OH})-$ ), 73.01 ( $\text{O}=\text{C}-(\text{CH}(\text{OH}))_3-\text{CH}(\text{OH})-$ ), 48.07 ( $-\text{CH}_2-\text{N}_{\text{imidazole}}$ ), 40.11 ( $-\text{CH}_2-\text{NHCO}$ ). Anal. Calcd. for  $\text{C}_{20}\text{H}_{37}\text{N}_3\text{O}_6 \cdot \frac{1}{2} \text{H}_2\text{O}$ : C, 56.58; H, 9.02; N, 9.90. Found: C, 56.83; H, 8.62; N, 10.08.

**N-(2-(2-Imidazolyl)-ethyl)-D-gluconamide (6).** To 0.695 g (3.78 mmol) of histamine dihydrochloride were added 0.673 g (3.78 mmol, 1 equiv.) of 1,5-D-gluconolactone, 30 ml of methanol, and 0.946 g (9.35 mmol, 2.5 equiv.) of  $\text{Et}_3\text{N}$  (the latter in order to liberate the histamine from its hydrochloride salt). After 30 min. refluxing a clear solution was obtained. After refluxing for an additional 30 min. the solution was cooled. White crystals were formed which were washed with cold methanol. Yield 0.79 g (2.72 mmol, 72.6 %) of **6**, m.p. 161.1 °C. IR (KBr) 3670–2800  $\text{cm}^{-1}$  (broad, with peaks at 3476, 3379, 3324 and 3212, OH), 2960 and 2939 ( $=\text{C}-\text{H}$ ), 1645 (amide I), 1590 (aromate), 1529 (amide II).  $^1\text{H}$ -NMR (400 MHz,  $\text{DMSO}-d_6$ ),  $\delta$  7.739 ppm (t, 1H,  $\text{NHCO}$ , which disappeared after addition of one drop of  $\text{D}_2\text{O}$ ), ( $\text{DMSO}-d_6 + 1$  drop of  $\text{D}_2\text{O}$ )  $\delta$  7.536 ppm (s, 1H,  $\text{N}_{\text{im}}-\text{CH}-\text{N}_{\text{im}}$ ), 6.809 (s, 1H,  $\text{N}_{\text{im}}-\text{CH}-\text{C}(\text{CH}_2)-\text{N}_{\text{im}}$ ), 3.966 (d, 1H,  $J_{2-3} = 3.70$  Hz,  $\text{H}^2$ ), 3.873 (2d, 1H,  $J_{3-4} = 2.04$ ,  $\text{H}^3$ ), 3.557 (2d, 1H,  $J_{6a-5} = 2.54$  Hz,  $J_{6a-6b} = -10.92$  Hz,  $\text{H}_{6a}$ ), 3.461 (m, 2H,  $\text{H}^{4+5}$ ), 3.358 (m, 1H,  $\text{H}^{6b}$ ), 3.284 (t, 2H,  $J = 6.98$  Hz,  $-\text{CH}_2-\text{NHCO}$ ), 2.629 (t,  $J = 7.138$  Hz,  $-\text{CH}_2-\text{CH}_2-\text{NHCO}$ ). Anal. Calcd. for  $\text{C}_{11}\text{H}_{19}\text{N}_3\text{O}_6 \cdot \frac{1}{3} \text{H}_2\text{O}$ : C, 44.74; H, 6.71; N, 14.23. Found: C, 45.06; H, 6.45; N, 13.68.

**1-n-Hexadecylimidazole (8).** Synthesis of this compound was described in Chapter 3.

### 5.2.2 Measurements of isotherms

Isotherms were recorded on a home-built Langmuir trough equipped with a Wilhelmy balance. The trough was filled with Milli-Q<sup>®</sup> water, which was in some cases adjusted with  $\text{H}_2\text{SO}_4$  to pH=1 or buffered with Tris (pH=9). The compounds were dissolved in methanol (conc. of 2.5 mM) and an accurate amount of 40  $\mu\text{l}$  solution was added dropwise on the subphase (195  $\text{cm}^2$ ). After 5 min. of stabilization, the compression was started. The temperature deviation was within 0.2 °C, and on a clean surface the surface pressure ( $\pi$ ) stayed below 0.1 mN/m.

### 5.2.3 SAXS experiments

X-ray powder diffractograms were recorded on a Philips PW1710 powder diffractometer with a Ni filtered Cu source (40 kV, 55 mA,  $\lambda=1.54060$  Å). The aqueous suspensions were transferred to a silicon sample holder and rapidly lyophilized in a vacuum desiccator under high vacuum and in the presence of  $\text{P}_2\text{O}_5$ .

### 5.2.4 Electron microscopy

The equipment that was used for electron microscopy experiments, has been described in Chapter 4. The sample preparation was similar to the procedure described in Chapter 4, Section 4.2.5.

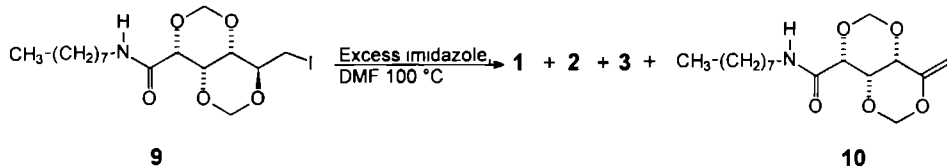


### 5.3 Results and discussion

#### 5.3.1 Preparation of the compounds

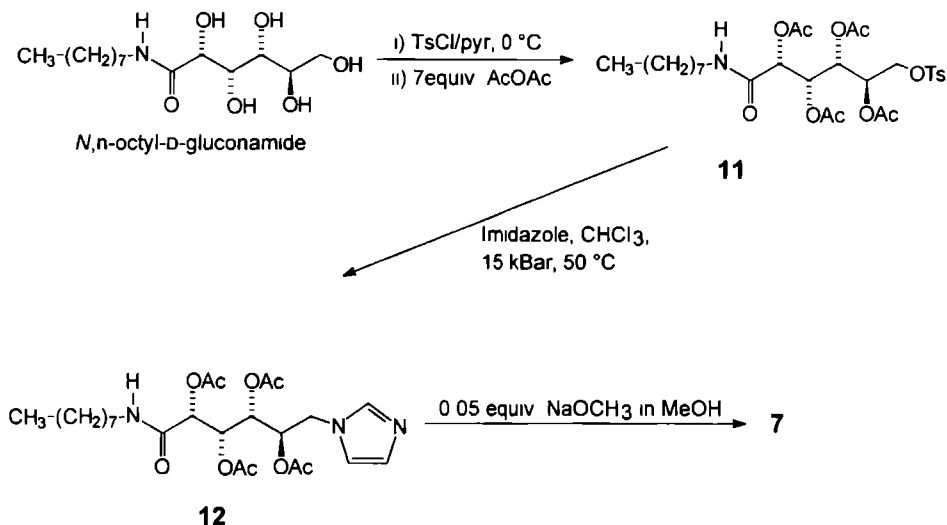
The synthesis of **1** has been described in Chapter 3. The attachment of the imidazole group to the gluconamide framework of **1** was carried out at 15 kBar to minimize the amount of elimination product. The reaction can also be carried out at normal pressure in DMF at 100 °C, with the disadvantage of low yields. If the tosylate in the above mentioned reaction (see Chapter 3) was substituted by an iodide (Scheme 5.1) the yield of **1** increased but the elimination product (**10**) was still the major component. In addition to **1** also compounds **2** and **3** (Scheme 5.1) were obtained, which could be isolated by column chromatography.

Scheme 5.1



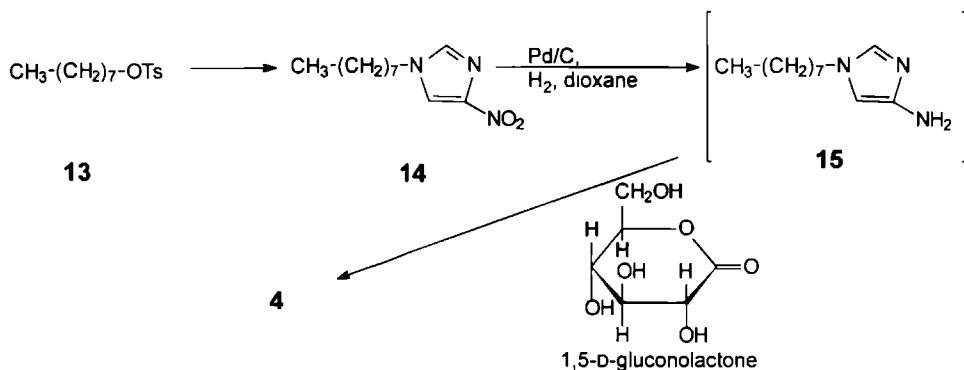
The synthesis of the non-protected 6-deoxy gluconamide **7** was performed as described in Scheme 5.2. The introduction of the imidazole group could be successfully carried out at high pressure.

Scheme 5.2



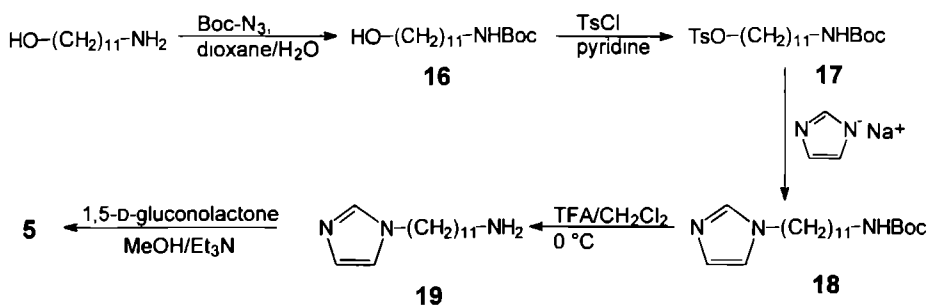
The synthesis of compound **4**, which has an imidazole group located between its head group and its alkyl chain, is outlined in Scheme 5.3. Compound **15**, which carries an amino substituted imidazole group, is air sensitive, and, therefore, was used in the subsequent reaction step to **4** without isolation.

Scheme 5.3



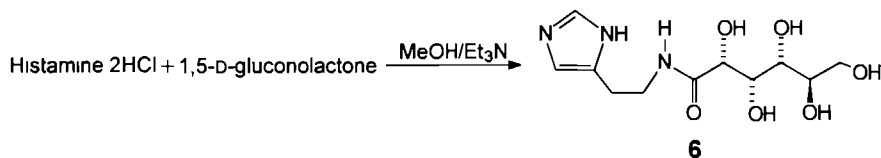
Compound **5**, in which the imidazole group is connected to the end of the alkyl chain, was synthesized according to Scheme 5.4.

Scheme 5.4



The synthesis of compound **6**, in which the imidazole group is connected to the amide nitrogen via an ethylene spacer is described in Scheme 5.5. Compound **6** by itself is not amphiphilic, but in combination with other metal ligating molecules, *e.g.* 1-imidazolyl-n-hexadecane (**8**) and metal ions, it may show amphiphilic behavior.

Scheme 5-5



### 5.3.2 $pK_a$ determination

The apparent  $pK_a$  ( $pK_a^*$ ) of **1** in a methanol-water mixture (95:1, v/v), is 6.28 which is only slightly lower than the  $pK_a$  values of imidazole and methyl imidazole (see Chapter 4).<sup>7</sup> The  $pK_a^*$  of compound **7** (7.02) was found to be rather similar to that of **1**. Apparently, the influence of the free hydroxyl groups in **7** on the acid-base character of the imidazole group is insignificant, although both types of groups are located next to each other. We assumed, therefore, that the  $pK_a^*$  values of compounds **2**, **3**, **5** and **6** were similar to those of imidazole and methylimidazole. Titration of compound **4**, in which the imidazole group is placed between the aliphatic chain and the amide function, did not result in the expected titration curve for imidazole-containing compounds (see Chapter 4, Figure 4.1). Instead of the usual buffer zone between the two inflection points, only one steep rise in  $pH^*$  was observed. The titration curve turned out to be similar to the titration of the blanco, which means that in solution **4** is not able to accept a proton from the titrant  $HClO_4$ . This lack of protonation may be due to the fact that the  $N^2$  nitrogen atom of the imidazole group is blocked because it is involved in an intramolecular hydrogen bond with the amide hydrogen atom. IR-experiments confirmed this hypothesis (see next Section).

### 5.3.3 IR experiments

Compound **4** and *N*,*n*-octyl-D-gluconamide were recrystallized from deuterated methanol in order to exchange the hydroxyl and amide hydrogens for deuterium atoms. The IR-spectrum of deuterium exchanged *N*,*n*-octyl-D-gluconamide showed a considerable shift of the hydroxyl stretching vibrations, viz. from a broad peak between 3620 and 3100  $cm^{-1}$  to one between 2750 and 2150  $cm^{-1}$ . The amide II peak (N-H bend) was shifted from 1528 to 1463  $cm^{-1}$  upon deuterium exchange of *N*,*n*-octyl-D-gluconamide. The IR-spectrum of **4** recrystallized from  $CD_3OD$  also showed a shift of the hydroxyl stretching vibrations, viz. from a set of peaks between 3680 and 3180  $cm^{-1}$  to a set of peaks between 2680 and 2030  $cm^{-1}$ . In contrast to *N*,*n*-octyl-D-gluconamide, deuterium exchanged **4** did not show a shift of the amide II vibration, indicating that the amide hydrogen was not exchanged for deuterium. This lack of exchange is probably due to the presence of a very strong *intramolecular* hydrogen bond with the imidazole group in **4** (vide supra).

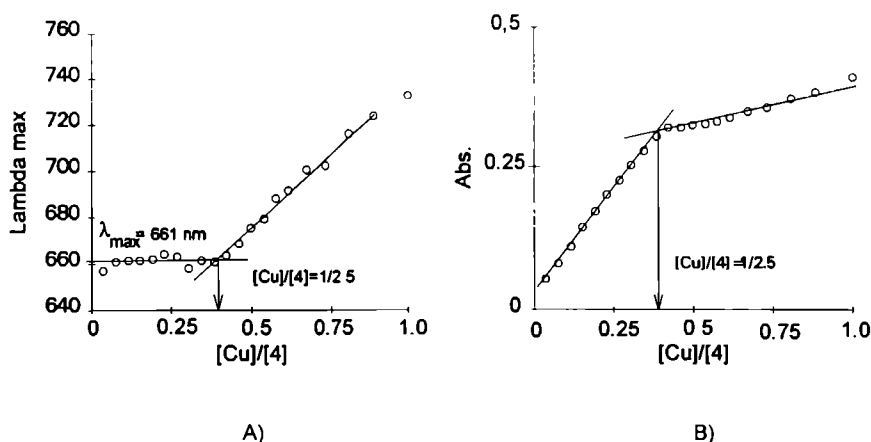
### 5.3.4 UV-vis spectroscopy

In order to determine the stoichiometry of the Cu(II) imidazole complexes, UV-vis titrations were carried out with compounds **1**, **4**, **6**, and **7** monitoring the d-d transition at approximately 600 nm.<sup>8</sup>

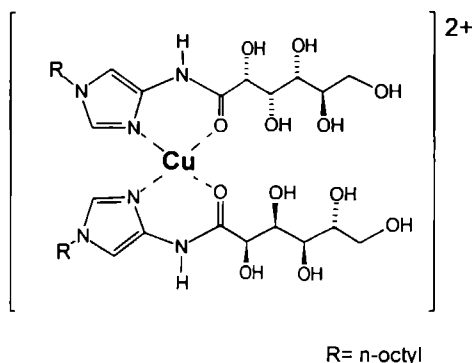
We assumed that the copper complexation behavior of compounds **2** and **3** was similar to that of **1**, *i.e.* 4 ligands surrounding the copper ion in Cu(ClO<sub>4</sub>)<sub>2</sub> (Chapter 4). The copper complexation of compound **7**, which formed 1/4 (Cu/Ligand) complexes with Cu(ClO<sub>4</sub>)<sub>2</sub>, is rather similar to the complexation behavior of compound **1** (Table 5 1). Apparently, the hydroxyl groups do not dramatically disturb the stoichiometry of the copper complex, although the free hydroxyl groups could have acted as additional ligating groups.

Compound **4** showed a deviating copper complexation behavior. In the graphs of the  $\lambda_{\max}$  and the absorption at  $\lambda_{\max}$  versus the copper perchlorate/ligand ratio inflection points were found at a Cu/ligand ratio of 1/2.5, indicating the formation of 1:2 or 1:3 complexes (see Figure 5.2). Although it is known from the literature that copper(II) ions can be ligated by 3 imidazole groups,<sup>9</sup> we believe that in our case, it is probable that 1:2 copper-ligand complexes are present, due to crowding of the ligands. It is not unlikely that in the case of the 1:2 complexes the oxygen atoms of the amide function take part in the complexation (*cf.* Figure 5.3).

Graphs of  $\lambda_{\max}$  and the absorption at  $\lambda_{\max}$  plotted versus the copper/ligand ratio obtained from a UV-vis titration of **4** with CuCl<sub>2</sub>, showed inflection points at a Cu/ligand ratio of 1/2.5, indicating that in the case of this metal salt similar copper complexes are obtained as in the case of Cu(ClO<sub>4</sub>)<sub>2</sub>. It should be noted that the  $\lambda_{\max}$  values of both the Cu(ClO<sub>4</sub>)<sub>2</sub> and CuCl<sub>2</sub> complexes (661 and 672 nm, respectively, the solutions are green), are different from those of the traditional blue-colored imidazole copper(II) complexes.



**Figure 5.2** UV-vis titration of [Cu][ClO<sub>4</sub>]<sub>2</sub> with **4** in methanol, A)  $\lambda_{\max}$  vs the [Cu]/[4] ratio B) Absorption at  $\lambda_{\max}$  vs the [Cu]/[4] ratio



**Figure 5.3** Possible structure of the complex of **4** with Cu(II) ions

**Table 5.1** Stoichiometry of complexes between Cu(ClO<sub>4</sub>)<sub>2</sub> and various imidazole ligands <sup>a</sup>

Ligand	Solvent <sup>b</sup>	Complexation	$\lambda_{\max}$ of complex (nm)
Melm <sup>c</sup>	H <sub>2</sub> O/MeOH (1.4)	1/4 1	610
<b>1</b>	CHCl <sub>3</sub> /MeOH (1 3)	1/4 4	602
<b>4</b>	CHCl <sub>3</sub> /MeOH (1 3)	1/2 5	661
<b>6</b>	H <sub>2</sub> O	1/4 0	585
<b>7</b>	CHCl <sub>3</sub> /MeOH (1 1)	1/3 7	613

<sup>a</sup> Obtained from UV-vis titrations. Cu(II)/ligand ratios were determined from the intersection of the tangents in the curves of  $\lambda_{\max}$  vs the Cu/ligand ratio (e.g. see Fig 5.2A)

<sup>b</sup> Ratio of solvents (v/v) in parenthesis

<sup>c</sup> 1-Methylimidazole

Compound **6** was titrated with Cu(ClO<sub>4</sub>)<sub>2</sub> in water, and showed an inflection point at 1/4.0 (Table 5.1). Apparently, the carbonyl oxygen atom of the amide function in this compound is not in a favorable position to participate in the complexation of the copper(II) center. In contrast to the 1:2 copper-ligand complexes obtained from gluconamide **4**, the copper complex of **6** displayed a dark blue color. In order to investigate the possibility of forming a mixed complex of copper(II) with **6** and 1-n-hexadecylimidazole (**8**), UV-vis spectra of the pure complexes of [(**6**)<sub>4</sub>Cu][ClO<sub>4</sub>]<sub>2</sub>, ((**6**)<sub>4</sub>Cu) and [(**8**)<sub>4</sub>Cu][ClO<sub>4</sub>]<sub>2</sub>, ((**8**)<sub>4</sub>Cu) were recorded as well as of a mixture of **6**, **8** and Cu(ClO<sub>4</sub>)<sub>2</sub> in a (2+2):1 ratio. The solvent appeared to be a limiting factor for the preparation of the afore mentioned complexes. Solvent mixtures of chloroform and methanol resulted in precipitation of both (**6**)<sub>4</sub>Cu and (**8**)<sub>4</sub>Cu. All complexes, therefore, were prepared in DMSO (the concentrations of the Cu complexes of **7**, **8** and combinations of these ligands were kept the same). The  $\lambda_{\max}$  values of the complexes are given in Table 5.2. It should be noted that the  $\lambda_{\max}$  values of the mixed complex are in between those of the pure complexes, but not at the arithmetical average. Although this is not yet a definite proof we believe that complexes with

mixed ligands were formed. Attempts to confirm the formation of mixed copper complexes with FAB-MS failed.

**Table 5.2**  $\lambda_{\max}$  Values of complexes between  $\text{Cu}(\text{ClO}_4)_2$  and various imidazole ligands

Complex <sup>a</sup>	$\lambda_{\max}$ (nm)
$[(1)_4\text{Cu}][\text{ClO}_4]_2$	647
$[(4)_2\text{Cu}][\text{ClO}_4]_2$	678
$[(6)_4\text{Cu}][\text{ClO}_4]_2$	650
$[(7)_4\text{Cu}][\text{ClO}_4]_2$	684
$[(8)_4\text{Cu}][\text{ClO}_4]_2$	677
$[(6)_2+(8)_2\text{Cu}][\text{ClO}_4]_2$	657

<sup>a</sup> In DMSO The concentration of the complexes is 45 mmolar

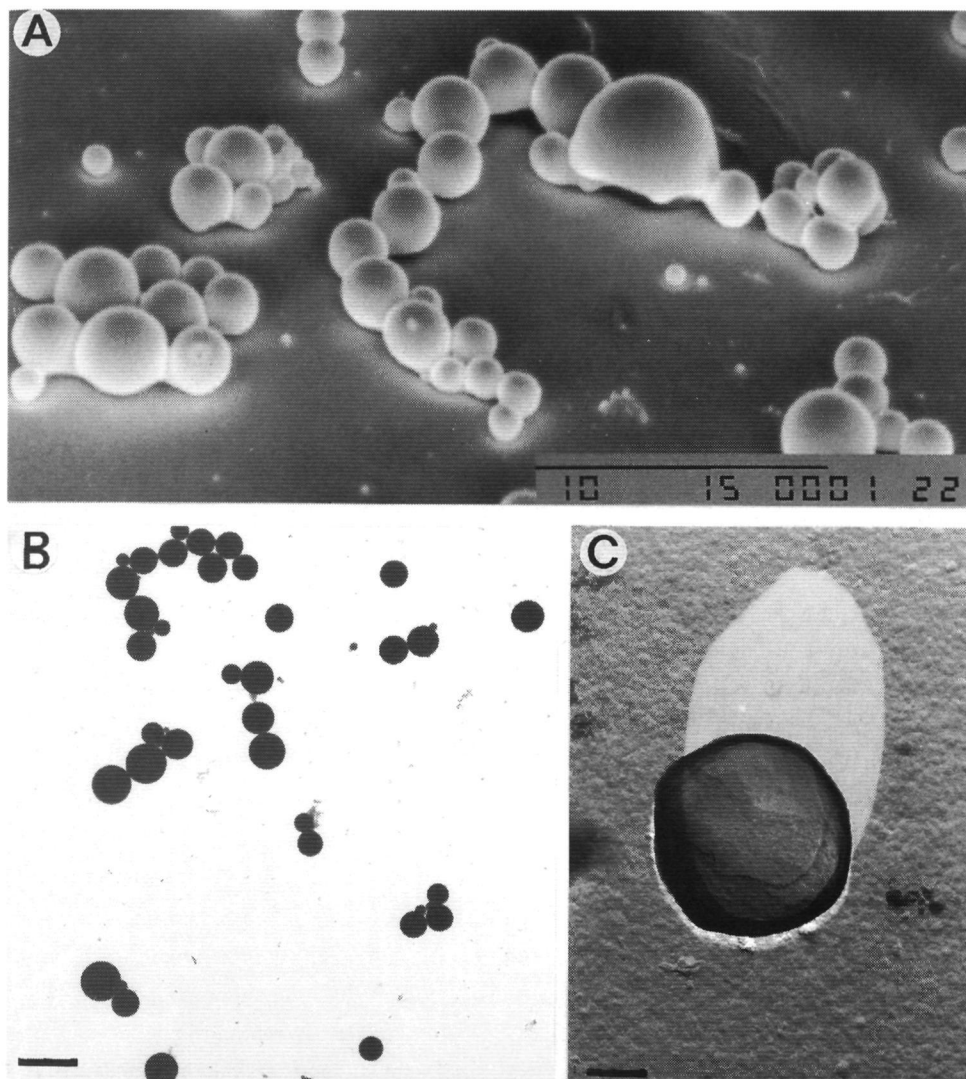
### 5.3.5 Electron microscopy

In Chapter 4, we reported that gluconamides containing imidazole groups can form vesicles, fibers, tubes or braids depending on the pH or the addition of metal ions. In this section the aggregates of compounds **2-8** and their copper complexes in aqueous solutions are described as visualized by transition electron microscopy (TEM). In addition, an attempt to prepare amphiphilic complexes in water by mixing **6** and **8** in combination with  $\text{Cu}(\text{ClO}_4)_2$ , is presented.

*6-Deoxy-5-(1-imidazolyl)-2,4,3,5-dimethylene-N,n-octyl-D-gluconamide (2)*. This compound dissolved readily in both warm ( $T = 60^\circ\text{C}$ ) acetic acid/sodium acetate buffered ( $\text{pH}=4.5$ ) water and warm Tris buffered ( $\text{pH}=8.5$ ) water. In both cases the solution remained clear upon cooling and no well-defined supramolecular structures of either the protonated form of **2** in acetate buffer or the non-protonated form of **2** in Tris buffer could be discerned by TEM. Upon addition of 0.25 equivalents of  $\text{Cu}(\text{ClO}_4)_2$  to a hot ( $T=80^\circ\text{C}$ ), clear aqueous solution of **2**, a pale blue turbid suspension was obtained. After sonicating the suspension for 5 minutes at  $70^\circ\text{C}$ , perfectly spherical vesicles with diameters ranging from 270 to 7000 nm, were observed by SEM (see Figure 5.4A). From the intense black color of the TEM pictures which were made without addition of staining agents, it was concluded that the aggregates contained copper ions (Figure 5.4B). Freeze-etching experiments revealed that the vesicles were multilamellar aggregates (Figure 5.4C). The vesicular suspension was stable for a short period only and started to precipitate after one day standing at room temperature.

*6-Deoxy-5-(1-imidazolyl)-2,4,3,5-dimethylene-N,n-octyl-D-idoonamide (3)*. Despite the change of the carbohydrate framework from gluconamide to idoconamide, and the change in stereochemical environment of the imidazole group, the aggregation behavior of compound **3** was very similar to that of compound **2**. Both the protonated (in acetate buffered solution) and neutral form (in Tris buffered solution) of **3** remained dissolved in water without forming aggregates when the warm clear aqueous solutions of this compound were cooled to room temperature.

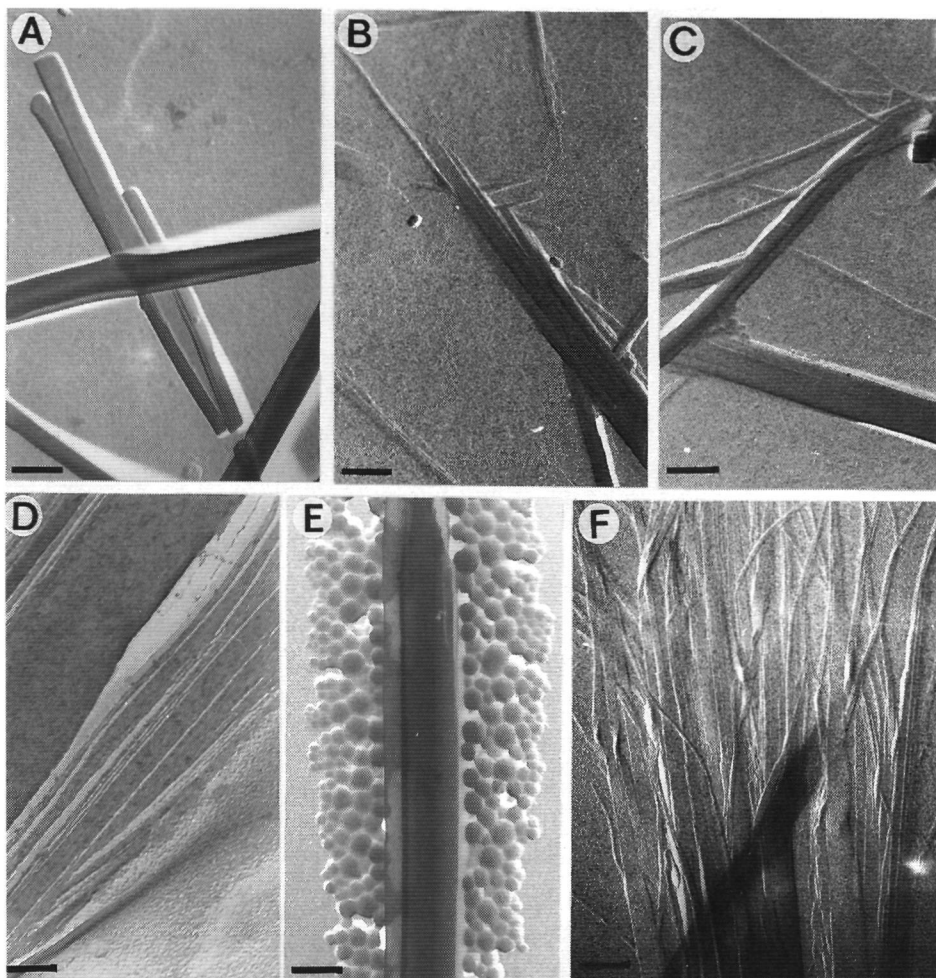
According to TEM and SEM, the copper complex ( $[(3)_4\text{Cu}][\text{ClO}_4]_2$ ) self-assembled in water to give multi lamellar spherical vesicles with a broad size distribution (pictures not shown). The diameters of the aggregates ranged from 130 nm - 6800 nm.



**Figure 5.4** Electron micrographs of vesicles of  $[(2)_4\text{Cu}][\text{ClO}_4]_2$ . A) SEM picture, bar is 10  $\mu\text{m}$ . B) TEM picture of dried vesicles, bar is 2.60  $\mu\text{m}$ . C) Freeze-etched electron micrograph showing multilamellar vesicles, bar is 298 nm.

*1-(n-Octyl)-4-imidazolyl-N-D-gluconamide (4)*. This compound dissolved in hot water and formed a gel upon cooling to room temperature. The gel crystallized after a few hours. TEM pictures taken from the gel showed ribbons (Figure 5.5A), which were composed of fibers (Figures 5.5B and C). According to freeze-etching experiments, the ribbons had a multilayer

structure (Figure 5.5D). The same type of ribbons was formed on cooling a warm clear solution of **4** in methanol (pictures not shown).



**Figure 5.5** TEM pictures of **4** in water (Pt shadowing), A) ribbons, bar is 275 nm, B) + C) ribbons showing fibers at their ends (bars are 260 and 250 nm, respectively), D) electron micrographs of a freeze-etched ribbon, bar is 75 nm, E) ribbons and vesicles obtained from an aqueous mixture of **4** and  $\text{Co}(\text{ClO}_4)_2$  (molar ratio  $\text{Co}/4 = 1/6$ ), bar is 231 nm, F) fibers formed in a mixture of **4** and  $\text{Ni}(\text{ClO}_4)_2$  in water (molar ratio  $\text{Ni}/4 = 1/4$ ), bar is 244 nm.

The 1:2 metal to ligand complex of **4** and  $\text{Cu}(\text{ClO}_4)_2$  yielded vesicles in water with an uniform diameter of 90 nm (pictures not shown). Mixing **4** and  $\text{Co}(\text{ClO}_4)_2$  in water in a 1:6 metal to ligand ratio<sup>10</sup> gave, according to TEM, both ribbons and vesicles (Figure 5.5E). Adding  $\text{Ni}(\text{ClO}_4)_2$  to a hot clear solution of **4** in a 1:4 metal to ligand ratio yielded after cooling ribbons and fibers (Figure 5.5F), while mixing  $\text{Mn}(\text{ClO}_4)_2$  and **4** in a 1:6 metal to ligand ratio gave fibers



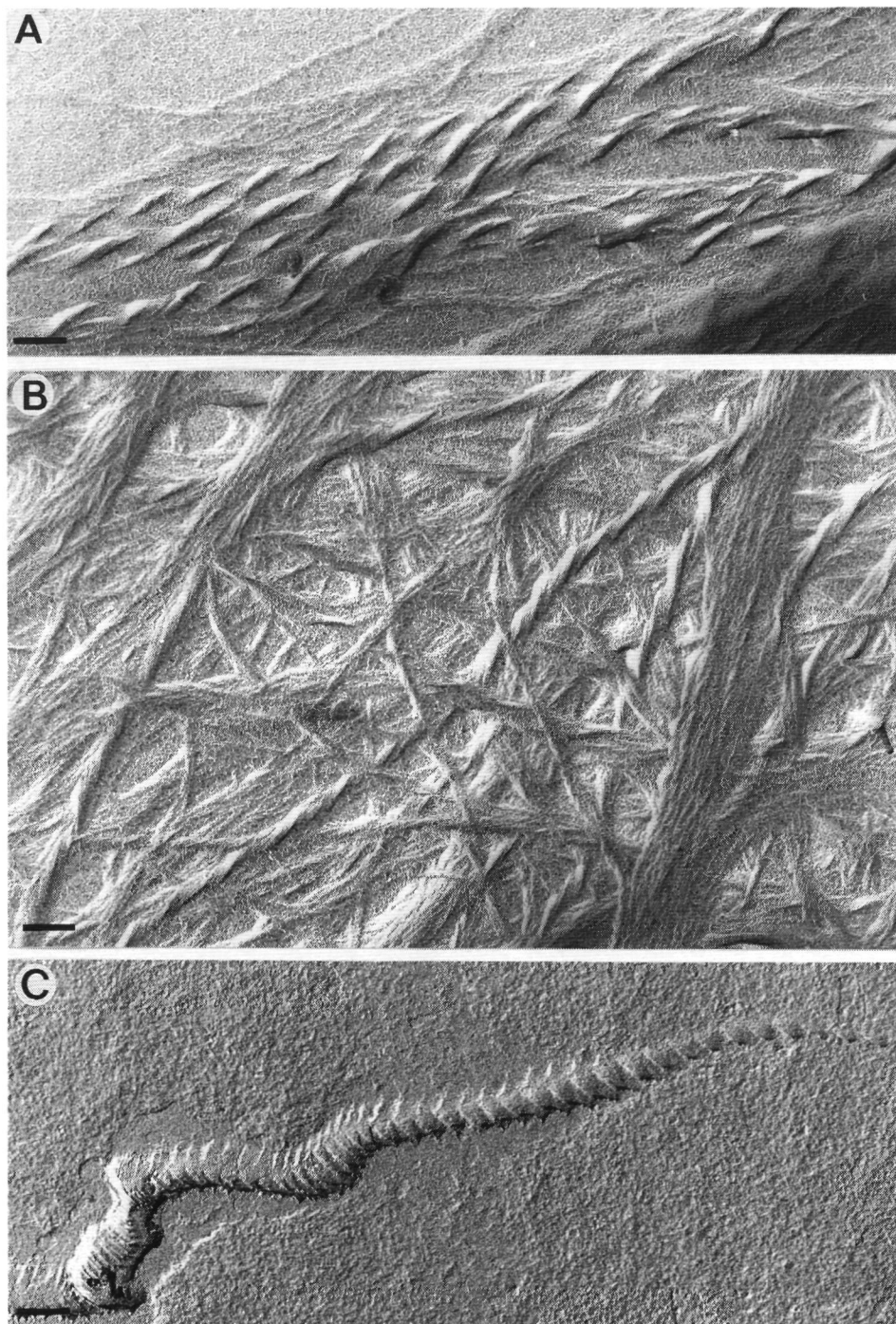
only (pictures not shown) The complexation behavior of  $\text{Co}(\text{ClO}_4)_2$ ,  $\text{Mn}(\text{ClO}_4)_2$  and  $\text{Ni}(\text{ClO}_4)_2$  with **4** was not studied further in detail All dispersions gave precipitates after a while

*N*-(11-(1-Imidazolyl)-*n*-undecyl)-*D*-gluconamide (**5**) This compound was readily soluble in acidic (acetic acid/sodium acetate buffer, pH=4.5) and alkaline (Tris buffer, pH=8.5) solutions Both the protonated (acetate buffer) and the neutral form (Tris buffer) of **5** did not form turbid solutions or gels in water like *N*,*n*-octyl-*D*-gluconamide and *N*,*n*-dodecyl-*D*-gluconamide did The suspension of neutral **5** was investigated with TEM Amorphous droplets with irregular offshoots were visible Although TEM showed some irregularly shaped structures, we believe that these are formed during the quick drying process, because the aqueous solution of **5** remained clear even after cooling, indicating that **5** did not form superstructures in solution Addition of  $\text{Cu}(\text{ClO}_4)_2$  (1:4 metal to ligand ratio),  $\text{Co}(\text{ClO}_4)_2$  (1:6 ratio),  $\text{Ni}(\text{ClO}_4)_2$  (1:4 ratio),  $\text{Mn}(\text{ClO}_4)_2$  (1:6 ratio) and  $\text{Zn}(\text{ClO}_4)_2$  (1:4) to hot clear solutions of **5** in water in all cases resulted in turbid mixtures in which no well-defined aggregates could be observed by TEM, except for the Mn complex in which case planar bilayer structures were visible (picture not shown)

*Mixture of N*-(2-(2-imidazolyl)-ethyl)-*D*-gluconamide (**6**) and 1-imidazolyl-hexadecane (**8**). Before studying the aggregation behavior of mixed complexes of compounds **6** and **8** with  $\text{Cu}(\text{ClO}_4)_2$ , we first prepared the separate complexes  $[(\mathbf{6})_4\text{Cu}][\text{ClO}_4]_2$  ( $(\mathbf{6})_4\text{Cu}$ ) and  $[(\mathbf{8})_4\text{Cu}][\text{ClO}_4]_2$  ( $(\mathbf{8})_4\text{Cu}$ ) and investigated these complexes with TEM Complex  $(\mathbf{6})_4\text{Cu}$  dissolved in water without giving suprastructures while  $(\mathbf{8})_4\text{Cu}$  formed ill-defined droplets (no vesicles)<sup>11</sup> A mixture of **6** (2 equiv), **8** (2 equiv) and  $\text{Cu}(\text{ClO}_4)_2$  (1 equiv) in water,<sup>12</sup> however, showed the presence of vesicles with diameters in the range of 150 to 500 nm (pictures not shown)

In order to obtain further information about the physical properties of the complexes we also recorded DSC thermograms of  $(\mathbf{6})_4\text{Cu}$  and  $(\mathbf{8})_4\text{Cu}$ , separately and the mixed complex of **6** and **8** with  $\text{Cu}(\text{ClO}_4)_2$  in water The complex  $(\mathbf{6})_4\text{Cu}$  dissolved in water at room temperature giving a dark blue solution, which showed no phase transition upon heating or cooling, while the complex  $(\mathbf{8})_4\text{Cu}$  in water was found to display a broad transition between 32 and 74 °C (maximum at 56 °C) The mixed complex of **6**, **8** and  $\text{Cu}(\text{ClO}_4)_2$  (2:2:1 molar ratio) in water showed on heating a thermogram which was almost similar to that of  $(\mathbf{8})_4\text{Cu}$  in water Thus the phase transition temperatures in the mixed complex are merely determined by ligand **8**, i.e. by the aliphatic chain and not by the carbohydrate head group A strong influence of the aliphatic tail on the aggregation behavior of gluconamide amphiphiles was also found in the thermotropic LC behavior of these compounds (see Chapter 3)

6-Deoxy-6-(1-imidazolyl)-*N*,*n*-octyl-*D*-gluconamide (**7**) This compound was dissolved in an acetic acid/sodium acetate buffer (pH=4.5, **7** is protonated) but formed no aggregates after cooling In a Tris buffered solution of **7** (pH=8.5, **7** is in neutral form) twisted ribbons with regular twists in one direction and fibers were visible by TEM (see Figure 5.6A and B) The copper complex  $[(\mathbf{7})_4\text{Cu}][\text{ClO}_4]_2$  showed, after freeze-etching, an interesting but rather strange aggregate (Figure 5.6C), which is probably a helix or a braid torn apart during the freeze-etching experiment



**Figure 5.6** TEM pictures of **7** and its copper (II) complex in water (Pt shadowing) A) twisted ribbons and B) fibers of **7**. C) Freeze-etched electron micrograph of  $[(7)_4Cu][ClO_4]_2$  dispersed in water.

### 5.3.6 Isotherms

In order to investigate why compound **5** fails to exhibit amphiphilic behavior, isotherms were recorded using the Langmuir film balance technique. For comparison similar experiments were carried out with *N*,*n*-dodecyl-D-gluconamide and compound **8** in the neutral and charged form. The latter compound appeared to form unstable monolayers both on an aqueous subphase which was buffered with Tris (pH=8.5, **8** in the neutral form) and on a subphase buffered with acetic acid/sodium acetate (pH=4.5, **8** is positively charged). *N*-*n*-Dodecyl-D-gluconamide showed an isotherm without any plateau area. From the onset of the surface pressure - surface area curve a molecular area of  $19.9 \text{ \AA}^2$  could be calculated, which did not change very much when the temperature or pH was changed. When **5** was spread on a Tris buffered subphase the surface pressure did not increase upon decreasing the surface area, which indicated that the molecules dissolved in the subphase without forming a monolayer. A similar result was obtained on an acetate buffered subphase indicating that the monolayer was not stable. Because of this negative result no further experiments were carried out with **5**.

### 5.3.7 X-ray powder diffraction experiments

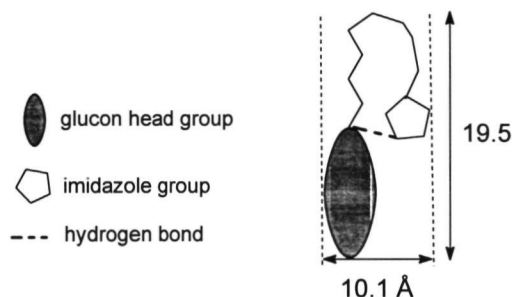
Powder diffractograms of lyophilized unprotonated **7** were recorded which showed that this compound is packed in layers with an interlayer distance similar to that of compound **1** (see Table 5.3 and Chapter 3). This suggests that the alkyl chains of **7** are interdigitized (Table 5.3). Although lyophilization can disturb the packing, we believe that by rapid cooling of the samples the ordering of the molecules in the aggregates is maintained. For lyophilized **4** a periodicity of  $38.5 \text{ \AA}$  was measured, which indicates that the molecules are packed in bilayers with their tails facing each other.<sup>13</sup> This packing is similar to the packing of *N*,*n*-octyl-D-gluconamide in aqueous aggregates,<sup>14</sup> but different from the monolayered head to tail packing found in the crystal structures of gluconamides, e.g. *N*,*n*-undecyl-D-gluconamide ( $19.5 \text{ \AA}$ ).<sup>13</sup>

**Table 5.3** Results of powder diffraction experiments on lyophilized samples of various gluconamides

Compound	d (Å)	Packing mode
<b>1</b>	25.5	bilayer (interdigitized)
<b>4</b>	38.5	bilayer (tail to tail)
<b>7</b>	26.5	bilayer (interdigitized)
<b>5H<sup>+</sup></b>	10.1 and 19.7	folded chain

Compound **5**, freeze-dried from Tris buffered solution, did not give a useful diffractogram indicating that the packing of the molecules was irregular. To our surprise lyophilization of **5** from an acetate buffered solution gave (according to the powder diffractogram), a highly ordered sample. Two periodicities, viz.  $10.1 \text{ \AA}$  and  $19.7 \text{ \AA}$ , were observed. According to CPK models,  $19.7 \text{ \AA}$  is a too small length for a stretched out molecule and, hence, also for molecules packed in an interdigitized bilayer. This length may indicate, however, that the alkyl chains of the

molecules are folded back, allowing the imidazole groups to form intramolecular hydrogen bonds with the amide groups. The 10 Å periodicity derived from the powder diffractograms, is also consistent with an alkyl chain that is folded back (see Figure 5.7). This folding disturbs the length-width ratio which is outside the range required for amphiphilic behavior of the molecule,<sup>15</sup> and is probably the reason why **5** does not form a stable monolayer on the air water interface and does not form aggregates in water.



**Figure 5.7** Schematic drawing of gluconamide **5** with a folded alkyl chain.

### 5.3.8 Thermotropic L.C. behavior

Experiments in the literature<sup>16</sup> and our own experiments,<sup>17</sup> have indicated that the amide function in a gluconamide is not very important for generating thermotropic L.C. behavior. The presence of a long alkyl chain and a glucon head group is thought to be sufficient for the molecules to display this behavior. DSC experiments carried out on **4** showed that this compound is not liquid crystalline although it had the required properties. Despite the absence of an intermolecular amide hydrogen bonding array, the melting point of **4** (172.3 °C) is higher than that of comparable non-modified gluconamides (e.g. *N*,*n*-octyl-D-gluconamide, m.p. 159.2 °C or *N*,*n*-undecyl-D-gluconamide m.p. 156.7 °C<sup>16</sup>). Apparently the interaction between the imidazole groups of neighboring molecules is very strong. Compound **5** did not show thermotropic L.C. behavior either, which is probably due to the folding of the alkyl chain, that prevents the molecules to adopt the rod-shaped form required for generating liquid crystalline behavior.

### 5.4 Concluding remarks

In the previous chapters we have shown that the imidazole groups in our gluconamides are of great importance to obtain (tunable) aggregation behavior in aqueous solution and to generate thermotropic L.C. behavior.<sup>17</sup> Based on the results described in this chapter, we may add to this that also the location of the imidazole group in the gluconamide is important for the aggregation behavior of this molecule. The ability to form highly organized aggregates is lost when in the gluconamide the imidazole group is moved from carbon atom C<sup>6</sup> to carbon atom C<sup>5</sup> (compare the generation of non-uniform sized vesicles from [(2)<sub>4</sub>Cu][ClO<sub>4</sub>]<sub>2</sub> with the braids formed from [(1)<sub>4</sub>Cu][ClO<sub>4</sub>]<sub>2</sub> (see Chapter 4). In the case of **5**, where the imidazole is located at the terminus of the hydrophobic part of the molecule, the alkyl chain was shown to folded back and to form an

intramolecular hydrogen bond with the amide function. As a result the conformation of the gluconamide was not fit for proper amphiphilic character.<sup>15</sup> A possible solution to overcome this problem is the introduction of a rigid segment in the alkyl chain, *e.g.* diacetylene function, but also in this case the risk of losing amphiphilic character is present (see Chapter 4).

In compound **4**, the imidazole is located between the head group and the alkyl chain. The carbohydrate part including the amide group of this compound is similar to that of *N*,*n*-octyl-D-gluconamide. One would expect, therefore, similar aggregation behavior for these two compounds,<sup>18</sup> because the hydroxyl groups in both cases can form inter-molecular hydrogen bonds which are important for the aggregation process, especially in aqueous solutions.<sup>19</sup> In theory, the packing of the molecules of **4** in the aggregates should be looser than that in aggregates of *N*,*n*-octyl-D-gluconamide, because the imidazole group is more bulky than one or two methylene groups. Remarkably, the packing in the former case appeared to be tighter than that in the latter case. An indication for this is the melting point of **4** which was found to be higher than that of the unmodified gluconamide, and melting points reflect the strength of the crystal packing (see Chapter 3). The aggregation behavior of **4** was not dependent on the solvent (methanol or water), whereas the aggregation of *N*,*n*-octyl-D-gluconamide was (see Chapter 6). The imidazole groups of molecules of **4** presumably show  $\pi$ - $\pi$  stacking interactions as they do in the aggregates of gluconamide **1** (see Chapters 3 and 6).

It is questionable whether it is possible to use **4** as an amphiphilic matrix for the anchoring of catalytically active metal complexes as was suggested in the Introduction. The metal complexing behavior of this compound is disturbed due to its bulkiness (only 1:2 metal to ligand complexes with  $\text{Cu}(\text{ClO}_4)_2$  were observed), and this bulkiness will prevent further coordination of substrates, which is necessary for catalysis. In addition, dissociation of **4** from the coordination sphere of the metal, which is needed for aziridination reactions (see Chapter 7), is very unlikely given the inflexibility of the ligand. This inflexibility was demonstrated by the presence of a strong hydrogen bond between the amide function in **4** and the imidazole group.

In principle, it is possible to create amphiphilic metal complexes by binding ligand molecules with different character, *i.e.* hydrophobic and hydrophylic, to a metal center. We have demonstrated that this idea is viable by mixing the hydrophobic imidazole derivative **8** and the hydrophylic imidazolyl derivate **6**, in water with copper (II) ions. The resulting complex displayed amphiphilic behavior and formed vesicles.

## 5.5 Literature

<sup>1</sup> Kunitake, T., Ishikawa, Y.; Shimomura, M. *J Am Chem Soc* **1986**, *108*, 327

<sup>2</sup> a) Menger, F M., Lee, J.-J.; Hagen, S. *J Am Chem Soc* **1991**, *113*, 4017, b) Kimizuka, N., Handa, T., Ichinose, I., Kunitake, T. *Angew Chem* **1994**, *106*, 2576, *Ibid Int Ed Eng* **1994**, *33*, 2483

<sup>3</sup> Ishikawa, Y., Kunitake, T. *J Am Chem Soc* **1986**, *108*, 8300.

<sup>4</sup> a) Brown, J M., Bunton, C.A. *J Chem Soc., Chem Commun* **1974**, 969; b) Kunitake, T., Ihara, H., Okahata, Y. *J Am Chem Soc* **1983**, *105*, 6070; c) Cleij, M.C., Drenth, W., Nolte, R.J.M. *Recl Trav Chim Pays-Bas* **1993** *112*, 1

- <sup>5</sup> Al-Shaar, A H M , Gilmour, D W , Lythgoe, D J , McClenaghan, I , Ramsden, C A *J Chem Soc Perkin Trans I* **1992**, 2779
- <sup>6</sup> McCaldin, D J *Chem Rev* **1960**, 60, 39
- <sup>7</sup> The pK<sub>a</sub>\* of imidazole in methanol/water is 6.96, see Chapter 4 and CRC Handbook of Chem and Phys 51<sup>st</sup> edition, Ed R C Weast, CRC Press, Cleveland Ohio, **1970**, D-118
- <sup>8</sup> Bernarducci, E , Schwindinger, W F , Hughey, IV, J L , Krogh-Jespersen, K , Schugar, H J *J Am Chem Soc* **1981**, 103, 1686
- <sup>9</sup> Tang, C C , Davalian, D , Huang, P , Breslow, R *J Am Chem Soc* **1978**, 100, 3918
- <sup>10</sup> The stoichiometry of the complexes between imidazole ligands and Co(ClO<sub>4</sub>)<sub>2</sub>, Ni(ClO<sub>4</sub>)<sub>2</sub>, and Mn(ClO<sub>4</sub>)<sub>2</sub> is (ligand to metal) 6 : 1, 4 : 1, and 6 : 1, respectively, cf Reedyk, J *Recl Trav Chim Pays-Bas*, **1969**, 1451
- <sup>11</sup> Compound **8** did not dissolve in water, not even after prolonged heating. The ligand, therefore, was dissolved in methanol, mixed with [Cu][ClO<sub>4</sub>]<sub>2</sub> (which resulted in a turbid mixture) and injected in water
- <sup>12</sup> The components were mixed before adding the copper(II) salt. Compound **8** was brought in water by injection
- <sup>13</sup> A tail-to-tail packing of *N*-n-undecyl-D-gluconamide shows a periodicity of 39.5 Å, see also Jeffrey, G A , Maluszinska, H *Carbohydr Res* **1990**, 207, 211
- <sup>14</sup> Svenson, S , Köning, J , Fuhrhop, J -H *J Phys Chem* **1994**, 98, 1022
- <sup>15</sup> Israelachvili, J N , Marcelja, S , Horn, R G *Quart Rev Biophys* **1980**, 13, 121
- <sup>16</sup> Pfannemüller, B , Welte, W , Chin, E , Goodby, J W *Liq Cryst* **1986**, 1, 357
- <sup>17</sup> See Chapters 3 and 4
- <sup>18</sup> a) Pfannemüller, B , Kühn, I *Macromol Chem* **1988**, 189, 2433, b) Tavel, F T , Pfannemüller, B *Macromol Chem* **1990**, 191, 3097
- <sup>19</sup> a) Fuhrhop, J -H , Schnieder, P , Rosenberg, J , Boekema, E *J Am Chem Soc* **1987**, 109, 3387, b) Fuhrhop, J -H , Schnieder, P , Boekema, E , Helfrich, W *J Am Chem Soc* **1988**, 110, 2861, c) Fuhrhop, J -H , Boettcher, C *J Am Chem Soc* **1990**, 112, 1768-1776, d) Köning, J , Boettcher, C , Winkler, H , Zeitler, E , Talmon, Y , Fuhrhop, J -H *J Am Chem Soc* **1993**, 115, 693, e) Svenson, S , Kirste, B , Fuhrhop, J -H *J Am Chem Soc* **1994**, 116, 11969, g) Frankel, D A , O'Brien, D F *J Am Chem Soc* **1994**, 116, 10057



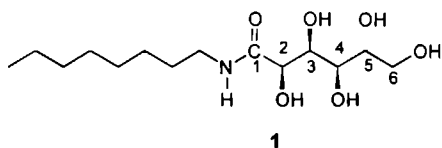
# Chapter 6

## Organo-gels from carbohydrate amphiphiles

### 6.1 Introduction

In supramolecular chemistry, assemblies of molecules held together by non-covalent interactions such as electrostatic interactions, VanderWaals interactions and H-bonding are receiving great interest. Amphiphiles consisting of a carbohydrate head group<sup>1</sup> to which an aliphatic alkyl chain is connected by an amide function are known to form fibrous aggregates upon dispersion in water<sup>2,3</sup>. Recently, we described imidazole containing carbohydrate amphiphiles which self assemble to give aggregates of which the structure can be tuned by changing the solvent conditions and by addition of copper ions<sup>4</sup>.

The behavior of supramolecular aggregates to some extent is comparable to that of macromolecules, for example repetitive units linked to each other by non-covalent or covalent bonds, can give a network resulting in a gel-like structure. A difference, however, is that gels obtained from supramolecules can be disintegrated by addition of a cosolvent or by raising the temperature because the connections are non-covalent bonds, whereas network structures obtained from macromolecules disintegrate only by breaking chemical bonds.



*N*-octyl-D-gluconamide **1** is known to form a highly viscous gel in aqueous solutions. Using transition electron microscopy (TEM) in combination with image analysis,<sup>5</sup> DSC<sup>6</sup> and NMR<sup>7</sup> it was proposed that this gel consists of 4 intertwined superhelices.<sup>8</sup> The self-assembly of **1** into helices has been ascribed to the formation of an intermolecular hydrogen bonding network, from which, during the aggregation, water molecules are expelled.<sup>2,9</sup> Different proposals regarding the packing arrangement of the gluconamide molecules in the aggregates have been made, viz head to tail<sup>10</sup> as found in the crystal structure<sup>11</sup> of **1** and head to head<sup>12</sup> which is seen more commonly for amphiphilic molecules in water. We believe that the latter packing is the most likely one given the powder diffraction experiments on lyophilized fibers which were recently published in the literature.<sup>10</sup>

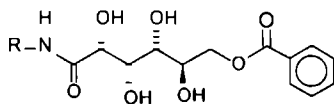
Neither the length of the alkyl chain nor the introduction of a diacetylene function into this chain was found to have a dramatic influence upon the aggregation behavior of molecules of type **1** in water.<sup>13</sup> Variations in the head group, however, dramatically changed the type of clustering.<sup>5a,13</sup> Gluconamide **1** has also been reported to gelate in 1,2-xylene,<sup>5</sup> forming bilayer scrolls, but this organogel was found to be very unstable.<sup>5</sup> Unfortunately, **1** is scarcely soluble in



common organic solvents like acetone, chloroform and dioxane, and, therefore, is not an ideal molecule for an extensive study of its gelation effects in organic solvents

Gelation in organic solvents has so far been observed for lecithins,<sup>14</sup> cholesterol derivatives,<sup>15</sup> peptides,<sup>16</sup> two-component gelling agents,<sup>17</sup> calixarenes,<sup>18</sup> semifluorinated *n*-alkanes<sup>19</sup> or silanes,<sup>20</sup> phenols<sup>21a</sup> and phthalocyanines<sup>21b</sup>. Despite the fact that a relatively broad range of compounds displays gelation, no rules of thumb for the design of such compounds have been given in the literature. This contrasts the situation for the classical amphiphilic compounds where such rules have been proposed.<sup>22</sup> Some factors, however, are known to stimulate gelation behavior, *viz* the possibility to form hydrogen bonds (as found in amide<sup>17</sup> and urethane<sup>16c</sup> gels) and a rod-shape geometry of the building block.<sup>15b</sup>

As part of our program aimed at the design and synthesis of supramolecular structures from carbohydrate amphiphiles and more particularly the fine-tuning of these structures, we synthesized compound **2a**. To our surprise **2a** formed gels at low concentrations in common organic solvents like chloroform, ethyl acetate and acetone. The introduction of the benzoate ester apparently changed the characteristic features of the carbohydrate moiety which is now located between two hydrophobic groups: the alkyl chain connected via the amide function and the ester group coupled at the C<sup>6</sup> end of the carbohydrate group.

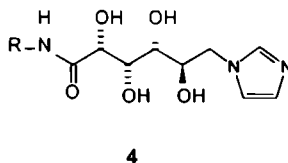
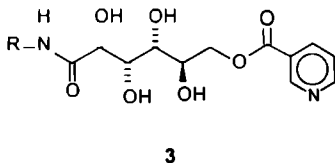


**2a** R= n-octyl  
**2b** R= n-hexadecyl

Stimulated by this finding we decided to study in more detail the organogel forming properties of *n*-alkyl-D-gluconamides. The results are described in this chapter. The investigations have been carried out using electron microscopy (EM), differential scanning calorimetry (DSC), NMR, UV-vis spectroscopy, X-ray powder diffraction (SAXS) and FT-IR. In order to be able to understand the driving forces behind organogel formation and hopefully to present suggestions for the design of new amphiphilic organo-gelators, a number of gluconamide derivatives based on gluconamide **1** have been synthesized and investigated. The rationale behind the choice of derivatives is presented below.

#### *Derivatives with aromatic nitrogen substituents on C<sup>6</sup>*

In order to probe the influence of an electron donor site in the aromatic head group, compounds **3** (pyridyl group) and **4** (imidazolyl group) have been synthesized.

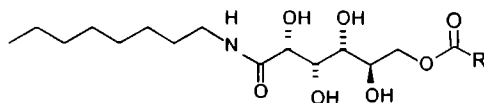


R = n-octyl

From investigations on the aggregation behavior of the imidazolyl compound **11** in water (see below) we know that the imidazole function plays an important role in the self assembly behavior of the amphiphiles (see Chapters 3 and 4). A crystal structure of **11** revealed that H-bonding by entrapped water molecules is important for the aggregation behavior of this compound. By comparing **3** and **4** with gluconamide **2**, we hoped to get insight in the influence of H-bonding by entrapped water molecules on the gelation behavior. Besides that, pyridyl and imidazolyl groups are metal complexing groups and therefore **3** and **4** are potentially interacting building blocks for catalytic systems which is part of another research program, see Chapter 7.

#### *Derivatives with aliphatic substituents on C<sup>6</sup>*

The benzoate ester (**2a**), 3-pyridine carboxylic ester (**3**) and imidazolyl (**4**) substituents are all aromatic moieties and can display  $\pi$ - $\pi$  stacking interactions. For comparison we have also synthesized a series of aliphatic ester functionalized gluconamides compounds **5-6**, which cannot give  $\pi$ - $\pi$  stacking. To investigate the effect of a bulky substituent we have also prepared compound **7**. The n-octanoic ester (see **6**) also is a relatively bulky group, but for compound **6** still a tight packing of the head groups can be expected because non-branched aliphatic chains tend to aggregate in a regular manner.



**5** R = CH<sub>3</sub>

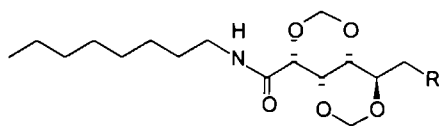
**6** R = (CH<sub>2</sub>)<sub>6</sub>ClCH<sub>3</sub>

**7** R =

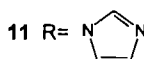
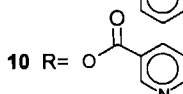
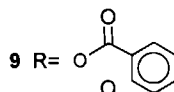
#### *Methylene protected derivatives*

Although the hydroxyl functions in carbohydrates of type **1** are generally considered to be important for the formation of a hydrogen bonding network,<sup>1,13</sup> we found that carbohydrate amphiphiles with protected hydroxyl groups can still form suprastructures in water (see Chapter 4).<sup>4</sup> The 2,4,3,5 dimethylene gluconamides **8-11** all have their secondary hydroxyl groups protected but contain the same functional groups that are present in **1**, **2a**, **3** and **4** (hydroxyl).

benzoyl, 3-pyridyl, and imidazolyl respectively) These compounds therefore have been included in this study for reasons of comparison

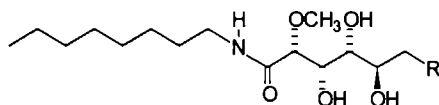


**8** R= OH

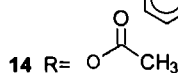
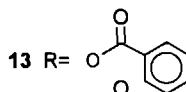


#### *Derivatives protected on C<sup>2</sup> with a methoxy group*

Compound **12** is special in the sense that it contains a methoxy group on the carbon atom C<sup>2</sup> which prohibits 1,3-*syndiaxial* interactions<sup>5a,7b 12 23</sup> between the -OH functions on C<sup>2</sup> and on C<sup>4</sup>. These *syndiaxial* interactions are believed to induce a bend in the glucon head group leading to a sickle-type of conformation<sup>23</sup>. We decided to include this compound in our study. It should be noted that the bulkiness of the methoxy group by itself can cause a bending in the head group. In general a disturbed linearity of the head group will increase the solubility of the amphiphile in water and may contribute to the formation of highly curved aggregates like helical micellar rods<sup>5a</sup>.



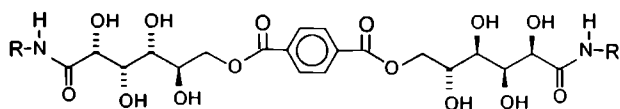
**12** R= OH



Too much bending, however, will not be advantageous for molecular ordering,<sup>22b</sup> which makes it difficult to predict the behavior of **12**. For comparison, we also prepared the derivatives **13** and **14**, which contain a benzoate and acetate function on C<sup>6</sup> respectively.

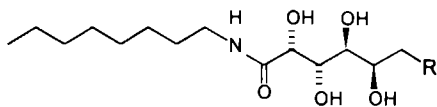
### Dimers of *N*,*n*-octyl-*D*-gluconamides

The introduction of an aliphatic substituent on the head group, as in **6** gives a gluconamide with two equally long alkyl chains at either end. In addition to compound **6**, we also prepared **15** which contains two *N*,*n*-octyl-*D*-gluconamide moieties linked up together at their head groups via a terephthalate spacer. This type of amphiphile has been previously reported by Menger and was named gemini surfactant.<sup>24</sup> For gemini surfactants, inverted bilayer structures with both alkyl chains facing the solvent can be expected.<sup>25</sup> Packing constraints are important in the understanding of the process of building up the aggregates.<sup>12, 13, 22a</sup> From the crystal structures of several gluconamides with aliphatic chains it is known that these molecules tend to crystallize in a head to tail manner.<sup>26</sup> Using **6** and **15** we hoped to obtain a monolayered packing of the amphiphiles, which has a head to head ordering. The idea is somewhat similar to the membrane spanning bolaamphiphiles,<sup>27</sup> which form monolayers of molecules having head groups on both ends. Since in **6** the head group is in the center, this molecule could be called a reversed bolaamphiphile, while **15** fits the gemini surfactant description.<sup>24</sup>

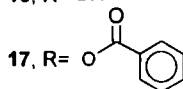


**15** R= *n*-octyl

For comparison we also synthesized the galactonamides **16** and **17**. Open-chain galactonamides do not have a bent head group like gluconamides have. In the case of compound **16** this results in a decreased solubility in water and a complete insolubility in 1,2-xylene. The low tensile gel which can be prepared at low concentrations in water, has been reported to contain helically twisted ribbons.<sup>5a</sup>



**16**, R= OH



**17**, R=

## 6.2 Experimental section

### 6.2.1 Syntheses

All solvents were distilled before use and dried on Mol Sieves 3 or 4 Å. Special care was taken with pyridine (distilled from CaH<sub>2</sub>), because this solvent is hygroscopic.

Analytical instruments and electron microscopes used, were identical to those described in the previous chapters.

The melting points were obtained from DSC measurements (the average of onset and peak of the melting transition). The synthesis of compound **1** has been described by Pfannemüller et al.<sup>2</sup>

***N,n*-Octyl-D-gluconamide-6-benzoate (2a).** Benzoyl chloride (1 306 g, 9.29 mmol 1.08 equiv.) was dissolved in 5 ml of pyridine and added dropwise to a cooled (ice bath) and stirred gelated solution of 2.650 g (8.62 mmol) of *N,n*-octyl-D-gluconamide (**1**) in 40 ml of pyridine. The apparatus was purged with dried nitrogen gas. Over a period of 2 hrs. whilst stirring in which the temperature was raised from 0 to 60 °C, the resulting clear yellow mixture was poured into  $\pm$  600 ml of saturated NaHCO<sub>3</sub>/icewater. The precipitate was purified by column chromatography (silica gel, eluent CHCl<sub>3</sub>/MeOH 95:5, v/v), yield 3.22 g (7.83 mmol, 90 %), m.p. 145.9 °C IR (KBr) 3660-3030 cm<sup>-1</sup> broad (OH), 1720/1703 (C=O, ester), probably more than one conformation in the solid state, only one peak in solution (THF) 1722, 1666 (amide I), 1546 (amide II). <sup>1</sup>H-NMR (DMSO-d<sub>6</sub>)  $\delta$  8.014 ppm (d, 2H, ArH), 7.636 (2 d, 1H, ArH), 7.516 (t, 2H, ArH), carbohydrate skeleton protons see Table 6.6, 3 063 (9 peaks, 2H, -(CH<sub>2</sub>)<sub>6</sub>-CH<sub>2</sub>-NHCO), 1 397 (t, 2H, -(CH<sub>2</sub>)<sub>5</sub>-CH<sub>2</sub>-CH<sub>2</sub>NHCO), 1.226 (broad s, 10H, CH<sub>3</sub>-(CH<sub>2</sub>)<sub>5</sub>-CH<sub>2</sub>-), 0.842 (t, 3H, CH<sub>3</sub>-). EI-MS *m/z* 412 (M+H)<sup>+</sup>, 156 (C<sub>8</sub>H<sub>17</sub>-NHC=O)<sup>+</sup>, 105 (ArC=O)<sup>+</sup>, 77 (C<sub>6</sub>H<sub>5</sub>). Anal. Calcd. for C<sub>21</sub>H<sub>33</sub>NO<sub>7</sub>: C, 61.30; H, 8.08; N, 3.40. Found: C, 61.22; H, 7.97; N, 3.40.

***N,n*-Dodecyl-D-gluconamide-6-benzoate (2b).** For the synthesis of this compound the procedure described for compound **2a** was followed using 3.081 g (8.476 mmol) of *N,n*-dodecyl-D-gluconamide (for the synthesis of this compound see Chapter 3) and 1.059 g (7.534 mmol) of benzoyl chloride. Yield 0.23 g (0.49 mmol, 6.5 %, not optimized), m.p. 153.0 °C. IR (KBr) similar to the spectrum found for **2a**. <sup>1</sup>H-NMR similar to the NMR spectrum obtained for **2a**, except for the integral of the methylene protons of the alkyl chain, which was equivalent to 18 protons. EI-MS *m/z* 468 (M+H)<sup>+</sup>, 212 (C<sub>8</sub>H<sub>17</sub>-NHC=O)<sup>+</sup>, 105 (ArC=O)<sup>+</sup>, 77 (C<sub>6</sub>H<sub>5</sub>). Anal. Calcd for C<sub>25</sub>H<sub>41</sub>NO<sub>7</sub>: C, 64.22; H, 8.84; N, 3.00. Found: C, 64.28; H, 8.97; N, 2.95.

***N,n*-Octyl-D-gluconamide-6-(3-pyridyl)-carboxylate (3).** This compound was prepared in an analogous manner to compound **2a** using 3 023 g (9.83 mmol) **1** and 1.1417 g (10 01 mmol) of 3-pyridinecarboxyl chloride (prepared from 3-pyridinecarboxylic (nicotinic) acid and thionyl chloride) instead of benzoyl chloride. The removal of the excess of pyridine (70 ml) was carried out under reduced pressure and at elevated temperature. Yield 0 35 g (0.85 mmol, 9 %, not optimized), after column chromatography (silica, eluent Et<sub>3</sub>N/EtOH/CHCl<sub>3</sub>, 1:20:79 v/v/v), m p 155.9 °C. IR (KBr) 3600-3050 cm<sup>-1</sup>, broad (OH), 1711 (C=O, ester), 1624 (amide I), 1540 (amide II). <sup>1</sup>H-NMR (DMSO-d<sub>6</sub>)  $\delta$  9.160 ppm (d, 1H, ArH), 8.651(2d, 1H, ArH), 8.347 (2d, 1H, ArH), 7 636 (t, 1H, NHCO), 7.574 (2d, 1H, ArH), carbohydrate skeleton protons see Table 6.6, 3.073 (9 peaks, 2H, -(CH<sub>2</sub>)<sub>6</sub>-CH<sub>2</sub>-NHCO), 1.404 (t, 2H, (CH<sub>2</sub>)<sub>5</sub>-CH<sub>2</sub>-CH<sub>2</sub>NHCO), 1.262 (broad s, 10H, CH<sub>3</sub>-(CH<sub>2</sub>)<sub>5</sub>-CH<sub>2</sub>-), 0 846 (t, 3H, CH<sub>3</sub>-); EI-MS *m/z* 412 M<sup>+</sup>, 156 (C<sub>8</sub>H<sub>17</sub>-NHC=O)<sup>+</sup>, 106 (PyrC=O)<sup>+</sup>, 78 (Pyr)<sup>+</sup>. Anal. Calcd. for C<sub>20</sub>H<sub>32</sub>N<sub>2</sub>O<sub>7</sub>: C, 58 24; H, 7.82; N, 6.79. Found C, 58.25, H, 7.64; N, 6.76.

**6-Deoxy-6-(1-imidazolyl)-*N,n*-octyl-D-gluconamide (4).** The synthesis and characterization of this compound are described in Chapter 5.

***N,n*-Octyl-D-gluconamide-6-acetate (5).** Acetic acid anhydride (1.031 g, 10.1 mmol, 1.01 equiv.) was dissolved in 15 ml of pyridine and added dropwise to a stirred (partly gelated) solution of 1.030 g (10.0 mmol) of *N,n*-octyl-D-gluconamide in 60 ml of pyridine at room temperature. The reaction vessel was purged with dry nitrogen. After 2 hrs. of stirring the solvent was evaporated at elevated temperature. The crude product was purified by column chromatography (silica gel, eluent CHCl<sub>3</sub>/MeOH, 9:1 v/v) and recrystallized from EtOAc. Yield

0.40 g (1.14 mmol, 11 %, not optimized), m.p. 130 °C IR (KBr) 3650-3030  $\text{cm}^{-1}$  broad (OH), 1736 (C=O, ester), 1640 (amide I), 1550 (amide II)  $^1\text{H-NMR}$  ( $\text{DMSO-d}_6$ )  $\delta$  7.598 ppm (t, 1H, NHCO), carbohydrate skeleton protons see Table 6.6, 3.053 (9 peaks, 2H,  $(\text{CH}_2)_6\text{-CH}_2\text{-NH}$ ), 1.994 (s, 3H, O-CO- $\text{CH}_3$ ), 1.389 (t, 2H,  $-(\text{CH}_2)_5\text{-CH}_2\text{-CH}_2\text{NHCO}$ ), 1.227 (broad s, 10H,  $\text{CH}_3\text{-(CH}_2)_5\text{-CH}_2\text{-}$ ), 0.846 (t, 3H,  $\text{CH}_3\text{-}$ ), EI-MS  $m/z$  350 ( $\text{M}+\text{H}$ ) $^+$ , 276 ( $\text{C}_8\text{H}_{17}\text{-NHCO(CHOH)}_4$ ) $^+$ , 156 ( $\text{C}_8\text{H}_{17}\text{-NHC=O}$ ) $^+$ , 43 ( $\text{CH}_3\text{C=O}$ ) $^+$ , Anal. Calcd for  $\text{C}_{16}\text{H}_{31}\text{NO}_7$ : C, 55.00, H, 8.94, N, 4.01. Found: C, 54.57, H, 9.01, N, 4.41.

***N,n*-Octyl-D-gluconamide-6-(n-octalate) (6).** The synthetic procedure was analogous to that described for compound **2a**. Instead of benzoyl chloride, 1.633 g (10.04 mmol) of caprylyl chloride (prepared from octanoic acid and thionyl chloride, distilled prior to use) and 3.093 g (10.06 mmol) of **1** were used. To keep the acid chloride mixture fluid, gentle heating was applied. The vessel, however, containing the gluconamide mixture to which the caprolyl chloride was added, was kept at 0 °C. The precipitate obtained from pouring the clear reaction mixture into  $\text{NaHCO}_3/\text{ice}$  was purified by column chromatography (silica, eluent  $\text{CHCl}_3/\text{MeOH}$ , 9:1 v/v) and recrystallized from EtOAc. Yield 0.18 g (0.42 mmol, 4 %, not optimized), m.p. 146.8 °C IR (KBr) 3640-3060  $\text{cm}^{-1}$  broad (OH), 1736 (C=O, ester), 1640 (amide I), 1545 (amide II),  $^1\text{H-NMR}$  ( $\text{DMSO-d}_6$ )  $\delta$  7.604 ppm (t, 1H, NHCO), for the carbohydrate skeleton protons see Table 6.6, 3.056 (10 peaks, 2H,  $-(\text{CH}_2)_6\text{-CH}_2\text{-NH}$ ), 2.274 (t, 2H, O-CO- $\text{CH}_2\text{--}(\text{CH}_2)_5$ ), 1.377 (t, 2H,  $(\text{CH}_2)_5\text{-CH}_2\text{-CH}_2\text{NHCO}$ ), 1.265 (broad s, 18H,  $(\text{CH}_2)_5\text{-CH}_2\text{-NHCO}$  and O-CO- $\text{CH}_2\text{-(CH}_2)_5$ ), 0.846 (t, 6H,  $\text{CH}_3\text{-}$ ), EI-MS  $m/z$  433 ( $\text{M}^+$ ), 156 ( $\text{C}_8\text{H}_{17}\text{-NHC=O}$ ) $^+$ , 127 ( $\text{CH}_3\text{-(CH}_2)_6\text{-C=O}$ ) $^+$ , Anal. Calcd for  $\text{C}_{22}\text{H}_{43}\text{NO}_7$ : C, 60.94, H, 10.00, N, 3.23. Found: C, 60.03, H, 10.01, N, 3.38.

***N,n*-Octyl-D-gluconamide-6-cyclohexanoate (7).** The synthetic procedure was analogous to that of compound **2a**, using 2.658 g (8.65 mmol) of **1**, and 1.337 g (9.12 mmol) of cyclohexanecarboxyl chloride (prepared from cyclohexanecarboxylic acid and thionyl chloride and distilled prior to use) instead of benzoyl chloride. Yield 2.16 g (5.18 mmol, 60 %) The compound was purified by column chromatography (silica eluent  $\text{CHCl}_3/\text{MeOH}$ , 96:4 v/v) m.p. 122.3 °C IR (KBr) 3650-3100  $\text{cm}^{-1}$  broad (OH), 1715 (C=O, ester), 1626 (amide I), 1544 (amide II)  $^1\text{H-NMR}$  ( $\text{DMSO-d}_6$ )  $\delta$  7.614 ppm (t, 1H, NHCO), for the carbohydrate skeleton protons see Table 6.6, 2.289 (9 peaks, 1H,  $\text{OCHC}_5\text{H}_{10}$ ), 1.812 (d, 2H, cyclohexyl  $\text{CH}_2$ ), 1.655 (2d, 2H, cyclohexyl  $\text{CH}_2$ ), 1.570 (d, 1H, C-H from cyclohexyl group), 1.41-1.29 (7H, C-H +  $2\text{*CH}_2$  from cyclohexyl group +  $(\text{CH}_2)_5\text{-CH}_2\text{-CH}_2\text{NHCO}$ ), 1.231 (broad s, 10H,  $\text{CH}_3\text{-(CH}_2)_5\text{-CH}_2\text{-}$ ), 0.846 (t, 3H,  $\text{CH}_3\text{-}$ ), EI-MS  $m/z$  417 ( $\text{M}^+$ ), 290 ( $\text{C}_8\text{H}_{17}\text{-NHCO(CHOH)}_4\text{CH}_2$ ) $^+$ , 276 ( $\text{C}_8\text{H}_{17}\text{-NHCO(CHOH)}_4$ ) $^+$ , 156 ( $\text{C}_8\text{H}_{17}\text{-NHC=O}$ ) $^+$ , 111 ( $\text{C}_6\text{H}_{11}\text{C=O}$ ) $^+$ , 83 ( $\text{C}_6\text{H}_{11}$ ) $^+$ . Anal. Calcd for  $\text{C}_{21}\text{H}_{39}\text{NO}_7$ : C, 60.41, H, 9.41, N, 3.35. Found: C, 60.48, H, 9.41, N, 3.29.

The syntheses and characterization of compounds **8** and **11** are described in Chapter 3.<sup>4</sup>

**2,4,3,5-Dimethylene-*N,n*-octyl-D-gluconamide-6-benzoate (9)** Benzoyl chloride, 0.853 g (5.93 mmol, 2 equiv.) was dissolved in 10 ml of chloroform and added dropwise to a stirred solution of 0.826 g (2.49 mmol) of 2,4,3,5-dimethylene-*N,n*-octyl-D-gluconamide (**8**) and 0.258 g (2.55 mmol) of triethyl amine in 20 ml of chloroform which was placed in an ice bath. The reaction vessel was purged with dried nitrogen gas. After stirring overnight at room temperature and additional refluxing for 2 hrs., the mixture was washed with water, and the compound was purified by recrystallization from ethyl acetate. Yield 0.50 g (1.15 mmol, 46 %, not optimized), m.p. 148.0 °C IR (KBr) 3285  $\text{cm}^{-1}$  sharp (NH), 1719 (C=O, ester), 1660 (amide I), 1549 (amide II)  $^1\text{H-NMR}$  ( $\text{CDCl}_3$ )  $\delta$  8.042 ppm (d, 2H, ArH), 7.590 (t, 1H, ArH), 7.464 (t, 1H, ArH), 6.552 (t, 1H, amide H), 5.276 and 4.833 (2 times d, 2H, methylene bridge H), 5.059 and 5.002 (2 times d, 2H, methylene bridge H) for the carbohydrate skeleton protons see Table 6.6, 3.309 (q, 2H,  $-(\text{CH}_2)_6\text{-CH}_2\text{-NHCO}$ ), 1.510 (m, 2H,  $(\text{CH}_2)_5\text{-CH}_2\text{-CH}_2\text{NHCO}$ ), 1.262 (broad s,

10H,  $\text{CH}_3\text{-(CH}_2\text{)}_5\text{-CH}_2\text{-}$ ), 0 875 (t, 3H,  $\text{CH}_3\text{-}$ ) EI-MS  $m/z$  435 (M)<sup>+</sup>, 156 ( $\text{C}_8\text{H}_{17}\text{-NHC=O}$ )<sup>+</sup>, 105 ( $\text{C}_6\text{H}_5\text{C=O}$ )<sup>+</sup>, 77 ( $\text{C}_6\text{H}_5$ )<sup>+</sup>, Anal Calcd for  $\text{C}_{23}\text{H}_{33}\text{NO}_7$  C, 63 43, H, 7 64, N, 3 22 Found C, 63 43, H, 7 56, N, 3 22

**2,4,3,5-Dimethylene-*N,n*-octyl-D-gluconamide-6-(3-pyridyl) carboxylate (10)** The synthetic procedure was analogous to that described for compound 9 In the present case 0 829 g (2 50 mmol) of 8 and 0 386 g (2 73 mmol) of 3-pyridine-carboxylic acid chloride were used The crude product was purified by column chromatography (silica, eluent EtOAc/MeOH, 95 5 v/v), yield 0 25 g (0 57 g, 49 %, not optimized), m p 135 2 °C IR (KBr) 3281  $\text{cm}^{-1}$  sharp (NH), 1723 (C=O, ester), 1661 (amide I), 1549 (amide II), <sup>1</sup>H-NMR ( $\text{CDCl}_3$ )  $\delta$  9 251 ppm (broad s, 1H, ArH), 8 826 (broad s, 1H, ArH) these two peaks are broadened probably due to dimer formation, in which water acts as a hydrogen bond donor to the pyridyl groups, at 2 507 ppm, a broad peak due to a water molecule is visible which integrates to one water molecule per two pyridyl ligands, 8 326 (d, 1H, ArH), 7 450 (2d, 1H, ArH), 6 566 (t, 1H, amide H), the patterns and chemical shifts of the methylene bridge and carbohydrate skeleton protons are similar to those of 9, 3 311 (q, 2H,  $\text{-(CH}_2\text{)}_6\text{-CH}_2\text{-NHCO}$ ), 1 513 (m, 2H,  $\text{-(CH}_2\text{)}_5\text{-CH}_2\text{-CH}_2\text{NHCO}$ ), 1 263 (broad s, 10H,  $\text{CH}_3\text{-(CH}_2\text{)}_5\text{-CH}_2\text{-}$ ), 0 876 (t, 3H,  $\text{CH}_3\text{-}$ ), EI-MS  $m/z$  350 (M+H)<sup>+</sup>, 276 ( $\text{C}_8\text{H}_{17}\text{-NHCO(CHOH)}_4$ )<sup>+</sup>, 156 ( $\text{C}_8\text{H}_{17}\text{-NHC=O}$ )<sup>+</sup>, 43 ( $\text{CH}_3\text{C=O}$ )<sup>+</sup>, Anal Calcd for  $\text{C}_{22}\text{H}_{32}\text{N}_2\text{O}_7 \cdot \frac{1}{2} \text{H}_2\text{O}$  C, 59 31, H, 7 47, N, 6 29 Found C, 59 44, H, 7 36, N, 6 31

**2-Methoxy-*N,n*-octyl-D-gluconamide (12)** To a mixture of 4 140 g (13 47 mmol) of *N,n*-octyl-D-gluconamide (1) and 1 105 g (19 70 mmol, 1 5 equiv) of powdered KOH in 35 ml of DMSO, was added dropwise 1 758 g (13 94 mmol, 1 03 equiv) of dimethyl sulfate<sup>28</sup> dissolved in 15 ml of DMSO After stirring the reaction mixture for 4 hrs, ethanol was added to inactivate the excess of dimethyl sulfate Prior to evaporation of DMSO the excess KOH was neutralized with 1 30 g (21 65 mmol) of acetic acid anhydride The residue was purified by column chromatography (silica, eluent  $\text{CHCl}_3/\text{MeOH}$ , 93 7 v/v), yield 0 61 g (1 89 mmol, 14 %), m p 129 2 °C IR (KBr) 3660-3060  $\text{cm}^{-1}$  broad (OH), 1656 (amide I), 1564 (amide II) <sup>1</sup>H-NMR ( $\text{DMSO-d}_6$ )  $\delta$  7 840 ppm (t, 1H, NHCO), for the carbohydrate skeleton protons see Table 6 6, 3 260 (s, 3H,  $\text{OCH}_3$ ), 3 057 (m, 2H, 2H,  $\text{(CH}_2\text{)}_6\text{-CH}_2\text{-NHCO}$ ), 1 398 (t, 2H,  $\text{(CH}_2\text{)}_5\text{-CH}_2\text{-CH}_2\text{NHCO}$ ), 1 230 (broad s, 10H,  $\text{CH}_3\text{-(CH}_2\text{)}_5\text{-CH}_2\text{-}$ ), 0 844 (t, 3H,  $\text{CH}_3\text{-}$ ), EI-MS  $m/z$  321 (M+H)<sup>+</sup>, 276 ( $\text{C}_8\text{H}_{17}\text{-NHCO(CHOCH}_3\text{)(CHOH)}_3\text{CH}_2\text{OH}$ )<sup>+</sup>, 260 ( $\text{C}_8\text{H}_{17}\text{-NHCO(CHOCH}_3\text{)(CHOH)}_2$ )<sup>+</sup>, 230 ( $\text{C}_8\text{H}_{17}\text{-NHCO(CHOCH}_3\text{)CHOH}$ )<sup>+</sup>, 156 ( $\text{C}_8\text{H}_{17}\text{-NHC=O}$ )<sup>+</sup>, Anal Calcd for  $\text{C}_{15}\text{H}_{31}\text{NO}_6$  C, 56 05, H, 9 72, N, 4 36 Found C, 56 04, H, 9 79, N, 4 42

**2-Methoxy-*N,n*-octyl-D-gluconamide-6-benzoate (13)** This compound was synthesized as described for compound 2a In this procedure 0 219 g (1 56 mmol) of benzoyl chloride and 0 338 g (1 05 mmol) of compound 8 were used The work up and purification procedure was similar to that described for compound 5 Yield 0 13 g (0 31 mmol, 29 %), m p 111 3 °C IR (KBr) 3660-3020  $\text{cm}^{-1}$  broad (OH), 1697 (C=O, ester), 1654 (amide I), 1539 (amide II) <sup>1</sup>H-NMR (90 MHz,  $\text{CDCl}_3$ )  $\delta$  8 058 ppm (d, 2H, ArH), 7 483 (m, 3H, ArH), 6 787 (t, 1H, NH-CO), 3 450 (s, 3H,  $\text{OCH}_3$ ), 1 258 (broad s, 10H,  $\text{CH}_3\text{-(CH}_2\text{)}_5\text{-CH}_2\text{-}$ ), 0 875 (t, 3H,  $\text{CH}_3\text{-}$ ) EI-MS  $m/z$  426 (M+H)<sup>+</sup>, 290 ( $\text{C}_8\text{H}_{17}\text{-NHCO(CHOCH}_3\text{)(CHOH)}_3$ )<sup>+</sup>, 260 ( $\text{C}_8\text{H}_{17}\text{-NHCO(CHOCH}_3\text{)(CHOH)}_2$ )<sup>+</sup>, 230 ( $\text{C}_8\text{H}_{17}\text{-NHCO(CHOCH}_3\text{)CHOH}$ )<sup>+</sup>, 156 ( $\text{C}_8\text{H}_{17}\text{-NHC=O}$ )<sup>+</sup>, 105 (ArC=O)<sup>+</sup>, 77 ( $\text{C}_6\text{H}_5$ )<sup>+</sup> Anal Calcd for  $\text{C}_{22}\text{H}_{35}\text{NO}_7$  C, 62 09, H, 8 29, N, 3 29 Found C, 61 94, H, 8 26, N, 3 23

**2-Methoxy-*N,n*-octyl-D-gluconamide-6-acetate (14)** The synthetic procedure was analogous to that described for compound 5, using 0 171 g (1 67 mmol) of acetic anhydride and 0 493 g (1 54 mmol) of compound 12 The work up and purification procedure was similar to that for compound 7 Yield 0 17 g (0 47 mmol, 30 %), m p 101 9 °C IR (KBr) 3660-3125  $\text{cm}^{-1}$  broad (OH), 1717 (C=O, ester), 1650 (amide I), 1539 (amide II) <sup>1</sup>H-NMR ( $\text{DMSO-d}_6$ )  $\delta$  7 614 ppm (t,

1H, NHCO), for the carbohydrate skeleton protons see Table 6.6, 3.263 (s, 3H, OCH<sub>3</sub>), 3.059 (m, 2H, -(CH<sub>2</sub>)<sub>6</sub>-CH<sub>2</sub>-NHCO), 1.991 (s, 3H, OCOCH<sub>3</sub>), 1.402 (t, 2H, (CH<sub>2</sub>)<sub>5</sub>-CH<sub>2</sub>-CH<sub>2</sub>NHCO), 1.232 (broad s, 10H, CH<sub>3</sub>-(CH<sub>2</sub>)<sub>5</sub>-CH<sub>2</sub>-), 0.843 (t, 3H, CH<sub>3</sub>-). EI-MS: *m/z* 363 (M+H)<sup>+</sup>, 290 (C<sub>8</sub>H<sub>17</sub>-NHCO(CHOCH<sub>3</sub>)(CHOH)<sub>3</sub>)<sup>+</sup>, 260 (C<sub>8</sub>H<sub>17</sub>-NHCO(CHOCH<sub>3</sub>)(CHOH)<sub>2</sub>)<sup>+</sup>, 230 (C<sub>8</sub>H<sub>17</sub>-NHCO(CHOCH<sub>3</sub>)(CHOH))<sup>+</sup>, 201 (C<sub>8</sub>H<sub>17</sub>-NHCO(CHOCH<sub>3</sub>))<sup>+</sup>, 156 (C<sub>8</sub>H<sub>17</sub>-NHC=O)<sup>+</sup>, 43 (CH<sub>3</sub>C=O). Anal. Calcd. for C<sub>17</sub>H<sub>33</sub>NO<sub>7</sub>: C, 56.18; H, 9.15; N, 3.85. Found: C, 56.03; H, 9.14; N, 3.88.

**Di-(6-*N*,*n*-octyl-D-gluconamide)-terephthalate (15).** To a partly gelated solution of 2.538 g (8.23 mmol) of **1** in 40 ml of pyridine, was added dropwise over a period of 20 min. 0.883 g (4.35 mmol) of terephthaloyl dichloride which was dissolved in 10 ml of DMF. After stirring for 1 hr. at 0 °C and an additional 1 hr. at room temperature, the clear yellow solution was heated for 2 hrs. at 60 °C. After cooling the clear solution was poured into ± 500 ml of saturated NaHCO<sub>3</sub>/ice and the precipitate was washed with hot methanol. Yield 1.13 g (1.51 mmol, 37 %), m.p. 203.4 °C (dec.). IR (KBr) cm<sup>-1</sup> 3650-3030 broad (OH), 1724/1701 (C=O, ester); since the peak of the ester function was split into two values, it was assumed that this function is present in the solid state in more than one conformation, 1624 (amide I), 1543 (amide II). <sup>1</sup>H-NMR (DMSO-d<sub>6</sub>) δ 8.133 ppm (s, 4H, ArH), 7.628 (t, 2H, ArH), for the carbohydrate skeleton protons see Table 6.6, 3.065 (9 peaks, 2H, (CH<sub>2</sub>)<sub>6</sub>-CH<sub>2</sub>-NHCO), 1.396 (t, 2H, (CH<sub>2</sub>)<sub>5</sub>-CH<sub>2</sub>-CH<sub>2</sub>NHCO), 1.223 (broad s, 10H, CH<sub>3</sub>-(CH<sub>2</sub>)<sub>5</sub>-CH<sub>2</sub>-), 0.837 (t, 3H, CH<sub>3</sub>-); EI-MS *m/z* 744 (M+H)<sup>+</sup>, 156 (C<sub>8</sub>H<sub>17</sub>-NHC=O)<sup>+</sup>, 105 (ArC=O)<sup>+</sup>, 77 (C<sub>6</sub>H<sub>5</sub>). Anal. Calcd. for C<sub>36</sub>H<sub>60</sub>N<sub>2</sub>O<sub>14</sub>: C, 58.03; H, 8.12; N, 3.76. Found: C, 57.59; H, 7.92; N, 3.66.

***N*,*n*-Octyl-D-galactonamide (16).** The synthesis and characterization of this compound has been described in the literature<sup>5a</sup> The analytical data (<sup>1</sup>H-NMR, IR, elemental analysis) were satisfactory.

***N*,*n*-Octyl-D-galactonamide-6-benzoate (17).** The synthetic procedure for this compound was similar to that described for compound **2a**. In the present case 0.765 g (5.44 mmol) of benzoyl chloride and 1.520 g (4.94 mmol) of *N*,*n*-octyl-D-galactonamide<sup>5a</sup> (compound **16**) were used. The precipitate obtained after pouring the reaction mixture into saturated NaHCO<sub>3</sub>/ice was purified by column chromatography (silica, eluent CHCl<sub>3</sub>/MeOH, 93:7 v/v), followed by recrystallization. Yield 0.33 g (0.80 mmol, 16 %), m.p. 188.2 °C (dec.). IR (KBr) 3669-3020 cm<sup>-1</sup> broad (OH), 1721/1711 (2×C=O, ester), 1665/1624 (amide I), 1543 (amide II). <sup>1</sup>H-NMR (DMSO-d<sub>6</sub>) δ 7.988 ppm (d, 2H, ArH), 7.650 (t, 1H, ArH), 7.522 (t, 2H, ArH), 5.169 (d, 1H, O<sup>2</sup>H), 4.711 (d, 1H, O<sup>5</sup>H), 4.510 (d, 1H, O<sup>4</sup>H), 4.397 (d, 1H, O<sup>3</sup>H), 4.297 (2d, 1H, C<sup>6</sup>H), 4.226 (2d, 1H, C<sup>6</sup>H), 4.143 (d, 1H, C<sup>2</sup>H), 4.061 (q, 1H, C<sup>5</sup>H), 3.854 (t, 1H, C<sup>3</sup>H), 3.476 (t, 1H, C<sup>4</sup>H), 3.077 (m, 2H, (CH<sub>2</sub>)<sub>6</sub>-CH<sub>2</sub>-NHCO), 1.399 (t, 2H, (CH<sub>2</sub>)<sub>5</sub>-CH<sub>2</sub>-CH<sub>2</sub>NHCO), 1.234 (broad s, 10H, CH<sub>3</sub>-(CH<sub>2</sub>)<sub>5</sub>-CH<sub>2</sub>-), 0.845 (t, 3H, CH<sub>3</sub>-); EI-MS *m/z* 411 (M)<sup>+</sup>, 156 (C<sub>8</sub>H<sub>17</sub>-NHC=O)<sup>+</sup>, 105 (ArC=O)<sup>+</sup>, 77 (C<sub>6</sub>H<sub>5</sub>). Anal. Calcd. for C<sub>21</sub>H<sub>33</sub>NO<sub>7</sub>·0.5H<sub>2</sub>O: C, 59.98; H, 8.15; N, 3.33. Found: C, 60.02; H, 7.87; N, 3.39.

## 6.2.2 Physical measurements

### Determination of *T*<sub>gel</sub>

A typical procedure for the preparation of the organogels was as follows: in a test tube, approximately 0.5 ml of solvent was added to 5 mg of powdered sample. The tube was closed and gently heated, in most cases until the mixture started to boil. Subsequently, the mixture was vortexed until a clear solution was obtained and thereafter allowed to cool to room temperature. When the gel had a viscosity high enough to turn the test tube upside down without damaging the structure, the sol-to-gel temperature was determined according to a method described in the



literature<sup>29</sup> A glass ball was placed on top of the gel and the test tube was subsequently placed in a thermostatted water bath and heated at 1.5 °C/min. The temperature at which the ball started to fall through the gel was denoted as  $T_{\text{gel}}$ .

#### *DSC measurements*

The thermograms were recorded on a Perkin Elmer DSC 7 instrument using closed stainless steel cups. Gelator (0.5 mg) was placed in the cups and 50  $\mu\text{L}$  of solvent was added with the help of a pipette. After sealing the cups were heated to 20 °C above the boiling point of the solvent, before the first run was recorded. The scan rate for both the heating and cooling runs was 5 °C/min. At least 2 heating and 2 cooling runs per sample were recorded. Loss of solvent during the runs was checked by weighing the cups before and after the measurements. In all cases no loss of weight was found. For the calibration of the instrument cyclohexane and indium samples were used.

The thermograms of the samples without solvent were recorded in 30  $\mu\text{L}$  aluminium pans. Calibration was carried out with zinc and indium samples (scan rate of 5 °C/min).

#### *Electron Microscopy*

The electron micrographs were recorded on TEM Philips EM201 and TEM Jeol JEMCXII instruments. The gels were transferred to carbon-coated 150 mesh copper grids. After 30 sec. of acclimatization the excess material was removed and the grids were covered with Pt deposited at an angle of 45°.

#### *X-ray powder diffraction*

X-ray powder diffractograms were recorded on a Philips PW1710 powder diffractometer with a Ni filtered Cu source (40 KV, 55 mA,  $\lambda = 1.54060 \text{ \AA}$ ). The 1 % (weight/volume) gels were transferred to a silicon sample holder and rapidly dried under high vacuum.

#### *FT-IR spectroscopy*

FT-IR spectra were recorded on a Bio Rad Digilab Division (FTS-25) instrument. The gels and solutions were measured between NaCl windows and corrected for the solvents. Solid samples were measured as KBr pellets.

## **6.3 Results**

### **6.3.1 Gelation behavior**

Compounds **1-17** were studied with regard to their gelation behavior in 5 organic solvents. The results are compiled in Table 6.1. The gels obtained were either clear or slightly turbid. Those possessing a viscosity so high that the test tube could be turned upside down without damaging the structure are denoted as (G) in Table 6.1. Gels with this behavior could be made from the gluconamide (**1**), the benzoate (**2a**), the cyclohexanoate (**7**) and the C<sup>2</sup> methoxy protected derivative **12**. The gels obtained from the imidazole and acetate derivatives **4** and **5** showed a significantly higher viscosity than expected for a solution or a vesicular dispersion, but were not as viscous as the afore mentioned gels, those are earmarked as (T). In some cases the compound remained dissolved (S) upon cooling without forming a gel while others formed crystalline powders within one hour (R). Insolubility is denoted as (I).

Compound **1** is capable of forming a very strong hydrogen bonding network which can only be split by very polar solvents like water and ethanol or by high temperature, *i.e.* in solvents

with high boiling points like 1,2-xylene (b.p. 144 °C). Introduction of substituents on the gluconamide framework leads to enhancement of the solubility (see Table 6.1). Both aromatic and aliphatic substituents on carbon atom C<sup>6</sup> gave soluble products, which in some cases recrystallized from ethyl acetate, but formed gels in 1,2-xylene and chloroform. When the secondary hydroxyl groups of the gluconamide derivatives were protected, the compounds became too soluble for most organic solvents and in most cases no gels or turbid mixtures were formed upon cooling. Even protection of only one of the hydroxyl groups (*viz* C<sup>2</sup>), increased the solubility too much for the formation of gels (except for compound **12** in 1,2-xylene). n-Hexane turned out not to be a suitable solvent for the formation of organo-gels. Even **6** and **15** did not dissolve in this solvent, which is somewhat surprising, since in both compounds the hydrophilic carbohydrate moiety is located in between two hydrophobic alkyl chains which should give **6** a relatively hydrophobic character.

**Table 6.1** Gelation behavior of gluconamides in organic solvents <sup>a</sup>

Compound	Protected <sup>b</sup>	Substituent <sup>c</sup>	n-hexane	1,2-xylene	CHCl <sub>3</sub>	EtOAc	EtOH
<b>1</b>	No	OH	I	G	I	I	R
<b>2a</b>	No	Aromatic	I	G	G	G	G
<b>3</b>	No	Aromatic	I	R	I	R	S
<b>4</b>	No	Aromatic	I	T	G	R	S
<b>5</b>	No	Aliphatic	I	G <sup>d</sup>	G <sup>d</sup>	R	S
<b>6</b>	No	Aliphatic	I	S	T	R	R
<b>7</b>	No	Aliphatic	I	G	G	G	S
<b>8</b>	Dimethylene	OH	R	T	S	S	S
<b>9</b>	Dimethylene	Aromatic	R	S	S	S	S
<b>10</b>	Dimethylene	Aromatic	R	S	S	S	S
<b>11</b>	Dimethylene	Aromatic	I	R	S	S	S
<b>12</b>	C <sup>2</sup> methoxy	OH	I	G	S	S	S
<b>13</b>	C <sup>2</sup> methoxy	Aromatic	I	R	S	S	S
<b>14</b>	C <sup>2</sup> methoxy	Aliphatic	I	R	S	S	S
<b>15</b>	No	Dimer	I	I	I	I	I
<b>(16)<sup>e</sup></b>	No	OH	I	I	I	I	R
<b>(17)<sup>e</sup></b>	No	Aromatic	I	T	T	R	R

<sup>a</sup> G the compound gels the solvent resulting in a high viscosity mixture upon cooling S compound dissolves without gelation I the compound is insoluble after prolonged heating R compound recrystallizes upon cooling within 1 h T upon cooling a turbid mixture with a slightly increased viscosity is obtained, but no gel is formed

<sup>b</sup> Protection of the hydroxyl groups

<sup>c</sup> Substituents on the C<sup>6</sup> of the carbohydrate

<sup>d</sup> Gel with low viscosity

<sup>e</sup> Galactonamide derivatives

In fact the octyl derivative **6** was hardly soluble in any solvent: only in boiling chloroform a clear solution could be obtained, which turned cloudy and viscous but did not form a firm gel. The gemini surfactant **15** was insoluble in almost every solvent, only in DMSO this compound could be dissolved. Apparently the packing in the solid phase is very strong, which was also evident from the very high melting point (203 °C, dec.) of this compound. Introduction of a benzoyl group in the gluconamide resulted in gelation of almost every solvent. Placing the benzoyl function on the galactonamide framework (**17**) resulted in an increase of the solubility of the compound, but unlike the gluconamide derivative, gelation was weak. Only in 1,2-xylene a gel with a very low tensile strength was formed.

All gels were thermoreversible, *i.e.* they turned into clear, low viscosity solutions upon heating and gelation returned after cooling. The temperature at which the gel vanishes is denoted as the gel-to-sol temperature  $T_{\text{gel}}$ . For the benzoate derivative **2a**, we studied  $T_{\text{gel}}$  in a variety of solvents (Table 6.2). We tried to relate physical constants like polarization index according to Snyder,<sup>30</sup> Rohrschneider constants,<sup>31</sup> dielectrical constants, surface tension and boiling points of the solvents to the  $T_{\text{gel}}$  values, but unfortunately no clear correlation could be obtained.

**Table 6.2** Temperatures at which the gel of the benzoate derivative **2a** vanishes in different solvents <sup>a</sup>

Solvent	$T_{\text{gel}}$ (°C) <sup>b</sup>	Pol index <sup>c</sup>	Boiling point (°C) <sup>e</sup>
Water	R	9 0	100
Methanol	17	6 6	65
Ethanol	28	5 2	79
Acetonitril	50	6 2	82
Acetone	28	5 4	56
Dioxane	15	4 8	101
Chloroform	66	4 4	62
Ethyl acetate	42	4 3	77
Tetrahydrofurane	S	4 2	66
Dichloromethane	43	3 4	40
Toluene	101	2 3	111
Ether	I	--- <sup>d</sup>	35
n-Hexane	I	--- <sup>d</sup>	69
Benzene	95	--- <sup>d</sup>	80
1,2-Xylene	102	--- <sup>d</sup>	144

<sup>a</sup> Determined by the Takahashi method, see Ref 29

<sup>b</sup> Explanation of symbols see Table 6 1

<sup>c</sup> Polarization index according to Snyder, see Ref 30

<sup>d</sup> Polarization index not known

<sup>e</sup> Boiling points of pure solvents.

In contrast to the gels of **1** in water and in 1,2-xylene where precipitation occurred after a couple of days,<sup>5,6</sup> the gels of **2a** in various solvents were very stable and did not change over a

period of several months. Transition electron microscopy (TEM) pictures of an aged sample in chloroform showed exactly the same texture as TEM carried out on a freshly prepared sample. The stability of the gel was only affected by raising the temperature.

In some cases (chloroform, dichloromethane, and benzene see Table 6.2) the  $T_{\text{gel}}$  of **2a** exceeded the boiling point of the solvent. Boiling only occurred upon decomposition of the gel ( $T_{\text{gel}} = \text{boiling}$ ).

Elongation of the alkyl chain length from n-octyl to n-hexadecyl in compound (**2b**) resulted in a slower gelation process. Only after one day of conditioning at ambient temperature, a gel in chloroform was formed, which is considerably slower than the time required for the octyl derivative **2a**, which gelled within several minutes upon cooling. This effect was also observed in aqueous gels of unsubstituted *N,n*-alkyl-D-gluconamides, which tend to crystallize with a rate depending on the length of the alkyl chain,<sup>2</sup> and in gels of maltobionamides, of which the fibers of the long chain compounds are not as regularly oriented as those of the short chain ones.<sup>2</sup>

### 6.3.2 DSC measurements

In order to obtain information about the enthalpy changes that accompany the formation and collapse of the gels, differential scanning calorimetry (DSC) experiments were carried out with compound **2a**. Both the heating and cooling curves showed in all cases very broad peaks, indicating that the transitions took place gradually. This can be attributed to the relatively low degree of ordering that is present in the gel, compared to the crystalline structures, which normally give sharp peaks (*e.g.* crystal-crystal transitions or melting). Although the large peak width reduced the accuracy of the thermograms,<sup>32</sup> certain trends could be distinguished.

**Table 6.3** Heat transformation upon gel formation,  $\Delta H(\text{gel})$  for **2a** in various solvents, obtained from DSC cooling thermograms

Solvent	kJ/mole gelator <sup>a</sup>
Dichloromethane	- 19
Chloroform	- 21
Ethanol	(14) <sup>b</sup>
Benzene	- 44
Toluene	- 37
1,2-Xylene	- 38

<sup>a</sup> Corrected to 50  $\mu\text{l}$  1 % gel (values  $\pm$  15 %)

<sup>b</sup> Value obtained upon heating. Gel formation upon cooling was too slow for accurate DSC measurements

The  $\Delta H(\text{gel})$  values were measured in several solvents. Thermograms of the gels showed that in chlorinated solvents  $\Delta H(\text{gel})$  is much lower than in aromatic solvents. In the case of ethanol an even lower  $\Delta H(\text{gel})$  value was observed (see Table 6.3). The latter is probably due to the fact that ethanol can accept and donate hydrogen bonds and hence disturb the *inter*-molecular hydrogen bonding network of **2a**. In order to investigate the influence of H-bonding from the

solvent, it would be of interest to do experiments in other solvents that are either H-bond donating or H-bond accepting. Compound **2a** dissolved in H-bonding accepting solvents like DMSO or THF but, unfortunately, remained in solution upon cooling, while gelation in dioxane was too slow (2 days) for performing accurate DSC measurements. On the other hand **2a** did not dissolve at all in water (H-bond donating) while gelation in methanol again was too slow (16 hrs.) for accurate DSC recording. For comparison we recorded the energy transfer that takes place when the aqueous gel of **1** is dissolved. As can be seen in Table 6.4 the energy transfers of **1** in water and **2a** in ethanol are in the same range.

**Table 6.4** Heat transfer upon dissolving the gels of **1** and **2a** <sup>a</sup>

Compound	kJ/mole gelator
<b>1</b> in water	11
<b>2a</b> in ethanol	14

<sup>a</sup> Data obtained from DSC heating thermograms

We also measured  $\Delta H(\text{gel})$  values for other gelators than **2a** in an organic solvent. In order to make it possible to compare different gelators in one solvent, experiments were carried out in 1,2-xylene. Since not every compound described so far gelled in 1,2-xylene, the choice was limited to **1**, **2a**, **12**, and **17**. Table 6.5 shows that the  $\Delta H(\text{gel})$  upon disruption of the gels in 1,2-xylene is nearly independent of the gelator type. Even the galactonamide derivative (compound **17**) does not deviate from this trend, although this compound formed a turbid mixture instead of a highly viscous gel.

**Table 6.5** Heat transfer upon formation of the gels in 1,2-xylene obtained from DSC cooling thermograms

Compound	kJ/mol gelator
<b>1</b>	- 42
<b>2a</b>	- 38
<b>12</b>	- 38
<b>17</b> <sup>a</sup>	- 37

<sup>a</sup> This compound does not form a highly viscous gel, but a turbid mixture

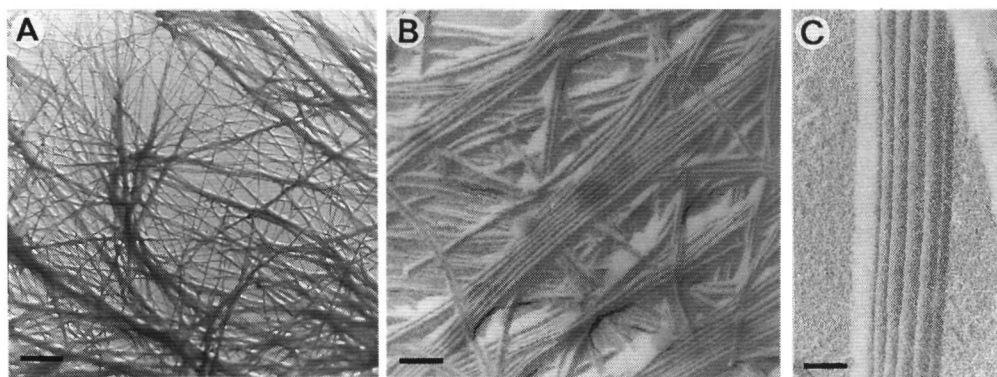
### 6.3.3 Electron microscopy

The high viscosity of the gels suggests that network structures are formed from the gluconamide building blocks, which we decided to investigate by transmission electron microscopy (TEM) in combination with Pt shadowing. In the following the TEM pictures obtained from the various compounds are discussed in some detail.

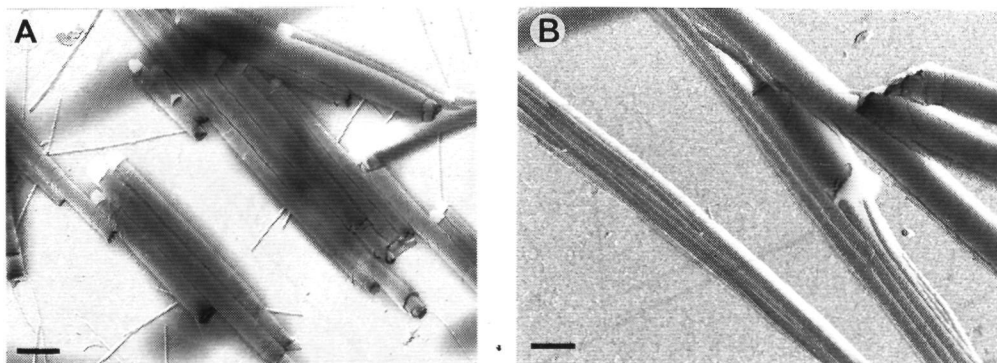
### 6.3.3.1 Gluconamides with aromatic substituents on C<sup>6</sup>

#### Benzoate derivatives **2a** and **2b**

The TEM pictures of the organogels formed from the benzoate derivative **2a** showed a network of whisker-type fibers (see Figure 6.1A, TEM picture, of a gel from **2a** in chloroform). Despite the relatively low concentration (1 % w/v), the network is finely meshed, which explains why the gel is rigid and why it can exist above the boiling point of the solvent without collapsing. The fibers are often bundled like the strings in a rope (see Figure 6.1B), but neither the individual fibers nor the bundles of fibers showed chirality. Apparently, in contrast with **1** in water, the chirality of the head group of **2a** is not expressed in the supramolecular structure. The fibers have an average diameter of 31 nm and hence must be composed of more than one monolayer or bilayer (2.4 nm and 4.9 nm, respectively, as estimated from CPK models) or must be hollow. From the TEM micrographs it can not be distinguished if the rodlike structures of **2a** are hollow tubes, or solid rods.



**Figure 6.1** TEM pictures of a gel of **2a** in chloroform (Pt shadowing). A) network of fibers, bar is 1.5  $\mu\text{m}$ . B) Bundles of whisker-type fibers, bar is 240 nm. C) Intertwined bundles of fibers; bar is 80 nm.



**Figure 6.2** TEM pictures of a gel of **2b** in chloroform (Pt shadowing). A) Cigar-like tubes from rolled-up multilayers; bar is 870 nm. B) Whisker-type fibers and cigar-like tubes, bar is 340 nm.

More insight would have been obtained if freeze-fracture and negative staining experiments could have been performed, but the organic solvent like chloroform prohibited the

application of these preparative techniques. The aspect ratio (length to width) of the fibers was very high, viz up to 500. Although the  $T_{\text{gel}}$  and  $\Delta H(\text{gel})$  values were dependent on the solvent, the shapes of the textures were not. Micrographs recorded from gels of **2a** in ethyl acetate, ethanol, or 1,2-xylene all showed fiber-like structures with the same dimensions as those seen for **2a** in chloroform.

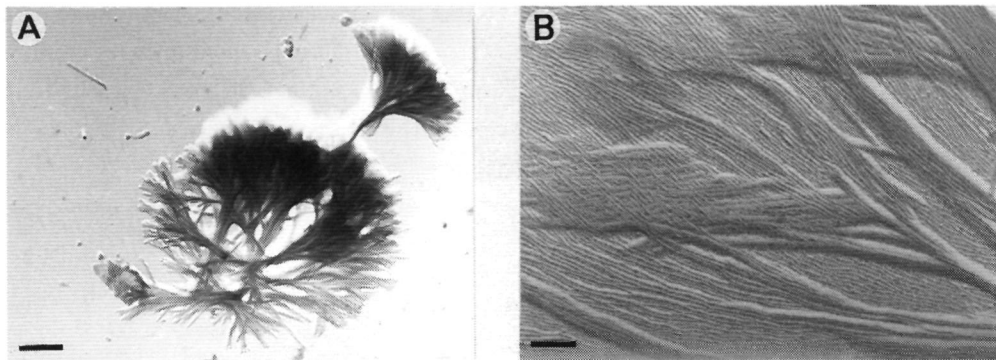
In electron micrographs of gels of **2b** two aggregation forms could be discerned: cigar-like rolled up multilayers (see Figure 6 2A) and whisker-type fibers (see Figure 6 2B) which were also present in gels of **2a** in chloroform (see Figure 6 1B). The multi-layered cigar-like structures had diameters ranging from 200 to 500 nm, whereas the fibers had a much smaller average diameter of 65 nm. These fibers must either consist of several layers or be hollow, because the estimated monolayer thickness is only 3.1 nm.

### *3-Pyridyl-carboxylate derivative 3*

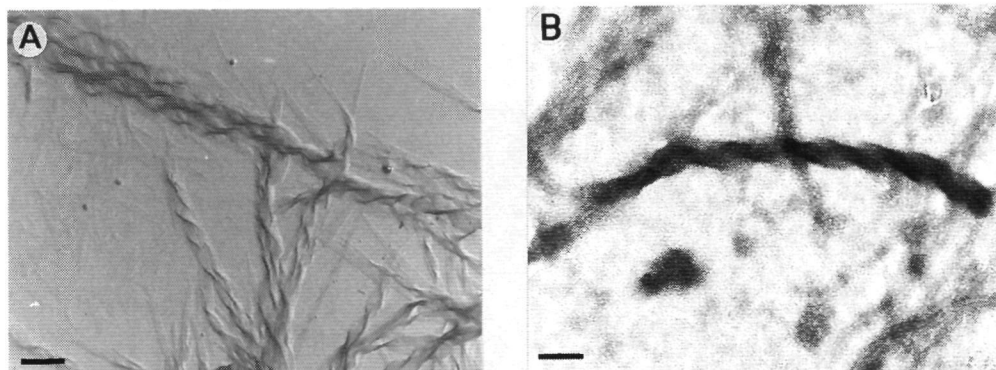
A TEM picture of a gel of **3** in dioxane showed fiber-like structures which assembled to form larger rod-like aggregates (the diameter of the fibers was approximately 10 nm, the average diameter of the rods was 40 nm, see Figure 6 3). Gluconamide **2a** also formed rod-like structures of approximately 30 nm, but the finer fibers of 10 nm as observed in the gels of the pyridine-carboxylic acid ester **3** were absent in the gels of **2a**. Chiral suprastructures like chiral twists or helical ropes, were not observed for compound **3**.

### *Imidazolyl derivative 4*

Compound **4** which contains the aromatic substituent imidazole was found to gelate in chloroform (see Section 6 3 1). TEM pictures of the gels revealed the presence of twisted ribbon-like structures (see Figure 6 4A). The direction of the twist was for all ribbons similar. For comparison we also studied the aggregation behavior of **4** in aqueous solution. The imidazole group of **4** has a  $\text{p}K_{\text{a}} = 7.02$  (see Chapter 5) and will be partly protonated in neutral water. In order to study the effect of protonation on the aggregation behavior as was done for the imidazole compound **11** (see Chapter 4), **4** was dissolved in Tris buffered (pH= 8.5) and acetic acid/sodium acetate buffered (pH= 4.5) water. In the former solution, compound **4** slowly formed a gel in which the same type of twisted ribbons were present as in the gel in chloroform. Attempts to obtain freeze etched electron micrographs of **4** in Tris buffered water failed, presumably because the alkyl chains in the bilayers intercalate, which prohibits clear fracturing. Staining of the samples with uranyl acetate, resulted in micrographs with relatively contrast-rich regions (Figure 6 4B). This might indicate that in the aggregates the hydrophilic parts of **4**, which bind the uranyl acetate, are in direct contact with the aqueous phase. We believe that the aggregates of **4** in chloroform have a similar molecular arrangement as the aggregates in water. The hydrophilic head groups of **4** and not the hydrophobic alkyl chains are probably facing the chloroform phase. Aggregation of **4** in water was found to be much slower than aggregation in chloroform or in dichloromethane. The clear solution of neutral **4** in water gelled only after 1 day, whereas the clear solution of **4** in chloroform gelled within 1 hour. Dissolving **4** in the acetate buffer of pH=4.5 resulted in a clear solution without the formation of any aggregates.



**Figure 6.3** TEM picture of a gel of **3** in 1,4-dioxane. A) Overview bar is 570 nm. B) Visible are rods which are build up from fibers. (Pt shadowing); bar is 140 nm.



**Figure 6.4** TEM pictures of **4**. A) Gel in chloroform. Visible are twisted ribbons (Pt shadowing), bar is 212 nm. B) Gel in Tris buffered solution pH 8.5 (neg. staining with  $\text{U}(\text{OAc})_2$  1 %). Visible are twisted ribbons; bar is 73 nm.

### 6.3.3.2 Gluconamides with aliphatic substituents on $\text{C}^6$

#### *Acetyl derivative 5*

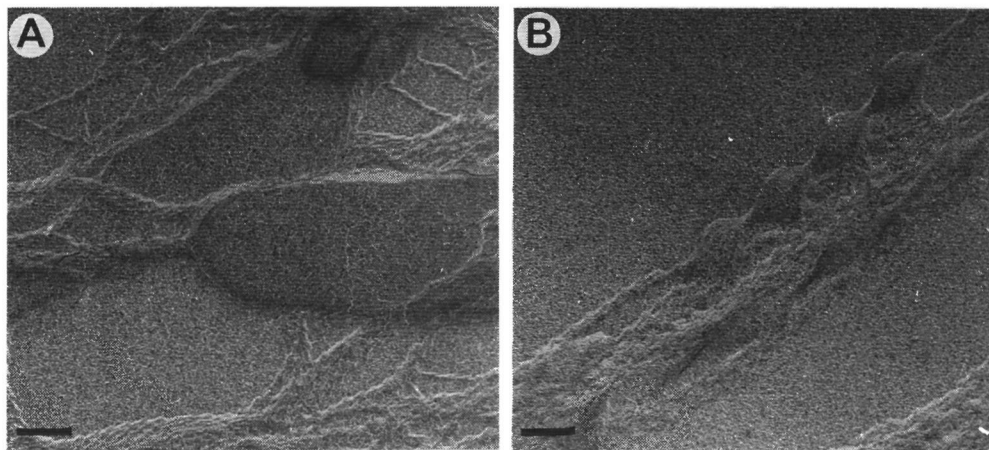
Compound **5** has a relative small hydrophobic substituent on carbon atom  $\text{C}^6$  of the glucon moiety. It is therefore not surprising that **5** is readily soluble in water at elevated temperatures and is capable of forming a gel upon cooling. Compound **5** also gels in organic solvents (*vide supra*). Gels formed from **5** in water and in chloroform were investigated by TEM. The aqueous gel of **5** had a lower viscosity than the gel obtained from **1** in water or from **2a** in chloroform. Electron micrographs of **5** in water showed the presence of multilayered ribbons, which rolled up to give helices (not shown). In chloroform similar types of chiral aggregates were present (see Figure 6.5A + 6.5B). This would suggest that the way compound **5** aggregates is solvent independent. Apparently, small hydrophobic groups (imidazole, see above, and acetate) allow the gluconamides to form gels in both water and chloroform. These groups do not disturb the packing of **5** and as a result the molecular chirality can be expressed in the suprastructures.

#### *n-Octyl derivative 6*

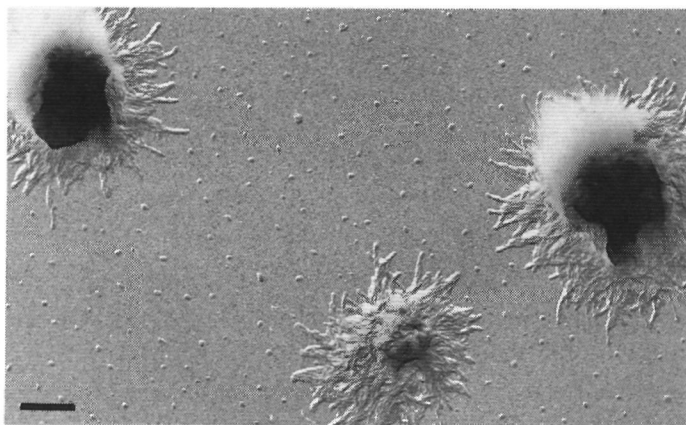
Since the size, shape, and structure of the substituent are important for the generation of the suprastructures, it was of interest to investigate what type of aggregates were present in gels of compound **6**, which has a longer alkyl substituent than **5**. Micrographs of a turbid mixture of **6**



in chloroform showed helical suprastructures, with an average diameter of 35 nm (Figure 6.6), but with a much smaller aspect ratio (maximum of ratio was 13) than the suprastructures obtained from *e.g.* **1** in water and **5** in water or chloroform. The observed helical forms originate from amorphous droplets of material and do not form a network as was observed for *e.g.* **2a** in chloroform. This explains why **6** does not form a *rigid* gel.



**Figure 6.5** TEM pictures of gels of **5** in chloroform (Pt shadowing). A) Flat ribbons which twist to give a helix, the bar is 140 nm. B) Helix, which changes into a twisted ribbon and back into a helix, bar is 110 nm.

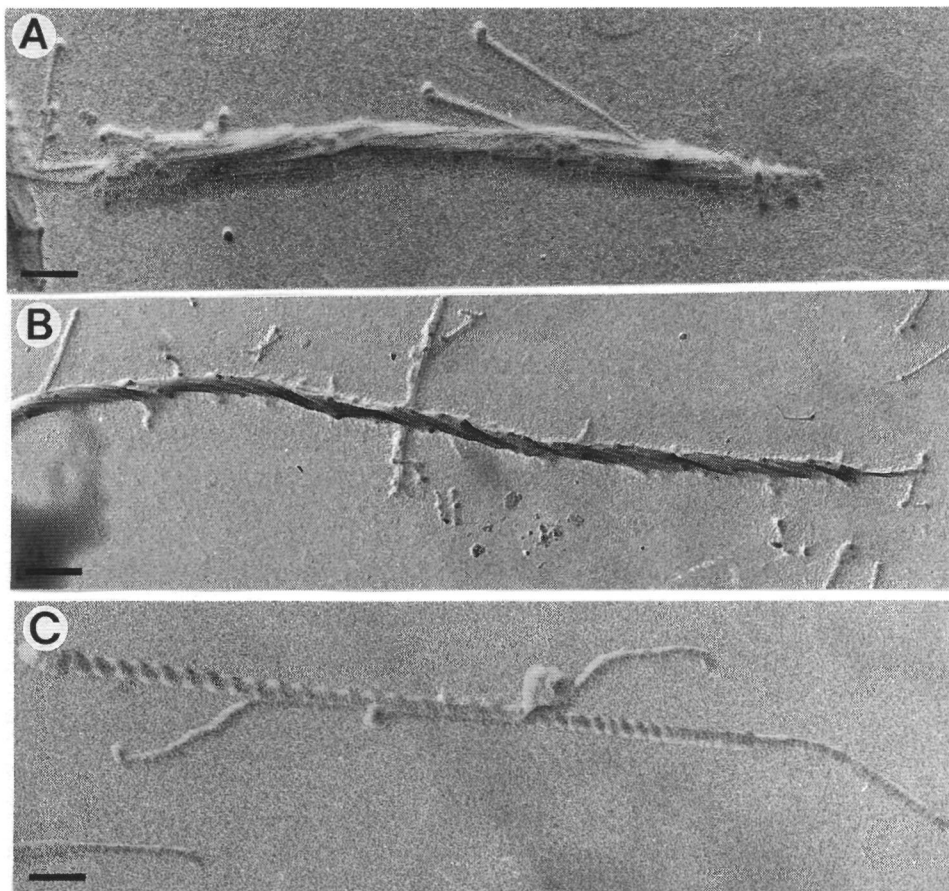


**Figure 6.6** TEM picture of a gel of **6** in chloroform (Pt shadowing). Helices are shown, which originate from an amorphous droplet, bar is 100 nm.

### Cyclohexanoyl derivative **7**

In benzene and ethyl acetate **7** forms gels in which fiber-like structures are present (Figure 6.7A). These fibers are not so well defined as those obtained from **2a** in ethyl acetate, 1,2-xylene or chloroform. They intertwine to form bundles. Many fibers have at both ends a remarkable knob-shaped enlargement (see Figure 6.7A and B). Careful inspection of the fibers reveals that they are helical and very tightly wound (see Figure 6.7C). Although the cyclohexanoate substituent is very bulky and comparable in size to the benzoate group, it does not prevent the

formation of chiral aggregates as the latter group does. Cyclohexane rings probably can stack in an orientation that fits the packing directed by the glucon group. Similar conclusions were drawn from the X-ray structure of (1S,2S)-1,2-bis(D-gluconamido)cyclohexane,<sup>33</sup> which has a hydrogen bonding network with exactly the same connectivity as compound **1**.<sup>11</sup>



**Figure 6.7** TEM pictures of a gel of **7** in ethyl acetate (Pt shadowing). A) Several fibers are visible that are twined to form a rope, bar is 114 nm. B) Fibers with knobs at their ends, bar is 430 nm. C) Helically wound fiber. The winding gets tighter at the end of the fiber, to the extent that a helical structure can no longer be detected, bar is 110 nm.

Comparing the aggregation forms of the C<sup>6</sup> substituted gluconamides discussed above, we may conclude that the size and the shape of the substituent is important for the transfer of chirality from the molecular level to the supramolecular level. The shape of the substituent seems to be more important than its size. The hydrogen bonds of the gluconamide moiety normally force the molecules to adopt a chiral packing.<sup>2,5,7,10,11</sup> Gluconamides with C<sup>6</sup>-substituents can still have these hydrogen bonding interactions, but when substituents are aromatic groups,  $\pi$ - $\pi$  interactions may partly overrule the hydrogen bonding scheme. As a result the chirality of the assembly is lost. The imidazole group in compound **4** is probably too small, to display strong  $\pi$ - $\pi$  interactions and the carbohydrate moiety can still direct the aggregation pattern. Chiral

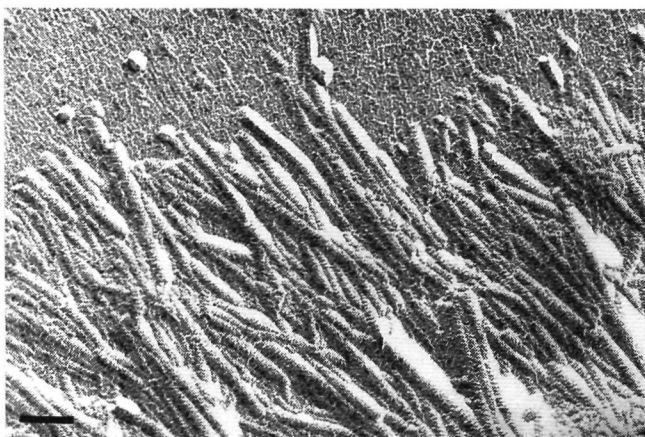
suprastructures, therefore, are still formed with this compound. Aliphatic substituents cannot  $\pi$ - $\pi$  stack and again the carbohydrate moieties regulate the aggregation process, resulting in chiral assemblies.

### 6.3.3.3 Gluconamides without C<sup>6</sup> substituents

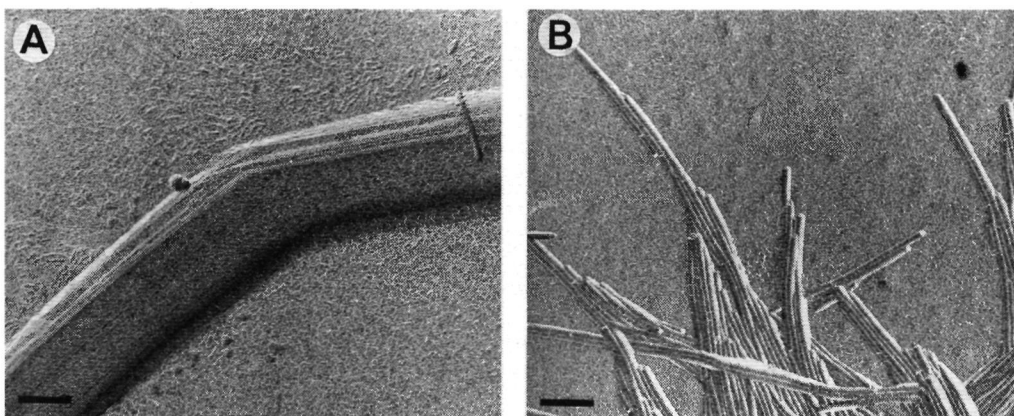
Gluconamide **1** forms gels in water, 1,2-xylene, and in pyridine. The gel in pyridine is only stable at temperatures below 10 °C. The type of aggregates displayed by **1** is solvent dependent: in water helices are generated,<sup>2</sup> in 1,2-xylene scrolls,<sup>5a</sup> and in pyridine fibers (see Figure 6.8). The fibers have an average diameter of 31 nm. We can not explain why in pyridine the chirality is not expressed in the aggregate structure.

#### C<sup>2</sup> methoxy derivative **12**

In water **12** crystallizes within 15 minutes. When a freshly prepared solution, however, is dried, stacked layers are observed by TEM (see Figure 6.9A). A highly viscous gel is formed in benzene, which shows fiber-like structures under the electron microscope (see Figure 6.9B).



**Figure 6.8** TEM picture of rods formed in gels of **1** in pyridine (Pt shadowing), bar is 100 nm.



**Figure 6.9** TEM pictures of aggregates formed by **12** in different solvents, Pt shadowing. A) Multilayers formed in water, bar is 170 nm. B) Whisker-type of fibers formed in a gel in benzene, bar is 110 nm.

These fibers have an average diameter of 22 nm and are similar to those formed by **2a** in organic solvents, *e.g.* ethyl acetate. The above mentioned fibers and bilayers do not show any chirality.

The gluconamides with methylene protected OH groups and substituents on C<sup>6</sup> (**8-11**) and the gluconamides with a C<sup>2</sup> methoxy group and a C<sup>6</sup> substituent (**13** and **14**) did not form gels or turbid mixtures in organic solvents and were therefore not investigated with electron microscopy.

Compounds with a C<sup>6</sup> substituent (**2a**, **4**, and **5**) yield aggregates of which the structure is not controlled by the type of solvent. Compounds without a C<sup>6</sup> substituent (**1** and **12**) form solvent-dependent-type of aggregates. A possible explanation for this behavior is that in the latter case solvent molecules are incorporated in the aggregates, whereas in the former case the aggregates are solvent free.

The ordering present in the gels can also be observed by a polarization microscope as shown in Figure 6.10 for the gel from **2a** in chloroform. It is clear from this Figure that the gel of **2a** does not contain small crystalline parts in a matrix of non-ordered solvent molecules, but is ordered throughout the sample. The magnification of the light microscope was too low to distinguish the fibers that were observed by TEM.



**Figure 6.10** Microscopic picture of a gel prepared from **2a** in chloroform. The gel was placed between crossed polarizing filters.

#### 6.3.4 NMR study

The type of chiral superstructures formed by our gluconamides seems to be determined by the steric constraints of the carbohydrate head groups and the possibility of these head groups to form extended hydrogen bonding patterns.<sup>12,34</sup> Even within the set of compounds described in the previous sections, which are all derived from glucose (with the exceptions **16** and **17**), several differences in gelation behavior are observed. On the basis of electron microscopy data, we may

conclude that the packing in the aggregates of the C<sup>6</sup> substituted gluconamides is still directed by the hydrogen bonding schemes of the carbohydrate moieties. Large aromatic substituents, however, interfere with these H-bonding schemes and as a result no chiral aggregates are formed in these cases. Although the gels to some extent may have a crystalline character they are still considered to be lyotropic systems in which the vast majority of the material consists of solvent molecules (gelator concentration is 1 % w/v). In order to investigate what the differences in head group conformation of the gluconamide are, we decided to perform a NMR study of the gels. Preliminary experiments were carried out with compound **2a**. Unfortunately, the gels of this compound in both chloroform and methanol were too unstable under the conditions of high spinning rates required for the measurements, and consequently we were unable to perform solid state <sup>13</sup>C-NMR.<sup>12,27,35</sup> In solution, the conformation of the carbohydrate head groups can be different from the conformations in the crystalline or gel state aggregate structures. Nevertheless, we decided to compare the solution <sup>1</sup>H-NMR spectra of the C<sup>6</sup> substituted derivatives of gluconamide **1** (*viz* **2-5**, **7**) with the spectrum of **1** itself. For comparison the C<sup>2</sup> methoxy derivatives **12** and **14** and the methylene protected derivative **11** were also measured. To simplify the coupling patterns, the hydrogen atoms of the hydroxyl groups were exchanged with deuterium through addition of D<sub>2</sub>O.

**Table 6.6** <sup>1</sup>H-NMR data of gluconamides derivatives <sup>a</sup>

Compound									
	<b>1</b>	<b>2a</b>	<b>3</b>	<b>4<sup>b</sup></b>	<b>5</b>	<b>7</b>	<b>12</b>	<b>14</b>	<b>11</b>
2-H	3 956	2 994	4 021	(4 176)	3 952	3 945	3 609	3 607	4 159
3-H	3 877	3 900	3 957	(4 067)	3 844	3 831	3 761	3 758	4 279
4-H	3 440	3 582	3 606	(3 492)	3 456	3 448	3 264	3 285	3 740
5-H	3 462	3 819	3 860	(3 875)	3 669	3 657	3 426	3 641	4 342
6-H	3 558	4 420	4 467	(4 326)	4 177	4 158	3 548	4 171	4 563
6'-H	3.348	4 205	4 265	(4.063)	3 909	3 916	3 317	3 880	4 271
<i>J</i> <sub>2,3</sub>	3 60	4 20	4 00	(3.65)	3 90	4.10	5 95	6 10	1 50
<i>J</i> <sub>3,4</sub>	2 30	2 50	2 40	(2 35)	2 70	2 55	2 40	2 15	--
<i>J</i> <sub>4,5</sub>	8 50	8 50	8 45	(8 50)	8 20	8 35	8 30	8 55	--
<i>J</i> <sub>5,6</sub>	2 80	2 55	2 35	(2 45)	2 65	2 55	3 25	2 40	6 25
<i>J</i> <sub>5,6</sub>	5 50	6 15	6 35	(7 10)	6 85	6 35	6 20	6 75	7 05
<i>J</i> <sub>6,6</sub>	11 20	11 35	11 25	(14 20)	11 30	11 30	11 05	11 35	11 85

<sup>a</sup> Spectra were recorded in DMSO-d<sub>6</sub> after addition of a small amount of D<sub>2</sub>O. Chemical shifts and *J*-couplings were checked by simulation with GenMR.

<sup>b</sup> Solvent CD<sub>3</sub>OD instead of DMSO-d<sub>6</sub>.

The proton signals and *J*-couplings of **2-5**, **7**, **11**, **12**, and **14** are listed in Table 6.6. Examination of the *J* values shows, that for all compounds *J*<sub>3,4</sub> is between 2.1-2.7 Hz and *J*<sub>4,5</sub> in the range of 8.2-8.6 Hz. In the literature,<sup>12,23</sup> the *J*<sub>3,4</sub> and *J*<sub>4,5</sub> coupling constants for **1** in DMSO-

$d_6$  have been reported to be 3.40 Hz and 3.00 Hz, respectively. These coupling constants are based on NMR simulations using the RACCOON simulation program.<sup>12,23</sup> From our measurements with compound **1** in DMSO- $d_6$  we calculated different  $J$ -couplings, viz  $J_{3,4} = 2.30$  Hz and  $J_{4,5} = 8.50$  Hz using GeNMR simulation program.<sup>36</sup> The  $J$  values for **1** obtained in our measurements are more in line with those found for the ester and imidazole derivatives (**2-5, 7**). According to the literature<sup>12</sup> gluconamide **1** in DMSO displays a sharp bend at C<sup>4</sup> giving the molecule a so-called  ${}_4G^+$  conformation. This proposed conformation is based on calculated <sup>1</sup>H-NMR data.<sup>12</sup> According to our measurements and calculations based on  $J_{3,4}$  and  $J_{4,5}$ , a significant difference in the percentage of *anti*<sup>37</sup> conformation (explanation see below) for the H-C<sup>4</sup>-C<sup>5</sup>-H bond can be seen, resulting in only a very small bend at C<sup>4</sup>, which is in contrast with the above mentioned  ${}_4G^+$  conformation model suggested in the literature.<sup>12</sup> We also note that the  $J_{2,3}$  (3.60 Hz) value is slightly smaller than the value previously reported for **1**  $J_{2,3}$  4.50 Hz,<sup>12</sup> but this may be due to an effect of the added D<sub>2</sub>O. Since the solvent can have a tremendous influence on the conformation of the gluconamide we also measured the <sup>1</sup>H-NMR spectra of **2a**, **5**, and **12**, in CD<sub>3</sub>OD. Except for the  $J_{2,3}$  coupling constant we were unable to find any significant difference in  $J$ -couplings between the samples measured in DMSO- $d_6$  (with a small amount of D<sub>2</sub>O) and in CD<sub>3</sub>OD, see Table 6.7 The gluconamide group is a flexible moiety and therefore not amenable to a strict determination of the dihedral angles between adjacent hydrogen atoms using the modified Karplus relation described by Altona.<sup>38</sup> As, however, there is a difference in vicinal  $J$  coupling when the hydrogen atoms are in the *syn* or in the *anti* position, it is possible to make a rough estimate of the percentages of conformations present in the *anti* position ( $P_{anti}$ ) in the molecules, using equation (1).<sup>39</sup>

**Table 6.7** Comparison of the  $J$  coupling constants of the carbohydrate moieties of gluconamide derivatives in different solvents

	<b>2a</b>			<b>6</b>			<b>12</b>		
	DMSO- $d_6$	CD <sub>3</sub> OD	$\Delta^a$	DMSO- $d_6$	CD <sub>3</sub> OD	$\Delta^a$	DMSO- $d_6$	CD <sub>3</sub> OD	$\Delta^a$
$J_{2,3}$	4.20	3.70	0.50	3.90	3.20	0.70	5.95	5.55	0.40
$J_{3,4}$	2.50	2.40	0.10	2.70	2.40	0.30	2.40	2.40	0.00
$J_{4,5}$	8.50	8.40	0.10	8.20	8.40	0.20	8.30	8.20	0.10
$J_{5,6}$	2.55	2.40	0.15	2.65	2.50	0.15	3.25	3.25	0.00
$J_{5,6}$	6.15	5.85	0.30	6.85	6.30	0.55	6.20	5.95	0.25
$J_{6,6}$	11.35	11.55	-0.20	11.30	11.35	-0.05	11.05	11.10	-0.05

<sup>a</sup> $\Delta = J$  in DMSO- $d_6$  -  $J$  in CD<sub>3</sub>OD

$$\text{anti} = \frac{J_{\text{obs.}} - (J_{60^\circ} + J_{-60^\circ})/2}{J_{\text{anti}} - (J_{60^\circ} + J_{-60^\circ})/2} \quad (1)$$

**Table 6.8** Observed vicinal  $J$  couplings in DMSO- $d_6$ , and calculated  $J$  couplings according to the modified Karplus relation <sup>a</sup>

Substituent		$J_{\text{Obs}}$ (Hz)	60°	180°	-60°	$P_{\text{anti}}$ (%)	
1	None	$J_{2-3}$	3 60	0 54	9 57	4 02	18
		$J_{3-4}$	2 30	4 03	9 72	0 54	0
		$J_{4-5}$	8 50	2 27	9 57	2.29	85
		$J_{5-6}$	2 80	0 90	10 68	5 02	0
		$J_{5-6}$	5 50	3 07	10 68	2 84	33
2a	C <sup>6</sup> Benzoyl	$J_{2-3}$	4 20	0 54	9 57	4 02	26
		$J_{3-4}$	2.50	4 03	9 72	0 54	3
		$J_{4-5}$	8 50	2 27	9 58	2 29	85
		$J_{5-6}$	2 55	0 90	10 68	5 02	0
		$J_{5-6}$	6 15	3 07	10 68	2 84	41
4	C <sup>6</sup> Imidazolyl	$J_{2-3}$	(3 65) <sup>b</sup>	0 54	9 57	4 02	19
		$J_{3-4}$	(2 35) <sup>b</sup>	4 03	9 72	0 54	1
		$J_{4-5}$	(8 50) <sup>b</sup>	2 24	9 42	2 30	87
		$J_{5-6}$	(2 45) <sup>b</sup>	1 58	10 96	4 53	0
		$J_{5-6}$	(7 10) <sup>b</sup>	2 59	10 96	3 52	51
5	C <sup>6</sup> Acetyl	$J_{2-3}$	3 90	0 54	9 57	4 02	22
		$J_{3-4}$	2 70	4 03	9 72	0 54	6
		$J_{4-5}$	8 20	2 27	9 58	2 29	81
		$J_{5-6}$	2 65	0 90	10 68	5 02	0
		$J_{5-6}$	6 85	3 07	10 68	2 84	50
12	C <sup>2</sup> Methoxy	$J_{2-3}$	5 95	0 67	9 66	3 96	49
		$J_{3-4}$	2 40	4 03	9 72	0 54	2
		$J_{4-5}$	8 30	2 27	9 57	2 29	83
		$J_{5-6}$	3 25	0 90	10 68	5 02	4
		$J_{5-6}$	6 20	3 07	10 68	2 84	42

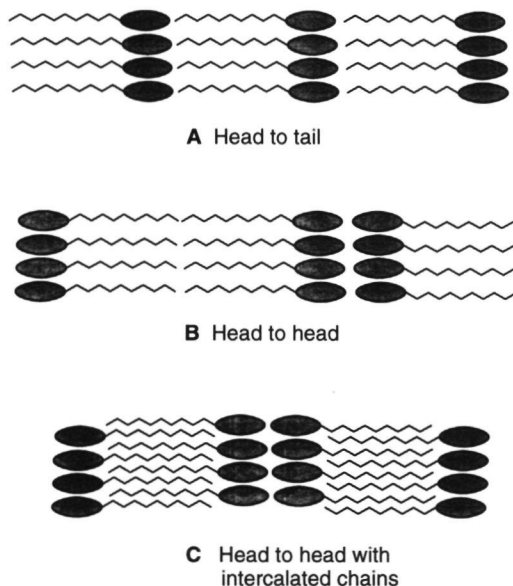
<sup>a</sup> See Ref 38. The percentage anti conformation ( $P_{\text{anti}}$ ) was calculated with equation (1)<sup>b</sup> Spectrum recorded in CD<sub>3</sub>OD

The results of these calculations are presented in Table 6.8. It is clear from Table 6.8 that substitution on C<sup>6</sup> (compare **1**, **2a**, **4**, and **5**, see Table 6.8) does not lead to large deviations in the overall conformation of the glucon unit. This confirms the hypothesis that, despite C<sup>6</sup> substitution, the conformation of the carbohydrate part of the head group is only slightly affected. Hence, packing of the gluconamides in the aggregates must in principle be similar for the unsubstituted (**1**) and the C<sup>6</sup>-substituted compounds. In the case of the larger aromatic

substituents (**2a** and **3**), however, additional  $\pi$ - $\pi$  stacking interactions may play a disturbing role, as discussed above. The C<sup>2</sup> methoxy derivative **12** shows an increase in the percentage of *anti* conformation around C<sup>2</sup>-C<sup>3</sup>. This means that a large bend is present in the carbohydrate head group at C<sup>2</sup> (the larger P<sub>anti</sub>, the bigger the bend), which reduces the overall length of the molecule. This decrease in length is also observed in powder diffraction spectra (see below). The major *d* spacing for **12** is 1.8 Å smaller than the spacing for **1**.<sup>40</sup> The aggregate structure of **12** appeared to be solvent dependent (*vide infra*). A possible explanation is that solvent molecules are incorporated in the superstructures. This is feasible because the packing of the amphiphiles is relatively loose due to the large bend at C<sup>2</sup>.

### 6.3.5 X-ray powder diffraction

It is of great importance to know how the molecules are packed in the suprastructures which form the gel. X-ray powder diffraction can help resolve a number of questions, *e.g.* whether the molecules are in layered structures or not. Using X-ray, it is possible to distinguish between a head to tail, a head to head packing with or without intercalated aliphatic tails (Figure 6.11). We expected our molecules to display predominantly head to tail packing, since in most cases the hydrophilic glucose unit is situated in between two hydrophobic groups. This feature is one of the reasons why **1** packs in a head to tail arrangement.<sup>41</sup>



**Figure 6.11** Several packing arrangements of amphiphilic gluconamides.



The crystal structure of compound **1**,<sup>11</sup> has revealed that this molecule has a V-shaped conformation with a torsion angle of  $112^\circ$  around the  $C^1$ - $C^2$  bond. This V-shaped structure is due to an intramolecular H-bond between  $C^2$ -OH and the carbonyl function of the amide group. For the molecules synthesized by us (**2-7**), we expect similar V-shaped conformations. In order to predict the lengths of our gluconamides, we used the crystal structure coordinates of molecule **1**<sup>11</sup> as a basis for the overall geometry of the molecules and substituted the OH on  $C^6$  by the respective ester or imidazole group. It should be noted, however, that the overall length of the molecule changes considerably when the  $C^6(H^6)$ - $O^6(C=O)$  torsion angle is varied since the substituents on  $C^6$  in our compounds are far more bulky than the OH group in **1**. When it is assumed that this torsion angle is similar to the one present in the crystal structure of **1**, the overall length is probably calculated incorrectly. In the crystal structure of **1**, the  $C^6$ -OH is involved in a hydrogen bond with the  $C^4$ -OH group of an adjacent molecule, which is not very likely in the  $C^6$  substituted gluconamides. We solved this problem by varying the  $C^6(H^6)$ - $O^6(C=O)$  torsion angles and calculated the lengths of the molecules. The maximum values obtained after these variations were taken as the predicted *d*-value. They are presented in column 3 of Table 6.9. These calculations were carried out using the molecular dynamics program Quanta-Charm.

Fuhrhop and coworkers<sup>23</sup> have shown that **1** can adopt more than one rigid conformation, depending on the preparation of the sample. Lyophilized **1** displays a head to head packing of the molecules ( $d=36$  Å).<sup>23</sup> If the sample is crystallized from methanol a *d*-spacing of 17.9 Å is observed (head to tail packing),<sup>23</sup> which is in line with the crystal structure of **1**.<sup>11</sup> In our work we found that organogels of **1** in pyridine<sup>42</sup> and in 1,2-xylene have *d*-spacings of 36.2 Å and 35.9 Å, respectively (see Table 6.9). Our powder diffraction studies on lyophilized **1** revealed a head to tail packing<sup>43</sup> of the molecules (*d*-spacing 16.1 Å) while the organogels of **1** showed a head to head packing (see Table 6.9 entries 1-3). The packing behavior of gluconamide **1** is therefore subject to confusion. We propose that the packing of **1** is solvent dependent, which was also concluded from our EM studies.

It is a remarkable fact that most of the gels prepared from gluconamides with substituents on  $C^6$  are packed in a head to tail manner (Table 6.9). Galactonamide derivatives behaved similarly: the lyophilized aqueous gel of the non-substituted derivative **16** showed a head to head packing, whereas the benzoyl substituted compound **17** displayed a head to tail packing.

The pyridyl ester **3**, and the imidazole gluconamide derivative **4** are packed in head to head geometries. These head to head packings may be a result of the presence of water molecules, which link the nitrogen atoms of the pyridyl or imidazolyl groups in two successive layers. We have observed such intercalating water molecules in the crystal structure of compound **11**.<sup>44</sup> The imidazole compound **4** probably forms bilayers in which the alkyl chains are interdigitized (Figure 6.11C). This can be concluded from the measured periodicity, which is larger than the predicted thickness of a monolayer but smaller than the thickness of a bilayer (Table 6.9). Bilayers with interdigitized alkyl chains were also found to be present in the crystal structure of the imidazole gluconamide **11** (see Chapter 3).

**Table 6.9** d-Spacings for gluconamide derivatives gelled in organic solvents.<sup>a</sup>

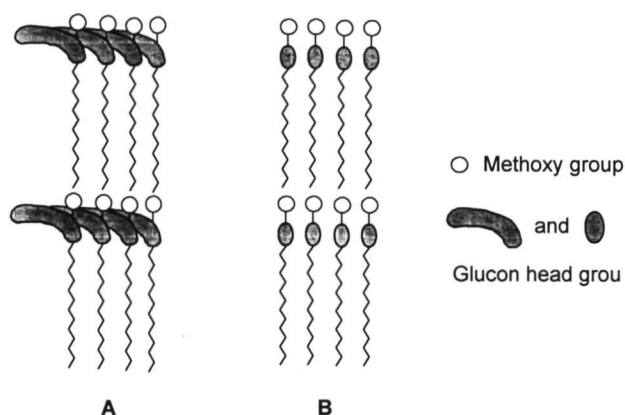
Compound	Substituent	Predicted monolayer thickness (Å)	Measured periodicity (Å)
<b>1</b>	None	17.9	16.1 <sup>b</sup>
<b>1</b> (pyridine)	None	17.9	36.2
<b>1</b> (1,2-xylene)	None	17.9	35.9
<b>2a</b> (ethanol)	C <sup>6</sup> Benzoyl ester	24.7	(24.3) <sup>c</sup>
<b>2a</b> (chloroform)	C <sup>6</sup> Benzoyl ester	24.7	23.3
<b>2a</b> (o-xylene)	C <sup>6</sup> Benzoyl ester	24.7	24.4
<b>2b</b>	C <sup>6</sup> Benzoyl ester	34.9	31.6
<b>3</b>	C <sup>6</sup> (3-Pyridyl ester)	23.0	43.2
<b>4</b>	C <sup>6</sup> Imidazolyl	21.1	26.3
<b>5</b>	C <sup>6</sup> Acetyl ester	21.8	21.3
<b>6</b>	C <sup>6</sup> Octyl ester	29.4	27.5
<b>7</b>	C <sup>6</sup> Cyclohexyl ester	25.1	24.0
<b>12</b>	C <sup>2</sup> Methoxy	17.9	16.0
<b>(16)</b>	None	37.0 <sup>d</sup>	37.2 <sup>b</sup>
<b>(17)</b>	C <sup>6</sup> Benzoyl	25.3	23.9

<sup>a</sup> Predicted values were calculated using the crystal structure of **1** in combination with the Quanta-Charm program (see text). The measured values were obtained from powder diffraction measurements (SAXS).

<sup>b</sup> Lyophilized from gel in water.

<sup>c</sup> Recrystallized from EtOH.

<sup>d</sup> Value as obtained from literature (see Ref. 12).



**Figure 6.12** Shoulder to tail packing as proposed for the C<sup>2</sup> methoxy gluconamide **12**. A and B are different projections in which the layers are rotated 90°.

The periodicity measured for the C<sup>2</sup>-methoxy gluconamide **12** suggests that the molecules of this compound are arranged in a head to tail packing (Table 6.9, entry 13). From the NMR study we know however, that a large bend is present in the molecule at C<sup>2</sup>, which will affect the packing. We believe therefore that molecules of **12** are packed like spoons in a box and that the methyl groups of the methoxy substituents are touching the tails of nearby layers (see Figure 6.12). This packing is more likely than a packing in which the C<sup>6</sup> ends of the head groups touch the termini of the alkyl chains. We propose the name “shoulder to tail” packing for this type of arrangement of the molecules.

### 6.3.6 IR experiments

The observation that the methylene-protected gluconamides **8-11** do not form gels (Section 6.3.1) suggests that an intermolecular hydrogen bonding network is necessary for gel formation. The possible existence of such a network in gels was investigated by FT-IR spectroscopy. The wavenumbers of the hydroxyl functions, the amide groups, and the ester groups of compounds **1**, **2a**, **4** and **12** in the gel state were compared to those in solution and in the solid state (crystalline compound or powder). The results are compiled in Tables 6.10 - 6.12.

The  $\nu(\text{O-H})$  peaks of compounds **2a** and **12** in the gel state were relatively sharp and even sharper than those in the solid samples (see Table 6.10), whereas the  $\nu(\text{O-H})$  peaks of **1** and **4** were relatively broad, resembling the solution spectra. This indicates that the H-bonding network in the case of compounds with a head to tail packing, **2a** and **12**, is more defined in the gels than in the solid state. There appears to be no well-defined H-bonding network in gels of compounds with a head to head packing (**1** and **4**).

**Table 6.10** Wavenumbers cm<sup>-1</sup> for the hydroxyl groups of gluconamide derivatives in the solid state (KBr) and gel state

KBr					Gel			
<b>1</b>	3532	3389	3358	3314	3508 <sup>a</sup>	3327 (broad) <sup>a</sup>		
<b>2a</b>	3521	3446	3368	3309	3512 <sup>b</sup>	3444 <sup>b</sup>	3358 <sup>b</sup>	3246 <sup>b</sup>
<b>4</b>	3500	3424	3366	-----	----- <sup>b</sup>	3375 <sup>b</sup>	3323 <sup>b</sup>	----- <sup>b</sup>
<b>12</b>	-----	3416	3348	3248	----- <sup>b</sup>	3408 <sup>b</sup>	3341 <sup>b</sup>	3282 <sup>b</sup>

<sup>a</sup> Gel in 1,2-xylene

<sup>b</sup> Gel in chloroform

The amide peaks in the spectra measured in solution were almost identical for all compounds (see Table 6.11). This was expected for the C<sup>6</sup> substituted compounds **2a** (benzoate) and **4** (imidazole), but not for compound **12** which has an amide function which is located next to a bulky substituent, viz. the methoxy group on C<sup>2</sup>. This means that differences in absorption or frequency between the solution and the solid or gel states can be attributed to differences in hydrogen bonding patterns.

The amide I band of **1** has been shifted to a higher wavenumber when going from the solid (crystalline) state to the gel state (1,2-xylene), whereas for the benzoate **2a** and the methoxy

derivative **12** this band is in a similar position for the gel and the solid states (see Table 6.11). This result can be explained in terms of packing arrangements. According to powder diffraction, **1** has in the solid state a head to tail packing whereas in the gel-state a head to head bilayer structure is present. This difference in packing is also evident from the IR data: in the bilayer geometry the (amide) carbonyl bond is stronger (probably due to a weaker hydrogen bond) than in the monolayer geometry. The packing for **2a** and **12** in the gel and solid states are presumably similar, *i.e.* head to tail packing, which results in similar wavenumbers for the amide I bands (Table 6.11). In contrast, the amide I band of the imidazole compound **4** shows a shift towards a lower value when going from the solid state to the gel state. This suggests that the amide carbonyl group is involved in a stronger hydrogen bond in the gel than in the solid state. The powder diffraction spectrum of **4** indicated a head to head packing in the gel with interdigitized alkyl chains. The crystal structure of the comparable imidazole gluconamide **11** (containing methylene protection groups) also revealed a head to head packing with interdigitized alkyl chains (see Chapter 3). It should be noted that these crystals were obtained from aqueous solutions which may have resulted in a different packing. It is possible that compound **4** still has a head to head packing with interdigitized alkyl chains in the solid state, but that due to an unfavorable position of the amide functions no intermolecular amide hydrogen bonds can be formed. This was confirmed by comparing the peaks of the amide II vibrations (N-H swing), which showed a lower wavenumber in the solid state than in the gel state, suggesting a weaker hydrogen bond in the former case (see below).

The wavenumber of the amide II absorption of **1** is similar in solution and in the solid state, but higher in the gel state, which indicates H-bond formation. The value for the gel is the same as that reported<sup>12</sup> for bilayer packing (in lyophilized fibers). The similarity between solid state and solution is somewhat surprising as the crystal structure shows the presence of a bifurcated intermolecular hydrogen bond which is expected to be broken in solution due to isotropic disordering. Our data suggest that the NH group is not involved in a hydrogen bond in the crystalline state but only in the gel state.

**Table 6.11** IR absorptions values (amide I/amide II vibrations) of gluconamide gelators in the solid state, gel state and in isotropic solution

	KBr pellet	Gel <sup>a</sup>	Packing in the gel	Solution
<b>1</b>	1646 / 1528	1654 / 1545	Bilayer (head to head)	1669 / 1527
<b>2a</b>	1631 / 1552	1633 / 1544	Monolayer (head to tail)	1678 / 1531
<b>4</b>	1646 / 1541	1635 / 1550 <sup>b</sup>	Bilayer (intercalated)	1674 / 1532
<b>12</b>	1656 / 1564	1655 / 1564	Monolayer (shoulder to tail)	1676 / 1530

<sup>a</sup> Gel in 1,2-xylene

<sup>b</sup> Gel in chloroform

The value of the amide II band for **2a** in the gel state is lower than that in the crystalline state but still considerably higher than that for **2a** in solution. This suggests that the N-H group in

the gel state is involved in a weaker H bond than in the solid state, while the strengths of the H bonds to the carbonyl group in the gel and the solid state are the same (see above). It is possible that the carbonyl groups in the gel state and the solid state do not form H-bonds with the amide N-H functions. Instead, one of the hydroxyl groups of an adjacent molecule may function as a hydrogen bond donor to the amide carbonyl group. Unfortunately, we do not have further support for this hypothesis.

The wavenumbers of the amide I and II bands in compound **12** (C<sup>2</sup> methoxy) are similar for the gel state and the solid state, indicating a related packing. Powder diffraction and <sup>1</sup>H-NMR suggested that the molecules are in an unusual “head to shoulder” monolayer packing. However, the amide I wavenumbers are more comparable to those of a bilayer arrangement (cf. Table 6.11, compound **1** in the gel state and **1** in the solid state). Remarkable is the large difference in wavenumber of the amide II absorption band of **12** when this band is compared with that of **1** in the solid state and that of **2a** in the gelated state, while all these compounds are packed in a monolayered arrangement. The wavenumbers of the amide II band in solution are similar for all these compounds, which means that the differences have to be induced by the different orderings. The strong bend causing the unusual head to shoulder packing of **12** may prohibit an ordering of the amide functions as observed for **2a**. The packing is less tight than the head to head packing of **1** in the gel state.

Surprisingly, the IR frequencies of the gluconamides in the gel state depend on the type of solvent in which the gel is made. For instance, in the case of **2a** the difference in wavenumbers of the amide I bands of the gel in chloroform and in toluene is substantial (see Table 6.12), although the suprastructures formed from **2a** in these solvents appear to be the same by TEM. The ester carbonyl vibration of **2a** showed a splitting in chloroform, which is absent in toluene suggesting that in the former gel more than one packing arrangement of the gluconamides is present. In one of the packing geometries, the ester is in a non H-bonded arrangement, because the value of one of the wavenumbers is similar to that in solution. The splitting of the ester vibrations is also observed in the solid state, which suggests that the fibers in the gel have a similar packing as in the solid state.<sup>26</sup>

**Table 6.12** Selected IR absorptions from gels of **2a** in different solvents, of **2a** in solution and of **2a** in the solid state

Solvent	Ester carbonyl	Amide I / II
chloroform <sup>a</sup>	1727 / 1702	1626 / 1548
toluene <sup>a</sup>	1717	1643 / 1548
1,2-xylene <sup>a</sup>	1721 / 1703	1633 / 1544
Solution <sup>b</sup>	1722	1678 / 1531
Solid state <sup>c</sup>	1722 / 1712	1631 / 1552

<sup>a</sup> Gels

<sup>b</sup> Dioxane

<sup>c</sup> KBr technique

## 6.4 Discussion

The formation of gels from our gluconamides is a fascinating phenomenon, especially if one realizes that this process occurs at concentrations as low as 1 % w/v. Molecular dynamics calculations using the Quanta Charm program reveal that only 24 chloroform molecules can make a close contact with **2a** forming a 4 Å shell around the gelator. In a 1 % w/v gel of **2a** in chloroform, the ratio solvent/gelator molecules, however, is over 500. For some reason not all solvent molecules have to be in close contact with the gelator for gelating the solvent.<sup>45</sup>

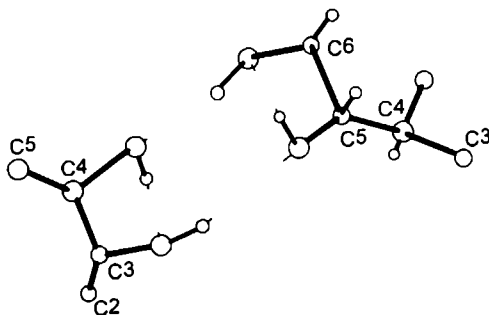
With exception of the n-octyl derivative **6**, all gel forming gluconamides form fibers with a high aspect ratio. These structures are found throughout the gel; however, the solvent molecules cannot be entrapped as glass is in the steel threads in security glass, because the meshes of the network for this kind of entrapping are too large. The observation that sometimes the same types of texture are formed in a variety of solvents, as shown for the benzoate derivative **2a**, suggests that the gelator molecules can exhibit really strong cohesive forces. In other cases, the textures are very dependent on the solvent as in the case of compound **1** which forms helical fibers in water,<sup>2</sup> multilayered sheets in 1,2-xylene,<sup>5</sup> and rod-like structures in pyridine. It has been reported that the n-octyl aldonamides mannuronamide, gulonamide and talonamide do not produce any chiral structures in gels in 1,2-xylene which has been ascribed to a lack of solvation of the carbohydrate groups.<sup>5a</sup> The carbohydrate part of the benzoyl derivative **2a** is probably also shielded from the solvent, since in the gels in chloroform, ethyl acetate, ethanol, and 1,2-xylene no helical but whisker-type fibers are formed. These whisker-type fibers have also been described in the literature.<sup>46</sup>

The influence of the substituent on the aggregation behavior of the gluconamide is substantial. Aromatic substituents on carbon atom C<sup>6</sup> can exhibit  $\pi$ - $\pi$  stacking which may help assemble the molecules into a supramolecular structure.  $\pi$ - $\pi$  Stacking, however, is not the only driving force since aggregates of **2a** are also formed in aromatic solvents like benzene, toluene, and 1,2-xylene. The benzoyl and pyridyl carboxylate groups are relatively large substituents which probably disturb the hydrogen bonding network of the gluconamide and, as a result, prevent the process of chiral recognition between the chiral head groups of the molecules. For **2a** and **3** therefore no chiral superstructures are obtained. The imidazole groups are less bulky than the afore mentioned groups which might explain why for this substituent the molecular chirality is expressed at the supramolecular level. The gluconamides with bulky cyclohexyl and n-octyl substituents, however, can still form helical twisted aggregates, suggesting that the bulkiness is not the only factor determining the formation of chiral superstructures.

DSC measurements showed that the type of solvent has a larger effect on the  $\Delta H$  of gelation than the type of gelator. Although the types of aggregates that are formed are the same for each solvent, indicating that the cohesive forces that lead to the supramolecular structures are independent of the solvent, the heat transfer and the gelation temperature are dependent on the solvent and not on the gelator. The energy transfer measured is therefore a gain in entropy and not a gain in enthalpy. We may conclude that the formation of organogels is a process which is determined by the entropy.

As shown in Section 6.3.6 IR experiments, in particular in the region of the OH stretching vibrations, can give valuable information on the packing of the gluconamide molecules in the gel state. This information cannot always be obtained from the amide vibrations. The differences in amide wavenumbers are relatively small for the various systems (Table 6.11) and the peaks do not sharpen-up going from the solution to the gel state. The trends in the shifts, however, can help clarify variations in the hydrogen bond patterns in the gel and solid state and can provide insight in the way the molecules are packed, e.g. head to head, head to tail or shoulder to tail.

From the crystal structure of **1**<sup>11</sup> it is known that this molecule forms (homo)dromic hydrogen bond cycles which involves the hydroxyl groups on the carbon atoms C<sup>6</sup>, C<sup>5</sup>, C<sup>4</sup>, and C<sup>3</sup>. These cycles extend within the layers (see Figure 6.13).

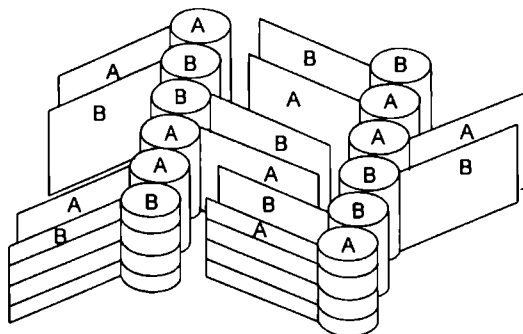


**Figure 6.13** A representation of a four-membered homodromic H-bond cycle found in the crystal structure of compound **1**<sup>11</sup>

After substitution with an ester or imidazole function, the compound lacks the hydroxyl on the C<sup>6</sup> atom and is no longer able to form such hydrogen bond cycles. In *N*,*n*-octyl-6-deoxy-D-gluconamide in which the terminal CH<sub>2</sub>OH is converted into a CH<sub>3</sub> group, a homodromic hydrogen bond cycle cannot be formed either. In this molecule on both ends hydrophobic CH<sub>3</sub> groups are present and this compound is therefore comparable to the organo-gel forming compounds **2-7**. The crystal structure of this deoxy gluconamide has recently been reported,<sup>47</sup> and the molecule appeared to crystallize in a packing that deviates from the normal head to head or head to tail arrangement. The asymmetric crystal consisted of molecules with two significantly different conformations (A,B). The head groups are packed in a AABBAABB fashion while the tails are packed in a ABABABAB manner (see Figure 6.14). Although a similar type of packing for our molecules was expected, we know from X-ray powder diffraction that **2-7** pack differently (see Table 6.9). Powder diffraction, <sup>1</sup>H-NMR and IR experiments have revealed that one of the gluconamides designed by us (**12**) exhibits another, yet unknown type of packing, viz. a shoulder to tail packing.

The head to tail packing of amphiphiles in aggregates is quite unusual.<sup>11,48</sup> Gluconamide **1** shows in the crystalline state a head to tail packing but this is changed into a head to head

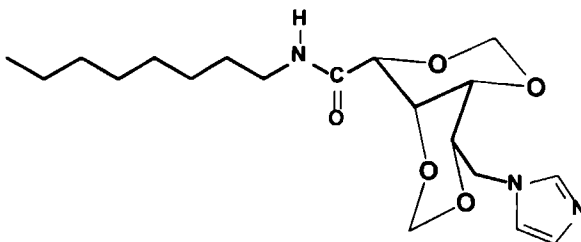
packing in the gel state (both in water and in organic solvents).<sup>12</sup> This kind of rearrangement is also known for the thermotropic liquid crystalline (L.C.) system since *N*,*n*-undecyl-D-gluconamide, also changes to a head to head packing in the smectic phase.<sup>49</sup>



**Figure 6.14** Crystal packing of 6-deoxy-N,n-alkyl-D-gluconamide

Upon entering the L.C. phase<sup>50</sup> the gluconamide molecules are proposed to retain a "core" of stacked alkyl chains rather than a network of hydrogen bonded carbohydrate moieties.<sup>51</sup> A study of the thermotropic L.C. properties of the C<sup>6</sup> substituted gluconamides would have been of interest to get more insight in the binding interactions of the head to tail packed molecules, since **2a**, **2b** and **5-7** retain their head to tail packing in the supramolecular aggregates. Unfortunately, **2a** and **5-7** exhibited no thermotropic L.C. behavior. For comparison, the longer chain derivative **2b** was also tested but this compound neither showed thermotropic L.C. behavior.

The compounds with the protected hydroxyl groups (**8-11**) do not show gelation behavior. This may be explained from the fact that the hydrogen bonding capacities of the sugar head groups are removed, and in principle also because there is no rotational freedom around the C<sup>2</sup>-C<sup>3</sup>, C<sup>3</sup>-C<sup>4</sup>, and C<sup>4</sup>-C<sup>5</sup> bonds. The head group is now more or less fixed in a so-called *cis*-decalin structure (see Figure 6.15).



**Figure 6.15** Schematic drawing of the *cis*-decaline structure in 6-deoxy-6-(1-imidazolyl)-2,4,3,5-dimethylene-N,n-octyl-D-gluconamide



Glycolic acid derivatives also contain a *cis*-decaline structure and are reported to form micelles upon dispersion in water.<sup>52</sup> These molecules do not give gels. Cholesterol derivatives, on the contrary, have a *trans*-decalin structure and exhibit strong gelation behavior.<sup>15</sup> This *trans*-decaline conformation is flatter than the *cis*-decalin conformation which will lead to a better packing of the molecules. This may explain why our compounds (**8** - **11**) do not and cholesterol derivatives do form organogels.

The gluconamides with a methoxy group on C<sup>2</sup>, and an additional group on C<sup>6</sup> (**13**, and **14**) were readily soluble in *e.g.* chloroform, ethyl acetate and 1,2-xylene, without any gelation upon cooling. The lack of formation of organogels by the compounds that have their C<sup>2</sup> hydroxyl group blocked is probably due to a strong bend in the head group caused by the methoxy group at C<sup>2</sup>. This strong bend probably prevents the tight packing needed for the aggregation in organic solvents. The exceptional behavior by compound **12** (C<sup>2</sup> methoxy and C<sup>6</sup> hydroxyl) which forms a gel is not yet fully understood.

### 6.5 Concluding remarks

We have shown that gluconamides can be easily modified to give compounds that form organogels with a high viscosity. Although *N*,*n*-octyl-D-gluconamide, which contains on one side a hydrophobic tail, forms an organogel in the high boiling solvent 1,2-xylene, the gluconamides generally have to contain a hydrophobic part on both sides of the carbohydrate framework to make them suitable as gelators in organic solvents with lower boiling points. In the organogels, the molecules are packed in a head-to-tail fashion. If there is the possibility to form inter-layer hydrogen bridges like in the case of *N*,*n*-octyl-D-gluconamide or *N*,*n*-octyl-D-gluconamide-6-(3-pyridyl)-carboxylate (in the latter case probably via an additional water molecule), the molecules are packed in a head-to-head fashion. It is not possible to alter this head to head packing by addition of equimolar quantities of hydrogen bond donors. The head-to-tail packing is probably favored by most compounds, because it allows the molecules to form *inter*-molecular *intra*-layer hydrogen bonds and in addition this packing allows van der Waals interactions between the hydrophobic layers of the C<sup>6</sup> substituent derivatives.

Some compounds are able to express their molecular chirality in the supramolecular structures while others are not. The gluconamides containing a large aromatic substituent on carbon atom C<sup>6</sup> yield aggregates that are not chiral, whereas the gluconamides with aliphatic substituents give chiral aggregates in all cases. The inability of the former compounds to generate chiral architectures is probably due to interfering  $\pi$ - $\pi$  stacking interactions by the substituents.

DSC experiments suggest that the formation of the gel is an entropy driven process. A different  $\Delta H$  upon gelating is measured for the same compound in different solvents, whereas different gelators in the same solvent show similar  $\Delta H$  values.

## 6.6 Literature

- <sup>1</sup> Jeffrey, G A , Wingert, L M *Liq Cryst* **1992**, *12*, 179-202
- <sup>2</sup> Pfannemüller, B , Welte, W *Chemistry Lipids Phys* **1985**, *37*, 227
- <sup>3</sup> Fuhrhop, J -H , Helfrich, W *Chem Rev* **1993**, *93*, 1565-1582
- <sup>4</sup> Hafkamp, R J H, Feiters, M C , Nolte, R J M *Angew Chem* **1994**, *106*, 1054, *Ibid Int Ed Engl* **1994**, *33*, 986
- <sup>5</sup> a) Fuhrhop, J -H , Schnieder, P , Boekema, E , Helfrich, W *J Am Chem Soc* **110**, **1988**, 2861-2867, b) Koning J Boettcher C , Winkler H , Zeitler E , Talmon Y , J -H Fuhrhop, *J Am Chem Soc* **1993**, *115* 693
- <sup>6</sup> Pfannemüller, B , Kuhn, I *Macromol Chem* **1988**, *189*, 2433
- <sup>7</sup> a) Taraval, F R , Pfannemüller, B *Macromol Chem* **1990**, *191*, 3097 b) J-H Fuhrhop, S Svenson, C Boettcher, E Rössler, H Vieth, *J Am Chem Soc* **1990** *112*, 4307
- <sup>8</sup> Fuhrhop, J -H, Koning, J Membranes and Molecular Assemblies The Synkinetic Approach, part of the series "Monographs in Supramolecular Chemistry", series ed Stoddart, J F , The Royal Society of Chemistry, Cambridge (UK) **1994**, pag IX
- <sup>9</sup> Fuhrhop, J -H , Schnieder, P , Rosenberg, J , Boekema, E *J Am Chem Soc* **1987**, *109*, 3387
- <sup>10</sup> Koning, J , Boettcher, C , Winkler, H , Zeitler, E , Talmon, Y , J -H Fuhrhop, *J Am Chem Soc* **1993**, *115*, 693
- <sup>11</sup> Zabel, V , Müller-Fahrnow, A , Hilgenfeld, R , Saenger, W , Pfannemüller, B Enkelmann, V Welte, W *Chemistry Phys Lipids* **1986**, *39*, 313
- <sup>12</sup> Svenson, S , Koning, J , Fuhrhop, J -H *J Phys Chem* **1994**, *98*, 1022
- <sup>13</sup> O'Brien, D F , Frankel, D A *J Am Chem Soc* **1994**, *116*, 10057
- <sup>14</sup> Scartazzini, R , Luisi P L *J Phys Chem* **1988**, *92*, 829-833
- <sup>15</sup> (a) Lin, Y -C , Weiss, R G *Macromol* **1987**, *20*, 414, (b) Lin, Y -C , Kacher, B , Weiss, R G *J Am Chem Soc* **1989**, *111*, 5542, (c) James, T D , Murata, K , Harada, T , Ueda, K , Shinkai, S *Chem Lett* **1994**, 273, (d) Murata, K , Aoki, M , Suzuki, T , Harada, T , Kawataba, H , Komori, T , Ohseto, F , Ueda, K , Shinkai, S *J Am Chem Soc* **1994**, *116*, 6664 and references cited therein
- <sup>16</sup> a) Hanabusa, K , Okui, K , Karaki, K , Koyama, T , Shirai, H *J Chem Soc Chem Commun* **1992**, 1371 b) Vries, de E J , Kellog, M *J Chem Soc Chem Commun* **1993**, 238 c) Hanabusa, K , Tange, J , Taguchi, Y , Koyama, T , Shirai, H *J Chem Soc Chem Commun* **1993**, 390 d) Takafuji, M , Ihara, H , Hirayama, C , Hachisako, H , Yamada, K *Liq Cryst I* **1995**, *18*, 97 and references cited therein
- <sup>17</sup> Hanabusa, K , Miki, T , Taguchi, Y , Koyama, T , Shirai, H *J Chem Soc , Chem Commun* **1993**, 1382
- <sup>18</sup> a) Aoki, M , Murata, K , Shinkai, S *Chem Lett* **1991**, 1715 b) Aoki, M , Nakashima, K , Kawataba, H , Tsutsui, S , Shinkai, S *J Chem Soc Perkin Trans 2* **1993**, 347
- <sup>19</sup> a) Twieg, R J , Russell, T P , Siemens, R , Rabolt, J F *Macromol* **1985**, *18*, 1361, b) Ishikawa, Y , Kuwahara, H , Kunitake, T *J Am Chem Soc* **1994**, *116*, 5579, in the latter publication aggregation is described instead of gelation
- <sup>20</sup> Lenk, T J , Siemens, R , Hallmark, V M , Miller, R D , Rabolt, J F *Macromol* **1991**, *24*, 1215
- <sup>21</sup> a) Brotin, T , Untermöhlen, R , Fages, F , Bouas-Laurant, H , Desvergne, J -P *J Chem Soc Chem Commun* **1991**, 416, b) Tata, M , John, V T , Waguespack, Y Y , McPherson, G L *J Phys Chem* **1994**, *98*, 3809
- <sup>22</sup> a) Israelachvili, J N , Marcelja, S , Horn, R G *Quart Rev Biophys* **1980**, *13*, 121 , b) Kunitake, T , Okhahata, Y Shimomura, M , Yasunami, S -I, Takarabe, K *J Am Chem Soc* **1981**, *103*, 5401

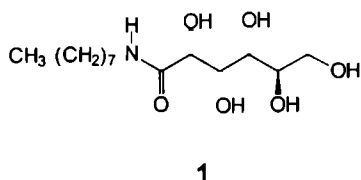
- <sup>23</sup> Svenson, S., Schäfer, A., Fuhrhop, J.-H. *J Chem Soc Perkin Trans 2* **1994**, 1023.
- <sup>24</sup> Menger, F.M., Littau, C.A. *J Am Chem Soc* **1993**, 115, 10083.
- <sup>25</sup> Fendler, J.H., *Membrane Mimetic Chemistry* New York, **1982**
- <sup>26</sup> Examples of crystal structures resolved are *N*,*n*-octyl-D-gluconamide, see Ref. 11; *N*,*n*-dodecyl-D-gluconamide see, Vollhardt, D., Gutberlet, T.; Emrich, G.; Fuhrhop, J.-H. *Langmuir* **1995**, 11, 2661, *N*-trideca-5,7-diyne-D-gluconamide see, André, C.; Luger, P., Fuhrhop, J.-H. *Carbohydr Res* **1994**, 230, 31
- <sup>27</sup> Fuhrhop, J.-H.; Fritsch, D. *Acc Chem Res* **1986**, 19, 130.
- <sup>28</sup> Precautions should be taken when dimethylsulfate is used, because this compound is known to be very toxic and carcinogenic
- <sup>29</sup> Takahashi, A., Sakai, M.; Kato, T. *Polym J* **1980**, 12, 335
- <sup>30</sup> Snyder, L.R. *J Chrom* **1974**, 92, 223.
- <sup>31</sup> Snyder, L.R. *J Chromatogr Sci* **1978**, 16, 223
- <sup>32</sup>  $T_{gel}$  was defined as the average between the onset and the peak values of the transition in the heating curve. The  $T_{gel}$  values determined from the DSC thermograms were similar to the  $T_{gel}$ 's determined by the glass ball method, deviations were obtained for the aromatic solvents
- <sup>33</sup> André, C., Luger, P., Nehmzow D., Fuhrhop, J.-H. *Carbohydrate Res* **1994**, 261, 1.
- <sup>34</sup> Fuhrhop, J.-H.; Schnieder, P.; Rosenberg, J.; Boekema, E. *J Am Chem Soc* **1987**, 109, 3387
- <sup>35</sup> Svenson, S., Kirste, B., Fuhrhop, J.-H. *J Am Chem Soc* **1994**, 116, 11969.
- <sup>36</sup> geNMR V 3.3 (1990), simulation package, Budzelaar, P.H.M.; IvorySoft®, Amsterdam, The Netherlands.
- <sup>37</sup> When the dihedral angle of two adjacent hydrogen atoms equals 180° the latter in an *anti* position, see Ref. 23
- <sup>38</sup> Haasnoot, C.A.C.; Leeuw, de F.A.A.M., Altona, C. *Tetrahedron* **1980**, 36, 2783
- <sup>39</sup> Hoffman, R.E.; Rutherford, T.J.; Mulloy, B.; Davies, D.B. *Magn Res Chem* **1990**, 28, 458
- <sup>40</sup> *d*-Spacing as obtained from the crystal structure, 17.9 Å, *d*-spacing from 12 was obtained from a rapidly dried benzene gel (see also Table 6.9)
- <sup>41</sup> The hydroxyl group on the C<sup>6</sup> is bend in such a way that the hydrophobic CH<sub>2</sub> group is in contact with the tail CH<sub>3</sub> of a molecule in a succeeding layer (see also Ref. 11).
- <sup>42</sup> The gel in pyridine is only formed at low temperatures <0°C and at concentration >10% w/v.
- <sup>43</sup> The gel was rapidly freeze dried in a vacuum desiccator over P<sub>2</sub>O<sub>5</sub> and under reduced pressure.
- <sup>44</sup> The crystal structure is described in Chapter 3.
- <sup>45</sup> Leloup, V.M., Colonna, P.; Ring, S.G. *Macromolecules* **1990**, 23, 862.
- <sup>46</sup> Fuhrhop, J.-H.; Boettcher, C. *J Am Chem Soc* **1990**, 112, 1768.
- <sup>47</sup> Herbst, R.; Steiner, T.; Pfannemüller, B., Saenger, W. *Carbohydrate Res* **1995**, 269, 29
- <sup>48</sup> Darbon, P.N.; Odon, Y.; Lacombe, J.M.; Dacoster, E., Pavia, A.A. *Acta Cryst* **1974**, C40, 1105
- <sup>49</sup> Jeffrey, G.A., Maluszynska, H. *Carbohydrate Res* **1990**, 207, 211.
- <sup>50</sup> Upon heating the rearrangement of the molecules changes head to tail on to head to head.
- <sup>51</sup> Doren, van H.A.; Geest, van der R.; Keuning, C.A.; Kellogg, R.M.; Wynberg, H. *Liq Cryst* **1989**, 5, 165
- <sup>52</sup> Guthrie, J.P.; Cullimore, P.A.; McDonald, R.S.; O'Leary, S. *Can J Chem* **1982**, 60, 747

# Chapter 7

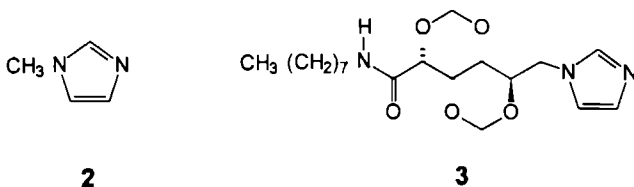
## Catalysis using supramolecular aggregates

### 7.1 Introduction

Enzymes are the best catalysts known. They combine highly selective substrate binding with supreme catalytic activity resulting in high turnover numbers. Very often enzymes are embedded in membranes, which are thought to fine-tune the properties of these biocatalysts. As part of our program aimed at the development of novel supramolecular catalytic systems<sup>1</sup> we decided to investigate the catalytic activity of copper(II) complexes as very simple enzyme mimics in chiral matrices.<sup>2</sup> From the studies described in the previous chapters, we have learned that gluconamide amphiphiles based on *N*,*n*-octyl-D-gluconamide (**1**) can form chiral aggregates in both water and organic solvents.



Our aim was to use these aggregates as matrices for catalysis. This kind of approach may be compared with traditional heterogenic catalysis, in which zeolites are used as the matrices. The advantage of using amphiphiles instead of *e.g.* zeolites is the possibility to introduce chirality in the matrix. In addition, by changing the chemical nature of the amphiphiles, the matrix can be fine tuned. Since **1** forms stable chiral aggregates in water, we investigated the possibility to use this compound as a support for catalytic centers. In our case, the catalytic center is a metal ion, and in order to place this metal ion in the aggregates, it has to be complexed with a (hydrophobic) ligand, *e.g.* methylimidazole (**2**) which is known to form complexes with copper(II) ions. Another approach is the use of aggregate-forming ligands with built-in metal complexing groups. In this option the metal complexes will certainly be located in the aggregates. Compound **3** has been proven to be amphiphilic and to form tunable supramolecular structures in water. It can therefore be used as a matrix for anchoring copper (II) centers in aqueous solutions.



Aziridines and epoxides both are versatile building blocks for the synthesis of a great variety of chemicals.<sup>3</sup> In our prospect, we decided to focus in our project on the metal catalyzed synthesis of these compounds. The first report of a metal catalyzed aziridination reaction involved a manganese porphyrin and was published in 1983.<sup>4</sup> In this catalytic system, however, a stoichiometric amount of porphyrin was needed. Some improvement was obtained by using an iron porphyrin.<sup>5</sup> Recently Evans<sup>6</sup> and Jacobsen<sup>7</sup> reported a copper-catalyzed olefin aziridination reaction which proceeds with high yields at room temperature. Given the efficiency of the copper ions in this reaction and given the fact that these ions easily form complexes with **3** as described in the previous chapters, we embarked a study of aziridination reactions in aqueous dispersions of complexes of the type  $\text{Cu}(\mathbf{3})_4\text{X}_2$  ( $\text{X} = \text{ClO}_4$  and  $\text{OTf}$ ). With this system,<sup>8</sup> we hoped to eventually achieve a transcription of chirality from the aggregate to the catalyst, and to obtain an enantioselective reaction. Besides aziridination, we also studied the effect of the supramolecular copper complexes on epoxidation reactions.

## 7.2 Experimental

The analytical instruments were the same as those described in Chapter 3. Gas liquid chromatography (GLC or, in short, GC) was performed with a Varian Model 3700 apparatus in combination with a Hewlett-Packard HP 3395 integrator, using a Chrompack WCOT column (length 25 meters) and a coating of CP-SIL5CB ( $\text{DF}=0.25\ \mu\text{m}$  or  $0.12\ \mu\text{m}$ ).

Solvents were distilled prior to use and stored on mol sieves 4Å. *N*-Methylimidazole was distilled under reduced pressure and stored in the dark. Styrene was filtered over basic alumina before use, in order to remove traces of styrene epoxide.

The copper salts were used as hydrates,  $\text{Cu}(\text{ClO}_4)_2$  as hexahydrate (Across Chimica) and copper triflate ( $\text{Cu}(\text{OTf})_2$ ) as tetrahydrate (see Chapter 3).

Titration was carried out as described in Chapters 3 and 4.

The presence of an enantiomeric excess of the (*R*) or (*S*) conformer of *N*-(*p*-tolylsulfonyl)-2-phenylaziridine was checked with a polarimeter, HPLC (column Chiralcel ODH), and  $^1\text{H-NMR}$  (400 MHz,  $\text{CDCl}_3$ ) in combination with a chiral shift reagent [ $\text{Eu}(\text{hfc})_3$ ]<sup>3+</sup>.

### 7.2.1 Syntheses

The syntheses of *N*,*n*-octyl-D-gluconamide (**1**) and (6-deoxy-6-(1-imidazolyl)-2,4,3,5-dimethylene-*N*,*n*-octyl-D-gluconamide **3** and 2-(1-imidazolyl)ethanol (**8**) were described before.<sup>9</sup> The compounds **2**, **4**, **7**, **10**, **11** and **13** were commercially available.

**(*N*-(*p*-Tolylsulfonyl)imino)phenyliodinane (**5**,  $\text{PhI}=\text{NTs}$ )** This compound was synthesized as described in the literature.<sup>10</sup> The reaction was carried out in methanol with 1.73 g (10.1 mmol) of tosylamide and 1.55 g (27.7 mmol) of KOH. Yield 2.41 g (6.46 mmol, 64 %) of pale yellow powder. *Mp* 103 °C (decomp). The product was stored in the freezer.

***N*-(*p*-Tolylsulfonyl)-2-phenylaziridine (styrene aziridine, **6**)** This compound was the reaction product of the catalysis experiments. The yields that were obtained, varied with the applied reaction conditions (see Section 7.3.1 and 7.3.2), *mp* 87.0 °C. TLC (silica eluent, *n*-hexane/EtOAc 2:1, v/v), FT-IR (KBr) and  $^1\text{H-NMR}$  ( $\text{CDCl}_3$ , 100 MHz) data were similar to data described in the literature.<sup>4</sup>

**Tosyl azide (TsN<sub>3</sub>, 9)** This azide was synthesized according to a literature procedure,<sup>11</sup> using 0.70 g (10.73 mmol) of sodium azide and 1.83 g (9.60 mmol) of tosyl chloride. <sup>1</sup>H-NMR (100 MHz, CDCl<sub>3</sub>) δ 7.90 ppm (d, 2H, ArH), 7.40 (d, 2H, ArH), 2.50 (s, 3H, CH<sub>3</sub>).

**Iodobenzene (12)** This compound was synthesized from 2.10 g (6.52 mmol) of iodobenzene diacetate using 50 ml of aqueous 2 N NaOH as described in the literature.<sup>12</sup> Warning! This compound can be explosive in powder form.

### 7.2.2 Catalytic aziridinations. General remarks.

The reaction product styrene aziridine (**6**) could not be determined accurately by GC, due to decomposition on the column even at relatively low temperatures. One of the side products of the catalytic reaction, iodobenzene (**5**), was therefore used to follow the reaction by GC (*vide infra*). Mesitylene was chosen as an internal standard. The GC-samples of 0.100 ml were filtrated through a piece of cotton wool before injecting in the gas chromatograph. For selected reactions the products were isolated by column chromatography and identified by comparing them with samples that had been synthesized separately. The reaction could be followed visually by the disappearance of the solid PhI=NTs, which is barely soluble in organic solvents (acetonitrile, chloroform) and in water. Yields of aziridine are based on the amount of PhI=NTs used.

### 7.2.3 Aziridinations in acetonitrile

In a typical experiment 0.014 mmol of the catalyst was weighed in a reaction vessel (Schlenk-tube) and 1 ml of MeCN was added. The air atmosphere was changed for nitrogen by evacuation followed by venting with nitrogen (three times). Styrene (0.145 mg, 1.4 mmol) was injected by a syringe through a septum and under a nitrogen-flow PhI=NTs was added (0.103 g, 0.28 mmol). During the course of the reaction, the mixture was covered with a nitrogen blanket. For the GC-monitored experiments, 0.175 ml (1.4 M) of mesitylene in acetonitrile was also added to the reaction mixture. When the reaction mixture was purified by column chromatography (silica, eluent EtOAc/n-hexane 1/4, v/v), the result was first checked by TLC (silica, EtOAc/n-hexane 1/4, v/v). This was done after a preset reaction time or when the *N*-donor had disappeared.

*Aziridination of styrene using Cu(OTf)<sub>2</sub> as the catalyst* The general procedure was followed using 6.1 mg (0.014 mmol) of catalyst, 0.15 g (1.44 mmol) of styrene and 0.103 g (0.28 mmol) of *N*-donor. The color of the solution changed from very light blue to green to yellow-green after the *N*-donor had been added. The reaction was followed by GC (0.100 ml samples were injected). After 5 min. no *N*-donor was left, and it was assumed that the reaction was completed. The experiment was carried out in duplicate: one reaction was followed by GC and in the other the products were isolated by column chromatography (yields 84 and 85 %, respectively).

*Aziridination of styrene using [Cu(MeIm)<sub>4</sub>][OTf]<sub>2</sub>* Following the general procedure 0.0090 g (0.013 mmol) of catalyst, 0.151 g (1.45 mmol) of styrene and 0.1045 g (0.28 mmol) of PhI=NTs were mixed. After adding the *N*-donor, the color of the reaction mixture changed from blue to pale gray and then gradually to pale blue. After 30 min., the solid PhI=NTs had disappeared which indicated the end of the reaction. The reaction was carried out in duplicate, one followed by GC (yield 92 %) the other by using column chromatography (silica, eluent EtOAc/n-hexane, 1/4, v/v yield 90 %).

*Aziridination of styrene using [Cu(3)<sub>4</sub>][OTf]<sub>2</sub>* The reaction was carried out following the general procedure using 0.0245 g (0.013 mmol) of catalyst, 0.148 g (1.42 mmol) of substrate, and

0.104 g (0.28 mmol) of *N*-donor. After addition of the *N*-donor the color changed from blue to pale gray and then slowly back to blue. The reaction was stirred for 3.5 hrs, yield 60 % (GC).

**Aziridination of styrene using  $[\text{Cu}(\mathbf{3})_4][\text{ClO}_4]_2$**  The copper complex was prepared *in situ* by mixing ligand **3** and  $\text{Cu}(\text{ClO}_4)_2$  in a 4:1 ratio. 0.0214 g (0.056 mmol) of **3** was dissolved in 0.80 ml of MeCN and added to 0.0053 g (0.014 mmol) of  $[\text{Cu}(\text{H}_2\text{O})_6][\text{ClO}_4]_2$  in 0.20 ml of MeCN, resulting in a dark blue solution. Thereafter, the general procedure was followed using 0.146 g (1.40 mmol) of styrene and 0.101 g (0.27 mmol) of  $\text{PhI}=\text{NTs}$ . After 6 hrs, the reaction was stopped and the product was purified by column chromatography, yield 79 %.

## 7.2.4 Aziridinations in chloroform

The procedures for the catalytic reactions in chloroform were similar to the reactions in acetonitrile. A 1.48 M solution of mesitylene in chloroform was used as the internal standard for GC.

**Aziridination of styrene using  $\text{Cu}(\text{OTf})_2$**  The general procedure was followed using 0.0050 g (0.012 mmol) of catalyst, 0.146 g (1.40 mmol) of substrate, and 0.104 g (0.28 mmol) of *N*-donor. Although the catalyst did not dissolve in chloroform, attempts were made to follow the reaction by TLC and GC. After 4.5 hrs, no aziridine could be detected by TLC, but according to GC, 34 % *N*-donor had been converted. The reaction was stopped at this point.

**Aziridination of styrene using  $[\text{Cu}(\text{MeIm})_4][\text{OTf}]_2$**  The general procedure was followed using 0.0077 g (0.012 mmol) of catalyst, 0.148 g (1.42 mmol) of substrate, and 0.104 g (0.28 mmol) of *N*-donor. According to GC, only 8 % of the *N*-donor had been converted to iodobenzene after 2 hrs. TLC did not show any spot that could be attributed to aziridine.

**Aziridination of styrene using  $[\text{Cu}(\mathbf{3})_4][\text{OTf}]_2$**  The general procedure was followed, using 0.025 g (0.013 mmol) of catalyst, 0.148 g (1.42 mmol) of substrate, and 0.104 g (0.28 mmol) of *N*-donor. After 2 hrs the reaction was stopped. At that time only 8 % of the *N*-donor had been converted to iodobenzene and no aziridine (**6**) was detected (TLC).

## 7.2.5 Aziridinations in aqueous dispersions

**Aziridination of styrene using  $\text{Cu}(\text{OTf})_2$**  The catalyst (0.006 g, 0.014 mmol) was weighed into a Schlenk-tube reaction vessel and dissolved in 1.00 ml of  $\text{H}_2\text{O}$ , giving a light blue solution. In this solution, 0.150 g (1.44 mmol) of styrene was injected and while stirring 0.105 g (0.28 mmol) of  $\text{PhI}=\text{NTs}$  was added. The mixture was stirred for 2 hrs. The aqueous mixture was washed with 3 ml of  $\text{CHCl}_3$ . According to TLC (silica, EtOAc/hexane 1:2, v/v), no aziridine was present in either the aqueous or organic phase.

**Aziridination of styrene using  $[\text{Cu}(\text{MeIm})_4][\text{OTf}]_2$**  The catalyst (0.009 g, 0.013 mmol) was weighed in a Schlenk-tube and dissolved in 1.00 ml  $\text{H}_2\text{O}$ . To this solution, 0.149 g (1.43 mmol) styrene was added and 0.104 g (0.28 mmol) of  $\text{PhI}=\text{NTs}$ . After 2 hrs the reaction was stopped and the aqueous reaction mixture was washed with 1 ml of  $\text{CHCl}_3$ . No aziridine was formed according to TLC (silica, eluent EtOAc/hexane 1:2, v/v).

## General Procedure for the catalytic reactions with the Cu aggregates in water

Water used for catalytic experiments was distilled twice. The aggregate containing the  $\text{Cu}(\text{II})$  complex was made *in situ*. In a typical experiment 0.0214 g (0.056 mmol) of **3** was dissolved in 0.80 ml of water by gentle heating.<sup>13</sup> The Cu salt (0.014 mmol  $\text{Cu}(\text{ClO}_4)_2 \cdot 6\text{H}_2\text{O}$  or  $\text{Cu}(\text{OTf})_2 \cdot 4\text{H}_2\text{O}$ ), dissolved in 0.20 ml of water, was added to the warm solution, immediately forming a more viscous opalescent mixture (indicating the formation of aggregates [catalyst] =

0.014 M) Subsequently 1.40 mmol (145.0 mg) of styrene was added, stirring was started and 0.28 mmol (103.0 mg) of  $\text{PhI}=\text{NTs}$  was added. The reaction was monitored for 3 hrs at RT by TLC. At the end of the reaction, 1 ml of  $\text{CHCl}_3$  was added to extract the product from the water layer. TLC (silica, EtOAc/hexane 1:2, 1:3 or 1:4, v/v) was used to check that no aziridine remained in the water layer. The product was purified by column chromatography (silica, eluent EtOAc/hexane 1:4, v/v). The yield was calculated on the basis of added  $\text{PhI}=\text{NTs}$ . In the following further details are given for each of the experiments.

*Aziridination of styrene using  $[\text{Cu}(\text{3})_4][\text{ClO}_4]_2$*  Reaction conditions: 0.0208 g (0.060 mmol) of **3**, 0.146 g (1.40 mmol) of styrene, and 0.109 g (0.29 mmol) of  $\text{PhI}=\text{NTs}$ , yield 25 %

*Aziridination of styrene using  $[\text{Cu}(\text{3})_4][\text{OTf}]_2$*  Reaction conditions: 0.0214 g (0.056 mmol) of **3**, 0.151 g (1.45 mmol) of styrene and 0.104 g (0.28 mmol) of  $\text{PhI}=\text{NTs}$ , yield 22 %

*Aziridination of styrene using  $[\text{Cu}(\text{3})_4][\text{ClO}_4]_2$  at 50 °C* Reaction conditions: 0.0214 g (0.056 mmol) **3**, 0.146 g (1.40 mmol) of styrene and 0.108 g (0.31 mmol) of  $\text{PhI}=\text{NTs}$ . After aggregates had been formed the reaction vessel was thermostatted in an oil-bath at a temperature of 50 °C. Styrene was injected and while stirring,  $\text{PhI}=\text{NTs}$  was added. Yield 33 % (after 3 hrs)

*Aziridination of styrene using  $[\text{Cu}(\text{3})_4][\text{ClO}_4]_2$  at 70 °C* Reaction conditions: 0.0214 g (0.056 mmol) of **3**, 0.141 g (1.35 mmol) of styrene and 0.097 g (0.28 mmol) of  $\text{PhI}=\text{NTs}$ . The reaction vessel was thermostatted at 70 °C. After 1.5 hr, a clear green solution was obtained indicating that the aggregates had disassembled. The stirring was stopped after 2 hrs. Yield 32 %

*Aziridination of styrene using  $[\text{Cu}(\text{3})_4][\text{ClO}_4]_2$  with **9** as N-donor* Reaction conditions: 0.0214 g (0.056 mmol) of **3** and 0.142 g (1.36 mmol) of styrene, and 0.0552 g (0.28 mmol) of  $\text{TsN}_3$  (**9**). After 3 hrs stirring was stopped. No aziridine was formed according to TLC.

*Aziridination of styrene using  $[\text{Cu}(\text{3})_4][\text{ClO}_4]_2$  with **9** as N-donor at 40 °C* Reaction conditions: 0.0215 g (0.056 mmol) of **3**, 0.151 g (1.45 mmol) of styrene, and 0.059 g (0.30 mmol) of  $\text{TsN}_3$ . The reaction mixture was thermostatted at 40 °C in an oil bath. After 3 hrs, the stirring was stopped. No aziridine was formed according to TLC.

*Aziridination of styrene using  $([\text{Cu}(\text{3})_4][\text{ClO}_4]_2)$  with a catalyst concentration of 0.0047 M* Reaction conditions: 0.0018 g (4.72  $\mu\text{mol}$ ) of **3** in 1 ml of water, 0.146 g (1.40 mmol) of styrene and 0.101 g (0.28 mmol) of  $\text{PhI}=\text{NTs}$ . Yield according to GC 14 %

*Aziridination of styrene using  $([\text{Cu}(\text{3})_4][\text{ClO}_4]_2)$  with a catalyst concentration of 0.0016 M* Reaction conditions: 0.0006 g (1.58  $\mu\text{mol}$ ) of **3** in 1.00 ml of water, 0.143 g (1.38 mmol) of styrene, and 0.104 g (0.28 mmol) of  $\text{PhI}=\text{NTs}$ . A very small spot was visible on TLC, which was ascribed to aziridine. The product was purified by column chromatography (silica, eluent EtOAc/hexane 1:4, v/v). The amount of aziridine obtained was too small for further characterization.

*General procedure for aziridinations in water using aggregates without covalently bound metal complexes*

In a typical experiment, 0.020 mmol of *N*,*n*-octyl-D-glucosamide was mixed with 1.00 ml of water and heated until a clear solution was obtained ( $T > 80^\circ\text{C}$ ). Upon cooling to room temperature, the solution started to gelate to a highly viscous white gel.<sup>14</sup> To this gel 0.014 mmol of catalyst was added, followed by the substrate styrene. The mixture was stirred, which resulted in pieces of gel mingled with water, and the  $\text{PhI}=\text{NTs}$  was added. After 3 hrs the stirring was



stopped and the water layer was washed with  $\text{CHCl}_3$  (1 ml). Both the organic and water layers were checked for the presence of aziridine by TLC (silica, eluent EtOAc/hexane 1/3 or 1/4, v/v). Aziridine, when present, was further purified by column chromatography (silica, eluent EtOAc/hexane 1/4 or 1/5, v/v).

*Aziridination of styrene using  $\text{Cu}(\text{OTf})_2$  as the catalyst* Reactions conditions: 0.0058 g (0.019 mmol) of **1**, 0.0046 g (0.014 mmol) of  $\text{Cu}(\text{OTf})_2$ , 0.146 g (1.40 mmol) of styrene, and 0.097 g (0.28 mmol) of  $\text{PhI}=\text{NTs}$ . Yield: 9 %.

*Aziridination of styrene using  $\text{Cu}(\text{OTf})_2$  as catalyst (stepwise addition of the N-donor)* Reactions conditions: 0.0068 g (0.022 mmol) of **1**, 0.0046 g (0.014 mmol) of catalyst, 0.146 g (1.40 mmol) of styrene. The N-donor **5** was added in three portions of 35.0, 33.0, and 35.0 mg, respectively, with intervals of 1 hr. No aziridine was formed.

*Aziridination of styrene using  $[\text{Cu}(\text{MeIm})_4][\text{ClO}_4]_2$  as the catalyst* Reactions conditions: 0.0052 g (0.017 mmol) of **1**, 0.0071 g (0.012 mmol) of catalyst, 0.146 g (1.40 mmol) of styrene and 0.094 g (0.27 mmol) of  $\text{PhI}=\text{NTs}$ . Yield: 52 %.

*Aziridination of styrene at 70 °C using  $[\text{Cu}(\text{MeIm})_4][\text{ClO}_4]_2$  as the catalyst* Reactions conditions: 0.0058 g (0.019 mmol) of **1**, 0.0065 g (0.011 mmol) of catalyst, 0.146 g (1.40 mmol) of styrene, and 0.097 g (0.28 mmol) of  $\text{PhI}=\text{NTs}$ . The mixture was thermostatted at 70 °C. Yield: 59 %.

*Aziridination of styrene using  $[\text{Cu}(\text{MeIm})_4][\text{ClO}_4]_2$  as the catalyst (stepwise addition of N-donor)* Reactions conditions: 0.0071 g (0.023 mmol) of **1**, 0.0077 g (0.013 mmol) of catalyst and 0.146 g (1.40 mmol) of styrene. The N-donor was added in three portions of 39.0, 33.0, and 31.0 mg, respectively, with intervals of 1 hr. Yield: 53 %.

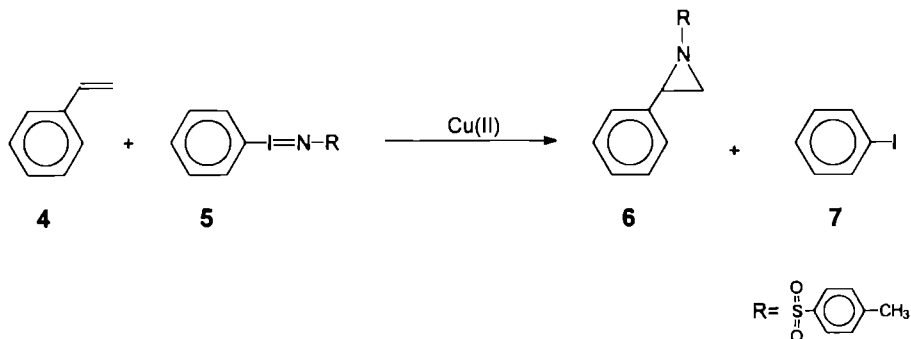
### 7.2.6 General procedure for the epoxidation reactions

The catalyst (0.01–0.1 mmol) was dissolved in 5.00 ml of acetonitrile, which was purged with nitrogen for several min. This solution was placed in a Schlenk tube, which had been evacuated three times and reevacuated with nitrogen. To this solution was added from a syringe 0.1–0.2 mmol of  $\alpha$ -pinene (**13**), filtered over basic alumina in order to remove  $\alpha$ -pinene oxide. The oxygen donor,  $\text{Ph-I}=\text{O}$  (**12**) (0.2–0.88 mmol), was added under a counter current flow of nitrogen. In the Cu(II) catalyzed experiments the color of the solution changed from light blue to green upon addition of the O-donor. After a few minutes the color turned to gray. In the case of the Co(II) catalyzed experiments the color changed from red to gray-brown. For analysis by GC, samples of 1  $\mu\text{l}$  were required.

## 7.3 Results and discussion

In this study, we mainly focussed on the catalytic aziridination of styrene (**4**), with *N*-(*p*-tolylsulfonyl)imino-phenyliodinane (**5**,  $\text{PhI}=\text{NTs}$ ) as the nitrogen donor. The reaction is shown in Scheme 7.1. The reaction products are *N*-(*p*-tolylsulfonyl)-2-phenylaziridine (**6**) and iodobenzene (**7**).

Scheme 7.1



In studies in the literature it is known that this aziridination reaction can be carried out successfully, giving high yields in short reaction times, using Cu(I) pyrazole and copper complexes of bis(oxazolines) as the catalysts<sup>6c 7 15</sup> When protic solvents like water or methanol are present, the yields of **6** are very low due to hydrolysis of the active copper species<sup>16 17</sup> In order to get more information about the effect of the solvent we decided to perform reactions in both organic solvent and water

### 7.3.1 Aziridination in organic solvents

One of the first problems we encountered in our study was the instability of **6** during its gas-chromatographic detection, even at relatively low temperatures HPLC of **6** resulted in very high retention times which made this procedure unreliable As a result, the amount of product formed could only be determined at the end of the reaction after having performed column chromatography We found however, that the other product of the reaction, iodobenzene, was stable during the GC detection and could be used as a monitoring agent This method should be used with caution, however, because Cu=NTs, which is an intermediate of the reaction, can react with water,<sup>17</sup> resulting in the formation of **7** without concomitant formation of **6** Several control experiments including blank reactions without catalyst present, in which the amounts of both **6** and **7** were determined by GC and column chromatography, showed that monitoring of **7** by GC is a reliable method for following the formation of **6** in organic solvents

In acetonitrile, Cu(OTf)<sub>2</sub> appeared to be an excellent catalyst for the aziridination of styrene Within 5 minutes, 85 % of product was obtained (see Table 7 1) The yield of aziridine could be further improved when the copper(II) complex of 1-methylimidazole ([((2)<sub>4</sub>Cu][OTf]<sub>2</sub>)<sup>18</sup> was used, although the reaction time was longer The copper(II) complexes of the gluconamide ligand **3** turned out to be good catalysts as well but the reaction times were rather long (see Table 7 1)

**Table 7.1** Aziridination of styrene in acetonitrile

Catalyst	Yield (%)	Reaction time <sup>a</sup>
Cu(OTf) <sub>2</sub>	85	≤ 5 min
[Cu(2) <sub>4</sub> ][OTf] <sub>2</sub>	92	30 min
[Cu(3) <sub>4</sub> ][OTf] <sub>2</sub>	60 <sup>b</sup>	3.5 hrs
[Cu(3) <sub>4</sub> ][ClO <sub>4</sub> ] <sub>2</sub>	79	6 hrs

<sup>a</sup> The reaction was stopped after the insoluble PhI=NTs had disappeared<sup>b</sup> The yield probably can be improved when the reaction time is extended

For the formation of the catalytically active species, one of the imidazole ligands has to dissociate from the copper(II) center in order to allow the nitrogen donor **5** to coordinate to the vacant site and to form the copper nitrene Cu=NTs complex.<sup>7b-d,17</sup> This dissociation may explain why the other copper imidazole complexes of Table 7.1 require longer reaction times than Cu(OTf)<sub>2</sub>. The complexes [(3)<sub>4</sub>Cu][X]<sub>2</sub> (X=ClO<sub>4</sub>, OTf) have the additional disadvantage that their imidazole ligands are bulky and carry long aliphatic tails. This will cause further shielding of the copper (II) center for the nitrogen donor **5**.

The copper(II) catalyzed aziridination reaction was also carried out in chloroform. To our surprise, no product was formed, neither with nor without imidazole ligands present (see Table 7.2). The amount of iodobenzene formed was also small (< 9 % after 2 hrs. of reaction). For unknown reasons, the active nitrene complex probably cannot be formed in chloroform. The related solvent dichloromethane has been tested in the literature and was found to be a suitable medium for the aziridination reaction.<sup>6,7,17</sup>

**Table 7.2** Aziridination of styrene in chloroform

Catalyst	Yield (%)
Cu(OTf) <sub>2</sub> <sup>a</sup>	0
[(MeIm) <sub>4</sub> Cu][OTf] <sub>2</sub>	0
[(3) <sub>4</sub> Cu][OTf] <sub>2</sub>	0

<sup>a</sup> Catalyst did not dissolve in CHCl<sub>3</sub>

### 7.3.2 Aziridination in water

The aziridination reaction was also carried out in aqueous solutions and dispersions. In these experiments, the monitoring of **7** by GC was not a reliable method for following the reaction. The amount of **5**, therefore, was determined by column chromatography.

Compound **5** turned out to be stable in water for days. The copper catalysts did not show any catalytic activity in water (see Table 7.3), presumably due to solvent trapping,<sup>16,17</sup> i.e. the hydrolysis of the active nitrene intermediate Cu=NTs. On the other hand, the catalysts built into aggregates retained their activity, although a lower amount of aziridine was obtained compared to

the reaction carried out in acetonitrile. In a first set of experiments, aggregates prepared from **1**<sup>19</sup> were used as the matrices for the catalytic reaction. The copper salt or its 1-methylimidazole complex was mixed with **1** in a 1:1.5 ratio and dispersed in water. The amount of substrate and *N*-donor were similar to the reactions carried out in organic solvents. Due to the turbidity of the dispersions, the disappearance of PhI=NTs could not be visually monitored. The reaction was therefore stopped after a preset time.

It is clear from Table 7.3 that the copper ions ligated by 1-methylimidazole have a much higher catalytic activity in the aggregates of **1** than the non-complexed copper ions. In comparison to the simple copper salts, the metal complexes with 1-methylimidazole have a more hydrophobic character, allowing them to penetrate more deeply into the hydrophobic area of the aggregates. This area is more comparable to an organic solvent and therefore more suitable for aziridination, as water molecules, which would cause solvent trapping of the nitrene complex, are less likely to penetrate it. Cu(OTf)<sub>2</sub> is very soluble in water and remains in the aqueous phase or in the head group region of the aggregated amphiphiles, making that solvent trapping is still possible.

**Table 7.3** Aziridination of styrene in aqueous media

Catalyst	Aggregates of <b>1</b> present	PhI=NTs, Steps of addition	Temperature (°C)	Yield <sup>a</sup> (%)
Cu(OTf) <sub>2</sub>	No	1	20	0
[Cu(2) <sub>4</sub> ][OTf] <sub>2</sub>	No	1	20	0
Cu(OTf) <sub>2</sub>	Yes	1	20	9
Cu(OTf) <sub>2</sub>	Yes	3	20	0
[Cu(2) <sub>4</sub> ][ClO <sub>4</sub> ] <sub>2</sub>	Yes	1	20	52
[Cu(2) <sub>4</sub> ][ClO <sub>4</sub> ] <sub>2</sub>	Yes	3	20	53
[Cu(2) <sub>4</sub> ][ClO <sub>4</sub> ] <sub>2</sub>	Yes	1	70	59

<sup>a</sup> Reaction time was 3 hrs except for the solutions without aggregates where this time was 2 hrs. The yield was calculated with respect to PhI=NTs.

In order to avoid saturation of the aggregates with PhI=NTs (the aggregates tend to flocculate upon addition of a large portion of PhI=NTs), in some experiments the *N*-donor was added in 3 portions (see Table 7.3). This step-wise addition of *N*-donor did not result in an increase of aziridine formation. Only a small improvement in the yield of aziridine was observed when the temperature was raised. Despite the fact that a chiral environment is created by using aggregates of **1**, no enantioselectivity was found in the aziridinations of styrene.

In a subsequent series of experiments aggregates derived from the amphiphile with the “built-in” metal complexing imidazole group (**3**) were tested. The copper complexes [Cu(3)<sub>4</sub>][ClO<sub>4</sub>]<sub>2</sub> have been shown to form chiral structures like braids and scrolls (see Chapter 4). The layered arrangement of the copper centers in these structures makes them suitable for catalyzing the aziridination reaction, because in the layers the copper ions are shielded from the

aqueous phase and therefore the Cu-nitrene intermediates will be protected from being hydrolyzed. This hypothesis appeared to be correct, since  $[\text{Cu}(\mathbf{3})_4][\text{ClO}_4]_2$  displayed catalytic activity in water (see Table 7.4).

**Table 7.4** Aziridination of styrene in water catalyzed by copper (II) complexes of ligands **2** and **3**

Catalyst	Reaction time (hrs )	Yield (%)
$[\text{Cu}(\mathbf{2})_4][\text{OTf}]_2$	2	0
$[\text{Cu}(\mathbf{3})_4][\text{OTf}]_2^a$	2	22
$[\text{Cu}(\mathbf{3})_4][\text{ClO}_4]_2^b$	3	25

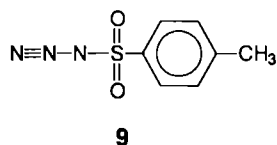
<sup>a</sup> Forms ill-defined vesicular structures in water

<sup>b</sup> Forms braids and scrolls in water

Although the amount of aziridine formed was lower than in the case of mixing  $[\text{Cu}(\mathbf{2})_4][\text{OTf}]_2$  with aggregates of **1**, copper complexes made from **3** appeared to be suitable catalysts. The observed lower yield is not surprising, since dissociation of the imidazole ligand from the copper center in order to create a free coordination site will be more problematic with **3** than with other ligands, because **3** is a supporting part of the amphiphilic aggregate. In addition, the individual molecules of **3** are organized in a tight lamellar packing (see Chapter 4).

Despite the direct connection between the metal and the chiral ligand, no chiral induction was observed in the aziridination reaction. Apparently, the chirality of the aggregate (braid and scroll) can not be transferred into enantioselective catalytic activity.

Attempts to improve the catalytic activity by using the *N*-donor tosyl azide (**9**), which is a liquid at room temperature, failed. Despite the better mixing of the reactants, which is possible with this formulation, the reactivity of **9**<sup>6d</sup> was too low for aziridination to occur in aqueous dispersions.



The amount of aziridine formed was slightly improved when the temperature was raised (see Table 7.5). Increasing the temperature has the advantage of accelerating the chemical reaction and enhancing the mobility of the individual amphiphilic molecules, which is favorable for the dissociation of the imidazole ligands. On the other hand, the penetration of water molecules into the hydrophobic area will be enlarged by increasing the temperature, which can lead to hydrolysis of the active nitrene complex. Unfortunately, the aggregates disintegrated after 1.5 hrs. of reaction when the temperature was too high, *i.e.* just below the  $T_{\text{Krafft}}$  (74 °C).

**Table 7.5** Variation of the reaction temperature in the aziridination of styrene in aqueous dispersions of  $[\text{Cu}(\mathbf{3})_4][\text{ClO}_4]_2$ 

Temperature (°C)	Reaction time (hrs)	Yield (%)
20	3	25
50	3	33
70	1.5 <sup>a</sup>	32

<sup>a</sup> Aggregates disintegrated after 1.5 hrs and the reaction was stopped

Decreasing the concentration of the catalyst resulted in an increase of the turnover (TO) number<sup>\*</sup> (Table 7.6), but the amount of product formed after 3 hrs. decreased. It is possible that the turnover number can be further increased by “diluting” the catalyst with free **3**, but this was not investigated.

**Table 7.6** Variation of the concentration of  $[\text{Cu}(\mathbf{3})_4][\text{ClO}_4]_2$  in the aziridination of styrene in aqueous dispersions<sup>a</sup>

Catalyst concentration <sup>b</sup>	% catalyst <sup>c</sup>	Yield (%) <sup>c</sup>	TO number
14.0	5.6	25	5
4.7	1.7	15	9
1.4	0.6	Trace <sup>d</sup>	--

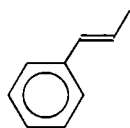
<sup>a</sup> Reaction time 3 hrs

<sup>b</sup> (mMolar) The concentration substrate and *N*-donor was not varied

<sup>c</sup> With respect to PhI=NTs

<sup>d</sup> Small spot on TLC, but no product was found after column chromatography

Besides styrene, we also used *trans*- $\beta$ -methyl-styrene (**10**) and cyclohexene (**11**) as olefins in the aziridination reaction in water with  $[\text{Cu}(\mathbf{3})_4][\text{ClO}_4]_2$  as catalyst, but according to TLC, only small traces of aziridine product were formed, which could not be isolated by column chromatography.

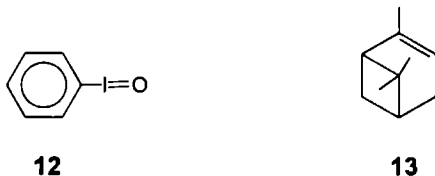
**10****11**

### 7.3.3 Epoxidation

In a final series of experiments, we investigated the epoxidation of olefins with iodosylbenzene (**12**) catalyzed by copper(II) complexes in acetonitrile. Copper catalyzed epoxidations of olefins have been described in the literature.<sup>20</sup> Despite the use of a reactive

<sup>\*</sup> Turnover number = (x mol product)/(y mol catalyst)

alkene, viz.  $\alpha$ -pinene (**13**), copper(II) salts and imidazole complexes of copper(II) perchlorate were not effective epoxidation catalysts in our hands (Table 7.7). The color of the reaction mixture changed from dark blue to green upon addition of iodobenzene, which indicated that a reaction with the copper complex took place. In addition, according to GC, iodobenzene was formed, also indicating



that the oxidant underwent a reaction. From the literature<sup>20</sup> it is known that traces of water can have a negative influence on the course of the reaction. We therefore, dried the reaction mixture on mol sieves after addition of the copper salt or complex. These precautions, however, did not result in any positive effect. Raising the temperature to 80 °C was not successful either in increasing the catalytic activity.

**Table 7.7** Epoxidation of  $\alpha$ -pinene using copper(II) catalysts <sup>a</sup>

Catalyst	Solvent dried	Reaction temperature (°C)	Yield (%) <sup>b</sup>
Cu(OTf) <sub>2</sub>	no	25	Trace
Cu(OTf) <sub>2</sub>	yes	25	0
Cu(ClO <sub>4</sub> ) <sub>2</sub>	yes	25	Trace
[Cu(2) <sub>4</sub> ][ClO <sub>4</sub> ] <sub>2</sub>	no	25	Trace
[Cu(2) <sub>4</sub> ][ClO <sub>4</sub> ] <sub>2</sub>	yes	25	Trace
[Cu(2) <sub>4</sub> ][ClO <sub>4</sub> ] <sub>2</sub> <sup>c</sup>	yes	25	Trace
[Cu(2) <sub>4</sub> ][ClO <sub>4</sub> ] <sub>2</sub>	yes	80	Trace

<sup>a</sup> Solvent acetonitrile, oxidant iodobenzene (**12**)

<sup>b</sup> With respect to PhI=O, the reaction time was 30 min

<sup>c</sup> Blanco reaction without PhI=O

Cobalt imidazole complexes ([Co(Im)<sub>6</sub>][ClO<sub>4</sub>]<sub>2</sub>) were also tested as catalysts in the epoxidation of  $\alpha$ -pinene, but the results were not positive enough to justify further studies. It was concluded, therefore, that copper or cobalt imidazole complexes are not suitable as catalysts for the epoxidation of olefins. Further studies with these metal complexes in the form of aggregates in water were not undertaken.

#### 7.4 Concluding remarks

We have shown that copper(II) imidazole complexes are suitable catalysts for olefin aziridination, although with respect to the free copper(II) salts the rate of the reaction was reduced by the introduction of the imidazole ligands. The reactions are very sensitive to water and cannot

be carried out in this solvent unless aggregates of amphiphiles are used. These aggregates contain a hydrophobic interior, which can accommodate the catalytic copper-imidazole complexes and shield the intermediate copper nitrene species from reaction with water. The catalytic complexes can be either physically adsorbed or covalently linked to the amphiphiles. In the latter case the yield of aziridine is lower. Unfortunately, the chirality of the amphiphilic molecules and the suprastructures did not lead to enantioselective reactions.

It has been demonstrated that copper-imidazole or cobalt-imidazole complexes are not very efficient catalysts in the epoxidation of olefins.

## 7.5 Literature

- <sup>1</sup> Feiters, M C *Supramolecular technology and applications* vol 10, part III Chap. 16 *supramolecular catalysis* vol. ed Reinhoudt, D N., part of the series "Comprehensive Supramolecular Chemistry", ed. Lehn, J.-M., Pergamon Press Elsevier Sci. Ltd., Oxford (UK) 1995
- <sup>2</sup> Kunitake, T., Shinkai, S. *Adv. Phys. Org. Chem.* **1980**, 17, 435
- <sup>3</sup> Tanner, D. *Angew. Chem.* **1994**, 106, 626, *Ibid. Int. Ed. Eng.* **1994**, 33, 599
- <sup>4</sup> Groves, J. T., Takahashi, T. *J. Am. Chem. Soc.* **1983**, 105, 2073
- <sup>5</sup> (a) Mansuy, D., Mahy, J.-P., Dureault, A., Bedi, G., Battioni, P. *J. Chem. Soc. Chem. Commun.* **1984**, 1161, (b) Mahy, J.-P., Bedi, G., Battioni, P., Mansuy, D. *J. Chem. Soc. Perkin Trans. II* **1988**, 1517, (c) Mahy, J.-P., Bedi, G., Battioni, P., Mansuy, D. *Tetrahedron Lett.* **1988**, 29, 1927
- <sup>6</sup> (a) Evans, D. A., Woerpel, K. A., Hinman, Faul, M. M. *J. Am. Chem. Soc.* **1991**, 113, 726, (b) Evans, D. A., Faul, M. M., Bilodeau, M. T. *J. Org. Chem.* **1991**, 56, 6744, (c) Evans, D. A., Faul, M. M., Bilodeau, M. T., Anderson, B. A., Barnes, D. M. *J. Am. Chem. Soc.* **1993**, 115, 5328, (d) Evans, D. A., Faul, M. M., Bilodeau, M. T. *J. Am. Chem. Soc.* **1994**, 116, 2742
- <sup>7</sup> (a) Li, Z., Conser, K. R., Jacobsen, E. N. *J. Am. Chem. Soc.* **1993**, 115, 5326, (b) Zhang, W., Lee, N. H., Jacobsen, E. N. *J. Am. Chem. Soc.* **1994**, 116, 425, (c) Hansen, K. B., Finney, N. S., Jacobsen, E. N. *Angew. Chem.* **1995**, 107, 750, *Ibid. Int. Ed. Eng.* **1995**, 35, 676 (d) Li, Z., Quan, R. W., Jacobsen, E. N. *J. Am. Chem. Soc.* **1995**, 117, 5889
- <sup>8</sup> Fendler, J. H. *Membrane Mimetic Chemistry*, John Wiley, New York **1982**, Fuhrhop, J.-H., Mathieu, J. *Angew. Chem.* **1984**, 96, 125, *Ibid. Int. Ed. Eng.* **1984**, 23, 100, Ringsdorf, H., Schlarb, B., Venzmer, J. *Angew. Chem.* **1988**, 100, 117, *Ibid. Int. Ed. Eng.* **1988**, 27, 113
- <sup>9</sup> For synthesis and characterization see Chapter 3
- <sup>10</sup> Yamada, Y., Yamamoto, T., Okawara, M. *Chem. Lett.* **1975**, 361
- <sup>11</sup> Doering, van W. E., DePuy, D. H. *J. Am. Chem. Soc.* **1953**, 75, 5955, Regitz, M., Hocker, J., Liedhegener, A. *Org. Synth. V* **1975**, 179
- <sup>12</sup> *Organic synthesis* ed. McKusick, B. C., **1963**, 43, 60
- <sup>13</sup> See also Chapter 4
- <sup>14</sup> For rope-like structures see Chapters 4 and 6 and references cited therein
- <sup>15</sup> Noda, K., Hosoya, N., Irie, R., Ito, Y., Katsuki, T. *Synlett* **1993**, 469
- <sup>16</sup> White, R. E. *Inorg. Chem.* **1987**, 26, 3916



<sup>17</sup> Perez, P J , Brookhart, M , Templeton, J L *Organometallics* **1993**, 12, 261

<sup>18</sup> For the complexation behavior of imidazole with Cu(OTf)<sub>2</sub>, see Chapter 3

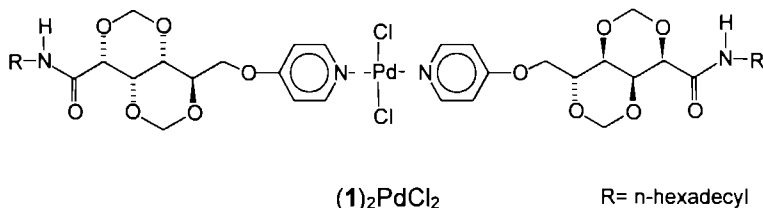
<sup>19</sup> For helical fibers see Pfannemüller, B , Welte, W *Chem Phys Lipids* **1985**, 37, 227

<sup>20</sup> a) VanAtta, R B , Franklin, C C , Valentine, J S *Inorg Chem* **1984**, 23, 4123, b) Tai, A F , Margerum, L D , Valentine, J S *J Am Chem Soc* **1986**, 108, 5006

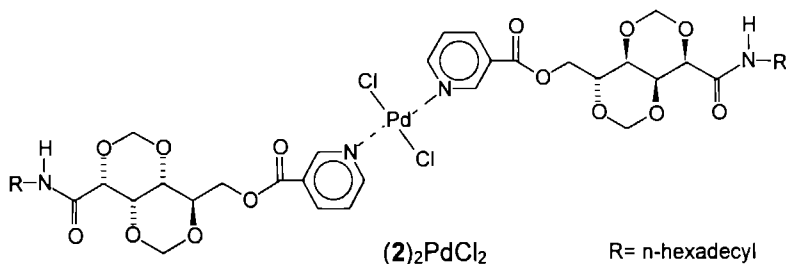
# Appendix 1

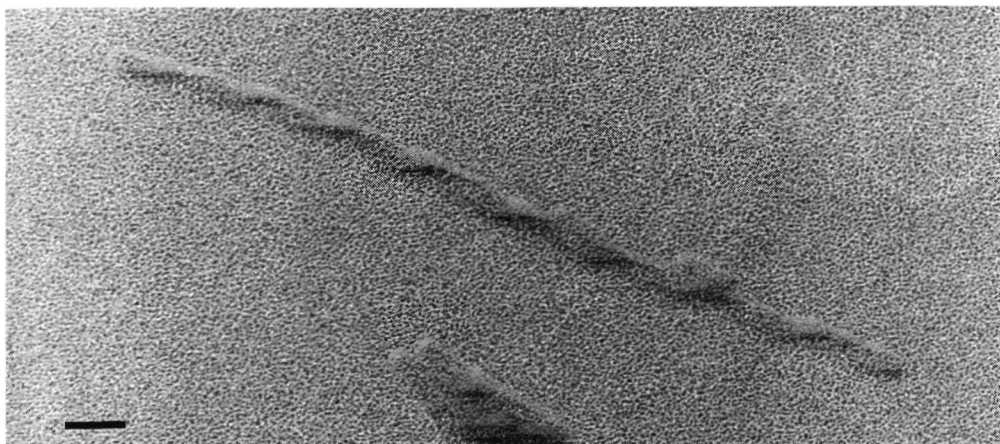
## Suprastructures from Pd complexes made of pyridyl substituted gluconamides

Pyridine ligands are known to give stable palladium (II) complexes.<sup>1</sup> Starting from *trans*-bis[benzonitrile]-palladium(II) chloride, *trans*-bis[6-(4-pyridyl)-2,4,3,5-dimethylene-*N*,*n*-hexadecyl-D-gluconamide]PdCl<sub>2</sub> ((1)<sub>2</sub>PdCl<sub>2</sub>) was synthesized.



This compound dissolved in chloroform but precipitated from water. In THF a rigid gel (organo-gel) was obtained, which did not change shape upon shaking the test tube. Organo-gels from gluconamide derivatives have been observed before,<sup>2</sup> but this is the first example of an organogel made from a metal complex of a gluconamide derivative. In addition, this is the first organo-gel of a methylene protected gluconamide and no gels in THF have been described before. The gel was investigated by TEM, which showed helical ribbons (width 36 nm) with a regular twist (pitch 110 nm) and a (maximum) aspect ratio of 25 (see Figure A1.1). The architecture of the aggregates was investigated with FT-IR, powder diffraction and DSC. Unfortunately, the results did not allow us to draw conclusions with respect to the architecture of the aggregates. The FT-IR spectra were not significantly different from the spectra of the non-complexed ligand, while powder diffraction and DSC spectra did not show relevant peaks. A PdCl<sub>2</sub> complex of 2,4,3,5-dimethylene-*N*,*n*-hexadecyl-D-gluconamide-6-(4-pyridine-carboxylic acid ester) ((2)<sub>2</sub>PdCl<sub>2</sub>) was also prepared. This complex dissolved in THF without giving a gel.





**Figure A 1.1** TEM picture of a helical ribbon formed by the complex  $(1)_2\text{PdCl}_2$  in THF. The aggregates were stained with a Pt shadow, bar is 285 nm.

There is no obvious explanation why  $(1)_2\text{PdCl}_2$  forms an organo-gel in THF and  $(2)_2\text{PdCl}_2$  not. A slight difference is expected between the conformations of  $(1)_2\text{PdCl}_2$  and  $(2)_2\text{PdCl}_2$ , because in the latter compound the pyridyl ring is meta substituted and the connection to the carbohydrate via an ester group is more extended. These alterations can cause a bend in the overall shape of the molecule which is not favorable for gelating solvents according to the rule of thumb: ‘gelators of organic fluids should have the capability of adopting rodlike shapes in their extended conformations’.<sup>3</sup>

## Experimental

The syntheses and characterizations of 6-(4-pyridyl)-2,4,3,5-dimethylene-*N*,*n*-hexadecyl-D-gluconamide (**1**) and 2,4,3,5-dimethylene-*N*,*n*-hexadecyl-D-gluconamide-6-(pyridyl-carboxylic acid ester) (**2**) were described in Chapter 3.

***Trans*-bis[6-(4-pyridyl)-2,4,3,5-dimethylene]-*N*,*n*-hexadecyl-D-gluconamide]-palladium(II)dichloride ( $(1)_2\text{PdCl}_2$ ).** The pyridyl compound **1** (37.3 mg, 0.072 mmol) was dissolved in  $\text{CHCl}_3$  and while stirring 13.1 mg (0.5 equiv.) of *trans*-bis(benzonitrile)-palladium(II) chloride was added. After 24 hrs. of stirring at room temperature, the starting materials had disappeared (according to TLC on silica, eluent  $\text{EtOH}/\text{CH}_2\text{Cl}_2$  (1:9, v/v)), and the  $\text{CHCl}_3$  was removed by evaporation. The yield was quantitative, m.p. 286 °C. IR (KBr): 3321  $\text{cm}^{-1}$  (NH), 1663 (amide I), 1540 (amide II).  $^1\text{H}$ -NMR (100 MHz,  $\text{CDCl}_3$ )  $\delta$  8.65 (d, 4H,  $J=6.8$  Hz, ArH, 0.16 ppm downfield shift due to complexation with Pd); 6.87 (d, 4H,  $J=7.1$  Hz, ArH). The assignments made for the chemical shifts and  $J$ -coupling values of the carbohydrate framework, amide and aliphatic chain are similar to those of **1**. FAB-MS  $m/z$ : 1219 ( $\text{M}+1$ )<sup>+</sup>, 1181 ( $(1)_2\text{PdCl}-1$ )<sup>+</sup>, 1146 ( $(1)_2\text{Pd}$ )<sup>+</sup>, 626 ( $(1)\text{Pd}$ )<sup>+</sup>.

***Trans*-bis[2,4;3,5-dimethylene-*N*,*n*-hexadecyl-D-gluconamide-6-(4-pyridine-carboxylic acid ester)]-palladium(II)dichloride ((**2**)<sub>2</sub>PdCl<sub>2</sub>).**

*Trans*-bis(benzonitrile)palladium(II) chloride (0.015 g, 0.0375 mmol) was added to a solution of 0.0413 g (0.075 mmol) of **2** in 15 ml of CHCl<sub>3</sub>. After stirring for 3 days, the solvent and the benzonitrile were removed by evacuation. Yield 0.038 g (0.03 mmol, 79.0 %), m.p. 194 °C. <sup>1</sup>H-NMR (CDCl<sub>3</sub>, 100 MHz) δ 9.46 ppm (d, 2H, ArH), 9.06 (2d, 2H, ArH), 8.44 (2t, 2H, ArH), 7.47 (m, 2H, ArH). The assignments of the chemical shifts of the carbohydrate frame work, amide and aliphatic chains are similar to those of **2**. FAB-MS *m/z* 1238 ((**12**)<sub>2</sub>PdCl + 1)<sup>+</sup>, 654 ((**12**)Pd)<sup>+</sup>.

## Literature

<sup>1</sup> Hudson, S A., Maitlis, P M *Chem Rev* **1993**, 93, 861

<sup>2</sup> See Chapter 6 and literature references cited therein

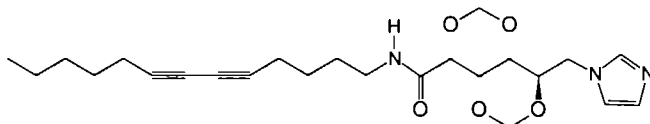
<sup>3</sup> Lin, Y -C , Kachar, B , Weiss, R G *J Am Chem Soc* **1989**, 111, 5542



## Appendix 2

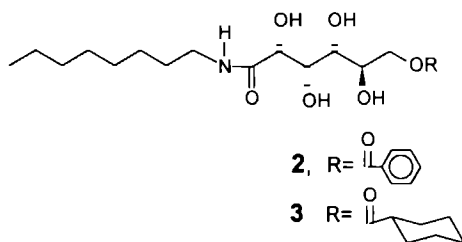
### Polymerization of suprastructures

Supramolecular aggregates can be stabilized by a polymerization reaction. Polymerization of vesicles<sup>1</sup> was first described in 1979 by Ringsdorf *et al*.<sup>2</sup> Several approaches towards vesicle polymerization have been reported.<sup>3</sup> Carbohydrate-based amphiphiles containing a diacetylene alkyl chain, forming monolayers<sup>4</sup> and superstructures like tubes<sup>5</sup> and fibrous aggregates<sup>6</sup> have been polymerized. Unfortunately, we failed to obtain suprastructures from the methylene-protected gluconamide with a diacetylenic function in the alkyl chain (**1**) (see Chapter 4), which prevented us from carrying out polymerization reactions with **1** in aggregated form.

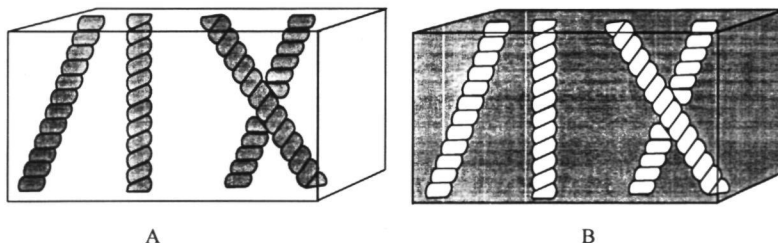


**1**

Gluconamide derived compounds like **2** and **3** form superstructures in organic solvents like chloroform and ethyl acetate.<sup>7</sup> We found that aggregates can also be obtained in a mixture of methyl methacrylate and *n*-butyl methacrylate, which made it possible to incorporate aggregates of gluconamides in a polymerized matrix. This approach is different from the one in which the aggregates themselves are stabilized by polymerization (Figure A2.1).



Compounds **2** and **3** gave well-defined aggregates with high aspect ratios in the above mentioned mixture of methyl methacrylate and *n*-butyl methacrylate (1/4, v/v). This dispersion of the aggregates was readily polymerized in a radical polymerization reaction using UV light, yielding a rigid polymer which did not collapse upon removing the reaction vessel.



**Figure A2.1** Schematic representation of aggregates in polymerizable solvents A) Before polymerization, aggregates forming an organogel, B) after polymerization and removal of the aggregates, leaving a block of polymer with well defined nanosized channels.



**Figure A2.2** TEM pictures of channels, bar is 1.35  $\mu\text{m}$

Using a microtome a slab of this polymer was sliced in thin couples (90 nm), which were allowed to float on a water surface before they were transferred to electron microscopy grids. The couples showed well-defined holes and channels according to TEM. Apparently the aggregates were extracted spontaneously from the polymeric matrix in water or removed as a consequence of the surface tension of water, leaving well-defined channels (see Figure A2.2). Although dispersions of compound **3** showed helical aggregates,<sup>7</sup> unfortunately, the channels that were observed in the polymeric matrix did not show helical structures.

### Experimental

The synthesis and characterization of compounds **1-3** were described in the Chapters 3 and 6. The procedure for taking electron micrographs was described in Chapter 4.

The gelators **1-3** (1 % w/v) were dissolved in a warm mixture of methyl methacrylate and n-butyl methacrylate (4:1 v/v) containing 0.5 % (w/v) polymerization catalyst (benzoin ethyl

ether). The mixtures were transferred into gelatin cups and irradiated overnight with UV light ( $\lambda = 365$  nm) in a refrigerator (5 °C).

Slices (90 nm) of the polymeric material were cut using a glass knife and a diamond microtome.

## Literature

<sup>1</sup> For reviews see a) Bader, H , Dorn, K , Hupfer, B , Ringsdorf, H *Adv Polym Sci* **1985**, 64, 1, b) Ringsdorf, H , Schlarb, B , Venzmer, J *Angew Chem* **1988**, 100, 117, *Ibid Int Ed Eng* **1988**, 27, 113

<sup>2</sup> Day, D, Hub, H H , Ringsdorf, H *Isr J Chem* **1979**, 18, 325

<sup>3</sup> Ringsdorf, H , Schlarb, B , Tyminski, P N , O'Brien, D F *Macromol* **1988**, 21, 671

<sup>4</sup> Bader, H , Ringsdorf, H , Skura, J *Angew Chem* **1981**, 93, 109, *Ibid Int Ed Eng* **1981**, 20, 91

<sup>5</sup> a) Frankel, D A , O'Brien, D F *J Am Chem Soc* **1991**, 113, 7436, b) O'Brien, D F , Frankel, D A *J Am Chem Soc* **1994**, 116, 10057

<sup>6</sup> Fuhrhop, J -H , Blumtritt, P , Lehmann, C , Luger, P *J Am Chem Soc* **1991**, 113, 7437

<sup>7</sup> See Chapter 6





## Appendix 3

### Atomic positional and vibrational parameters (with esd's) for compound 1a (Chapter 3)

Atom	x	y	z	$U_{eq}$ ( $\text{\AA}^2$ )
O(1)	0 6203(12)	0 4517(12)	0 0813(2)	0 039(4)
O(2)	0 5063(12)	0 8326(15)	0 0793(2)	0 065(5)
O(3)	0 7178(14)	0 5989(14)	0 1198(2)	0 044(5)
O(4)	0 5658(12)	0 9658(13)	0 1192(2)	0 056(5)
O(5)	1 0971(2)	0 8394(15)	0 1587(2)	0 054(4)
N(1)	1 089(18)	0 0723(19)	0 0356(2)	0 068(7)
N(2)	0 9833(15)	0 349(2)	0 0430(2)	0 060(7)
N(3)	0 6738(3)	0 8611(15)	0 1678(2)	0 043(5)
C(1)	1 147(19)	0 223(3)	0 0486(3)	0 058(5)
C(2)	0 8559(2)	0 1196(19)	0 0237(3)	0 031(3)
C(3)	0 792(2)	0 291(2)	0 0270(3)	0 058(4)
C(4)	1 005(2)	0 528(2)	0 0529(3)	0 049(4)
C(5)	0 744(2)	0 548(2)	0 0652(3)	0 047(4)
C(6)	0 759(2)	0 759(2)	0 0795(3)	0 041(4)
C(7)	0 853(2)	0 7325(19)	0 1065(3)	0 030(3)
C(8)	0 732(2)	0 446(2)	0 1059(3)	0 041(4)
C(9)	0 8200(19)	0 900(2)	0 1236(3)	0 041(4)
C(10)	0 508(3)	0 989(3)	0 0934(3)	0 076(6)
C(11)	0 875(2)	0 864(2)	0 1522(3)	0 040(4)
C(12)	0 706(2)	0 836(2)	0 1954(3)	0 049(4)
C(13)	0 4549(18)	0 841(2)	0 2100(2)	0 043(4)
C(14)	0 490(2)	0 8244(19)	0 2396(3)	0 050(4)
C(15)	0 236(2)	0 836(2)	0 2546(3)	0 047(4)
C(16)	0 264(2)	0 829(2)	0 2841(2)	0 049(4)
C(17)	0 0060(18)	0 8388(19)	0 2994(2)	0 034(3)
C(18)	0 0366(19)	0 835(2)	0 3277(2)	0 046(4)
C(19)	-0 223(2)	0 838(2)	0 3423(3)	0 060(4)

Table continues next page

Atom	x	y	z	$U_{eq}$ ( $\text{\AA}^2$ )
H(1)	1 289(3)	0 236(3)	0 0604(3)	0 07
H(2)	0.7502(19)	0 0402(19)	0 0142(3)	0 037
H(3)	0.650(2)	0.354(2)	0.0198(3)	0.069
H(3A)	0 5161(15)	0.8750(15)	0 1613(2)	0.051
H(4A)	1.051(2)	0.608(2)	0 0384(3)	0.058
H(4B)	1 145(2)	0 535(2)	0 0662(3)	0 058
H(5)	0.622(2)	0.603(2)	0 0501(3)	0 057
H(6)	0.882(2)	0.837(2)	0 0700(3)	0.05
H(7)	1 042(2)	0.7016(19)	0 1059(3)	0.036
H(8A)	0 646(2)	0 353(2)	0.1162(3)	0 049
H(8B)	0.918(2)	0.414(2)	0 1040(3)	0.049
H(9)	0 9486(19)	0 989(2)	0 1174(3)	0 049
H(10A)	0.639(3)	1 069(3)	0.0856(3)	0.091
H(10B)	0.335(3)	1.046(3)	0 0919(3)	0 091
H(12A)	0 823(2)	0 928(2)	0 2023(3)	0.059
H(12B)	0.792(2)	0.723(2)	0 1985(3)	0 059
H(13A)	0.3423(18)	0.745(2)	0 2038(2)	0 052
H(13B)	0 3644(18)	0 952(2)	0 2061(2)	0 052
H(14A)	0 575(2)	0 7115(19)	0 2436(3)	0 06
H(14B)	0 609(2)	0 9177(19)	0.2457(3)	0 06
H(15A)	0.148(2)	0 946(2)	0 2499(3)	0 057
H(15B)	0.121(2)	0.740(2)	0 2490(3)	0.057
H(16A)	0 377(2)	0.926(2)	0 2897(2)	0 059
H(16B)	0 354(2)	0 719(2)	0 2888(2)	0.059
H(17A)	-0.0854(18)	0.9474(19)	0 2945(2)	0.041
H(17B)	-0.1061(18)	0.7401(19)	0 2940(2)	0.041
H(18A)	0 1428(19)	0 936(2)	0 3333(2)	0 055
H(18B)	0.1328(19)	0 728(2)	0.3327(2)	0 055
H(19A)	-0.193(3)	0 811(12)	0 3608(4)	0.09
H(19B)	-0.341(7)	0.752(2)	0.3347(12)	0 09
H(19C)	-0.301(9)	0.954(2)	0.3408(15)	0 09

## Summary

This thesis describes the synthesis and aggregation behavior of glucose derivatives with unbranched alkyl chains containing 8 or 16 carbon atoms and their metal complexes. These molecules can exhibit amphiphilic behavior, *i.e.* they can self-assemble in water to give aggregates or suprastructures based on non-covalent interactions. It was known from the literature that *N*,*n*-alkyl-D-gluconamides form helices in water. We intended to use these chiral aggregates as matrices for catalysis and, in order to achieve this, metal binding imidazolyl and pyridyl groups were coupled to the glucose derivatives. The secondary hydroxyl groups of the gluconamides were first protected with methylene bridges resulting in the loss of amphiphilic behavior. After substitution of the primary hydroxyl group on carbon atom C-6 with an imidazolyl group, however, aggregates were formed in water as was shown by electron microscopy. The supramolecular structures could be fine-tuned by changing the pH and by adding metal ions. We decided to systematically investigate the possibility of fine-tuning the aggregates by variation of both the structure of the amphiphile molecule as well as the metal ions added. Although the form of the suprastructures in water was found to be different, in many cases the underlying molecular pattern was the same, *viz.* a layered structure. Apparently, the carbohydrate moiety determines the basic mode of molecular assembly of the amphiphilic molecule, while the fine tuning of the higher organization is achieved by the metal ions or protons present. In order to vary the distance of the complexed ion to the surface of the aggregate, the location of the imidazolyl groups in the gluconamide amphiphiles was modified. When the imidazole group was linked to the hydrophobic end of the molecule, an *intramolecular* hydrogen bond was formed between this imidazolyl group and the amide group which prevented the molecule to adopt a stretched out conformation, which would be required to exhibit amphiphilic behavior according to the packing parameter concept. When, however, the imidazole group was placed between the alkyl chain and the carbohydrate framework, aggregates could be formed in water although the copper coordinating behavior of these molecules was different from those with imidazole groups present at the carbohydrate terminus of the molecules.

Gluconamide based aggregates proved to be useful as a matrix for anchoring catalysts. The interior of the aggregates acted as a hydrophobic medium for aziridination reactions, which normally can not be carried out in the presence of water since the proposed intermediate ( $\text{Cu}=\text{N}-\text{R}$ ) is very water-sensitive. Unfortunately, the chirality of the amphiphilic molecules and the suprastructures did not lead to enantioselective reactions.

Besides lyotropic liquid crystalline behavior, carbohydrates with a long aliphatic chain can display thermotropic liquid crystalline (LC) behavior. This dualistic character of these molecules (which make them "schizophrenes") was used to investigate the binding forces (non-covalent interactions) that are operative in the suprastructures. In most carbohydrate-based LC compounds the sugar moiety acts as a mesogenic group forming an extensive *intermolecular* (dynamic)

hydrogen bonding network with its hydroxyl groups. In the case of the gluconamides the amide function also participates in the hydrogen bonding scheme, but in the 6-substituted-2,4,3,5-dimethylene-D-gluconamides no hydrogen bonding network can be formed since the carbohydrate has no free hydroxyl groups. By applying structural variation of the gluconamides, it was found that *interlayer* interactions are needed for thermotropic LC behavior. This idea was confirmed in a crystal structure of one of the compounds, which showed that water molecules in the supramolecular aggregates can form *interlayer* hydrogen bonds and act as a lubricant in the LC (smectic A) state. The absence of *intermolecular* hydrogen bonds between the amides functions in the LC state was surprising. Upon complexation of the gluconamides to copper ions (via attached imidazole functions), forming metallomesogens, the water molecules were replaced by copper(II) ions, and in this case the layer of counter ions was found to act as a lubricant.

Substitution of the C-6 hydroxyl groups of the *N,n*-alkyl-D-gluconamides gave compounds that formed suprastructures in other solvents than water *viz* organic solvents like chloroform, ethanol and ethyl acetate. Aggregation led to the formation of rigid gels. Transmission electron micrographs of dried gels showed fibrous aggregates with high aspect ratios. In some cases, the fibers displayed chirality, *viz* helices and twisted bilayers. Aliphatic and small aromatic substituents on C-6 resulted in compounds that formed chiral aggregates, while large aromatic groups gave rise to non chiral aggregates. The gels collapsed upon heating (in some cases at temperatures far above the boiling temperature of the solvent) but they were formed again upon cooling. The stacking of the substituted gluconamides in the organogels was investigated with FT-IR, X-ray powder diffraction and DSC. It was found that generally the gluconamides are packed in a head to tail fashion, except for the molecules that can form *interlayer* hydrogen bridges, which have head to head packing. From DSC results it was concluded that the formation of the gels is an entropy driven process. Preliminary experiments showed that organogels can also be obtained in a mixture of methyl and *n*-butyl methacrylate. After polymerization of the solvent the aggregates were removed and well-defined channels were obtained.

# Samenvatting

In dit proefschrift wordt de synthese en het aggregatiegedrag van glucosederivaten met onvertakte alkylketens bestaande uit 8 of 16 koolstofatomen en de metaalcomplexen daarvan beschreven. Dit soort moleculen zijn amfifielen, dat wil zeggen dat in water door zelf-associatie op basis van niet-covalente bindingen aggregaten of suprastructuren worden gevormd. Uit de literatuur was bekend dat *N,n*-alkyl-D-gluconamides in water helices vormen. De bedoeling was deze helices te gebruiken als chirale matrix voor katalyse. Om dit te bereiken werden metaalbindende imidazool- en pyridyl-groepen aan de gluconamides bevestigd. De secundaire hydroxylgroepen van de gluconamides werden beschermd met methyleenbruggen; hetgeen resulteerde in niet-amfifiële verbindingen. Echter, na substitutie van de primaire hydroxylgroep met een imidazoolgroep, werden in water weer aggregaten gevormd, zoals te zien was met elektronenmicroscopie. De vorm van de suprastructuren kon worden ingesteld door verandering van de pH of door toevoeging van metaalionen. De mogelijkheid tot variatie van de vorm van de suprastructuren werd systematisch onderzocht door verandering in de structuur van de amfifielen aan te brengen en door metaalionen toe te voegen. Hoewel de vorm van de suprastructuren in water kon verschillen, bleek in veel gevallen de moleculaire opbouw dezelfde te zijn, te weten een gelaagde structuur. Het bleek dat het koolhydraatgedeelte het aggregatieproces domineerde, terwijl de hogere structuur werd bepaald door metaalionen of protonen. Om de lokatie van mogelijke metaalcomplexen binnen het aggregaat te variëren werd de plaats van de imidazoolgroep in het gluconamide-molecuul veranderd. Bij verplaatsing van de imidazoolgroep naar het hydrofobe eind van het molecuul verdween het amfifiële karakter omdat een *intramoleculaire* waterstofbrug tussen de imidazoolgroep en de amidegroep werd gevormd die het molecuul krom trekt, waardoor het niet meer voldoet aan het pakkings-parameterconcept. Wanneer de imidazoolgroep tussen de kopgroep en de alkylstaart geplaatst werd, bleef het amfifiële karakter wel behouden en werden aggregaten in water gevormd.

Aggregaten op basis van gluconamides bleken bruikbare matrices voor de verankering van katalysatoren te zijn. Het aggregaat fungeerde als hydrofoob medium voor aziridineringsreacties, die normaal in aanwezigheid van water niet kunnen plaatsvinden omdat het voorgestelde intermediair ( $\text{Cu}=\text{N}-\text{R}$ ) gevoelig is voor dit oplosmiddel. Helaas bleek de chiraliteit van de amfifiële liganden en de suprastructuren niet over te worden gedragen op de katalytische reacties, zodat er geen enantioselectieve katalyse werd waargenomen.

Naast lyotroop-vloeibaar-kristallijn gedrag kunnen suikers met een lange alkylstaart ook thermotroop-vloeibaar-kristallijn (LC) gedrag vertonen. Dit dualistisch karakter van de moleculen (waardoor ze “schizofreen” worden genoemd) werd gebruikt om de niet-covalente interacties binnen de suprastructuren te onderzoeken. In de meeste LC-koolhydraten, fungeert het suikergedeelte als een mesogene groep die een uitgebreid dynamisch *intermoleculair* waterstofbrugnetwerk vormt. Bij gluconamides participeert de amidegroep ook in dit waterstofbrugnetwerk. In het geval van 6-gesubstitueerde-2,4,3,5-dimethyleen-D-gluconamides kan geen netwerk worden gevormd omdat het koolhydraat geen vrije hydroxylgroepen meer

bevat Door structurele variatie in de verbindingen aan te brengen werd gevonden dat interacties tussen de verschillende lagen nodig is voor thermotroop LC gedrag Dit idee werd bevestigd door opheldering van de kristalstructuur van een van de gluconamides, waarin duidelijk werd dat watermoleculen waterstofbruggen vormen tussen de verschillende bilagen in de aggregaten en daarbij dienen als smeermiddel voor de bilagen in de vloeibaar-kristallijne (smectisch A) fase Verrassend was de afwezigheid van *intermoleculaire* waterstofbruggen in de LC-fase Bij complexering van de imidazoolderivaten aan koper(II)ionen werden de watermoleculen vervangen door deze koperionen en dienden de tegenionen als smeermiddel in de LC-fase

Substitutie van de C-6 hydroxylgroepen van *N,n*-alkyl-D-gluconamides resulteerde in de vorming van suprastructuren in andere oplosmiddelen dan water zoals chloroform, ethanol en ethylacetaat Door aggregatie werden stijve gellen gevormd Uit transmissie-elektronenmicroscopie opnamen van gedroogde gellen werd duidelijk dat deze bestaan uit vezels met een grote lengte/diameter-verhouding De vezels vertoonden in sommige gevallen chiraliteit in de vorm van helices en gedraaide bilagen Alifatische en kleine aromatische substituenten in het gluconamide leidden tot chirale aggregaten, terwijl grotere aromatische groepen niet-chirale aggregaten tot gevolg hadden De gelering verdween bij verwarming (in sommige gevallen pas bij temperaturen boven het kookpunt van het oplosmiddel) maar keerde terug bij afkoeling De pakking van de gesubstitueerde gluconamides in de organogelen werd onderzocht met behulp van FT-IR, Röntgen poederdiffractie en DSC Gluconamides blijken over het algemeen in een kopstaart-pakking te aggregeren, behalve als de moleculen de mogelijkheid hebben tot het vormen van een waterstofbrug tussen de verschillende lagen Uit DSC-experimenten werd duidelijk dat de vorming van de gellen een entropie gedreven proces is In oriënterende experimenten werd een organogel verkregen in een mengsel van methyl- en n-butylmethacrylaat Na polymerisatie van de hars werden de aggregaten verwijderd en goed gedefinieerde kanalen bleven achter

# Curriculum Vitae

Op 6 Juli 1966 werd in Dieren de auteur van dit proefschrift geboren. In 1983 werd het HAVO-diploma aan het Thomas a Kempis College te Arnhem behaald. Daarna werd begonnen met de HLO-studie, differentiatie Organische Chemie aan de OLAN te Arnhem, waarbij de stage- en de afstudeeropdracht bij Akzo research in Arnhem (afdeling CRH, exploratieve organische en polymeerchemie) werden uitgevoerd. Aansluitend op het behalen van het diploma in 1987 werd een vaste baan bij Akzo research aanvaard. In augustus 1988 is de auteur begonnen met de deeltijdstudie Scheikunde aan de Rijks Universiteit Utrecht welke met succes werd afgerond in april 1991 met als hoofdvak Fysisch-organische Chemie (Prof. W. Drenth), in een samenwerkingsproject met de afdeling TUD (Prof. W. Mijs) en Akzo research (afdeling CRH). Per 1 december 1991 heeft de auteur Akzo verlaten en was van 1 november 1991 tot en met 31 oktober 1995 in dienst van de Katholieke Universiteit Nijmegen. Tijdens de laatst genoemde aanstelling werd het onderzoek onder leiding van Prof. R.J.M. Nolte en Dr. M.C. Feiters, beschreven in dit proefschrift, uitgevoerd. Als onderwijstaken heeft de auteur 2 maal de herfstcursus voor middelbare scholieren georganiseerd en werkcolleges aan eerstejaars-chemiestudenten gegeven. Sinds 1 februari 1996 is de auteur in dienst van Unilever Research te Vlaardingen (afdeling Biological Cleaning).







